RENEWABLE ENERGY AND ENVIRONMENTAL SUSTAINABILITY USING BIOMASS FROM DAIRY AND BEEF ANIMAL PRODUCTION

Final Report
Volume I of Three Volume Reports

VOLUME 1: THERMO-CHEMICAL CONVERSION AND DIRECT COMBUSTION METHODS

DE-FG36-05GO85003
June 1, 2005 to April 30, 2012

Submitted by
Kalyan Annamalai[1],
John M. Sweeten[2],
Brent W. Auvermann[2],
Saqib Mukhtar[3],
Sergio Caperada[3]
Cady R. Engler[3],
Wyatte Harman[4]
Reddy JN[1]
Robert Deotte[5]

[1]Department of Mechanical Engineering, Texas Engineering Experiment Station (TEES), Texas A&M University (TAMU), College Station, TX 77843-3123

[2]Texas AgriLife Research (formerly Texas Agricultural Experiment Station), Texas A&M University System (TAMUS), Texas AgriLife Research & Extension Center-Amarillo 6500 Amarillo Blvd West, Amarillo, TX 79106-1796

[3] TAMU Biological and Agricultural Engineering Department (BAEN) & Texas AgriLife Research, Texas A&M University, 217 Scoates Hall, College Station, TX 77843-2117

[4]Blackland Research and Extension Center, Texas AgriLife Research (formerly Texas Agricultural Experiment Station)-Temple 720 E. Blackland Road, Temple, TX 76502

[5]Department of Agricultural Sciences & Engineering,
West Texas A&M University, Canyon, TX 79016-0001

April 26, 2012

Submitted to

US Department of Energy-Golden Field Office,
MS1501, 1617 Cole Blvd., Golden, CO80401, USA

ACKNWOWLDGEMENT: This final report is based upon work supported by the U. S. Department of Energy under Award No. DE-FG36-05GO85003.

DISCLAIMER: This report was prepared as an account of work sponsored by an agency of the United States Government. Neither the United States Government nor any agency thereof, nor any of their employees, makes any warranty, expressed or implied, or assumes any legal liability or responsibility for the accuracy, completeness, or usefulness of any information, apparatus, product, or process disclosed, or represents that its use would not infringe privately owned right. Reference herein to any specific commercial product, process, or service by trade name, trademark, manufacturer, or otherwise does not necessarily constitute or imply its endorsement, recommendation, or favoring by the Untied States Government or any agency thereof. The views and opinions of authors expressed herein do not necessarily state or reflect those of the United States Government or any agency thereof.

Executive Summary for the Three Volume Final Report

Renewable Energy and Environmental Sustainability Using Biomass from Dairy and Beef Animal Production Facilities

Texas Engineering Experiment Station and
Texas AgriLife Research & West Texas A&M University
Texas A&M University, College Station, TX 77843-3123

USDOE Award No. DE-FE3605GO85003

The Texas Panhandle is regarded as the "Cattle Feeding Capital of the World", producing 42% of the fed beef cattle in the United States within a 200-mile radius of Amarillo generating more than 5 million tons of feedlot manure /year. Apart from feedlots, the Bosque River Region in Erath County, just north of Waco, Texas with about 110,000 dairy cattle in over 250 dairies, produces 1.8 million tons of manure biomass (excreted plus bedding) per year.

While the feedlot manure has been used extensively for irrigated and dry land crop production, most dairies, as well as other concentrated animal feeding operations (CAFO's), the dairy farms utilize large lagoon areas to store wet animal biomass. Water runoff from these lagoons has been held responsible for the increased concentration of phosphorus and other contaminates in the Bosque River which drains into Lake Waco—the primary source of potable water for Waco's 108,500 people. The concentrated animal feeding operations may lead to land, water, and air pollution if waste handling systems and storage and treatment structures are not properly managed. Manure-based biomass (MBB) has the potential to be a source of green energy at large coal-fired power plants and on smaller-scale combustion systems at or near confined animal feeding operations. Although MBB particularly cattle biomass (CB) is a low quality fuel with an inferior heat value compared to coal and other fossil fuels, the concentration of it at large animal feeding operations can make it a viable source of fuel. The overall objective of this interdisciplinary proposal is to develop environmentally benign technologies to convert low-value inventories of dairy and beef cattle biomass into renewable energy. Current research expands the suite of technologies by which cattle biomass (CB: manure, and premature mortalities) could serve as a renewable alternative to fossil fuel. The work falls into two broad categories of research and development.

Category 1 – Renewable Energy Conversion. This category addressed mostly in volume I involves developing. Thermo-chemical conversion technologies including cofiring with coal, reburn to reduce nitrogen oxide (NO, N2O, NOx, etc.) and Hg emissions and gasification to produce low-BTU gas for on-site power production in order to extract energy from waste streams or renewable resources.

Category 2 – Biomass Resource Technology. This category, addressed mostly in Volume II, deals with the efficient and cost-effective use of CB as a renewable energy source (e.g. through and via aqueous-phase, anaerobic digestion or biological gasification).

The investigators formed an industrial advisory panel consisting fuel producers (feedlots and dairy farms) and fuel users (utilities), periodically met with them, and presented the research results; apart from serving as dissemination forum, the PIs used their critique to red-direct the research within the scope of the tasks.

The final report for the 5 to 7 year project performed by an interdisciplinary team of 9 professors is arranged in three volumes: Vol. I (edited by Kalyan Annamalai) addressing thermo-chemical conversion and direct combustion under Category 1 and Vol. II and Vol. III (edited by J M Sweeten) addressing biomass resource Technology under Category 2. Various tasks and sub-tasks addressed in Volume I were performed by the Department of Mechanical Engineering (a part of TEES; see Volume I), while other tasks and sub-tasks addressed in Volume II and IIII were conducted by Texas AgriLife Research at Amarillo; the TAMU Biological & Agricultural Engineering Department (BAEN) College Station; and West Texas A&M University (WTAMU) (Volumes II and III).

The three volume report covers the following results: fuel properties of low ash and high ash CB (particularly DB) and MB (mortality biomass and coals, non-intrusive visible infrared (NVIR) spectroscopy techniques for ash determination, dairy energy use surveys at 14 dairies in Texas and California, cofiring of low quality CB with high quality coal, emission results and ash fouling behavior, using CB as reburn fuel for NOx and Hg reduction, gasification of fuels to produce low quality gases, modeling of reburn, pilot scale test results, synthesis of engineering characterization, geographical mapping, a transportation cost study to determine potential handling and transportation systems for co-firing with coal at regional coal-fired power plants, software analyses for the design of off-site manure, pre-processing and storage systems for a typical dairy farm or beef cattle feedlot, recursive production functions/systems models for both cattle feedlots , systems modeling, stocks and flows of energy involved in the CAFO system, feedback from an Industry Advisory Committee (IAC) to the investigators on project direction and task emphasis and economics of using CB as cofiring and reburn fuel,

TABLE OF CONTENTS-VOL I Page

Executive Summary of Accomplishments **22**

INTRODUCTION **26**

Overall Objective **30**

Team and Investigators **30**

Summary of Proposed Project Tasks and Assigned Investigators **32**

Industrial Advisory Committee Members **36**

Summary of Tasks performed under Thermo-Chemical Energy Conversion (Volume I) **36**

References **37**

1. FEEDLOT AND DAIRY MANURE RESOURCES AND FUEL PROPERTIES **40**

- **1.1. Introduction** **41**
- **1.2. Literature review** **41**
  - *1.2.1.* Coal 41
  - *1.2.2.* Feedlot Manure or Feedlot Biomass (FB) 43
  - *1.2.3.* Dairy Manure or Dairy Biomass (FB) 44
  - *1.2.4.* Hog or Swine Biomass 44
- **1.3. Fuel Properties** **46**
  - *1.3.1.* Coal 47
  - *1.3.2.* Feedlot Biomass 50
  - *1.3.3.* Dairy Biomass 53
  - *1.3.4.* Natural Gas 63
  - *1.3.5.* Blend of Coal: DB 64
  - *1.3.6.* Ash Analyses 65
- **1.4. Impact on Tasks due to Industrial Advisory Committee feed back** **68**
- **1.5. Summary** **69**
- **1.6. References** **69**
- **1.7. Acronyms** **71**
- **1.8. Education** **73**
- **1.9. Other support** **73**
- **1.10. Dissemination** **73**

2. FUEL PYROLYSIS AND IGNITION **74**

2.1. Introduction **75**
2.2. Literature Review **75**
2.2.1. Manure Collection Techniques 75
2.2.2. Fuel Properties 76
2.2.3. Ignition 80
2.3. Objectives **80**
2.4. Experiments and Procedure **81**
2.5. Results and discussion **82**
2.5.1. Pyrolysis Characteristics 82
2.5.2. Ignition Characteristics 88
2.5.3. Pyrolysis Model 89
2.5.4. Ignition introduction 105
2.5.5. Effect of Fuel 105
2.5.6. Effect of Particle Size 106
2.6. Summary and Conclusions **108**
2.7. Acronyms **109**
2.8. Education and Training **110**
2.9. References **110**
2.10. Other support **110**
2.11. Dissemination **110**

3. COFIRING **112**

3.1. Introduction **113**
3.2. Literature review **113**
3.3. Objectives **121**
3.4. Experimental setup and procedure **122**
3.4.1. Experimental Facility 122
3.4.2. Instrumentation 127
3.4.3. Experimental Procedure 127
3.5. Results and discussion **128**
3.5.1. Introduction 128
3.5.2. Fuel Properties 129
3.5.3. Experimental Parameters 130
3.5.4. O_2 and Equivalence Ratio 131
3.5.5. CO and CO_2 Emissions 133
3.5.6. Burnt Fraction 136
3.5.7. NO_x Emissions 138
3.5.8. Fuel Nitrogen Conversion Efficiency 142
3.6. Impact on Tasks due to Industrial Advisory Committee feed back **144**
3.7. Summary **145**
3.8. Acronyms and symbols **145**
3.9. References **146**
3.10. Education and Training **148**
3.11. Other support **148**
3.12. Dissemination **148**

4. REBURN FOR NOX REDUCTION **151**

4.1. Introduction **152**

4.2. Literature review **152**
4.3. Objectives **159**
4.4. Experimental setup **159**
4.5. Results and discussion **163**
4.6. Impact on Tasks due to Industrial Advisory Committee feed back **176**
4.7. Summary **177**
4.8. Acronyms and symbols **178**
4.9. References **180**
4.10. Education and Training **182**
4.11. Other support if any **182**
4.12. Dissemination **182**
4.13. Patents if any **184**

5. GASIFICATION **185**

5.1. Introduction **186**
5.2. Literature review **186**
5.3. Objectives **188**
5.4. Experiments **189**
5.4.1. Experimental facility 189
5.4.2. Experimentation 190
5.4.3. Enriched oxygen mixture Gasification 190
5.4.4. Experimental procedure 191
5.4.5. Experimental Procedure for enriched oxygen gasification 192
5.4.6. Modeling 192
5.5. Results and discussion **194**
5.5.1. Fuel properties 194
5.5.2. Modeling Results and discussion for air gasification 195
5.5.3. Experimental Results and discussion for air gasification 201
5.5.4. Experimental results and discussion for enriched air gasification 210
5.6. Impact on Tasks due to Industrial Advisory Committee feed back **215**
5.7. Summary **215**
5.7.1. Gasification facility 215
5.7.2. Modeling studies 215
5.7.3. Experimental studies 216
5.8. Acronyms **217**
5.9. References **219**
5.10. Education and Training **221**
5.11. Other support **221**
5.12. Dissemination **222**

6. PILOT SCALE TESTS ON COFIRING AND REBURN FOR HG REDUCTION **223**

6.1. Introduction **225**
6.2. Pilot scale facility selection **227**
6.3. Problems and solutions regarding pilot test conditions **228**
6.4. Operating conditions **231**
6.5. Pilot scale research facility **237**

6.6. Diagnostics **243**
6.7. Results **244**
6.8. Summary **250**
6.9. Acknowledgements **252**
6.10. Acronyms and symbols **252**
6.11. References **253**
6.12. Education and training **254**
6.13. Other support if any **254**
6.14. Dissemination **254**
6.15. Patents if any **254**

7. REBURN MODELING **254**

7.1. Introduction **255**
7.2. Literature review **256**
7.2.1. NO_x formation 256
7.2.2. Control of NO_x emission 257
7.2.3. Parameters that influence the NO_x reduction in reburner process 257
7.2.4. Reburning with different fuels 258
7.3. Objective and tasks **258**
7.4. Explanation of model **258**
7.4.1. General outline of the reburn model 259
7.4.2. Main burner modeling 260
7.4.3. Natural gas composition 261
7.4.4. Reburner modeling 262
7.4.5. Mixing model 267
7.4.6. Chemical reactions 268
7.5. Results and discussion **276**
7.5.1. Discussion of the numerical model 276
7.5.2. NO_x results 277
7.5.3. Fuel Nitrogen emission modeling 289
7.5.4. NO reaction kinetics 291
7.5.5. Ammonia content 293
7.5.6. Particle size distribution 294
7.5.7. Reburn Thermal Energy 295
7.5.8. Reburner Inlet Temperature 296
7.6. Summary **296**
7.7. Acronyms **297**
7.8. References **297**
7.9. Education and Training **299**
7.10. Other support **299**
7.11. Publications **299**

8. DIRECT COMBUSTION **300**

8.1. Introduction **300**
8.2. Literature Review **300**
8.3. Objectives **307**
8.4. Experiential Procedure **308**

8.4.1. Modeling Small-Scale, On-the-farm Manure-Based Biomass Combustion Systems 308
8.4.2. Combustion System for High Moisture Manure-based Biomass 308
8.4.3. Combustion System for Scraped Solids and Lower Moisture Biomass 315
8.5. Results And Discussion 316
8.5.1. Base Run 316
8.5.2. Flushing Systems and Solids Separation 318
8.5.3. Effect of Drying Solids Before Combustion 321
8.5.4. Combustion of Dried Biomass Solids 322
8.5.5. Operation of Fire-tube Boiler 325
8.5.6. Additional Fueling for Complete Wastewater Disposal 326
8.6. Summary And Conclusions 327
8.7. Acronyms 328
8.8. References 329
8.9. Student's & Training 330
8.10. Other support 330
8.11. Dissemination 330

9. ASH CHARACTERIZATION 331

10. ECONOMIC MODELING OF CATTLE BIOMASS ENERGY SYSTEMS332

10.1. Introduction 332
10.2. Literature Review 333
10.2.1. Co-firing Coal with Biomass 333
10.2.2. Reburning Coal with Biomass 336
10.2.3. Competing NO_x Control Technologies 337
10.2.4. Dollar Values of Emissions 337
10.3. Objectives 338
10.4. Experimental Procedure 338
10.4.1. Biomass Drying Models 338
10.4.2. Biomass Transportation Model 354
10.5. Economics of Manure-based Biomass Combustion in Large-scale Coal-fired Power Plants 358
10.5.1. Co-firing 359
10.5.2. Reburning 385
10.5.3. Economic Estimations for Small-scale Manure-based Biomass Systems 401
10.6. Impact on Tasks due to Industrial Advisory Committee feed back 404
10.7. Summery and Conclusions 404
10.7.1. Economics of Co-firing 404
10.7.2. Economics of Reburning 405
10.8. Acronyms 406
10.9. References 407
10.10. Education and Training 410
10.11. Other support 410
10.12. Dissemination 410

11. CO-FIRE AND REBURN FOR HG REDUCTION 412

11.1. Introduction 414

11.2. Literature review **416**
11.3. Objectives **429**
11.4. Experimental facility and procedure **430**
11.5. Results and discussion **437**
11.6. Impact on Tasks due to Industrial Advisory Committee feed back **447**
11.7. Summary and conclusions **447**
11.8. Acronyms and symbols **448**
11.9. References **450**
11.10. Education and training **452**
11.11. Other support if any **452**
11.12. Dissemination **452**
11.13. Patents/disclosures if any **454**

List of Figures **Page**

Figure 0.1. Overview on Energy Conversion Methods……26

Figure 1.2.1 Coal fields in the United States [EIA, 2005] 42
Figure 1.2.2 Feedlot cattle on large confined animal feeding operation [FactoryFarm.org, 2007] 43
Figure 1.2.3 Total inventory of hogs and pigs by state in the US in 2007 (NASS, 2007) 45
Figure 1.3.1 Manure production and environmental effects 48
Figure 1.3.2 Feedlot biomass collection at paved surfaced feed 49
Figure 1.3.3 Feedlot biomass collection at soil surfaced feed yards 49
Figure 1.3.4 Higher heating values for cattle ration, raw FB, partially composted FB, finished composted FB, coal, and respective FB+5% crop residue blends [adopted from Sweeten et al., 2003] 51
Figure 1.3.5 Screen solid-liquid separator. 53
Figure 1.3.6 Current dairy and feedlot manure disposal [adapted from Schmidt et al., 1988] 54
Figure 2.5.1: TGA and DTA trace of TXL. 86
Figure 2.5.2: TGA and DTA trace of PRB 86
Figure 2.5.3: TGA and DTA trace of LA-PC-DB-SepSol. 87
Figure 2.5.4: TGA and DTA trace of HA-PC-DB-SoilSurf 88

Figure 2.5.5: Example of ignition of TXL coal. Ignition is the point where the difference curve begins to deviate from 0%. 92
Figure 2.5.6: Ultimate Analysis of LA-PC-FB. 93
Figure 2.5.7: Variation of Fuel Properties for HA-RM-FB. 94
Figure 2.5.8 : Single Reaction Model Rigorous Solution Activation Energy for As Received Classification. 97
Figure 2.5.9: Single Reaction Model Rigorous Solution Activation Energy for LA-PC-FB, Effect of Particle Size 98
Figure 2.5.10: Activation Energy Results Obtained Using the Slope Approximation. ... 99
Figure 2.5.11: DAEM Activation Energy of AR Biomass Fuels. 99
Figure 2.5.12: DAEM Standard Deviation of AR Biomass Fuels. 100
Figure 2.5.13: DAEM Activation Energy of 60 Micron Class Biomass Fuels. 100
Figure 2.5.14: DAEM Standard Deviation of 60 Micron Class Biomass Fuels. 100
Figure 2.5.15: DAEM Activation Energies of 22.5 Micron Class Biomass Fuels. 101
Figure 2.5.16: DAEM Standard Deviations of 22.5 Micron Class Biomass Fuels. 101
Figure 2.5.17: Average Activation Energy of Biomass Fuels for DAEM as a Function of TXL Coal Percentage in Blend. 102
Figure 2.5.18: DAEM Activation Energy of LA-PC-FB 103
Figure 2.5.19: DAEM Standard Deviation for LA-PC-FB. 103
Figure 2.5.20: DAEM Activation Energies for HA-PC-FB. 103
Figure 2.5.21: DAEM Standard Deviations for HA-PC-FB. 104
Figure 2.5.22: Ignition Temperature for the As Received Particle Class. 106
Figure 2.5.23: Ignition Temperatures for the 60 Micron Particle Class. 106
Figure 2.5.24: Ignition Temperatures for the 22.5 Micron Particle Class. 106
Figure 2.5.25: Ignition Temperatures for LA-PC-FB. 107
Figure 2.5.26: Ignition Temperatures for LA-RM-FB. 107
Figure 2.5.27: Ignition Temperatures for HA-PC-FB. 107
Figure 2.5.28: Ignition Temperatures for HA-RM-FB. 108
Figure 3.2.1. Schematic of a 450 kg (1000 lb) cattle waste production process from excretion to collection. 114
Figure 3.2.2. U.S. annual milk production distribution. Despite the decrease in the number of small dairies, total dairy production is increasing due to the number of large dairies increasing. 115
Figure 3.2.3. U.S. annual milk production per cow. Increased dairy efficiency leads to higher milk production per head of cow. 116
Figure 3.2.4. Western expansion of dairies. 117
Figure 3.2.5. Tillman's (2000) NO_x reduction from cofiring coal with AB fuels. Note the measured NO_x trend line is lower than the predicted NO_x trend line. 120
Figure 3.4.1.1. Schematic of boiler burner facility at Coal and Biomass Laboratory at Texas A&M University. 123
Figure 3.4.1.2. Dimensioned 100,000 BTU/hr furnace constructed by Thien (2002). .. 125
Figure 3.4.1.3. Dimensioned cross-section of greencast 94 refractory sections used in furnace. 126
Figure 3.4.1.4. Detailed cross-section of fins used to mix primary and secondary air. . 127

Figure 3.5.4.1. Equivalence ratio based on air flow rates and the calibrated fuel flow rate vs. equivalence ratio based on O2% in exhaust for TXL and TXL:DB blended fuels. 132
Figure 3.5.4.2. Equivalence ratio based on air flow rates and calibrated fuel flow rate vs. equivalence ratio based on O_2% in exhaust for TXL and TXL:DB blended fuels.133
Figure 3.5.5.1. Effect of fuel on CO_2 for TXL and TXL:DB blended fuels. 134
Figure 3.5.5.2. Effect of fuel on CO for TXL and TXL:DB blended fuels. 134
Figure 3.5.5.3. Effect of fuel on CO_2 for WYO and WYO:DB blended fuels.....135
Figure 3.5.5.4. Effect of fuel on CO for WYO and WYO:DB blended fuels. 136
Figure 3.5.6.1. Effect of fuel on BF for TXL and TXL:DB blended fuels. Note that in the rich regime, the BF overlaps for all fuels. This indicates that the same percentage of all fuels was burnt. 137
Figure 3.5.6.2. Effect of fuel on BF for WYO and WYO:DB blended fuels. Note that the data points come close to overlapping for all equivalence ratios. Thus, BF was independent of fuel type. 137
Figure 3.5.7.1. Effect of fuel on NO_x for TXL and TXL:DB blended fuels. Note that blended fuels have lower NO_x values at stoichiometric and in rich combustion. ..138
Figure 3.5.7.2. Effect of fuel on NO_x for TXL and TXL:DB blended fuels corrected to 3% O_2. 139
Figure 3.5.7.3. Effect of fuel on NO_x for TXL and TXL:DB blended fuels in kg/GJ. ..139
Figure 3.5.7.4. Effect of fuel on NO_x for WYO and WYO:DB blended fuels. Note how NO_x decreases in the near lean region for blended fuels.....140
Figure 3.5.7.5. : Effect of fuel on NO_x for WYO and WYO:DB blended fuels corrected to 3% O_2. 141
Figure 3.5.7.6. Effect of fuel on NO_x for WYO and WYO:DB blended fuels in kg/GJ. 142
Figure 3.5.8.1. Effect of fuel on nitrogen conversion efficiency for TXL and TXL:DB blended fuels. Note that the conversion efficiency is less than coal for almost all TXL:DB blended fuels. 143
Figure 3.5.8.2. Effect of fuel on nitrogen conversion efficiency for WYO and WYO:DB blended fuels. Note that the conversion efficiency is less than coal for almost all WYO:DB blended fuels. 144
Figure 4.2.1. Reburn zones.....153
Figure 4.2.2. NOx Formation And Reduction Paths By Fuel-N Depending On The Stoichiometry 154
Figure 4.4.1. DB and FB Fuels – Classification.....160
Figure 4.4.2.A schematic of the small-scale 30 kWt (100,000 Btu/h) downward fired boiler burner facility. 161
Figure 4.5.1. Properties of the fuel blends on a dry basis: (a) Cl and Hg and (b) Fuel-N, ash loading and HHV 167
Figure 4.5.2. Particle size (Rosin Rammler) distributions of the reburn fuels.....169
Figure 4.5.3. TGA results during pyrolysis (N2) and oxidation (air) 170
Figure 4.5.4 TEMPERATURE DISTRIBUTIONS OF THE FLUE GAS ALONG THE FURNACE 171

Figure 4.5.5 . NO_x levels for FB and Coal with a 0° injection angle. 174
Figure 4.5.6. Comparison of vitiated vs. non-vitiated reburn experiments.....175
Figure 4.5.7. NOx reductions during the reburning experiments with Coal as Reburn fuels 176
Figure 4.5.8. NO_x EMISSIONS USING DAIRY BIOAMSS (DB) AND COALS AS REBURN FUELS 176
Figure 4.7.1. Top view of slag or melted ash deposits in furnace.....177
Figure 5.4.1 Schematic Gasification Facility 189
Figure 5.5.1: Effect of the ER_M on CO, CO2, CH4 and H_2 production for FB, DB, TXL, and WYC with AOF at 0.25 and temperature at 800 K, estimated with atom balance 197
Figure 5.5.2: Effect of the ASTR on CO, CH_4, CO_2 and H_2 production for FB, DB, TXL, and WYC with ER_M at 2 and temperature at 800 K, estimated with atom balance 198
Figure 5.5.3: Effect of the ASTR on production of H_2, CO, and CH_4 for FB, DB, and TL with ER_M at 2, estimated with equilibrium model 199
Figure 5.5.4: Effect of the ER and ASTR on production of H_2 and CO for DB and FB, estimated with equilibrium model.....200
Figure 5.5.5: Effect of the ASTR and ER_M on HHV for DB, FB and TXL.....201
Figure 5.5.6: Effect of the ASTR and ER_M on energy recovery for DB, FB and TXL. 202
Figure 5.5.7 (a) Temperature Profile during a Typical Gas Analysis at ER=3.18 and SF=0.8 (b) Temperature Profile along of Gasifier Axis for Several ERs and S: F =0.68, (c) Peak Temperature Profile vs ER for Several S: F ratios. 203
Figure 5.5.8 (a) Gas Composition vs. time for a Typical Experiment at ER= 4.24 and S: F=0.35, (b) Gas Composition for Several ERs and S: F=0.68 206
Figure 5.5.9 (a) Hydrogen % vs ER for Several S: F ratios, (b) Carbon Monoxide % vs ER for Several S: F ratios (c) Carbon Dioxide % vs ER for several S: F ratios, (d) Mass of gases produced per kg of DAF DB on a dry tar free basis for gasification of pure DB 208
Figure 5.5.10. Temperature profile for ER = 2.1 and S:F = 0.....210
Figure 5.5.11. Temperature profile for ER = 4.2 and S:F = 0.....211
Figure 5.5.12. Temperature profile for ER = 4.2, S:F = 0.33.....212
Figure 5.5.13. Gas composition for ER = 2.11, S:F = 0.....213
Figure 5.5.14. Gas composition for ER = 4.2 and S:F = 0.....213
Figure 5.5.15. Gas composition for ER = 4.2 and S:F = 0.33.....214
Figure 5.5.16. Gas heating value for ER = 4.2 and different S:F.....214
Figure 6.4.1. Reburn Fuel Pallets Prepared and shipped by TAES-Amarillo/Bushland236
Figure 6.5.1. Combustion Research Facility (CRF) at SRI.....237
Figure 6.5.2. Temperature-time profile of the Combustion Research Facility (CRF). .238
Figure 6.5.3. Schematic of Pilot Scale Facility 239
Figure 6.5.4. Mercury speciation data with spike and recovery.....242
Figure 6.7.1. Estimated Equivalence Ratio (ϕ) of main burner and Equivalence Ratio the facility ; Note: there is no O2 supply from main burner; FEO: 3.7 %; Standard Flow at 60 F (376 SCF per lb mole).....246

Figure 6.7.2. Mercury speciation data for the ESP inlet, taken Wednesday, May 30th 247
Figure 6.7.3. Estimated % NOx reduction vs. estimated Reburn Zone Equivalence ratio RBZ using Galatia baseline coal at SRI preliminary tests 249
Figure 6.7.4. Mercury speciation data for the ESP inlet, taken Friday, May 25th. 250
Figure 7.4.1 Facility Schematics 258
Figure 7.4.2 Schematics of the Reburner Zone 259
Figure 7.5.1 Choice of Temporal Step, Texas Lignite 276
Figure 7.5.2 Effect of class size distribution on devolatilization rate 277
Figure 7.5.3 Temperature profile for LAPC, pure air, ER = 1 278
Figure 7.5.4 Comparison between temperature profile for Texas Lignite and LAPC, pure air, ER = 1 279
Figure 7.5.5 Temperature profile for LAPC, vitiated air, ER = 1 280
Figure 7.5.6 Comparison of temperature profiles for pure and vitiated air, LAPC, ER = 1 281
Figure 7.5.7. Comparison between temperature profile with real distribution and monosize, LAPC, pure air, ER = 1 282
Figure 7.5.8 Volatile emission rate LAPC, pure air, ER = 1 283
Figure 7.5.9 Comparison of normalized pyrolysis rate for pure and vitiated air, LAPC, ER = 1 284
Figure 7.5.10 Specific mass per Particle LAPC, pure air, ER = 1. 284
Figure 7.5.11 Fixed Carbon fraction LAPC, pure air, ER = 1 285
Figure 7.5.12 Comparison with experimental data LAPC, pure air 286
Figure 7.5.13 Comparison with experimental data LAPC, vitiated air 286
Fig.7.5.14. NO and oxygen concentration along the furnace, LAPC, pure air, ER = 1 . 287
Figure 7.5.15 Comparison of NO concentration along the furnace, pure and vitiated air, LAPC 288
Figure 7.5.16 Reaction rate involving NO, LAPC, pure air, ER = 1 289
Figure 7.5.17 Effect of different FN models 290
Figure 7.5.18 Effect of different FN emission model, Texas Lignite 291
Figure 7.5.19 Effect of different NO kinetics on the results, LAPC biomass 292
Figure 7.5.20 Effect of different NO kinetics on the results, Texas Lignite 292
Figure 7.5.21 Effect of ammonia fraction, LAPC biomass 293
Figure 7.5.22 Effect of ammonia fraction, Texas Lignite, pure air, ER = 1 294
Figure 7.5.23 Effect of SMD or real distribution on NO emission, Texas Lignite 295
Figure 7.5.24 Effect of reburner thermal power fraction 295
Figure 7.5.25 Effect of the Reburner Inlet Temperature on the NO_x emissions 296
Figure 8.2.1 Design for a wastewater treatment plant for large confined animal feeding operations and drainage of anaerobic treatment lagoons (Kolber, 2001) 301
Figure 8.2.2 Components of the covered waste processor in the wastewater treatment plant discussed by Kolber (2001) 302
Figure 8.2.3 The Elimanure^{TM} System developed by Skill Associates (2005) 303
Figure 8.2.4 Black box thermodynamic model of a manure energy conversion system (Carlin, 2005) 303

Figure 8.2.5 Required manure biomass solids composition needed to completely convert manure waste to combustion gases, water vapor, dry ash, and to maintain a desired system temperature of 373 K (Carlin, 2005) 304
Figure 8.2.6 Conceptualized model for manure biomass thermo-chemical energy conversion system for a CAFO (Carlin, 2005) 305
Figure 8.2.7 Waste disposal efficiency of conceptualized manure biomass energy conversion system vs. mass of additional fuel used for combustion (Carlin, 2005) 306
Figure 8.2.8 Schematic of a moving grate manure biomass combustor (adapted from Mooney *et al*., 2005) 307
Figure 8.4.1 Conceptualized design of MBB thermo-chemical energy conversion system for large free stall dairies or large indoor piggeries with flush waste disposal systems 309
Figure 8.4.2 Mass and energy balance of wastewater in fire-tube boiler 312
Figure 8.4.3 Conceptualized design of MBB thermo-chemical energy conversion system for large feedlot corrals or open lot dairies that produce low moisture manure 315
Figure 8.5.1 Sample output from computer spreadsheet model of small-scale on-the-farm manure biomass combustion system 317
Figure 8.5.2 Usable steam produced from combustion system vs. number of animals housed at the feeding operation 318
Figure 8.5.3 Usable steam, remaining wastewater, and disposal efficiency vs. moisture percentage of the flushed manure 319
Figure 8.5.4 Disposal efficiency and steam production vs. moisture content of the separated MBB solids 320
Figure 8.5.5 Boiler and disposal efficiency vs. the amount of solids remaining in the wastewater after the solid separator 320
Figure 8.5.6 Adiabatic flame temperature and wastewater mass flow vs. moisture percentage of the dried solids 321
Figure 8.5.7 Steam production and use vs. moisture percentage of the dried solids 322
Figure 8.5.8Effects of preheating combustion air 323
Figure 8.5.9Boiler efficiency vs. excess air percentage and stack temperature 323
Figure 8.5.10 Disposal efficiency vs. excess air percentage and stack temperature 324
Figure 8.5.11 Flame temperature, Steam production, and steam usage vs. ash percentage in the MBB solids 325
Figure 8.5.12The effect of ash percentage in the MBB solids on disposal efficiency 325
Figure 8.5.13 Steam production and disposal efficiency vs. moisture percentage of boiler blow down solids 326
Figure 8.5.14 The effect of additional fueling on the disposal efficiency 327
Figure 10.2.1 Schematic of a blended-feed co-firing arrangement for a pulverized coal boiler (adapted from DOE, 2004) 335
Figure 10.2.2 Schematic of a separate-feed co-firing arrangement for a pulverized coal boiler (adapted from DOE, 2004) 335
Figure 10.4.1 Mass and energy flow diagram for conveyor belt dryers (adapted from Kiranoudis et al., 1994) 339

Figure 10.4.2 Dryer air flow rate vs. air exit temperature and exit relative humidity at fixed chamber temperature drop, ΔTchamber = 10 K. MBB being dried from 60% to 20% moisture at a rate of 0.56 kg/s (2 metric tons/hour) 343
Figure 10.4.3Dryer air flow rate vs. air exit temperature and drying chamber temperature drop at fixed exit relative humidity = 20%. MBB being dried from 60% to 20% moisture at a rate of 0.56 kg/s (2 metric tons/hour) 344
Figure 10.4.4 Dryer heat consumption and air mass flow rate in drying chamber vs. rate of manure-based biomass 345
Figure 10.4.5 Comparison of two drying models for perpendicular air flow dryers by monitoring Reynolds number against characteristic biomass particle size and sphericity. Biomass application thickness on conveyor belt = 80 mm 346
Figure 10.4.6 Comparison of two drying models for perpendicular air flow dryers by monitoring Reynolds number against characteristic biomass particle size and biomass application thickness on conveyor belt 347
Figure 10.4.7 Determination of appropriate manure-based biomass application thickness 349
Figure 10.4.8 Comparison of fuel consumption between conveyor belt dryer and rotary steam-tube dryer 351
Figure 10.4.9 Temperature of entrained vapor and temperature of biomass solids in the drying zone vs. molar fraction of steam in vapor phase 352
Figure 10.4.10 Temperature of entrained vapor vs. characteristic particle size of biomass solids 353
Figure 10.4.11 The effect of holdup on the slope, biomass residence time, and biomass speed through a rotary steam-tube dryer 354
Figure 10.4.12 Montone 33.6 m3 (44 yd3) dump trailer (Montone Trailers, LLC., 2008) 355
Figure 10.4.13 Number of hauling vehicles and hauling weight vs. moisture percentage of transported manure based biomass 356
Figure 10.4.14 Total diesel fuel consumption from hauling vehicles vs. moisture percentage of transported manure based biomass 356
Figure 10.4.15 Total diesel fuel consumption and number of trucks required vs. biomass transport distance and trailer volume 357
Figure 10.4.16 Number of trucks required for hauling MBB vs. hauling schedule and annual number of hauling days 358
Figure 10.5.1 Flow diagram of computer spreadsheet model for coal/manure-based biomass co-firing system on an exiting coal-fired power plant. 359
Figure 10.5.2 Overall cash flows for the base case run of the manure-based biomass co-fire economics model 371
Figure 10.5.3 Biomass drying and transportation cost and annualized cost/revenue of biomass co-fire system vs. the biomass co-fire rate 372
Figure 10.5.4 Fueling rates for Wyoming sub-bituminous coal and low-ash dairy biomass vs. co-fire rate 372
Figure 10.5.5 Annualized cost/revenue and net present worth vs. year 1 coal price 373

Figure 10.5.6 Annualized cost/revenue and net present worth vs. year 1 farmer's asking price for manure 374
Figure 10.5.7 Annualized cost/revenue and net present worth vs. the value of CO2 375
Figure 10.5.8 Specific CO2 reduction cost/revenue vs. the value of CO2....376
Figure 10.5.9 Effect of flue gas desulphurization on the annualized cost/revenue of co-firing manure-based biomass with coal....377
Figure 10.5.10 Ash emission vs. co-fire rate when replacing Wyoming sub-bituminous coal with low-ash dairy biomass 378
Figure 10.5.11 Ash emission vs. co-fire rate when replacing Texas lignite with low-ash dairy biomass....378
Figure 10.5.12 Ash emission vs. co-fire rate when replacing Texas lignite with high-ash feedlot biomass....379
Figure 10.5.13 Matching coal-fired power plants and areas with high agricultural biomass densities, adapted from (Virtus Energy Research Associates, 1995) and (Western Region Ash Group, 2006)....380
Figure 10.5.14 Manure-based biomass co-fire O&M cost components vs. distance between plant and animal feeding operations 380
Figure 10.5.15 Manure-based biomass co-fire capital cost components vs. distance between plant and animal feeding operations 381
Figure 10.5.16 Annualized cost/revenue and net present worth vs. manure-based biomass transport distance....382
Figure 10.5.17 Annualized cost/revenue vs. natural gas price....383
Figure 10.5.18 Overall fuel costs for coals and low-ash dairy biomass at different drying requirements 384
Figure 10.5.19 Number of trucks and dryers and manure-based biomass fueling rate vs. power plant capacity....385
Figure 10.5.20 Flow diagram of computer spreadsheet model for reburning coal with manure-based biomass in an exiting coal-fired power plant along with comparisons to SCR and SNCR systems 386
Figure 10.5.21 Overall cash flows for the base case run of the manure-based biomass reburn economics model 391
Figure 10.5.22 Overall cash flows for the base case run of the SCR economics model 392
Figure 10.5.23 Drying and transport O&M costs and annualized cost/revenue vs. percentage of plant's heat rate supplied by manure-based biomass reburn fuel 393
Figure 10.5.24 Fueling rates of Wyoming sub-bituminous coal and low-ash dairy biomass vs. percentage of plant's heat rate supplied by the biomass reburn fuel ..394
Figure 10.5.25 Annualized cost/revenue and net present worth of manure-based biomass reburning and SCR vs. coal price....394
Figure 10.5.26 Annualized cost/revenue and net present worth vs. the value of CO2 ..395
Figure 10.5.27 Annualized cost/revenue for both MBB reburning and SCR vs. the value of NOx....396
Figure 10.5.28 Annualized cost/revenue vs. NOx levels achieved by primary NOx controllers....397

Figure 10.5.29 Specific NOx reduction cost/revenue for manure-based biomass reburning vs. the value of NOx 398
Figure 10.5.30 The effect of sulfur emissions on annualized cost during reburning 399
Figure 10.5.31 Ash emission vs. heat rate supplied by biomass reburn fuel for Wyoming sub-bituminous coal being replaced by low-ash dairy biomass 399
Figure 10.5.32 Annualized cost and net present worth of both reburning and SCR vs. manure-based biomass transport distance 400
Figure 10.5.33 Number of required trucks and dryers and biomass fueling rate vs. plant capacity 401
Figure 10.5.34 Simple payback period vs. the capital investment of the fire-tube boiler of the small-scale MBB combustion system 403
Figure 11.1.1. Layout of a coal fired power plant [Endress+Hauser, Coal Fired Power Plant, http://www.endress.com, August 2007] 415
Figure 11.2.1. Mercury loadings (in pounds of Mercury per 1012 British thermal units 419
Figure 11.2.2. Equilibrium speciation of mercury in flue gas as a function of temperature [14] 422
Figure 11.2.3. Effect of chlorine in coal with mercury emissions [18] 423
Figure 11.2.4. Mercury in flue gas path [32] 425
Figure 11.2.5. Effect of blending coal with biomass on mercury oxidation [22] 429
Figure 11.4.1. Dimensions of the furnace 431
Figure 11.4.2. Vertical section of the boiler 431
Figure 11.4.3. Schematic layout of the furnace and accessories 432
Figure 11.4.4. VM 3000 Mercury Vapor Monitor 433
Figure 11.4.5. Wet chemistry based flue gas conditioning system 434
Figure 11.4.6. Schematic of experimental setup 436
Figure 11.5.1. Variation of Cl and Heating values for different blends 438
Figure 11.5.2. Base case mercury results for Coal 439
Figure 11.5.3. Elemental Hg for TXL and its blends with Sep. Sol. PC-DB 440
Figure 11.5.4. Elemental Hg for WYC and its blends with Sep. Sol. PC-DB 441
Figure 11.5.5. Effect on elemental mercury ($\mu g/m^3$) when blending DB with coal on flue gas concentration basis 442
Figure 11.5.6. Effect on elemental mercury with chlorine content in fuel 443
Figure 11.5.7. Effect of NOx on elemental mercury 443
Figure 11.5.8.. Hg emissions using dairy bioamss (db) and prb/wyc as reburn fuels 445
Figure 11.5.9. Sorbed Hg Fraction: 15°C case for both chlorinated carbons 447

List of Tables **Page**

Table 1.2.1 Ultimate and heat value analyses of major coals mined in the US [Probsein et al., 2006a] 42
Table 1.2.2 proximate, and heat value analyses of various hog or swine manures 45
Table 1.3.1 Ultimate, proximate, and heat value analyses of coals 47
Table1.3.2 Ultimate and heat value analyses of cattle feed ration and feedlot manure from Bushland, Texas [Sweeten et al., 2003] 50
Table 1.3.3 Ultimate analysis for fuels when used as Reburn Fuels. 52
Table1.3.4 Averaged ultimate, proximate, and heat value analyses of dairy 55
Table 1.3.5 Averaged ultimate, proximate, and heat value analyses for dairy manure solids collected by various methods for various dairies in Texas [Mukhtar et al., 2008] 56
Table 1.3.6 Ultimate, proximate, heat value analysis, and adiabatic flame temp (as received basis) of DB samples 58
Table 1.3.7 Ultimate, proximate and heat value analysis (DAF basis) of DB samples ... 58
Table 1.3.8. Fuel properties (Compare with natural gas: 55000 kJ/kg (23,641Btu/lb)) .. 59
Table 1.3.9 Ultimate and heat value analyses of dairy manure 61
Table 1.3.10 Fuel properties for reburn fuels on an as received basis. 62
Table 1.3.11 Gas compositions of NG used in the reburn experiment 63
Table 1.3.12 Characterization of 90% DB: 10% WYC (mass %) 64
Table 1.3.13 Ash elemental analysis (% mass, ash was calcined @ 600°C (1100°F) prior to analysis) 66
Table 1.3.14 Ash loading and DAF chemical Formula 67
Table 1.3.15 Proximate analysis for reburn fuels. 68
Table 2.2.1. Proximate and ultimate analysis of plant base biomass. 76
Table 2.2.2. Proximate and ultimate analysis of selected animal waste biomass fuels. .. 77
Table 2.2.3. Proximate and ultimate analysis of selected coals. 78
Table 2.5.1. Test Parameters. 93
Table 2.5.2: TGA Analysis of Fuels. 93
Table 2.5.3: Ultimate and Proximate Analyses (As Received), Average of 3 Samples. .94
Table 2.5.4: Ultimate and Proximate Analyses (DAF), Average of 3 Samples 95
Table 2.5.5: Combustion Properties of Test Fuels, Average of 3 Samples. 96
Table 2.5.6: Sieve Results and SMD for all Fuels, Average of 3 Samples. 97
Table 2.5.7: Average Summed Error for the Single Reaction Model Grouped by Fuel Ratio. 105
Table 2.5.8: Average Summed Error for the Single Reaction Model Grouped by Particle Size. 105
Table 2.5.9: Average Summed Error for the Distributed Activation Energy Model Grouped by Fuel Ratio. 105
Table 2.5.10: Average Summed Error for the Distributed Activation Energy Model Grouped by Particle Size. 105
Table 3.2.1. Firing rates of fuels investigated by Miller. 118
Table 3.2.2. Proximate, ultimate, and ash analyses of fuels investigated by Miller. 119

Table 3.2.3. Collectible quantities of dry manure available per animal. 121
Table 3.4.1.1. Natural gas composition. 123
Table 3.4.1.2. Composition of greencast 94. 126
Table 3.4.1.3. Quarl and blade angle details. 127
Table 3.5.2.1. Ultimate and proximate fuel properties 130
Table 3.5.2.2. Size distribution parameters. 130
Table 4.2.1 Literature review on reburn articles 157
Table 4.4.1 Primary combustion zone (PRZ) operating conditions 163
Table 4.5.1 Average fuel compositions for all fuels in pure form 164
Table 4.5.2 Proximate and ultimate analyses for fuels. 165
Table 4.5.3 Derived properties of fuels on a dry basis. 165
Table 4.5.4 Proximate and ultimate analyses for coals and CB 166
Table 4.5.5 Fuel particle size distribution 168
Table 4.5.6 Biomass ash composition [Goughnour] 172
Table 5.4.1. Air and oxygen flows in SCFH (ft^3/hr) 191
Table 5.5.1: ultimate and proximate analyses of DB 195
Table 5.5.2. Proximate analysis values for LAPCDB 195
Table 5.5.3: Energy density of the gases (kJ /Standard temperature and pressure (SATP) m^3) for several ERs and S: Fs. 209
Table 5.5.4: Energy conversion efficiency (ECE) for several ERs and S:Fs estimated by tom balance 210
Table 5.5.5. Theoretical T_{peak} values. 211
Table 6.3.1 Choctaw America Coal 228
Table 6.3.2 SRI Pilot Scale Facility: Initially-estimated feed rates using Choctaw America Coal as baseline 229
Table 6.4.1 Input data on reb-lownox excel based program 232
Table 6.4.2 OUTPUT for Stack O_2 = 3% for 3,500,000 BTU/hr, 10% Heat Input via Reburn, Φmain = 0.95 (5% excess air) & 235
Table 6.5.1 SRI 1 MWth Pilot Scale Facility and Furnace Firing Parameters Main Burner, baseline firing conditions 240
Table 6.7.1 Galatia HvB Bituminous coal analysis (from coal feeder discharge). 244
Table 6.7.2 Properties of Reburn Fuels. 245
Table 6.7.3 Results on Flue Gas Composition 248
Table 8.5.1 Base case values for modeling the small-scale on-the-farm MBB combustion system 316
Table 10.2.1 Capital investment costs of installing a biomass co-firing system on an existing coal-fired power plant, taken from various sources 334
Table 10.2.2 Capital investment costs of installing a reburning system on an existing coal-fired power plant, taken from various sources 336
Table 10.4.1 Empirical constants required for drying constant (km) model for perpendicular air flow dryers 347
Table 10.4.2 Base case parameters for rotary steam-tube manure-based biomass dryer 350

Table 10.5.1 Base case input parameters for coal-fired power plant operating conditions and emissions 359
Table 10.5.2 Base case input parameters for co-firing and SOx controls 361
Table 10.5.3 Base case input parameters for manure-based biomass drying system.....362
Table 10.5.4 Base case input parameters for manure-based biomass transportation system 365
Table 10.5.5 Base case economics input parameters 366
Table 10.5.6 Base case fueling and emissions results for a 300 MWe coal plant operating before any co-firing or reburning system is installed.....368
Table 10.5.7 Base case fueling and emissions results for a 300 MWe coal plant operating while co-firing manure-based biomass (5% by mass).....369
Table 10.5.8 Comparison of base case Year 1 costs for power plant operation before and during manure-based biomass co-firing (300 MWe plant, 5% biomass by mass).370
Table 10.5.9 base case inputs for reburning coal with manure-based biomass.....387
Table 10.5.10 Base case fueling and emissions results for a 300 MWe coal plant operating while reburning coal with manure-based biomass (10% by heat) 389
Table 10.5.11 Comparison of base case Year 1 costs of selected NOx control technology arrangements (300 MWe plant, 10% biomass by heat for reburn case) 390
Table 10.5.12 Base case run for the economics of the small-scale MBB combustion system when no additional fuel is burned 402
Table 10.5.13 Economic results for the small-scale MBB combustion system when additional fuel is used to completely vaporize all waste from the animal feeding operation 403
Table 11.2.1 Estimates of total release of mercury to the global environment [L. Levin, 2004].....416
Table 11.2.2 Sources of mercury in US [www.iit.edu/~ipro356s05/bg_sources.html] .417
Table 11.2.3. Mercury values in selected U.S. coal areas from the COALQUAL database [Finkelmann,2003] 418
Table 11.2.4. Mercury on equal energy basis, mean values for samples in selected U.S. coal areas [Finkelmann, 2003] 418
Table 11.2.5. Percentage of women aged 16-49 years with blood mercury (Hg) levels ≥ 5.8μg/L, by race/ethnicity − National Health and Nutrition Examination Survey, United States, 1999-2002 [Mhaffey, 1999].....420
Table 11.2.6.Average mercury capture by existing post-combustion control configurations used for PC-fired boilers [20] 427
Table 11.5.1. Proximate and Ultimate Analysis of fuels used– Hg Cofiring Experiments 437
Table 11.5.2. Mercury measurements with time 444
Table 11.5.3. Hg removals in fuel-rich conditions with wyc as the primary fuel-reburn[Hyukjin et al 2011] 446

Executive Summary of Accomplishments

VOLUME 1: THERMO-CHEMICAL CONVERSION AND DIRECT COMBUSTION METHODS

The common Manure-based biomass (MBB) includes cattle manure or cattle biomass (CB) which includes feedlot manure (or feedlot biomass, FB) and dairy manure (DB) , chicken manure or termed as litter biomass (LB)a and other animal manures. The focus of volume I is on thermo-chemical energy conversion from CB fuels. The Volume I deals with i) generation of fuel properties for feedlot manure (or feedlot biomass, FB) , dairy manure (or dairy biomass, DB), and coals including Texas lignite (TXL) and Wyoming Powder River Basin coal (WYO), ii) co-firing of CB with coal: low ash CB blends, iii) reburn tests for NOx and Hg reduction and iv) gasification for high ash and finally the economics on use of CB as fuel. Test results show that CB can be used to reduce NOx in coal fired plants. The CB represents both DB and FB while chicken manure is termed as litter biomass (LB). An overview on various energy conversion methods is presented. Fuel properties are presented for coals, feedlot manure (or feedlot biomass, FB) and dairy manure (DB) used in cofiring, reburn and gasification experiments. It was found that dry ash free (DAF) CB has approximately 20,000 kJ/DAF kg which is 2/3 of the heating value of DAF coal (30,000 kJ/DAF coal) , twice the volatile matter of coal (80 % for CB vs 40 % for coal), and four times the N content of coal on heat basis. The CB contains more Cl compared to cola which could aid in Hg capture in coal fired plants. The main value of composting for combustion fuel is to improve physical properties and to provide homogeneity. The energy potential of CB diminished with composting time and storage; however the DAF HHV is almost constant for ration and CB.

Fuel Properties: Proximate and ultimate analyses and TGA/DSC studies were conducted on CB and Coal. The CB fuels have much higher nitrogen (kg/GJ) and ash content (kg/GJ) than coal. The HHV of TXL and WYO coal as received were 14,000 and 18,000 kJ/kg, while the HHV of the LA-PC-DB-SepS and the HA-PC-DB-SoilS were 13,000 and 4,000 kJ/kg. The HHV based on stoichiometric air were 3,000 kJ/kg for both coals and LA-PC-DB-SepS and 2,900 kJ/kg for HA-PC-DB-SoilS. The nitrogen and sulfur loading for TXL and WYO ranged from 0.15 to 0.48 kg/GJ and from 0.33 to 2.67 for the DB fuels.

TGA/DSC Studies. . The pyrolysis kinetics and ignition temperatures of different types of CB as well as blends of each biomass with Texas lignite coal were obtained. Activation energy results for pure samples of each fuel using the single reaction model were as follows: 45 kJ/mol (low ash raw manure, LARM), 43 kJ/mol (low ash partially composted, LAPC), 38 kJ/mol (high ash raw manure, HARM), 36 kJ/mol (high ash partially composted, HAPC), and 22 kJ/mol (Texas lignite, TXL). Using the distributed activation energy model the activation energies were found to be: 169 kJ/mol (LARM), 175 kJ/mol (LAPC), 172 kJ/mol (HARM), 173 kJ/mol (HAPC), and 225 kJ/mol (TXL). Ignition temperature results for pure samples of each of the fuels were as follows: 734 K (461°F, LARM), 745 K (471°F, LAPC), 727 (454°F , HARM), 744 K (471°F, HAPC), and 592 K (319°F, TXL).

Cofiring: Cofiring of CB with coal offers a technique of utilizing CB for power/steam generation, reducing greenhouse gas concerns, and increasing financial returns to dairy

operators. The effects of cofiring coal and CB have been studied in a 30 kW (100,000 BTU/hr) burner boiler facility. Experiments were performed with TXL as a base line fuel. Two forms of partially composted CB fuels were investigated: low ash separated solids and high ash soil surface. Two types of coal were investigated: TXL and WYO. The results for cofiring of DB with coal are reported below. The NOx emissions for equivalence ratio (ϕ) varying from 0.9 to 1.2 ranged from 0.34 to 0.90 kg/GJ (0.79 to 0.16 lb/mmBTU) for pure TXL. They ranged from 0.35 to 0.7 kg/GJ (0.82 to 0.16 lb/mmBTU) for a 90:10 TXL:LA-PC-DB-SepS blend and from 0.32 to 0.5 kg/GJ (0.74 to 0.12 lb/mmBTU) for a 80:20 TXL:LA-PC-DB-SepS blend over the same range of ϕ. In a rich environment, DB: coal cofiring produced less NOx and CO than pure coal. This result is probably due to the fuel bound nitrogen in DB is mostly in the form of urea which reduces NOx to non-polluting gases such as nitrogen (N2). The high ash CB must be avoided in pulverized coal (PC) boilers since HA PC FB causes severe slag buildup and cause ash fouling problems.

Reburn tests: Reburning experiments involving CB and coal were performed in a small-scale 30 kW_t (100,000 Btu/h) downward fired boiler burner facility. The results show that the pulverized CB can serve as a supplementary fuel for the coal-fired boilers, and combustion of the CB with coals shows reductions in NO_x emissions. The FB appears to be an effective reburn fuel for reduction of NO_x up to 90%-95%. It is believed that 1) most of the fuel-nitrogen in the CB existed in forms of NH_3 or urea which led the high NO_x reductions. The equivalence ratio (ϕ), an inverse value of the stoichiometric ratio, was considered as a key parameter to achieve high NO_x reductions. The effect of equivalence ratio on the NO_x reduction was found to be significant, and the NO_x emissions decreased with an increase in the equivalence ratio, proportion of the feedlot biomass (CB) in the fuel blend, and vitiation of the air (i.e. lowered O2 concentration) used to inject the reburn fuel and decrease in ash content. In addition, burning CB fuels containing high Cl and low Hg resulted in low Hg emissions when cofired and reburnt. Pulverized CB can be used as a supplementary fuel in existing coal-fired power plants and is very effective on the reductions of NO_x and Hg emissions.

Reburn Modeling: A zero D reburn model has been developed to predict NO_x. The model accounts for finite rate of heating of solid fuel particles, mixing with NO_x laden hot gases, size distribution, finite gas phase and heterogeneous chemistry, and oxidation and reduction reactions for NO_x. After model is validated by comparison with experimental findings, extensive parametric studies have been performed to evaluate the parameters controlling NO_x reduction. The model recommends the following correlations for optimum reduction of NO_x: Equivalence Ratio should be above 1.05; mixing time should be below 100ms (especially for biomass); pure air can be used as carrier gas; the thermal power fraction of the reburner should be between 15% and 25%; residence time should be at least 0.5s and the SMD of the size distribution should be as small as possible, at least below 100 μm.

Cofiring and Reburn for Hg Reduction: Unlike other trace metals that are emitted in particulate form, mercury is released in vapor phase in elemental or oxidized form. The oxidized form of mercury can be captured in traditional emission control devices such as wet flue gas desulfurization (WFGD) units, since oxidized mercury is soluble in water. The chlorine concentration present during coal combustion plays a major role in mercury oxidation. For Wyoming coal the concentration of chlorine is 100 ppm, while for Low Ash Partially Composted Dairy Biomass it is 1,400 ppm. After conducting the study of mercury reduction using dairy biomass blends in coal, it was determined that increase in biomass to coal-biomass blends aids in

mercury oxidation. To summarize, elemental Hg reduces by 75% from pure TXL to 80:20 blend of TXL: LA PC-DB, where oxidized Hg is as high as 88%, 72% from pure WYC to 80:20 blend of WYC: LA PC-DB, where oxidized Hg is as high as 87%. The optimum fuel blend would be coal and Sep. Sol. PC-DB in a blend ratio of 90:10 on mass basis. During reburn tests, the effect of unburned carbon (UBC) on Hg emissions was found to be significant. The more amounts of the UBC, the more captures of Hg^0 in the flue gas and the higher Hg^0 removals. During reburn tests, with an increase in the proportion of the DB in the reburn fuels, the amounts of Cl increase while those of Hg decrease; hence the Hg emissions were reduced.

Gasification: While the cofiring of high ash CB with coal leads to poor performance and ash fouling problems, the concentrated production of low quality (i.e high ash , high moisture) CB at these feeding operations serves as a good feedstock for in situ gasification for syngas (CO and H2) production and subsequent use in power generation. A small scale (10 kW) counter current fixed bed gasifier was rebuilt to carry out gasification studies under quasi-steady state conditions using dairy biomass (DB) as feedstock and various air-steam mixtures as oxidizing sources. A DB-ash (from DB) blend and a DB-Wyoming coal blend were also studied for comparison purposes. Two main parameters were investigated in the gasification studies with air-steam mixtures: i) equivalence ratio ER which is the ratio of stoichiometric air to actual air and ii) the steam to fuel ratio (S: F). Prior to the experimental studies, atom conservation with limited product species and equilibrium modeling studies with a large number of product species were performed on the gasification of DB in order to determine suitable range of operating conditions (ER and S: F ratio). Results on bed temperature profile, gas composition (CO, CO_2, H_2, CH_4, C_2H_6, and N_2), HHV, and Energy Conversion Efficiency (ECE) are presented. Both modeling and experimental results show that gasification under increased ER and S: F ratios tend to produce H_2 and CO_2 richer mixtures but poorer mixtures in CO. Increased ER produces gases with higher HHV but decreases the ECE due to higher tar and char production. Gasification of DB under the operating conditions $1.59<ER<6.36$ and $0.35<S: F<0.8$ yielded gas mixtures with composition as given below: CO (4.77 - 11.73 %), H_2 (13.48 - 25.45%), CO_2 (11-25.2%), CH_4 (0.43-1.73 %), and C_2H_6 (0.2-0.69%). In general, the bed temperature profiles present a peak which ranged between 519 and 1032°C for DB gasification and the peak temperature increased with increase in oxygen concentration in the incoming gasification medium. The gasification data shows that the product gas has a heat value of about 10-15 % of heat value of natural gas due to high nitrogen content of air used for gasification.

Pilot Scale Tests: With cost sharing from Texas Commission on Environmental Quality (TCEQ), pilot scale tests were performed over 2.5 days during May 24, 25 and 30, 2007 in the (1 MW_{th}, thermal) pilot scale Combustion Research Facility (CRF) at Southern Research Institute (SRI), Environment and Energy Department, AL. The main burner operated near stoichiometry almost simulating a low NOx burner (LNB) instead of operating at 5% excess air as performed in small scale experiments. The preliminary data from SRI tests indicated NO_x reduction of about 75% for each of the different reburn fuel types, including the raw manure (LAFB-Raw or LA-RM) and low ash partially composted manure (LAFB-PC or LAPC) and almost independent of firing conditions tested so far. The NOx reduction of 75% is attributed due to almost staged

combustion like behavior of the main burner and the reburner. The fuel used for the main burner is Galatia coal, which had very low mercury content but somewhat higher Cl level compared with Wyoming Powder River Basin (PRB) coal used in the TAMU small-scale tests. The SRI results indicated negligible elemental Hg was emitted for most of the tests due to high Cl in the main burner and reburn fuel. The pilot scale tests demonstrated the difficulties in incorporating the changes in a large scale utility boiler and valuable experience was gained from these preliminary tests. As a result, the test procedure, operating conditions and injection geometry need to be improved for the future pilot scale tests.

Direct Combustion Model: Exploratory thermodynamic studies have been performed whether one can directly fire wet ash high moisture MBB. A base case run of a mathematical model describing a small-scale, on-the-farm MBB combustion system that can completely incinerate high-moisture (over 90%) manure biomass was developed and completed. The conceptualized MBB combustion system, under base assumptions, could potentially incinerate about 50% of all the high moisture manure waste emanating from a 500-cow dairy, while producing over 750 kg/hr of 300 $kPa_{(gage)}$ saturated steam that could be used for external thermal processes. Drying separated solids and pre-heating combustion air greatly improve the efficiency of the MBB combustion system and increase the amount of usable steam that can be produced. Higher ash contents in the MBB solids (greater than 30% on a dry basis) were found to be detrimental to the performance of the small-scale combustion system. Interestingly, the results from the parametric study of the small-scale MBB combustion system seem to suggest that the rotary steam-tube dryer removes moisture from the manure waste stream more effectively than the fire-tube boiler.

Economics: The objective of this study is to model the potential fueling, emission, and economic savings from reburning coal with CB and compare those savings against competing technologies. A spreadsheet program was developed to compute capital, operation, and maintenance costs for CB reburning, selective catalytic reduction (SCR) and selective non-catalytic reduction (SNCR). An initial run of the economics modeling program, with input parameters found in research and literature review, showed that a CB reburn system retrofitted on an existing 500 MW coal plant (9,750 Btu/kWh and 80% capacity factor) was found to have a net present worth (NPW) of $43.7 million with a rate of return of 15.6% and a six year seven month simple payback period. Comparatively, an SCR system under the same base case input parameters was found to have a NPW of $6.45 million with a rate of return of 6.59% and a 13 year six month simple payback period. An SNCR system, under the same conditions, would not generate enough revenue from NOx credits to payoff initial investments. The profitability of a CB reburning system retrofit on an existing coal-fired power plant can decrease with lower coal prices, shorter operation periods, lower values on NOx emission credits, and more efficient primary NOx controllers. Biomass transport distances and the unavailability of suitable, low-ash CB may require future research to concentrate on smaller capacity coal-fired units between 50 and 300 MW

INTRODUCTION

Texas A&M University System has formed the Texas Agriculture and Engineering BioEnergy Alliance (TAEBEA) comprising Texas Agricultural Experiment Station (TAES), and Texas Engineering Experiment Station (TEES), the two leading pillars (A&M) of The Texas A&M University System. The purpose of the BioEnergy Alliance is to focus resources on CO_2 neutral biomass feedstock and processing to produce products for energy, chemicals and feed and to help Texas and the U.S. build a highly productive bioenergy/bioproducts industry

The biomass fuels, that include energy crops and a wide range of material such as agricultural and forestry residues and municipal, industrial, and animal wastes, could serve as a renewable source for energy conversion processes including biological and thermal gasification and direct combustion. The inclusion of biomass as feedstock in thermal conversion processes does not increase the concentration of CO2 in the atmosphere, since biomass is a carbon neutral fuel. .

The National Agricultural Statistics Service of the United States Department of Agriculture (USDA) estimated that the US livestock and poultry produced in excess of 920,000 Mg of manure dry matter per day [Jawson, 2001]. Among dairy cattle, feeder steers or heifers, each animal of mass ranging from 0.540 to 1.150 Mg produces between 27 and 57 kg of wet manure per day (5-6 % body mass) containing 85-90 % moisture and 10-15 % solids (including volatile matter, nutrients, ash and combustibles). Accounting for growth, the amount of manure collected from one animal over a five month period was approximately found as 1 Mg with 35 % moisture and 65 % solids (combustibles + ash) on an as collected basis [Sweeten, 2003]. The animal-residue biomass (e.g. harvested cattle manure or cattle biomass (CB), and mortalities called as mortality biomass, MB) is a major byproduct from concentrated animal feeding operations (CAFOs including feedlots and dairy farms) within Texas and certain regions of the U.S. A cattle of 1000 lb produce 5 air dry (45-50 % moisture) tons per year ; According to the USDA , more than 335 million tons of "dry matter" wastes are produced from farms per year in USA which is about 1/3 of the total municipal and industrial wastes; (1 cow waste $\approx$ Human wastes of 160 residents). In many cases, the production of biomass from one or more animal species is in excess of what can safely be applied to farmland in accordance with nutrient management plans, and the stockpiled waste poses economic and environmental liabilities. Hence, biomass can contribute to surface or ground water contamination and air pollution problems with the release of greenhouse gases.

Texas ranks 1st nationally in fed beef production and slaughter and is among the top 10 nationally in dairy, broiler and caged layer production. Concentrated animal feeding operations (CAFOs) bring in about $9 billion per year to Texas. CAFOs produce biomass residuals—manure, wastewater, and carcasses. All are sources of nutrients and renewable energy, not just potential sources of air, water, or soil pollution. Along with the economic benefits, an estimated 8 million dry tons of animal manure/residues are produced in Texas' concentrated animal feeding operations (CAFOs), which are regulated by both state and federal policies protecting water and air quality. Cattle feedlot manure is produced principally in the High Plains of Texas, with one-third of the cattle on feed for slaughter produced within a 150 mile radius of Amarillo

TX and 42% of cattle on feed are within 200 mile radius, which includes neighboring states of NM, OK, KS & CO. Currently, dairy production and resulting dairy manure production is divided between North Central Texas, East Texas, and the Texas High Plains. To illustrate the rapid translocation and influx of dairies to the High Plains that has occurred this decade, in June 2006, 7 of the top 10 milk producing counties were located in the Texas High Plains, whereas in 2000 only one of the High Plains counties ranked in the top 10 milk producing counties of the state! Over 90% of Texas' swine production occurs in the top two tiers of the Texas Panhandle, north of the Canadian River. By contrast, poultry production including broilers, caged layers and turkeys is concentrated in East Texas and Central Texas. In the Texas Panhandle region, which covers portions of New Mexico and Oklahoma, there are approximately 7.5 million head of cattle (33.4 million in USA) sent through feeding operations annually. Disposal of the vast quantity of manure produced as a by-product of the cattle feeding industry is one of the major operating tasks of the industry. It is both an economic burden on the industry and a potential environmental hazard to air, water, and land. Traditional uses of manure from cattle feedlots or feedlot biomass (FB) in West Texas, dairy manure or dairy biomass, (DB) in Central Texas, and poultry manure (or poultry biomass, PB) in East and Central Texas have involved land application as fertilizer on crop or pasture land. The term "Cattle Biomass (CB)" will refer to both feedlot biomass (FB) and dairy biomass (DB) However, environmental concerns with over-application of phosphorus in some watersheds have lead to total maximum daily loads (TMDLs) for some stream segments (e.g., the North Bosque River system). Reduced irrigation water availability and higher pumping costs have reduced irrigation water use. Consequently, growers are shifting to lower water use crops that require lower nutrient applications per acre and hence reduced manure applications. The cost burden of CB disposal during the short early spring and fall seasons have spurred research into environmentally friendly and economically viable means of disposal.

Similarly depending on animal species, mortalities have traditionally been rendered for by-product recovery (e.g. beef or dairy cattle or swine), incinerated (poultry), or buried on-site (poultry). However, rendering has recently become more costly, and some operators have embraced the alternative of composting carcasses along with collected manure, enhancing the animal residue biomass feedstock stream. Alternative higher-valued uses of collectable animal manure and mortalities must be developed to assure long term sustainability of concentrated animal agriculture in Texas. Several large, commercial feed yards have successfully incorporated carcass composting with feedlot manure [Auvermann & Sweeten 2005].

An alternative and attractive way of overcoming the disposal threat is to develop processes that make use of manure as a resource using conversion of biomass into renewable energy and other co-products. Some of the possible methods include utilizing the generated manure as fuel or as raw materials in other industries. These will alleviate the ever-increasing burden placed both on the industry and the natural resources

There are several distinct modes in which renewable energy may be extracted from CB. Further the manure can also serve as a "reburn fuel". "Reburn Technology" is being developed now for reducing the "smog" causing NOx from existing power plants by introducing coal or natural gas beyond the combustion zone. If coal is used as reburn fuel, and then the capture of NOx is limited by volatile matter of coal. However manure has higher volatile matter, N mostly in the form of urea and hence it is more than likely to capture more NOx. By blending with coal, one controls the volatile matter, N content and as well as heating value of fuel fired. Presentations were made before TCFA and SPS (Southwestern Public Service Company) in

Spring 1994 now known as XCEL energy and at the workshop organized by the Texas Renewable Industries Association in summer 1997. At the conclusion of Spring 94 meeting, pilot plant experiments were suggested. The summer 97 workshop concluded that the best option for the utilities companies is to use the cofiring technology and direct combustion in existing burners.

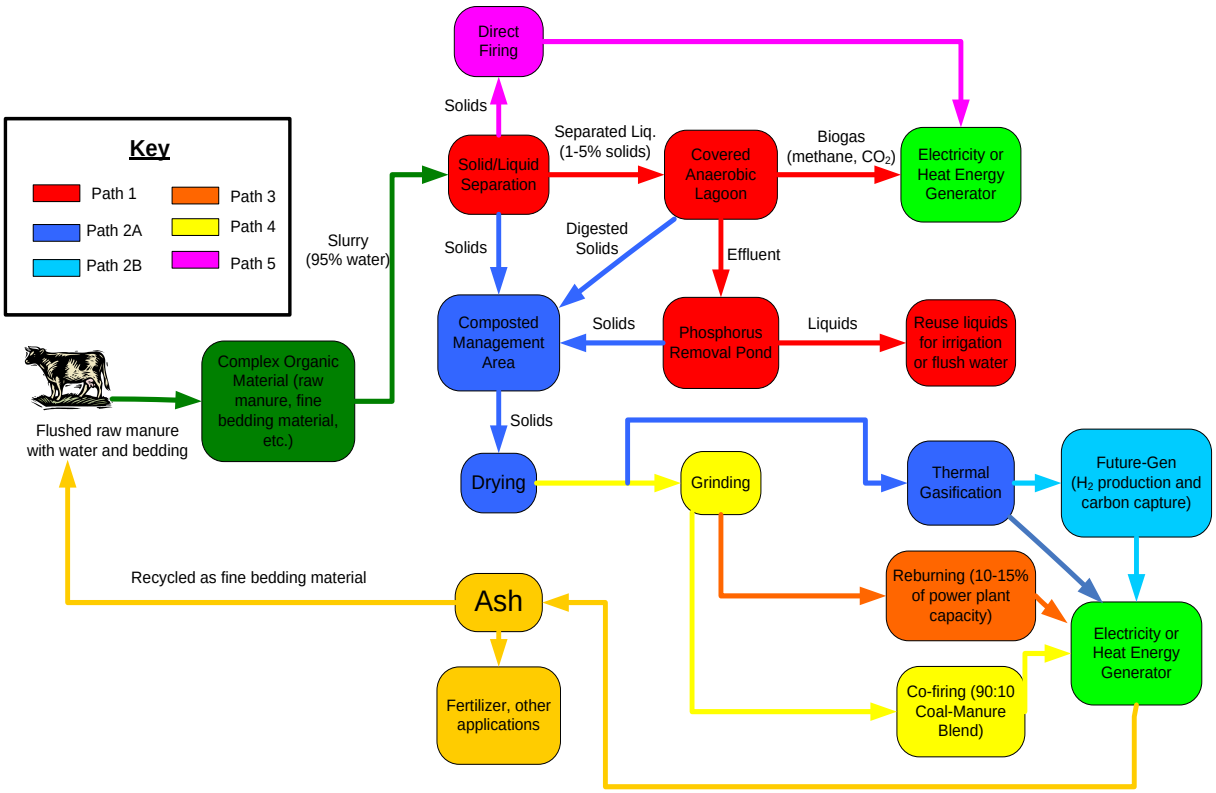

Figure 0.1. Overview on Energy Conversion Methods

Extensive research has been performed at Texas A&M university (TAMU) by investigators Kalyan Annamalai of TAMU-TEES and John M Sweeten of TAMU-TAES over several years but intermittently depending upon funding sources and amounts with FB i) as a fuel in fluidized bed combustors (FBC) , ii) as cofired fuel with coal in boiler burners, iii) as reburn fuel in coal fired boilers to reduce NOx and as well as Hg, iv) finally as fuel for gasification using fixed bed gasifiers . Patents and several disclosures of invention have been obtained. An overview on energy conversion methods is shown in Figure 1. The earlier studies include combustion fluidized bed (Sweeten et al, 1986; Annamalai et al, 1987), co-firing in a boiler burner (Annamalai et al. 2003, Arumugam et al. 2005-b; Annamalai et al 2003), gasification [Priyadarsan et al. 2002, 2005a and 2005 b; Raman et al; young and Pian 2005] in fixed beds , or reburn processes for NOx reduction [Annamalai et al, 2003b, Thien and Annamalai, 2001; Freeman et al., 2003; Annamalai and Sweeten, 2005a, Arumugam et al. 2005-a]. The low NOx burner development, co-firing and reburn processes to reduce the NOx emission produced by combustion of coal in electric power plants by [Annamalai K ,2003],

[Sami M ,2001] and [Carlin N, 2007], gasification of biomass with steam-air by [Galloway el al., 2002] and [Kalisz S el al.,2004], steam by [Jangsawang W el al.,2006] and [Ferdous D el al.,2001], pure oxygen, pure oxygen and steam by [Gil J.,1999], and gasification of coal and wastes [Pinto F,2007] blends are new emerging technologies around the world.

Prior research with FB combustion in the 1980s and 1990s was conducted in fluidized-bed combustors operated in conventional and recirculating modes (Annamalai et al., 1987a; Sweeten et al., 1986). Some of these technologies have met with limited success due to the highly variable properties of cattle manure and the associated flame stability problem in combustion systems. Furthermore, while ash is 2 – 10% in woody biomass and 10% in coal, the ash content in FB and DB can range from 20 – 50%, leading to lower heating values. However combustion processes with pure biomass fuel prefer biomass with high heat value (high grade) and low ash content since those with low heat value lead to poor combustion stability and those with high ash content can cause fouling and slagging problems in the boilers according to [Demirbas A, 2005]. Direct combustion and partial oxidation of wood and biomass-derived charcoal with air have been amply studied over the last few decades by [Klass DL, 1998] and [DI Blasi C, 1999]. The renewable fuels are being extensively experimented either as co-fired fuels or as reburn fuels. Co-firing is defined as the firing of two dissimilar fuels in the boiler. In the mixed method of the co-firing technique, the alternate fuel is mixed with coal before the coal feeder, and the blend is fired in existing pulverized coal-fired boiler burners. In the reburn process of the co-firing technique, an additional fuel usually natural gas (NG) is injected downstream of coal-fired boiler burners and burn under fuel-rich conditions in order to reduce NOx generated by coal burners [Annamalai et al.,1987a] and [Sami et al., 2001] summarized the various energy conversion technologies (non-bio) which mostly utilize FB as an energy source. The review deals with literature on energy conversion using co-firing and manure as sole fuel source. Most of the literature on co-firing (except Texas A&M University studies) is concerned with agricultural and forestry-based biomass fuels. The biomass fuels follow the same sequence of pyrolysis, volatilization and combustion as in low-rank coal combustion. However, there are differences. Typically, the energy density of coal is higher compared to biomass fuels. Biomasses as collected usually contain a higher moisture content, but contain 70-80% volatile matter (VM) on a dry, ash free (DAF) basis, whereas coal consists of only 10-60% VM on a DAF basis.

Under several programs supported by DOE, Texas Advanced Technology Program (ATP), and USDA for the conversion of animal waste to energy conversion technology, a 30 kW boiler burner facility has been built and instrumented at A&M. The details of facility along with detailed fuel characteristics have been recently reported elsewhere (Annamalai et al., 2003a, Sweeten et al., 2003). Small scale and pilot scale tests were performed on co-firing of coal with FB (80: 20 coal: FB and 90:10 blend) at 30 kW (100,000 BTU/hr) Texas A&M (TAMU) Boiler Burner facility and 150 kW NETL-DOE facility (Annamalai et al., 2003a-b; Frazitta et al., 1999). Coals and coal: FB (manure) and coal: LB (chicken litter biomass) blends have been fired before in the burner for determining the combustion and emission performance. Since the test results on co-firing 90% coal and 10% high N feedlot biomass under similar thermal output yielded lesser or comparable NO_x for co-firing compared to coal in spite of increase in N% (from 0.82 to 1.29 lb N per mm BTU), it is believed that the FB can serve as effective reburn fuel. The co-firing facility was modified to conduct reburn experiments using coal, biomass, and a 50:50 coal: biomass blend, and a 90:10 coal: biomass blend.

In the past, NOx reduction in coal-fired plants has been achieved by using reburn systems in which natural gas (NG) is injected under slightly rich conditions into combustion products emanating from primary coal-fired burners. Recently, the high cost of NG has inspired research into alternate solid reburn fuels including micronized coal and agricultural biomass (AB). However, lesser reductions have been found with micronized coal (about 40%-50%) compared NG (about 60%). Thus, only a limited number of coal power plants in the USA use reburn systems for NOx reduction. A few plants have opted for selective catalytic reduction (SCR, >90% reduction) and selective non-catalytic reduction (SNCR, about 35% NOx reduction in large plants over 50 MW). Yet there are some major drawbacks to SCR and SNCR, including possible ammonia exposure and high installation costs, which have made many plant owners reluctant to invest in these technologies. Recent experiments conducted at the Texas A&M Coal and Biomass Energy Laboratory have shown that reburning with cattle manure (or feedlot biomass, FB) can reduce NOx emission up to 90% due to its high volatile content, rapid release of volatile matter (VM) during combustion, and release of fuel bound nitrogen in the form of ammonia, NH3; however the reburn effectiveness decreases when FB is blended with coal. US patent 6,973,883 has been obtained in 12/ 2005for the methodology and basic fuel preparation. In order to validate the small-scale test data, additional tests were performed at 150 kW NETL-DOE facility that yielded similar or better results (Freeman et al. 2003).

Overall Objective

The overall purpose of this interdisciplinary proposal is to develop environmentally benign technologies to convert low-value inventories of dairy and beef cattle biomass into renewable energy. This research expands the suite of technologies by which cattle biomass (CB: manure, and premature mortalities) could serve as a renewable alternative to fossil fuel. The work falls into two broad categories of research and development.

Category 1 – Renewable Energy Conversion. This category involves developing technologies to extract energy from waste streams or renewable resources through co-firing with coal, combustions as a reburn fuel to reduce nitrogen oxide (NO, N2O, NOx, etc.) and Hg emissions from coal-fired power plants, and thermo-chemical (non-biological) gasification to produce low-BTU gas for on-site power production.

Category 2 – Biomass Resource Technology. The goal is to use cattle biomass C efficiently and cost-effectively as a renewable energy source (e.g. through and via aqueous-phase, anaerobic digestion or biological gasification). The sources must be (a) characterized with respect to its net thermal energy potential and (b) quantified both temporally and spatially. The CB production, collection, harvesting and processing systems are examined and refined to make the CB suitable for energy production. The task involves a synthesis of engineering characterization, geographical mapping, quality assessment, systems modeling, sensitivity and economic analysis of the sources, stocks and flows of energy involved in the CAFO system. The biomass resources were evaluated by a) obtaining fuel characteristics of the feed; manure biomass of varying forms (e.g. solid, semi-solid, slurry, liquid, etc.); and comparing with composted manure, b) developing innovative and producer-friendly information-management systems to process, synthesize, and mine the enormous quantities of data generated by modern and future data-acquisition systems

Team and Investigators

Prof. Kalyan Annamalai served as Program Manager and Principal Investigator (PI) for TEES in coordinating the tasks and timely delivery of progress reports. Dr. Annamalai was responsible for preparing Volume I, which is focused primarily on CB conversion experiments and results.

Dr. John M. Sweeten served as Principal Investigator (PI) for Texas AgriLife Research. Dr. Sweeten was responsible for preparing Volumes II and III of this report, which summarized the work of a team of biological and agricultural engineers, environmental engineers, and agricultural economists, which focused on cattle biomass as a viable feedstock. This team examined CB production, harvesting, analysis, characterization, transportation, logistics, and economic tradeoffs, in comparison with lignite or coal, for use in the conversion processes described by Dr. Annamalai et al. in Volume I.

The detailed list of co-principal investigators of various sub-tasks under goals 1, 2, 3 and 4 including the PI's or Co-PI's are listed alphabetically below. Abbreviations of the PI's and Co-PI's are included in parentheses

Principal Investigators:

- Dr. Kalyan Annamalai (KA), Paul Pepper Professor of Mechanical Engineering, Texas A&M University, College Station, TX.77843-3123; Texas Engineering Experiment Station (TEES),979-845-2562, kannamalai@tamu.edu, http://www1.mengr.tamu.edu/cabel
- Dr. John Sweeten, (JS), Resident Director and Professor of Biological and Agricultural Engineering, Texas AgriLife Research, Texas AgriLife Research (TALR) & Extension Center, Amarillo & Vernon, TX. 806-677-5600; j-sweeten@tamu.edu

Co-Principal Investigators (alphabetical):

- Dr. Brent Auvermann (BA), Professor of Biological and Agricultural Engineering, Texas AgriLife Research, Amarillo, TX, TALR, (806) 677-5663; b-auvermann@tamu.edu
- Dr. Sergio C. Capareda, Associate Professor of Biological and Agricultural Engineering, Texas AgriLife Research, College Station, Texas A&M University, College Station, TX 77843-2117; TALR, (979)-458-3028; scapareda@tamu.edu
- D. Robert DeOtte (RD), Associate Professor of Environmental Science and Engineering, West Texas A&M University, WTAMU Box 60998, Canyon, TX 79016-0001. TALR, (806) 651-8780; rdeotte@mail.wtamu.edu
- Dr. Cady Engler (CE), Professor of Biological & Agricultural Engineering Department, Texas AgriLife Research, College Station, TX. TALR, (979)-845-3685; c-engler@tamu.edu
- Dr. Wyatte Harman (WH), Professor of Agricultural Economics, Texas AgriLife Research, Texas AgriLife Research, Blackland Res. and Ext. Center 720 E. blackland Rd, Temple, TX 76502. TALR, (254)774-6104 ; harman@brc.tamus.edu;
- Dr. Saqib Mukhtar, Associate Professor of Biological and Agricultural Engineering, Texas AgriLife Research, 303-B Scoates Hall, 2117 TAMU, College Station, TX 77843-2117College Station, TX. TALR (979)458-1019 ; mukhtar@tamu.edu
- Dr. David B. Parker, former Associate Professor, Agricultural Sciences and Engineering, West Texas A&M University, West Texas A&M University , Canyon, TX 79016-0001; (806) 651-5281 ; dparker@mail.wtamu.edu
- Dr. Reddy JN, Distinguished Professor and Wyatt Chair , Mechanical Engineering, Texas A&M University, College Station, TX.77843-3123; TEES 979-845-2562, TEES, (979) 862-2417; jnreddy@tamu.edu

- Dr. B.A. Stewart, Professor, Agricultural Sciences and Engineering, West Texas A&M University, Canyon, TX. (806)-651-2299, bstewart@wtamu.edu

The final report for the 5 year project performed by an interdisciplinary team of 9 professors is arranged in two volumes: Vol. I addressing several tasks and results and discussion for each task under Category 1 and Vol. II addressing several tasks and results and discussion for each task under Category 2. The responsibility of these faculty members for various tasks and subtasks is indicated within the text of this report.

As advised by DOE, the investigators formed an industrial advisory committee (IAC) panel consisting fuel producers (feedlots and dairy farms) and fuel users (utilities), periodically met with them, and presented the research results; apart from serving as dissemination forum, the PIs used their critique to red-direct the research within the scope of the tasks.

Due to the feedback from IAC, tasks include "several different paths to achieve energy conversion until "one " catches fire; it is for the industry to adopt the technology suitable to their need and suitability of their feedstock; for e.g. high ash FB suitable for gasification while low as FB suitable for cofiring or reburn". Under summary section of most of the tasks, comments from IAC members (in quotes) and the impact of their comments on the progress of research are included.

Summary of Proposed Project Tasks and Assigned Investigators

The detailed list of various sub-tasks under goals 1, 2, 3 and 4 including the PI's or Co-PI's who are responsible for the tasks are listed alphabetically below. These were originally proposed; however a few tasks were slightly modified and additional tasks were performed which are indicated in the three volumes.

Goal 1 – Renewable Energy Conversion (covered mostly in Vol I)

Task A: Thermochemical conversion and direct combustion methods

- Task A.1. (JS, BA, SM, SC, KA): Fuel resources and ash characterization for open-lot beef cattle feedlot and dairy manure biomass.
  - Task A.1.1. (JS, BA, SM, SC): Determine Fuel Characteristics of cattle biomass (CB), including feedlot manure biomass (FB), dairy biomass (DB) from free-stall barns and open lots, solids collected in a lagoon, vacuumed DB, settled solids in digesters and composted mixtures of CB and animal mortality carcasses.
  - Task A.1.2. (JNR): Improve quality of cattle biomass slurry (CBS) by reduction of water in CBS for application to direct firing.
  - Task A.1.3. (BA): Preparation and characterization of composted mixtures of CB and cattle carcasses for firing in gasifier and combustion unit.

- Task A.2. (KA): Fuel pyrolysis
  - Task A.2.1. TGA fundamental studies on the pyrolysis of DB and FB, and evolution of nitrogenous species (N in the form of NH3 and HCN).
  - Task A.2.2. Relate ultimate and proximate analyses to volatile composition and evolution during controlled pyrolysis of DB.

- Task A.3. (KA): Co-firing
  - Task A.3.1. Co-firing with WYC and/or TXLC.
  - Task A.3.2. Co-fire the CB with low grade TXLC and chlorinated carbon.

- Task A.4. (KA): Reburn Process
  - Task A.4.1. Reburn experiments using FB and DB as reburn fuels, and measurements of fuel-N in the form of NH3 and HCN.
  - Task A.4.2. Reburn experiments for reducing Hg emissions (Two different solid fuels).

- Task A.5. (KA): Gasification to produce low-BTU gas for on-site energy conversion
  - Task A.5.1. Modification of facility, air-steam gasification of CB, and measurements of HCN and NH3.
  - Task A.5.2.a. Steam gasification of CB to produce chlorinated (in N2) and activated carbon (in H2O) for Hg emission reduction.
  - Task A.5.2.b. Pyrolysis with the gasifier using N2/inerts and study of ash and gas quality.
  - Task A.5.3. Gasification of CB with the mixture of pure O2 and H2O (g) (IGCC or FutureGen).

- Task A.6. (KA, JS): Pilot-scale studies
  - Task A.6.1. As a sub-contract to TEES, a pilot-scale facility will be used to generate the reburn data.
  - Task A.6.2. Pilot scale tests on Hg reduction using CB as “Hg-reburn” fuel and testing chlorinated activated carbon for Hg capture.

- Task A.7. (KA): Reburn modeling and exploratory studies
  - Task A.7.1. The modeling study includes zero dimensional reburn modeling with different CB streams as reburn fuels.
  - Task A.7.2. Reburn modeling for the new fuels and development of Fluent Code for reburn application.

- Task A.8. (KA): Exploratory Overall Energy Conversion studies
  - Task A.8.1. Exploratory global modeling studies; a) firing waste streams (DB + water) directly, b) replacing natural gas with DB as fuel in cement kilns around

Waco and use the resulting ash on-site for various in-house purposes, and c) using DB as fuel in coal-fired power plants near Waco.
  - Task A.8.2. Direct firing of low quality CB slurry with regenerator.

- Task A.9. (JS, DP, RDO): Ash characterization for value-added uses
  - Task A.9.1. Characterize the ash from combustion and gasification experiments.
  - Task A.9.2. Engineering & fertility evaluation of fly ash utilization of combustion ash from fluidized beds.
  - Task A.9.3. Use of ash in flowable fill mixture
  - Task A.9.4. Use of fly ash as a soil amendment to reduce shrink-well capacity of soil
  - Task A.9.5. Technology Transfer. Dissemination and use of information
  - Task A.9.6. Use of bottom ash and cyclone ash as road surface application for winter weather.

Task B: Anaerobic Digestion Methods (CE, BA, and SM) (covered mostly in Vol II)

- Task B.1. (CE, SM): Engineering analysis of a commercial digester
  - Task B.1.1. Engage in an intensive monitoring scheme to assess the net energy production of a new covered lagoon anaerobic digester and phosphorus reduction system.
  - Task B.1.2. Whole farm energy analysis when operating with the digester.
- Task B.2. (BA): Building research capacity for anaerobic digestion of mortality biomass
  - Task B.2.1. Build and test a research-scale, plug-flow, mesophilic, anaerobic digester.
  - Task B.2.2. Build a second research-scale anaerobic digester to provide parallel treatments (viz. treatment vs. control) in terms of substrate, operating variables and loading rates.

<u>Goal 2 – Biomass Resource Technology (covered mostly in Vol II)</u>

Task C: Biomass Characterization and Inventory (SM, SC)

- Task C.1. (SM, SC): Database development for CB as energy feedstock.
- Task C.2. (SM, SC, JS): Dairy biomass characterization survey.
- Task C.3. (SM, SC): Conduct robust analysis of the ash content in the DB and relate to slagging characteristics.

Task D: Biomass Handling Methods (BA)

- Task D.1. (BA): Stabilizing bovine carcasses for thermochemical gasification via carcass composting.

- Task D.2. (SC, SM): Efficient collection, harvest and transport.

Goal 3 – Energy System modeling (covered mostly in Vol II)

Task E: Inventory, Characterization and Transport of Cattle Biomass (SC, SM)

- Task E.1. (SC, SM): GIS-based inventory and transport analysis.
- Task E.2. (SM, SC, JS, BA): Use of DB as a renewable energy source.
- Task E.3. (JS, BA, SM, and SC): Quantitative Dairy and feed yard CAFO systems models.

Task F: Sensitivity Analysis of CAFO Energy Systems (BA)

- Task F.1. (SC, WH): Feasibility work.
- Task F.2. (BA, SM, and SC): Developing strategies for an efficient utilization of manure.
- Task F.3. (BA, SM): Addressing engineering and other farm issues arising from manure-to-energy projects.

Task G: Industry Input into Energy-systems Model Development (JS)

- Task G.1 (JS, KA): Establishment of a project Industry Advisory Committee (IAC).
- Task G.2. (JS, KA): Use IAC feedback and output to guide research and technology transfer.

Task H: Economic Modeling of Cattle Biomass Energy Systems (WH)

- Task H.1. (WH, KA, JS): Economic Analyses of co-firing, reburning, and gasification of CB.
- Task H.1.1. Includes a benefit/cost analysis for using CB as fuel with or without coal.
- Task H.2. (WH): Estimate the opportunity cost (per unit of energy produced) of using non-renewable energy sources.
- Task H.3. Adapt and utilize the IMPLAN Economic Model (University of Minnesota).

Goal 4 – Process Sensitivity Analyses, Instrumentation and Information Technology (covered mostly in Vol II)

Task I: Energy Analysis of Dairy Farms and Feed Yards (SM, SC, BA)

- Task I.1. Utilize the 12 Dairies identified in biomass characterization study.

Task J: Process Sensitivity Analysis, Instrumentation and Information Technology (BA, SM)

- Task J.1. Effects of fuel preparation including drying at lower and higher temperatures.
- Task J.2. Net energy budgets for dairy and beef production systems in relation to CB and energy production potential.

Industrial Advisory Committee Members

Fuel Producers/Suppliers

Mr. Ben Weinheimer, Texas Cattle Feeders Association, Amarillo, TX

Mr. John Cowan, Texas Association of Dairymen Grapevine, TX

Mr. Ned Meister, Texas Farm Bureau, Waco, TX

Utilities:

Mr. Paul Joiner, The Panda Group, Dallas, TX

Mr. Cliff Clark, TX U Power, Dallas, TX

Mr. Olon Plunk, VP Environmental Services, Xcel Energy, Golden, CO 80403

Summary of Tasks performed under Thermo-Chemical Energy Conversion (Volume I)

The tasks and results under each task are presented in subsequent sections of Volume I: Each section follow the task list summarized below:

Section 1: Task A-1. Fuel resources and ash characterization for open-lot beef cattle feedlot and dairy manure biomass. Fuel properties of coal, agricultural biomass, and animal waste; detailed elemental composition and proximate analyses including heat values are presented.

Section 2: Task A-2. Fuel pyrolysis. The TGA traces are given for limited samples

Section 3: Task A-3. Co-firing. Two types of coal (Texas lignite, TXL and Wyoming Powder River Basin coal, WYO) were used for cofiring. Effect on Hg emission is dealt in Section 11

Section 4: Task A-4. Reburn tests with CB and Coal: CB blends. The results from reburning experiments involving CB as reburn fuel show that the pulverized CB can reduce NOx by as much as 90 %.; Effect on Hg emission is dealt in Section 11

Section 5: Task A-5. Gasification to produce low-BTU gas for on-site energy conversion. The gasification experiments were also performed on CB and the effects of equivalence ratio (ER) and steam to fuel ratio (S: F) ratio on peak temperature and gas yield were investigated. The data shows that the peak temperature is about 1325 K and gas has a heat value of about 10-15 % of heat value of natural gas due to high N2 content

Section 6: Task A-6. Pilot-scale studies. As a sub-contract to TEES, a pilot-scale facility was used to generate the reburn data.

Section 7: Task A-7: Reburn modeling and exploratory studies. Modeling results are presented and compared with experimental data.

Section 8: Task A-8. Exploratory Overall Energy Conversion studies. A Thermodynamic analysis of direct combustion of Wet CB/waste streams is presented and results are presented for maximum water and ash contents in wet CB.

Section 9: Task A-9. Ash characterization for value-added uses Characterization studies on as from combustion and gasification were performed and value-added uses (fertility evaluation) are presented (Reader should refer to Vol. II for results)

Section 10: Task A-10. Economics of CB as Renewable Energy (Task H under Category 2 or Vol. II; but addressed in detail in Vol. I). An economics model and deterministic computer program were also developed to model capital, operation, and maintenance costs for CB reburning, SCR, and selective non-catalytic reduction (SNCR

Section 11: (New task) Effect of Cofiring and Reburn on Hg The Cl can combine with Hg and produce soluble HgCl2 thereby reducing elemental Hg emission. The % reduction of elemental Hg was as much as 75% with 20 % addition of CB with coal.

References

1. Annamalai, K., Freeman, M., Sweeten, J. M., Mathur, M., O'Dowd, W., Walbert, G., and Jones, S., "Co-firing of coal and cattle biomass (FB) fuels. Part III: Fouling result from a 500,000 Btu/h pilot plant scale burner, "Fuel 2003; 82:1195-1200. Fuel, V. 82, 10, 1195-1200, 2003.
2. Annamalai, K., Ibrahim, Y. M., and Sweeten, J. M., J. Energy Resources Tech., 109 (2) (1987) 49-57
3. Annamalai, K., Thien, B., and Sweeten, J. M., Fuel 82 (2003a) 1183-1193

4. Annamalai, K, Thien B, Sweeten, J., Heflin, K., and Greene, L W, " Feedlot Manure as Reburn Fuel for NOx reduction in Coal Fired Plants, "3 rd International Symposium on Combustion on Agricultural Air Pollution, Raleigh, NC, Oct 12-15, 2003b.

5. Arumugam, S., Annamalai, K., Priyadarsan, S., Thien, B., and Sweeten, J. M., "A Novel Application of Feedlot Biomass (Cattle Manure) as Reburning Fuel for NOx Reduction in Coal Fired Power Plants," Symposium, State of the Science, Animal Manure and Waste Management (USDA), January 5-7, 2005, San Antonio, Texas.

6. Annamalai K, Puri I. Combustion Science and Engineering.1st ed. CRC Press; 2006.

7. Annamalai K, Carlin NT, OH H, Gordillo AG, Lawrence B, Arcot U, Sweeten JM, Heflin K, Harman WL. Thermo-chemical energy conversion using supplementary wastes with coal. ASME International Mechanical Engineering Congress and Exposition, Seattle, Washington, USA 2007.

8. Annamalai K, Priyadarsan S, Arumugam S, Sweeten JM. Energy conversion: principles of coal, animal waste, and biomass fuels. Encyclopedia Energy Eng Technol 2007; 1(1):476-497.

9. Auvermann, B.W., J. M. Sweeten. 2005. "Methodological Challenges to a Systems Approach to the Management of Animal Residuals". In: Proceedings of State of the Science: Animal Manure and Waste Management, Jan. 4-7, 2005, San Antonio. CDROM

10. Department of Energy, USA, Energy Information Administration, Annual Energy Outlook 2004 with Projections to 2025, January 2004.

11. Carlin N, Annamalai K, Sweeten JM, Mukhtar S. Thermo-chemical conversion analysis on dairy manure-based biomass through direct combustion. Int. J Green Energy 2007; 4:1-27.

12. Demirbas A. Potential applications of renewable energy sources, biomass combustion problems in boiler power systems and combustion related environmental issues. Prog. Energy Combust Sci. 2005; 31:171-192.

13. Di Blasi C, Signorelli G, Portoricco G. Countercurrent fixed-bed gasification of biomass at laboratory scale. J Ind. Eng. Chem. Res. 1999; 38: 2571-2581

14. Di Blasi C. Modeling wood gasification in a countercurrent fixed-bed reactor. J AIChe 2004; 50 (9):2306-2318.

15. Ferdous D, Dalai AK, Bej SK, Thring RW. Production of H2 and medium heating value gas via steam gasification of Lignin in fixed-Bed reactors. J Can Chem Eng 2001;.79:913-922

16. Frazzitta, S., Annamalai, K., and Sweeten, J. M., J. Propulsion and Power, 15 (2) (1999) 181-186

17. Freeman, M, Annamalai, K and Sweeten, J., "NOx Reduction with Feedlot Biomass as a Reburn Fuel in a 150 kW Pilot Scale Boiler Burner Facility, "Electric Power Conf, George Brown Conference Center, Houston, March 4-6, 2003.

18. Galloway T, Waidl J, Annamalai K, Sweeten JM, Tomlinson T, Weigle D. Energy resources recovery applications using gasification and steam reforming. Bi-annual Incineration and Thermal Alternatives. New Orleans: Conference 2002.

19. Gil J, Corella J, Azner MP, Caballero MA. Biomass gasification in atmospheric and bubbling fluidized bed: effect of the type of gasifying agent on the product distribution. J Biomass and Bioenergy 1999; 17:389-403.

20. Jawson, M.D., Wright, R. J., Buck, D. A., Lindsay, J. A., Robens, J. F., Smith, L. W., and Weltz, M. A., National Program Annual Report, 2001

21. Jangsawang W, Klimanek, Gupta AK. Enhanced yield of hydrogen from wastes using high temperature steam gasification. J. Energy Res. Technol 2006; 128:179-185

22. Kalisz S, Lucas C, Jansson A, Blasiak W, Szewczyk D. Continuous high temperature air/steam gasification (HTAG) of biomass. Victoria, Canada: 6th Int. Conference on Science in Thermal and Chemical Biomass Conversion 2004

23. Klass, D. L. (1998). Biomass for Renewable Energy, Fuels and Chemicals. San Diego: Academic Press

24. Pinto F, Lopez H, Neto RA, Gulyurtlu I, and Cabrita I. Effect of catalysts in the quality of syngas and by-products obtained by co-gasification of coal and wastes. !. Tars and nitrogen compounds abatement. J Fuel 2007; 86:2052-2063

25. Priyadarsan, S. Fixed bed gasification studies on coal-feedlot biomass and coal-chicken litter biomass under batch mode operation. Master' Thesis, Texas A&M University, 2002.

26. Priyadarsan, S., Annamalai, K., Sweeten, J. M., Holtzapple, M., and Mukhtar, S., Proceedings of the 30th Symposium (International) on Combustion, 30(2005a) 2973-2980.

27. Priyadarsan S, Annamalai K, Sweeten JM, Mukhtar S, Holtzapple MT. Fixed bed gasification of feedlot and poultry litter biomass Trans ASAE 2005b; 47:1689-1696

28. Raman KP, Walawender WP, Fan LT. Gasification of feedlot manure in a fluidized bed reactor. The effect of temperature. J Ind Eng Chem Process Des Dev 1980; 19: 623-629.

29. Sami, M., Annamalai, K., and Wooldridge, M., "Co-firing of coal and biomass fuel blends," Prog. Energy and Combust. Sci., 27 (2001) 171-214.

30. Sweeten, J. M., Annamalai, K., Thien, B., and McDonald, L. A., Fuel, 82 (2003) 1167-1182

31. Thien B., and Kalyan Annamalai, "Reduction of NO Through Reburning With Coal and Feedlot Biomass" , National Combustion Conference, Oakland, Ca. March 25-27, 2001

32. Young L, and Pian C. High temperature, air-blown gasification of dairy-farm wastes for energy production. J Energy. 2003; 28:655-672.

1. FEEDLOT AND DAIRY MANURE RESOURCES AND FUEL PROPERTIES

Task A-1: Fuel resources and ash characterization

ABSTRACT:

The use of cattle manure (referred to as Cattle Biomass, CB) as a fuel source has the potential to solve both waste disposal problems and reduce fossil fuel based CO_2 emissions. Fuel properties are presented for coals, feedlot manure (or feedlot biomass, FB) and dairy manure (DB) used in cofiring, reburn and gasification experiments. The CB represents both DB and FB. . It was found that CB has approximately half the heating value of coal, twice the volatile matter of coal, and four times the N content of coal on heat basis. The main value of composting for combustion fuel would be to improve physical properties and to provide homogeneity. The energy potential of CB diminished with composting time and storage; however the DAF HHV is almost constant for ration and CB, The fuel N per GJ is considerably high compared to coal, which may result in increased NOx emissions.

1.1. Introduction

The biomass fuels, that include energy crops and a wide range of material such as agricultural and forestry residues and municipal, industrial, and animal wastes, could serve as a renewable source for energy conversion processes including biological and thermal gasification and direct combustion. The inclusion of biomass as feedstock in thermal conversion processes does not increase the concentration of CO_2 in the atmosphere, since biomass is a carbon neutral fuel. Emissions, flame temperatures, and heat energy outputs from burning biomass are required to determine the effectiveness and profitability of biomass energy conversion systems. However, in order to estimate these outputs, fuel properties of both coal and biomass must be known. The following is a review of the fuel properties of coals and some manure-based biomasses. A brief discussion of the supply of manure biomasses will also be included.

1.2. Literature review

1.2.1. Coal

The type of coal consumed for a particular plant usually depends on what type of coal is mined at nearby coal fields; although, recently many plants around the country have begun to import low-sulfur sub-bituminous coal from the Power River Basin. Figure 1.2.1is a map of major coal fields in the Unites States, The largest coal deposits are in the Power River Basin, the North Dakota or Fort Union Region, the Four Corners or Southwest Region, the Appalachian Basins and the Illinois Basins. The rank of coal is usually determined by the carbon content. Higher ranked coals have higher percentages of carbon on a dry, ash-free basis, and generally have a greatest higher heating value, or calorific value. A proximate analysis of the fuel can provide the moisture, ash, fixed carbon, and volatile matter contents of the fuel. Volatile matter is the part of the solid fuel that will vaporize, or pyrolize, in an inert environment when heated. Fixed carbon is material that will not vaporize in inert environments, but will oxidize when a reactant (usually air or oxygen) is heated along with the fuel. The ash is the inert portion of the solid fuel that is left even after the reaction with the oxidizer. Yet, for this study, an ultimate analysis of the fuels, which includes the elemental contents of the fuel (Carbon, Hydrogen, Nitrogen, Oxygen, and Sulfur) along with moisture and ash, will be required for emissions and energy release calculations.

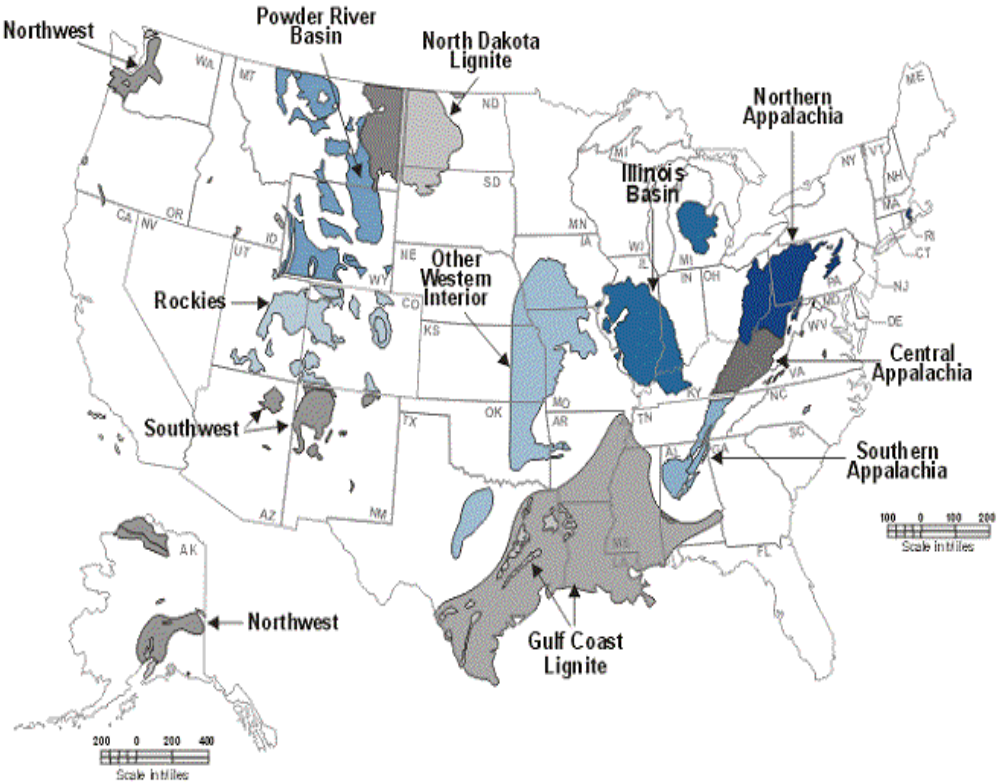

Figure 1.2.1 Coal fields in the United States [EIA, 2005]

Table 1.2.1 Ultimate and heat value analyses of major coals mined in the US [Probsein et al., 2006a]

	Fort Union Lignite	**Powder River Basin (PRB) Sub-bituminous**	**Four Corners Sub-bituminous**	**Illinois C Bituminous**	**Appalachia Bituminous**
(by mass)	As received				
Moisture	36.2	30.4	12.4	16.1	2.3
Ash	8.6	7.8	25.6	7.4	9.7
Carbon	39.9	45.8	47.5	60.1	73.6
Hydrogen	2.8	3.4	3.6	4.1	4.9
Nitrogen	0.6	0.6	0.9	1.1	1.4
Oxygen	11	11.3	9.3	8.3	5.3
Sulfur	0.9	0.7	0.7	2.9	2.8
HHV (kJ/kg)	15,600	18,400	19,600	24,900	31,200

Ultimate analyses of several representative coals in the US are presented in Table 1.2.1on an as-

Figure 1.2.2 Feedlot cattle on large confined animal feeding operation [FactoryFarm.org, 2007]

received basis. These coals follow the general trend for ranking coal. Lignite coals generally have less carbon, but more oxygen, than higher ranked sub-bituminous and bituminous coals on a dry, ash-free basis. Heat values also increase for higher ranked coals.

1.2.2. Feedlot Manure or Feedlot Biomass (FB)

The three largest cattle states are Texas, Kansas and Nebraska, respectively. See Figure 1.2.2. These three states produce more feedlot cattle than the other 47 states combined. Most of the Texas feedlots are concentrated in the Panhandle region of the state [NASS, 2007]. Feedlots in the Texas and Oklahoma Panhandle regions can range between 5,000 and 75,000 head [Harman, 2004]. Moreover, feedlot cattle can produce 5 to 6% of their body weight in manure each day; roughly 5.5 dry kg (12 lb) per animal per day [DPI&F, 2003]. According to the [ASAE, 2005] standard, full grown beef cattle excrete 6.6 dry kg (15 lb) of manure per animal per day. However, only about 5.0 dry kg (11 lb) per animal per day is collectable when scraped from earthen lots. Beef cow manure from earthen lots can range between 53 and 87% ash (dry basis), and 24 and 42% moisture. Thus, nearly 18 million dry metric tons (19.8 million tons) of cattle manure per year comes from large feedlot CAFOs. Texas alone produces over 27% of this annual total. If the manure is roughly 70% ash (dry basis), and the dry ash-free heating value of the manure is roughly 20,000 kJ/kg(8,597Btu/lb), the thermal energy conversion of the

collectable manure from large feedlot operations in the US can produce about 109 million GJ/yr (103 million MMBtu/yr).

1.2.3. Dairy Manure or Dairy Biomass (FB)

There are certain areas of the country, such as the Bosque River Watershed near Waco, Texas and many parts of California that contains dozens of large dairy operations, each with over 500 milking cows. The dairy cows in the Bosque River watershed make up about 25% of the total number of dairy cows in Texas. The California counties of Tulare (26%), Merced (14%) and Stanislaus (10%), house about 50% of the 1.74 million dairy cows in California [CDFA, 2006]. Full- grown milking cows can produce 7- 8% of their body weight in manure per day; roughly 7.3 dry kg (16lb) per animal per day according to [Schmidt et al.,1998] .The American Society of Agriculture engineer (ASAE) standard, as excreted, manure production from a full grown lactating cow is 8.9 kg (20lb) per animal per day. The manure is roughly 87% moisture when excreted [ASAE, 2005]. If about 70% of this manure can be collected, then 21.2 million dry metric tons (23.3 million tons) of dairy manure per year can be utilized in the US. Texas daily cows produce about 890,000 tons dry metric (980,000 tons) of manure per year. If dairy manure solid are roughly 40% ash on average, and the dry ash-free heating value of the manure is about 20,000kJ/kg(8597Btu/lb), then the thermal energy conversion of dairy manure in the US can potentially produce about 255 million GJ/yr(242 million MMBtu/yr).

1.2.4. Hog or Swine Biomass

Most of the discussion in this dissertation will center on cattle manure. However, much of the same findings and modeling equations presented here can be used for hog or swine MBB in combustion systems as well. In 2007, Iowa had the largest inventory of hogs and pigs with over 19 million head. This was almost twice as much as the second largest state inventory, which belonged to North Carolina with about 10 million head. Minnesota, Illinois, and Indiana were the next largest swine states in 2007. In Figure 1.2.3, the East North Central census region of the US was shown to be the largest coal consuming region. Four of these states (Illinois, Indiana, Michigan, and Ohio) are all among the states with the largest swine inventories.

Figure 1.2.3 is graph of hog and pig inventory by state in 2007.

The ultimate, proximate, and heat value analyses from three different studies of swine manure may be found in Table 1.2.2. Like cattle manures, swine manure is 70 to 80% volatile matter with a dry, ash free higher heating value of about 20,000 kJ/kg. Swine manure is also, at many times, flushed from indoor piggeries and stalls, and very high in moisture, as can be seen in the table. However, the ash content of this high moisture swine manure is about 30 to 35% on a dry basis, which is slightly higher than low-ash dairy manure, which is also generally flushed from free stall barns.

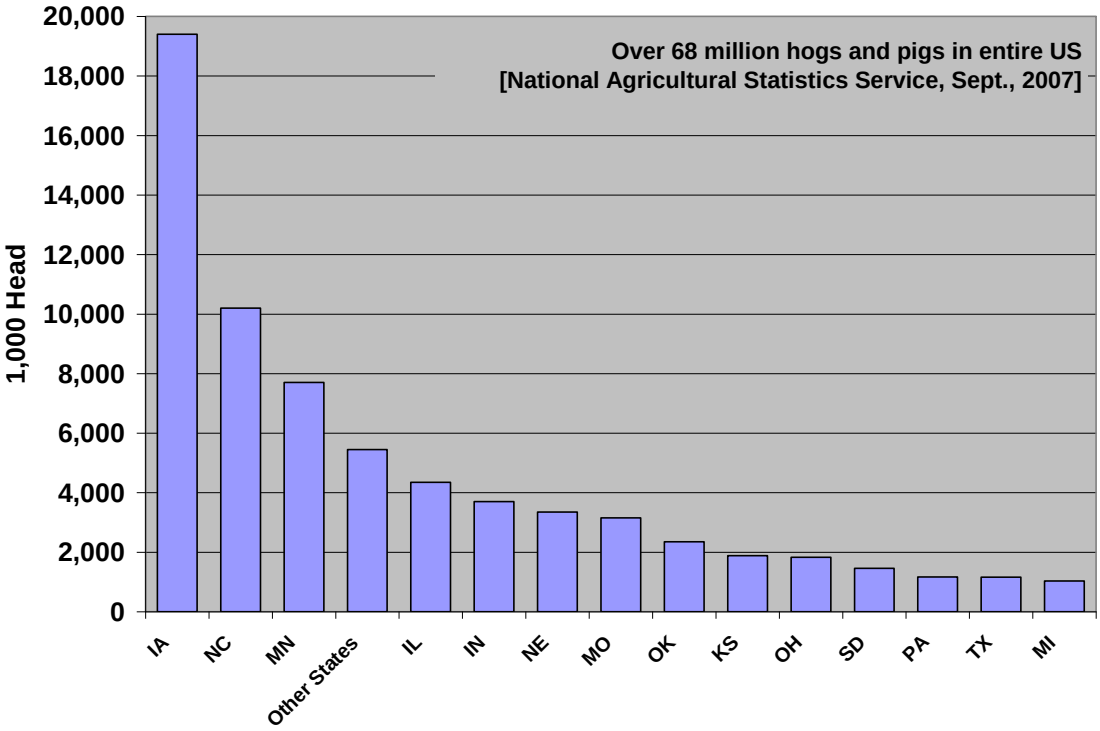

Figure 1.2.3 Total inventory of hogs and pigs by state in the US in 2007 (NASS, 2007)

Table 1.2.2 proximate, and heat value analyses of various hog or swine manures

	Air-dried Raw Hog Manure	High Moisture Swine Manure	High Moisture Pig Manure
(by mass)	As received		
Moisture	7.2	72.57	92.1
Ash	29.1	NRd	2.8
Fixed Carbon	11.3	NRd	1.0
Volatile Matter	52.3	23.94	4.1
Carbon	34.3	12.53	2.8
Hydrogen	5.0	1.77	0.3
Nitrogen	3.5	0.95	0.2
Oxygen	27.4	8.59	1.7
Sulfur	0.7	0.1	NR
HHV (kJ/kg)	14,511	NR	1,089
	Dry		
Moisture	0.0	0.0	0.0
Ash	31.4	NR	35.4

	Air-dried Raw Hog Manure	High Moisture Swine Manure	High Moisture Pig Manure
Fixed Carbon	12.2	NR	12.7
Volatile Matter	56.4	87.3	51.9
Carbon	37.0	45.7	35.4
Hydrogen	5.4	6.5	3.8
Nitrogen	3.7	3.5	2.8
Oxygen	29.5	31.3	21.5
Sulfur	0.7	0.4	NR
HHV (kJ/kg)	15,640	NR	13,785
	Dry, ash-free		
Moisture	0.0	0.0	0.0
Ash	0.0	0.0	0.0
Fixed Carbon	17.8	NR	19.6
Volatile Matter	82.2	NR	80.4
Carbon	53.9	NR	54.9
Hydrogen	7.9	NR	5.9
Nitrogen	5.5	NR	4.3
Oxygen	43.0	NR	33.3
Sulfur	1.0	NR	NR
HHV (kJ/kg)	22,798	NR	21,353

a Jensen et al., 2003
b He et al., 2000
c ECN, 2003
d Ash + fixed carbon is 3.49% on an as received basis
NR: Not reported

According to the ASAE (2005) standard, gestating sows excrete about 0.5 dry kg (1.1 lb) of manure per animal per day, lactating sows excrete 1.2 dry kg (2.5 lb) of manure per animal per day, and boars excrete about 0.38 dry kg (0.84 lb) of manure per animal per day. About 0.32 dry kg (0.70 lb) of manure per animal per day is collectable from flushed manure from indoor piggeries. Liquid flushed manure from indoor piggeries is generally about 98% moisture. Roughly 7.9 million dry metric tons (8.7 million tons) of swine manure can be collected every year in the US. If the manure solids are 40% ash on average, then the thermal energy conversion of swine manure can potentially generate about 95 million GJ/yr (90.3 million MMBtu/yr).

1.3. Fuel Properties

A proximate analysis of fuel can provide the moisture, ash, fixed carbon, and volatile matter contents of the fuel. Volatile matter is the part of the solid fuel that will vaporize, or pyrolize, in an inert environment when heated. Fixed carbon is material that will not vaporize in inert environments, but will oxidize when a reactant (usually air or oxygen) is heated along with the fuel. The ash is the inert portion of the solid fuel that is left even after the reaction with the

oxidizer. The ultimate analysis of the fuels includes the elemental contents of the fuel: Carbon, Hydrogen, Nitrogen, Oxygen, and Sulfur and sometimes trace elements like Chlorine and Hg. The ultimate analyses provide empirical chemical formulae and as well as aids in mass balances of elements, deduction of an overall empirical formulae for volatiles and emission reporting of NOx and SOx. Additional fuel properties are presented in Volume II of this final report.

1.3.1. Coal

Fuel analyses of Texas lignite from the Gulf Coast lignite field and Wyoming sub-bituminous from the Powder River Basin will be used during simulations. The ultimate, proximate and heat value analyses of these coals are presented in

Table 1.3.1 Ultimate, proximate, and heat value analyses of coals modeled in this study (TAMU, 2006)

	Texas Lignite	**Wyoming Sub-bituminous**
(by mass)	**As received**	
Moisture	**38.3**	**32.9**
Ash	**11.5**	**5.6**
Fixed Carbon	**25.4**	**33.0**
Volatile Matter	**24.8**	**28.5**
Carbon	**37.2**	**46.5**
Hydrogen	**2.1**	**2.7**
Nitrogen	**0.7**	**0.7**
Oxygen	**9.6**	**11.3**
Sulfur	**0.6**	**0.3**
HHV (kJ/kg)	**14,290**	**18,194**
	Dry, ash-free	
Moisture	**0.0**	**0.0**
Ash	**0.0**	**0.0**
Fixed Carbon	**50.6**	**53.7**
Volatile Matter	**49.4**	**46.3**
Carbon	**74.1**	**75.7**
Hydrogen	**4.2**	**4.4**
Nitrogen	**1.4**	**1.1**
Oxygen	**19.1**	**18.4**
Sulfur	**1.2**	**0.4**
HHV (kJ/kg)	**28,467**	**29,594**

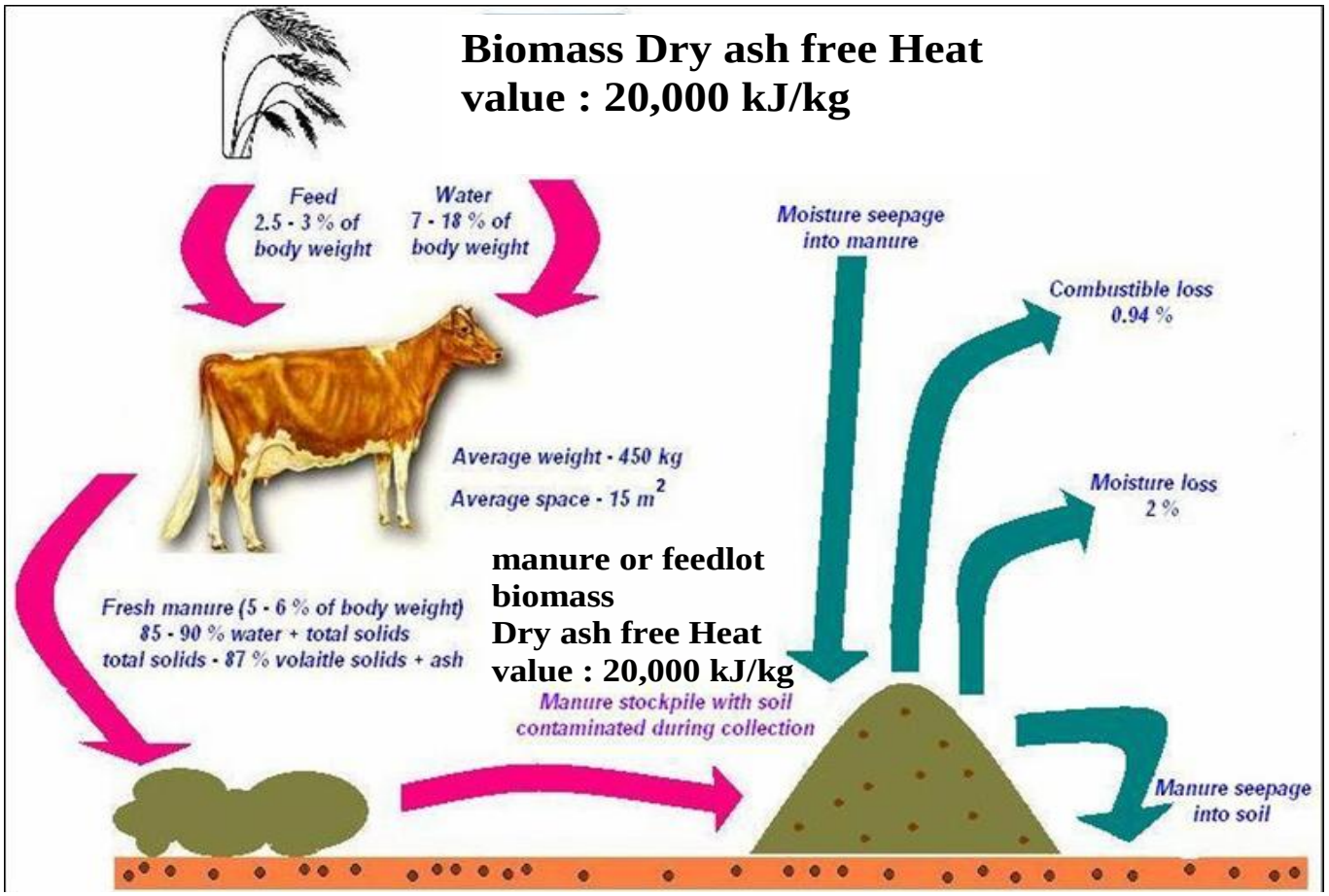

Figure 1.3.1 Manure production and environmental effects

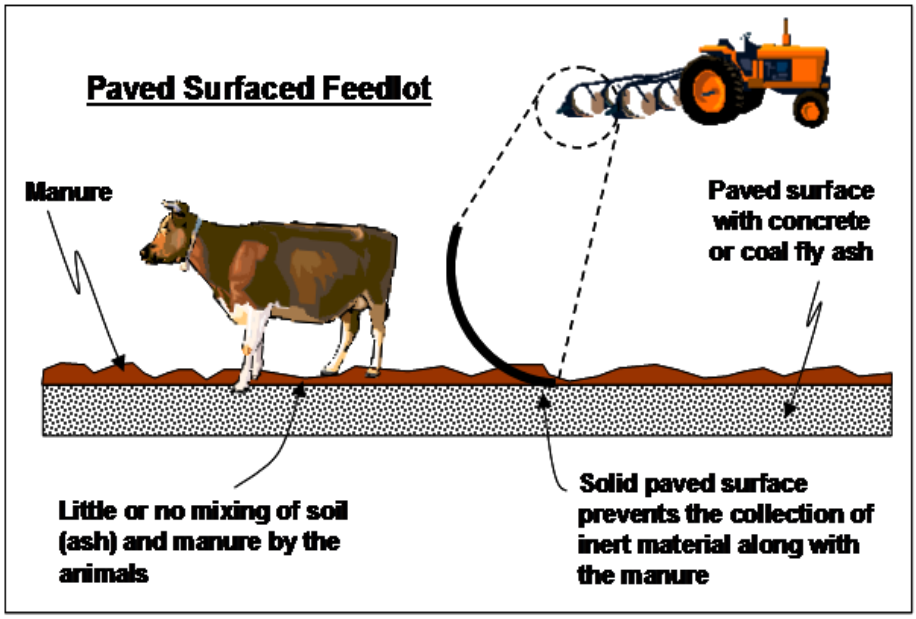

Figure 1.3.2 Feedlot biomass collection at paved surfaced feed

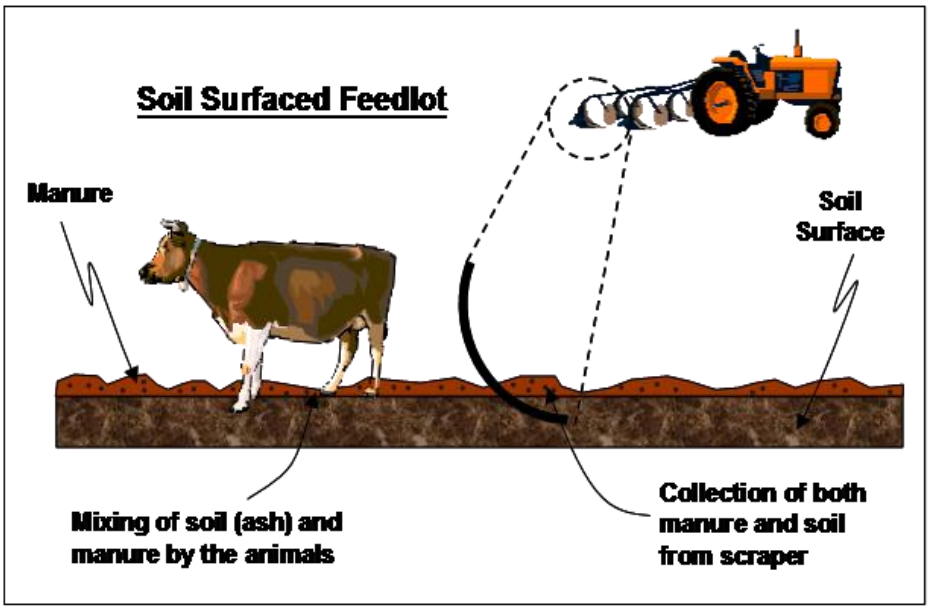

Figure 1.3.3 Feedlot biomass collection at soil surfaced feed yards

1.3.2. Feedlot Biomass

Ultimate and heat value analyses are presented in Table1.3.2,for cattle feed ration, low-ash feedlot manure, and high-ash feedlot manure collected at an experimental feedlot facility at Bushland, Texas by Mr. Kevin Heflin. The primary concern with FB is the ash content in the manure. Hence, the way the manure is collected and how the feed cattle are kept is important. Most cattle on feed at large feedlot operations are kept in large feed yards or corrals, similar to open lots discussed previously for dairies. The important distinction between feedlots that produce low-ash FB and feedlots that produce high-ash FB is the type of surfacing of the feed yards (Figure 1.3.3, Figure 1.3.2). Feedlots that are not paved (Figure 1.3.3) or only paved with soil tend to produce high ash manure, about 45% on a dry. On the other hand, as seen in feedlots paved with either cement or fly ash byproduct from coal combustion can produce FB that is very low in ash (Figure 1.3.2).

Table1.3.2 Ultimate and heat value analyses of cattle feed ration and feedlot manure from Bushland, Texas [Sweeten et al., 2003]

	Cattle Feed Ration[b]	**Low-ash Feedlot Manure[c]**	**High-ash Feedlot Manure[c]**
(by mass)	As received		
Moisture	19.8	29.3 [a]	27.3 [a]
Ash	3.6	9.6	32.9
Fixed Carbon	17.9	12.9	7.3
Volatile Matter	59.5	48.0	32.5
Carbon	35.9	35.1	23.5
Hydrogen	5.0	4.2	2.8
Nitrogen	1.6	2.4	1.7
Oxygen	34.0	19.1	11.5
Sulfur	0.1	0.4	0.3
HHV (kJ/kg)	14,700	13,222	8,189
	Dry		
Moisture	0.0	0.0	0.0
Ash	4.5	13.6	45.2
Fixed Carbon	22.3	18.2	10.0
Volatile Matter	74.2	67.9	44.7
Carbon	44.8	49.6	32.3
Hydrogen	6.2	5.9	3.9
Nitrogen	2.0	3.3	2.3
Oxygen	42.4	27.0	15.8
Sulfur	0.1	0.5	0.4
HHV (kJ/kg)	18,329	18,688	11,266
	Dry, ash-free		
Moisture	0.0	0.0	0.0
Ash	0.0	0.0	0.0
Fixed Carbon	23.4	21.2	18.4
Volatile Matter	77.6	78.5	81.7

	Cattle Feed Ration[b]	Low-ash Feedlot Manure[c]	High-ash Feedlot Manure[c]
Carbon	46.9	57.4	59.1
Hydrogen	6.5	6.8	7.0
Nitrogen	2.1	3.9	4.2
Oxygen	44.4	31.3	28.9
Sulfur	0.1	0.6	0.8
HHV (kJ/kg)	19,191	21,626	20,572

a Moisture in manure samples is low due to solar drying prior to fuel analysis

b Sweeten et al., 2003

c Sweeten and Heflin, 2006

In Figure 1.3.4, it may be seen that raw FB, partially composted (PC) FB, fully/finished composted (FC) FB, and cattle ration (cattle feed) all fall under this dry, ash-free (DAF) HHV range. Similar results are also found when blending 5% crop residues with each FB fuel. On a

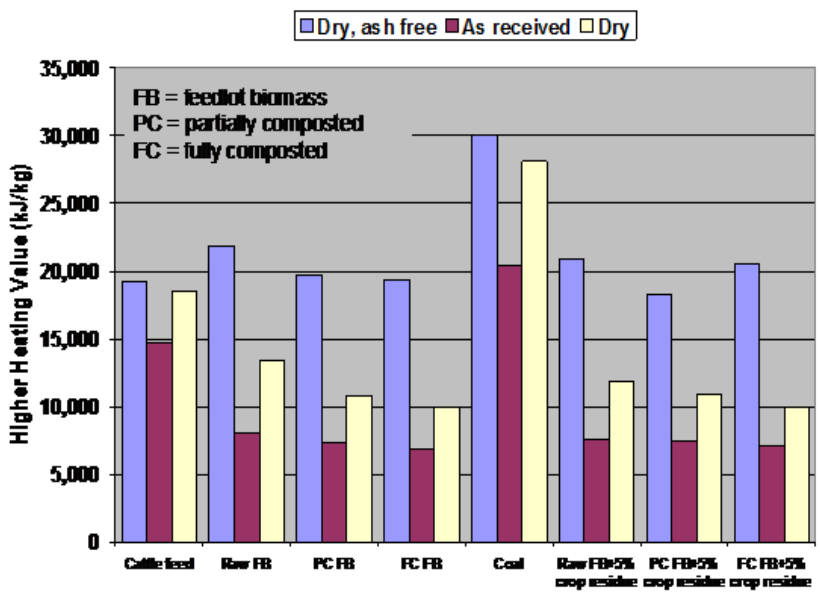

Figure 1.3.4 Higher heating values for cattle ration, raw FB, partially composted FB, finished composted FB, coal, and respective FB+5% crop residue blends [adopted from Sweeten et al., 2003]

dry, ash-free basis, the combustible contents of low-ash FB and high-ash FB are similar to the feed ration given to the animals[Sweeten et al., 2003] reported that the higher heating value (HHV) of FB on a dry, ash-free basis tends to generally is around 20,000 ±2000

kJ/kg(44,000±4,400lb) depending on the animal's feed ration. However, also like dairies, very few feedlots produce low-ash biomass, because the vast majority of feedlots are unpaved. There are concerns of how the hard surfaces of paved lots will affect the animals. Moreover, paving feedlots is expensive, and since many operations are so large, a tremendous amount of concrete or coal ash would be needed to completely convert an entire feedlot operation to paved surfaces. Over time, maintenance and repaving may also be required, since the animals are heavy and generate a great amount of force when they stomp on the ground. This in turn may add to the cost of operating the feedlot [Heflin, 2008].

Table 1.3.3 Ultimate analysis for fuels when used as Reburn Fuels.

Average Fuel Compositions								
	HAPC-FB		LAPC-FB		TX Lignite		Wyoming	
Ultimate (%)	As Rec.	Dry	As Rec.	Dry	As Rec.	Dry	As Rec.	Dry
Carbon	14.92	17.97	33.79	42.05	37.18	60.30	46.52	69.32
Hydrogen	1.39	1.68	3.65	4.55	2.12	3.44	2.73	4.06
Nitrogen	1.13	1.36	1.97	2.45	0.68	1.11	0.66	0.98
Oxygen	11.40	13.73	23.94	29.78	9.61	15.58	11.29	16.83
Sulfur	0.31	0.38	0.51	0.64	0.61	0.98	0.27	0.41
Ash	53.85	64.88	16.50	20.53	11.46	18.59	5.64	8.40
Moisture	17.00	0.00	19.64	0.00	38.34	0.00	32.88	0
Total	100.00	100.00	100.00	100.00	100.00	100.00	100.00	100.00

	HAPC-FB	LAPC-FB	TX Lignite	Wyoming
Ash Loading (kg/GJ)	65.31	9.51	4.55	2.02
DAF Chemical Formula	$CH_{1.11}N_{0.065}O_{0.57}S_{0.008}$	$CH_{1.28}N_{0.05}O_{0.53}S_{0.006}$	$CH_{0.68}N_{0.02}O_{0.19}S_{0.006}$	$CH_{0.7}N_{0.01}O_{0.18}S_{0.002}$

Various samples of reburn fuels are such as High Ash Partially Composted Feedlot Biomass (HAPCFB) composted manure collected with more amounts of soil, Low Ash Partially Composted Feedlot Biomass (LAPCFB) composted manure collected with less soil or specially paved feedlots, Low Ash Partially Composted Separated Solid Dairy Biomass (LASSDB) which solids separated from water flushed dairy manure, Texas Lignite Coal (TXLC), and Wyoming

Sub bituminous Coal (WYC) were collected from feedlots in Amarillo, Texas and analyzed for the proximate and ultimate analyses on an as received (as rec.) and dry basis. Three samples of each fuel were analyzed and the average values are listed in Table 1.3.3. LAPCFB and LASSDB contain about 2.5 times more fuel-N contents than coals on a dry basis

1.3.3. Dairy Biomass

In the TAMU experiments, all fuels were supplied by the Texas A&M Agricultural Research & Extension Center, Amarillo Texas. Figure 1.3.3 and Figure 1.3.2 illustrate the most common ways DB and FB are collected. They are then treated and used at most animal feeding operations. The manure collection processes at dairies generally depend on how the animals are kept. Most dairies keep cows primarily in open lots or corrals paved with soil. Manure is periodically removed by scraping the corrals with a tractor and box blade, usually when the cows are at the milking center. However, large amounts of dirt and other inert material is also scraped along with the manure, making the DB from open lot dairies high in ash and unsuitable for most direct combustion processes. Scraping manure from soil surfaced open lot can produce 16.1 dry kg or 35.5lb) of recoverable solids per animal per day. About 43% of these solids are inert material or ash. The moisture percentage of scraped solids from soil surfaced lots can range between 39 and 69% [ASAE, 2005]. Hybrid daily facilities have open lots plus free stalls. Free stalls are covered, open air barn structures, typically paved with concrete, Bedding, which can be straw, sand, or composted manure, is usually placed on the concrete flood for the animals' comfort. Sometime loafing beds are placed on the concrete floods to further increase the animals' comfort level as well [Mukhtar et al., 2008].

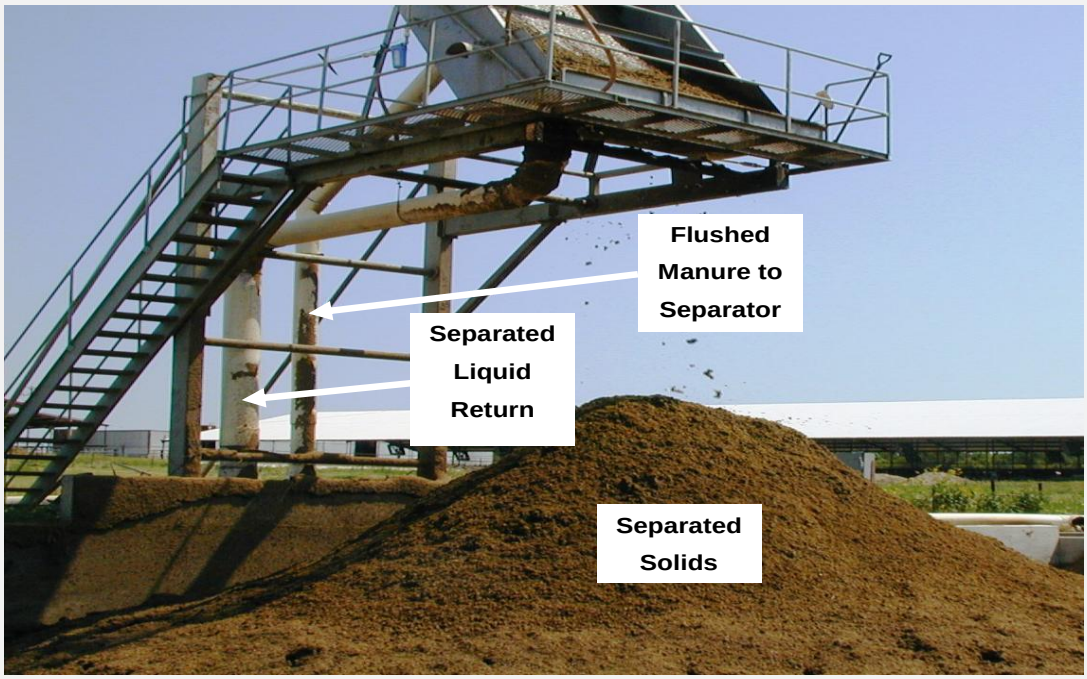

Figure 1.3.5 Screen solid-liquid separator.

Manure may be removed from free stall barns in several ways. The manure, along with the bedding material can be washed or flushed with water, which usually flows downhill from one end of the free stall barn to the other. At the bottom end of the barn, some dairies have solid separators that remove some of the solids from the liquid flushed manure. The separated solids are either stored or composed and are eventually used as fertilizer on nearby plots of land or discarded at landfills. The remaining wastewater from the separator is typically sent to a treatment pond or lagoon, where the remaining solids are diluted and broken down by anaerobic processes. Any inorganic matter in the wastewater will sink to the bottom of the lagoon and create a layer of sludge. After treatment, the water in the lagoon is typically used for further flushing in the free stall, or as irrigation water [Mukhtar, 1999]. Alternatively, a vacuum machine can collect the manure and bedding into a "slurry wagon". After manure is vacuumed, it is taken either to fields and used as fertilized or spread and dries. If flushing or vacuum systems are not available, free stalls can be also be scraped to remove manure [Mukhtar et al., 2008]. About 11.2 dry kg (24.7lb) of manure per animal per day can be removed when scraping concert surfaces. Whereas only 5.36 dry kg (12 lb) per animal per day can be recovered from flushed DB slurry. The slurry will be roughly 92% moisture [ASAE, 2005].

The proximate content of DB, unlike coal and woody biomass fuels, varies greatly for a number of reasons. As excreted, DB typically has a moisture content of about 88%. However, since plenty of bedding (about 6 kg (13.2lb) of bedding per 50 kg (110lb) of excreted DB) is also present in the freestalls, the moisture content of DB on the ground (excreted plus bedding) in a freestall is usually lower [Carlin et al, 2006]. Nevertheless, depending on how the biomass is collected and how long it is stored, the ash and moisture contents of DB can be very different. The flushed dairy biomass from a freestall can have much less ash and up to 97% moisture. Furthermore, mechanical solid separators, augers, and settling basins can each change moisture

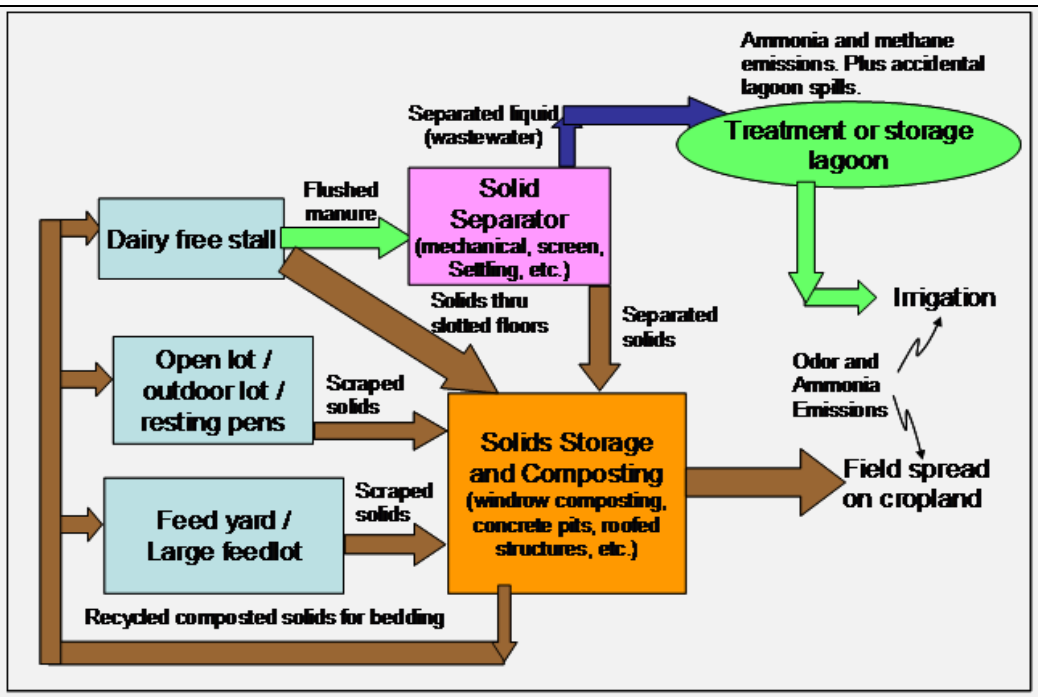

Figure 1.3.6 Current dairy and feedlot manure disposal [adapted from Schmidt et al., 1988]

and ash contents of separated DB solids or lagoon water to different degrees. Therefore, it is difficult to say how much moisture and ash is in a manure stream at any given time.

The makeup of the combustible or dry biomass is ash-free portion of the manure biomass is largely determined by the feed or ration that the animals eat just as was the case for cattle cows. In Table1.3.4, the mean proximate, ultimate and heat value analyses of the cattle feed, as excreted manure, and aged manure solids are listed for a number of dairies in Texas obtained by [Mukhtar el al., 2008]. On an as received basis and on a dry basis (i.e. all moisture removed) the heat value of the excreted manure was less than the heat value of the original ration that was feed to the animals. However, on a dry, ash free basis, the heat values for excreted manure and cattle feed was very similar. On a dry basis, it may also be seen that the heat value for age's solids was lower compared to the excreted manure. This decrease in heat value was predominantly due to the loss of volatiles during composting or storage of manure solids

Table1.3.4 Averaged ultimate, proximate, and heat value analyses of dairy cow feed, as-excreted manure, and aged solids for various dairies in Texas [Mukhtar et al., 2008]

	Dairy Cattle Feed	**As Excreted Dairy Manure**	**Aged Solid Dairy Manure**
(by mass)	As received		
Moisture	41.4	84.1	36.2
Ash	5.2	3.2	41.7
Fixed Carbon	11.2	2.3	0.7
Volatile Matter	42.2	10.4	21.4
Carbon	26.3	6.8	11.1
Hydrogen	3.2	0.8	1.2
Nitrogen	1.5	0.4	1.0
Oxygen	21.7	4.7	8.6
Sulfur	0.2	0.0	0.3
HHV (kJ/kg)	9,159	1,161	2,810
	Dry		
Moisture	0.0	0.0	0.0
Ash	8.9	20.1	65.4
Fixed Carbon	19.1	14.5	1.1
Volatile Matter	72.0	65.4	33.5
Carbon	44.9	42.8	17.4
Hydrogen	5.5	5.0	1.9
Nitrogen	2.6	2.5	1.6
Oxygen	37.0	29.6	13.5
Sulfur	0.3	0.0	0.5
HHV (kJ/kg)	15,792	7,354	4,519
	Dry, ash free		
Moisture	0.0	0.0	0.0
Ash	0.0	0.0	0.0
Fixed Carbon	21.0	18.1	3.2

	Dairy Cattle Feed	As Excreted Dairy Manure	Aged Solid Dairy Manure
Volatile Matter	79.0	81.9	96.8
Carbon	49.3	53.5	50.2
Hydrogen	6.0	6.3	5.4
Nitrogen	2.8	3.1	4.5
Oxygen	40.6	37.0	38.9
Sulfur	0.4	0.0	1.4
HHV (kJ/kg)	16,644	16,788	13,045

In Table 1.3.5, the ultimate, proximate, and heat value analyses for dairy manure solids collected by various methods are presented from the same study by [Mukhtar et al. 2008]. Scraped DB solids were collected at open lots and hybrid lots in both central Texas and the Texas Panhandle region. Separated solids from flushed systems on hybrid lots were also collected in these two Texas regions. Vacuumed DB solids were collected from two hybrid lots in central Texas as well. First, notice the moisture percentage on an as received basis. Scraped DB, which was once 80% moisture as excreted, mixes with either bedding or soil in open lots and is dried in the sun to about 40% moisture; however, on a dry basis the DB's ash percentage increases from 20% as excreted to about 36%, on average, when scraped. Scraped solids can be as high as 70% ash on a dry basis, depending on the open lot surfacing and the care taken by the box blade operator when collecting the manure.

On the other hand, mechanically and gravitationally separated solids are extremely high in moisture as they are screened or settled from streams of high moisture flushed dairy manure. Mechanically separated solids were found to be very low in ash, as much of the inert material in the DB is made-up of smaller particles that pass through screen meshes more easily than the combustible, organic material. This data confirms the same hypothesis by [Carlin .2005] and [Carlin et al., 2007a], who found that separated DB solids from a dairy in Hico, Texas were only 11% ash on a dry basis. However, gravitationally separated solids are higher in ash since the small inert particles settle to the bottom of settling basins along with the combustible material.

Table 1.3.5 Averaged ultimate, proximate, and heat value analyses for dairy manure solids collected by various methods for various dairies in Texas [Mukhtar et al., 2008]

	Scraped Dairy Solid Manure	Mechanically Separated Dairy Solids	Gravitationally Separated Dairy Solids	Vacuumed w/ Sand Bedding	Vacuumed w/ Compost Bedding
(by mass)	As received				
Moisture	40.8	83.2	69.9	52.0	83.6
Ash	21.2	1.3	12.4	38.6	3.6
Fixed Carbon	5.3	10.5	8.5	6.7	5.6
Volatile	32.7	5.0	9.2	2.7	7.2

	Scraped Dairy Solid Manure	Mechanically Separated Dairy Solids	Gravitationally Separated Dairy Solids	Vacuumed w/ Sand Bedding	Vacuumed w/ Compost Bedding
Matter					
Carbon	18.8	8.0	12.0	5.9	6.8
Hydrogen	2.2	0.9	1.4	0.7	0.8
Nitrogen	1.3	0.3	0.5	0.3	0.4
Oxygen	13.8	6.2	8.2	2.4	4.7
Sulfur	0.3	0.1	0.1	0.1	0.1
HHV (kJ/kg)	6,433	2,554	3,777	2,258	2,740
	Dry				
Moisture	0.0	0.0	0.0	0.0	0.0
Ash	35.8	7.7	41.2	80.4	22.0
Fixed Carbon	9.0	62.5	28.2	14.0	34.1
Volatile Matter	55.2	29.8	30.6	5.6	43.9
Carbon	31.8	47.6	39.9	12.3	41.5
Hydrogen	3.7	5.4	4.7	1.5	4.9
Nitrogen	2.2	1.8	1.7	0.6	2.4
Oxygen	23.3	36.9	27.2	5.0	28.7
Sulfur	0.5	0.6	0.3	0.2	0.6
HHV (kJ/kg)	11,361	15,480	11,452	4,854	14,813
	Dry, ash free				
Moisture	0.0	0.0	0.0	0.0	0.0
Ash	0.0	0.0	0.0	0.0	0.0
Fixed Carbon	13.9	67.7	48.0	71.3	43.8
Volatile Matter	86.1	32.3	52.0	28.7	56.3
Carbon	49.5	51.6	67.8	62.8	53.1
Hydrogen	5.8	5.8	7.9	7.4	6.3
Nitrogen	3.4	1.9	2.8	3.2	3.1
Oxygen	36.3	40.0	46.3	25.5	36.7
Sulfur	0.8	0.6	0.6	1.1	0.8
HHV (kJ/kg)	17,667	16,788	18,255	23,949	19,130

The type of material used as bedding in free stalls and open lots plays a significant role in how much inert material is collected along with the DB. In Table 1.3.5, fuel analyses for vacuumed DB solids are also presented. It can be seen that vacuumed solids from free stalls with sand bedding had significantly higher ash contents than from free stalls with compost bedding. According to [Sweeten and Heflin, 2006], this higher ash content from free stalls bedded with sand is also true for flushed manure and the related separated solids. In general, sand bedding causes ash contents in manure to be extremely high, no matter what collection technique is employed, and thus making the DB unsuitable for most any thermo-chemical conversion process. On a dry basis, the results for vacuumed manure from free stalls with

compost bedding seem promising, with a mean ash percentage of only 22%. Vacuum machines can collect almost all of the manure from the free stalls, along with the bedding.

On a dry, ash free basis, the compositions and heat values of each of the manure samples in Table 1.3.5 should be similar; however, since these numbers are averages of samples taken from several dairies in different parts of Texas, there seems to have been some variation in the combustible contents of the DB samples. The low-ash DB sample was taken from separated solids from a free stall using composted manure as bedding of a dairy in Comanche, Texas. The high-ash sample is from scraped DB from an open lot at the same dairy.

Table 1.3.6 Ultimate, proximate, heat value analysis, and adiabatic flame temp (as received basis) of DB samples

As Received					
Parameter (by mass)	**Separated Solid**	**PC-3-4 weeks Windrow**	**Fully Comp. 3-4 months**	**Flushed DB**	**Lagoon DB**
Moisture	80.94	76.01	57.40	93.31	93.23
Ash	2.14	3.26	13.12	3.43	1.83
FC	3.64	4.83	7.04	0.45	--
VM	13.28	15.90	22.44	2.81	--
C	9.39	11.44	16.25	1.85	--
H	0.98	1.09	1.46	0.17	--
N	0.36	0.51	0.92	0.16	--
O	6.14	7.64	10.70	1.04	--
S	0.05	0.05	0.15	0.04	--
HHV (kJ/kg)	3468	4266	5965	668	--
T_ad (K)	719.96	948.79	1368.66	--	--

T_{ad}: adiabatic flame temperature for as received fuel

Table 1.3.7 Ultimate, proximate and heat value analysis (DAF basis) of DB samples

Dry, Ash Free Basis					
Parameter (by mass)	**Separated Solid**	**PC-3-4 weeks Windrow**	**Fully Comp. 3-4 months**	**Flushed DB**	**Lagoon DB**
Moisture	0.00	0.00	0.00	0.00	0.00
Ash	0.00	0.00	0.00	0.00	0.00
FC	21.51	23.30	23.88	13.80	--
VM	78.49	76.70	76.12	86.20	--
C	55.50	55.19	55.12	56.75	--
H	5.79	5.26	4.95	5.21	--
N	2.13	2.46	3.12	4.91	--
O	36.29	36.85	36.30	31.90	--
S	0.30	0.24	0.51	1.23	--
HHV (kJ/kg)	20494	20579	20234	20505	--
Empirical Formulae	$C_{0.78}H_{0.97}N_{0.03}O_{0.38}S_{0.002}$	$C_{0.95}H_{1.08}N_{0.04}O_{0.48}S_{0.002}$	$C_{1.35}H_{1.45}N_{0.07}O_{0.67}S_{0.005}$	$C_{0.15}H_{0.17}N_{0.01}O_{0.07}S_{0.001}$	--

Table 1.3.8. Fuel properties (Compare with natural gas: 55000 kJ/kg (23,641Btu/lb))

	HA-PC-DB-SoilS	**LA-PC-DB-SepS**	**TXL**	**WYO**
Ash	59.89	14.86	11.46	5.64
Dry Loss (% Moisture)	12.21	25.26	38.34	32.88
FC	3.92	13.00	25.41	32.99
VM	23.99	46.88	24.79	28.49
Carbon, C	18.04	35.21	37.18	46.52
Hydrogen, H	1.45	3.71	2.12	2.73
Nitrogen, N	1.15	1.93	0.68	0.66
Oxygen, O (diff)	7.07	18.60	9.61	11.29
Sulfur, S	0.19	0.43	0.61	0.27
Empirical Formulae	$CH_{0.96}N_{0.055}$ $O0_{.29}S_{0.0039}$	$CH_{1.25}N_{0.047}$ $O_{0.40}S_{0.0046}$	$CH_{0.68}N_{0.016}$ $O_{0.19}S_{0.0061}$	$CH_{0.70}N_{0.012}$ $O_{0.18}S_{0.0022}$
CO2 max, Mole%	19.36	18.93	19.66	
HHV , kJ/kg As Received (BTU/lb)	4312(1854	12844(5522)	14287(6142)	18193(7822)
HHV , kJ/kg Dry (BTU/lb)	4911(2111)	17186(7389)	23169(9961)	27107(11654)
HHV , kJ/kg DAF, (BTUlb)	15452(6643)	21450(9222)	28460(12236)	29593(12723)
HHV, kJ/kg of stoich Air, (BTU/lb)	1931(830)	2886(1241)	3156(1357)	3192(1372)
Boie HHV, kJ/kg, (BTU/lb)	7340(3156)	14799(6362)	14582(6269)	18348(7888)
VM, HHV, kJ/kg (BTU/lb)	12625(5429)	18312 (7874)	24046(10340)	25916(11144)
VM heat Control, %	81.7	66.8	41.7	40.6
A:F AR	2.23	4.45	4.53	5.70
A:F DAF	8.11	7.44	8.77	9.22

FC DAF	14.04	21.72	50.62	53.66
VM DAF	85.96	78.28	49.38	46.34
Ash kg/GJ	138.90	11.57	8.02	3.10
HV of VM	12624	18310	24046	25921
Heat % by VM	70	67	42	41
Nitrogen kg/GJ(lb/mmBTU)	2.67(6.21)	1.50(3.49)	0.48(1.12)	0.36(.837)
Sulfur kg/GJ (lb/mmBTU)	0.43(1.00)	0.33(.768)	0.42(.977)	0.15(.349)
SMD (μm) from Sieve Analysis	84.69	88.84	94.72	114.17
SMD (μm) from Rosin Rammler Distribution	70.86	98.80	88.88	100.95

The high heating value of the fuel can be computed using Boie equation [Annamalai et al, 1987]

$$HHV(kJ*kg^{-1}) = 35160*Y_C + 116225*Y_H - 11090*Y_O + 6280*Y_N + 10465*Y_S .$$

Where Y_C, mass fraction of element carbon in fuel.

Table 1.3.8 presents the analyses of DB fuel in cofiring and derived fuel properties [Lawrence et al, 2006]. Note that the DB fuels are much higher in nitrogen than coal fuels. This is different from most agriculture fuels (e.g. saw dust, corn stalks, switch grass, nut shells, rice hulls, etc.) which are lower in nitrogen than coal. Manure based biomass is the exception to this generality. The ash in high ash, partially composted, soil surface, dairy biomass (HA-PC-DB-Soil Surf) was more than 10 times that of Wyoming Powder River Basin coal. The heat values of HA-PC-DB- DB solid are unreliable due to very high ash content. The SMD's were calculated based on the sieve and they are presented in

Table 1.3.8.

Low ash, partially composted, separated solids, dairy biomass (LA-PC-DB-SepSol) was almost 3 times richer in nitrogen than Wyoming Powder River Basin coal. Although, low ash separated solids dairy biomass was more than 4 times lower in ash than high ash soil surface dairy biomass, it was still higher in ash than either coal. On a dry ash free basis, the dairy biomass fuels contained almost twice the volatile matter of coal, and hence less fixed carbon. Since HHV of DAF fuel is approximately given as: $HHV_{DAF} \approx VM_{DAF} * HHV_{VM} + FC_{DAF} * HV_{FC}$

where HHV DAF is the dry ash free higher heating value, $FC_{DAF} = 1 - VM_{DAF}$, $HV_{FC} = 32806$ kJ/kg (14,102Btu/lb) of C , the HV_{VM} can be estimated; the % heat contribution by VM is then computed using the relation: % heat by VM = $HHV_{DAF} = \{VM_{DAF} * HHV_{VM}\} * 100 / HHV_{DAF}$

It is seen from

Table 1.3.8 that even though the DB VM % is higher by twice the amount of VM of coal, the heat % contribution is not twice that of coal due to lower HV of VM from DB. On a heat basis, the DB fuels had higher nitrogen contents than coal.

The combustible contents of these two samples on a dry, ash free basis seem similar, although the heat value for the high ash sample is significantly lower, even on a dry, ash-free basis. This lower heat value for higher ash manure samples has been observed on several occasions over the course of this study and previous work; however, physically the low-ash and high-ash samples should be almost identical on a dry, ash-free basis if the manure samples are from the same feeding operation and the animals are given the same ration. The discrepancy may be from the fuel testing itself. Higher heat values are typically determined from bomb calorimeters, and it may be that part of the combustible content is shielded or diluted in the high ash content of the fuel and not burned during the calorimetric test. Ash analyses of these fuels as well as other coals and agricultural based biomasses can be found at the Texas A&M Coal and Biomass Energy Laboratory website (TAMU, 2006): http://www1.mengr.tamu.edu/CABEL/TAMU%20FDB.htm

Table 1.3.9 Ultimate and heat value analyses of dairy manure from a dairy in Comanche, Texas (Sweeten and Heflin, 2006)

	Low-ash Dairy Manure	**High-ash Dairy Manure**
(by mass)	As received	
Moisture	25.3	12.2
Ash	14.9	59.9
Fixed Carbon	13.0	3.9
Volatile Matter	46.9	24.0
Carbon	35.2	18.0
Hydrogen	3.1	1.6
Nitrogen	1.9	1.2
Oxygen	19.2	6.9
Sulfur	0.4	0.2
HHV (kJ/kg)	12,843	4,312
	Dry	
Moisture	0.0	0.0
Ash	20.0	68.2
Fixed Carbon	17.4	4.4
Volatile Matter	62.8	27.3
Carbon	47.1	20.5
Hydrogen	4.2	1.8
Nitrogen	2.6	1.3

	Low-ash Dairy Manure	High-ash Dairy Manure
Oxygen	25.6	7.9
Sulfur	0.6	0.2
HHV (kJ/kg)	17,183	4,912
	Dry, ash-free	
Moisture	0.0	0.0
Ash	0.0	0.0
Fixed Carbon	21.7	14.0
Volatile Matter	78.4	86.0
Carbon	58.9	64.6
Hydrogen	5.2	5.7
Nitrogen	3.2	4.1
Oxygen	32.0	24.9
Sulfur	0.7	0.6
HHV (kJ/kg)	21,475	15,467

a Moisture in manure samples is low due to solar drying prior to fuel analysis, typically 80% moisture for low-ash dairy manure before drying, moisture of scraped high-ash solids is variable before drying

It is noted that even though the HHV of as received fuels range from 5207 to 18196 kJ/kg(11,479 to 40,114lb), the HHV in kJ per kg of stoichiometric air is approximately same for coals and CB as shown from 3055 to 3425 kJ/kg(6735 to 7550lb) which implies that the oxygen consumption will be same when same thermal output is maintained; i.e. the same air flow rate is maintained when switching the fuels and the fuel flow is adjusted until similar O_2% in exhaust is maintained when operated under slightly fuel-lean conditions (Table 1.3.10).

Table 1.3.10 Fuel properties for reburn fuels on an as received basis.

	HAPCFB	**LAPCFB**	**LASSDB**	**TXLC**	**WYC**
HHV, kJ/kg (BTU/lb)	**5207 (2240)**	**13267 (5705)**	**12844 (5520)**	**14289 (6145)**	**18196 (7823)**
HHV in kJ per kg Stoich Air, (BTU/lb)	**3055 (1315)**	**3235 (1390)**	**3425 (1475)**	**3115 (1340)**	**3150 (1355)**
HHV in kJ per kg Stoich O2, (BTU/lb)	**13285 (5710)**	**14065 (6045)**	**14845 (6380)**	**13540 (5820)**	**13690 (5885)**
DAF HHV, kJ/kg (BTU/lb)	**17865 (7680)**	**20775 (8930)**	**21474 (9232)**	**28465 (12240)**	**29600 (12725)**

Ash Loading, kg/GJ	**103.42**	**12.44**	**11.62**	**8.02**	**3.10**
Chemical Formula	**CH1.11 N0.065 O0.57 S0.008**	**CH1.28 N0.05 O0.53 S0.006**	**CH1.06 N0.05 O0.41 S0.005**	**CH0.68 N0.02 O0.19 S0.006**	**CH0.7 N0.01 O0.18 S0.002**

1.3.4. Natural Gas

Natural gas (NG) is used as the primary fuel during reburn tests, and its gas compositions are shown in

Table 1.3.11. The compositions of NG consisted of 94.3% methane (CH_4), 1.7% carbon dioxide (CO_2), 2.4% ethane (C_2H_6), 0.7% nitrogen (N_2), 0.5% propane (C_3H_8) and trace amounts of several other gases. Its overall empirical chemical formula is CH3.87N0.0068O0.033 with a higher heating value (HHV) of 37050 kJ/m3. For most calculations performed in the current research, the NG composition was assumed to be pure CH_4 with a heating value of 36340 kJ/m3 indicating that actual value is about 2% higher in heating value. The compositions of NG used during the fouling experiments were different from the NG compositions as shown in figure 1.5. The compositions of NG used in ash fouling consisted of 94.5% CH_4, 1.7% CO_2, 2.3% C_2H_6, 0.5% N_2, and 0.6% C_3H_8. Its chemical formula is $CH_{3.84}N_{0.0086}O_{0.032}$ with a heating value of 37055 kJ/m3.

Table 1.3.11 Gas compositions of NG used in the reburn experiment

Gas Analysis Report

(August 19, 2007)

Analysis id: 93006400 | Test Number: 361454

Source Information

Operator	Texas A & M University
Source	Texas A&m Power Plant(ireland Dr)
County	Brazos
State	Tx
Freq	Daily

Field Data

Date Sampled from to 08/10/2007

Static Pressure (psia)	253
Diff Pressure (inches)	0
Flowing Temp (deg. f.)	91
Water Vapor (lbs/mmcf)	2
Hydrogen Sulfide (ppm)	0
Sampled by	BOND
Field BTU @ 14.65D	1022
Field Rel Den (R)	0.592

Analysis Results

Constituent	MOL %	Gal/MCF
Helium	0.00	
Carbon Dioxide	1.69	
Oxygen	0.00	
Nitrogen	0.69	
Methane	94.32	
Ethane	2.40	0.64
Propane	0.49	0.13
Isobutane	0.10	0.03
N-Butane	0.12	0.04
Isopentane	0.05	0.02
N-Pentane	0.03	0.01
Hexanes+	0.11	0.05
Hydrogen Sulfide	0.00	
Totals	100.00	0.92

Laboratory Data

Calculated BTU @ 14.65 Dry	1022.513
Calculated BTU @ 14.65 Saturated	1004.62
Relative Density(real)	0.5983
Total Inerts	
Interchange Factor	1306
Date Reported	08/19/2007

Composite Contract Quality Requirements

	Minimum	Maximum
BTU	950	1100
Relative Density		0
Interchange	0	0
Water Vapor(lbl/mmcf)		7
Carbon Dioxide(%)		2
Oxygen(%)		0.05
Nitrogen(%)		
CO2+N2		
Total Inerts(%)		4
Hydrogen Sulfide(gr/ccf)		0.25
Hydrocarbon Dew Pt(F)		40

Remarks

Approved by DC

1.3.5. Blend of Coal: DB

The characterization of DB: WYC blend fuel is presented in

Table 1.3.12. The properties of the blend were obtained using the weighted properties of coal and DB.

Table 1.3.12 Characterization of 90% DB: 10% WYC (mass %)

Fuel Name	90% DB: 10% WYC
Dry loss %	25.015
Ash %	14
VM %	45.606
FC %	15.38
VM_{DAF} %	0.75
FC_{DAF}%	0.25
C %	37.15
H %	3.13
N %	1.791
O %	18.498
S %	0.417
HHV (kJ/kg)	13698.1
DAF HHV(kJ/kg)	22315
Dry HHV (kJ/kg)	18237
Emprical Formulae	$CH_{1.03}N_{0.043}O_{0.39}S_{0.001}$
$ER_{MAX\ FC \rightarrow CO}$	5.14
Stochiometric air:fuel ratio, mol basis	5.06
$ER_{FC \rightarrow CO + H2 + N2}$	8.37
$AOF_{FC \rightarrow CO + H2 + N2}$	0.61
$HHH_{FC \rightarrow CO}$ (kJ/kg gas)	8192.00
$HHV_{FC \rightarrow CO + H2}$ (kJ/kg gas)	11730.00

1.3.6. Ash Analyses

The ash contents are typically high in FB and DB (

Table 1.3.15). Even though mass based ash content of LAPCFB is 50 % higher compared to lignite, the ash content on heat basis is almost 2 times that of lignite due lower heat value of LAPCFB. The pure HAPCFB has the highest ash loading and only limited tests have been conducted due to safety concerns.

The mineral analysis of ash for the reburn fuels tested are very important since it affects the deposition rate, fusion and melting points, corrosion rate, and erosion rate of HEX tubes. The mineral analysis is presented in Table **1.3.13**. Higher alkaline oxide contents (Calcium, Magnesium, Sodium, and Potassium) result in a higher probability of fouling due to the oxide layers on a HEX surface growing faster. The LAPCFB has high alkaline contents probably due to the collection of FB from fly ash paved feedlots. The dominant compositions of reburn fuels are silicon (SiO_2), aluminum (Al_2O_2), and calcium (CaO). The total amounts of ash acids (SiO_2, Al_2O_3, TiO_2) are higher than that of basic components (Fe_2O_3, CaO, MgO, Na_2O, and K_2O) for HAPCFB, TXLC, and WYC. Though the ash fusion temperatures are typically hard to obtain,

they depend upon the ratio of ash acid and the basic components [Hyukjin et al., 2007] higher the amount of basic components, the lower the fusion temperature.

Table 1.3.13 Ash elemental analysis (% mass, ash was calcined @ 600°C (1100°F) prior to analysis).

Compositions	**HAPCFB**	**LAPCFB**	**TXLC**	**WYC**	**Melting Point (°C)**
Silicon, SiO_2	65.55	20.78	48.72	31.73	1712.85
Aluminum, Al_2O_3	11.2	4.94	16.04	17.27	2040
Titanium, TiO_2	0.52	0.22	0.85	1.35	1829.85
Iron, Fe_2O_3	2.99	1.71	7.44	4.61	1564.85
Calcium, CaO	7.47	21	11.70	22.20	2298.85
Magnesium, MgO	2.29	7.54	1.93	5.62	2799.85
Sodium, Na_2O	1.38	5.26	0.29	1.43	1132
Potassium, K_2O	4.66	14.6	0.61	0.67	763
Phosphorus, P_2O_5	2.43	13.77	0.1	0.8	300
Sulfur, SO_3	1.3	4.47	10.80	10.40	16.9
Chlorine, Cl	0.41	5.07	<0.01	<0.01	-101.55
Carbon dioxide, CO_2	0.51	0.59	0.08	0.37	-57

Source: [Annamalai *et al.*2006] Pyrolysis, Ignition, and Fuel Characteristics of Coal, Feedlot Biomass, and Coal: Feedlot Biomass Blends. Final Report for TCEQ, March 31, 2006 which was used as cost share for DOE project.

Table 1.3.14 Ash loading and DAF chemical Formula

Average Fuel Compositions				
	HAPC	**LAPC**	**TX Lignite**	**Wyoming**
Ash Loading (kg/GJ)	65.31	9.51	4.55	2.02
DAF Chemical Formula	$CH_{1.11}N_{0.065}O_{0.57}S_{0.008}$	$CH_{1.28}N_{0.05}O_{0.53}S_{0.006}$	$CH_{0.68}N_{0.02}O_{0.19}S_{0.006}$	$CH_{0.7}N_{0.01}O_{0.18}S_{0.002}$

In order to evaluate the ash "fouling" behavior in a small boiler burner and its effect on the overall heat transfer rate to water tubes and air tubes, it is essential to determine the composition of ash. Further the loss on ignition (LOI) is a widely used method to estimate the carbon content of ash. Organic matter is oxidized to CO_2 and ash at 500 – 550ºC (932-1022 F), and carbon remains at 900 – 1000ºC (1652-1832F) LOI is typically obtained by the weight loss during the process by weighing the samples before and after heating. In the current study, the combustible loss which is defined as the ratio of unburnt combustibles in the ash to initial combustibles in the fuel is estimated instead of carbon contents. All ash samples were dried in the lab and sent for analysis. The contents of moisture and volatile combustible matter (VCM) in the ash samples were measured. The measurement of the moisture content was performed by overnight drying at 105ºC (221F) to constant weight. For the measurement of the VCM, ash samples were placed in a 950ºC (1742F) oven for 15 minutes and removed, and then heated in an oven at 575ºC (1067F) overnight to a constant weight.

The ash analyses are also useful for the determination of a burnt fraction (BF) which is defined as the ratio of combustibles burnt to combustibles in, a brief overview of the BF analysis is presented. For a dry solid fuel with an ash fraction A and a combustible fraction F,

$$A_0 = \frac{m_{A,0}}{m_{A,0} + m_{F,0}} \tag{1-1}$$

where A0 denotes the initial ash fraction on a dry basis, mA,0 is the initial mass of ash in the dry solid fuel and mF,0 is the initial mass of combustible in the dry solid fuel. After combustion, the mass of ash remains constant but the amount of combustibles decreases. Therefore, the ash fraction increases.

$$A = \frac{m_A}{m_{A,0} + m_F} \tag{2-2}$$

where A represents the ash fraction in a dry sample after combustion. Therefore, the burnt fraction is expressed by equations (2.3) .

$$BF = 1 - \frac{(1-A)A_0}{(1-A_0)A} \tag{2-3}$$

Therefore, the combustible loss can be expressed as

$$Combustible\ loss = 1 - BF \tag{2-4}$$

Table 1.3.15 Proximate analysis for reburn fuels.

Proximate (%)	**HAPCFB**		**LAPCFB**		**LASSDB**		**TXLC**		**WYC**	
	As Rec.	**Dry**	**As Rec.**	**Dry**	**As Rec.**	**Dry**	**As Rec.**	**Dry**	**As Rec.**	**Dry**
Moisture	17.00	0	19.64	0	25.26	0	38.34	0	32.88	0
Ash	53.85	64.88	16.50	20.53	14.93	19.97	11.46	18.59	5.64	8.40
Volatile Matter	25.79	31.07	52.33	65.11	46.86	62.70	24.79	40.20	28.49	42.45
Fixed Carbon	3.36	4.05	11.54	14.36	12.95	17.33	25.41	41.21	32.99	49.15
HHV, kJ/kg (BTU/lb)	5207 (2240)	6247 (2685)	13267 (5705)	16507 (7095)	12844 (5522)	17182 (7387)	14289 (6145)	23172 (9960)	18196 (7823)	27114 (11655)

1.4. Impact on Tasks due to Industrial Advisory Committee feed back

1. There was concern about high N and impact NOx emission. But it is believed that the FB Nitrogen is in mostly in the form of urea and hence it may aid in reduction of NOx when co-fired with coal (see Task A-7)
2. There was concern from utility that there is more than 1-1.5% of Sodium (Na) in FB and may cause slagging in coal-fired plants. The effect of cofiring FB with coal on ash fouling and heat transfer characteristics to heat exchanger tubes were investigated [see results under task A-3]
3. Low ash FB and DB were recommended for cofiring ; however low ash requires specially paved surfaces. “Paving feed pens may not pay out considering animal performance. Industry has problems with hard-surfaced pen surfaces and thus may need to find other uses for manure ash and other technologies for use of high ash FB and DB”. “Grinding cost increase with ash contents”. Gasification experiments were performed since it can handle high ash FB and DB [see Task A-5]. Further whether the fly ash produced from cofiring can be used as supplemental material with cement. [See results under task A-9]
4. There is 25-30% fat in beef carcasses; consider that if considering use as biofuel; the properties of composted carcasses were determined. (see Volume II under Task A.1.1 , properties)
5. CAFO techniques require improvement in quality of raw material; suggested approach is to use ash separation (See Volume II).

1.5. Summary

A majority of proposed task was performed. The following is a summary of results.

1. The DAF-HHV was almost constant for most CB fuels (20,000 kJ/kg) about2/3 of the DAF heat value of coals (30,000 kJ/kg).
2. The fuel N, per mmBTU, in FB, was high compared to coal which may result in increased NOx emission
3. The volatile matter is almost twice that of coal but the heat value of volatiles of CB per unit mass of volatiles is lesser than that of VM of coal
4. The HHV per unit stoichiometric oxygen mass is roughly constant (13000 to 14000 kJ/kg O_2) for most fuels
5. The ash loading per unit heat value even for low ash CB is almost twice that of TX lignite; ash loading from 3.10to 8.0 kg/GJ for the coals and from 11.57 to 139 kg/GJ for the DB fuels.
6. The nitrogen loadings of CB on heat basis are almost 3 times that of coal while sulfur loadings are about 2 times that of coal.

1.6. References

ASAE D384.2 MAR 2005. ”Manure production and characteristics: ASAE standard. American Society of Agricultural Engineers”.

ASAE. 2005. Manure production and characteristics: ASAE standard. American Society of Agricultural Engineers. ASAE D384.2 MAR2005

Annamalai K, Sweeten JM, Freeman M, Mathur M, O’Dowd W, Walbert G, Jones S, 2003. “Co-firing of coal and cattle biomass (FB) fuels”. Part III: Fouling result from a 500,000 Btu/h pilot plant scale burner. Fuel; 82:1195-1200.

Carlin, N. T. 2005. “Thermo-chemical conversion of dairy waste based biomass through direct firing”. MS Thesis. Texas A&M University: College Station, Texas.

Carlin, N., Annamalai, K., Sweeten, J., and Mukhtar, S. 2007a.” Thermo-chemical conversion analysis on dairy manure-based biomass through direct combustion”. *International Journal of Green Energy* 4(2): 133-159

Carlin N, Annamalai K, Sweeten JM, Mukhtar S, 2007. “Thermo-chemical conversion analysis on dairy manure-based biomass through direct combustion”. Int J Green Energy; 4:1-27.

CDFA. 2006. “California dairy facts. California Dairy Research Foundation of the California Department of Food and Agriculture”. Available online at: http://www.cdrf.org. (Accessed on November 2007).

DI Blasi C, Signorelli G, Portoricco G ,1999. “Countercurrent fixed-bed gasification of biomass at laboratory scale”. J Ind. Eng. Chem. Res.; 38: 2571-2581

DPI&F. 2003. Feedlot waste management series: manure production data. Department of Primary Industries and Fisheries. Government of Queensland, Australia. Available online at: http://www.dpi.qld.gov.au/environment/5166.html. (Accessed on September 2005).

Demirbas A ,2005. "Potential applications of renewable energy sources, biomass combustion problems in boiler power systems and combustion related environmental issues". Prog Energy Combust Sci; 31:171-192.

ECN. 2003." Phyllis: the composition of biomass and waste". Energy Research Centre of the Netherlands. Available online at: http://www.ecn.nl/phyllis/. Last updated in May 2003. (Accessed on January 2009).

Ferdous D, Dalai AK, Bej SK, Thring RW,2001. "Production of H_2 and medium heating value gas via steam gasification of Lignins in fixed-Bed reactors". J Can Chem Eng ;.79:913-922

Galloway T, Waidl J, Annamalai K, Sweeten JM, Tomlinson T, Weigle D 2002. "Energy resources recovery applications using gasification and steam reforming". Bi-annual Incineration and Thermal Alternatives. New Orleans: Conference 2002.

Gil J, Corella J, Azner MP, Caballero MA ,1999. "Biomass gasification in atmospheric and bubbling fluidized bed: effect of the type of gasifying agent on the product distribution". J Biomass and Bioenergy ; 17:389-403.

Harman, W. L. 2004. "Pen cleaning costs for dust control, Southern Great Plains feedlots". Texas Agricultural Experiment Station, Texas A&M University, Blackland Research Center Report No. 04-01.

Heflin K. 2008. Personal contact. Extension Associate. Texas AgriLife Extension Service, Amarillo and Bushland, Texas.

He B. J., Zhang Y., Yin Y., Funk T. L., and Riskowski G.L. 2000. "Operating temperature and retention time effects on the thermochemical conversion process of swine manure". *Transactions of the ASAE* 43(6): 1821-1825.

Jangsawang W, Klimanek, Gupta AK ,2006." Enhanced yield of hydrogen from wastes using high temperature steam gasification". J. Energy Res. Technol ; 128:179-185

Jensen M. D., Timpe R. C., Laumb J. D. 2003. "Advanced heterogeneous reburn fuel from coal and hog manure". Final report to the US Department of Energy – National Energy Technology Laboratory (DOE-NETL). Award No. DE-FG26-02NT41551.

Kalisz S, Lucas C, Jansson A, Blasiak W, Szewczyk D ,2004. "Continuous high temperature air/steam gasification (HTAG) of biomass". Victoria, Canada: 6th Int. Conference on Science in Thermal and Chemical Biomass Conversion

Klass DL ,1998. "Biomass for Renewable Energy, Fuels, and Chemicals". San Diego: Academic press;.

Miller, B.G., S. F. Miller, A. W. Scaroni, 2002." Utilizing agricultural by-products in industrial boilers: Penn State's experience and coal's role in providing security for our nation's food supply", Nineteenth Annual International Pittsburgh Coal Conference, Pittsburgh, PA. 23-27.

Mukhtar, S. 1999. Proper lagoon management to reduce odor and excessive sludge accumulation. Texas A&M University, Texas Agricultural Extension Service. Available at: http://tammi.tamu.edu/pdf%20pubs/lagoonmanagement.pdf. (Accessed on October 2005).

Mukhtar S., Goodrich B., Engler C., and Capareda S,2008. "Dairy biomass as a renewable fuel source". AgriLife Extension, Texas A&M System, L-5494, 02-08.

NASS. 2007. "Farms, land in farms, and livestock operations: 2006 summary". National Agricultural Statistics Service of the United States Department of Agriculture. Available online at: http://usda.mannlib.cornell.edu/usda/nass/FarmLandIn//2000s/2007/FarmLandIn-02-02-2007.pdf. (Accessed on January 2009).

Pinto F, Lopez H, Neto RA, Gulyurtlu I, and Cabrita I ,2007. "Effect of catalysts in the quality of syngas and by-products obtained by co-gasification of coal and wastes. !. Tars and nitrogen compounds abatement". J Fuel; 86:2052-2063.

Schmidt, G. H., Van Vleck, L. D., and Hutjens, M. F,1988. "Principles of dairy science, second edition, Chapter 27: Dairy cattle housing". Englewood Cliffs, New Jersey: Prentice Hall.

Sweeten, J. M. and Heflin, K. 2006. Preliminary interpretation of data from proximate, ultimate and ash analysis, results of June 7, 2006, samples taken from feedlot and dairy biomass biofuel feedstocks at TAES/USDA-ARS, Bushland, TX. Amarillo/Bushland/Etter, TX: Texas A&M Agricultural Research & Extension Center.

Sweeten, J M., Kevin Heflin, Kalyan Annamalai, Brent W. Auvermann, Ph.D.,F.Ted McCollum, and David B. Parker, P , 2006 ASABE Annual International Meeting, Oregon Convention Center, Portland, Oregon 9 - 12 July 2006

Sweeten, J. M., Annamalai, K., Thien, B., McDonald, L,2003." Co-firing of coal and cattle feedlot biomass (FB) fuels, Part I: feedlot biomass (cattle manure) fuel quality and characteristics". *Fuel* 82(10): 1167-1182.

Sami M, Annamalai K, Wooldridge M ,2001. "Co-firing of coal and biomass fuel blends". J Prog Energy Combust Sci; 27:171-214.

1.7. Acronyms

AFB: Advanced Feedlot Biomass

APF: Annular Primary Fuel

ARS: Agricultural Research Station

ASTM: American Society for Testing and Materials

ATP: Texas Advanced Technology Program
AW: Agricultural Wastes
AWDF: Animal Waste Derived Biomass Fuels
BL: Broiler Litter
CAB: Coal: Agricultural Biomass Blend
CAFO: Concentrated Animal Feeding Operations
CB; Cattle biomass
CFB: Coal: Feedlot Biomass (Cattle Manure)
CFB: Coal: Feedlot Biomass
CHFB: Coal: High Ash Feedlot Biomass
CLB: Coal: Litter (Poultry Waste) Biomass
DAF: Dry Ash Free
DB: Dairy Biomass
DOE: Department of Energy
FB: Feedlot biomass (Cattle manure – conventional, i.e., high ash)
FB: Feedlot biomass (Cattle manure or Cattle Biomass CB)
FC: Fixed Carbon
HA-PC-FB: High Ash Partially Composted Feedlot Biomass
HA-FB-Raw: High Ash Feedlot Biomass Raw form
HFB: High ash Feedlot Biomass
HHV: Higher or Gross heating value
HT: Hemispherical Temperature
HV: Heating value
LA-PC-FB: Low Ash Partially Composted Feedlot Biomass
LA-FB-Raw: Low Ash Feedlot Biomass
LAHP: Low ash/High Phosphorus feedlot biomass
LALP: Low ash/Low Phosphorus feedlot biomass
LASSDB: Low Ash Partially Composted Separated Solid Dairy Biomass
LB: Livestock Biomass
MAF: Moisture Ash Free, Dry Ash Free
mmBTU: million BTU
MMF: Mineral Matter Free
MSW: Municipal Sewage Waste
NETL: National Energy Technology Laboratory
PC: Partially composted (45 days)
PCGC2: Pulverized Coal Gasification and Combustion- 2 Dimensional
PM: Particulate Matter
PM: particulate matter
RDF: Refuse Derived Fuel
RM; Raw Manure
SFB: Simulated Feedlot Biomass artificially created with similar ash content
SR: Stoichiometric ratio, Air: Fuel/ (Air: Fuel) stoich

SS: Soil surfaced or high ash feedlot biomass
SSFB: Soil Surfaced Feedlot Biomass
TAES: Texas Agricultural Extension Service/Experiment Station
TAMU: Texas A&M University
TBP: Boiling Point Temperature
TCEQ: Texas Commission on Environmental Quality
TCFA: Texas Cattle Feeders Association
TEES: Texas Engineering Experiment Station
TSP: Total Suspended Particles
TXLC: Texas Lignite Coal
USDA: US Dept of Agriculture
USDA: US Dept of Agriculture
VM: Volatile matter
WYC: Wyoming Sub bituminous Coal

1.8. Education

Hyuk Jin Oh, PhD Dissertation
Nicholas Thomas Carlin, PhD Dissertation
Gerardo Gordillo Ariza, PhD Dissertation
Ben Lawrence, Master Thesis

1.9. Other support

None

1.10. Dissemination

The fuel properties form part of publications under other Chapters/Sections

Sweeten, J M, Heflin, K, Annamalai, K, Auvermann, B., Mc Collum, and Parker, D B, "Combustion-Fuel Properties of Manure Compost from Paved vs. Un-paved Cattle feedlots, ", ASABE 06-4143, Portland, Oregon, July 9-12, 2006

Kalyan Annamalai, Invited participant , "Energy Conversion research-An Overview, " Workshop on Energy , Materials and Systems , January 10 - 11, 2008, Anna University, Guindy, India; Seminar on Energy Materials and Systems, pp 5-6, 2008;

Brandon Martin, Ben Thien, Kalyan Annamalai and Bukur, Dragomir, " Pyrolysis and Group Ignition of Coal, Feedlot Biomass and Blends under TGA Conditions," CSS-CI ; May 21-23, 2006, Cleveland, OH

2. FUEL PYROLYSIS AND IGNITION

Task A-2: Fuel Pyrolysis Studies

ABSTRACT

Increases in demand, lower emission standards, and reduced fuel supplies have fueled the recent effort to find new and better fuels to power the necessary equipment for societies needs. Often, the fuels chosen for research are renewable fuels derived from biomass. Current research at Texas A&M University is focused on the effectiveness of using cattle manure biomass as a fuel source in conjunction with coal burning utilities. The scope of this project includes fuel property analysis, pyrolysis and ignition behavior characteristics, combustion modeling, emissions modeling, small scale combustion experiments, pilot scale commercial combustion experiments, and cost analysis of the fuel usage for both feedlot biomass and dairy biomass. This paper focuses on fuel property analysis and pyrolysis and ignition characteristics of feedlot biomass. Deliverables include a proximate and ultimate analysis, pyrolysis kinetics values, and ignition temperatures of different types of biomass as well as blends of each biomass with Texas lignite coal. Activation energy results for pure samples of each fuel using the single reaction model rigorous solution were as follows: 45 kJ/mol (LARM), 43 kJ/mol (LAPC), 38 kJ/mol (HARM), 36 kJ/mol (HAPC), and 22 kJ/mol (TXL). Using the distributed activation energy model the activation energies were 169 kJ/mol (LARM), 175 kJ/mol (LAPC), 172 kJ/mol (HARM), 173 kJ/mol (HAPC), and 225 kJ/mol (TXL). Ignition temperature results for pure samples of each of the fuels were as follows: 734 K (LARM), 745 K (LAPC), 727 (HARM), 744 K (HAPC), and 592 K (TXL). There was little difference observed between the ignition temperatures of the 50% blends of coal with biomass and the pure samples of coal as observed by the following results: 606 K (LARM), 571 K (LAPC), 595 K (HARM), and 582 K (HAPC).

2.1. Introduction

Pyrolysis by definition is the decomposition or transformation of a biomass caused by heat. Thus, the fundamental characteristics of coal and CB require not only fuel properties based on ultimate and proximate analyses but also the rate at which the volatiles are evolved from the fuel during pyrolysis and the rate at which char oxidizes in air. The fuels of interest are cattle biomass and coal. While coal contains 40-50% volatile matter, the CB can release up to 80% gases on dry ash free basis thus providing more heat input via volatiles than char.

There are two major steps to the pyrolysis of most solid fuels. First, any moisture in the fuel will evaporate, and second, volatile compounds (CH_4, CO, CO_2, H_2, C_2H_6, etc.) will be driven off. While, extensive data is available for coal, data on pyrolysis and oxidation of CB are very limited. The objectives of this task are to generate the kinetic data on pyrolysis of coal FB and coal:FB blends using single and parallel reaction model and the corresponding ignition characteristics. The kinetic information is useful in modeling, and the fundamental knowledge obtained will provide insight into the combustion behavior of coal-biomass blends. The pyrolysis data is generated using TGA of fuel samples in inert gas (N_2) and ignition data in air. The data in N_2 is interpreted with the parallel reaction model while data on ignition may be interpreted with the "group ignition" model (Tognotti et al, 1985). The review by Annamalai et al (1995) revealed that the experiments involving variations of sample masses resulted in different volatile yields: ASTM: 1000 mg, TGA: 15-30 mg, Crucible Experiments: 10-20 mg, Heated Grids: 5-10 mg, Flash heating <10 mg. Thus, apart from kinetic and thermo-physical parameters, the size of sample or group effects will also affect the volatile yields. While extensive data is available for coal, only limited studies have been conducted on pyrolysis of animal waste. An extensive review on pyrolysis and ignition of isolated particles and groups of coal particles has been conducted (Annamalai et al, 1995).

2.2. Literature Review

2.2.1. Manure Collection Techniques

Feedlot biomass fuel properties (chiefly ash content) depend greatly on the collection technique used when the manure is gathered from the feedlots; this is due in large part to the surface of the feedlot. Most feedlots have a soil base with an interfacial layer which consists of mixed soil and manure. If the manure is not harvested carefully some of the interfacial layer will be disturbed or collected with the manure. This leads to higher ash content in the manure. Collection techniques vary between feedlots but usually one of the following methods is used: wheel loader alone, chisel-plow followed by wheel loader, and elevating scraper.

The first manure harvesting method is to use a wheel loader to scrape and collect the manure from the surface of the feedlot. However, this is not the most effective method since wheel loaders can easily damage the interfacial layer. The quality of the collected manure depends greatly on the skill of the operator. A more efficient technique (tons/hour) is to use a chisel-plow to loosen the manure and then collect the manure with the wheel loader. Again, this method can easily damage the interfacial layer. Another disadvantage of this method is that it requires two-pieces of equipment rather than just one. The most effective method of manure collection is the elevating scraper. The scraper is pulled behind a tractor, and can be set to collect at a certain depth. This ensures that the interfacial layer will not be damaged and increases the quality of the harvested manure. Since the scraper needs to be pulled along, corners of a feedlot pen cannot be reached with the scraper, requiring the use of a box-blade or other equipment for collection in those areas. Due to its versatility, the wheel loader is the most common collection technique. Some feedlots are paved with fly ash. A wheel loader is used for

collection from these pens since there is no interfacial layer to disturb. Ash content of manure from these pens is lower than the ash content of the soil surfaced pens since no soil is collected during harvesting.

2.2.2. Fuel Properties

Due to the growing demand for renewable fuels, there are a wide variety of biomass fuels either being used in pilot scale plants or under laboratory investigation. The majority of these fuels fall into one of two categories, plant based biomass and animal waste biomass. The ultimate and proximate analyses as well as the higher heating value both on a dry and dry ash free basis of the plant based biomass fuels are given in Table 2.2.1. These fuels were analyzed as part of a study conducted for the National Renewable Energy Laboratory on the fouling characteristics of biomass fuels. Fouling is directly related to the ash content of the fuel and is a major concern for direct firing of biomass fuels.

Table 2.2.1. Proximate and ultimate analysis of plant base biomass.

Fuel:	Red Oak Sawdust	Mixed Paper	Sugar Cane Bagasse	Wheat Straw	Almond Shells
Proximate Analysis (% as recieved)					
Moisture	11.45	8.75	10.39	7.04	6.93
Fixed Carbon	11.92	6.78	10.70	16.47	19.28
Volatile Matter	76.35	76.87	76.72	69.97	70.73
Ash	0.28	7.60	2.19	6.52	3.06
Ultimate Analysis (% dry ash free)					
Carbon	50.12	52.35	49.86	48.31	50.98
Hydrogen	5.94	7.23	6.02	5.87	6.17
Oxygen (diff)	43.91	40.19	43.92	45.17	42.02
Nitrogen	0.03	0.15	0.16	0.47	0.79
Sulfur	0.01	0.08	0.04	0.17	0.04
Higher heating value (Dry)					
MJ/kg	19.42	19.05	18.53	16.68	18.85
Btu/lb	8348	8190	7967	7172	8102
Higher heating value (Dry Ash Free)					
MJ/kg	19.48	20.78	18.99	17.94	19.49
Btu/lb	8374	8934	8166	7714	8378

The as received proximate analysis shows a lot of similarity among the plant based biomass fuels; the major component being the volatile matter (70 – 77 % as received). The ultimate analysis again reveals the similarity between these fuels with carbon and oxygen contents varying by less than 5%. Both heating values given are also very similar for all but the wheat straw biomass.

Table 2.2.2 gives the characteristics of different types of animal waste biomass fuels (AWBF). The selected fuels are all derived from animal manure, but other types of animal biomass could be included, i.e. animal carcasses (part of the future work at Texas A&M Universities Renewable Energy Lab). The four cattle biomass fuels on the left of the table are the test fuels for this research, while the data on the other fuels was gathered from literature. The diary biomass analysis is part of research gathered into the feasibility of an advanced gasification system for a dairy farm in Upstate New York that could be used to eliminate excess dairy waste. The data on sheep biomass was gathered by a research team at Pennsylvania State University.

They are investigating the hardware, development, fuel evaluations, and emissions characteristics of biomass fuels and coal in industrial boilers. The chicken litter biomass information was gathered at Texas A&M University as part of ongoing research by the Renewable Energy Lab into the disposal and utilization of excess animal waste.

Table 2.2.2. Proximate and ultimate analysis of selected animal waste biomass fuels.

Fuel:	HAPC* Cattle Biomass	LAPC* Cattle Biomass	HARM* Cattle Biomass	LARM* Cattle Biomass	Dairy Cattle Biomass	Sheep Biomass	Chicken Litter Biomass
Proximate Analysis (% as recieved)							
Moisture	17.00	19.64	19.81	20.27	69.60	47.80	7.57
Fixed Carbon	3.36	11.54	6.02	12.16	N/A	7.30	8.41
Volatile Matter	25.79	52.33	27.08	51.47	N/A	34.00	40.22
Ash	53.85	16.50	47.10	16.10	8.96	10.90	43.80
Ultimate Analysis (% dry ash free)							
Carbon	51.19	52.91	52.56	53.99	44.65	51.33	45.14
Hydrogen	4.77	5.72	6.36	6.55	5.85	6.45	6.06
Oxygen (diff)	39.10	37.49	35.35	34.73	38.18	38.81	42.02
Nitrogen	3.87	3.08	4.70	3.90	2.05	2.65	5.41
Sulfur	1.08	0.79	1.03	0.84	0.31	0.76	1.37
Higher heating value (Dry)							
MJ/kg	6.27	16.51	7.86	16.81	18.22	16.04	9.98
Btu/lb	2697	7097	3380	7229	7834	6895	4291
Higher heating value (Dry Ash Free)							
MJ/kg	17.86	20.77	19.05	21.07	18.22	20.27	18.97
Btu/lb	7680	8930	8190	9058	7834	8715	8155

The as received analyses of the animal biomass fuels are much more varied than the plant biomass fuels, with moisture varying from 7-70%. The ash content of these fuels is also much higher than for the plant biomass fuels. However, the fuels are very similar when compared on a dry ash free (DAF) basis as in the ultimate analysis and the DAF higher heating value. There is also a lot of similarity between the plant based biomass fuels (PBF) and the AWBF on a DAF basis. This is likely due to the strong relation between animal ration and animal waste, since cattle metabolic efficiency is approximately 20%.

Since much of the research on biomass fuels deals with co-combustion with coal, a table of various coals tested in literature is also presented here, Table 2.2.3. The table gives data from the two research coal being used at Texas A&M University, Texas lignite and Wyoming sub-bituminous, as well as four other coals. The data on the Cyprus bituminous and Alaskan lignite coals was gathered from the Korean Institute of Energy Research in which different candidate coal were compared to improve efficiency and reduce emissions through coal gasification. The Greek lignite and Colombian coals were studied in conjunction with meat and bone meal (MBM) biomass in a study by the University of Crete, which looks into the combustion of MBM biomass as a means of waste disposal.

The proxiamte analyses conducted on these fuels shows how coals vary in different regions of the world. Even in the dry ash free ultimate anlayses, many differences can be noted, specifically carbon and oxygen contents. Overall, however, coals are much higher in heating value than biomass. For this reason, most research into biomass fuel technology is restricted to biomass being used as a suplemntary fuel (i.e. co-firing or reburn).

Kinetics of Pyrolysis

Pyrolysis by definition is the decomposition or transformation of a compound caused by heat. There are two major steps to the pyrolysis of most fuels. First, any moisture in the fuel will evaporate, and second, volatile compounds, CH_4, CO, CO_2, etc., will be driven off. Kinetics

Table 2.2.3. Proximate and ultimate analysis of selected coals.

Fuel:	Texas* Lignite Coal	Wyoming* Sub-bit. Coal	Cyprus Coal (USA)	Alaskan Coal	Greek Lignite	Colombian Coal
Proximate Analysis (% as recieved)						
Moisture	38.34	32.88	9.97	22.32	24.32	4.20
Fixed Carbon	25.41	32.99	44.22	29.19	30.59	53.00
Volatile Matter	24.79	28.49	42.25	36.75	31.30	36.60
Ash	11.46	5.64	3.56	11.75	13.79	6.20
Ultimate Analysis (% dry ash free)						
Carbon	74.06	75.68	66.36	48.24	61.25	83.40
Hydrogen	4.22	4.43	5.44	6.07	5.13	6.25
Oxygen (diff)	19.14	18.37	27.09	44.95	31.05	8.01
Nitrogen	1.35	1.07	0.95	0.62	1.83	1.56
Sulfur	1.22	0.45	0.16	0.12	0.73	0.78
Higher heating value (Dry)						
MJ/kg	23.17	27.11	25.33	22.60	20.16	28.23
Btu/lb	9962	11657	10890	9718	8666	12135
Higher heating value (Dry Ash Free)						
MJ/kg	28.46	29.60	26.37	26.63	24.65	30.18
Btu/lb	12236	12726	11338	11449	10598	12975

parameters such as activation energy and pre-exponential factor can be determined from measured parameters such as weight change, time, and temperature recorded during pyrolysis. Measurements are made using a thermogravimetric analyzer (TGA) for relatively slow heating rates, i.e. < 100 K/min. The basic first order kinetics model of pyrolysis is given below:

$$-\frac{dm_v}{m_v} = k_0 \cdot \exp\left(-\frac{E}{\overline{R} \cdot T}\right) dt$$

Where m_v is the mass of the volatiles remaining in the sample, k_o is the frequency factor or pre-exponential factor, E is the activation energy, $\overline{R}$ is the universal gas constant, T is the temperature, and t is time. The preceding reaction is known as the single reaction model . Details to the solution of this equation are given in chapter V. It has been shown that the single reaction model does not adequately represent the kinetics of pyrolysis for coal or biomass fuels since the fuel consists of several decomposable polymers which break down into monomers and other compounds. Consequently, a new model was needed.

Dutta et al. (1977) conducted pyrolysis of Pittsburgh HVab coal and Illinois no 6 coal using a Fisher TGA. The coal pyrolysis is complete around 350°C to 400°C and the volatile yields correspond to the proximate yields. Anthony *et al*. (1974) conducted experiments using 5-10 mg monolayer samples of lignite and bituminous coal in the range of 400°C to 1000°C and found that the weight loss depends on the final temperature, but not on heating rate for heating

rates less than 10,000 K/s. They formulated a distributed activation energy model, where a Gaussian distribution represented the activation energy.

$$-\frac{dm_{v_i}}{\left(m_{v,i}\right)} = k_{0,i} \cdot \exp\left(-E_i / \overline{R}T\right) \cdot dt$$

The subscript *i* implies that the activation energy does not have a single value but rather has multiple values. Anthony *et al*. further theorized that the distribution of activation energies could be fit to a Gaussian distribution *f(E)* with mean activation energy E_m and standard deviation s. Using the model they were able to determine the kinetics values for several species of coal with reasonably accurate results; however, the solution to equation requires a complex double integration as seen in equation. Anthony *et al*. found the mean activation energies for two coals, Montana Lignite and Pittsburgh Seam Bituminous, to be 236 kJ/mol and 212 kJ/mol with standard deviations 46 kJ/mol and 29 kJ/mol, respectively.

$$\left(\frac{m_v}{m_{v,0}}\right) = \int_{E_m-3\sigma}^{E_m+3\sigma} \exp\left\{-\int_{T_0}^{T} \frac{k_0}{\beta} \cdot \exp\left(-\frac{E_i}{\overline{R}T}\right) \cdot dT\right\} f\left(E\right) dE$$

Later, Raman *et al*. (1981) applied the distributed activation energy model to feedlot biomass to determine the effects TGA parameters had on the activation energy and standard deviation. The manure used in this study was collected from paved feedlots at Kansas State University's Beef Research Center. They concluded that thermogravimetric parameters such as heating rate, size fraction, and purge gas flow rate had no effect on E_m, but was affected by the heating rate and purge gas flow rate. Their results indicated a mean activation energy of 176 kJ/mol with standard deviation 27 kJ/mol.

The review by Annamalai et al (1995) revealed that the experiments involving variations of sample masses resulted in different volatile yields: ASTM: 1000 mg, TGA: 15-30 mg, Crucible Experiments: 10-20 mg, Heated Grids: 5-10 mg, Flash heating <10 mg. Thus, apart from kinetic and thermo-physical parameters, the size of sample or group effects will also affect the volatile yields. While extensive data is available for coal, only limited studies have been conducted on pyrolysis of animal waste.

More recent work in this area has been to make improvements to the distributed activation energy model to make the equation easier to solve and/or to better approximate results. One alteration of the DAEM was proposed by Donskoi and McElwain (1998); they related the activation energy and pre-exponential factor directly to the heating rate. Their model was applicable to models with a large number of heating rates, and it significantly cut down on the time for calculation without an appreciable change in the accuracy of the calculation. Another approach taken by Donskoi and McElwain (2000) was to use a modified Gauss-Hermite Quadrature method to evaluate the double integration in equation (3) in order to lower the error of integration as well as reduce the computation time. Other attempts to reduce computation time were proposed by Please et al. (2003) in which asymptotic expansions were used to rapidly arrive at a solution. Two assumptions of the distributed activation energy model are that the distribution, *f(E)*, is Gaussian and the k_o term in equation (II.3) is constant ($1.67*10^{13}$ 1/s). The assumption for a constant k_o is valid for small values of , but not for wider activation energy ranges. The fuels being tested at Texas A&M University's Renewable Energy Lab were tested using distributed activation energy model with a constant value for k_o to simplify the calculation. Jinno et al (2004) studied the decomposition behavior of surrogate solid wastes (cellulose, polyethylene, polypropylene, polystyrene and polyvinyl chloride) in inert (N_2) and oxidizing (air) gases. They extracted the pyrolysis kinetics using single global first order reaction model and determined half decomposition (50 % mass loss) temperatures as 344-395 C for cellulose

(lower heating rate (HR): 5 C/min, higher HR: 50 C/min), 430-490 C for polypropylene, 388-457 C for polystyrene, and 290-340 C for polyvinyl chloride. The corresponding values in air were consistently lower with values of 325, 298, 281, 362 and 279 C respectively at HR= 5 C/min. It should be noted that these samples were homogeneous in makeup, and a single reaction model could be used. For fuels with a wide variety of components, the parallel reaction model produces results that are more accurate.

2.2.3. Ignition

When TGA is performed in N_2, only pyrolysis occurs. If the experiment is repeated in air, oxidation can also occur simultaneously. The experiments in air can also be used to define the onset of ignition of fuel samples in TGA. Tognotti et al (1985) used TGA techniques to determine the ignition temperature of coal particles and found that the ignition temperature of sample is lower than the single particle ignition temperature.

2.3. Objectives

The overall objective of this research is to evaluate the pyrolysis and ignition behavior of four types of feedlot biomass (FB), Texas lignite coal (TXL), and blends of biomass with TXL. The fuels being considered are High Ash Raw Manure (HARM), Low Ash Raw Manure (LARM), High Ash Partially Composted Manure (HAPC), Low Ash Partially Composted Manure (LAPC), Texas Lignite Coal (TXL), and Wyoming Sub-bituminous Coal (WSB). Low ash samples of each FB will be collected from feedlot pens with a fly ash surface, while high ash samples will be collected from soil surfaced enclosures. The FB samples are representative of the types of fuels which may be fired in a utility boiler either as reburn fuel or co-firing fuel. In order to achieve the overall objective, the following tasks were performed:

a. Obtain fuel samples and determine fuel characteristics
   i. The fuel samples will be gathered from members of our research team in the Amarillo, TX area. Once prepared, the samples will be sent to the renewable energy lab (REL) in College Station, TX.
   ii. The fuel characteristics will be obtained using a commercial testing company
b. Write speciation for and obtain thermogravimetric analyzer TGA
   i. This task requires an investigation into commercially available thermogravimetric analyzers and a review of the needs of the REL research group. Once completed, the TGA can be purchased through bid process.
c. Classify fuel samples by particle size
   i. The prepared fuel samples will be sieved and classified according to particle size using available REL equipment.
   ii. Particle sizes selected for testing will be: As Received, 60 micron and 22.5 micron based on sieve sizes available.
d. Determine blend ratios and blend fuels for testing
   i. The biomass fuels will be mixed with coal in varying amounts to determine what effect this has on the kinetics parameters under investigation. Specific blend ratios will be determined through coordination with other group members to ensure consistency in results. Blends are on a mass basis.
   ii. Blend ratios to be tested will be as follows (FB/TXL): 100/0, 50/50, 30/70, 10/90, and 0/100
e. Test fuel sample in TGA in both N2 and air environments

i. The specification for the TGA will include requirements for a software package and necessary training for operation of the equipment. Testing can begin after training has been completed. N2 will be provided via a gas cylinder obtained locally, and air will be provided from the physical plant supply lines running to the lab. The heating rate for testing will be maintained at 40 K/min.

f. Create methods for fuel characteristics calculations. (From available literature necessary formulas and theory have been gathered to make calculations.)

i. Create an Excel based spreadsheet to calculate activation energy using the single reaction model described in the literature review solving the following equations for activation energy E:

$$-\ln\left(\frac{m_v}{m_{vo}}\right)=\left(\frac{B}{\beta}\right)\cdot\left(\frac{E}{\overline{R}}\right)\cdot\left(\frac{\mathrm{E}_2(X)}{X}-\frac{\mathrm{E}_2(X_o)}{X_o}\right)$$

ii. Create an Excel based spreadsheet to determine the ignition temperature using the relationship (ignition temperature is the point where this statement is true and remains true as temperature increases):

$$\frac{(m\%)_{N2}-(m\%)_{air}}{\left[\frac{(m\%)_{N2}+(m\%)_{air}}{2}\right]}>5\%$$

iii. Create a MatLAB based program to calculate the activation energy using the distributed activation energy model to solve the following equation and obtain a value for activation energy E (this equation must be solved numerically, hence the necessity of a MatLAB based program):

$$\frac{m_v}{m_{v,0}}(T)=\frac{1}{\sigma\sqrt{2\pi}}\cdot\int_0^\infty \exp\left\{-\frac{k_0}{\beta}\cdot\left[T\cdot\mathrm{E}_2\left(\frac{E}{\overline{R}\cdot T}\right)-T_0\cdot\mathrm{E}_2\left(\frac{E}{\overline{R}\cdot T_0}\right)\right]-\frac{(E-E_m)^2}{2\cdot\sigma^2}\right\}dE$$

g. Use the created calculations tools to determine characteristics described in the objectives.

h. Report the results for kinetics of pyrolysis and comparative ignition behavior of biomass fuels, coal, and blends

2.4. Experiments and Procedure

The thermal analyzer must be preheated prior to the beginning of testing if it has had a significant amount of idle time. This is done by heating the furnace to 1273 K and letting it cool without a sample in one of the sample pans. The sample pans are made of alumina and have a 90 μL capacity. To begin testing, the furnace is opened, and the sample pans are checked to verify they are free of any residual material and cleaned if necessary. The furnace is then closed to tare the balances. The Q600 is a dual beam balance beam capable of measuring up to 350 mg per balance. After tarring the balances the furnace is opened and the sample pan is carefully removed using tweezers. The sample pan orientation should be noted before removal. The sample pan is nearest to the front of the machine; the other pan is a reference pan used for heat flow calculations.

Once removed, 10 mg of the sample is added to the pan. No excess material should be on the top or exterior of the sample pan as these can damage the platinum thermocouples embedded in the balance beams. The filled sample pan is then placed back on the beam in the same orientation it was in when the balance was tarred. The furnace is closed and testing begins.

The software package included in the purchase of the thermal analyzer is a windows based program that allows for easy changes to be made to the test procedure. A typical test procedure is as follows:

1. Select Gas (1 for N_2, 2 for Air)
2. Set Gas Flow Rate (200mL/min)
3. Heat at 40 K/min to 383.15K (110 ºC)
4. Hold at 383.15K for 5min
5. Set Gas Flow Rate (50mL/min)
6. Heat at 40K/min to 1373.15K (1100ºC)

Typically , the initial gas flow rate is set to 200mL/min to fully evacuate the furnace of gaseous impurities before the beginning of testing. This must be done for 5 minutes at that flow rate, hence the temperature hold at 383.15K (110ºC). This is also done to fully dry the sample, which ensures that any changes in the temperature/weight trend are due to volatile losses or ignition depending on the purge gas. The heating rate is set to 40K/min to maximize the slope of the temperature/weight trend for calculation purposes, the higher this value, the greater the slope. The Q600 TGA is capable of heating rates up to 100 K/min, but this causes excess wear to the machine.

2.5. Results and discussion

2.5.1. Pyrolysis Characteristics

Figure 2.5.1,

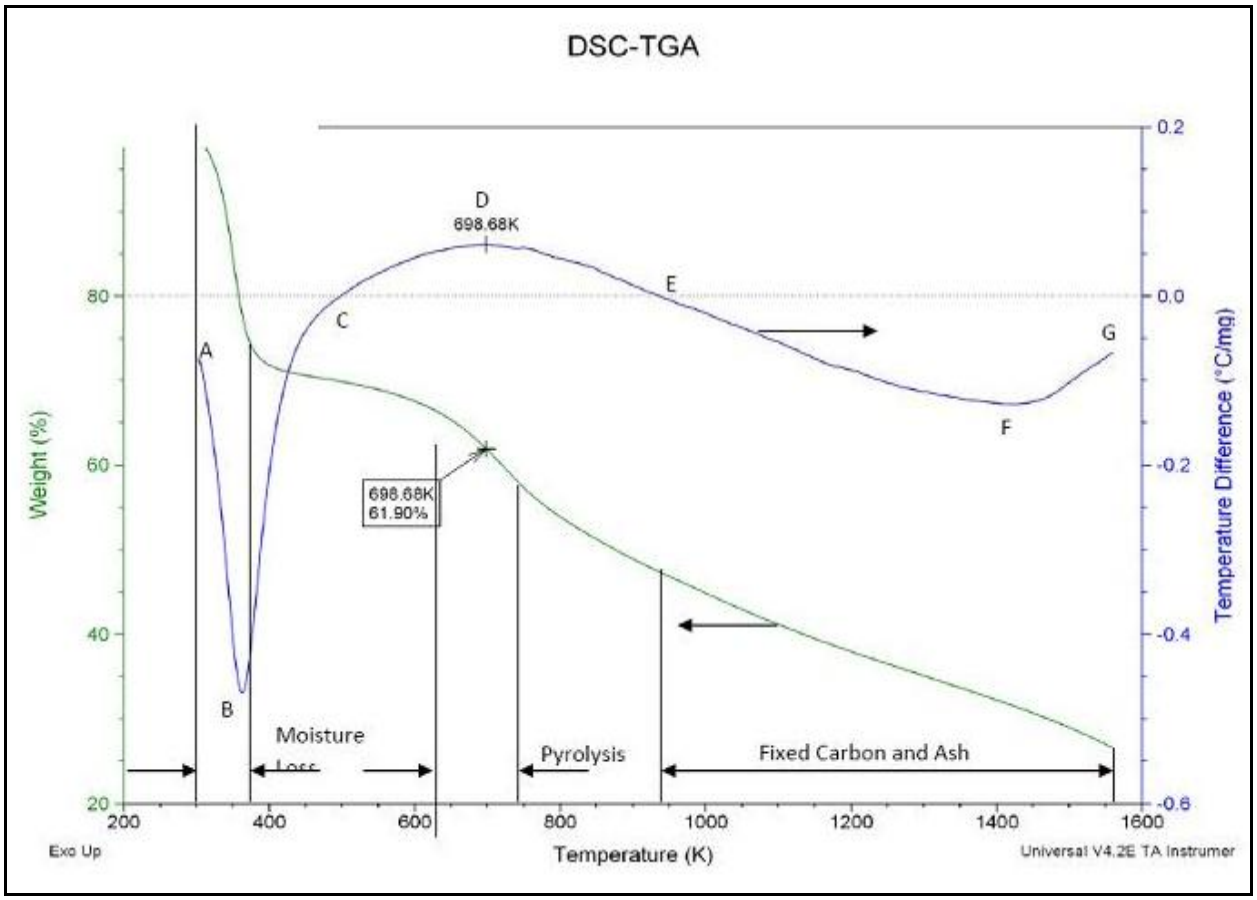

Figure 2.5.2, Figure 2.5.3 and

Figure 2.5.4 present the TGA and DTA traces for the fuels considered. Point A marks the beginning of the traces. Point B marks the peak of drying. Point C marks the beginning of the pyrolytic exotherm. Point D marks the peak of the exothermic portion of the pyrolytic process. Point E marks the end of the pyrolytic exotherm. Following pyrolysis, the remaining fixed carbon and ash is heated. Point F marks the peak of this heating endotherm. Point G marks the end of the trace. A horizontal line has been added to the figures at 0.0 on the DTA scale. All portions of the trace above this line are exothermic and all portions below are endothermic.

As moisture is removed from the fuel, less moisture remained and hence the rate of evaporation is slowed down and hence the BC curve indicates less endothermicity.

Of particular interests are the temperatures at which pyrolysis begins, ends, and the percentage of mass lost due to pyrolysis. The portion between points A and B on the TGA trace defines the amount of mass lost do to drying (moisture loss). The portion between points C and E on the TGA trace defines the amount of mass lost due to exothermic pyrolysis. The peak of the DTA trace has been marked. This is the point of maximum mass loss during pyrolysis. The

temperature and remaining mass at this point have been marked on the figures. Table 2.1 summarizes the data.

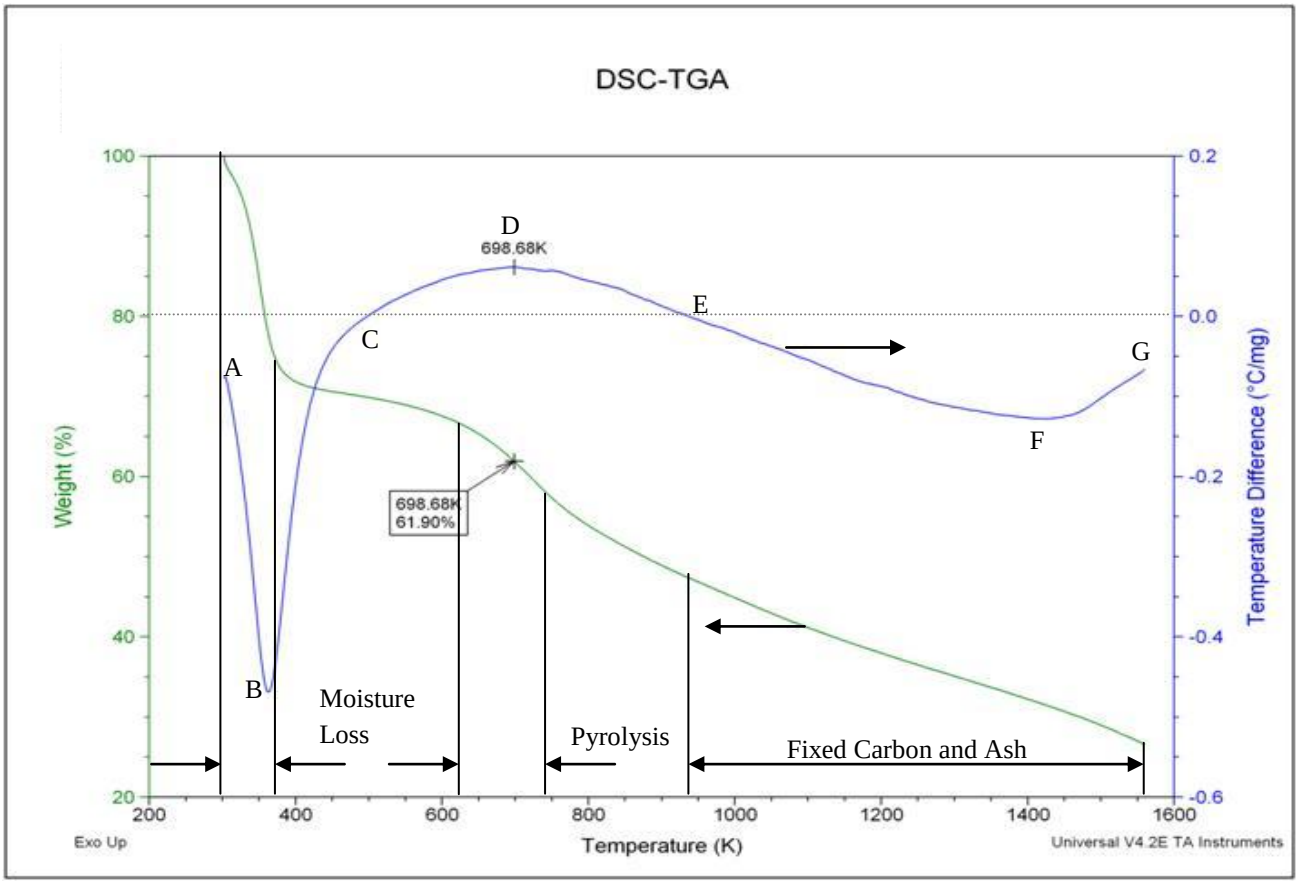

Figure 2.5.1: TGA and DTA trace of TXL.

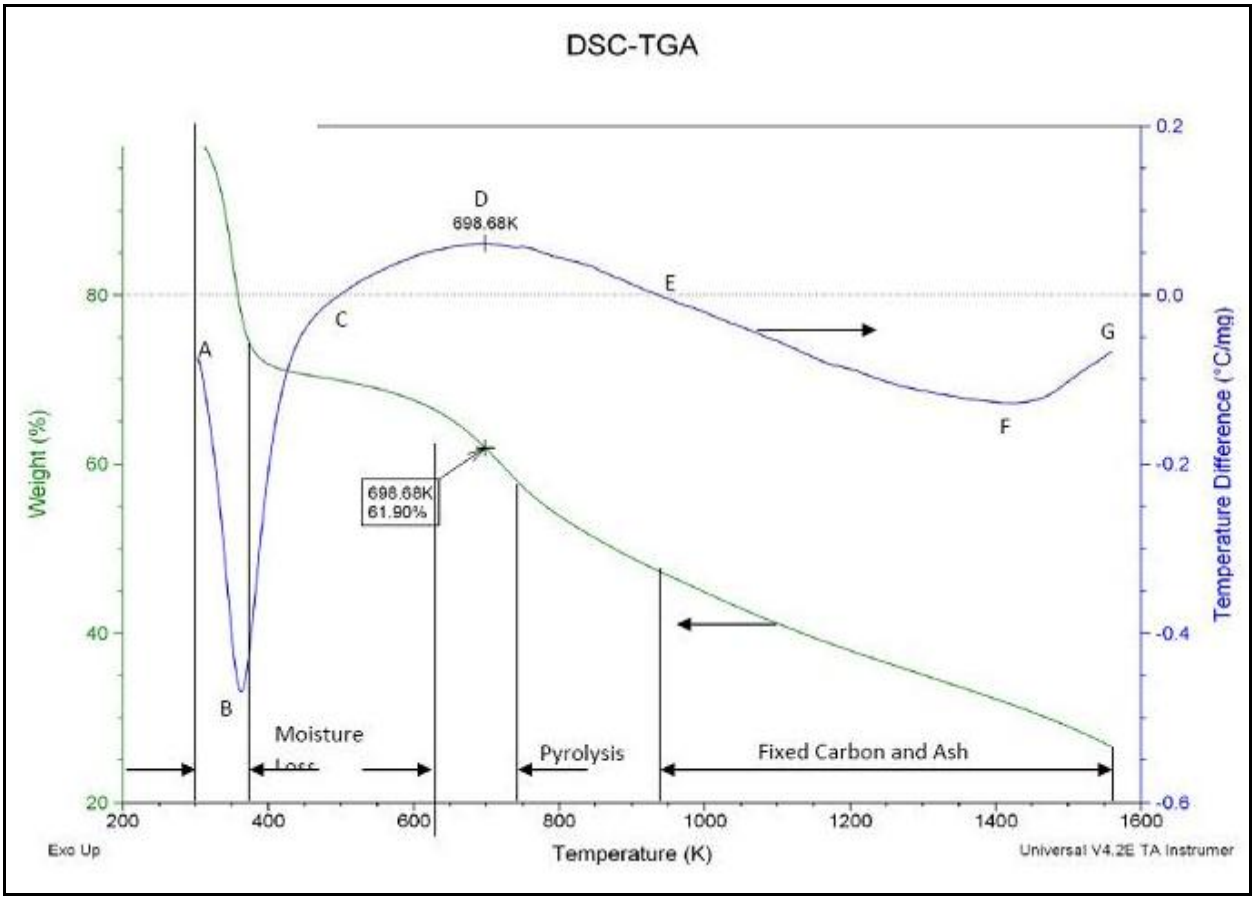

Figure 2.5.2: TGA and DTA trace of PRB

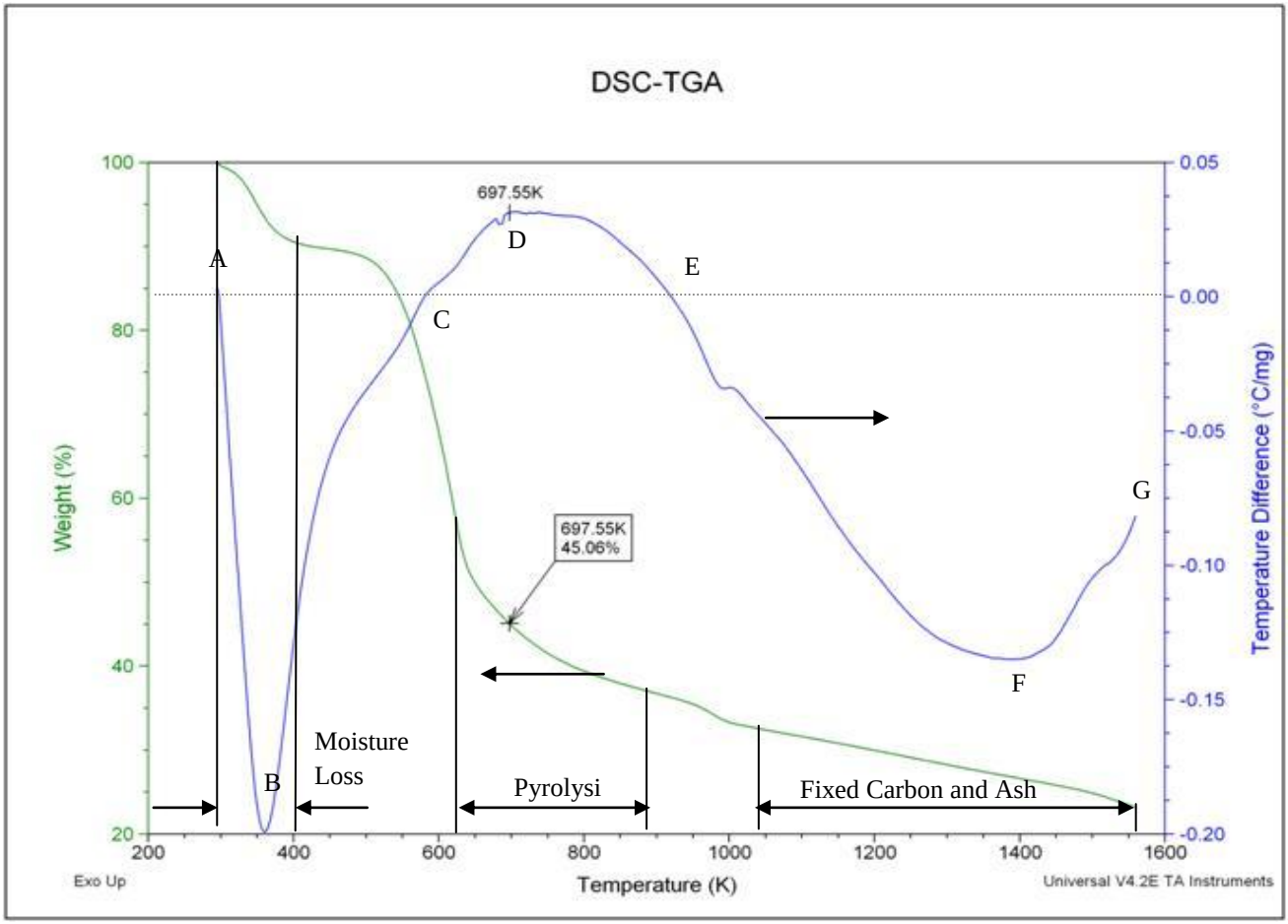

Figure 2.5.3: TGA and DTA trace of LA-PC-DB-SepSol.

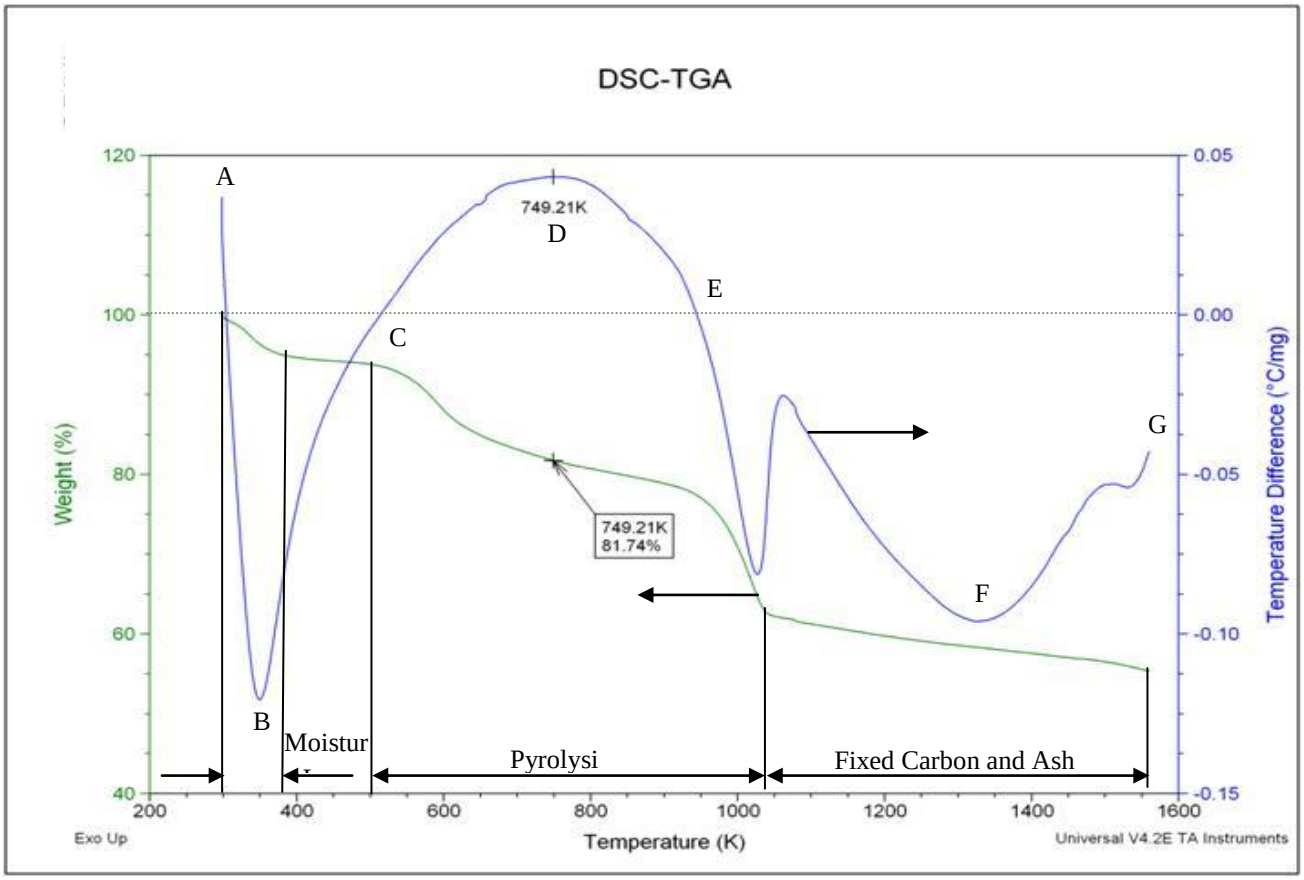

Figure 2.5.4: TGA and DTA trace of HA-PC-DB-SoilSurf.

2.5.2. Ignition Characteristics

TGA analysis can also be used to determine the ignition temperature of a fuel when experiments are performed in air. Tognotti et al (1985) used TGA techniques to determine the ignition temperature of coal particles and found that the ignition temperature of sample is lower than the single particle ignition temperature.

Each fuel was first analyzed in a nitrogen environment and then analyzed again in an air environment. The TGA traces of the two fuels began similar, but upon ignition, the fuel would oxidize if air was present. Ignition caused the two TGA traces to deviate. The temperature at which this deviation occurred was defined as the ignition temperature. The DTA traces of TXL and WYO look similar. The portions of the trace that are below 0.0 °C/mg are endothermic and the portions above are exothermic. The most significant endothermic process occurred at approximately 373K. This was the drying process, which is known to be endothermic. Pyrolysis was an exothermic process. This agrees with combustion theory which says that all pyrolysis must be an exothermic process.

2.5.3. Pyrolysis Model

Method A: Single reaction model

2.5.3.1. Derivation

The basic first order, single reaction model of pyrolysis is given by the following Arrhenius rate equation

$$-\frac{dm_v}{m_v} = Be^{\left(-\frac{E}{R_u T}\right)}dt \qquad 3.5.1.1$$

Typically measurements are made for m (t), mass of sample and T (t), temperature are recorded when they are heated at fixed heating rate β = dT/dt using a TGA for relatively slow heating rates, i.e. < 100 K/min. Rewriting 3.5.1.1

$$-d\big(ln(m_v)\big) = \frac{B}{\beta}e^{\left(-\frac{E}{R_u T}\right)}dT$$

Using Annamalai and Puri (2005) and with $X = \left(\frac{E}{R_u T}\right)$

$$-ln\left(\frac{m-m_{char}-m_{ash}}{m_o-m_{char}-m_{ash}-m_{H_2O}}\right) = \frac{B}{\beta}\frac{E}{R_u}\left(\frac{E_2(X)}{X} - \frac{E_2(X_o)}{X}\right) \qquad (2.1)$$

where E_2 is evaluated using the Abramovitz and Stegun, (1965) recurrence relation:

$$\frac{E_n(X)}{X} = \int_X^{\infty}\frac{e^{-X}}{X^n}dX \qquad (2.\ 2)$$

This is evaluated with:

$$E_1(X)Xe^X = \frac{\left(X^2 + a_1X + a_2\right)}{\left(X^2 + b_1X + b_2\right)} \qquad (2.3)$$

Where:

a_1=2.334733, b_1=3.330657, a_2=.250621, b_2=1.681534, for 1≤X<∞. Uing recurrence relations

$$E_n(X) = \exp(-X) - XE_{n-1}(X) \qquad (2.4)$$

We obtain

$$E_2(X) = \exp(-X) - XE_1(X) = \exp(-X)\left\{1 - \frac{\left(X^2 + a_1X + a_2\right)}{\left(X^2 + b_1X + b_2\right)}\right\} \qquad (2.\ 5)$$

$$E_2(X) = \exp(-X)C'(X) \ where \ C'(X) = \left\{\frac{(b_1 - a_1)X + b_2 - a_2}{\left(X^2 + b_1X + b_2\right)}\right\}, X = \left(\frac{E}{\overline{R}\cdot T}\right) \qquad (2.\ 6)$$

Method B: Slope Approximation

Since X<< X_0, and $E_2(X)/X$>>>> $E_2(X_0)/X_0$, one can assume E and k_o reach that error is minimized between theory and experiment, then

$$-\ \ln\left(\frac{(m - m_{char} - m_{ash})}{m_o - m_{char} - m_{ash} - m_{H2O}}\right) \approx \left\{\frac{B\ (E/R)}{dT/dt}\right\}\left[\frac{E_2(X)}{X}\right] \approx \left\{\frac{B\ C(X)\ \ (E/R)}{(dT/dt)}\right\}\exp(-X) \qquad (2.7)$$

$$where \ \ C(X) = \left\{\frac{(b_1 - a_1)X + b_2 - a_2}{X\left(X^2 + b_1X + b_2\right)}\right\},\ X = \left(\frac{E}{\overline{R}\cdot T}\right) \qquad (2.8)$$

$$\ln\left\{-\ln\left(\frac{(m-m_{char}-m_{ash})}{m_o-m_{char}-m_{ash}-m_{H2O}}\right)\right\}\approx\ln\left\{\frac{(E/R)B\{C(X)\}}{(dT/dt)}\right\}-\frac{E}{\overline{R}T}\ ,\ X=\left(\frac{E}{\overline{R}\cdot T}\right) \tag{2.9}$$

The variation of C(X) can be assumed in the form of A*exp(DX) and a fit reveals A= 0.092, D=- 0.032, 7.8<X<60 with R2= 0.94 or C(X) =0.092 exp(-0.032 X). If one ignores variation of C(X) with X, the plot of LHS vs 1/T is linear and hence E/R can be determined for single reaction model.

$$\ln\left\{-\ln\left(\frac{(m-m_{char}-m_{ash})}{m_o-m_{char}-m_{ash}-m_{H2O}}\right)\right\}\approx A-\frac{E}{\overline{R}T}\ \ where\ \ A=\ln\left\{\frac{(E/R)B\{C(X)\}}{(dT/dt)}\right\}=\ln\left\{\frac{(E/R)B}{(dT/dt)}\right\}+\ln\left\{\frac{(b_1-a_1)X+b_2-a_2}{X(X^2+b_1X+b_2)}\right\},X=\left(\frac{E}{\overline{R}\cdot T}\right)$$

The earlier literature with C(X) filled between for 20 < E/R_uT < 60 yields:

$$-\ln\left(\frac{m_v}{m_{vo}}\right)\cong 0.00482\cdot\frac{E\cdot B}{\overline{R}\cdot\beta}\cdot\exp\left(-1.052\cdot\left(\frac{E}{\overline{R}\cdot T}\right)\right) \tag{2. 10}$$

Equation (2.10) can be rewritten as

$$\ln\left[\ln\left(\frac{m_v}{m_{vo}}\right)\right]\cong\ln\left[-\left(\frac{B}{\beta}\right)\cdot\left(0.00482\cdot\frac{E}{\overline{R}}\right)\right]+\left(-1.052\cdot\left(\frac{E}{\overline{R}}\right)\cdot\left(\frac{1}{T}\right)\right) \tag{2. 11}$$

A solution for activation energy can be found by plotting $\ln(\ln(m_v/m_{vo}))$ vs. 1/T. The slope of the resulting line is $-1.052*E/R_u$. Then a check is made whether the approximation is correct by calculating E/R_uT and checking if the value falls between 20 and 60. Once the activation energy is obtained a resulting value for the frequency factor can be calculated.

Method C: Distributed Activation Energy Model

However, it has been shown that the single reaction model does not adequately represent the kinetics of pyrolysis for coal or biomass fuels. For this reason, a new model was needed. TGA analysis of feedlot biomass in N_2 was previously investigated by Raman et al. (1981) at heating rates between 40°C/min and 160°C/min. When TGA is performed in N_2, only pyrolysis occurs. If the experiment is repeated in air, oxidation can also occur simultaneously. Jinno et al (2004) studied the decomposition behavior of surrogate solid wastes (cellulose, polyethylene, polypropylene, polystyrene and polyvinyl chloride) in inert (N_2) and oxidizing (air) environments. They extracted the pyrolysis kinetics using single global first order reaction model and determined half decomposition (50% mass loss) temperatures as 344-395 ºC for cellulose (lower HR: 5 ºC/min, higher HR: 50 ºC/min), 430-490 ºC for polypropylene, 388-457 ºC for polystyrene, and 290-340 ºC for polyvinyl chloride. The corresponding values in air were consistently lower with values of 325, 298, 281, 362 and 279 ºC respectively at HR= 5 ºC/min. It should be noted that these samples were homogeneous in makeup, and a single reaction model could be used. For fuels with a wide variety of components, the parallel reaction model produces results that are more accurate. The experiments in air can also be used to define the onset of

ignition of fuel samples in TGA. Anthony et al. (1974) conducted experiments using 5-10 mg monolayer samples of lignite and bituminous coal in the range of 400°C to 1000°C and found that the weight loss depends on the final temperature, but not on heating rate for heating rates less than 10,000 K/s. They formulated a distributed activation energy model (parallel reaction), where a Gaussian distribution represented the variation of activation energy. Consider the first order pyrolysis reaction:

$$-\frac{dm_{v_i}}{\left(m_{v,i}\right)} = k_{0,i} \cdot \exp\left(-E_i / \overline{R}T\right) \cdot dt \tag{2.12}$$

The subscript *i* implies that the activation energy does not have a single value but rather has multiple values. Anthony and Howard further theorized that the distribution of activation energies could be fit to a Gaussian distribution with mean activation energy E_m and standard deviation σ. Using the model they were able to determine the kinetics values for several species of coal with reasonably accurate results; however, the solution to equation requires a complex double integration as seen in equation.

$$\left(\frac{m_v}{m_{v,0}}\right) = \frac{1}{\sigma \cdot \sqrt{2\pi}} \cdot \int_0^{\infty} \exp\left\{-\int_{T_0}^{T} \frac{k_0}{\beta} \cdot \exp\left(-E/\overline{R}T\right) \cdot dT\right\} \cdot \exp\left\{-\frac{\left(E - E_m\right)^2}{2 \cdot \sigma^2}\right\} dE \tag{2.13}$$

Later, Raman et al. (1981) applied the distributed activation energy model to feedlot biomass to determine the effects TGA parameters had on the activation energy and standard deviation. They concluded that thermogravimetric parameters such as heating rate, size fraction, and purge gas flow rate had no effect on E_m, but σ was affected by the heating rate and purge gas flow rate.

More recent work in this area has been to make improvements to the distributed activation energy model to make the equation easier to solve and/or to better approximate results. One alteration of the DAEM was proposed by Donskoi and McElwain (1998); they related the activation energy and pre-exponential factor directly to the heating rate. Their model was applicable to models with a large number of heating rates, and it significantly cut down on the time for calculation without an appreciable change in the accuracy of the calculation. Another approach taken by Donskoi and McElwain (2000) was to use a modified Gauss-Hermite Quadrature method to evaluate the double integration in equation in order to lower the error of integration as well as reduce the computation time. Other attempts to reduce computation time were proposed by Please et al. (2003) in which asymptotic expansions was used to rapidly arrive at a solution. Two assumptions of the DEAM are that the distribution, *f(E)*, is Gaussian and the k_o term in equation (2.3) is constant. The assumption for a constant k_o is valid for small values of σ, but not for wider activation energy ranges.

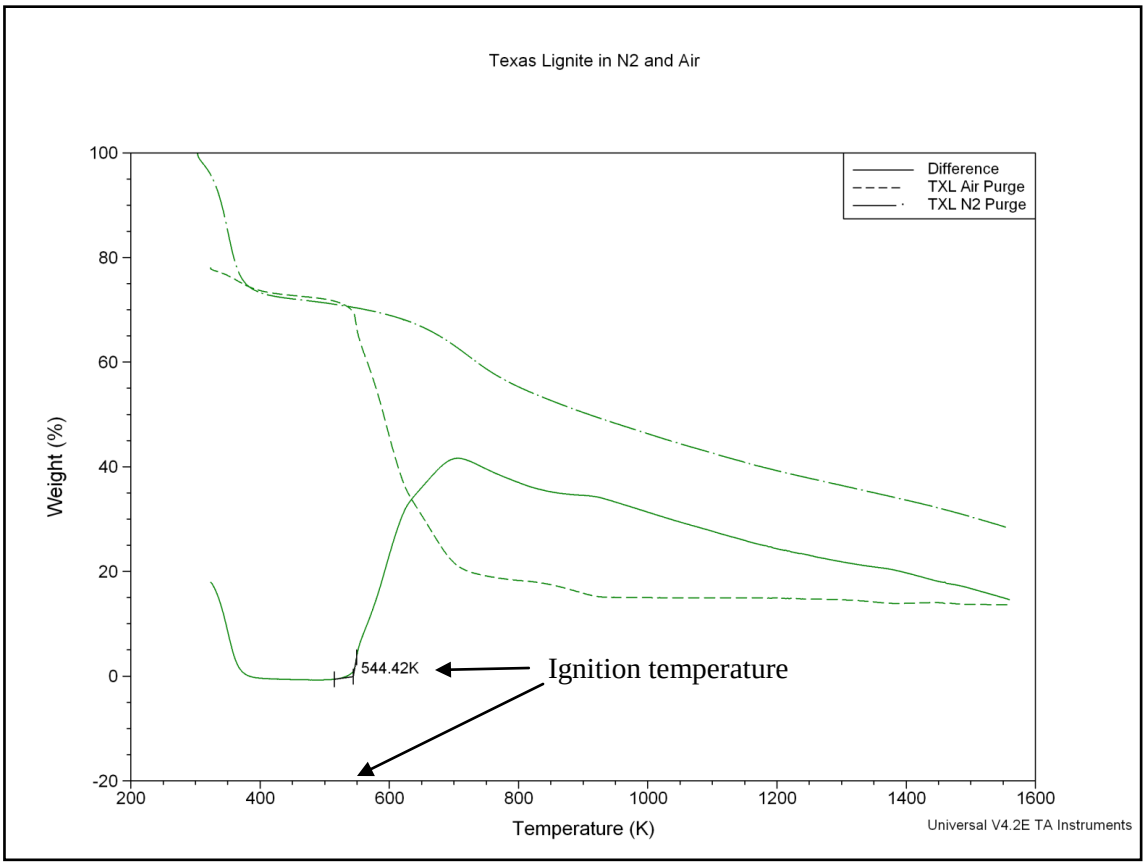

Figure 2.5.5: Example of ignition of TXL coal. Ignition is the point where the difference curve begins to deviate from 0%.

Table 2.5.1. Test Parameters.

Test Parameters		
Initial Temp	~300	(K)
Final Temp	1373	(K)
Heating Rate	40	(K/min)
Gas Flow Rate	50	(ml/min)
Sample Size	8-10	(mg)

Table 2.5.2: TGA Analysis of Fuels.

Fuel	TXL	WYO	HA-PC-DB-SoilS	LA-PCDB-SepS
Moisture Loss Onset Temperature (K)	373.09	375.71	367.45	386.19
Moisture Mass (%)	24.12	20.92	4.678	8.89
Pyrolysis Loss Onset Temperature (K)	637.93	657.15	529.23	513.6
Pyrolysis Mass (%)	18.95	21.01	32.53	56.01
10% of Pyrolysis Mass (%)	1.895	2.101	3.253	5.601
Mass at 10% of Pyrolysis Mass (%)	73.985	76.979	92.069	85.509
10% Pyrolysis Mass Loss Temperature (K)	661.11	685.44	552.99	536.27
90% of Pyrolysis Mass (%)	17.055	18.909	29.277	50.409
Mass at 90% of Pyrolysis Mass (%)	58.825	60.171	66.045	40.701
90% Pyrolysis Mass Loss Temperature (K)	748.78	759.83	1021.28	766.89
Peak Pyrolysis Mass (%)	61.9	66.21	45.06	81.74
Peak Pyrolysis Temperature (K)	698.68	702.5	697.55	749.21
FC and Ash Mass (%)	56.93	58.07	62.792	35.1
FC and Ash Loss Onset (K)	774.07	786.56	1037.1	990.95
Ignition Temperature (K)	544.42	571.78	509.43	526.06

Two of the biomass fuels were chosen to show the differences between the three samples of each fuel tested. LA-PC-FB is plotted in Figure 2.5.6 and high ash raw manure is plotted in Figure 2.5.7. For the LA-PC-FB sample, the largest differences are the moisture content, while for the HA-RM-FB sample variations can be seen in the carbon, oxygen, ash, and moisture contents. However, these variations are all less than 10% of the average value.

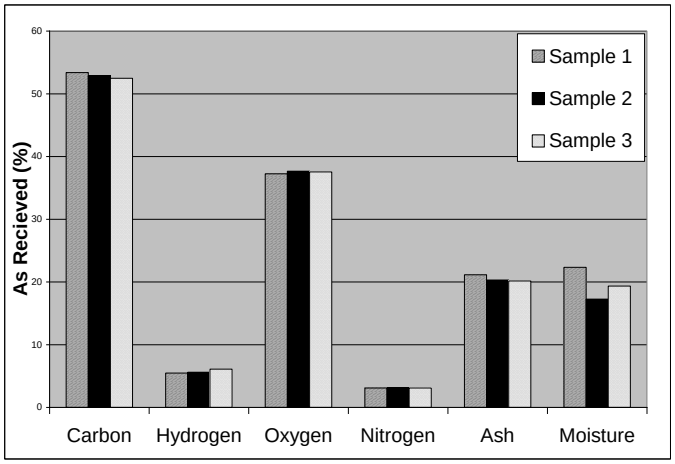

Figure 2.5.6: Ultimate Analysis of LA-PC-FB.

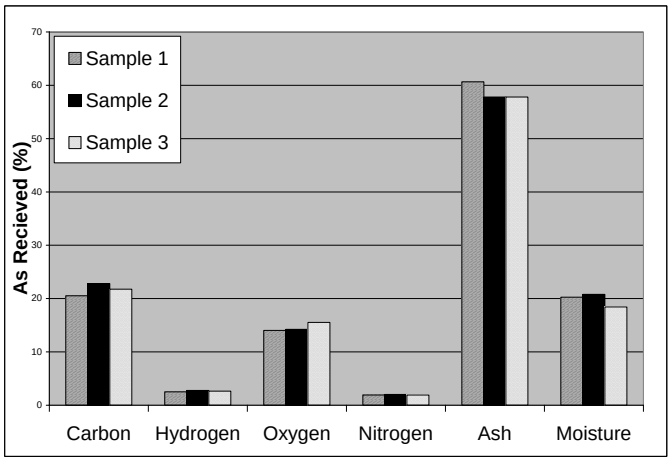

Figure 2.5.7: Variation of Fuel Properties for HA-RM-FB.

A summary of the as received results for the fuels is given in

Table 2.5.3. The moisture content of the four biomass fuels is very consistent with an average value of 19.2 %. There is also little variation between the RM samples and the partially composted samples, with the exception of the ash content of the two high ash fuels. The largest difference between the high ash and low ash samples is obviously the ash content. The low ash biomass had an average ash content of 16.3 %, while the ash content of the high ash biomass averaged 50.5 %. The high ash content presents a major concern for utility application because it could quickly be deposited on heat transfer surfaces inside a utility boiler, reducing the heat transfer rates from gases to water/steam. Texas lignite coal is also listed in the table, but the as received properties of the coal vary greatly from the biomass fuels.

Table 2.5.3: Ultimate and Proximate Analyses (As Received), Average of 3 Samples.

Ultimate and Proximate Analysis					
As Received (%)					
Fuel	HAPC	LAPC	HARM	LARM	TXL
Proximate:					
Moisture	17.00	19.64	19.81	20.27	38.34
Ash	53.85	16.50	47.10	16.10	11.46
Volatile	25.79	52.33	27.08	51.47	24.79
FC	3.36	11.54	6.02	12.16	25.41
Ultimate:					
Moisture	17.00	19.64	19.81	20.27	38.34
Carbon	14.92	33.79	17.39	34.35	37.18
Hydrogen	1.39	3.65	2.10	4.17	2.12
Nitrogen	1.13	1.97	1.56	2.48	0.68
Sulfer	0.31	0.51	0.34	0.53	0.61
Oxygen	11.40	23.94	11.70	22.10	9.61
Ash	53.85	16.50	47.10	16.10	11.46

To show how similar the biomass samples are and to give a better comparison to coal, the ultimate and proximate analyses are also given on a DAF basis, Table 2.5.4. As seen in the table, the primary combustion components of the biomass fuels are volatile compounds, > 80%. HA-PC-FB is the only inconsistency on a DAF basis, about 8% higher VM content compared to

the other biomasses. There is a large difference between the biomass samples and the coal sample in both VM and FC content. The FC content of TXL coal is just higher than 50%, indicating it will have a much higher HHV than the biomass samples, but the FC (char) burns slowly 200 ms to burn a 100 micron char particle. Another notable difference between the biomass fuels and coal is the oxygen content. The oxygen content of the biomass fuels is ~ 35 – 40% while the oxygen content of TXL coal is only 20 %. The oxygen content of biomass reduces the HHV due to the presence of oxygenated compounds such as CO, CO_2, and alcohols, etc.

Table 2.5.4: Ultimate and Proximate Analyses (DAF), Average of 3 Samples

Ultimate and Proximate Analysis					
Dry Ash Free (%)					
Fuel	HAPC	LAPC	HARM	LARM	TXL
Proximate:					
Moisture	0.00	0.00	0.00	0.00	0.00
Ash	0.00	0.00	0.00	0.00	0.00
Volatile	88.47	81.94	81.82	80.89	49.38
FC	11.53	18.06	18.18	19.11	50.62
Ultimate:					
Moisture	0.00	0.00	0.00	0.00	0.00
Carbon	51.19	52.91	52.56	53.99	74.06
Hydrogen	4.77	5.72	6.36	6.55	4.22
Nitrogen	3.87	3.08	4.70	3.90	1.35
Sulfer	1.08	0.79	1.03	0.84	1.22
Oxygen	39.10	37.49	35.35	34.73	19.14
Ash	0.00	0.00	0.00	0.00	0.00

Using the HHV as well as the ultimate and proximate analyses, several combustion properties were calculated (empirical formula, molecular weight of empirical formula, air/fuel ratio, and adiabatic flame temperature), see Table 2.5.5. The HHVs are given on an As Received, Dry, Dry Ash Free, and Volatile Matter basis. On an As Received basis, the low ash biomass fuels have comparable heating values to the Texas lignite coal, while the high ash fuels have a much lower heating value. Also, the raw manure samples have a higher heating value than the partially composted samples; this is consistent with the findings of Sweeten et al (1990). Once the moisture is factored out, the similarities between the low ash biomass and TXL coal disappear, with the coal having a much higher heating value. On a dry ash free basis, the high and low ash biomass fuels again show similarities with heating values between 18 and 20 MJ/kg.

Table 2.5.5: Combustion Properties of Test Fuels, Average of 3 Samples.

Combustion Properties					
Fuel:	HAPC	LAPC	HARM	LARM	TXL
HHV (kJ/kg):					
As Received	5208	13268	6305	13409	14290
Dry	6274	16510	7863	16818	23176
Dry Ash Free	17867	20775	19052	21074	28467
Volatile Matter	15948	18168	16041	18351	24229
Emperical Values:					
Formula					
Carbon	1.00	1.00	1.00	1.00	1.00
Hydrogen	1.11	1.29	1.44	1.44	0.68
Nitrogen	0.06	0.05	0.08	0.06	0.02
Sulfer	0.01	0.01	0.01	0.01	0.01
Oxygen	0.57	0.53	0.50	0.48	0.19
Mol.Wt.	23.5	22.7	22.9	22.2	16.2
$A:F_{stoich.}$	5.87	6.45	6.72	6.97	9.17
Adiabatic Flame Temp. (K)	1202	1407	1165	1341	1378

Table 2.5.5 also gives empirical values for fuel formula, molecular weight, stoichiometric air/fuel ratio, and adiabatic flame temperature. The empirical formulas have been normalized for 1 carbon atom. The stoichiometric air/fuel ratio for coal is much higher than the biomass fuels due in large part to the amount of oxygen already in the biomass fuels. Adiabatic flame temperature is higher for the low ash fuels compared to the high ash fuels and for partially composted compared to the raw manure samples.

The results of the sieve analysis as well as the calculation of SMD are summarized in table 2.5. The results show similarities between the raw and partially composted biomass samples; however, there are large differences for SMD between the high and low ash samples. This is most likely due to the size of the ash particles. The ash is related to the surface of the feedlot, and in the high ash case, it is directly related to the soil in the area of the feedlot. The major soil component in the Amarillo area is Pullman clay loam which has an SMD of 3 microns. It should be noted that the kinetics and ignition results assume spherical geometries for the particles for calculation purposes; however, these particles could be fibrous or elongated. This would artificially increase the particles in the larger size classifications.

Table 2.5.6: Sieve Results and SMD for all Fuels, Average of 3 Samples.

Particle Size Distribution					
Mean Dia. (μm)	**HARM** (%)	**LARM** (%)	**HAPC** (%)	**LAPC** (%)	**TXL** (%)
1596	0.02	0.05	0.02	0.06	0.00
1015	0.03	0.06	0.05	0.11	0.00
570	2.73	10.81	2.40	7.79	5.23
225	8.96	24.50	7.92	27.25	35.38
113	17.16	22.55	15.42	22.98	35.02
60	21.00	15.35	20.03	15.36	11.62
22.5	50.09	26.68	54.15	26.44	12.75
SMD (μm)	36.12	56.54	34.37	56.51	80.88

Two single reaction model solutions were described for calculating the activation energy and pre-exponential factor, method A: rigorous solution, method B: slope approximation. The rigorous solution results are discussed first, followed by the slope approximation.

Method A: Rigorous Solution

Detailed results for the rigorous solution are discussed first by comparing all four biomass fuels at various blend ratios with Texas lignite coal, and second, the individual biomass fuels are analyzed for differences in activation energy based on particle size. Figure 2.5.8 gives the activation energy results for the biomass fuels for as received.

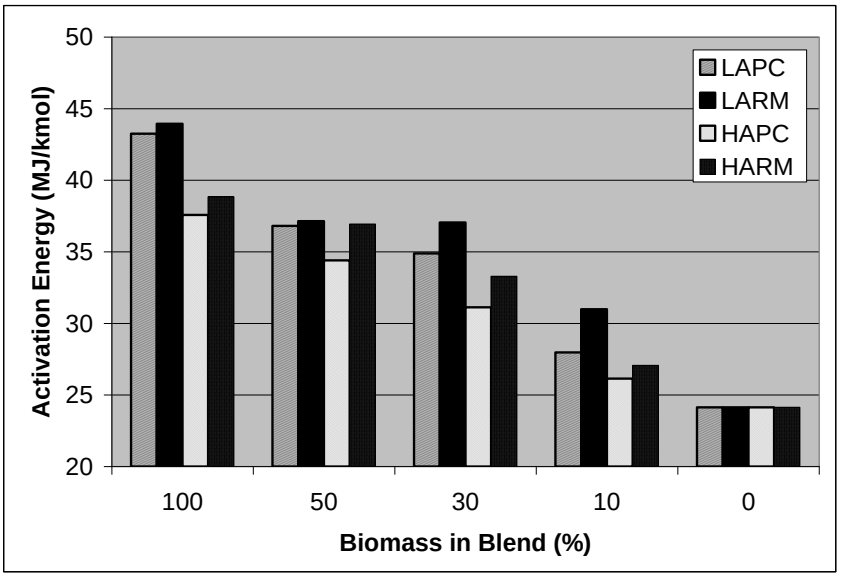

Figure 2.5.8 : Single Reaction Model Rigorous Solution Activation Energy for As Received Classification.

The results show that in general the activation energy decreases with increasing coal in the blend. As with the slope approximation, the raw manure samples tend to have higher activation energies than the partially composted samples. In addition, the high ash samples generally have lower or equivalent activation energy when compared to the low ash samples, indicating that the ash in the sample tends to lower the activation energy.

Figure 2.5.9 presents the rigorous solution activation energy grouped by particle size.

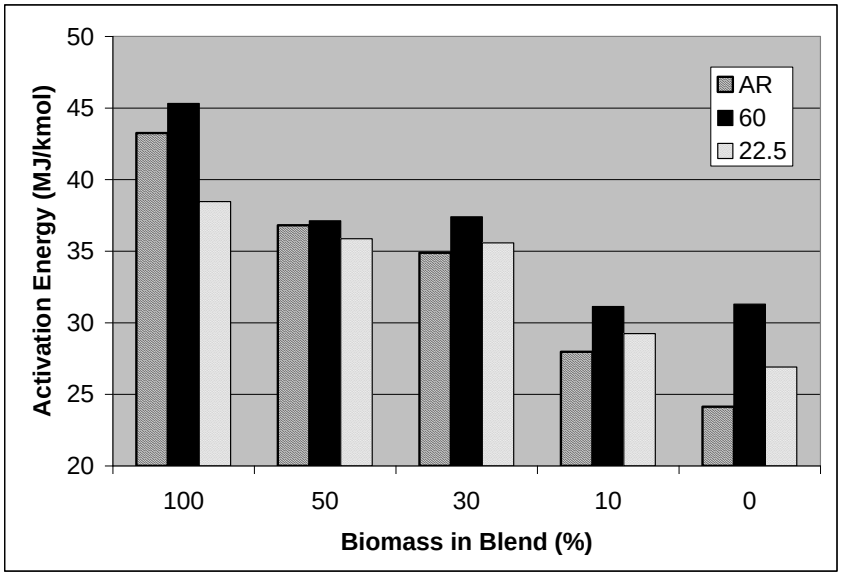

Figure 2.5.9: Single Reaction Model Rigorous Solution Activation Energy for LA-PC-FB, Effect of Particle Size

In all cases (pure biomass, pure coal, and blends) except the HA-RM-FB, the activation energies for the 60 micron particle size group are higher than the as received particle size group. This is most likely due to the fixed carbon content of the samples. The HA-RM-FB sample also had a lower dry ash free fixed carbon content compared to the other three biomass fuels. The activation energy for the 22.5 micron particle group is generally lower than the other two size classes for all four fuels. Also, the ash content of this size class is higher than the others as a result sieving as discussed earlier. This supports the case that higher ash content tends to lower the activation energy of the fuel.

The frequency factor was also calculated for each of the samples tested; however, the values were not consistent with the state theory assumption of 1.67E+13 s^{-1}. In most cases the frequency factor was below 500 s^{-1} with a maximum value of 2800 s^{-1}.

Method B: Slope Approximation

As mentioned earlier, the slope approximation is only valid for test results where the expression E/R_uT is between 20 and 60. None of the samples tested fell into the valid range for this expression; however, the results for pure samples of each fuel are presented in Figure 2.5.10 for brief discussion. The results indicate that the activation energy for low ash biomass is higher than that of high ash biomass for both raw and partially composted samples. Also, the raw manure samples have slightly higher activation energies than the partially composted samples. It is noted that a uniform particle temperature assumption has been used. The size effect on pyrolysis values comes through the temperature gradient within the particle; however, the particle sizes here are extremely small. In addition, the heating rates are low; thus, the size effect may not be responsible for different activation energies. The results also show the activation energy for Texas lignite coal to be lower than all four types of biomass, a result that is counter to results observed in the literature review. Again, the significance of these results is questionable since the validation for using the slope approximation failed. It should be noted that the two constants in the slope approximation formula, E and k_o, can be adjusted to better fit the data; however, once adjusted the valid range for the formula would be unknown.

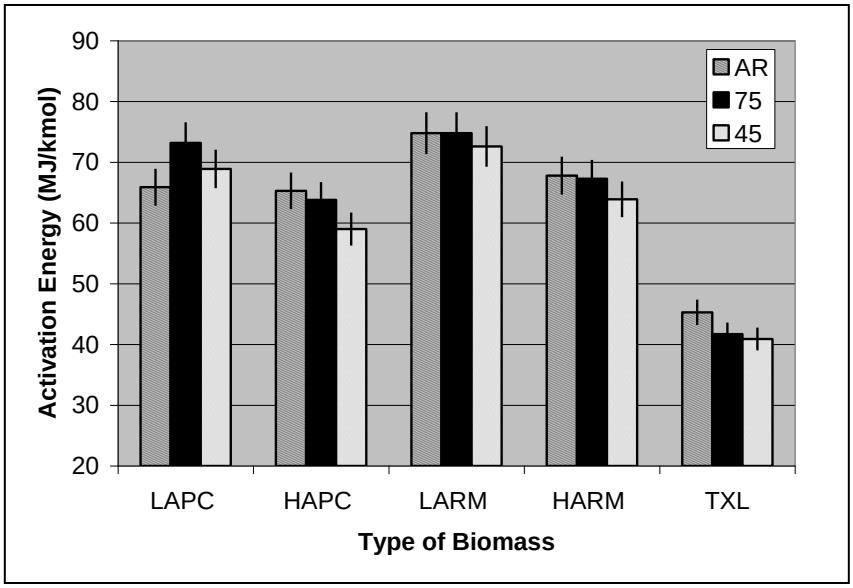

Figure 2.5.10: Activation Energy Results Obtained Using the Slope Approximation.

Method C: Distributed Activation Energy Model

The results for the DAEM are discussed first by comparing all four fuels at various blend ratios with TXL. Figure 2.5.11 presents the activation energies of the AR fuels. Figure 2.5.12 presents the standard deviations of the AR biomass fuels. Figure 2.5.13 presents the activation energies of the 60 micron class biomass fuels. Figure 2.5.14 presents the standard deviations of the 60 micron class biomass fuels. Figure 2.5.15 presents the activation energies of the 22.5 micron class biomass fuels. Figure 2.5.16 presents the standard deviations of the 22.5 micron class biomass fuels.

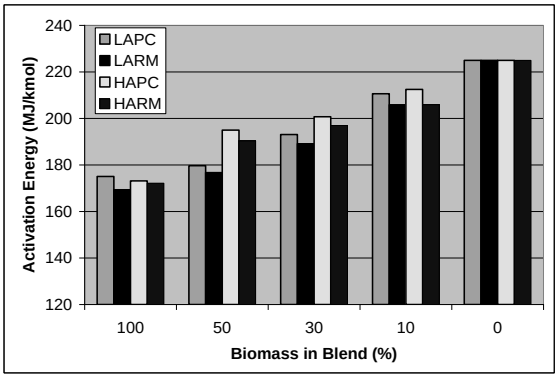

Figure 2.5.11: DAEM Activation Energy of AR Biomass Fuels.

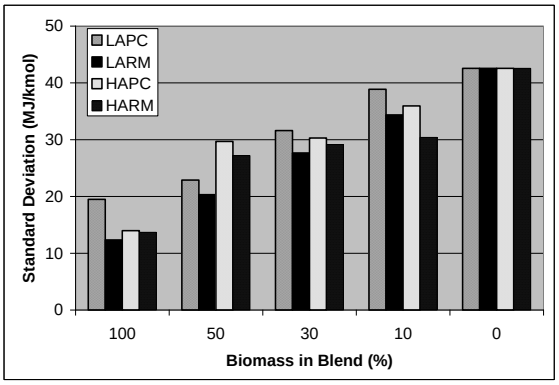

Figure 2.5.12: DAEM Standard Deviation of AR Biomass Fuels.

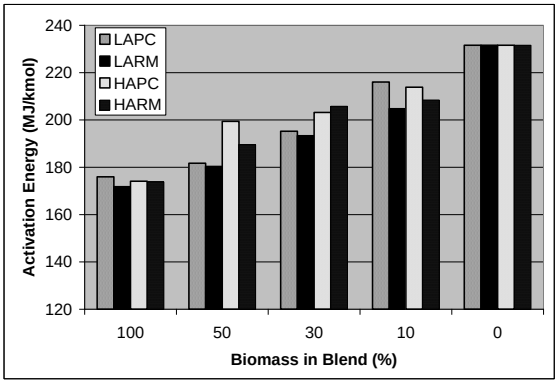

Figure 2.5.13: DAEM Activation Energy of 60 Micron Class Biomass Fuels.

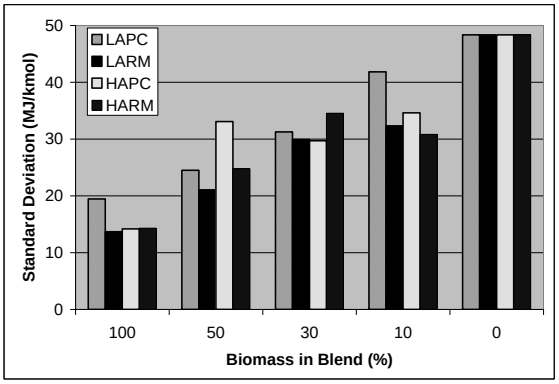

Figure 2.5.14: DAEM Standard Deviation of 60 Micron Class Biomass Fuels.

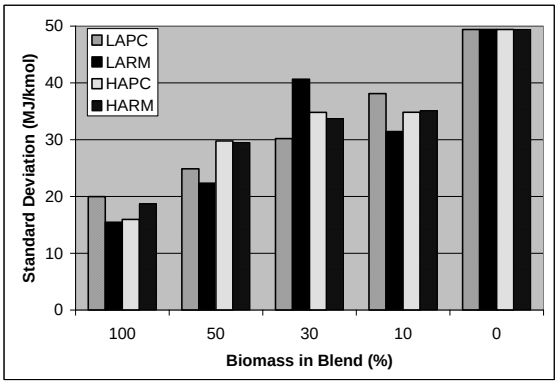

Figure 2.5.15: DAEM Activation Energies of 22.5 Micron Class Biomass Fuels.

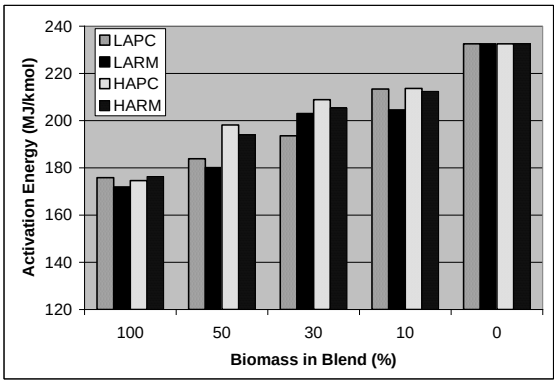

Figure 2.5.16: DAEM Standard Deviations of 22.5 Micron Class Biomass Fuels.

The average activation energies were 174 (kJ/mol) for feedlot biomass and 230 (kJ/mol) for Texas lignite coal. These values are very consistent with results from literature. In all cases, the activation energy increases as the amount of coal in the blend increases. However, the relationship between activation energy and blend ratio is nonlinear as seen in Figure 2.5.17; a linear relationship would indicate a direct relation to mass.

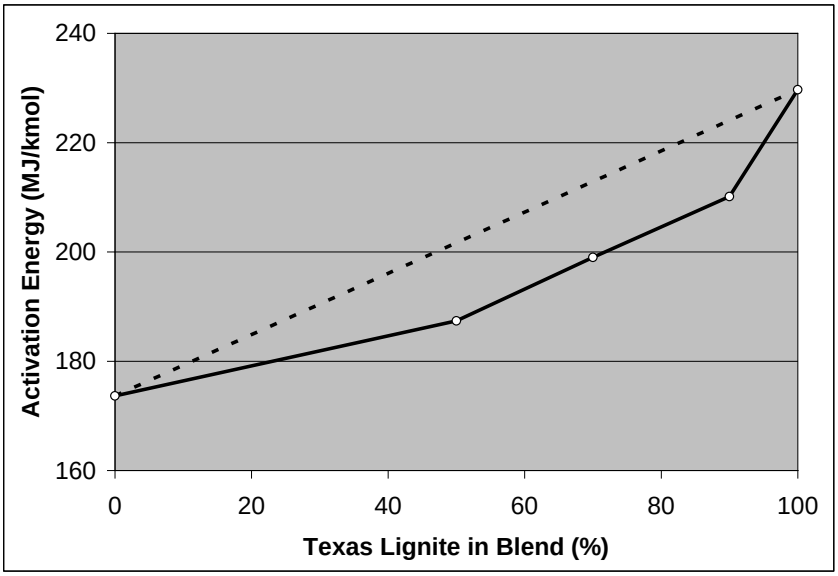

Figure 2.5.17: Average Activation Energy of Biomass Fuels for DAEM as a Function of TXL Coal Percentage in Blend.

The relationship between blend ratio and activation energy can be modeled by the following series of equations:

$$\frac{dm_v}{dt} = -\left[k_c \cdot \exp\left(-\frac{E_c}{\overline{R}T} \right) \cdot m_{v,c} + k_b \cdot \exp\left(-\frac{E_b}{\overline{R}T} \right) \cdot m_{v,b} \right] \quad \text{(a)}$$

Where the subscripts "*c*" and "*b*" designate coal and biomass respectively

$$m_{v,c} = m \cdot Y_{c,blend}(VM_c)$$
$$m_{v,b} = m \cdot Y_{b,blend}(VM_b) \quad \text{(b)}$$

$$\frac{dm_v}{dt} = -m \cdot \left[k_c \cdot \exp\left(-\frac{E_c}{\overline{R}T} \right) \cdot Y_{c,blend}(VM_c) + k_b \cdot \exp\left(-\frac{E_b}{\overline{R}T} \right) \cdot Y_{b,blend}(VM_b) \right] \quad \text{(c)}$$

Since E_c, E_b, $(VM)_c$, and $(VM)_b$ are different, one would not expect a linear relation.

The activation energies for the high ash biomass fuels tend to be higher in almost all cases. The only exceptions are the pure samples of partially composted biomass. Also, in general the partially composted samples have higher activation energies than the raw manure samples.

The trends for the standard deviations are similar to those found in the activation energies. As the amount of Texas lignite coal in the blend increases, the standard deviation also increases. The standard deviation is also higher for the partially composted samples compared to the raw manure samples; however, the standard deviation data is a bit more scattered and more exceptions are present. There is no discernible overall trend relating the high and low ash samples. In all the 50-50 blends, the high ash samples have a higher standard deviation, while in the 90-10 blends the low ash samples have a higher standard deviation. All of the results obtained thus far for the distributed activation energy model are in direct contrast to the results of the single reaction model. This will be discussed in greater detail later in the section.

Next, the fuels are individually compared based on particle size; Figure 2.5.18 presents the activation energies for LA-PC-FB. Figure 2.5.19 presents the standard deviations for LA-PC-

FB. Figure 2.5.20 presents the activation energies for HA-PC-FB. Figure 2.5.21 presents the standard deviations for HA-PC-FB.

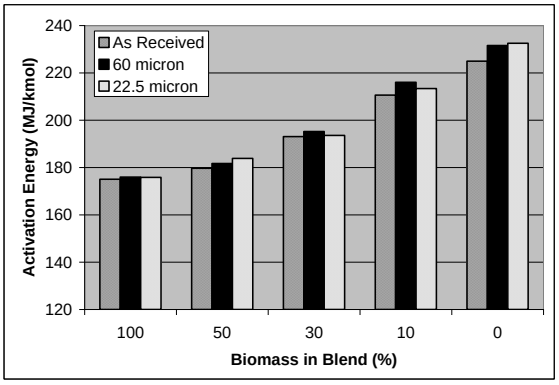

Figure 2.5.18: DAEM Activation Energy of LA-PC-FB

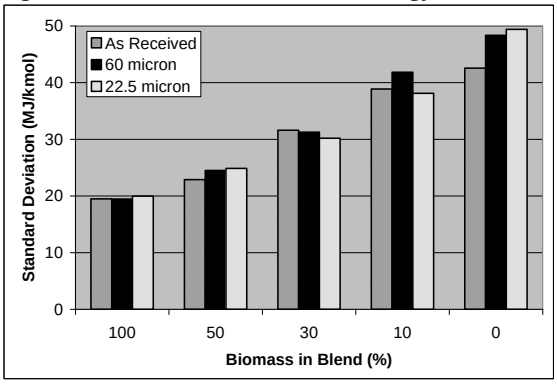

Figure 2.5.19: DAEM Standard Deviation for LA-PC-FB.

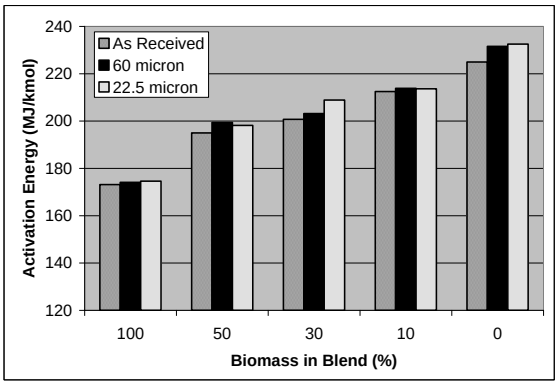

Figure 2.5.20: DAEM Activation Energies for HA-PC-FB.

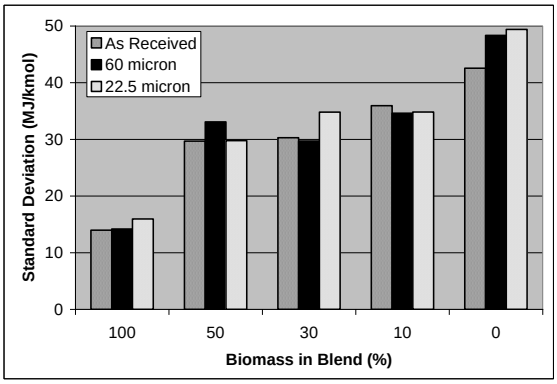

Figure 2.5.21: DAEM Standard Deviations for HA-PC-FB.

For the pure biomass samples, there is very little change in activation energy with respect to changes in particle size, with the 22.5 micron classification having only slightly higher activation energies. The three blended cases show that the activation energy increases as the particle size decreases. As mentioned in previous chapters it is likely that the percentage of ash in the smaller particle size classes is higher than for the as received samples since the ash particles are very small, indicating the activation energy is higher for samples with higher ash content. This result is supported by the results that showed the high ash biomass samples to have higher activation energy than the low ash samples unless catalytic effects are present. Higher ash can slow the flow of volatiles thereby increasing the "apparent" activation energy. Again, these trends are opposite the trends observed in the single reaction model results. Out of the 13 different comparisons of standard deviation change with respect to particle size, 6 show an increase in standard deviation for the 60 micron size class over the as received class, 4 show relatively little change, and 3 show a decrease. However, 10 of the 22.5 micron samples show an increase in standard deviation compared to the as received size class; this may be due to large ash content variation.

Since the results of the distributed activation energy model and the single reaction model tend to be in direct contrast, some discussion is warranted. Both calculations use an iterative process to arrive at the solution. The solution is determined by minimizing the squared error between the measured and theoretical thermograms. The average values for the squared error are as follows: SRM 0.90, DAEM 0.37. Table 2.5.7, and Table 2.5.8 give the average squared errors for the single reaction model rigorous solution grouped by fuel ratio and particle size respectively. The same information is given for the distributed activation energy model in Table 2.5.9 and Table 2.5.10. The SRM data shows that the high ash calculations more closely followed the data than did the low ash samples. The error also decreases with increased coal in the blend. Smaller particle sizes showed decreased error as well. The trends are not as apparent in the DAEM error results. The high ash samples did have lower errors, but the differences are not as large as those for the SRM. This implies that the DAEM model is much more applicable for different types of fuels. Also, the DAEM model uses a fixed value for frequency factor of 1.67E+13 s^{-1} obtained from the literature; whereas, the SRM allows this value to vary. However, the frequency factors obtained using the SRM were not consistent with the theoretical value. Finally, modeling results from the overall research project at Texas A&M University show that the activation energies obtained using the DAEM are more applicable.

Table 2.5.7: Average Summed Error for the Single Reaction Model Grouped by Fuel Ratio.

Biomass in Blend	LAPC	HAPC	LARM	HARM
100	5.638	0.572	6.559	0.966
50	1.439	0.037	1.722	0.124
30	0.257	0.007	0.439	0.019
10	0.011	0.014	0.039	0.010
0	0.047	0.047	0.047	0.047

Table 2.5.8: Average Summed Error for the Single Reaction Model Grouped by Particle Size.

Particle Size	LAPC	HAPC	LARM	HARM
AR	1.824	0.174	2.144	0.330
60	1.467	0.170	1.570	0.216
22.5	1.144	0.063	1.569	0.153

Table 2.5.9: Average Summed Error for the Distributed Activation Energy Model Grouped by Fuel Ratio.

Biomass in Blend	LAPC	HAPC	LARM	HARM
100	0.693	0.194	0.314	0.304
50	0.537	0.305	0.504	0.326
30	0.364	0.180	0.452	0.247
10	0.282	0.235	0.282	0.181
0	0.482	0.482	0.482	0.482

Table 2.5.10: Average Summed Error for the Distributed Activation Energy Model Grouped by Particle Size.

Particle Size	LAPC	HAPC	LARM	HARM
AR	0.465	0.272	0.373	0.283
60	0.525	0.323	0.413	0.314
22.5	0.426	0.243	0.434	0.327

Results and Discussion - Ignition

2.5.4. Ignition introduction

The ignition temperature results are grouped similarly to the activation energy results, discussing the effect of different types of biomass first followed by a discussion of particle size effects.

2.5.5. Effect of Fuel

Figure 2.5.22, Figure 2.5.23, and Figure 2.5.24 compare the ignition temperature results of the different types of biomass. The results indicate that the presence of coal in the sample has the greatest effect on the ignition temperature compared to other variables. The average ignition temperature of all samples with coal was 577 K (high: 611 K, low: 555 K, σ: 2.6%). While the samples without coal had an average ignition temperature of 744K (high: 790 K, low: 727 K, σ: 2.2%). In several of the blended samples the high ash samples had a higher ignition temperature than the low ash samples. This trend is not observed in the pure biomass samples. For the as received and 60 micron particle size groupings, the high ash partially composted sample had the

higher ignition temperature, while in those same classes the low ash raw manure had the higher ignition temperature.

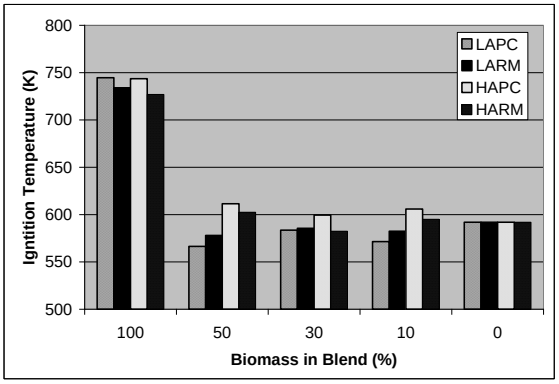

Figure 2.5.22: Ignition Temperature for the As Received Particle Class.

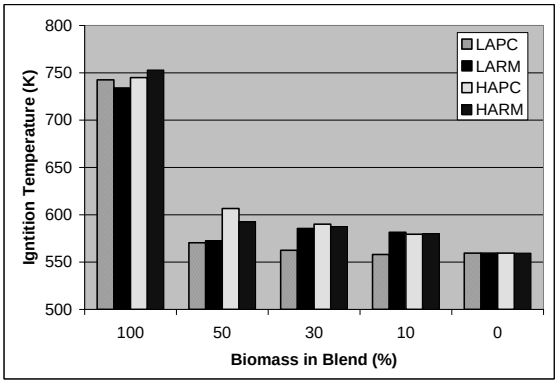

Figure 2.5.23: Ignition Temperatures for the 60 Micron Particle Class.

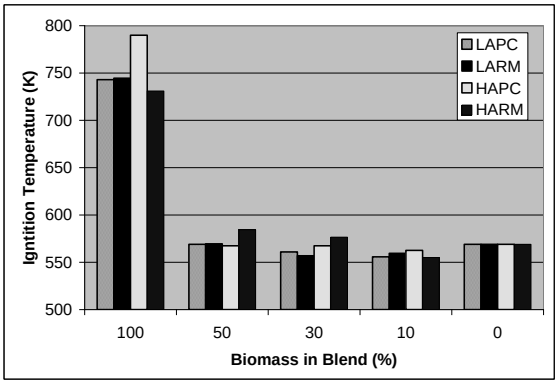

Figure 2.5.24: Ignition Temperatures for the 22.5 Micron Particle Class.

2.5.6. Effect of Particle Size

The effect of particle size on ignition temperature can be seen in Figure 2.5.25, Figure 2.5.26, Figure 2.5.27, and Figure 2.5.28. For the low ash samples the ignition temperature of the as received particle size group is noticeably higher than the other two classifications at blend percentages less than 30%. This result is also seen in the pure Texas lignite sample. For the high

ash samples, the as received particle size group has a higher ignition temperature for all but one of the blended samples. There is no distinguishable effect of particle size on pure biomass ignition temperature.

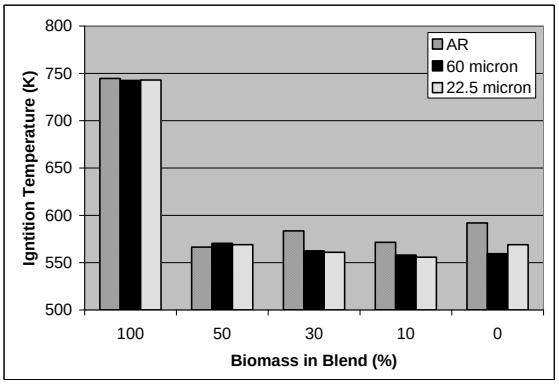

Figure 2.5.25: Ignition Temperatures for LA-PC-FB.

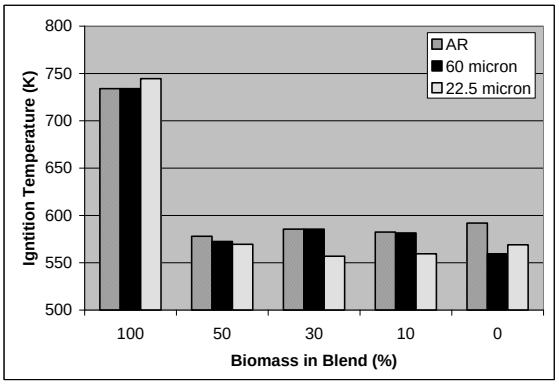

Figure 2.5.26: Ignition Temperatures for LA-RM-FB.

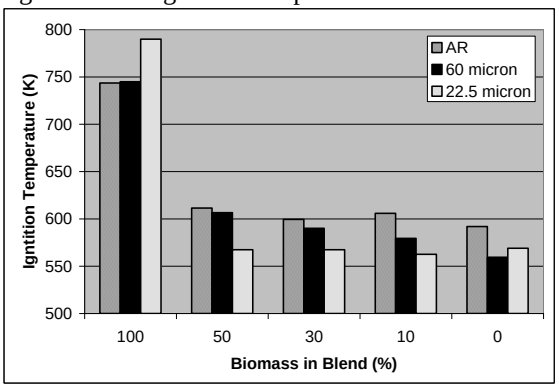

Figure 2.5.27: Ignition Temperatures for HA-PC-FB.

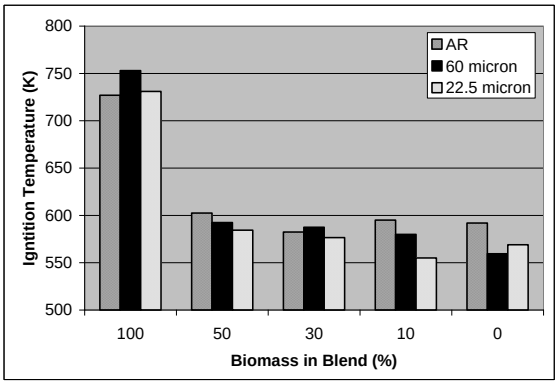

Figure 2.5.28: Ignition Temperatures for HA-RM-FB.

2.6. Summary and Conclusions

A majority of proposed task except for the composition of volatiles released during the pyrolysis of coal, FB and DB was performed. There were problems faced with FTIR operation and hence the instrument could not be fixed before the contract deadline. Instead of FTIR, we added the new sub-task investigating the effects of biomass % in the blend on ignition and developed several new methods for determining the kinetics of pyrolysis (See journal articles submitted on pyrolysis [Wei Chen et al, 2011]). Several conclusions can be drawn from the results obtained for feedlot biomass.

1. All three single reaction models (slope approximation, rigorous solution, and maximum volatile rate) yield a lower value for activation energy for lignite, biomass, and blends compared to the distributed activation energy model.
2. The distributed activation energy model provides more applicable results than the single reaction model for the pyrolysis behavior of feedlot biomass and blends of feedlot biomass with coal. This statement is supported by the wide use of the distributed activation energy model to study the behavior of non-uniform solid fuel particles as observed in the literature and the comparability of these results to literary results.
3. The relative accuracy of the distributed activation energy model is better since the average error was smaller.
4. The increased ash content of the biomass tends to increase the activation energy required for combustion of biomass fuels. This is observed directly in the calculation of activation energy using the distributed activation energy model.
5. While initial observation suggests that particle size tends to increase activation energy, the increased activation energy is more likely a result of increased ash content in the smaller sample sizes. Performing ultimate and proximate analysis on the sieved samples could confirm this hypothesis.
6. The ignition temperature results indicate that biomass fuels ignite at higher temperatures than coal despite the fact that biomass pyrolysis has lower activation energy. It is theorized that the increased volatile content of biomass fuels carries away a portion of the heat required for biomass ignition thereby delaying the onset of ignition as outlined in the literature review.

2.7. Acronyms

β	TGA Heating Rate
μm	Micrometer or Micron
B	Pre-exponential Factor
^{o}C	Degree Celsius
C_2H_6	Ethane
CB	Cattle Biomass (either FB or DB)
CH_4	Methane
CO	Carbon Monoxide
CO_2	Carbon Dioxide
DAF	Dry Ash Free
DB	Dairy Biomass
DEAM	Distributed Activation Energy Model
DSC	Differential Scanning Calorimetry
DTA	Differential Thermal Analysis
E	Activation Energy
$E(X_n)$	Exponential Integral of the nth Order
FB	Feedlot Biomass
FC	Fixed Carbon
FTIR	Fourier Transform Infra Red
H_2	Hydrogen
HA-PC-DB-SoilSurf	High Ash Partially Composted Dairy Biomass Soil Surface
HA-PC-FB	High Ash Raw Manure Feedlot Biomass
HA-RM-FB	High Ash Raw Manure Feedlot Biomass
HR	Heating Rate
HHV	Higher Heating Value
K	Degree Kelvin
LA-PC-DB-SepSol	Low Ash Partially Composted Dairy Biomass Separated Solids
LA-PC-FB	Low Ash Partially Composted Feedlot Biomass
LA-RM-FB	Low Ash Raw Manure Feedlot Biomass
MVRR	Maximum Volatile Release Rate
min	Minute
mL	Milliliter
m_v	Volatile Mass
N_2	Nitrogen
PRB	Powder River Basin Coal (a sub bituminous coal)
RM	Raw Manure
R_u	Universal Gas Constant
SMD	Sauter Mean Diameter
SRM	Single Reaction Model
t	Time
T	Temperature
T_e	Empty Pan Thermocouple
T_s	Sample Pan Thermocouple
TC	Thermocouple
TGA	Thermogravimetric Analysis

2.8. Education and Training

This work was used to partially fulfill the masters degree requirements for Brandon Martin and Ben Lawrence

Ben Lawrence, Master of Science Mechanical Engineering, "Cofiring coal and dairy biomass in a 100,000 BTU/hr furnace, "Master Of Science, Mechanical Engineering, Texas A&M University, College Station, TX December 2007

Martin , Brandon Ray, " Pyrolysis and Ignitions Behavior of Coal, Cattle Biomass and Coal/Cattle Biomass Blends, "Master Of Science, Mechanical Engineering, Texas A&M University, College Station, TX, Dec 2006..

2.9. References

Annamalai, K. and Puri, I. *Combustion Science and Engineering*, CRC Press, Boca Raton, FL., 2005.

Annamalai, K., Ryan, W., Dhanapalan, S., "Interactive Processes in Gasification and Combustion – Part III: Coal/Char Particle Arrays, Streams, and Clouds," *Progress in Energy and Combustion Science*, 1995, vol. 20, pp. 487-618.

Anthony, D. B., Howard, H. C., Hottel, H. C., Meissner, H. P., "Rapid Devolitization of Pulverized Coal", *Fifteenth Symposium (International) on Combustion*, 1974, pp. 1303-1317.

D. Jinno, Ashwani K. Gupta1 and K. Yoshikawa, "Determination of Chemical Kinetic Parameters of Surrogate Solid Waste, "Journal of Engineering for Gas Turbines and Power, 2004, Vol. 126, pp 685-692

Raman, P., Walawander, W. P., Fan, L. T.; Howell, Jerald A. "Thermogravimetric Analysis of Biomass. Devolitization studies on Feedlot Manure," *Ind. Eng. Chem Des. Dev.*, 1981, vol. 20, pp. 630-640.

Tognotti, L., Malotti, A., Petarca, L., Zanelli, S., "Measurement of Ignition Temperature of Coal Particles Using a Thermogravimetric Technique," *Combustion Science and Technology*, 1985, vol. 44, pp.15-28.

2.10. Other support

None

2.11. Dissemination

Annamalai, K., Texas A&M and Puri,I K, VA Tech, and Jog Milind, Univ. of Cincinnati Advanced Thermodynamics Engineering, , , Edition 2 :1096 page and 14 Chapters book

containing approximately 200 examples, 415 figures, 465 exercise problems and 45 tables. Taylor and Francis, Boca Raton, Florida.ISBN: 978-1-4398-0572-5, 3/2011.

Annamalai, Kalyan and Puri, Ishwar, Combustion Science and Engineering, 18 Chapter book on "Combustion Science and Engineering," , pages: 1121, Taylor and Francis, Orlando, Florida; ISBN: 0849320712; Dec 2006

Brandon Martin, Ben Thien, Kalyan Annamalai and Bukur, Dragomir, " Pyrolysis and Group Ignition of Coal, Feedlot Biomass and Blends under TGA Conditions," CSS-CI ; May 21-23, 2006, Cleveland, OH

Wei Chen, Ben Lawrence, Kalyan Annamalai, R. James Ansley, and Mustafa Mirik, "Kinetics of Pyrolysis of Mesquite and Juniper Biomass Fuels Fuel from TGA Data," J of Biomass and Energy, Under Review (2011)

3. COFIRING

TASK A-3: Co-firing coal with DB

ABSTRACT

DB is evaluated as a possible co-firing fuel with coal. Cofiring of DB offers a technique of utilizing dairy manure for power/steam generation, reducing greenhouse gas concerns, and increasing financial returns to dairy operators. The effects of cofiring coal and DB have been studied in a 30 kW (100,000 BTU/hr) burner boiler facility. Experiments were performed with TXL as a base line fuel. The combustion efficiency from co-firing is also addressed in the present work.

Two forms of partially composted DB fuels were investigated: low ash separated solids and high ash soil surface. Two types of coal were investigated: TXL and WYO.

Proximate and ultimate analyses were performed on coal and DB. DB fuels have much higher nitrogen (kg/GJ) and ash content (kg/GJ) than coal. The HHV of TXL and WYO coal as received were 14,000 and 18,000 kJ/kg, while the HHV of the LA-PC-DB-SepS and the HA-PC-DB-SoilS were 13,000 and 4,000 kJ/kg. The HHV based on stoichiometric air were 3,000 kJ/kg for both coals and LA-PC-DB-SepS and 2,900 kJ/kg for HA-PC-DB-SoilS. The nitrogen and sulfur loading for TXL and WYO ranged from 0.15 to 0.48 kg/GJ and from 0.33 to 2.67 for the DB fuels.

The NO_x emissions for equivalence ratio (ϕ) varying from 0.9 to 1.2 ranged from 0.34 to 0.90 kg/GJ (0.79 to 0.16 lb/mmBTU) for pure TXL. They ranged from 0.35 to 0.7 kg/GJ (0.82 to 0.16 lb/mmBTU) for a 90:10 TXL:LA-PC-DB-SepS blend and from 0.32 to 0.5 kg/GJ (0.74 to 0.12 lb/mmBTU) for a 80:20 TXL:LA-PC-DB-SepS blend over the same range of ϕ. In a rich environment, DB:coal cofiring produced less NO_x and CO than pure coal. This result is probably due to the fuel bound nitrogen in DB is mostly in the form of urea which reduces NO_x to non-polluting gases such as nitrogen (N_2).

3.1. Introduction

The overall objective of the current research is to evaluate the combustion and emission behavior of coal:DB blends. The combustion behavior was evaluated by measuring product gas composition. The coal fuels included TXL and WYO. The DB fuels considered were LA-PC-DB-SepS and HA-PC-DB-SoilS. LA-PC-DB-SepS was collected from the flushed manure from the milking house of a dairy. The flushed manure was then passed through a mechanical separator to remove most fine solids including ash prior to air drying and grinding. This made LA-PC-DB-SepS low in ash. HA-PC-DB-SoilS was scraped from dairy farms that used soil as open pen surface and was high in entrained soil including ash. The DB was blended (on a mass basis) with the two types of coals and cofired in a 100,000 BTU/hr furnace. The gas compositions of products were used to characterize the combustion efficiency and emission behavior. TGA analysis was also performed on the pure fuels to determine pyrolysis behavior.

The HHV of TXL and WYO coal as received were 14,000 and 18,000 kJ/kg, while the HHV of the LA-PC-DB-SepS and the HA-PC-DB-SoilS were 13,000 and 4,000 kJ/kg. However, the HHV based on stoichiometric air were 3,000 kJ/kg for both coals and LA-PC-DB-SepS and 2,000 kJ/kg for HA-PC-DB-SoilS. All solid fuels should have approximately the same HHV based upon stoichiometric air. The Boie equation was used to approximate the HHV of the fuels based upon the ultimate analysis of each fuel. The Boie HHV was within 13% of the experimental HHV for the coals and LA-PC-DB-SepS. The nitrogen and sulfur loading from fuel input into the boiler for TXL and WYO ranged from 0.15 to 0.48 kg/GJ and from 0.33 to 2.67 for the DBs.

TXL began to pyrolize at 640K and the WYO began to pyrolize at 660K. The DBs began to pyrolize at lower temperatures, 530K for the HA-PC-DB-SoilS and 510K for the LA-PC-DB-SepS. This lower pyrolysis temperature delayed NO_x formation in rich combustion during cofiring experiments. The maximum rate of volatile release occurred at 700K for both coals and HA-PC-DB-SoilS and at 750K for LA-PC-DB-SepS.

The emissions of NO_x for ϕ varying from 0.9 to 1.2 ranged from 340 to 90 kg/GJ for pure TXL. They ranged from 350 to 70 kg/GJ for a 90:10 TXL:LA-PC-DB-SepS blend and from 320 to 50 kg/GJ for a 80:20 TXL:LA-PC-DB-SepS blend over the same range of ϕ.

3.2. Literature review

Intensive animal feeding operations (dairy and cattle farms) create large amounts of animal waste that must be safely disposed of in order to avoid environmental degradation. CAFOs, which include cattle feedlot and dairy operations, are a cornerstone of the agricultural economy in Texas and neighboring states in the Southern Great Plains. In feedlots, cattle are confined to relatively small pens of 10 to 40 m^2/hd (100 to 430 ft^2/hd) and fed a high calorie

grain diet in preparation for slaughter. Figure 3.2.1 shows a schematic of a 450 kg (1000 lb) cattle waste production process from excretion to collection (Tranchida, 2007).

Among dairy cattle, each animal, having a live weight between 1200 and 2000 lb, produces between 60 and 125 lb of wet manure per day per animal. This manure contains 85-90 % moisture and 10-15 % solids (including volatile matter, nutrients, ash

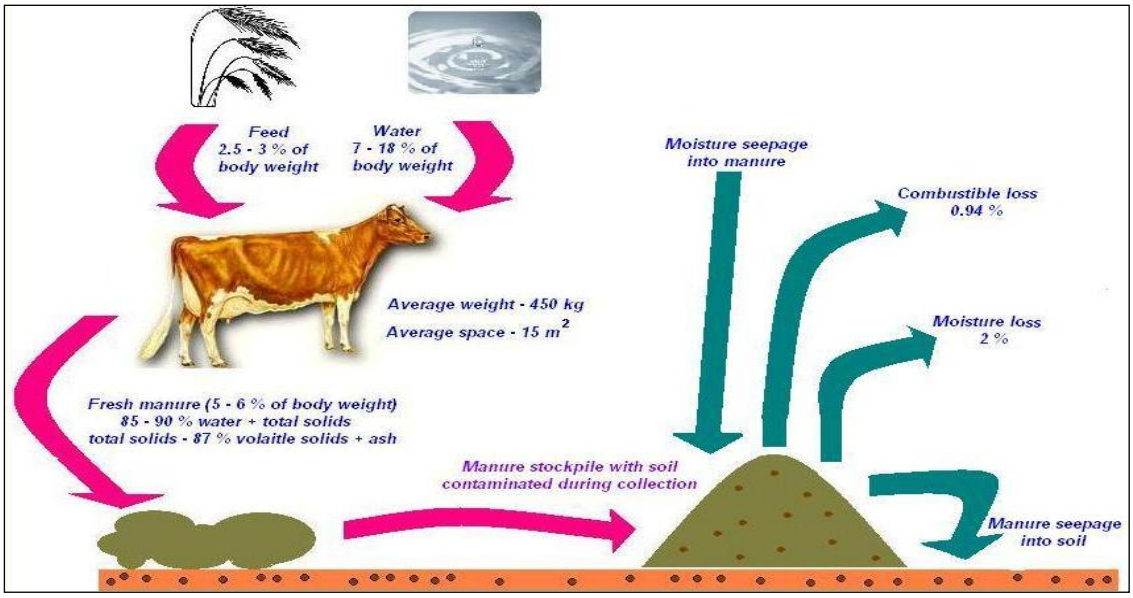

Figure 3.2.1. Schematic of a 450 kg (1000 lb) cattle waste production process from excretion to collection.

and combustibles) (Carlin et al., 2007). Manure collected from a feedlot is called FB, while manure collected from a dairy is called DB. The sum of FB and DB together is commonly called CB. Potentially harvestable CB from all of the CAFOs in the U. S. easily exceeds 100 million tons per year on a dry basis and 6-12 million dry tons in the Texas Panhandle alone.

Another example of CAFOs is chicken houses. In chicken houses, thousands of chickens are kept in close proximity. Biomass derived from chicken litter will be called little biomass. If FB, DB and LB are not beneficially utilized as fertilizer or properly disposed of, these by-products may become sources of air, water, or soil pollution in some areas of the U.S., including the Southern Great Plains.

When the CB gets very dry, the cattle's feet grind the dry manure, creating a dust problem. PM or dust from feedlot ranges from 8.5 to 12 microns (Sweeten, 1979). TSP in feedlot dust can range from 150 $\mu g/m^3$ to 400 $\mu g/m^3$ (Sweeten, 1979). The PM 10 regulation requires the concentration of particles less than 10 μm should be less than 150 $\mu g/m^3$.

FB, DB and LB could be used as a fuel by mixing it with coal and firing it in an existing coal suspension fired combustion systems. This technique is known as co-firing. The high temperatures produced by the coal will allow the biomass to be completely combusted. These biomass fuels are higher in ash, lower in heat content, higher in moisture, and higher in nitrogen and sulfur (which can cause air pollution) compared to coal. Previous work (Frazzitta et al.,

1999), (Arumugam et al., 2005), (Annamalai et al., 2006), (Annamalai et al., 2003a), (Sweeten et al., 2003) (Annamalai et al., 2003b) was concerned with cofiring FB with coal

With support from DOE-Golden, Colorado and TCEQ to develop new technologies for use of FB and DB as an alternative renewable fuel, a comprehensive inter-disciplinary research initiative is currently being undertaken.

DB fuel properties (chiefly ash content) depend greatly on the collection technique used when the manure is gathered from the dairy; this is due in large part to the surface of the dairy. Most dairies have a soil base with an interfacial layer which consists of mixed soil and manure. If the manure is not harvested carefully some of the interfacial layer will be disturbed or collected with the manure. This leads to higher ash content in the manure. Collection techniques vary between dairies but usually one of the following methods is used: wheel loader alone, chisel-plow followed by wheel loader, and box scraper (Sweeten, 1990).

When the milking herd is moved inside the concrete floored milking house, fresh manure is collected by flushing the milking house floor with water or scraping the manure. This manure does not contain soil. The flushing water is then passed through a mechanical separator to remove the volatile solids from the flushing liquids. This liquid can then be used as lagoon water. The removed volatile solids can be combusted. This technique was used to collect the LA-PC-DB-SepS (Stokes and Gamroth, 1999).

The United States dairy industry is currently in the middle of a paradigm shift. In general, the total number of dairies is decreasing, but the size of each individual dairy is increasing and dairies are moving west. The rate of size increase of individual dairies is outpacing the rate of decrease of total number of dairies. Thus, the total dairy production rate is increasing. Figure 3.2.2 summarizes how the number of small dairies is decreasing, while the number of large dairies is increasing. These trends are predicted to continue.

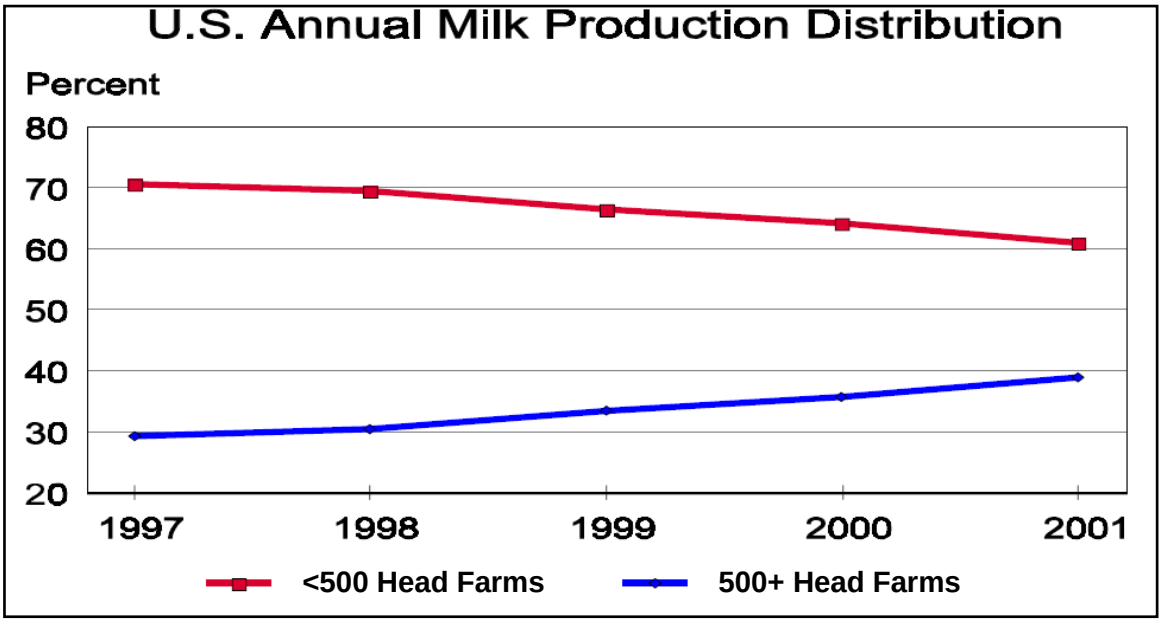

Figure 3.2.2. U.S. annual milk production distribution. Despite the decrease in the number of small dairies, total dairy production is increasing due to the number of large dairies increasing.

United States dairies are also becoming more efficient which means more milk is being produced per cow as demonstrated by Figure 3.2.3. The increased efficiency of dairy operation is due to increased research in the areas of animal diets and improved milking systems.

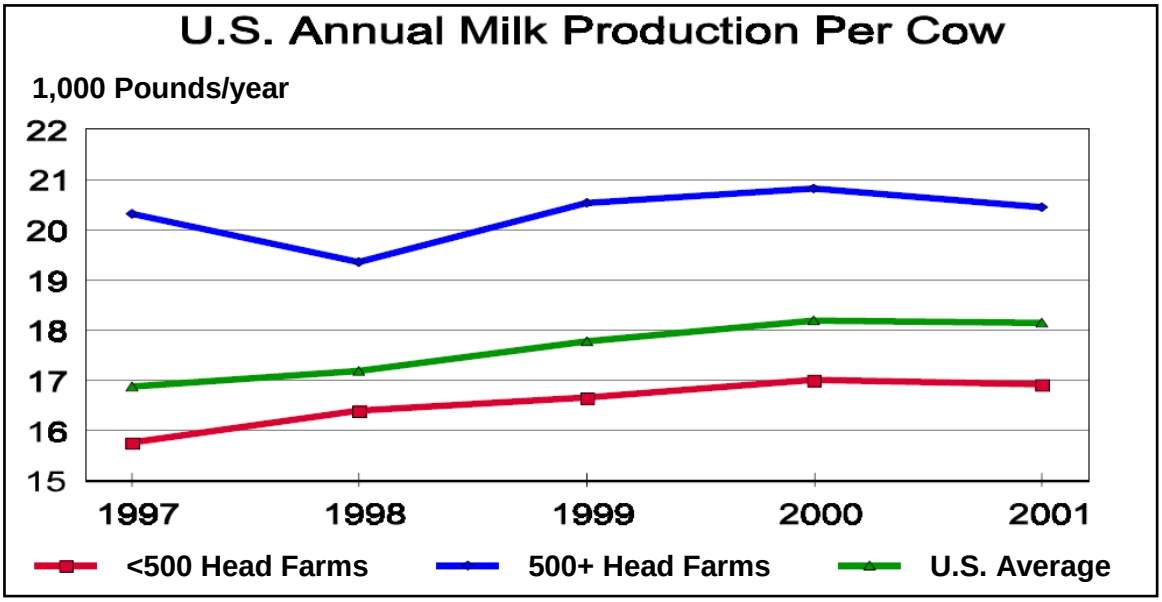

Figure 3.2.3. U.S. annual milk production per cow. Increased dairy efficiency leads to higher milk production per head of cow.

Figure 3.2.4, adapted from NASS (2002), illustrates the movement of dairies to the west. Note that the Midwest has seen a decline in the number of dairies, while the western states have seen a general increase in the number of dairies. Also note that the total milk production has increased in the western states. Note that the number of dairies in Iowa and the Dakotas has decreased, but the amount of milk produced in those states has either increased or stayed relatively unchanged. This further attests to how dairy production has become more efficient. Washington, Nevada, Oklahoma, and Montana also demonstrate this trend.

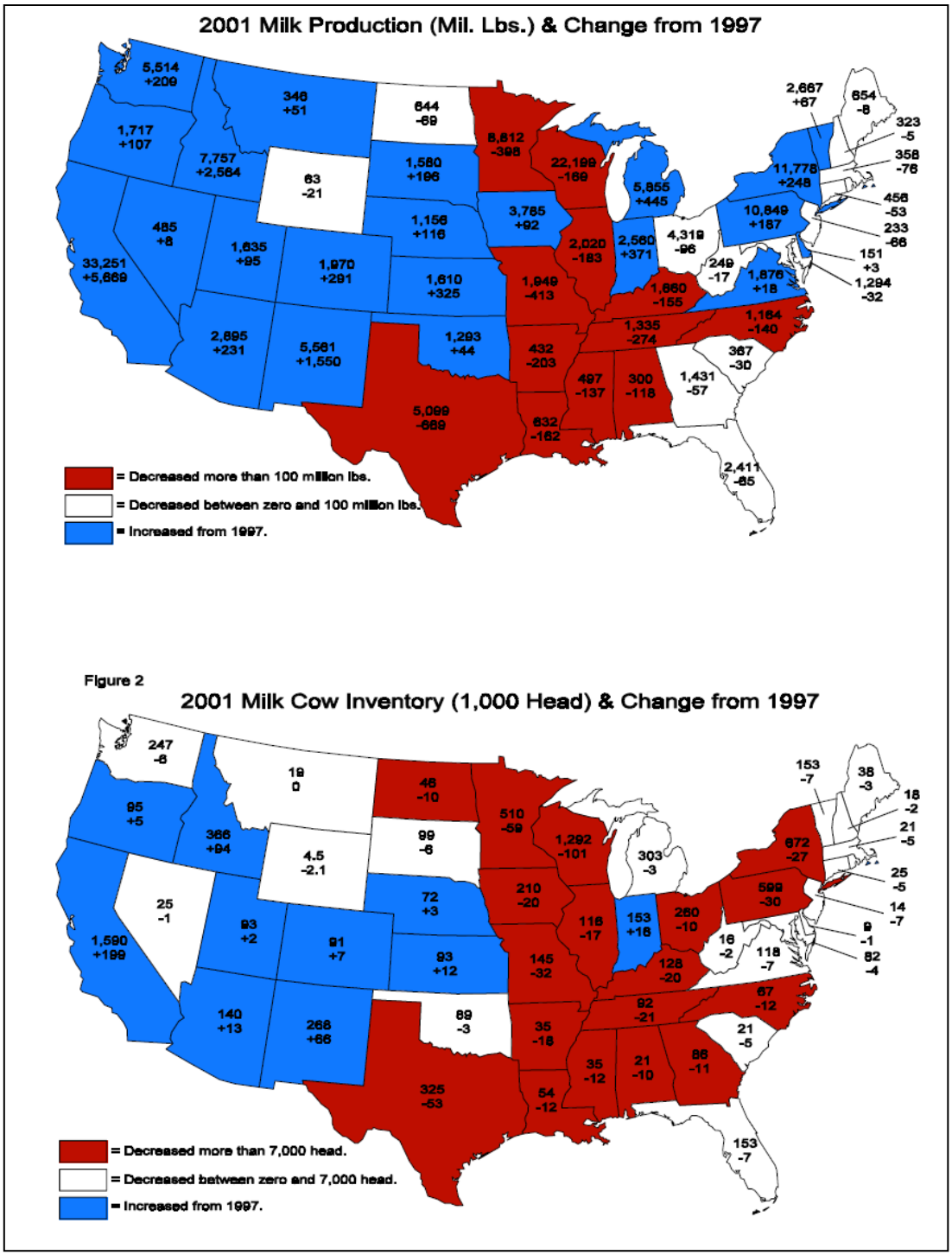

Figure 3.2.4. Western expansion of dairies.

Although this work is primarily concerned with biomass derived from dairy manure, this is not the sole source for biomass (Volk, et al., 2002). Biomass can also come from agricultural crop residues, energy plantations, and municipal and industrial wastes. Biomass is considered to be both a renewable fuel and a carbon neutral fuel. Although combustion of biomass does release carbon into the atmosphere, this carbon is in turn used by vegetation to create more biomass. Thus, the net carbon balance remains approximately level.

NO_x causes lung deterioration and affects blood hemoglobin which deprives the body of oxygen. NO_x also plays a role in altering ozone levels. NO_x is absorbed in the atmosphere to create acid rain. (Annamalai and Puri, 2007) CO is a poisonous gas which can be fatal to humans.

Lundgren (2002) studied using horse manure from ranches for onsite heat production. He found that the horse manure could be effectively disposed of by firing it in a small burner and the heat created could be used for onsite purposes. The primary drawback to this technique was the elevated NO_x emissions. Lundgren reported 370 mg/m^3 of NO_x at 10% excess O_2. He did not discuss any rich combustion results.

Miller et al. (2002) has cofired LB with coal. The primary focus of his research was rendering chicken fat into a useable fuel. However, he has provided detailed ash analyses for several different cofired fuels. His work suggests that DB has a higher energy content than FB and both CB have higher energy content than LB.

Table 3.2.1 summarizes the feed rates of coal and various forms of biomass Miller used in cofiring experiments in his 200 million BTU/hr furnace.

Table 3.2.1. Firing rates of fuels investigated by Miller.

Feedstock	Maximum Firing Rate (kg/hr AR)	Maximum Thermal Input (kW)
Coal	36744	46389
Sewage Sludge	1720	139
Swine Manure	1576	34.2
Dairy Manure	8378	3107
Beef Manure	650	277
Sheep Manure	168	85.1
Covered Barn Manure	741	149
Reed Canary Grass	377	108
Plastics	1.32	3.37
Wood Chips/Shavings	12566	8323

The full fuel properties and ash analysis of fuels used by Miller are presented in Table 3.2.2. Of particular note is that all of the biomass fuels are higher in moisture than the coal. On a DAF basis, the manure biomass and AB fuels are higher in VM than coal. This is typical of most AB fuels. All of the biomass fuels are lower in FC than the coal. The AB fuels have less nitrogen than the coal. Hence, the AB fuels being higher in volatiles and lower in nitrogen help contribute to NO_x mitigation when the AB fuels are cofired with coal.

Table 3.2.2. Proximate, ultimate, and ash analyses of fuels investigated by Miller.

	Cofire Coal	Pine Shavings	Reed Canary Grass	Sheep Manure	Dairy Free-Stall	Dairy Tie-Stall Manure	Misc. Manure	Poultry Litter
Moisture	5.0	45.0	65.2	47.8	70.3	69.8	50.5	20.0
Proximate analysis (wt.%, db)								
Volatile matter	24.16	84.7	76.1	65.2	30.6	30.1	21.8	55.3
Ash	14.70	0.1	4.1	20.9	62.3	62.5	73.5	17.0
Fixed carbon	61.14	15.2	19.8	14.0	7.1	7.4	4.8	7.7
Ultimate analysis (wt. %, db)								
Carbon	72.75	49.1	45.8	40.6	22.1	22.6	19.6	38.1
Hydrogen	3.91	6.4	6.1	5.1	2.9	2.9	2.5	5.6
Nitrogen	1.50	0.2	1.0	2.1	1.1	1.1	1.0	3.5
Sulfur	2.27	0.2	0.1	0.6	0.1	0.1	0.1	0.6
Oxygen	4.87	44.0	42.9	30.7	11.5	10.8	3.3	30.9
HHV (Btu/lb, db)	13,118	8,373	7,239	6,895	3,799	8,203	3,114	6,399
Bulk density (lb/ft^3)	--	11.9	3.12	23.1	50.5	50.5	43.7	--
Ash Analysis (wt.%)								
Al_2O_3	25.34	13.4	1.66	3.08	0.96	2.26	1.34	9.14
BaO	--	0.15	0.05	0.05	0.02	0.02	0.01	0.05
CaO	2.28	8.75	9.57	12.8	6.38	23.3	3.44	12.7
Fe_2O_3	18.34	5.94	1.47	1.95	1.29	1.37	0.93	4.04
K_2O	2.22	4.94	18.1	23.4	6.75	10.7	1.77	9.94
MgO	0.82	3.35	5.29	5.74	2.65	8.91	1.06	4.01
MnO	--	0.49	0.11	0.17	0.17	0.14	0.03	0.36
Na_2O	0.25	1.38	2.34	4.64	1.32	7.04	0.88	3.60
P_2O_5	0.4	1.44	13.8	9.21	2.90	14.7	2.54	14.0
SiO_2	48.2	57.2	43.0	29.3	74.98	26.0	84.82	39.4
SO_3	0.67	0.05	0.02	5.52	0.04	0.14	0.01	2.58
SrO	--	0.80	0.11	0.03	0.10	0.11	0.14	0.03
TiO_2	--	1.16	4.99	0.20	2.06	5.08	1.20	0.51

Tillman (2000) has investigated cofiring coal with all forms of biomass for several years for the Foster Wheeler Corporation. One of the most important topics he has studied is emissions mitigation through use of biomass. The results from Tillman's experiments on cofiring coal and biomass are summarized as follows:

1. blends of wood waste and coal will flow through bunkers to pulverizers or cyclone feeders with minimum bridging;
2. blends of wood waste and coal can be stacked and stored outside through summer months and, if the piles are constructed correctly, spontaneous combustion will not occur;
3. blends of wood waste or switch grass and coal can be burned with minimum impact on boiler operations; the blend may be largely transparent to the boiler operator if the percentage of biomass in the blend is low;
4. there are no technical show stoppers to cofiring biomass fuels with coal in existing boilers, although there are efficiency and emissions impacts and there can be capacity impacts.
5. The parametric test experience further documented the following impacts when cofiring biomass with coal:
    - reduced boiler efficiency, with the reduction being manageable;
    - reduced NO_x emissions, with reductions greater than originally expected;
    - reduced fossil CO_2 emissions, typically on the order of 3.15 ton fossil CO_2 avoided per ton of biomass burned;

Figure 3.2.5 demonstrates the synergistic effects of cofiring coal with biomass on NO_x emissions.

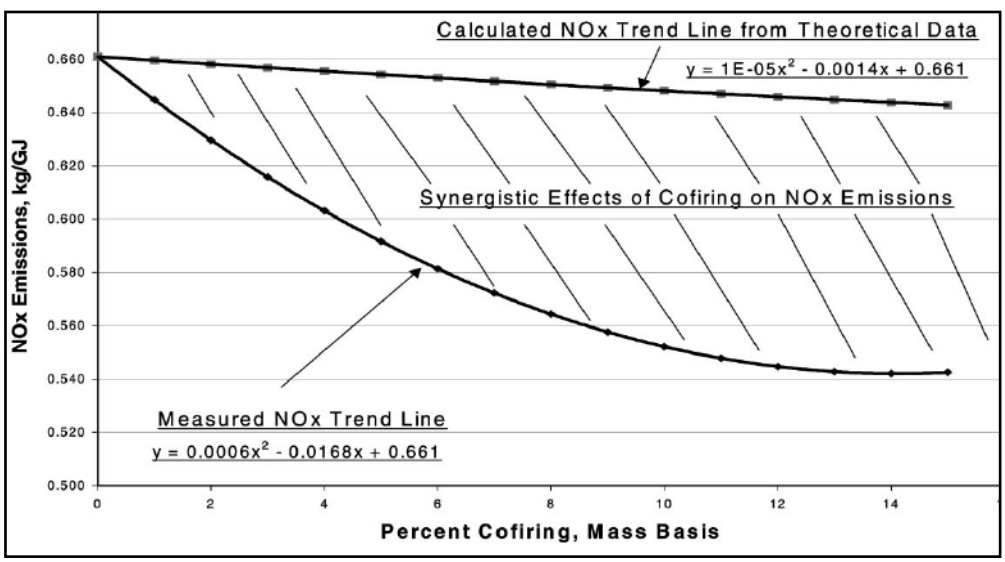

Figure 3.2.5. Tillman's (2000) NO_x reduction from cofiring coal with AB fuels. Note the measured NO_x trend line is lower than the predicted NO_x trend line.

Schmidt (2003) conducted an extensive study on biomass recovery opportunities for the utility industry. Table 3.2.3 helps identify promising biomass options by showing how much biomass is available. The first column gives the amount of manure produced. The second column gives the percentage of manure that can be collected. The third column gives the amount of manure that can be collected per animal per year. This table does not take into account the numbers of each animal. Note that of all forms of animal manure, dairy manure is the most plentiful on a per animal basis. This is due in large part to larger animal size, and high forage ratios that are lower in digestibility than a higher concentration ratio.

Di Nola (2007) used an FTIR instrument to measure the concentrations of HCN and NH_3 in the early flame stages of flames fired with coal and coal:LB blends. His work showed that coal alone can produce upwards of 700 ppm of HCN and approximately 80 ppm of NH_3. When 20% by mass LB was blended with the coal, HCN decreased to approximately 250 ppm and NH_3 increased to approximately 200 ppm. These experiments demonstrated that cofiring coal with LB has the potentially to reduce the formation of NO_x because it is known the high concentrations of HCN work to produce NO_x, whereas high concentrations of NH_3 work to reduce NO_x.

There is no previous research regarding cofiring DB with coal at the various equivalence ratios studied.

Table 3.2.3. Collectible quantities of dry manure available per animal.

Collectible Tons of Dry Animal Manure			
Livestock	Tons Dry Manure Excreted/Animal/Year	Percent of Manure Collectible	Tons Dry Manure Collectible/Animal/Year
Cattle and Calves	0.73	100	0.73
Milk Cows and Dairy Cattle	2.13	80	1.704
Hogs and Pigs	0.27	100	0.27
Chickens	0.01644	100	0.01644
Sheep and Lambs	0.106	50	0.053

3.3. Objectives

The overall objective of the present research was to develop energy conversion technologies for utilization of CB. The specific objective of current work was to study combustion and emission behavior when DB is cofired with coal. In order to achieve the objective, the following tasks were preformed:

Obtain thermo-chemical characteristics of coals and DB fuels including ultimate and proximate analyses.

Grind coals and DB fuels and obtain particle size distributions.

Perform cofiring experiments under constant heat input

Obtain combustion and emissions characteristics.

3.4. Experimental setup and procedure

3.4.1. Experimental Facility

All of the experiments were conducted using a 30 kW (100,000 BTU/hr) small scale furnace capable of firing most types of ground fuels. Solid fuel was fed at approximately 6.80 kg/hr (15 lb/hr). This furnace is part of the Coal and Biomass Laboratory of Mechanical Engineering at Texas A&M University. This facility operates with coal and coal:biomass blends and has been in operation for over 10 years. A schematic of the furnace is shown in Figure 3.4.1.1. Propane and natural gas (see Table 3.4.1.1 for composition) are used to heat the furnace to the operating temperature of 1100 C (2000 F). Type K (shielded, ungrounded) thermocouples are used to measure the temperature along the axial length of the furnace. These thermocouples provide a detailed temperature profile of the furnace throughout the combustion zone. A solid fuel hopper feeds coal and coal/biomass blends during experiments. Primary air is necessary to propel the solid fuel through the fuel line and to the furnace. Solid fuel comes out of the solid fuel line as a finely ground powder lightly dispersed in an air stream.

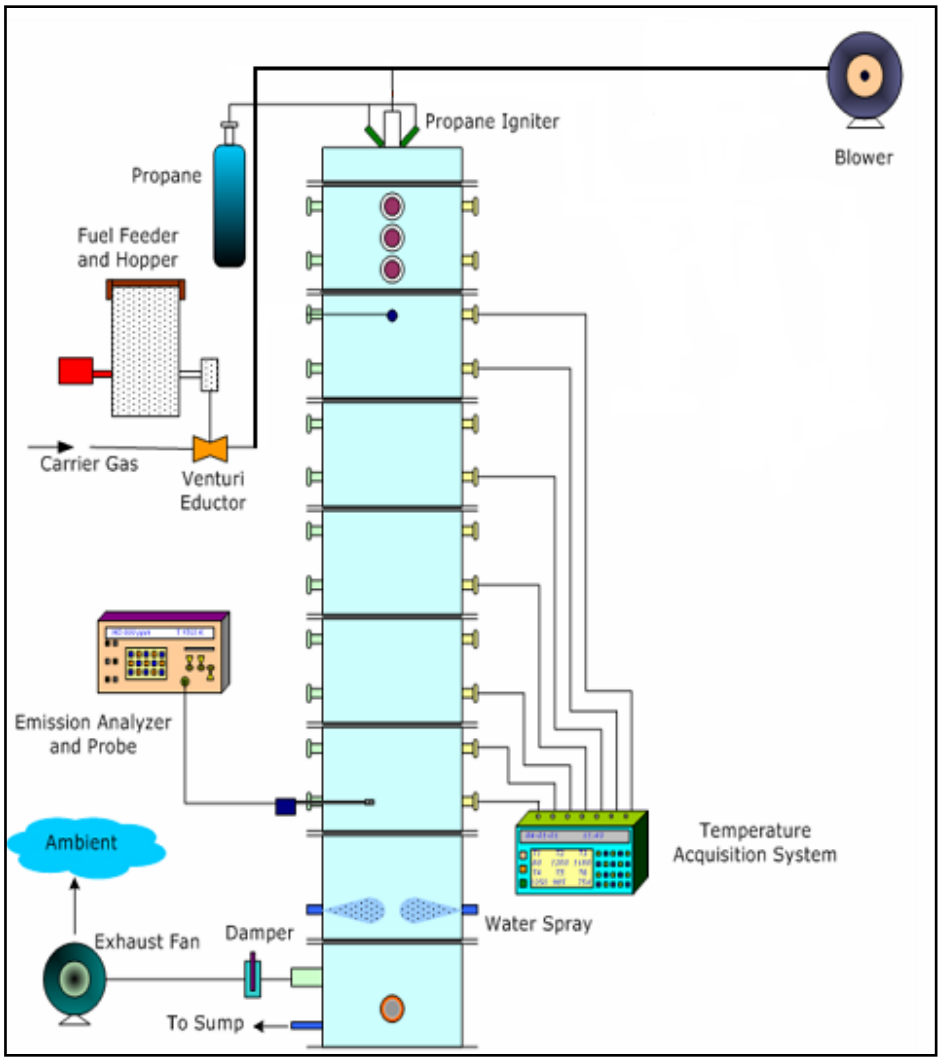

Figure 3.4.1.1. Schematic of boiler burner facility at Coal and Biomass Laboratory at Texas A&M University.

Table 3.4.1.1. Natural gas composition.

Natural Gas Composition	
Component	Mole Fraction
Methane	94.45
Ethane	2.34
Propane	0.59
Isobutane	0.12
N-Butane	0.14
Isopentane	0.06
N-Pentane	0.04
Hexanes	0.12
Carbon Dioxide	1.69
Nitrogen	0.45
HHV (kJ/kg)	55304

At the base of the furnace, a probe is used to sample the flue gases. Prior to ventilation, all exhaust gases pass through a water-cooling spray to significantly lower the temperature of the gases. A sump pump pumps this water out of the furnace. More details are provided in Frazitta et al. (1999), Arumugam et al. (2006), and Annamalai et al. (2005).

Thien (2002) built the current 100,000 BTU/hr furnace used. Figure 3.4.1.2 gives dimensions of the furnace.

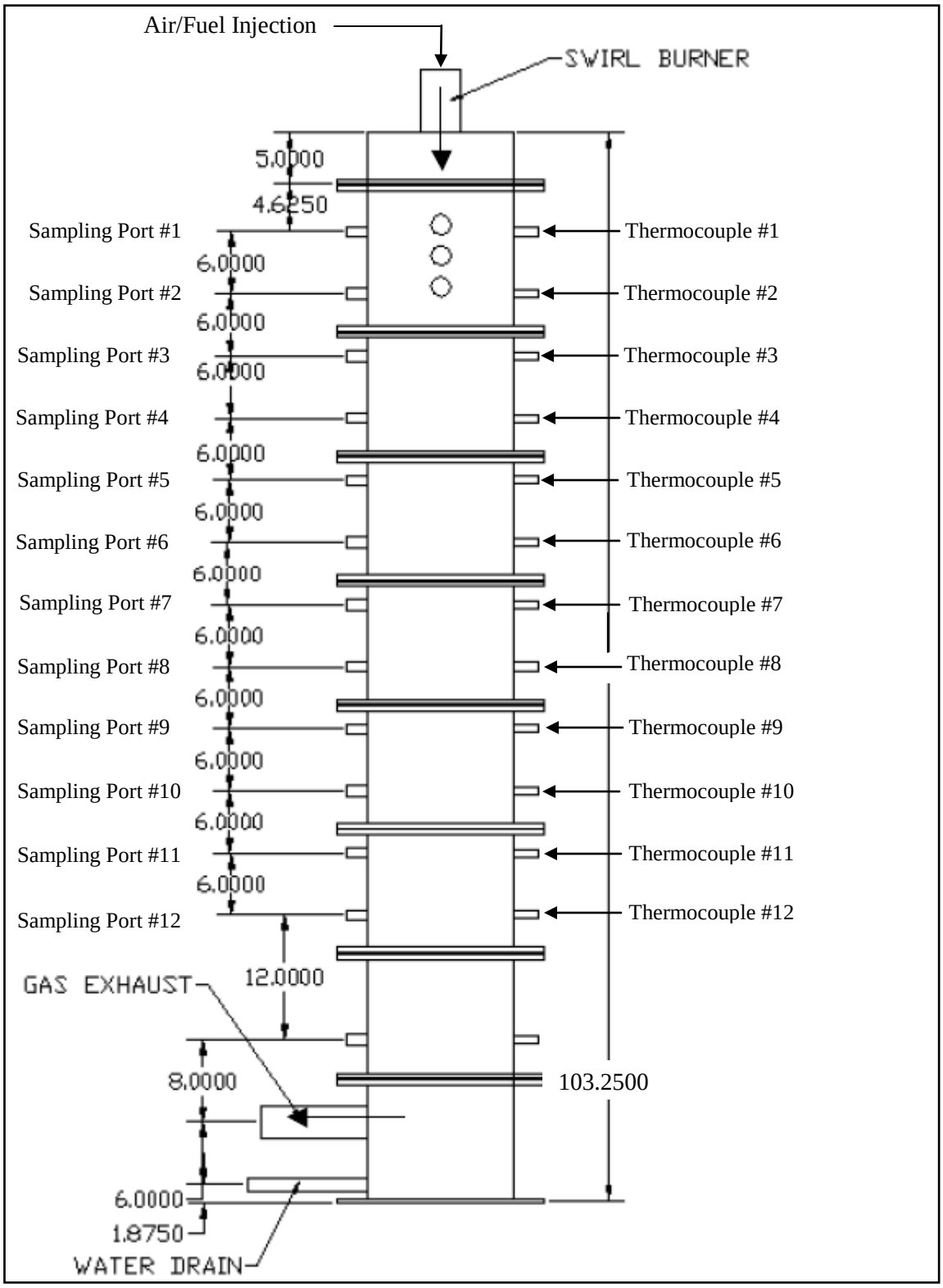

Figure 3.4.1.2. Dimensioned 100,000 BTU/hr furnace constructed by Thien (2002).

Figure 3.4.1.3 shows the cross section of one piece of the furnace. The refractory is made of greencast 94 ceramic. Table 3.4.1.2 following the figure gives the composition of greencast 94. The thermocouple ports are the same distance apart as the sampling ports: 6 inches. Also note that greencast 94 could react with SO_2 causing readings to be in error.

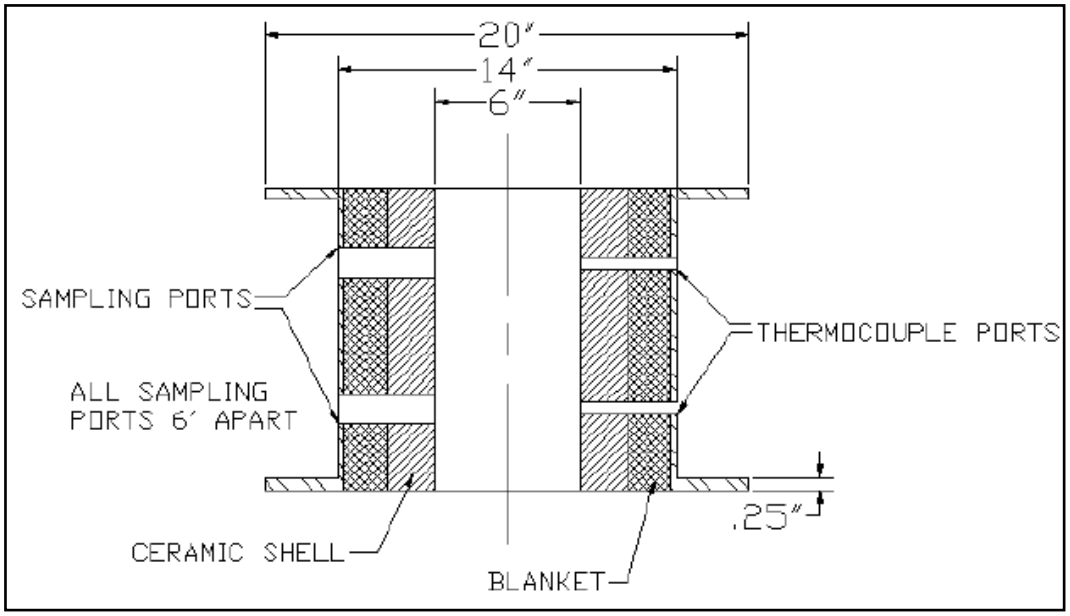

Figure 3.4.1.3. Dimensioned cross-section of greencast 94 refractory sections used in furnace.

Table 3.4.1.2. Composition of greencast 94.

Ingredient	Formula	Percent
Silica	SiO_2	0.2
Alumina	Al_2O_3	94.1
Titania	TiO_2	0.1
Iron Oxide	Fe_2O_3	0.2
Lime*	CaO	5.1
Magnesia*	MgO	0.1
Alkalis*	Na_2O+K_2O	0.2
* These alkaline oxides may react with SO_2		

The quarl at the top of the furnace is necessary to diffuse the coal and primary air into the secondary air stream and ensure sufficient mixing for thorough combustion. Figure 3.4.1.4 details the channels of the burner nozzle and swirlers which induce swirl to the secondary air. Table 3.4.1.3 details the parameters of the nozzle and gives the quarl angle of 24°.

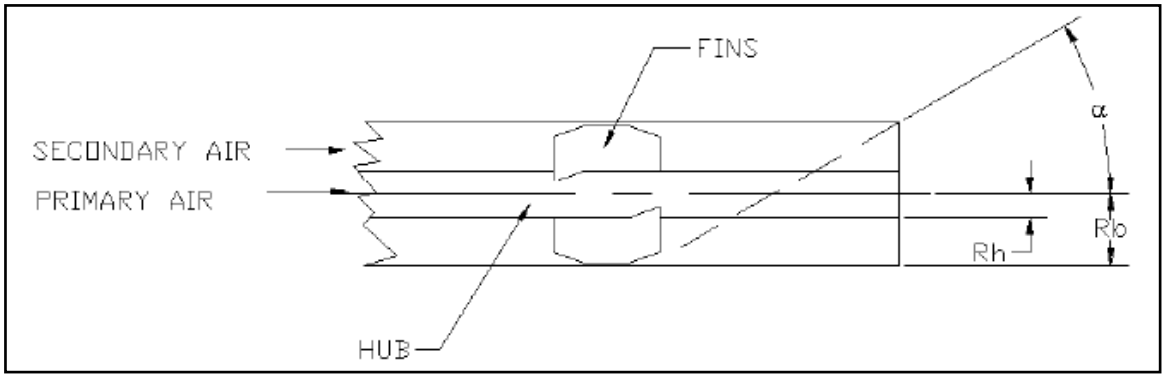

Figure 3.4.1.4. Detailed cross-section of fins used to mix primary and secondary air.

Table 3.4.1.3. Quarl and blade angle details.

Parameter	Value
Rh	0.0127m (.5in)
Rb	0.0206375m (.8125in)
Quarl Half Angle	24˚
Blade Angle	45˚
Swirl Number	0.7

3.4.2. Instrumentation

Flue gas concentrations were measured using an E-Instruments (2003) 8000 Portable Flue Gas Analyzer capable of detecting CO, CO_2, NO_x, SO_2, and O_2 in a flue gas stream. The analyzer uses electrochemical cells to detect flue gases in low range applications and NDIR in middle range applications.

Primary air flow measurements were made using Dwyer RMC Rate-Master Flow Meters. Two flow meters were used, one for motive air and one for eductor air. Each flow meter was calibrated to be accurate in the range of 20-200 SCFH of air with an accuracy of plus or minus 5 SCFH. Secondary air was measured using a Dwyer GFC Gas Mass Flow Controller. The flow meter was calibrated to be accurate in the range of 0-1000 SLPM of air with an accuracy of plus or minus 1.5% FS of the flow meter.

3.4.3. Experimental Procedure

The experimental procedure is as follows:

1. Secondary air flow is started.
2. A propane torch is used to fire natural gas into the furnace to heat the furnace to 650 C (1200 F) as indicated by thermocouple #1.
3. The air flow rate is gradually increased for about an hour until the flame is close to stoichiometric. This period is used to preheat the furnace.
4. At 650 C (as indicated by the first thermocouple), the propane line is shut off and the second half of the heating phase is done burning exclusively natural gas. Natural gas is used to heat the furnace to 1100 C. At this temperature, coal is able to self-ignite and maintain stable flame.
   The natural gas line is closed and the solid fuel line and feeder air lines are opened. The solid feeder is turned on. The furnace is visually inspected to ensure that flame is still present. The thermocouple readings can also verify that a flame is present in the furnace.
5. From the known HHV of the fuel, the required fuel and air flow rates to obtain a 100,000 BTU/hr flame are calculated for all desired equivalence ratios.
6. The feeder and air lines are set to the proper flow rates for stoichiometric combustion.
7. The secondary air is adjusted to achieve the desired equivalence ratio. The primary air must stay at a constant value for all experiments. This is a requirement for the solid feeder to operate properly. The blower output can be increased to provide more secondary air.
8. After allowing 30 minutes for the furnace to stabilize, an initial analysis of the flue gases is taken to verify that the flame is at stoichiometric. The flue gas analyzer will require three minutes to self-calibrate and self-zero. After the initial start up, the analyzer is connected to the exhaust port.
9. This air flow rate is recorded as it will be used to calculate other air flow rates for all equivalence ratios.
10. After the reading at stoichiometric combustion has been recorded, the air flow rate can be adjusted to achieve any desired equivalence ratio. It is important to wait 10 minutes between readings to allow transients to dampen out.
11. Once all readings have been taken, the furnace is shut down by turning off the solid feeder and closing the feeder air lines. The secondary air line is cut to 100 L/min and the furnace to cools to ambient conditions.

3.5. Results and discussion

3.5.1. Introduction

This chapter presents the fuel properties for the four fuels considered. Fuel properties played a significant impact on the burnt fraction and the emissions created by combustion. In addition, this chapter presents the results from the cofiring experiments performed and discusses their role in evaluating the combustion performance of the fuels. The performance was evaluated by measuring combustion efficiency (burnt fraction) and the emissions levels of pollutants which include NO_x and CO. In addition, overall fuel nitrogen conversion efficiency to NO_x was also determined. The mercury emissions are presented elsewhere.

When BF is very high, near unity, it implies that all of the fuel was combusted. When fuel nitrogen conversion efficiency is very low, it means that most fuel bound nitrogen is converted to something other than NO_x. Unfortunately, optimizing one criterion is often at the expense of another criterion. To increase BF, typically fuel nitrogen conversion efficiency may be increased as well.

3.5.2. Fuel Properties

Table 3.5.2.1 presents the fuel properties. Note that the DB fuels are much higher in nitrogen than coal fuels. However, most AB fuels (e.g. saw dust, corn stalks, switch grass, nut shells, rice hulls, etc.) are lower in nitrogen than coal. Manure based biomass is the exception to this generality. LA-PC-DB-SepS was almost 3 times richer in nitrogen than WYO. Both the DB fuels were higher in ash content than the coal fuels. The ash in HA-PC-DB-SoilS was more than 10 times more that of WYO. Although, LA-PC-DB-SepS was more than 4 times lower in ash than HA-PC-DB-SoilS, it was still higher in ash than either coal. The DB fuels contained less FC. The reduced FC for HA-PC-DB-SoilS caused the DB fuels to have a lower HHV. WYO had a 5.5 times larger HHV than HA-PC-DB-SoilS. The FC on a DAF basis was still low for HA-PC-DB-SoilS and lower even compared to LA-PC-DB-SepS.

TXL had the most sulfur, which is characteristic of a lignite coal. (Annamalai and Puri, 2007) WYO was lower in sulfur. It had less sulfur than LA-PC-DB-SepS, but more than HA-PC-DB-SoilS on a mass basis. On a heat basis, the biomass fuels had higher nitrogen and sulfur contents than coal.

Both of the biomass fuels had less moisture than either of the coals. This is due to the preparation of the biomass. Prior to grinding, the biomass fuels were composted for 90 days in a greenhouse. (Heflin and Sweeten, 2006) During the composting process, the biomasses were also air dried. Hence, specially prepared DB fuels contained less moisture. HA-PC-DB-SoilS had approximately the same amount of VM as the two coals. LA-PC-DB-SepS had almost twice the volatiles as HA-PC-DB-SoilS, TXL, or WYO.

The Boie HHV was the HHV predicted by the Boie equation (Annamalai and Puri, 2007):
$$HHV(kJ*kg^{-1}) = 35160*Y_C + 116225*Y_H - 11090*Y_O + 6280*Y_N + 10465*Y_S \,.$$
Eq. 5.2.1.

Table 3.5.2.1. Ultimate and proximate fuel properties

	HA-PC-DB-SoilS	LA-PC-DB-SepS	TXL	WYO
Dry Loss (% Moisture)	12.21	25.26	38.34	32.88
Ash	59.89	14.86	11.46	5.64
FC	3.92	13.00	25.41	32.99
VM	23.99	46.88	24.79	28.49
Carbon, C	18.04	35.21	37.18	46.52
Hydrogen, H	1.45	3.71	2.12	2.73
Nitrogen, N	1.15	1.93	0.68	0.66
Oxygen, O (diff)	7.07	18.60	9.61	11.29
Sulfur, S	0.19	0.43	0.61	0.27
HHV (kJ/kg) As Received	4311.63	12844.17	14286.82	18193.02
HHV (kJ/kg) Dry	4911.11	17185.90	23169.07	27106.57
HHV (kJ/kg) DAF	15452.02	21449.85	28459.80	29593.38
HHV (kJ/kg of stoich Air) AR	1931.41	2886.07	3155.51	3191.89
Boie HHV (kJ/kg)	7340.86	14799.49	14582.32	18347.96
A:F AR	2.23	4.45	4.53	5.70
A:F DAF	8.00	7.44	8.77	9.22
FC DAF	14.04	21.72	50.62	53.66
VM DAF	85.96	78.28	49.38	46.34
Ash kg/GJ	138.90	11.57	8.02	3.10
Nitrogen kg/GJ	2.67	1.50	0.48	0.36
Sulfur kg/GJ	0.43	0.33	0.42	0.15

See Table 3.5.2.2. Note that the coals had a larger SMD than the DB fuels. The dirt that got collected with the DB fuels passed through all of the sieves and collected in the pan. This caused the DBs to have a smaller SMD. The larger SMD of the coals caused clogging difficulties.

Table 3.5.2.2. Size distribution parameters.

Size Distribution Parameters				
	TXL	WYO	LA-PC-DB-SepS	HA-PC-DB-SoilS
n	1.2991	1.4369	1.0934	1.2612
b	0.000934	0.00042	0.0024	0.0013
SMD (microns)	396	396	96.7	91.6

3.5.3. Experimental Parameters

TXL was used as the base case fuel. TXL and WYO were fired as blends with two DB fuels. Each coal was blended with each DB fuel in 100-0, 95-5, 90-10, and 80-20 blends on a mass basis. This created 14 different fuel blends. For each blended fuel, the equivalence ratio was varied from 0.8 to 1.2 in 0.1 increments. The 80-20 blends were too rich in DB to be used in industrial applications, but were used in order to get more data points for the study. In the rich

regime (equivalence ratio > 1.0) the HA-PC-DB-SoilS quickly clogged the sampling port due to high ash content. Thus, a full set of data points could not be generated.

Primary air was provided from a compressed air line and was used to carry solid fuel to the burner nozzle. The amount of primary air was dictated by the feeder and was constant at 5.95 m^3/hr (15 - 25% of total air). However, secondary air (75 – 85% of total air) was provider by a separate compressed air line and could be adjusted to change the equivalence ratio. Note that on a heat basis, the percent of heat attributed to each fuel type was much less compared to percent mass basis. For example: for the 80:20 WYO:HA-PC-DB-SoilS fuel, 80% of the mass was WYO, but more than 94% of the heat came from WYO. All fuel and air flow rates were calculated from a program developed by Goughnour (2006). Combustion any leaner than 0.8 created a heavy strain on the compressor and was also useless for industrial applications.

Note that for pure coal and coal:biomass blends, the fuel flow rates and air flow rates remained relatively constant at the same equivalence ratio. This is in agreement with combustion theory. (Annamalai and Puri, 2007) The coal:biomass blends needed slightly more fuel in order to compensate for the lower energy content of biomass. Also note that the HHV on a stoichiometric air basis is roughly constant (except for HA-PC-DB-SoilS).

3.5.4. O_2 and Equivalence Ratio

The air fuel ratio, and hence the equivalence ratio, can be estimated from measured flow rates of air and fuel. It can also be computed using the measured O_2 percentage in the exhaust for lean mixtures. Using O_2 percentage data the equivalence ratio of the exhaust stream was approximated by:

$\phi_{flue} \approx 1 - 4.76 * O_2$; Eq. 4.4.4.1 $\quad \phi_{flue} < 1.0$ (Annamalai and Puri, 2007)

Equation 4.4.4.1 assumes that all the fuel has been gasified. If large particles are not gasified, the O_2 percentage will increase. This will cause the ϕ based on exhaust gases to decrease. Figure 3.5.4.1 plots the ϕ_{flue} computed from flue gas analysis versus the ϕ_{flow} computed from air and fuel flow rates. It is seen that ϕ_{flue} is less than ϕ_{flow}. This indicates that the BF is less than 1.0. Also note that the ϕ_{flow} requires knowledge of the fuel flow rate. Due to limitations of the feeder, only average flow rates could be measured.

Figure 3.5.4.2 presents the exhaust equivalence ratio for WYO and WYO:DB blended fuels. Ideally, the data points would follow a 45 line, indicating ϕ_{flue} and ϕ_{flow} were in perfect agreement. The real data points lie within the experimental uncertainty of each other. This indicates that the values are valid.

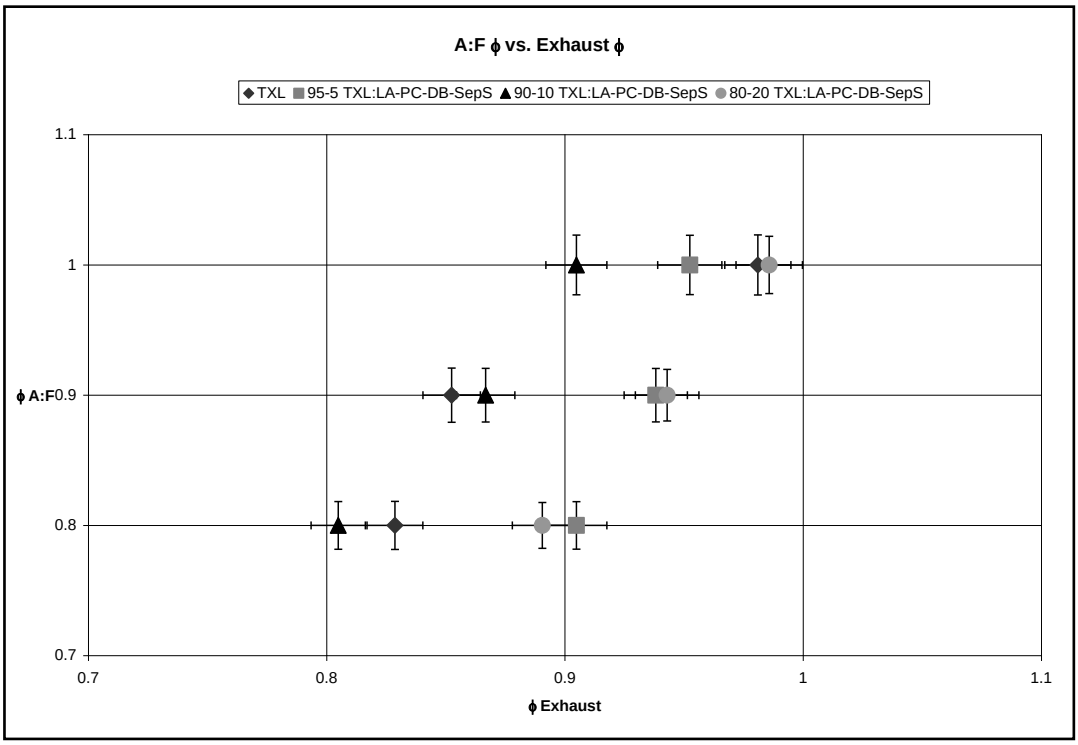

Figure 3.5.4.1. Equivalence ratio based on air flow rates and the calibrated fuel flow rate vs. equivalence ratio based on O2% in exhaust for TXL and TXL:DB blended fuels.

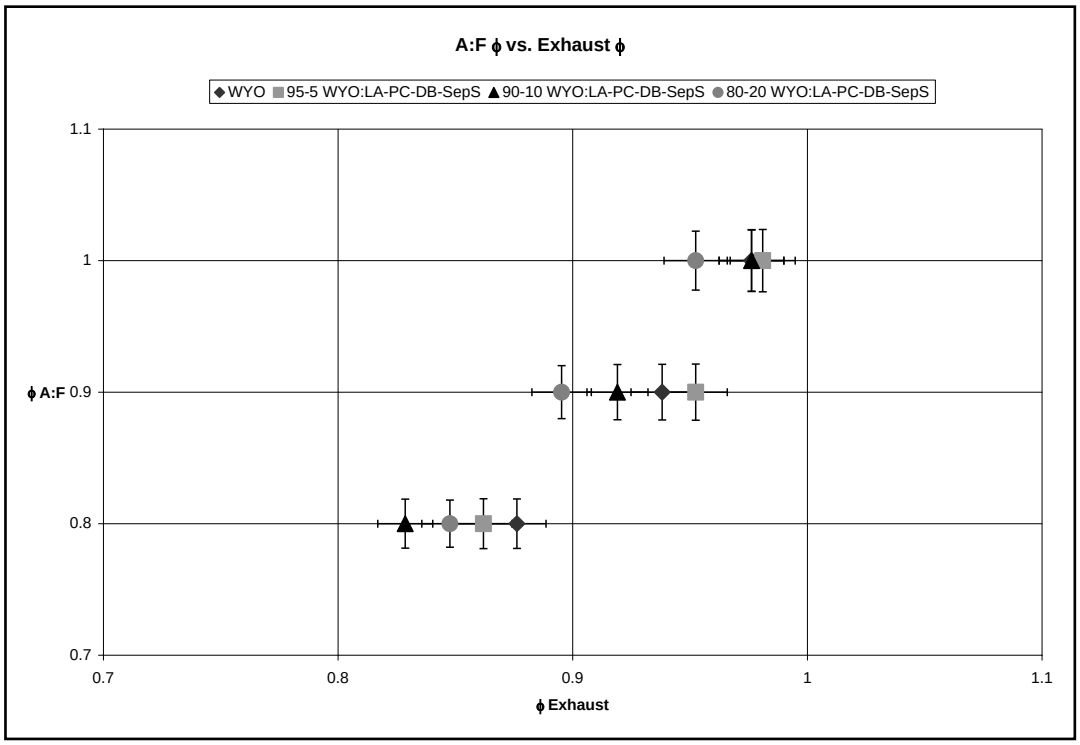

Figure 3.5.4.2. Equivalence ratio based on air flow rates and calibrated fuel flow rate vs. equivalence ratio based on O_2% in exhaust for TXL and TXL:DB blended fuels.

3.5.5. CO and CO_2 Emissions

Very little CO was formed in the lean regime. In lean combustion, there is sufficient oxygen for all the carbon to fully oxidize to CO_2. However, once combustion became oxygen deficient (rich) CO begins to be formed. In general, the blended fuels produced more CO because the DB fuels contained more oxygen.

Figure 3.5.5.1 and Figure 3.5.5.2 present the CO_2 and CO exhaust concentrations for TXL and TXL:DB blended fuels respectively. The equivalence ratio was based upon measured air and calibrated fuel flow rates. It is apparent that CO_2 peaked at approximately the stoichiometric condition. As air flow was increased from the stoichiometric point, the excess air diluted the flue gas concentrations. This dilution affect decreased the CO_2 percentage. On the other hand, if air flow was decreased below the stoichiometric air flow rate, less CO_2 was formed due to insufficient O_2 to oxidize fuel bound carbon. This explains why the peak in CO_2 was at approximately stoichiometric.

In all future plots, the ϕ represents the equivalence ratio based on measured air flow rates and the calibrated fuel flow rate.

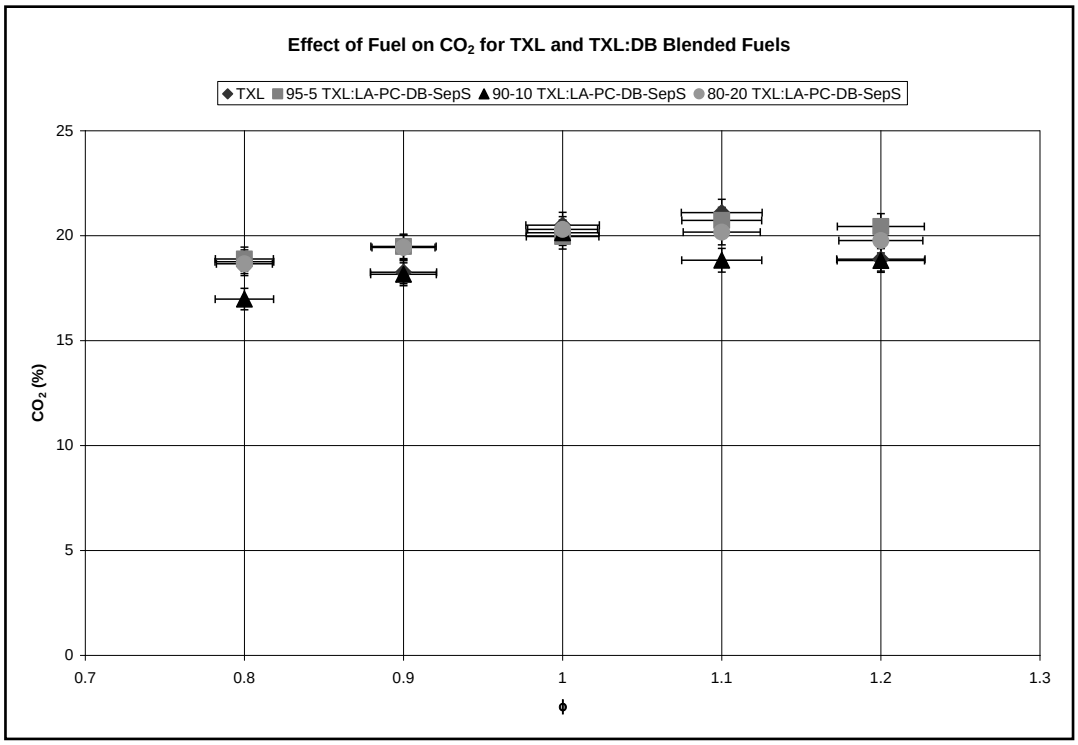

Figure 3.5.5.1. Effect of fuel on CO_2 for TXL and TXL:DB blended fuels.

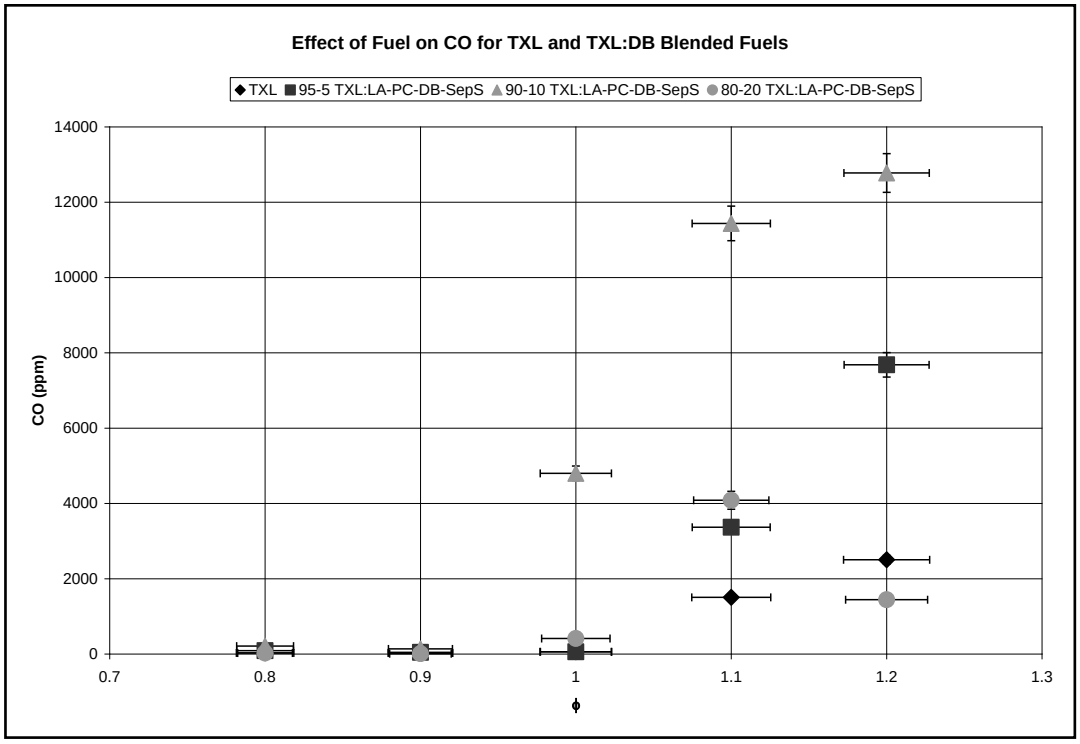

Figure 3.5.5.2. Effect of fuel on CO for TXL and TXL:DB blended fuels.

WYO presented trends similar to those of TXL:DB blends. Figure 3.5.5.3 and Figure 3.5.5.4 present the CO_2 and CO concentrations for WYO and WYO:DB blended fuels. The wider uncertainty bands for CO were due to the uncertainty in CO measurements being a percentage of the reading. The uncertainty bands overlap too much to draw any conclusions about the effect of blending coal with DB on CO production. The equivalence ratio was based upon air and fuel flow rates.

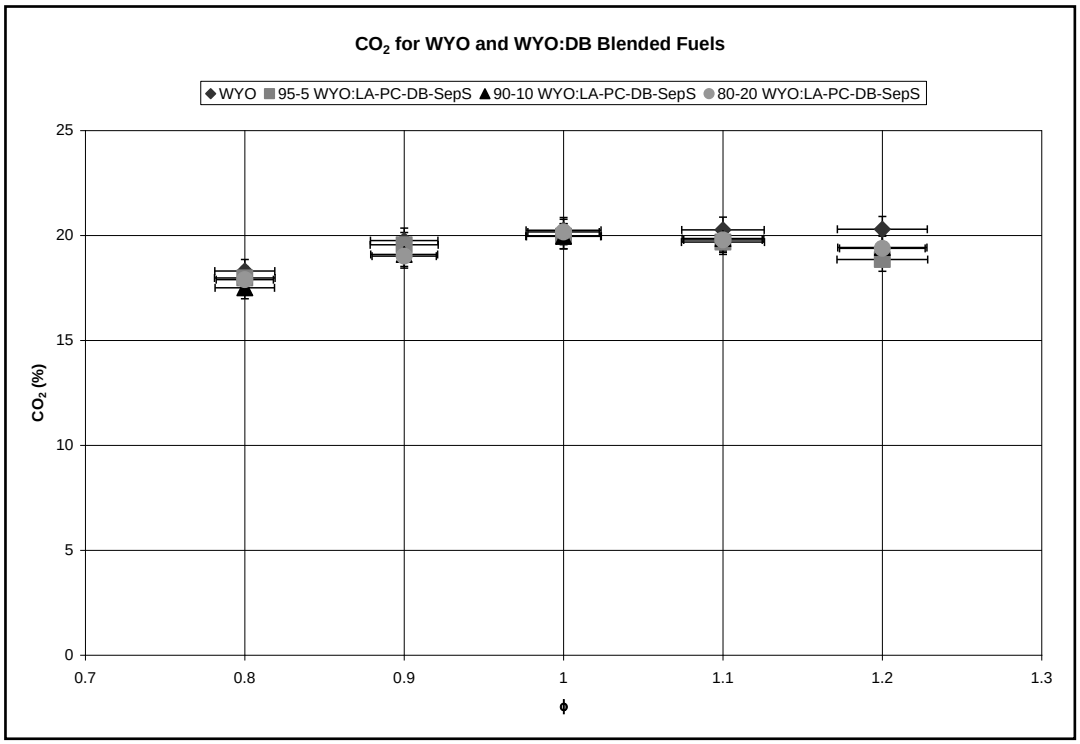

Figure 3.5.5.3. Effect of fuel on CO_2 for WYO and WYO:DB blended fuels.

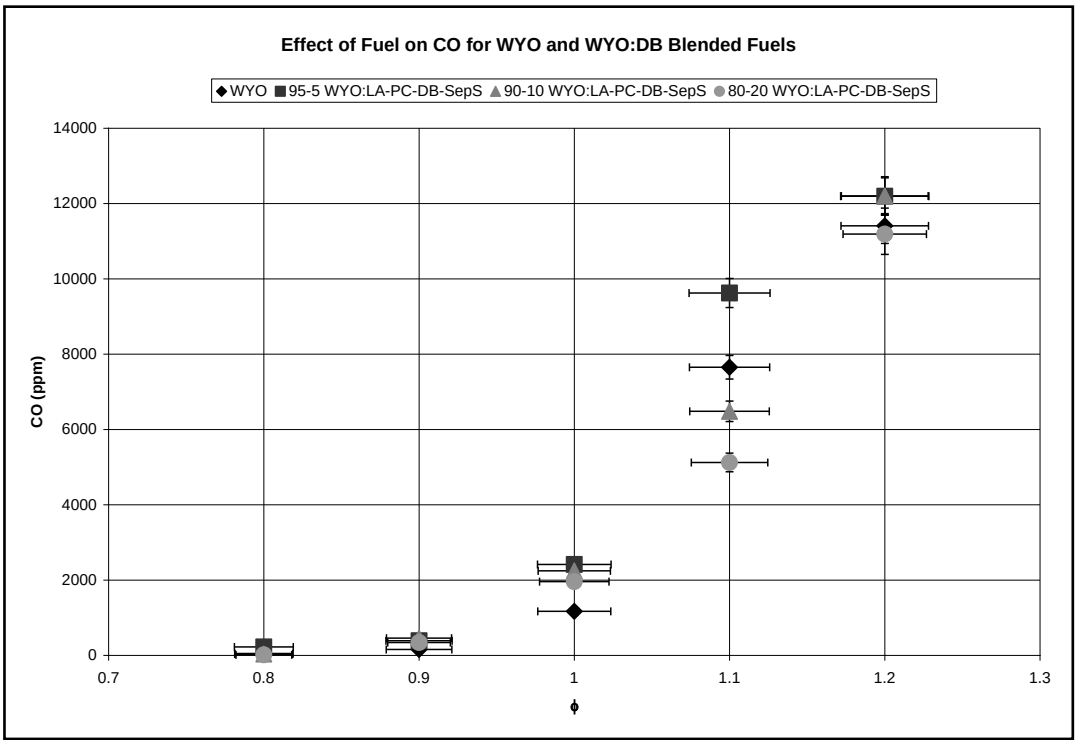

Figure 3.5.5.4. Effect of fuel on CO for WYO and WYO:DB blended fuels.

3.5.6. Burnt Fraction

Recall that O_2 in the exhaust is an indicator of ϕ used in experimentation. Thien (2002) derived an expression for the burnt fraction of a solid fuel can be approximated as:

$$BF \approx \frac{1}{\phi} * \left(1 - \frac{X_{O_2}}{X_{O_{2,A}}}\right); \text{ Eq. 4.4.6.1}$$

Where BF is the burnt fraction, ϕ is the measured equivalence ratio from flow rates, X_{O2} is the mole fraction of oxygen in the exhaust gases (dry basis), and $X_{O2,A}$ is the mole fraction of oxygen in the ambient air (dry basis). This equation can be used for rich or lean mixtures. Note that BF is larger than 1 for some of the extremely lean experiments. These values demonstrate the limitations of EQ. 4.4.6.1 as well as experimental uncertainties including fuel compositions. As to be expected, BF decreased with increasing equivalence ratio. In rich combustion, insufficient air was provided to completely oxidize all fuel carbon to CO_2, leaving unburned fuel in the ash. This caused the BF to be less than 1.

Figure 3.5.6.1 and Figure 3.5.6.2 present the BF for TXL and TXL:DB blended fuels and WYO and WYO:DB blended fuels, respectively. Even in the very rich combustion (ϕ=1.2), approximately 83% of the fuel was burnt.

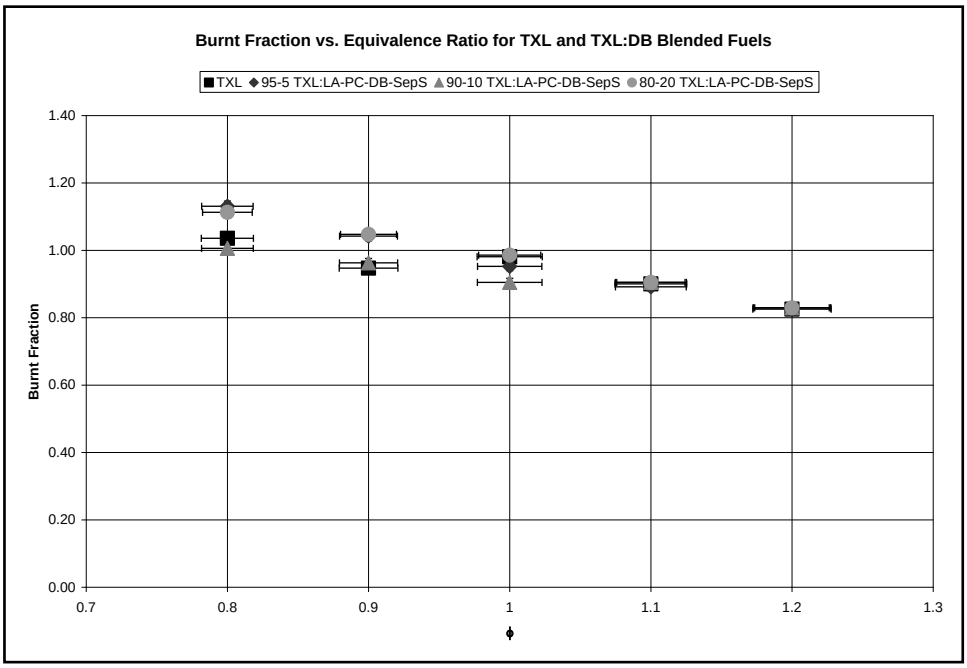

Figure 3.5.6.1. Effect of fuel on BF for TXL and TXL:DB blended fuels. Note that in the rich regime, the BF overlaps for all fuels. This indicates that the same percentage of all fuels was burnt.

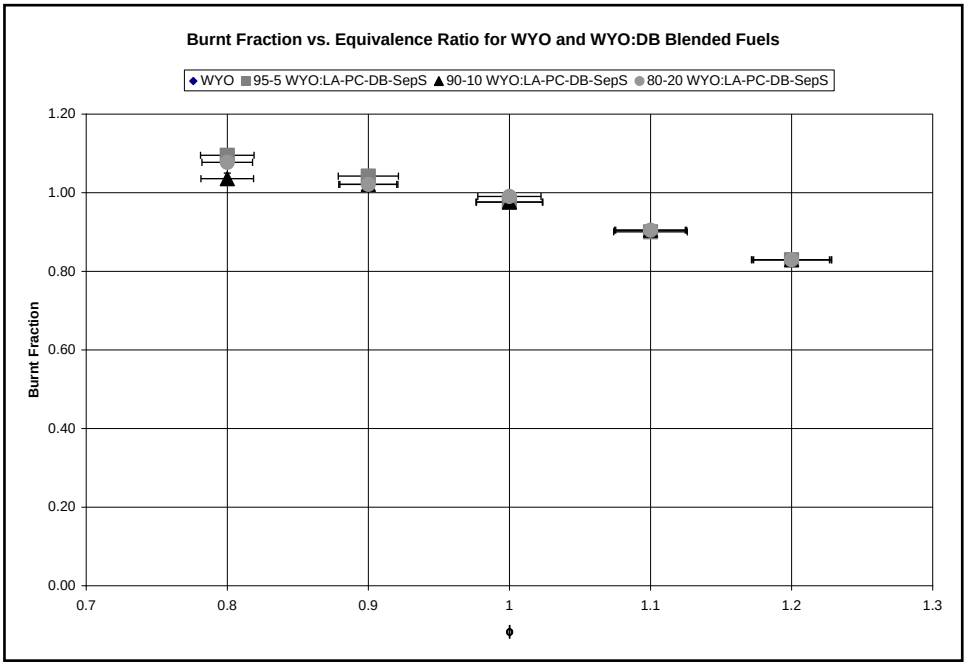

Figure 3.5.6.2. Effect of fuel on BF for WYO and WYO:DB blended fuels. Note that the data points come close to overlapping for all equivalence ratios. Thus, BF was independent of fuel type.

3.5.7. NO_x Emissions

With the exception of 95-5 TXL:HA-PC-DB-SoilS, all of the blended fuels produced more NO_x in the lean region than the pure TXL. This is due to the higher amount of fuel bound nitrogen present in the biomass binding with the excess oxygen to form NO_x. But, in the slightly rich region, the blended fuels produced less NO_x than the pure TXL. This is due to the fuel bound nitrogen being forced to form other nitrogen compounds due to the deficiency in oxygen and VM reacting quickly to absorb any available oxygen the might bound with nitrogen.. No experiments with 80:20 TXL:HA-PC-DB-SoilS were possible due to excessive amounts of particulate matter (mostly ash) clogging the flue gas analyzer. The instrument clogged faster than it was able to settle to a stable reading.

Figure 3.5.7.1 and Figure 3.5.7.2 presents the NO_x emissions for TXL and TXL:DB blended fuels in ppm and corrected to 3% O_2. Correcting to 3% O_2 is a common industry practice to prevent utilities from artificially diluting NO_x emissions with O_2. In the very lean regime, correcting caused the NO_x emissions to increase. However, for all other equivalence ratios, correcting caused the NO_x emissions to decrease because there is less than 3% O_2 in the exhaust prior to correcting.

Another method employed to prevent emission dilution is to report NO_x levels on a heat basis. Figure 3.5.7.3 presents the NO_x emissions in kg/GJ of heat input.

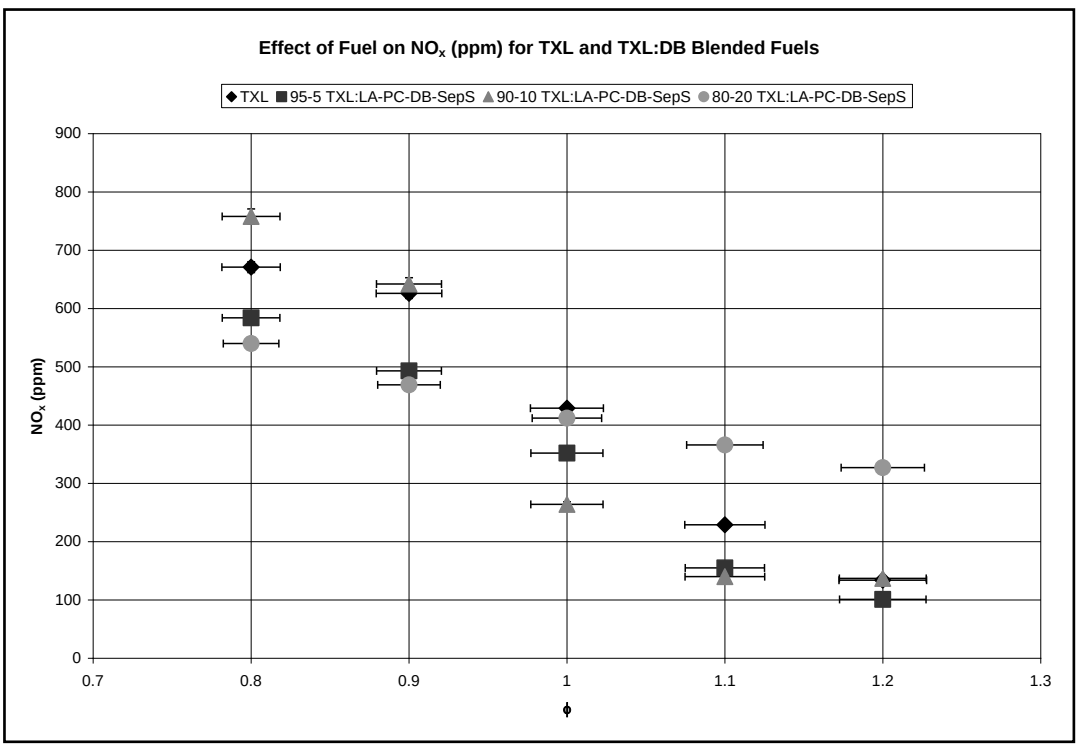

Figure 3.5.7.1. Effect of fuel on NO_x for TXL and TXL:DB blended fuels. Note that blended fuels have lower NO_x values at stoichiometric and in rich combustion.

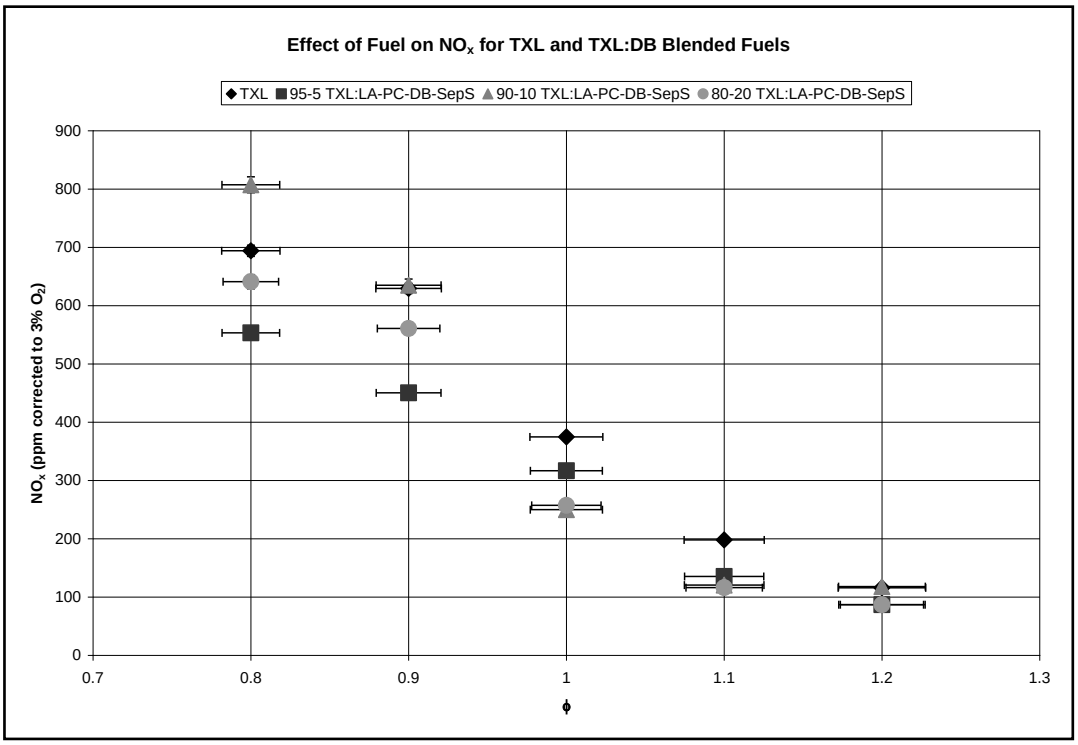

Figure 3.5.7.2. Effect of fuel on NO_x for TXL and TXL:DB blended fuels corrected to 3% O_2.

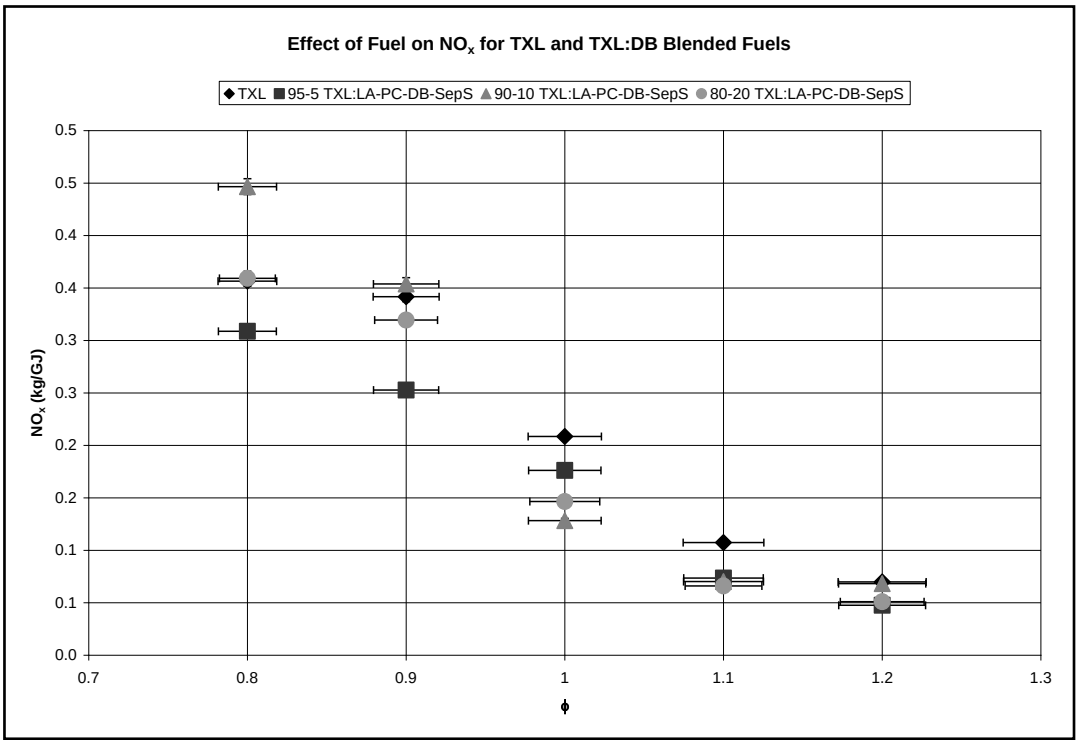

Figure 3.5.7.3. Effect of fuel on NO_x for TXL and TXL:DB blended fuels in kg/GJ.

Note that in the lean region, the blended fuels produce more NO_x than the pure WYO. In the slightly rich region, the blended fuels produce less NO_x than the pure WYO. The same explanation for TXL applies to the WYO fuels. Experiments in the rich region with 80-20 WYO:HA-PC-DB-SoilS were unsuccessful due to excessive amounts of particulate matter (mostly ash) clogging the flue gas analyzer.

Figure 3.5.7.4 and Figure 3.5.7.5 present the NO_x emissions from WYO and WYO:DB blended fuels in ppm and corrected to 3% O_2. Figure 3.5.7.6 presents the NO_x emissions from WYO and WYO:DB blended fuels in kg/GJ of heat input.

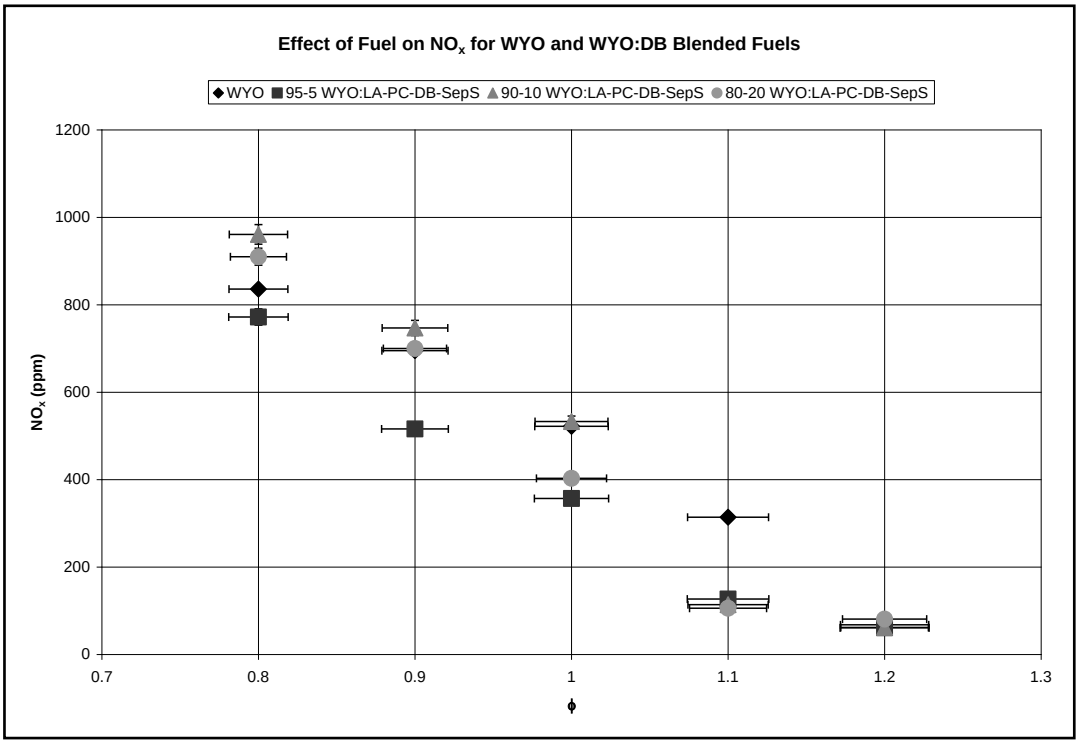

Figure 3.5.7.4. Effect of fuel on NO_x for WYO and WYO:DB blended fuels. Note how NO_x decreases in the near lean region for blended fuels.

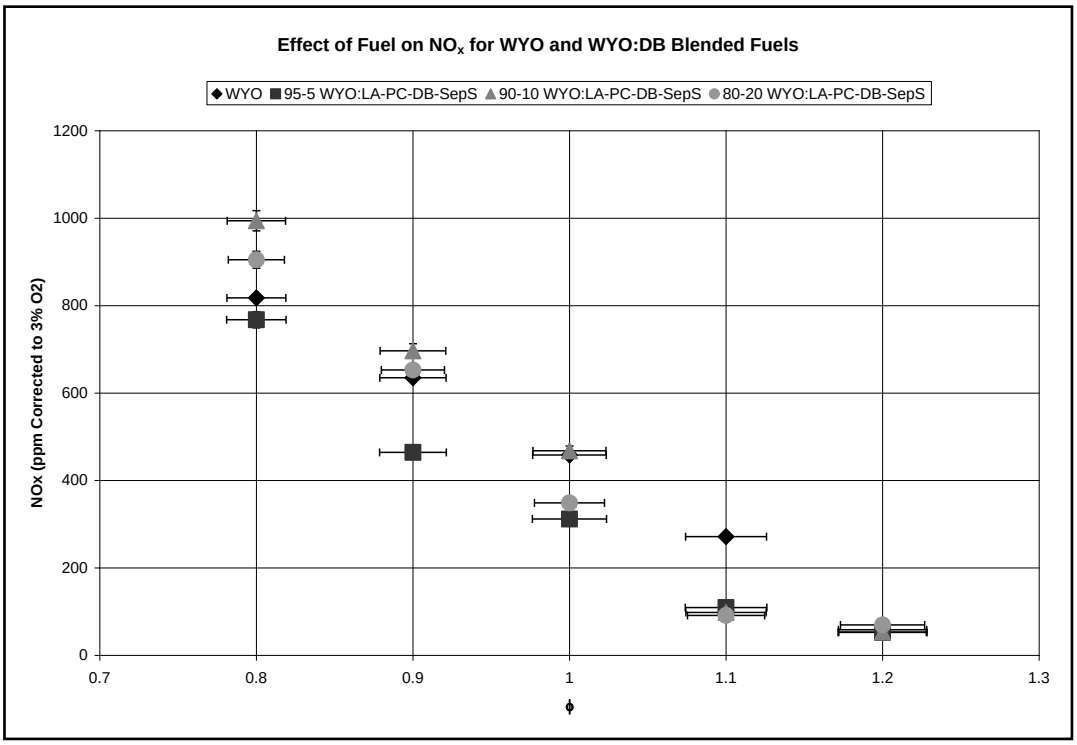

Figure 3.5.7.5. : Effect of fuel on NO_x for WYO and WYO:DB blended fuels corrected to 3% O_2.

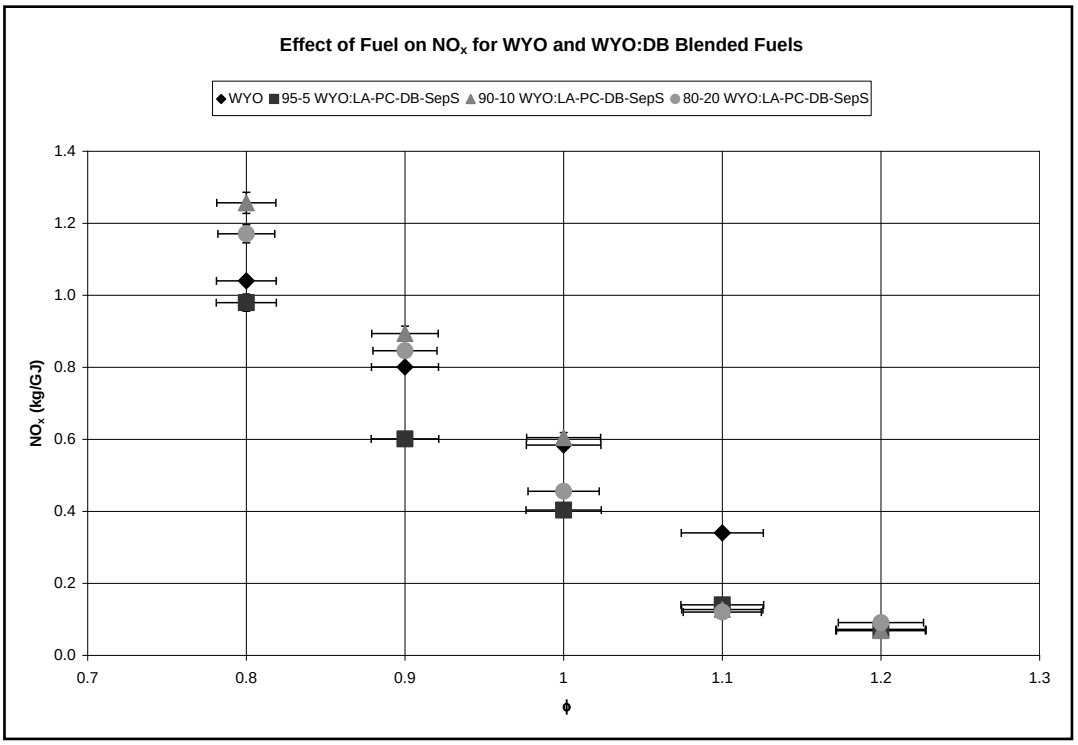

Figure 3.5.7.6. Effect of fuel on NO_x for WYO and WYO:DB blended fuels in kg/GJ.

3.5.8. Fuel Nitrogen Conversion Efficiency

In coal combustion, the majority of NO_x comes from fuel bound nitrogen bonding with available oxygen to form NO_x. This reaction is inhibited by carbon radicals bonding with available oxygen to form CO and CO_2. The nitrogen conversion efficiency is defined as the amount of fuel nitrogen that gets converted to NO_x. Annamalai and Puri (2007) showed that overall fuel nitrogen conversion efficiency can be approximated by:

$$N_{CONV} \approx \frac{(c/n) * X_{NO}}{X_{CO_2} + X_{CO}} \text{ ; Eq. 4.4.8.1}$$

Where c/n is the ratio of the empirical carbon and nitrogen respectively, X_{NO} is the mole fraction of NO_x, X_{CO2} is the mole fraction of CO_2, and X_{CO} is the mole fraction of CO. All gases were measured in the exhaust stream. Note that the equation assumes that all NO_x originates from fuel nitrogen and hence it presents an upper bound on fuel nitrogen conversion efficiency. Work should be done to investigate the validity of assuming all NO_x comes from the fuel. Burning a fuel that does not produce fuel NO_x (i.e. natural gas) at the same temperature profile as the solid fuel could measure the amount of thermal NO_x produced.

Note that as equivalence ratio increased, less nitrogen was converted to NO_x. In the extremely rich region, the conversion efficiency was nearly 0%. The largest decrease in

conversion occurred when the flame went from stoichiometric to rich. Figure 3.5.8.1 and Figure 3.5.8.2 present the fuel nitrogen conversion efficiency for TXL and TXL:DB blended fuels and WYO and WYO:DB blended fuels, respectively. Also note that in general, the DB blended fuels converted less nitrogen to NO_x. These fuels produced more NO_x than pure coal because there was more fuel bond nitrogen. If both fuels had the same amount of fuel bound nitrogen, the DB would have produced less NO_x than coal because a lower percentage of nitrogen.

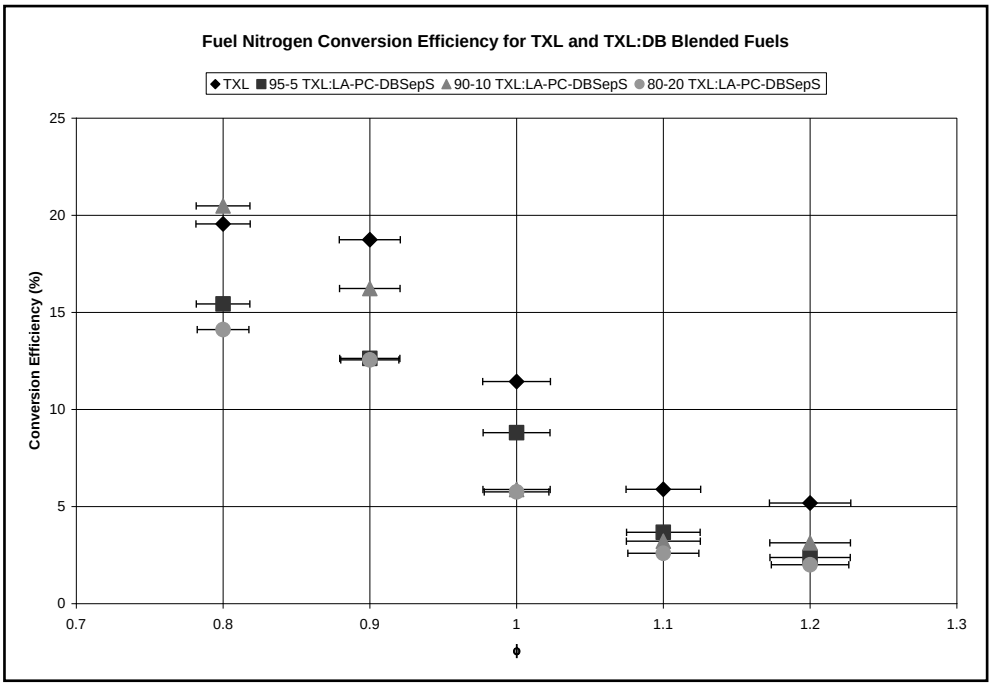

Figure 3.5.8.1. Effect of fuel on nitrogen conversion efficiency for TXL and TXL:DB blended fuels. Note that the conversion efficiency is less than coal for almost all TXL:DB blended fuels.

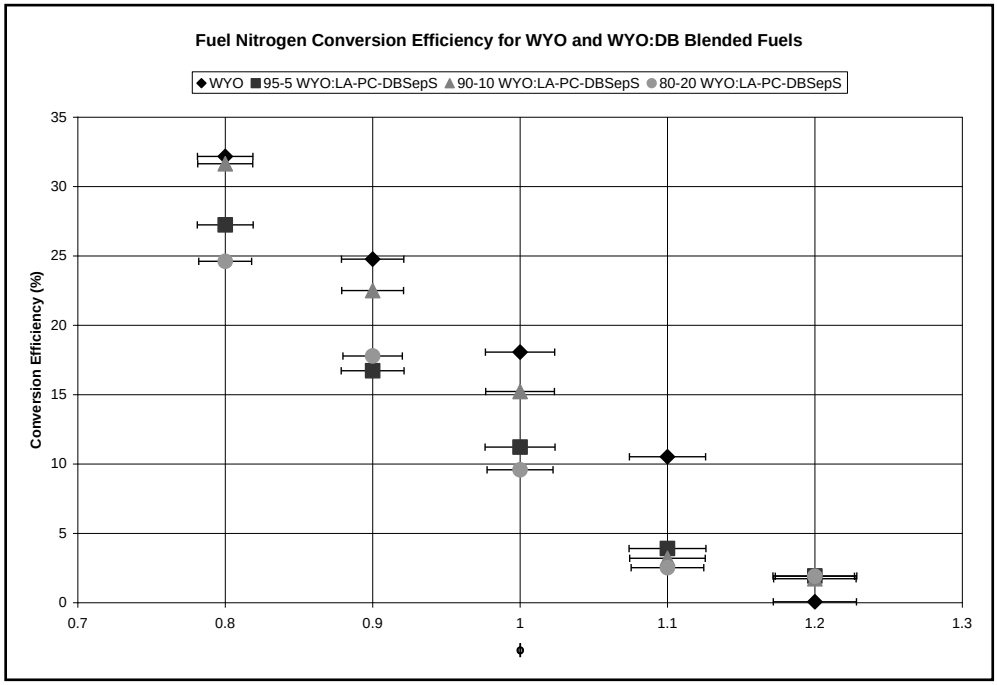

Figure 3.5.8.2. Effect of fuel on nitrogen conversion efficiency for WYO and WYO:DB blended fuels. Note that the conversion efficiency is less than coal for almost all WYO:DB blended fuels.

3.6. Impact on Tasks due to Industrial Advisory Committee feed back

1. Low ash FB and DB were recommended for cofiring ; however low ash requires specially paved surfaces. Paving feedpens may not pay out considering animal performance. Industry has problems with hard-surfaced pen surfaces and thus may need to find other uses for manure ash and other technologies for use of high ash FB and DB. . Further 90% of dairies in the High Plains use sand bedding which will result in high ash. Gasification experiments were performed since it can handle high ash FB and DB [see Task A-5]. Further whether the fly ash produced from cofiring can be used as supplemental material with cement. [See results under task A-9]
2. "Dairy biomass is more fibrous and hence more difficult to grind" ; thus it may be used in gasification (Task A-5)
3. "Feedlot operators: LAFB does not exist; should develop technologies for high ash FB; need scalable technologies" See task A-5.

3.7. Summary

All tasks were completed except for the effect of firing high Cl biomass char with coal to investigate its effect on elemental Hg. This was replaced with a new task on bench scale studies performed on "Sorption of Elemental Mercury by Chlorinated Carbons Made of Dairy Biomass, "by Andreas Jaeger Texas A&M University, 12/18/2008. A condensed version was included on p 411-413 (which deals with NOx and Hg reduction under Co-firing (Task A-3) and reburn (Task A-4) for NOx and Hg reduction) the major conclusions of this research are:

1. DB had a lower heat content due to less fixed carbon, more oxygen, and more ash; furthermore it contained more fuel bound nitrogen.
2. DB can be successfully blended with coal and cofired in a furnace.
   - Cofiring has minimal effect on burnt fraction.
   - BF was independent of fuel type. BF was almost unity when operating near stoichiometric.
   - DB fuels converted produced more NO_x due to greater fuel bound nitrogen percentages, however; they converted a lower percentage of fuel bound nitrogen to NO_x.
   - Cofiring increased NO_x in lean combustion, however; NO_x was reduced by blending coal with DB in rich combustion.
3. Blending of fuel by more than 90-10 was beyond practical limitations imposed by the high ash percentage in DB fuel.

High ash content of HA-PC-DB-SoilS made it a poor quality fuel.

3.8. Acronyms and symbols

AB	Agricultural Biomass
b	Pre-exponential Constant Used in Size Distribution Analysis
BF	Burnt Fraction
BTU	British Thermal Units
CAFO	Confined Animal Feeding Operation
CB	Cattle Biomass
CMF	Cumulative Mass Fraction
CO	Carbon Monoxide In Exhaust Gas Stream
CO_2	Carbon Dioxide In Exhaust Gas Stream
DAF	Dry Ash Free
DB	Dairy Biomass
DOE	Department Of Energy
DTA	Differential Thermal Analysis
FB	Feedlot Biomass
FC	Fixed Carbon
FS	Full Scale
ft^2/hd	Foot Squared per Head
GJ	Gigajoule
HA-PC-DB-SoilS	High Ash Partially Composted Dairy Biomass Soil Surfaced Pens
HHV	Higher Heating Value

kJ	Kilojoule
kW	Kilowatt
LA-PC-DB-SepS	Low Ash Partially Composted Dairy Biomass Separated Solids
lb	Pound
LB	Litter Biomass
m^2/hd	Meter Squared per Head
m^3	Meter Cubed
mmBTU	Million British Thermal Units
n	Exponential Constant Used in Size Distribution Analysis
NO_x	Nitrous Oxides In Exhaust Gas Stream
O_2	Oxygen In Exhaust Gas Stream
$O_{2,A}$	Oxygen In Ambient Air
PC	Partially Composted
PM	Particulate Matter
PPM	Parts Per Million
SCFH	Standard Cubic Feet Per Hour
Sep	Separated
SLPM	Standard Liters Per Minute
SMD	Sauter Mean Diameter
SO_2	Sulfur Dioxide
TCEQ	Texas Commission on Environmental Quality
TGA	Thermo-gravimetric Analysis
TSP	Total Suspended Particles
TXL	Texas Lignite Coal
VM	Volatile Matter
WYO	Wyoming Powder River Basin Coal (a sub bituminous coal)
X_i	Measured Value from Instrument I (Used in Uncertainty Analysis)
Y_i	Mass Fraction of Compound i
ϕ	Equivalence Ratio
ϕ_{flow}	Equivalence Ratio based upon fuel and air flow rates
ϕ_{flue}	Equivalence Ratio based on exhaust gas analysis
μg	Microgram

3.9. References

Annamalai, K., I. K. Puri, (2007) *Combustion Science and Engineering*, CRC Press, Taylor and Francis Group, Boca Raton, FL.

Annamalai, K., J. Sweeten, S. Mukhtar, B. Thien, G. Wei, S. Priyadarsan, S. Arumugam, K. Heflin, (2003a) Co-firing Coal: Feedlot and Litter Biomass (CFB and CLB) Fuels in Pulverized Fuel and Fixed Bed burners, Final DOE Report , DOE-Pittsburgh Contract # 40810.

Annamalai, K., J. Sweeten, S. Priyadarsan, S. Arumugam, (2006) Energy Conversion *in The Encyclopedia of Energy Engineering and Technology*/Ed. B. Capehart. Taylor and Francis Group, Boca Raton, FL.

Annamalai, K., B. Thien, J. Sweeten, (2003b) Co-firing of coal and cattle feedlot biomass (FB) fuels. Part II. Performance results from 30 kW_t (100,000) BTU/h laboratory scale boiler burner. *Fuel*, **82**(10), 1183-1193.

Arumugam, S., K. Annamalai, B. Thien, J Sweeten, (2005) *Int. National Journal of Green Energy*, **2**, 409-419.

ASTM Standard C136-06. (2006) Director V.A. Miller. **4**(2) ASTM International, Baltimore, MD.

Babcock and Wilcox. (1978) *Steam: It's Generation and Use*. Babcock and Wilcox. New York.

Carlin, N., K. Annamalai, J. Sweeten, S. Mukhtar, (2007) I*nt. National J of Green Energy*, in press.

Di Nola, G., (2007) Biomass Fuel Characterization for NO_x Emissions in Co-firing Applications, Ph.D. dissertation, Delft University of Technology, Delft, The Netherlands.

E-Instruments, (2003) Instruction Manual for Greenline 6000 and Greenline 8000. E-Instruments Group LLC Langhorne, PA.

Frazzitta, S., K. Annamalai, J. Sweeten, (1999) Performance of a burner with coal and coal–bio-solid fuel blends. *Journal of Propulsion and Power* 15(2), 181-186.

Goughnour, P., (2006) NO_x Reduction with the Use of Feedlot Biomass as a Reburn Fuel, M.S. Thesis, Texas A&M University, College Station, TX.

Heflin, K. and J. Sweeten (2006) Preliminary interpretation of data from proximate, ultimate and ash analysis, results of June 7, 2006 samples taken from feedlot and dairy biomass biofuel feedstocks at TAES/USDA-ARS, Bushland, TX Texas Agricultural Experiment Station, Texas A&M Agricultural Research & Extension Center Amarillo/Bushland/Etter, TX.

Kegel, T.M., (1996) Basic measurement uncertainty. *71st International School of Hydrocarbon Measurement*, April 9-11, Oklahoma City, OK. 1-7.

Kline, S.J., and F.A. McClintock, (1953) Describing uncertainties in single sample experiments. *Mechanical Engineering*. **75**(1), 3-8.

Lundgren, J., Pettersson, E., (2002) Combustion of horse manure for heat production. Technical Report, NIFES.

Miller, B.G., S. F. Miller, A. W. Scaroni, (2002) Utilizing agricultural by-products in industrial boilers: Penn State's experience and coal's role in providing security for our nation's food supply, *Nineteenth Annual International Pittsburgh Coal Conference*, Pittsburgh, PA. 23-27.

NASS, (2002) U.S. Dairy Herd Structure, National Agricultural Statistics Service, Agricultural Statistics Board, U.S. Department of Agriculture, Washington, DC.

Schmidt, D.D., V. S. Pinapati, (2003) "Opportunities For Small Biomass Power Systems." Final Technical Report. Prepared for U.S. Department of Energy Chicago Operations Office. DOE Contract No. DE-FGO2-99EE35 128.

Stokes, S., and M. Gamroth, (1999) Freestall Dairy Facilities in Central Texas, Texas A&M University, Texas Agricultural Extension Service. Available at: http://animalscience.tamu.edu/ansc/publications/dairypubs/15311-fresstalldairies.pdf. Accessed on October 17, 2005.

Sweeten, J.M., (1979) Texas Agricultural Extension Service Publication L-1094, Texas Agricultural Extension Service, Texas A&M University, College Station, TX.

Sweeten, J.M., (1990) Texas Agricultural Extension Service Publication B-1671, Texas Agricultural Extension Service, Texas A&M University, College Station, TX.

Sweeten, J.M., K. Annamalai, B. Thien, L. McDonald, (2003) Co-firing of coal and cattle feedlot biomass (FB) fuels, part I: feedlot biomass (cattle manure) fuel quality and characteristics *Fuel* **10**, 1167-1182.

Thien, B., (2002) Cofiring With Coal – Feedlot Biomass Blends, Ph.D. dissertation, Texas A&M University, College Station, TX.

Tillman. D.A., (2000) Biomass cofiring: the technology, the experience, the combustion consequences, *Biomass and Bioenergy* **19**, 365-384.

Tranchida, T., (2007) Cattle manure production, Available at: www.dpi.qld.gov.au/environment/5166.html.

Volk, T.A., *L.P. Abrahamson, E.H. White, E. Neuhauser, E. Gray,* et al., (2002) Biomass, Available at: http://en.wikipedia.org/wiki/Biomas

3.10. Education and Training

This work was used for partial completion of an MS thesis for Ben Lawrence (2007)

3.11. Other support

None

3.12. Dissemination

Annamalai, K., Carlin, N.T., Oh, H., Gordillo-Ariza, G., Lawrence, B., et al. (2008) "Thermo-Chemical Energy Conversion of Coal, Animal Waste Based Biomass, and Coal:Biomass Blends." *19th National and 8th ISHMT-ASME, Heat and Mass Transfer Conference*, January 3-5, 2008: JNTU Hyderabad, India.

Annamalai, K., Carlin, N.T., Oh, H., Gordillo-Ariza, G., Lawrence, B., et al. (2007) "Thermo-Chemical Energy Conversion Using Supplementary Animal Wastes with Coal." *Proceedings of the IMECE, 2007 ASME International Mechanical Engineering Congress and Exposition*, November 11-15, 2007: Seattle, WA, USA.

Annamalai, A. Udayasarathy, Hyukjin and Sweeten, JM, ," Mercury Emission And Control For Coal Fired Power Plants, pp 205-217, ISBN 978-81-8487-014-5, Book Edited Agarwal, AK, Kushari, A, Aggarwal, S K and Ruchai , AK, Narosa Publishing House, New Delhi,2009

Carlin, N.T., Annamalai, K., Oh, H., Gordillo-Ariza, G., Lawrence, B., et al. (2008) "Co-Combustion and Gasification of Coal and Cattle Biomass: A Review of Research and Experimentation." *Progress in Green Energy*.

Lawrence, B., Annamalai, K., Sweeten, J.M., (2007) "Performance of Small Scale Boiler Burner Fired with Blends of Coal and Dairy Biomass." *5th US Combustion Meeting Organized by the Western States Section of the Combustion Institute*, March 25-28, 2007: Sand Diego, CA, USA.

Lawrence, B., Annamalai, K., Sweeten, J., Heflin, K., "Cofiring Coal and Dairy Biomass in a 29 kWt Furnace." Applied Energy (2009) Vol. 96, pg. 2359-2372

Hyukjin Oh and Kalyan Annamalai, and John M. Sweeten "Effects of ash fouling on heat transfer during combustion of cattle biomass in a small-scale boiler burner facility under unsteady transition conditions **International Journal of Energy Research** , 2010 DOI: 10.1002/er.1768

Hyukjin Oh and Kalyan Annamalai, and John M. Sweeten "Investigations of Ash Fouling with Cattle Wastes as Reburn Fuel in a Small Scale Boiler Burner under Transient Conditions, " ***J of Air and Waste Management Association***, 58:517–529 (2007)

K.Annamalai, J. Sweeten, S.Priyadarsan, and S. Arumugam, Invited Article on " Energy Conversion Energy Conversion: Principles for Coal, Animal Waste, and Biomass Fuels, " ***Encyclopedia of Energy Engineering and Technology*** , Edited by Barney Capehart, Tyler and Francis, ISBN # 978-0-8493-3653-9; pp 476-497(2007). Total pages 1800 **{Energy Conversion Paths, Review, FutureGen}**

S.Arumugam, K Annamalai , Ben Thien and , J Sweeten, "Feedlot Biomass Co-firing: A Renewable Energy Alternative for Coal-fired Utilities," ***Int. National J of Green Ener***gy,Vol. 2, No. 4 , 409 – 419, 2005.

Hyukjin Oh, Annamalai, K., John M. Sweeten, Christopher Rynio, and Witold Arnold, “Combustion Of Cattle Biomass As A Supplementary Fuel In A Small Scale Boiler Burner Facility For NOx And Mercury Reduction, “ IMECE2009-12626, Proceedings of IMECEC2009, 2009 ASME International Mechanical Engineering Congress and Exposition, November 13-19, Lake Buena Vista, Florida, USA.

Kalyan Annamalai, “Thermo-chemical Energy Conversion of Coal, Animal Waste Based Biomass, and Coal:biomass Blends, “19th National & 8th ISHMT-ASME Heat And Mass Transfer Conference, January 3 - 5, 2008, ASME -ISHMT, Hyderabad, India, Jan 3-5, 2008. pp

K. Annamalai, N.T. Carlin, H. Oh, G. Gordillo Ariza, B. Lawrence, And U. Arcot V, J.M. Sweeten K. Heflin, W.L. Harman “ Thermo-Chemical Energy Conversion Using Supplementary Animal Wastes With Coal , “, Invited Key Note Presentation, 2007 ASME International Mechanical Engineering Congress and Exposition, November 11-15, 2007 Seattle, Washington, USA; IMECE2007-43386; CROSS LISTED UNDER INVITED LECTURE

S.Arumugam, KAnnamalai , Ben Thien and , J Sweeten, “Feedlot Biomass Co-firing: A Renewable Energy Alternative for Coal-fired Utilities,” IGEC-1, Proceedings of the International Green Energy Conference 12-16 June 2005, Waterloo, Ontario, Canada, Paper No. IGEC-1-128

4. REBURN FOR NOX REDUCTION

Task A-4 (KA): Reburn Process

Task A-4-1: Reburn experiments using FB and DB as reburn fuels, and measurements of fuel-N in the form of NH3 and HCN

Accomplishments: All proposed objective have been achieved except that the attempts have been made to measure NH3, HCN using Mass Spectrometer during experiments yielded inconclusive results.

Task A-4-2: Reburn experiments for reducing Hg emissions (Two different solid fuels)

Accomplishments: All proposed objective have been achieved.

ABSTRACT

Combustion of cattle biomass (CB) as a supplementary fuel has been proposed for reducing emissions of NO_x, Hg, SO_2, and nonrenewable CO_2 in large coal-fired power plants. It has benefits to power industries for lowering coal consumption and fuel costs and to animal industries for disposing burdensome agricultural wastes from large animal feeding operations. In order to develop environmentally friendly thermo-chemical energy conversion technologies that can utilize CB for NO_x and Hg reductions in existing coal-fired power plants, reburning experiments involving CB and coal were performed in a small-scale 30 kW_t (100,000 Btu/h) downward fired boiler burner facility. The reburning are mainly presented and discussed. The results show that the pulverized CB can serve as a supplementary fuel for the coal-fired boilers, and combustion of the CB with coals shows reductions in NO_x emissions. It is believed that 1) most of the fuel-nitrogen in the CB existed in forms of NH_3 or urea which led the high NO_x reductions. The equivalence ratio (ϕ), an inverse value of the stoichiometric ratio, was considered as a key parameter to achieve high NO_x reductions. Higher NO_x reductions were measured under fuel-rich conditions ($\phi > 1.0$).

4.1. Introduction

Co-combustion of animal waste/biomass (AnB) and coals in traditional coal-fired power plants is an option for the combined renewable and fossil energy application to reduce environmental impacts of fossil fuel combustion. The major environmental benefits of co-combustion of AnB and coals are low emissions of traditional pollutants (NOx, Hg, SOx, etc.) and lower net greenhouse gases (CO2, CH4, etc.). Co-combustion with AnB also offers a solution to manure disposal issues. The AnB includes cattle manure, poultry litter, hog manure, horse waste, swan waste, etc. Cattle manure/biomass (CB) has been proposed as a renewable, supplementary fuel, and its energy conversion technologies involve adapting and developing technologies to extract energy from waste streams or renewable resources through five processes as shown in Figure 4.2.1 [K.Annamalai, et al ASME 2007.]: 1) Anaerobic digestion (or biological gasification), 2) Thermo-chemical gasification/pyrolysis of high ash and wet CB, 3) Small-scale on-the-farm direct combustion, 4) Co-firing CB with coals in existing power plants, and 5) Combustion of CB as a reburn fuel.

The co-combustion techniques of CB and coals such as co-firing and reburning were investigated to develop alternative ways of disposing CB and control emissions, especially NOx and CO2 [K.Annamalai, et al., 2007, K. Annamalai, et al 2003, J.M. Sweeten, et al 2003; Thien 2002.]. Co-firing 10% CB with coals reduced NOx emissions by about 10% [Annamalai 2003]. Though reburning CB with coals needs an advanced boiler configuration indicating the higher investment for equipping the existing power plants with the reburn technology, the CB as a reburn fuel is possibly more effective and economical than natural gas (NG) .

4.2. Literature review

Many forms of air pollution are emitted during the combustion of coal. Nitrogen Oxides is considered one of the major pollutants emitted during fossil fuel combustion NOx is produced when fuel is burnt with air. The N in NOx can come from both the N containing fuel compounds (e.g. coal, biomass, animal waste) and from the N in the air. The NOx generated from fuel N is called fuel NOx, and NOx formed from the air is called thermal NOx. Typically, 75 % of NOx in boiler burners is from fuel N. The NOx and volatile organic compounds released from automobiles, utilities etc. react in the presence of sunlight and produce ozone or smog (approx. 0.08 ppm), which can damage cells in the lung's airways, causing inflammation. The uncontrolled NOx emissions in industrial boilers are : 43-129 g/GJ (0.1-0.3 lb per mmBTU) for natural gas and 86-172 (0.2-0.4) for distillate oil while coal produces 86-258 (0.2-0.6) for stoker fired and 215-387 (0.5-0.9) for wall tangentially and wall fired units. Thus, it is mandated that NOx, a precursor of smog, be reduced to 0.40 to 0.46 lb/mmBTU for wall and tangentially fired units under the Clean Air Act Amendments (CAAA). With approximately 40% of world electric power generation coming from coal fired utilities [Energy Information Administration 2006] improved methods for controlling this emission are necessary. The current technologies developed for reducing NOx include: combustion controls (e.g. staged combustion or low NOx burners LNB, reburn) and post combustion controls (e.g. Selective Non-Catalytic Reduction, SNCR using urea, etc

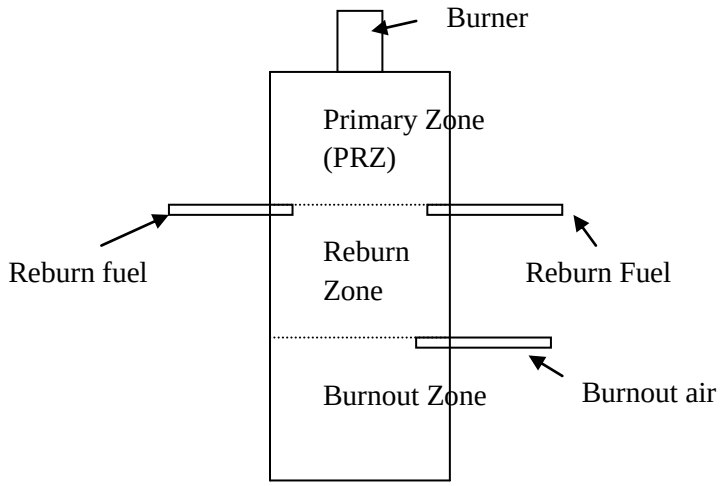

Figure 4.2.1. Reburn zones

In reburning, additional fuel (coal or natural or gas) is injected down stream from the primary combustion zone to create a fuel rich zone where NO_x is reduced through reactions with hydrocarbons. The nitrogen in the reburn fuel then recombines with oxygen to form NO_x, or combines with N to form N_2. After the reburn zone, additional air is injected in the burnout zone to complete the combustion process. A diagram of the entire process with the different combustion zones is shown in Figure 4.2.2. This process is somewhat similar to air staging where the fuel is first burnt in a rich primary zone to minimize the production of NO_x, and later air is injected to complete the combustion process.

There have been numerous studies on reburn technology found in the literature, the experiments conducted and the important results summarized in . The NOx reduction technologies include post combustion gas treatment: 30-90 % reduction, flue gas recirculation (5-60 %), etc. The use of biomass for combustion is favorable to utilities and scientists because it is a CO2 neutral fuel. CO2 neutral fuels are generally derived from plant material which absorbs CO2 during photosynthesis and then releases the CO2 back into the environment when combusted. Common biomass fuels used include wood, straw, animal waste, sugarcane residue, olive residue, sewage sludge, and municipal solid waste.

While past research essentially deals with reburning with coal, agricultural biomass, and natural gas, recent research is concerned with use of animal manure as a reburn fuel. In the Texas high plains area, beef cattle are fattened for slaughter in large pens known as feedlots. The manure produced by these operations can cause environmental degradation if not properly disposed of or used as fertilizer. Thus, research was conducted proposing (Frazzitta et al, 1999) that the manure be collected, dried, pulverized, and used as a reburn fuel. Previous attempts to use feedlot manure as a fuel source have met with only limited technical success, due to flame stability problems caused by its high ash and moisture combined with its low heating value. Previous research performed at the Texas A&M 100 kW Boiler Burner Facility followed by pilot plant tests at National Energy Technology Laboratory of DOE-Pittsburgh indicate that feedlot biomass can be co-fired with coal in conventional boiler burners. In this approach, the high temperatures produced by the coal allow for the successful combustion of the FB. Even though the N of FB is twice as high as compared to coal on mass basis, the NO emission with 90:10 blend cofiring is similar or less compared to coal. It is believed that most of the N in FB exists as NH3

and volatile matter of FB is twice that of coal. Since the feedlot manure has uses as a renewable energy source, and a reburn fuel, it will now be referred to as feedlot biomass (FB).

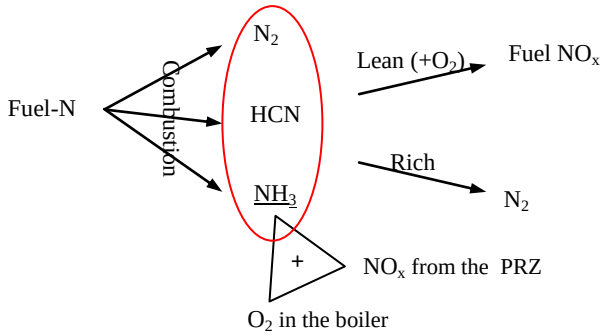

Figure 4.2.2. NOx Formation And Reduction Paths By Fuel-N Depending On The Stoichiometry

The review of the literature has shown that the effectiveness of the reburn process depends on a number of variables, as listed below:

Temperature: under reducing conditions of the reburn zone, a higher temperature will result in better NO reduction.

Turbulence or Reburn jet mixing: A high degree of mixing in the reburn zone is necessary for NO reduction.

Time -Residence: The longer the reburn zone residence time, the lower the NOx emission. The residence times required for gaseous reburn fuels are shorter than the time required for solid fuels. The first three variables are informally known as the three "T's" required for effective reburn.

Fuel Type: The fuel type does have an effect on the NO levels. Special care must be taken in using high nitrogen fuels to ensure that NO is not produced in the burnout zone.

Oxygen concentration: A lower oxygen concentration in the reburn zone will result in lower NO.

Reburn zone stoichiometry: This is the most important parameter. Experiments show that there is an optimum reburn stoichiometric ratio (SR), usually between SR 0.7 and 0.9. This does not seem to be a constant across all experiments, but changes with experimental conditions.

Coals contain approximately 1 ~ 2% nitrogen (N), which is called fuel-N, and its amounts depend on the rank of the coal. Unlike coals, fuel-N content in biomass can vary widely: wood, straw, sawdust, and corn residue contain less than 1%, FB contains 3 ~ 4%, poultry litter biomass contains 1 ~ 5%, and meat and bone meal contain 9 ~ 11% on a dry ash free (DAF) basis [Sweeten, et al 2003; Yang, Y.B. et al 1997]. Fuel-N is released to the gas phase during coal and biomass combustion and could either finally form NO_x in fuel-lean combustion and N_2 in fuel-rich combustion. These reactions are shown in Esq. (1), (2) and (3) and in Fig. 1, and. Also, fuel-N released from coal and biomass could be in the form of HCN and/or NH_3. The CB contains more fuel-N in the form of urea compared to coal. For most coal-fired boilers fuel NO_x contributes about 75% of the total NO_x emissions, and the mechanisms of fuel NO_x formations in a primary combustion zone (PRZ) and NO_x reductions in a reburn combustion zone (RBZ) are presented in Fig. 1.(?? where is RBZ in fig. 1??) Though it is

found that the fuel-N plays a fundamental role in the formation and reduction of NO_x, there are a few systematic studies [Di Nola, G., 2007] on the characterization of fuel-N in coal and biomass.

$$4NH_3 + 6NO \rightarrow 5N_2 + 6H_2O$$

$$4NH_3 + 4NO + O_2 \rightarrow 4N_2 + 6H_2O$$

$$4NH_3 + 5O_2 \rightarrow 4NO + 6H_2O$$

In typical power plants, the primary zone (PRZ) is typically maintained in slightly fuel-lean combustion ($\phi_{PRZ} < 1.0$), while the RBZ is kept in fuel-rich combustion ($\phi_{RCR} > 1.0$) for most effective NO_x reduction. In the reburn process, coal is burned into the PRZin fuel-lean conditions, and most fuel-N from the coal is converted to NO_x during the combustion. The combustion gas including NO_x enters the RBZ in which a fuel-rich mixture of reburn fuel is burned. Some of fuel-N from the reburn fuel is forms HCN and/or NH_3 in the RCR. Thus the NO_x produced in the PRZ is destructed in the RBZ by a reverse prompt NO_x reaction, that is, HCN and NH_3 produced from the reburn combustion react with NO_x to reduce it to harmless N_2. At the downstream, overfire air (OFA) is injected into the combustor to complete the combustion process. The most common reburn fuel is natural gas (NG). Table 1 presents some of recent reburn studies and their operating conditions [Thien 2002; Carpi 1997; Agarwal 2006; Gibb 2000; Cao 2005; Hall 1991; Laudal 2003; Sable 2007a, 2007b]. Most of reburn studies using NG or coals as reburn fuels show lower than 70% NO_x reductions, while results with biomass-type fuels presents up to 95% NO_x reductions.

Yang et al. (1997) investigated the use of eight different coals as reburn fuels. They used a downward-fired 0.2 MW furnace with a propane burner mounted on top. Further downstream, coal was injected and gas samples were taken at sampling ports with a water-cooled sampling probe. At the end of the furnace, a water spray cooled the gases, and the gases were exhausted. NO was created in the primary zone by premixing propane with ammonia and injecting it into the furnace. It was found that nearly all ammonia was converted to NO to create a NO concentration of approximately 600 ppm

The most common type of biomass used was a wood chip and in all of the cases it was reported that the biomass served as an acceptable reburn fuel. Rudiger et al (1996) report on the use of coal, straw, sewage sludge, wood, and their pyrolysis products as a reburn fuel. They found that all of the fuels tested resulted in a reduction of NOx to acceptable levels, with coal pyrolysis products being the most effective. The low cost of biomass and its availability make it ideal source of pyrolysis gas, which is a more effective reburn fuel than the main source fuel, which is typically coal. Kicherer et al (1993) investigated coal, straw, natural gas, and fuel oil. They found that reburning with straw biomass yielded results that were similar to the coal, natural gas, and fuel oil. Miller et al (1996) used a propane burner to simulate furnace gases, and then used a tire-derived fuel (TDF) as a reburn fuel. They found that TDF could successfully be used as a reburn fuel. The new renewable energy technology using biomass as reburn fuel is beneficial to both the operators of coal fired boilers.

When co-firing pine sawdust with coal, it was found that NOx levels and unburned carbon in the fly ash increased when the same grinder was used to pulverize the coal and sawdust. This increase was attributed to larger coal particle sizes and the moisture in the wood causing a delay in the ignition of the coal and biomass. It is recommended that separate coal and biomass grinders and separate feeding systems be used to ensure that the biomass does not cause the coal grinders to perform poorly.4

Another research group determined that it should be possible to achieve 45% NOx reduction using sawdust as a reburn fuel with air as the carrier gas. A 55 % reduction is possible when using re-circulated flue gas as the carrier. This level of reduction was achieved under only the best mixing setup,

opposed fired reburn injectors and overfire air injectors. They report that their results are consistent with other results showing a 60% reduction in NOx.5

Municipal solid waste (MSW) is another biomass commonly combusted. It is reported by Patumsawad6 that MSW can be co-fired with coal in fluidized bed combustors. He reports that the high ash content of the MSW reduces the combustion efficiency approximately 12% when firing 20% MSW by mass. It was also reported that there was less SO2 emissions because of the low SO2 content of the MSW and more CO emissions caused by a lower bed temperature.

In Germany, [Storm et al 2005] did considerable research with sewage sludge, straw, and Miscanthus Sinensis, a feedstock. They found that each of these biomasses reduce NOx emissions when they are used as reburn fuels in coal fired plants. For large particle sizes, a long residence time was needed to completely burn the biomass. The Miscanthus and straw also reduced the SO2 emissions due to their low levels of sulfur. SO2 emissions rose for the sewage sludge because there was a higher level of sulfur in the sludge than in the coals used.

Also in Germany, [Hartmann and Kaltschmitt, 1999] found that firing 10% straw or residual wood in an existing power plant reduces all investigated emissions. The straw reduced the emissions of NOx and SO2 by (Table 4.2.1) approximately 46% and 80% respectively. The residual wood had even better results with NOx and SO2 reduction of 66% and 95% respectively. These measurements were taken after desulphurization and denitrification treatments were performed. They concluded that the use of biomass for co-combustion is beneficial to the environment as compared to using only coal.

Annamalai et al. used cattle feedlot biomass for co-firing [Annamalai K, et l 2003; Annamalai et al 2003b, Arumugam et al 2003, Arumugam et al 2005]. Nitrogen oxides emission control through reburning with biomass in coal-fired power plants. Master's Thesis, Texas A&M University; 2004].. They found that the co-firing 10% biomass reduced NOx emissions by about 10 %, but the CO emissions increased. They suggest that the higher volatile matter in the feedlot biomass depletes the oxygen rapidly, which inhibits NOx formation. Also, it may be possible that the nitrogen in the fuel is released as NH3, which reacts with NOx to create N2. Further, it was reported that co-firing 20% biomass reduced NOx even more. It is not clear whether Stoichiometry or some other effect caused the NOx reduction.

The first ever reburn studies funded by Texas Advanced Technology Program [Texas ATP]:found that firing cattle feedlot biomass in the reburn stage of a coal fired power plant can reduce NOx emissions by as much as eighty percent under certain conditions [Ben Thien 2002]. In further research it was found that using feedlot biomass as a reburn fuel could reduce NOx by as much as 62% or five times greater than the reduction achieved with coal as the reburn fuel [Arumugam S. 2004]. He also found that a flat spray injector or an injector that has an oval exit provided better NOx reduction due to better mixing.

These reburn experiments were conducted with FB and Wyoming sub bituminous coal. These experiments focused on what type of injector would provide the greatest level of NOx reduction. The experiments showed that injectors that decrease the mixing time and increase the residence time in the reburn zone give better NOx reduction.3

Table 4.2.1 Literature review on reburn articles

Author	Reburn Fuel	Reburn minimum SR	Particle size	Temp	Residence time	Burnout zone	Max Reduction	Conclusion
Adams et all, 1998	Wood	0.9	1/16 to 1/32 in	1370 °C	.4 to 1.2 s	YES	55%	Wood can successfully used a reburn fuel in a cyclone combustor
Bilbao et al, 1994	Natural Gas	N/A	gas	1200-1500°C	98-280 ms	NO	<90%	Found that high temperature and low oxygen are good for NO reduction
Bilboa at al, 1995	Natural Gas	0.94	gas	1200 - 1500°C	95-280 ms	YES	95%	Successful reburn at temperatures above 1200°C
Bilbao et al, 1997	Natural gas, methane, ethane	0.93	gas	1100 °C	220 ms	NO	87.5%	Reburning with natural gas most effective at 0.93 SR
Chen et al 1996	Coal, and coal char	0.8 for those that reached a min	NA	1100 °C	.2 s	NO	80-95%	Heterogeneous mechanisms accounted for the majority of the NO_x reduction, chars can be used in reburning
Kicherer et al. 1993	Coal, natural gas straw, light fuel oil	minimum at 0.76, but little change after 0.85~0.9	2, 15, 30, 40 wt % <90 μm	NA	.5 to 1.3 seconds, NO continually decreasing	YES	77.6%	To maximize NO reduction: small particles, high volatile fuel, long residence time, good mixing
Maly, P. et	natural gas, coal, pond fines,		~200 μm	1430 °C	.2 to .9 s	YES	70-95%	Alternate fuels can be more effective than

al, 1999	RDF, Orimulsion, and wood							reburning with natural gas
Miller et al, 1996	Tire derived Fuel, and Natural gas	NA	< .25 in	1260° C – 820 °C	NA	YES	63%	TDF can be used successfully as a reburn fuel
Smart, J. et al 1994	Coal, Fuel oil, natural gas, and Coke oven gas	0.81	95% < 75 μm	1150-1250°C	NA	YES	88.7%	NOx reduction and the burnout were not greatly affected by the fuel type
Spliethoff et al, 1996	coal, pyrolysis gas, and methane	0.8~.85	.5% >90 μm	1000-1400 °C	.2 to 2	YES	87.5%	pyrolysis gas the best, longer residence time a lower NO_x concentration
Yang et al 1997	Coal	< 0.92	75% < 63 μm and 100%< 63μm	1325 °C	120-840 ms no effect beyond 450 ms	YES	65%	The reburn Stoichiometry is the most important factor, fuel nitrogen content does not have a large effect on burn out NO

4.3. Objectives

Solid fuels fired in boiler furnaces typically release N in the form of NH_3, HCN and N_2. The CB contains more N in the form of urea compared to coals; thus the investigators of the current study have hypothesized that the CB releases NH_3 rich compounds which react with NO_x to produce harmless N_2 under oxygen deficient conditions. The CB also contains higher amounts of Cl and thus releases Cl rich compounds (mainly HCl) when burned, which oxidizes elemental Hg to $HgCl_2$ that can be captured by SO_x and particulate control devices such as wet scrubbers. Past research at TAMU determined that FB reduced NOx emissions significantly. The use of feedlot biomass also relieves the cattle industry of the excess manure, which can itself cause adverse effects on the environment. By developing this technology, coal fired utilities can meet the NOx emissions requirements and also help the cattle industry dispose of their excess manure.

The overall objective of the current study is to develop environmentally friendly thermo-chemical energy conversion technologies for utilizing CB to reduce NO_x and Hg emissions from traditional pulverized coal-fired power plants. The specific objectives are to investigate combustion and emission behaviors during combustion of CB and coals in conventional coal-fired boilers and to study the effects of equivalence ratios (ϕ) and blending ratios on NO_x and Hg reductions.

The current research was conducted to determine what operating conditions provide the optimal levels of NOx reduction. The research experiments were conducted on a 29.3 kW (100,000 BTU/hr) downward fired furnace. The parameters of interest in this study were the equivalence ratio, reburn fuel injector angle, the effectiveness of biomass and coal mixtures, and the effects of vitiated air.

In order to achieve the objectives the following task s were performed: 1. Acquired the required amounts of pulverized biomass and coal. 2. Determined the physical and chemical properties of the fuels. 3. Modified the current burner facility for reburn experiments with 0° (lateral) and 45° injectors. 4. Investigated the effects of using different FB fuels for reburn. The reburn fuels used in this research include high-ash partially composted feedlot biomass (HA PC FB), low-ash partially composted feedlot biomass (LA PC FB), and mixtures of FB with Texas lignite coal. 5. Injected the reburn fuel with pure air and simulated vitiated air.

4.4. Experimental setup

Reburn Fuels:

Several fuels and fuel blends were used as reburn fuels. The fuels consisted of low-ash partially composed feedlot biomass (LA PC FB), high-ash partially composted feedlot biomass (HA PC FB), Texas Lignite Coal (TXL), Wyoming Sub bituminous coal (WYC), and blends of FB and TXL. Each of the fuels used and their respective ultimate and proximate analyses are listed inTable 4.5.2

Fuel Preparation

All of the biomass used for this project were collected and prepared at the Texas Engineering Experiment Station now called as Texas AgriLife Research and Extension Center in Bushland, TX and were then used during the study (Figure 4.4.1). The high-ash feedlot biomass was collected from feedlots with a soil surface and then composted in windrows for 55 days. The low-ash

feedlot biomass was collected from feedlots paved with fly ash. It was also composted in windrows for 55 days. Less soil is collected with the manure gathered from paved feedlots and therefore less ash is in the fuel. After composting the biomass, it was dried and finely ground. Powder River Basin Wyoming coal (PRB/WYC), Texas lignite coal (TXLC) and feedlot biomass (FB). WYC was selected as the base case fuel. The reburn fuel blends consisted of 70% LA PC FB/30% TXL, 50% LA PC FB/50% TXL, 10% LA PC FB/90% TXL, 70% HA PC FB/30% TXL, 50% HA PC FB/50% TXL, and 10% HA PC FB/90% on a mass basis. In addition WYC:LA PC FB blends were used. The fuels were well mixed in five gallon buckets prior to being placed in the fuel hopper of the reburn feeding system.

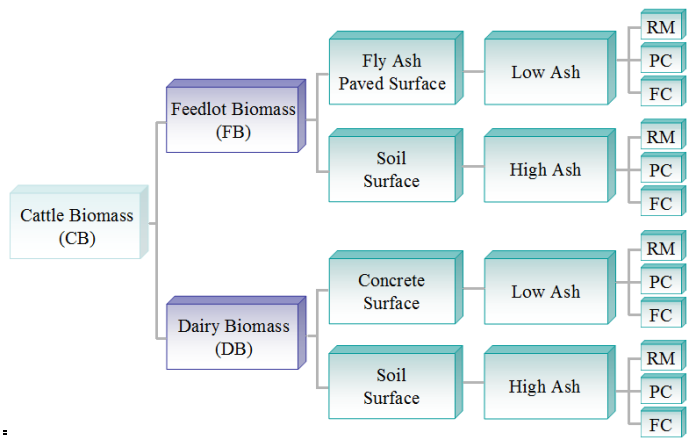

Figure 4.4.1. DB and FB Fuels – Classification

Reburn Facilities

A schematic of a small scale (30 kW or 100,000 BTU/h) boiler burner at TAMU is shown in Figure 4.4.2. It was fired with NG as a primary fuel and with coals, FB or coal:FB blends as reburn fuels. The average fuel composition was 96% methane. All other components of the fuel were in small quantities and were considered negligible. For all calculations performed for the current research, the total fuel composition was assumed to be methane The CB and coals, as reburn fuels, were fired downstream from the primary coal-fired boiler burners to explore the possibility of reducing NO_x generated by the primary coal burners. The boiler burner consisted of a 6 in (15.24 cm) diameter, 72 in (182.88 cm) long vertically down-fired combustor. The combustor was made with a steel frame containing a 2 in (5.08 cm) layer of

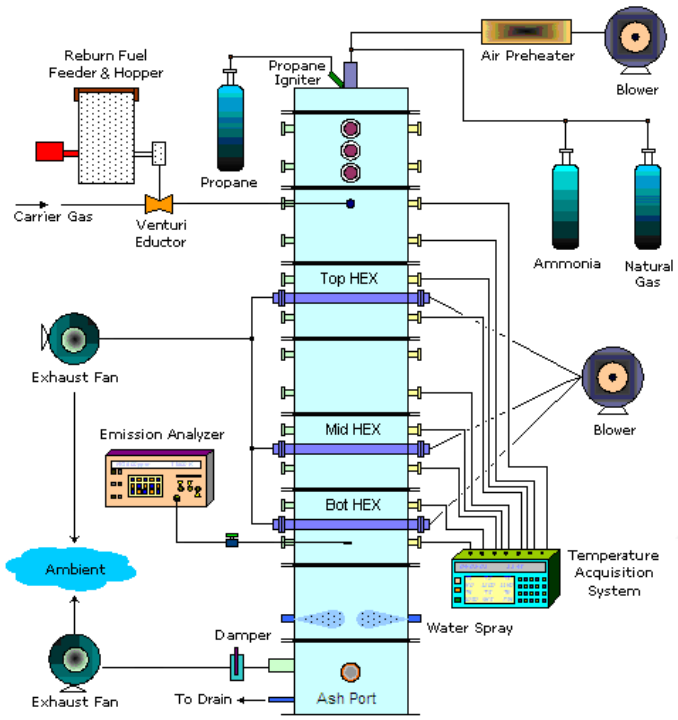

Figure 4.4.2.A schematic of the small-scale 30 kWt (100,000 Btu/h) downward fired boiler burner facility.

insulation and a 2 in (5.08 cm) section of refractory. Along the walls of the furnace there were several gas sampling ports and temperature measurements ports. The gas stream was cooled down by the jet water in the quenching area, and then the exhaust gases vented out through an exhaust system. The primary fuel (NG) and air were injected from the top into the primary combustion zone. The primary air was heated in an air pre-heater to 100°C before entering the furnace. The pre-heat temperature was varied to better control the maximum furnace temperature. Because the furnace operated at a relatively low temperature, the combustion gases were simulated by injecting propane air mixture along with a trace amount of NH3 into the primary reaction zone (PRZ), and generated 70% of the total heat (21 kW_t) under a slightly fuel-lean condition ($\phi = 0.95$). The reburn fuel and air (about 20% of total air) were injected into the reburn combustion zone (RBZ), and it produced 30% of the total heat (9 kW_t) under fuel-rich conditions ($\phi > 1.0$). The detailed information about the facility and operating conditions is described elsewhere [Oh,2008;Oh 2010]. The reburn fuel was injected into the burner laterally (0°). After the temperature in the reburn zone reached the steady state condition, the emission gas analyzer was used to determine concentrations of NOx, O2, CO, CO2, SO2, and combustibles (CxHy) at the measurement ports

Operational Conditions

The total heat input for each experiment was set to 30 kW (100,000 BTU/h). The primary combustion zone supplied 70% of the total heat (21 kW or 70,000 BTU/h) and the reburn zone supplied 30% of the total heat (9 kW 30,000 BTU/h). The primary zone combustion conditions were maintained the same for each experiment. The conditions of primary and reburn combustion

were calculated based on the following general equation (1). It should be noted that the main burner always operates under lean conditions with sulfur and nitrogen free fuel and hence d=0 and g=0. Eq (1) also allowed the control of NOx emissions to the reburn zone with the NH3 flow. It is important to maintain a fuel-lean combustion zone for the conversion of all NH3 to NOx. Using the higher heating value (HHV) of fuels, the fuel flow required for the primary and reburn combustion were calculated. The mass flow of the fuel changed for each experiment due to the variation of HHV of fuel (Table 4.5.1) so that same thermal output is maintained. With the mass flow and the ultimate analysis of the fuel, the air requirements were calculated. As established in the literature review, the Stoichiometry of the reburn zone has a large effect on the level of NOx reduction achieved in the combustion and reburn zone. The equivalence ratio (ER or φ) was varied by changing the amount of air injected with the reburn fuel. In actual power plants, typically ER (φpri) of the primary burner is maintained at a level less than one (fuel lean). The amount of air used through the reburn nozzle is varied to obtain desired equivalence ratio in the reburn zone (RZ). For the reburn zone, φreb is generally kept at a level greater than one (fuel rich). Each reburn fuel and fuel blend was fired for equivalence ratios from 1.00 to 1.15 in increments of 0.05. The equivalence ratio was varied by varying the motive airflow for the reburn fuel. The use of vitiated air in the reburn zone has also been reported to reduce NOx. It is difficult to re-circulate exhaust gases with the reactor used in this study; therefore the oxygen concentration of the motive air was reduced with nitrogen gas in an effort to simulate vitiated air. For the current studies, φ_{PRZ} was maintained at 0.95 and φ_{RBZ} was varied from 0.95 to 1.15 in increments of 0.05. The vitiated air in the reburn fuel injector was simulated by diluting the oxygen concentration with nitrogen. Since the required O2 flow must be same for desired ER in RZ, the vitiation will increase the injection velocity because there is more mass and volume flow through the reburn injectors.

The base case was considered the case of WYC reburn fuel in the conditions of the non-vitiation and lateral (0°) reburn injection without HEXs. In order to ensure that the furnace was near steady state and that temperature changes during the experiment would not affect the data, each operating condition was set and maintained until all reactor temperatures were near steady state. The reburn zone temperature for the experiments was held between 1120 and 1230 °C (2050 to 2250 °F). Each measurement consisted of several parameters including combustion gas temperature measurements in the following locations: at the reburn zone, 15.24 cm (6 in) below the reburn zone, 30.5 cm (12 in) below the reburn zone, 45.72 cm (18 in) below the reburn zone, 76.2 cm (30 in) below the reburn zone, and 137.16 cm (54 in) below the reburn zone. Wall temperature measurements were measured at 45.72 cm (18 in) below the reburn zone, 91.44 cm (36 in) below the reburn zone, and 137.16 cm (54 in) below the reburn zone.

In order to determine the level of NOx and excess oxygen present in the gas stream before the reburn zone, gas composition measurements were conducted before the reburn fuel was injected. After the level of NOx was determined and the primary zone equivalence ratio was at the desired level, the reburn fuel was fired. The levels of O2, NOx, CO, CO2, and combustibles (CxHy) were then measured 137.16 cm (54 in) below the reburn zone. After the measurements were taken, the reburn fuel was shut off and a check was done to ensure that the level of NOx generation was still consistent with the initial setting. This process was followed for each measurement [Annamalai et al, 2006; Goughnour P, 2006]. The operating conditions selected by Goughnour are as follows (Table 4.4.1)

Table 4.4.1 Primary combustion zone (PRZ) operating conditions

Primary Zone Heat Input	20.5 kW (70,000 BTU/hr)
Natural Gas Flow	30.1 SLPM (63.9 SCFH)
Primary Air Flow	320.3 SLPM (678.7 SCFH)
Ammonia Flow	0.123 SLPM (0.265 SCFH)
Equivalence Ratio	0.95

For the determination of the overall system uncertainty, possible error ranges of instruments and measurements were considered. Based on the flow fluctuations for the primary air, reburn motive air, reburn aspirated air, ammonia, natural gas, and HEX air, the error ranges of each flow meter were determined to be less than ±1.0%. The dominant uncertainty was the large fluctuation of the data reading. Finally, the overall system uncertainty was determined to be in the range of ±3.0 to ±5.3% . The repeatability was also estimated using LAPCFB and TXLC cases. The mean repeatability was found about 7.5% offset.

4.5. Results and discussion

Fuel Characterization

The higher heating values of HA PC FB and LA PC FB on a mass basis are 5207 and 13267 kJ/kg (2239 and 5704 BTU/lb) respectively. On a dry ash free basis, the heating values for LA PC FB and HA PC FB are 17865 and 20733 kJ/kg (7681 and 8931 BTU/lb) respectively. The HHV of LA PC FB is 2.5 times larger than HA PC FB on an as received basis whereas it is only 1.2 times larger for the dry ash free case. Ash and moisture content are not the only differences; however, the data shows that a large percentage of the difference can be attributed to ash and moisture. For more fuel information on the fuel compositions, see Chapter 1 .

Table 4.5.1 Average fuel compositions for all fuels in pure form

AVERAGE FUEL COMPOSITIONS								
	HA PC FB		LA PC FB		TXLC		WYC	
Proximate (%)	As Rec.	Dry	As Rec.	Dry	As Rec.	Dry	As Rec.	Dry
Moisture	17.00	0.00	19.64	0.00	38.34	0.00	32.88	0.00
Ash	53.85	64.88	16.50	20.53	11.46	18.59	5.64	8.40
Volatiles	25.79	31.07	52.33	65.11	24.79	40.20	28.49	42.45
Fixed C	3.36	4.05	11.54	14.36	25.41	41.21	32.99	49.15
HHV (kJ/kg)	5207	6274	13267	16507	14289	23172	18196	27114
DAF HHV (kJ/kg)	17865		20773		28465		29599	
	HA PC FB		LA PC FB		TXLC		WYC	
Ultimate (%)	As Rec.	Dry	As Rec.	Dry	As Rec.	Dry	As Rec.	Dry
Carbon	14.92	17.97	33.79	42.05	37.18	60.30	46.52	69.32
Hydrogen	1.39	1.68	3.65	4.55	2.12	3.44	2.73	4.06
Nitrogen	1.13	1.36	1.97	2.45	0.68	1.11	0.66	0.98
Oxygen	11.40	13.73	23.94	29.78	9.61	15.58	11.29	16.83
Sulfur	0.31	0.38	0.51	0.64	0.61	0.98	0.27	0.41
Ash	53.85	64.88	16.50	20.53	11.46	18.59	5.64	8.40
Moisture	17.00	0.00	19.64	0.00	38.34	0.00	32.88	0.00

As more fuel samples were acquired, the proximate and ultimate analyses of the tested fuels change slightly as shown in Table 4.5.1 . Other important properties of the fuels are also listed in Table 4.5.3. Compared to the properties in coals, it was found that FB contains a) higher fuel-N which can lead higher NO_x reductions if the fuel-N is released as NH_3, b) higher Cl which can lead higher Hg oxidations, c) lower Hg which can produce lower Hg emissions, and d) higher ash loadings which can cause severe fouling and slagging problems. TXLC contains less Cl and more Hg than WYC. The

properties of the fuel blends on a mass basis derived from Table 4.5.4 are presented in Figure 4.5.1. The amounts of Cl, fuel-N and ash increase with an increase in % of the FB in the fuel blends while Hg and HHV decrease

Table 4.5.2 Proximate and ultimate analyses for fuels.

	Fuels, dry		
	FB	TXLC	WYC
Ash	20.53	12.65	7.61
Volatile Matter, VM	65.11	46.75	42.52
Fixed Carbon, FC	14.36	40.60	49.87
Moisture (As Rec.)	19.64	30.46	20.86
Carbon, C	42.05	66.36	71.87
Hydrogen, H	4.55	5.02	4.49
Nitrogen, N	2.45	1.19	0.93
Oxygen, O	29.78	13.65	14.74
Sulfur, S	0.64	1.13	0.36

Table 4.5.3 Derived properties of fuels on a dry basis.

	Fuels, dry		
	FB	TXLC	WYC
Fuel-N (g/GJ)	1486	452	340
Cl (g/GJ)	550	3.27	53.5
Hg (mg/GJ)	4.52	18.7	3.39
Ash loading (kg/GJ)	12.44	4.79	2.79
HHV (kJ/kg)	16507	26400	27315

Table 4.5.4 Proximate and ultimate analyses for coals and CB

Properties	Fuels			
	WYC	TXLC	DB	FB
Proximate Analysis (%), dry				
Moisture (As Rec.)	20.86	30.46	10.14	19.64
Ash	7.61	12.65	34.95	20.53
Volatile Matter	42.52	46.75	53.90	65.11
Fixed Carbon	49.87	40.60	11.15	14.36
Ultimate Analysis (%), dry				
Carbon, C	71.87	66.36	33.72	42.05
Hydrogen, H	4.49	5.02	4.08	4.55
Nitrogen, N	0.93	1.19	2.87	2.45
Oxygen, O	14.74	13.65	23.77	29.78
Sulfur, S	0.36	1.13	0.60	0.64

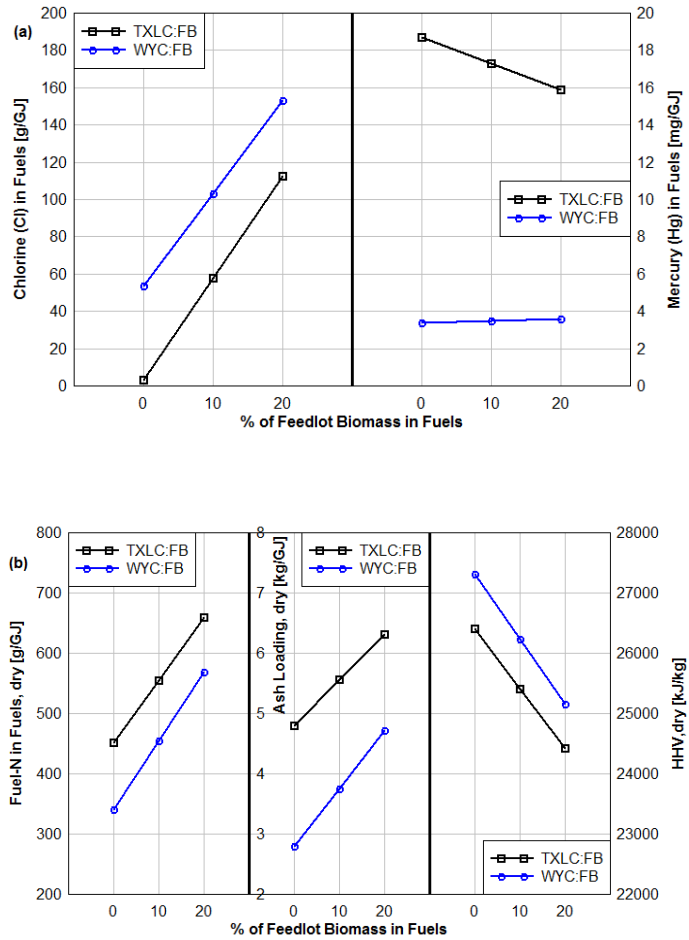

Figure 4.5.1. Properties of the fuel blends on a dry basis: (a) Cl and Hg and (b) Fuel-N, ash loading and HHV

The particle size distribution of the two fuels used in 2006 experiments is quite interesting (Table 4.5.5). A larger percentage of very small particles is found in the high ash fuel. This may suggest that the ash tends to be the smaller particles and the combustibles are larger. If this is the case, a method for removing portions of the ash from the fuel could be developed with the use of a particle size separator. Theoretically, the smaller particle sizes would heat faster, release their volatiles faster and thus reduce NO_x more readily. The HA FB does the opposite. As will be shown later, the HA FB does not reduce NO_x as well as LA FB. This is further evidence to suggest that the small particles may be primarily ash. It is also important to note that the soil in the Bushland, TX area is Pullman clay loam. The particle sizes for clay are <2 μm and the particle sizes for loam are from 2 to 50 μm.

Table 4.5.5 Fuel particle size distribution

Particle Size Distribution				
Mean Diameter (μm)	HA PC FB (%)	LA PC FB (%)	TXL (%)	WYC (%)
1596	0.01	0.05	0.01	0.0
1015	0.03	0.10	0.00	0.0
570	1.68	7.58	4.97	1.69
225	6.44	27.21	33.72	15.35
113	13.73	22.56	37.09	45.02
60	20.43	16.06	11.82	21.76
22.5	57.69	26.44	12.38	16.19
SMD	32.71	56.28	81.02	64.45

Size Distributions of Fuel Particles

Combustion of solid fuels is governed by the rate at which the oxidizers diffuse from the surrounding gases to the particle surface and by the release rate of volatiles from the particles. Thus smaller particles can heat up faster and release volatiles rapidly. The size of the fuel particles plays an important role in the reduction of local oxygen and hence their effects on NO_x emissions. In general, solid fuels used in utility boilers are about 70% of solid fuels having the particle size less than 75 μm (or 200-mesh screen) . Rosin Rammler distributions of the fuels tested are presented in Figure 4.5.2. The particle size distributions of TXLC and WYC were relatively to similar each other. The amounts of the fuel particles smaller than 75 μm were about 40-55% depending on the fuels. The proportions of the particles smaller than 53 μm were much higher for the FB than coals; however, the opposite trend was observed for the particles larger than 53 μm. Sauter mean diameters (SMD or d_{32}) are also presented in Table 4.5.5 Fuel particle size distribution. The SMD is typically used to determine the average diameter of solid fuel particles by representing particles having the same volume to surface area ratio. The SMD is 56 μm for FB, 81 μm for TXLC and 64.5 μm for WYC. The size distributions of the blended fuels can be determined by the linear combinations of the pure coals and FB distributions.

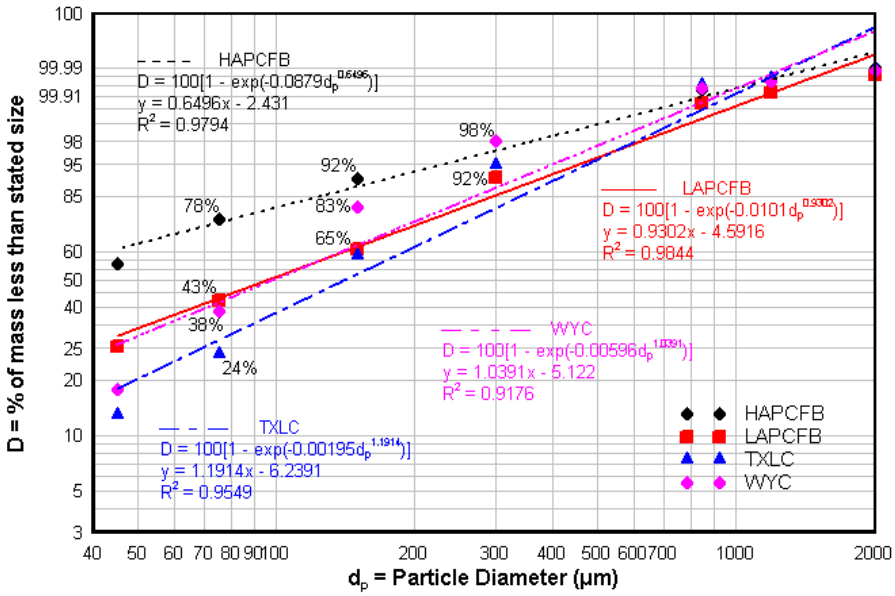

Figure 4.5.2. Particle size (Rosin Rammler) distributions of the reburn fuels

Thermogravimetric Analysis (TGA)

The pyrolysis and oxidation of the fuels were characterized by Thermogravimetric Analysis (TGA). The TGA traces in Figure 4.5.3 shows the thermal degradation of WYC during the pyrolysis using N_2 and the oxidation using air on a dry basis. The moisture loss was about 11% of the total weight. The major amounts of the volatiles seemed to be released between 200 and 600°C, and then the fixed carbon seemed to be released at temperatures slightly lower than 600°C. The residual at the end of the process was ash. Because of the presence of the oxygen, all stages took place at lower temperatures and much faster in the oxidation test compared to the pyrolysis test. It was found that the WYC was ignited near 300ºC (See Chapter on TGA/DSC analyses).

For analyzing the overall uncertainty of the experiment, the error ranges of instruments (i.e. flow meters of air, NH_3, and NG) and the fluctuations of the measurements (mainly NO_x readings) were considered. The dominant uncertainty was the large fluctuation of the data reading. The overall uncertainty was determined to be ±6.0% [Oh, 2008].

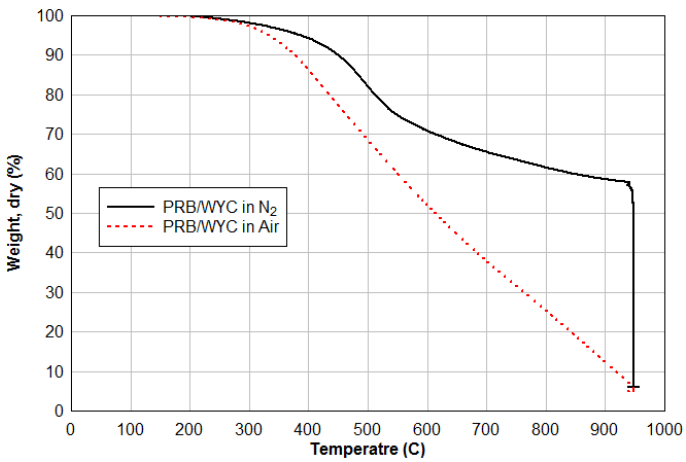

Figure 4.5.3. TGA results during pyrolysis (N2) and oxidation (air)

NO_x Reductions during Reburn Tests

Two reburn cases were conducted using pure coals: 1) TXLC as both the primary and reburn fuels and 2) WYC as both the primary and reburn fuels. The baseline concentrations of NO_x generated by the coal combustion in the PRZ were to be about 370 g/GJ for WYC and 320 g/GJ for TXLC. The RBZ equivalence ratio (ϕ_{RBZ}) was varied from 0.9 to 1.2 by changing the amount of air injected with the reburn fuel.

NOx Emission Relation

Typically for the measurement of NOx emissions, the O_2 concentration should be analyzed at the same point as NOx is analyzed and on the same basis (wet or dry). The NOx concentration should always be referred to the O_2 concentration. The representation of NOx emissions based on a 3% O_2 concentration or reference O_2 at the exhaust is suggested by EPA standards. The conversion formula for the corrected NOx concentration at 3% O_2 is represented [Sable et al 2007a; also Annamalai and Puri 2005]:

$$[NO_x]_{corr} = [NO_x]_{meas} \times \frac{O_{2,amb} - O_{2,ref}}{O_{2,amb} - O_{2,meas}} \tag{2}$$

where $[NOx]_{meas}$ is the measured NOx concentration in [ppm], $O_{2,amb}$ is the ambient O_2 percentage (20.9%), $O_{2,ref}$ is the reference O_2 percentage (3%), $O_{2,meas}$ is the measured O_2 percentage. However for reburn tests in small scale test facility without overfire air, the above method may not work since the reburn zone is typically operated under richer mode. Equation (2) can still be used for the reburn tests with overfire air. Thus the emissions of NOx and SO_2 on a thermal heat rate basis are recommended and described as below [Annamalai, et al 2003a]:

$$NO_x \ in \ (kg/GJ) = \frac{46.01 \times x_{NO_x} \times C \ fraction}{12.01 \times x_{CO_2} \times HHV \ (GJ/kg)} \tag{3}$$

$$SO_2 \ in \ (kg/GJ) \ = \ \frac{64.06 \ \times \ x_{SO_2} \ \times \ C \ \ fraction}{12.01 \ \times \ x_{CO_2} \ \times \ HHV \ \ (GJ/kg)} \tag{4}$$

where *C fraction* is the mass fraction of carbon in 'as received' fuel, *HHV* is the higher heating value of the 'as received' fuel, and *x* is mole fraction. Note that a molecular weight of 46.01 is used for NOx since all NO is eventually converted into NO_2 in the atmosphere. In Eq (3) and (4), the amount of CO is neglected, otherwise $x_{CO_2} + x_{CO}$ is used instead of x_{CO_2}.

Burnt fraction (BF) is defined as the ratio of combustibles burnt to combustibles in, and represented as Eq (5).

$$BF = 1 - \frac{(1-A)A_0}{(1-A_0)A} \tag{5}$$

where A_0 denotes the initial ash fraction on a dry basis and *A* represents the ash fraction in a dry sample after combustion.

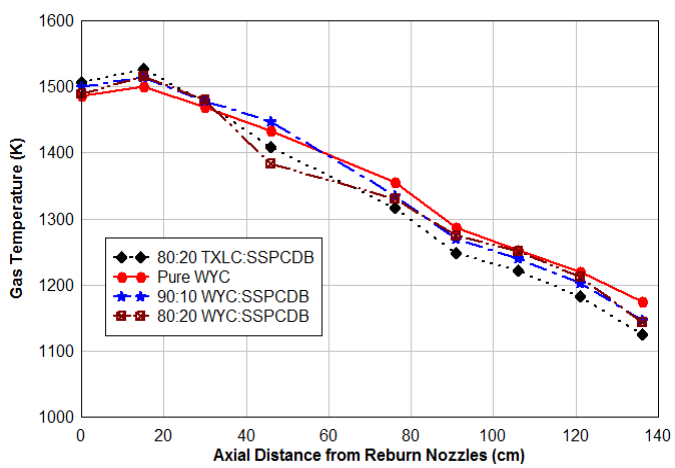

Figure 4.5.4 TEMPERATURE DISTRIBUTIONS OF THE FLUE GAS ALONG THE FURNACE

The distribution of the gas temperature is illustrated in Figure 4.5.4 and it resulted in a linear decrease along the reactor. The maximum temperatures were maintained below 1550 K in order to avoid a large production of thermal NO_x; thus most of the NO_x produced was fuel` NO_x. Results obtained by Goughnour are shown in Figure 4.5.7 [Goughnour, 2006] with 0° injection angles. The decreasing NO_x level with increasing equivalence ratio trend is evident in the observed data. Error bars were left off of this data because the purpose of the figure is to display the downward trend of NO_x level with increasing equivalence ratio.

High Ash Biomass vs. Low Ash Biomass

In all cases, better NOx reduction was achieved with LA PC FB as compared to HA PC FB. On a dry, ash free basis, the ultimate analysis of the two biomasses is essentially the same. This leads one to consider what effect the ash may have. The lower NOx reduction may be linked to the amount of heat required to heat the additional ash. This would retard the release of the volatiles and thus slow down the oxidation of the volatiles. This could affect the rate of NOx reduction and cause less NOx to be reduced. Another consideration is the catalytic or inhibiting effects of the ash. The effect of sodium and calcium was briefly discussed in the literature review. Based on the findings of the discussed study, sodium promotes NOx reduction and calcium inhibits the reduction. The concentration of Na and Ca in the HA FB is less than that found in LA FB, but when fired, the mass flow of Na and Ca for HA FB and LA FB is the same for both fuels. The similarity is because the largest source for calcium and sodium in the manure is from the ration fed to the cattle. Since the mass flow is the same, it is assumed that the effect of the two metals is the same for both fuels. The composition of the ash is shown in Table 4.5.6

Table 4.5.6 Biomass ash composition [Goughnour]

Ash Elemental Analysis (% mass)		
(Ash was calcined @ 1100 °F prior to analysis)		
	HA FB	LA FB
Silicon, SiO_2	64.68	25.55
Aluminum, Al_2O_3	7.72	1.94
Titanium, TiO_2	0.44	0.27
Iron, Fe_2O_3	2.90	1.37
Calcium, CaO	7.09	20.20
Magnesium, MgO	2.34	7.17
Sodium, Na_2O	1.38	4.94
Potassium, K_2O	4.50	12.70
Phosphorus, P_2O_5	2.81	11.11
Sulfur, SO_3	1.06	4.46
Chlorine, Cl	0.68	5.02
Carbon dioxide, CO_2	1.35	1.71
Total ash analysis	96.95	96.44
Metals in Ash, equal-weight-composite, mg/kg		
Arsenic	4.12	3.96

Barium	669	2,620
Cadmium	<1	2
Chromium	<20	20
Lead	20	20
Mercury	<0.01	<0.01
Selenium	<2	2
Silver	<2	<2
Total metals in ash	693.12	2,667.96

The particle size distribution indicates that there is a greater percentage of very small particles (< 60 µm) in the HA FB as compared to the LA FB. This may indicate that the particle size of ash is generally smaller than the particle size of combustible biomass. If this is the case, it may be possible to remove portions of the ash through screens, centrifugal, or other methods.

The difference in NOx reduction levels for HA PC FB compared to LA PC FB can be seen in Figure 4.5.5. For both the vitiated and the non-vitiated cases, the LA PC FB reduced NOx better when compared to HA PC FB.

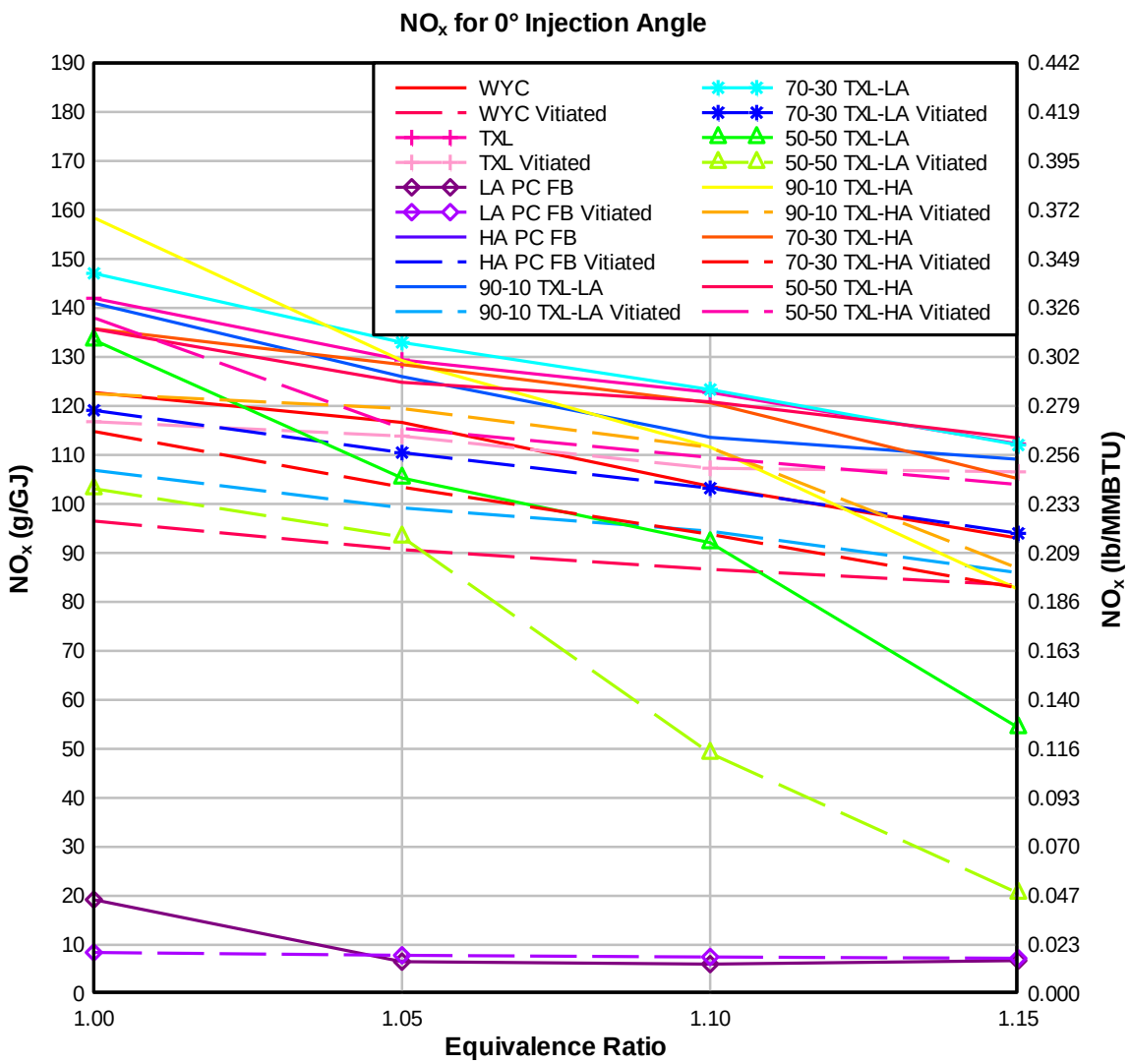

Figure 4.5.5 **.** NO_x levels for FB and Coal with a 0° injection angle.

The experiments at hand attempted to simulate exhaust gas recirculation by injecting nitrogen gas with the reburn fuel motive air. The same amount of air was used; however, the oxygen concentration was lowered to 12.5 %. The simulated exhaust gas recirculation will not take into account the NO_x reduced due to recirculation, but it should account for the other, more dominant reduction modes.

When simulated vitiated air is used, the reduction in NO_x caused by dilution must also be taken into account when reporting the NO_x in parts per million (ppm) or on a volume basis. In these experiments, the levels of NO_x are reported on mass per heat output basis. This reporting method allows for better comparison of the results between the vitiated and non-vitiated cases. Figure 4.5.6 compares the difference between non-vitiated and vitiated air. Another consideration that may be important is the specific heat of N_2 compared to CO_2. At a typical reburn zone temperature (1400 K or 2060 °F), the specific heat of nitrogen is 34.5 kJ/kmol-K while the specific heat of CO_2 is 57.7 kJ/kmol-K. When nitrogen gas is used to simulate vitiated air, there is no CO_2 in the exhaust. The actual CO_2 concentration of exhaust gas is around 12%. It is unknown whether the presence of the

CO_2 in the exhaust gas has an effect on NO_x reduction. This shows that vitiation has a greater effect on the NO reduction when a lateral injection is used.

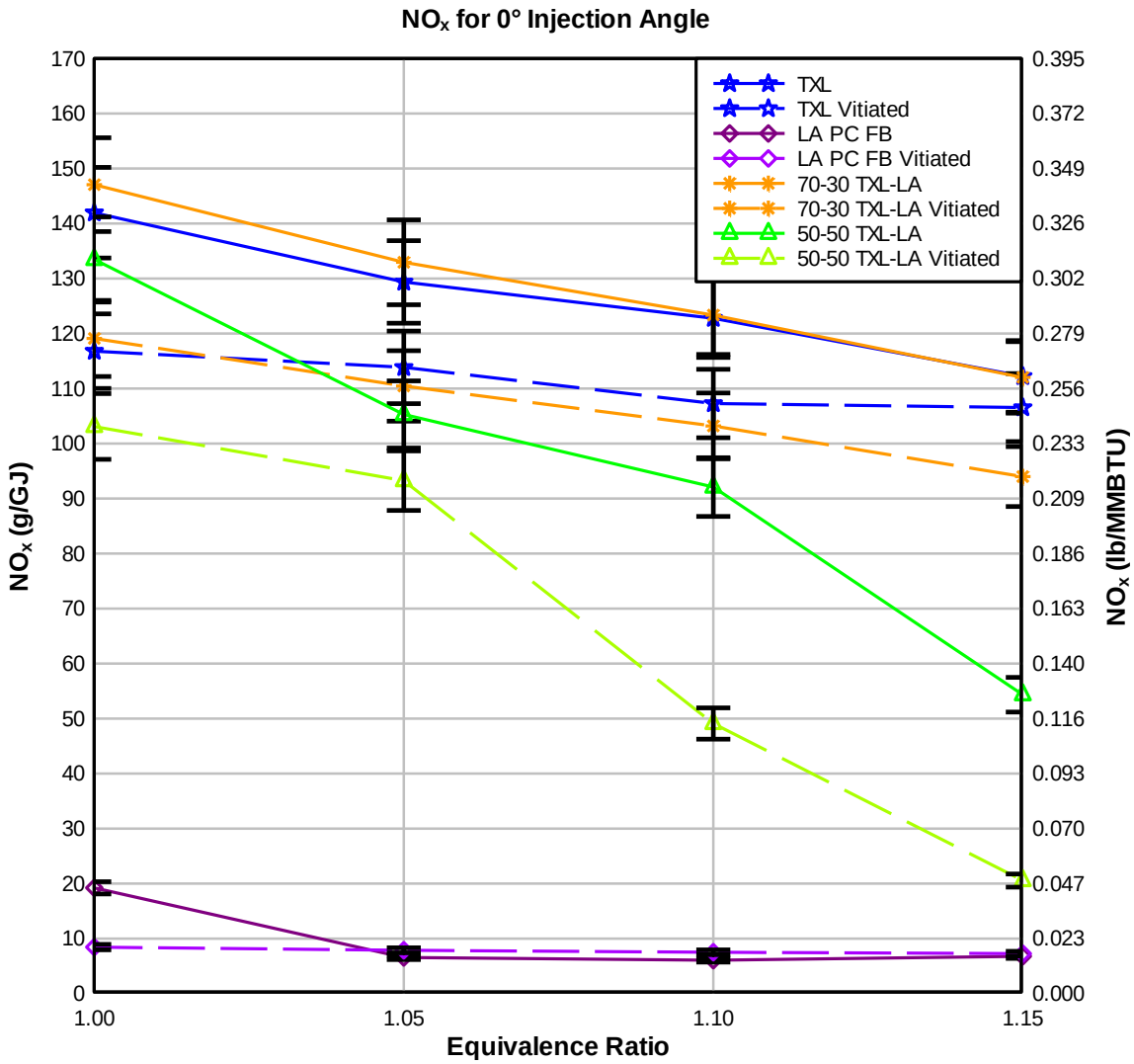

Figure 4.5.6. Comparison of vitiated vs. non-vitiated reburn experiments.

The results in Figure 4.5.7 and Figure 4.5.8 show that the NO_x reductions increased with an increase in the RBZ equivalence ratio, indicating a key operating parameter. The range of the NO_x reductions was found to be about 16 to 55% for WYC and 15 to 48% for TXLC. Figure 4.5.5 and Figure 4.5.6 indicate that higher NOx reduction with CB fuels compared to pure coals.

Once CB (FB or DB) is blended with coals as a reburn fuel, the higher NO_x reductions are expected because the CB may release NH_3 rich compounds which react with NO_x to produce harmless N_2 under O_2 deficient conditions.

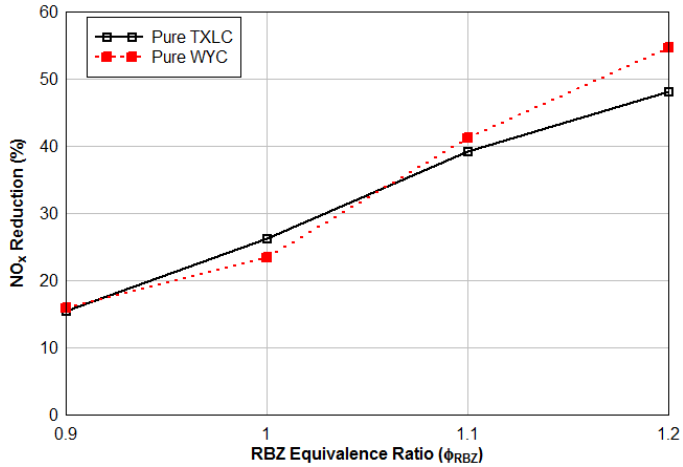

Figure 4.5.7. NOx reductions during the reburning experiments with Coal as Reburn fuels

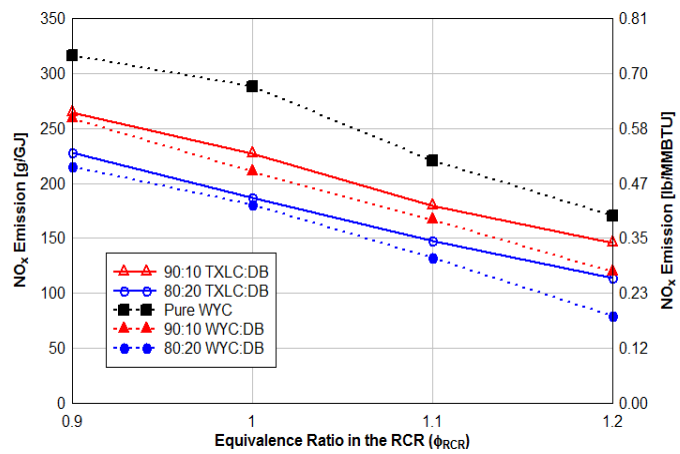

Figure 4.5.8. NO_x EMISSIONS USING DAIRY BIOAMSS (DB) AND COALS AS REBURN FUELS

4.6. Impact on Tasks due to Industrial Advisory Committee feed back

1. There was concern from utility that there is more than 1-1.5% of Sodium (Na) in FB and may cause slagging in coal-fired plants. The effect of cofiring FB with coal on ash fouling and heat transfer characteristics to heat exchanger tubes were investigated [see results under task A-3]
2. Low ash FB and DB were recommended for cofiring ; however low ash requires specially paved surfaces. Paving feedpens may not pay out considering animal performance. Industry has problems with hard-surfaced pen surfaces and thus may need to find other uses for manure ash and other technologies for use of high ash FB and DB. Gasification

experiments were performed since it can handle high ash FB and DB [see Task A-5]. Further whether the fly ash produced from cofiring can be used as supplemental material with cement. [See results under task A-9]

3. "Reburn – been around for many years; glad to use manure if can reduce NOx emissions; looks encouraging; can it scale up?" (See Task A-6 Pilot scale Test Results)
4. " Beginning to see some exciting results from some of the work, especially in the reburn area. Need to double check the work, but I'm seeing some rather exciting opportunities". "Hard to find commercial pilot plants to run replicated experiments". Next stage of research is to find source of funding to run a commercial testing.

4.7. Summary

A majority of proposed task was performed. After conducting the research mentioned in this report, it was determined that the optimal reburn fuel composition is pure LA PC FB. When this type of fuel is used, the effects of vitiation is very small. The other conclusions are summarized below:

Figure 4.7.1. Top view of slag or melted ash deposits in furnace.

i) The effect of equivalence ratio on the NO_x reduction was found to be significant, and the NO_x emissions decreased with an increase in the equivalence ratio.
ii) The NO_x emissions also decreased with an increase in the proportion of the feedlot biomass (FB) in the fuel blend.

iii) Burning fuels containing high Cl and low Hg resulted in low Hg emissions.
iv) The effect of unburned carbon (UBC) on Hg emissions was found to be significant.
v) Pulverized FB can be used as a supplementary fuel in existing coal-fired power plants and is very effective on the reductions of NO_x and Hg emissions.
vi) The high ash FB must be avoided for combustion in PC furnace since it leads to poor NOx reduction and ash fouling problems (Figure 4.7.1)
vii) Vitiating the air used to inject the reburn fuel reduces the level of NOx for both the 45° injection and the lateral injection.
viii) Higher equivalence ratios reduce NOx levels to a greater extent than lower equivalence ratios.
ix) LA PC FB reduces NOx to a greater extent when compared to HA PC FB.
x) HA PC FB causes severe slag buildup in the furnace and should not be used without special consideration of the effects of the ash.
xi) For blends of biomass and coal, the level of NOx reduction increases for greater than 50% biomass by mass. Lower percentages need further experimentation to determine their effectiveness.

4.8. Acronyms and symbols

A	Ash
AgB	Agricultural Biomass
AnB	Animal waste based Biomass
AF:	Air Fuel Ratio
ASTM	American Society for Testing and Materials
AW:	Agricultural Wastes
BF	Burnt Fraction
CAFO	Concentrated Animal Feeding Operations
CB	Cattle biomass
DAF	Dry Ash Free
DB	Dairy Biomass
DOE	Department of Energy
DSC	Differential Scanning Calorimetry
EPA	Environmental Protection Agency
FB	Feedlot biomass (Cattle manure or Cattle Biomass CB)
FC	Fixed Carbon
FTIR	Fourier Transform Infrared Spectroscopy
HA-FB-PC	High Ash Feedlot Biomass Partially Composted
HA-FB-Raw	High Ash Feedlot Biomass Raw form
HHV	Higher or Gross heating value
HV	Heating value

LA-FB-PC	Low Ash Feedlot Biomass Partially Composted
LA-FB-Raw	Low Ash Feedlot Biomass
LAHP	Low ash/High Phosphorus feedlot biomass
LALP	Low ash/Low Phosphorus feedlot biomass
LOI	Loss on ignition or % carbon in bottom and fly ash
mmBTU	million BTU
NETL	National Energy Technology Laboratory
NG	Natural gas
PC	Partially composted (45 days)
Pf	pulverized fuel fired
ϕ	Equivalence ratio
ϕ_{RBZ}	Equivalence ratio in the reburn zone
ϕ_{RSZ}	Equivalence ratio in the reburn supply zone
PM	particulate matter
PRZ	Primary combustion zone
RBZ	Reburn combustion zone
RM	Raw Manure
SA	Secondary Air
SCFH	Standard Cubic Feet per Hour
SMD	Sauter mean diameter
SR	Stoichiometric ratio, Air: Fuel/ (Air: Fuel) $_{stoich}$
TAMU	Texas A&M University
TCEQ	Texas Commission on Environmental Quality
TEES	Texas Engineering Experiment Station
TGA	Thermo-Gravimetric Analysis
TXLC	Texas lignite coal
USDA	US Dept of Agriculture
VM	Volatile matter
WYC	Wyoming coal

4.9. References

Agarwal, H/\., H.G. Stenger, S. Wu, Z. Fan, Energy and Fuels 20 (2006) 1068-1075.

Annamalai, K., and J. Sweeten, US Patent #6,973,883, 2005,

Annamalai K, Thien B, Sweeten B. Co-firing of coal and cattle feedlot biomass (FB) fuels. Part II. Performance results from 30 kW (100,000) BTU/h laboratory scale boiler burner. Fuel 2003a;82:1183-93;

Annamalai, K., Sweeten, J.M., Mathur, M., Thien, B., Wei, G., Priyadarsan, S., Arumugam, S., and Heflin, K., 2003b. Co-firing Coal: Feedlot and Litter Biomass (CFB and CLB) Fuels in Pulverized Fuel and Fixed Bed Burners. Final Report: National Energy Technology Laboratory (NETL) and Department of Energy (DOE). See also URL www.osti.gov/bridge/servlets/purl/822025-otOX2Z/native/ 822025.pdf.

Annamalai, K.T. , N.T. Carlin, H. Oh, G. Gordillo Ariza, B. Lawrence, U. Arcot V, J.M. Sweeten, K. Heflin, W.L. Harman, Proceedings of the IMECE, 2007 ASME International Mechanical Engineering Congress and Exposition, Seattle, WA, November 11-15, 2007.

Annamalai,K., J. Sweeten, US Patent #6,973,883, 2005.
Annamalai K., and Puri, I K, Comb Sc and Engineering, Taylor and Francis, 2005b

Annamalai, K., Goughnour, P.G., Oh, H., Arcot V, U., and Sweeten, J.M., 2006. NO_x and Hg Capture using Coal, Feedlot Biomass (Cattle Manure) as Reburn Fuels – Task 2: Reburn Experiments for NO_x and Hg Reduction. Final Report: Texas Commission on Environmental Quality (TCEQ), Austin, TX.

Arumugam, S., and Heflin, K., 2003. Co-firing Coal: Feedlot and Litter Biomass (CFB and CLB) Fuels in Pulverized Fuel and Fixed Bed Burners. Final Report: National Energy Technology Laboratory (NETL) and Department of Energy (DOE). See also URL www.osti.gov/bridge/servlets/purl/822025-otOX2Z/native/ 822025.pdf.

Arumugam S. Nitrogen oxides emission control through reburning with biomass in coal-fired power plants. Master's Thesis, Texas A&M University; 2004.

S.Arumugam, K Annamalai , Ben Thien and , J Sweeten, "Feedlot Biomass Co-firing: A Renewable Energy Alternative for Coal-fired Utilities," ***Int. National J of Green Ener***gy, Vol. 2, No. 4 , 409 - 419 , 2005.

Agarwal, H., H.G. Stenger, S. Wu, Z. Fan, Energy and Fuels 20 (2006) 10

Cao, Y., Y. Duan, S. Kellie, L. Li, W. Xu, J.T. Riley, W.P. Pan, P. Chu, A.K. Mehta, R. Carty, Energy and Fuels 19 (3) (2005) 842-854.

Carpi, A., Water, Air and Soil Pollution 98 (3-4) (1997) 241-254.

Di Nola, G., 2007. "Biomass Fuel Characterization for NOx Emissions in Co-firing Applications". PhD Dissertation, Mechanical Engineering, Universita' degli studi di Napoli, Italy]

Energy Information Administration, International Energy Outlook 2006. Accessed July 2006 http://www.eia.doe.gov/oiaf/ieo/electricity.html

Energy Information Administration, International Energy Outlook 2006; Accessed July 2006 http://www.eia.doe.gov/oiaf/ieo/electricity.html

Gibb,W.H., F. Clarke, A.K. Mehta, Fuel Processing Technology 65 (2000) 365-377.

Goughnour, Paul "NOx reduction with the use of Feedlot Biomass as Reburn Fuel, "Mech. Engg., Texas A&M, Aug. 2006

Hall,B., P. Schager, O. Lindqvist, Water, Air, and Soil Pollution 56 (1991) 3-14.

Hartmann D, Kaltschmitt M. Electricity generation from solid biomass via co-combustion with coal: energy and emission balances from a German case study. Biomass and Bioenergy 1999;16:397-406.

http://www.wcaslab.com/tech/tbftir.htm- On FTIR

Laudal, D.L., J.S. Thompson, J.H. Pavlish, L. Brickett, P. Chu, R.K. Srivastava, J. Kilgroe, C.W. Lee, Air and Waste Management Association's Magazine for Environmental Managers, February 2003, 16-22.

Oh, H., Ph.D. Dissertation, Mechanical Engineering, Texas A&M University, College Station, TX, 2008

Oh et al., Proceedings of the ASME/JSME 2011 8th Thermal Engineering Joint Conference, AJTEC, March 13-17, 2011, Honolulu, Hawaii, USA, AJTEC2011-44182

Oh Hyukjin, Kalyan Annamalai, John Sweeten, Witold Arnold, " Reburning Of Cattle Manure-Based Biomass With Coals In A Small Scale Boiler Burner Facility For NOx And Mercury Reduction, " Proceedings of the ASME/JSME 2011 8th Thermal Engineering Joint Conference, AJTEC2011-44182, March 13-17, 2011, Honolulu, Hawaii, USA (NOx and Hg Reduction)

Sable, S.P.,W. de Jong, R. Meij, H. Spliethoff, Energy and Fuels 21 (4) (2007a) 1883-1890

Sable,S.P., W. de Jong, R. Meij, H. Spliethoff, Energy and Fuels 21 (4) (2007b) 1891-1894.

Sweeten, J.M., Annamalai K., Thien B., and McDonald L.A., 2003. "Co-firing of Coal and Cattle Feedlot Biomass (FB) Fuels. Part I. Feedlot Biomass (Cattle Manure) Fuel Quality and Characteristics". *Fuel*, 82(10), pp. 1167-1182.

Thien, Thien Ph.D. Dissertation, Mechanical Engineering, Texas A&M University, College Station, TX, 2002.

Yang, Y.B., Naja, T.A., Gibbs, B.M., and Hampartsoumian, E., 1997. "Optimisation of Operating Parameters for NO Reduction by Coal Reburning in a 0.2 MW_t Furnace". *Journal of the Institute of Energy*, 70, pp. 9-16

Storm, C., Spliethoff, H., and Hein, K.R.G., 2005. "Generation of a Gaseous Fuel by Pyrolysis of Biomass and Sewage Sludge for Use as Reburn Gas in Coal-Fired Boilers". *Clean Air*, 6(3), pp. 289-328.

4.10. Education and Training

1. Paul Goughnour, MS, Goughnour, Paul "NOx reduction with the use of Feedlot Biomass as Reburn Fuel, "Mech. Engg., Texas A&M, Aug. 2006
2. Oh Hyuk Jin , Reburning Renewable Biomass For Emissions Control And Ash Deposition Effects In Power Generation, Mech. Engineering, Texas A&M University, PhD Thesis August 2008.

4.11. Other support if any

Only those involving reburn is presented here.

1. Feedlot Biomass: A Reburn Fuel For "Maximum NOx" Reduction In Coal-Fired Power Plants, Kalyan Annamalai, Dept. of Mechanical Engineering, Texas A&M University, and John Sweeten, Texas Agricultural Experiment station, Texas A&M Agricultural Research Extension Center, Amarillo, Texas, **Texas Commission on Environmental Quality**, 3/2005-5/2007; TCEQ Grant # 582-5-65591 0015 $ 341,933

2. Development And Application Of New Optical Sensors For Measurements Of Mercury Concentrations, Speciation, And Chemistry, **Department of Energy**, Robert Lucht of Purdue University, J. Caton and K. Annamalai of TAMU, 2004-2008, ($ 400,000 from DOE); Subcontract to TAMU: J. Caton and Annamalai, $135,480

4.12. Dissemination

1. **Combustion Science and Engineering**, 18 Chapter book on "Combustion Science and Engineering," by Annamalai, Kalyan and Puri, Ishwar, pages: 1121, Taylor and Francis, Orlando, Florida; ISBN: 0849320712; Dec 2006

2. Annamalai, A. Udayasarathy, Hyukjin and Sweeten, JM, ," Mercury Emission And Control For Coal Fired Power Plants, pp 205-217, ISBN 978-81-8487-014-5, Book Edited Agarwal, AK, Kushari, A, Aggarwal, S K and Ruchai , AK, Narosa Publishing House, New Delhi,2009.

Journal Publications printed, accepted, {subject area in parenthesis}

1. Hyukjin Oh and Kalyan Annamalai, and John M. Sweeten "Effects of ash fouling on heat transfer during combustion of cattle biomass in a small-scale boiler burner facility under unsteady transition conditions **International Journal of Energy Research** , 2010 DOI: 10.1002/er.1768
2. Carlin NT, Annamalai K, Harman WL, Sweeten JM, 2008, "The economics of reburning with cattle manure-based biomass in existing coal-fired power plants for NOx and CO2 emissions control". **J of Biomass and Energy,** 33 (2009), pp. 1139-1157

3. Magnuson, Jesse; Anderson, Thomas; Lucht, Robert, Vijayasarathy, Udayasarathy; Oh, Hyukjin; Annamalai, Kalyan; Caton, Jerald Title: "Application of a Diode-Laser-Based Ultraviolet Absorption Sensor for In Situ Measurements of Atomic Mercury in Coal Combustion Exhaust***", Energy & Fuels***, 22, **pp 3029–3036, 2008**

4. Hyukjin Oh and Kalyan Annamalai, and John M. Sweeten "Investigations of Ash Fouling with Cattle Wastes as Reburn Fuel in a Small Scale Boiler Burner under Transient Conditions, " ***J of Air and Waste Management Association***, 58:517–529 (2007)
5. Thomas N. Anderson and Robert P. Lucht , Soyuz Priyadarsan1, Kalyan Annamalai, and Jerald A. Caton, "In situ measurements of nitric oxide in coal-combustion exhaust using a sensor based on a widely-tunable external-cavity GaN diode laser," V 46, 3946-3957, ***J of Applied Optics***, July 2007.
6. S. Priyadarsan, K. Annamalai. Thien, J. M. Sweeten, M. T, and S. Mukhtar, "Animal Waste As A Source Of Renewable Energy," Chapter 16, ***USDA-Source Book on Animal Waste Animal Waste as a Source of Renewable Energy***, Edited by Outlaw , Chapter 16, 2005.
7. NOx Reduction using Cattle Feedlot Biomass as Reburn Fuel in Coal-Fired Boilers Hyukjin Oh,; Kalyan Annamalai ; Paul G Goughnour, Ben Thien, John M Sweeten ***J of Fuel*** , Submitted Nov 2010, under Review **.**

Paper prepared and ready to be submitted

8. Hyuk Jin Oh, Kalyan Annamalai, John M. Sweeten, " Potentials of Cattle Wastes/Biomass as Alternative Fuels in Coal-Fired Power Plants for Emissions Controls, **" to be Submitted**

Full paper refereed Conference Proceedings and Publications

9. Hyukjin Oh, Annamalai, K., John M. Sweeten, Christopher Rynio, and Witold Arnold, "Combustion Of Cattle Biomass As A Supplementary Fuel In A Small Scale Boiler Burner Facility For NOx And Mercury Reduction, " IMECE2009-12626, Proceedings of IMECEC2009, 2009 ASME International Mechanical Engineering Congress and Exposition, November 13-19, Lake Buena Vista, Florida, USA.
10. Kalyan Annamalai, "Thermo-chemical Energy Conversion of Coal, Animal Waste Based Biomass, and Coal:biomass Blends, "19th National & 8th ISHMT-ASME Heat and Mass Transfer Conference, January 3 - 5, 2008, ASME -ISHMT, Hyderabad, India, Jan 3-5, 2008.
11. K. Annamalai, N.T. Carlin, H. Oh, G. Gordillo Ariza, B. Lawrence, And U. Arcot V, J.M. Sweeten K. Heflin, W.L. Harman " Thermo-Chemical Energy Conversion Using Supplementary Animal Wastes With Coal , ", Invited Key Note Presentation, 2007 ASME International Mechanical Engineering Congress and Exposition, November 11-15, 2007 Seattle, Washington, USA; IMECE2007-43386; CROSS LISTED UNDER INVITED LECTURE
12. Giacomo Colmegna, Kalyan Annamalai, Udayasarathy Arcot V , "Hg Reduction During Reburn Process With The Use Of Cattle Biomass As A Reburn Fuel, " The 3rd International Green Energy Conference, IGEC-2007, Västerås, Sweden, June 17-20, 2007.

Conference Publications Under review , {subject area in parenthesis}

13. Hyukjin Oh, Kalyan Annamalai, John Sweeten, Witold Arnold, " Reburning Of Cattle Manure-Based Biomass With Coals In A Small Scale Boiler Burner Facility For NOx And Mercury Reduction, " Proceedings of the ASME/JSME 2011 8th Thermal Engineering Joint Conference, AJTEC2011-44182, March 13-17, 2011, Honolulu, Hawaii, USA (NOx and Hg Reduction)

Abstract reviewed Conference Publications and other non-reviewed Proceedings

14. Hyukjin Oh, Kalyan Annamalai1*, John M. Sweeten, Christopher Rynio(Ruhr-Universität-Bochum, Bochum, Germany 44780) , "Co-Combustion of Animal Wastes and Coals in a 30 kWt Boiler Burner Facility for Reductions of NOx and Mercury Emissions, " 11E4, US national Combustion Meeting, Ann Arbor, MI , May 17-20, 2009.

15. Kalyan Annamalai Invited participant for Combustion Work shop," Mercury Emission And Control For Coal Fired Power Plants, " Dec 31-Jan 2, 2008, Indian Inst of Technology (IIT), Kanpur, India. (CROSS LISTED UNDER INVITED SEMINARS)
16. Kalyan Annamalai, Invited participant , "Energy Conversion research-An Overview, " Workshop on Energy , Materials and Systems , January 10 - 11, 2008, Anna University, Guindy, India; Seminar on Energy Materials and Systems, pp 5-6, 2008; (CROSS LISTED UNDER INVITED SEMINARS)
17. Jesse K. Magnuson, Thomas N. Anderson, Robert P. Lucht, School of Mechanical Engineering, Purdue University , Udayasarathy A. Vijayasarathy, Hyukjin Oh, and Kalyan Annamalai, Texas A&M University, "Application of a diode-laser-based ultraviolet absorption sensor for in situ measurements of atomic mercury in coal combustion exhaust, "Paper G02 – Diagnostics, 5th US Combustion Meeting, March 25-28, 2007.
18. S. Arumugam, K. Annamalai, S. Priyadarsan, B. Thien and J. Sweeten, A "Novel Application of Feedlot Biomass (Cattle Manure) as Reburning Fuel for NOx Reduction in Coal Fired Power Plants," Symposium, State of the Science, Animal Manure and Waste Management (USDA), January 5-7, 2005 San Antonio, Texas.

4.13. Patents if any

1. Provisional Patent on " Reburn Injection System And Optimization With Animal Waste Based Biomass Fuels (AnB) For NOx Reduction In Power Plants" by Kalyan Annamalai, John M. Sweeten, AgriLife Mark Freeman, NETL-DOE, filed with US Patent Office; also Disclosure of Invention # 02-***TAMUS Disclosure # 1997, 2003 ; files for US patent in 2009***
2. US patent Application For United States Patent " A Method for the Production of Thermally Advanced Feedlot Biomass (TAFB) for Use as Fuel," by John M. Sweeten, Kalyan Annamalai, Mark Freeman (DOE) under review by US patent office , Fa09; Disclosure of Invention # 03-***TAMUS Disclosure # 1995, 2003***
3. US Patent # 6,973,883; 12/13/ 2005- A Reburn System with Feedlot Biomass for Maximum NOx Reduction in Power Plants with issued patent #6,973,883), ***Annamalai and Sweeten;*** Disclosure of Invention # 01- ***TAMUS Disclosure # 1726, 2002***

5. GASIFICATION

TASK A-5: Gasification to produce low-BTU gas for on-site energy conversion.

ABSTRACT

Concentrated animal feeding operations such as cattle feedlots and dairies produce a large amount of manure, cattle biomass (CB), which may lead to land, water, and air pollution if waste handling systems and storage and treatment structures are not properly managed. However, the concentrated production of low quality CB at these feeding operations serves as a good feedstock for in situ gasification for syngas (CO and H2) production and subsequent use in power generation. A small scale (10 kW) counter current fixed bed gasifier was rebuilt to carry out gasification studies under quasi-steady state conditions using dairy biomass (DB) as feedstock and various air-steam mixtures as oxidizing sources. A DB-ash (from DB) blend and a DB-Wyoming coal blend were also studied for comparison purposes. In addition, chlorinate char was also produced via pure pyrolysis of DB using N_2 and N_2- steam gas mixtures. The chlorinate char is useful for enhanced capture of Hg in ESP of coal fired boilers. Two main parameters were investigated in the gasification studies with air-steam mixtures. One was the equivalence ratio ER which is the ratio of stoichiometric air to actual air and the second was the steam to fuel ratio (S:F). Limited studies were done using oxygen enriched air to study for its effect on the temperature profile and gas quality. Prior to the experimental studies, atom conservation with limited product species and equilibrium modeling studies with a large number of product species were performed on the gasification of DB in order to determine suitable range of operating conditions (ER and S:F ratio).Results on bed temperature profile, gas composition (CO, CO_2, H_2, CH_4, C_2H_6, and N_2), HHV, and Energy Conversion Efficiency (ECE) are presented. Both modeling and experimental results show that gasification under increased ER and S:F ratios tend to produce H_2 and CO_2 richer mixtures but poorer mixtures in CO. Increased ER produces gases with higher HHV but decreases the ECE due to higher tar and char production. Gasification of DB under the operating conditions $1.59<ER<6.36$ and $0.35<S:F<0.8$ yielded gas mixtures with composition as given below: CO (4.77 - 11.73 %), H_2 (13.48 - 25.45%), CO_2 (11-25.2%), CH_4 (0.43-1.73 %), and C_2H_6 (0.2-0.69%). In general, the bed temperature profiles present a peak which ranged between 519 and 1032°C for DB gasification and the peak temperature increased with increase in oxygen concentration in the incoming gasification medium.

5.1. Introduction

There is a growing interest in reducing the dependence on crude oil, coal and natural gas and the resulting emissions due to the combustion of these fossil fuels. Increasing demand for energy, particularly in developing countries, has exacerbated the concerns over global warming caused by green house gas emissions from combustion of fossil-fuels. Research has increasingly included efforts to partially replace fossil fuels with renewable energy-sources in thermal conversion processes. Biomass is a CO_2 neutral organic fuel, which includes energy crops, municipal solid wastes, farm residues, and animal manure wastes. These potential fuels can serve as a renewable feedstock for sustainable heat and power generation (Klass et al, 1998).

Large concentrated animal feeding operations (CAFOs) produce a large amount of CB which may lead to land, water, and air pollution if waste handling systems and storage and treatment structures are not properly managed. However, the concentrated production of FB and DB serves as a good feedstock for *locally based* thermal conversion processes such as combustion to produce heat, co-firing with coal, reburning with coal to reduce NO_x emissions from power plants, and gasification to produce fuel gas (Annamalai et al, 2007). However, CB has high moisture and ash contents that make it a low quality fuel; in other words, the CB is a "low Btu" fuel more appropriate for gasification than for direct combustion processes. Typically, biomass gasification uses pure air (young et al, 2003 and Priyadarsan et al, 2005), steam (Ferdous et al, 2001 and Jangsawang et al, 2006), air-steam (Galloway et al, 2002 and Kalisz et al, 2004), and pure oxygen or pure oxygen plus steam (Klass et al, 1998 and Gill et al, 1999) for partial oxidation.

5.2. Literature review

Fixed-bed gasifiers are the oldest and historically most common reactors used to produce syngas, but in the last two decades large-scale (higher than 10 MW), fixed-bed reactors have lost a part of their industrial market (Hobbs et al, 1993). Yet, small scale (lower than 10 MW) fixed-bed gasifiers that have high thermal efficiency and require minimal pretreatment of the supplied biomass, have maintained a commercial interest especially for *locally based* power generation.

Pyrolysis, partial oxidation, and reforming are the three basic processes in biomass gasification (Klass et al, 1998). Pyrolysis is the thermal decomposition of fuel in the absence of oxygen. At about 600 K, pyrolysis produces light volatiles, charcoal, and tars (Lawrence et al, 2007) . At higher temperatures of about 1000 K, the tar cracks to produce volatiles such as hydrocarbons, carbon oxides, hydrogen, and steam. Under partial oxidation, the fixed carbon is oxidized to produce oxidized products. Reforming in the presence of steam involves reactions between charcoal and other secondary products with steam to produce CO and H_2; therefore, biomass gasification produces volatiles, partially oxidized products, and CO and H_2 after steam reforming.

In a fixed-bed gasifier, the gasification processes occur in four different zones (Priyadarsan et al,2005) known as combustion or oxidation, gasification or reduction, de-volatilization or pyrolysis, and drying. In the oxidation zone the oxygen and the steam react with the remaining char from the reduction zone to produce CO_2, CO, H_2, and heat. The heat produced in the oxidation zone is carried up by convection and diffusion to the higher zones to supply the energy required in gasification,

pyrolysis, and drying. In the reduction zone, the CO_2 and H_2, produced in the combustion zone by the reactions $C+O_2 \rightarrow CO_2$ and $C+H_2O \rightarrow CO+H_2$, and the remaining H_2O from the combustion zone react with char that descends from the pyrolysis zone to produce more CO, CH_4, and H_2. The homogeneous reactions of CO with steam occur in downstream zones.

In 1987, gasification of Texas lignite coal was studied by Rhinehart et al. (Rhinehart et al, 1987) in a pilot-scale fluidized bed reactor at 810 kPa using a mixture of pure oxygen and steam, preheated at 800 K as an oxidizer.

In 1980, Raman et al., studied the effect of the temperature on yield, gas composition, and energy recovery. Experiments were made in a fluidized bed gasifier using FB as feedstock and a mixture of gases (H_2O, O_2, and CO_2) produced by combustion of propane as oxidizing source. They concluded that increasing the temperature in the gasifier improves the yield and energy recovery. A typical gas mixture leaving the gasifier of 14.3% of H_2, 56.48% of N_2, 4.31% of CH_4, 11.07% of CO, 11.42% of CO_2, 1.75% of C_2H_6, and 0.44% of C_3H_6 was achieved at T=707 °C (980 K). For 627<T<717 the energy recovery ranged from ~20 to ~60%

In 2003, Young et al, developed a modeling study to estimate the feasibility of producing energy from non-adiabatic fluidized bed gasification of DB, using a system previously developed for gasification of coal. The modeling was developed under constant air temperature (1227 ºC), constant pressure (100 kPa), and variable air to fuel ratio. Results of performance calculations indicated energy recovery ranging from 65 to 85%, depending on the operating conditions. The gas composition was estimated with an equilibrium model at a reaction temperature of 1400 ºC, and the composition was predicted to be 26.9% CO, 6.1% CO_2, 17.1% H_2, and 49.9% N_2.

In 2005, Priyadarsan et al conducted gasification experiments in a small scale (10 KW) fixed-bed gasifier using two flows of pure air (1.27 SATP(standard ambient temperature and pressure) m^3/h and 1.7 SATP m^3/h) for partial oxidation of FB, Wyoming sub-bituminous coal (WYC), and WYC-FB blends. Two different particle sizes were tested but without an ash disposal system. Due to non-steady state conditions, the peak temperature (T_{peak}) started moving toward bed surface since ash was not removed and as much ash accumulated at the bottom creating a dead zone at the bottom of the bed. As such, steady state could not be maintained during the experiments. They concluded that particle size did not affect the species composition and the bed profile temperature. The gas composition of samples taken at the top of the gasifier was almost constant at (7-10% of H2), (27-30% of CO), (1-3% of CH4), and (2-6% of CO2).

In 2004, Zhang et al., investigated the catalytic destruction of tar produced in air blown fluidized bed gasification of seed corn wastes. A catalytic reactor and guard bed were designed in order to treat the gases produced in the gasifier. In the guard bed (small packed bed located downstream of the gasifier) dolomite was used as catalyst with the purpose of cracking the heavy tar while three nickel based steam-reforming catalysts (commercially known as ICI46-1, Z409, and RZ409) were evaluated

in the catalytic reactor. Chromatographic Analysis of gas samples reported that the catalysts used eliminated over 99% of heavy tar and increased the production of H_2 by (6-11% on a dry basis).

In 2007, Pinto et al., studied the effect of catalysis on the quality of syngas produced by co-gasification of carbon with pine, petcoke, and polyethylene based wastes. The catalysts tested were dolomite, olivine, nickel and magnesium oxides, and zing oxides (G-72D) and cobalt and molybdenum (C49-TRX) oxides. The experiments were performed in a bubbling fluidized bed gasifier using a mixture of oxygen and steam as oxidizing source. The results of this study showed that in general all the catalysts used in the experiments reduced the tar formation. The most reduction in tar formation (~76%), as compared to the absence of catalyst, was achieved by Ni-Mg catalyst. Ni-dolomite catalyst reduced the formation of tar by ~66% while the reduction was about 36% with dolomite.

In fluidized bed gasification, the oxygen concentration is maintained almost uniform along of the gasifier which seems to oxidize a fraction of H_2 produced by steam reforming reactions, and as such, H_2 production is typically less. Since the current study uses an adiabatic fixed-bed reactor with a temperature peak within the bed and oxygen is available only near the bottom of bed, the H_2 production should be enhanced with air-steam mixtures. Literature review revealed that there are no previous published studies on the catalytic effects of DB ash on gas composition and peak temperature. Additionally, the continuous analysis of gas samples also contributes to understand the dynamic of gas composition and to ensure a better accuracy of the data.

5.3. Objectives

The overall objective of the current research is to conduct an in situ gasification study with dairy biomass (DB) as a feedstock using a fixed bed gasifier. In order to achieve the overall objective the following tasks must be carried out.

1. Modify the gasifier facility (10 kW or 30000 BTU/h)
2. Build a steam generator for feeding steam into the gasifier plenum
   a. Construct an ash disposal system to run experiments under steady state conditions
   b. Acquire a Mass Spectrometer (MS) and the gas mixtures necessary to calibrate the MS.
   c. Perform calibration and analysis set-up on the MS
   d. Mount a temperature data acquisition system
   e. Develop a sampling system for preparing the gas samples to be analyzed by a Mass Spectrometer (MS)
   f. Install a heater unity to heat the gasifier
   g. Set up a control panel to control the operating conditions of the gasifier
   h. Assemble the gasification facility
3. Characterize the feedstocks
4. Perform global modeling studies on gasification to determine operating conditions
5. Conduct experiments on gasification with air, air-steam, oxygen enriched air and obtain data on bed temperature profile and gas composition under various operating conditions and verify that the system operate near adiabatic conditions.

5.4. Experiments

5.4.1. Experimental facility

The current experiments were performed using a modified small scale (10 KW) batch type fixed bed counter flow gasifier (FBCFG, Figure 5.4.1). The gasifier (72 cm tall) is divided into 4 sections which are joined by using ring type flanges of ½ in x 14 in x 20 in. The gasifier is constructed of castable alumina refractory tube (inner and outer diameter of 13.9 cm (6 in) and 24.5 cm (10 in) respectively) which is surrounded by 4.45 cm (1¾ in) of insulating blanket in order to minimize heat losses. The layer is then surrounded by a steel outer tube with an inner diameter of 34.3 cm (13½ in). Ash disposal system was installed to maintain quasi-steady operation. A conical gyratory cast iron grate drilled with a large number of ¼ in holes was coupled to a pneumatic vibrator of variable frequency that maintains the grate in continuous vibration in order to dispose the ash continuously from the bed. The rate of ash removed can be controlled by changing the vibrational frequency in the vibrator. The ash from the plenum was periodically removed. The fuel is supplied at the top of the gasifier while the mixture of air and steam is supplied at the bottom (plenum). The steam is generated by a steam generator built with a cylindrical 4 inch internal diameter vessel heated by a (1.2 kW) type tape heating element rolled around of the vessel with variable power output (0.1 to 1.2 kW); thus, the steam production rate can be controlled from 0.1 to 1.5 kg/h by changing the power supplied to the heater element. The sampling unit is composed of two condensers cooled with ice-cold water (0 º C) to condense out the tar and the H_2O in the products and a filter system to retain the particulate material. The temperature of the bed is measured every 60 seconds using K type thermocouples (Cr-Al) placed at 8 locations along the gasifier axis. The gas samples are analyzed by a mass spectrometer (MS) continuously at real time.

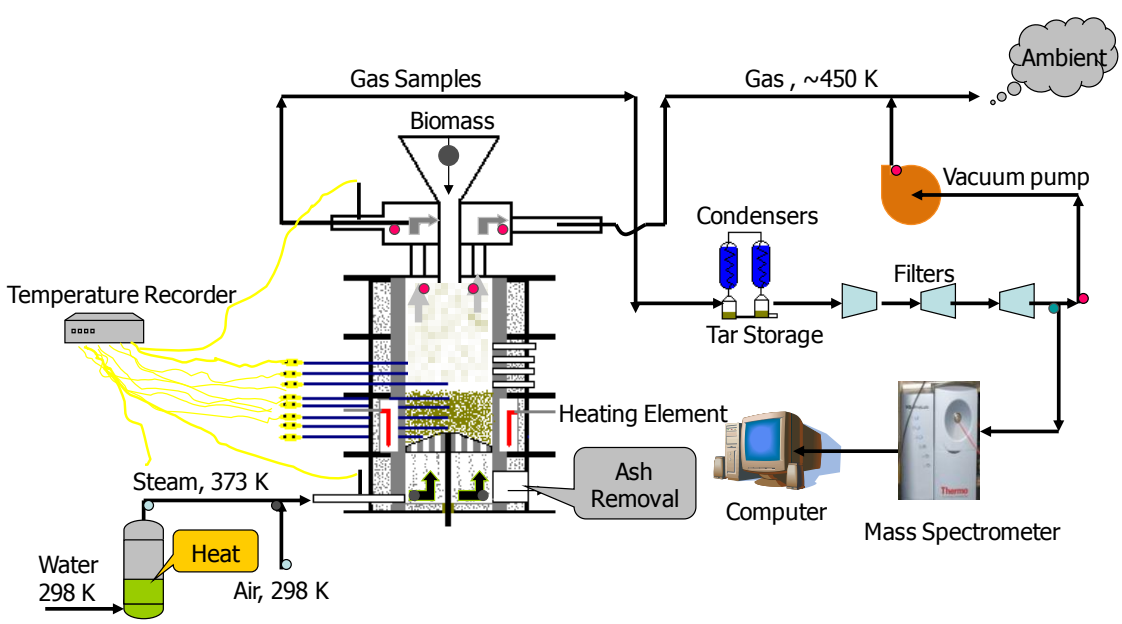

Figure 5.4.1 Schematic Gasification Facility

5.4.2. Experimentation

The gasification experiments were performed for the following cases:

a) Base case

- Bed height at 17 cm (~6 ¾”)
- Fuel: Low Ash Separated solids Dairy Biomass (LA-PC-SepSol-DB).
- Particulate size, dp = ~6.25 cm (1/4”) for DB and ~3 mm (~1/8”) for coal
- Fuel flow rate 1 kg h^{-1} (2.2046 lbm h^{-1})
- Air flow ~1.13 normal m^3h^{-1} (40 SCFH) at 298 K (536 R)
- Steam flow rate at 0.3 kg/h (~0.66 lb h^{-1})
- Equivalence ratio (ER) at 3.18
- Steam to fuel ratio (S:F) at 0.68

b) Parametric cases

- Fuel: LA-PC-SepSol-DB, Coal-LA-PC-SepSol-DB blend (90 % LA-PC-SepSol-DB, 10% Coal), and Ash - LA-PC-SepSol-DB blend (90 % LA-PC-SepSol-DB, 10% ash)
- Air flow between 0.57 and 2.26 normal m^3 h^{-1} (20 and 80 SCFH) at 298K (536.4 R)
- Steam flow rate between 0.18 and 0.5 kg h^{-1}(0.4 and 1.1 lb h^{-1}) at 373K (671.4 R)
- Equivalence ratio (ER) between 1.59 and 6.36
- Steam to fuel ratio (S:F) between 0.35 and 0.8

Experiments with i) DB-coal blends (90% DB-10% Coal) ii) DB-ash blends (90% DB-10% ash) were used in order to determine catalytic effect if any on gasification.

c) Enriched air cases

- Fuel: LA-PC-SepSol-DB.
- Air flow between 0.57 to 1.7 normal m^3 h^{-1} (20 and 60 SCFH) at 298K (536.4 R).
- Oxygen flow between 0.06 to 0.11 normal m^3 h^{-1} (2 and 4 SCFH) at 298K (536.4 R).
- Equivalence ratio (ER) between 2.1 and 4.2
- Steam fuel ratio between 0 and 0.33 kg of steam/kg of AR biomass.

5.4.3. Enriched oxygen mixture Gasification

A specified amount of oxygen is mixed with a known amount of air to obtain a mixture having desired oxygen percentages. Different air and oxygen flows used in the experiments are shown in Table 5.4.1.

Table 5.4.1. Air and oxygen flows in SCFH (ft^3/hr)

21%			24%			26%			28%		
air	O_2	ER	air	O_2	ER	air	O_2	ER	air	O_2	ER
60.00	0	2.11	50.67	2	2.10	44.40	3	2.15	41.14	4	2.10
40.00	0	3.16	-	-	-	29.60	2	3.23	30.86	3	2.80
30.00	0	4.21	-	-	-	-	-	-	20.57	2	4.20

For enriched oxygen gasification, equivalence ratio (ER) and steam fuel ratio (SF) are determined using the following formula.

$$ER=\frac{O_2 \text{ in actual air}}{\text{Stoichiometric } O_2 \text{ needed for complete combustion}} \quad (5.1)$$

$$SF=\frac{\text{kg of steam sent into gasifier}}{\text{kg of fuel fed intogasifier}} \quad (5.2)$$

The temperature profiles and the gas composition obtained at different equivalence ratios (ER) and steam fuel ratios (S:F) are discussed in detail in the following sections.

5.4.4. Experimental procedure

A normal experiment started with preheating the grate and the combustion chamber using a propane torch placed under the grate. When the temperature in the combustion chamber (2 cm above the grate) reached 800 º C (~after 2 hours), the torch was turned off and biomass was added to the gasifier. The addition continued until the bed height attained 17 cm; afterwards, the fuel port was closed and the flows of steam and air were adjusted to the desired experimental conditions. As the biomass was pyrolyzed and the char was burned the bed height started decreasing and the ash accumulated. Thus, biomass was added every 10 minutes and in batches as required. In the earlier batch experiments reported by Priyadarsan et al, there was no ash disposal system; as such temperature peak moved towards the bed surface due to ash accumulation at the bottom. In the current experiments the ash was disposed off continuously and quasi-steady state was assured by maintaining the peak temperature at the same location in the ash disposal system. When the peak temperature achieved a steady state (~1.0 hours) the gas sampling unit was turned on and the gas analysis was performed continuously during 20 minutes by the mass spectrometer (MS).

The flow rate of dairy biomass was maintained constant at 1 kg/h and the flows of air (0.56-2.26 SATP m^3/h (standard ambient temperature and pressure meter cube per hour)) at 15 °C and steam (0.19-0.43 kg/h) at 100 °C were changed in order to obtain the desired experimental conditions: ER=1.59, 2.12, 3.18, 4.24, and 6.36 and S: F=0.35, 0.56, 0.68, and 0.80. An air drier was used to dry the air before it was supplied to the gasifier. The gasifier was operated at 98 Pa vacuum pressure during all the experimentation. Temperatures along the gasifier were monitored at every 60 seconds by type K thermocouples located at 0.02, 0.04, 0.07, 0.13, 0.20, 0.24, and 0.28 m above of the grate.

Samples were taken at the top of the gasifier at the rate of 0.14 SATP m^3 h^{-1} and conditioned by the sampling unit in order to remove tar and particulate material. The mole fractions of CO_2, CO, CH_4, C_2H_6, O_2, H_2, and N_2 were measured every ten seconds by the MS.

5.4.5. Experimental Procedure for enriched oxygen gasification

The same procedure used for the air gasification was again employed for enriched air gasification with little changes. The gasifier was initially preheated using a propane torch until the temperature at a height of 2 cm from the grate reached a steady temperature of 800^0C. Once the desired temperature was reached the torch was removed and the gasifier was sealed perfectly thereby there was no air leak into the reactor. The pressure inside the reactor was maintained slightly below the atmospheric pressure using a suction fan. The fuel was added into the gasifier gradually until the bed height reached seven inches. The fuel is gasified and ash is discharged. The bed height tends to decrease. The bed is maintained at a constant height by adding fuel at regular time intervals. Air mixture having higher percentage of oxygen was sent into the reactor. The temperature profile within the bed is monitored continuously using thermocouples located at different heights along the axis of the gasifier. The ash produced as a result of gasification was removed using a pneumatic vibrator coupled to the grate. Once a steady temperature profile was obtained, the gases were analyzed for their composition using a mass spectrometer (MS). Gases for analysis are split and a fraction of gases was passed through a condensing system which condensed out the condensables and then through a set of filters to remove the particulates so that clean gases enter the MS without contaminating the MS. The time taken from the start of preheating to analyzing gases varies between 3 to 4 hours. The same procedure was repeated for different ER and S:F ratios.

5.4.6. Modeling

Typically, gasification of biomass with air yields principally a mixture of gases whose compounds are CO_2, CO, CH_4, H_2, and N_2. Other compounds are produced in trace amounts. The molar composition of these five products under gasification conditions can be predicted using: i) mass (or atom) and energy conservation equations for assumed species and ii) chemical equilibrium calculations with a larger number of species, including trace species.

5.4.6.1. Atom balance Model

Complete combustion (theoretical or stochiometric combustion) of any fuel containing C, H, N, O, and S, with air, means that all the combustible components in the fuel are burned completely with oxygen to yield sensible energy.

$$CH_hO_oN_nS_s + aO_2 \rightarrow bCO_2 + cH_2O + dSO_2 \qquad (5.3)$$

On the other hand, if insufficient air is supplied to the gasifier for partial oxidation of the fuel, which yields a low-Btu gas mixture. Many times, steam is also used in gasification in order to promote steam-reforming reaction to produce H_2-rich gas mixtures.

$$\begin{aligned} CH_hO_oN_nS_s &+ e(O_2 + 3.76N_2) + fH_2O \\ &\rightarrow gCO_2 + hCO + iCH_4 + jH_2S + kN_2 + lH_2 \end{aligned} \tag{5.4}$$

Equivalence ratio (ER), which is the ratio of the actual fuel-air ratio to the theoretical fuel-air ratio, defines the rich and lean regions of the reaction. In processes where the oxidizer used in gasification is a mixture of air and the steam, the equivalence ratio (ER) definition is modified as stoichiometric oxygen to actual oxygen supplied by both air and steam. Equation (5.5) defines the modified equivalence ratio (ER_M) used in this paper.

$$ER_M = \frac{\text{stoichiometric oxygen}}{\text{actual oxygen}} = \frac{2a}{2e + f} \tag{5.5}$$

The oxygen split between the air-steam mixtures in the gasification processes depends on the ratio between the oxygen supplied by the air to total oxygen supplied by both air and steam (ASTR).

$$ASTR = \frac{2e}{2e + f} = ER_M\left(\frac{e}{a}\right) \tag{5.6}$$

The definition provided by equation (4) yields a finite range of ASTR from 0 (gasification only with steam, e = 0) to 1 (gasification of DAF biomass only with air, f = 0).

Under adiabatic gasification, the energy conservation can be represented by Equation (5.7).

$$\sum_k N_{k,P} h_{k,P}(T_P) = \sum_k N_{k,R} h_{k,R}(T_R) \tag{5.7}$$

Where $N_{k,\,p}$ and $h_{k,p}$ are the moles and enthalpies of the products at temperature T_P and $N_{k,R}$ and $h_{k,R}$ the moles and enthalpies of the reactants at temperature T_R. Equations 5.5, 5.6, and 5.7 together with equations obtained from the atom balance of the five elements of the fuel (C, H, O, N, and S) define a system of 8 equation and 8 unknown (e to *l*) in equation (5.4) that can be solved to get the moles of CO_2, CH_4, H_2, CO, N_2, and H_2S as a function of the adiabatic temperature (T_p) in equation (5), ER_M, and ASTR. Annamalai et al used this method for 3 reactants (fuel, O_2, and steam) and 4 products (CO_2, H_2, N_2, and SO_2). Once solved for the product's species, the HHV of the gases and the ECE of the gasifier are calculated with Equations (5.8) and (5.9).

$$HHV_{Gases} = X_{CO} * HHV_{CO} + X_{CH_4} * HHV_{CH_4} + X_{H_2} * HHV_{H_2} \tag{5.8}$$

Where X_i and HHV_i are mole fraction and gross heating value (kJ normal m^{-3}) on a dry basis of the fuel gases respectively, i = CO, CH_4, and H_2. HHV_{Gases} is the energy density (kJ normal m^{-3}) of the product gases on a dry basis.

$$\eta_{Gas,E} = \frac{\mathrm{HHV_{Gases}}}{\mathrm{N_{Fuel}} * \mathrm{HHV_{Fuel}} + \mathrm{N_{steam}} * 18(\lambda + 4.18(373 - 298))} \tag{5.9}$$

Where, N_{Fuel} and N_{steam} correspond to the moles of fuel and steam supplied respectively to the gasifier by each normal m^3 of dry product gases and λ is the latent heat of steam. HHV_{Fuel} is the gross heat value (kJ $kmol^{-1}$ of DAF fuel) of the fuel and $\eta_{Gas,E}$ is ECE.

5.4.6.2. Equilibrium model under adiabatic gasification

Equilibrium modeling has also been used to estimate the adiabatic dry gas composition for about 150 species in the product gas. The NASA equilibrium code PC version was used to solve for species without the presence of $H_2O_{(g)}$ in the products and adiabatic temperature. Atom and equilibrium modeling is developed under the operating conditions.

5.5. Results and discussion

5.5.1. Fuel properties

Ultimate and proximate analysis (on an as received basis) of the DB used as feedstock in the current gasification experiments are presented in Table 5.5.1. Using as received analysis, dry and dry ash free (DAF) values are calculated and reported. Also, empirical chemical formulae and the ER and air to fuel ratio (A:F) in which all FC content in DB would go to CO ($C+1/2O_2 \rightarrow CO$) if the process was ideal are presented in Table 5.5.1 for gasification of DAF DB. Air gasification of DAF DB at ER > 5.8 (or A:F < 0.87) implies insufficient oxygen for the reaction ($C+1/2O_2 \rightarrow CO$) and hence, incomplete conversion of char, which means char as byproduct. On the other hand, at ER< 5.8 (or A: F >0.87) there is more oxygen than that required for the conversion of all FC to CO and the FC could be gasified completely to CO and CO_2. However, in gasification processes where the reaction time is not infinity (no ideal), incomplete conversion of char can be possible even with ER<5.8.

Table 5.5.1: ultimate and proximate analyses of DB

Dry loss %	25.26
Ash %	14.95
VM %	46.84
FC %	12.95
C %	35.27
H %	3.1
N %	1.9
O %	19.1
S %	0.42
HHV (kJ/kg)	12844
DAF HHV(kJ/kg)	21482
Dry HHV (kJ/kg)	17185
Emprical Formulae	$CH_{1.06}N_{0.047}O_{0.405}S_{0.0045}$
ER at which FC $\longrightarrow$ CO	5.8
Air:fuel ratio FC $\longrightarrow$ CO	0.87

Proximate analysis of the stored low ash partially composted dairy biomass (LAPCDB) is shown in Table 5.5.2. It was noted that the ash percentage in the fuel used for enriched oxygen gasification was higher compared to ash content of earlier experiments of Gerardo; this is possible due to decomposition of biomass or aging effect.

Table 5.5.2. Proximate analysis values for LAPCDB

Composition	Percentage
Dry loss %	13.23
Ash %	20.28
FC and VM %	66.49

5.5.2. Modeling Results and discussion for air gasification

5.5.2.1. Atom-balance model

5.5.2.1.1 Effect of ER_M

The effect of the ER_M on species production is shown on Figure 5.5.1. for ASTR at 0.25 and temperature at 800 K. Increasing ER_M at constant temperature and at constant ASTR implies lesser oxygen (lesser air and steam) supplied to the gasifier; hence, the oxidation of char takes place in a deficient O_2-H_2O ambient, which produces mixtures rich in CO. Also, since less C leaves with CO and CO_2 under increased ER_M, more C must leave with CH_4 and hence more H atoms must be with CH_4. Less H atoms are available for conversion to H_2. Figure 5.5.1 states that the ER_M must be kept below

about 4 for DB and WYC, 3.5 for TXL, and 8.5 for FB during the experiments with ASTR at 0.25 in order to produce H_2 at 800 K.

5.5.2.1.2 Effect of ASTR

The results from the atom balance model on production of CO, CH_4, and H_2 are presented in Figure 5.5.2as a function of ASTR at fixed ER of 2 and temperature of 800 K.

The decreasing of the ASTR at fixed ER_M implies increased atoms of hydrogen supplied to the reactor which leads to increased CH_4 and H_2 and low contents of CO and CO_2. The curves of Figure 5.5.2 suggest that at constant ER_M and constant temperature, H_2 can be produced within 0 < ASTR < 1. In other words, it is possible produce H_2 by gasification of biomass with air, steam or steam-air mixtures.

The atom model shows that the effect of changes in ER_M on H_2 is more significant than changes in ASTR. The production of CO and CH_4 is possible only under certain conditions. For instance, to produce CO with DB at $ER_M = 2$ and $T_P = 800$ K, the ASTR must be maintained higher than 0.3, while the production of CH_4 with FB is possible only for ASTR lower than 0.35. Alternatively, the atom model shows that the production of CH_4 and CO is very sensitive to changes of all parameters (ER, ASTR and T_P). Additionally, the curves in Figure 5.5.1 and Figure 5.5.2 illustrate that under the same conditions of operation of the gasifier (T_P, ER_M, and ASTR), FB is better than other biomasses to produce H_2 but it is not as good as the coals and DB to produce CH_4. This is due to higher hydrogen content in FB as compared with TXL, WYC, and DB.

5.5.2.2. Equilibrium model

The equilibrium model provides information on gas composition, HHV of gases, and energy recovery as functions of the ER_M and ASTR. Although, the study was performed for about 150 species, only significant species are reported here.

As discussed before, decreasing ASTR at constant ER_M decreases the air to steam ratio supplied to the gasifier and there are more H atoms available, which favor Reactions of C with steam and H_2 and CO with steam. Hence, the production of CH_4 and H_2 is increased but the production of CO is diminished (Figure 5.5.3). However at ER-= 2, ASTRs > 0.4 and ASTRs > 0.6 do not affect the production of CO from FB and TXL and DB respectively.

Increasing ER_M at constant ASTR implies decreasing the oxygen supplied with the air. Thus, there is less oxygen to produce CO from the reaction of carbon and oxygen that is exothermic resulting in lower temperatures not high enough for H_2 to be stripped from H_2O in the steam reforming reaction. The effect of ER_M on concentrations of CO and H_2 for DB and FB are illustrated in Figure 5.5.4 at various ASTRs.

The FB biomass has more oxygen and hydrogen in the fuel compared to DB; the availability of O in the fuel results in more production of CO which promotes the shift reaction of CO with steam to produce H_2 and CO_2. Additionally, more H in the fuel raises the production of H_2. Figure 5.5.4 shows that the production of H_2 with DB and FB is possible at 0.2 < ASTR < 0.8 and 2 < ER < 6, while the production of CO with DB is only possible for ER_M > ~0.20. Due to the higher hydrogen content in FB, the production of CO is even possible at lower ER_M as compared to that of DB.

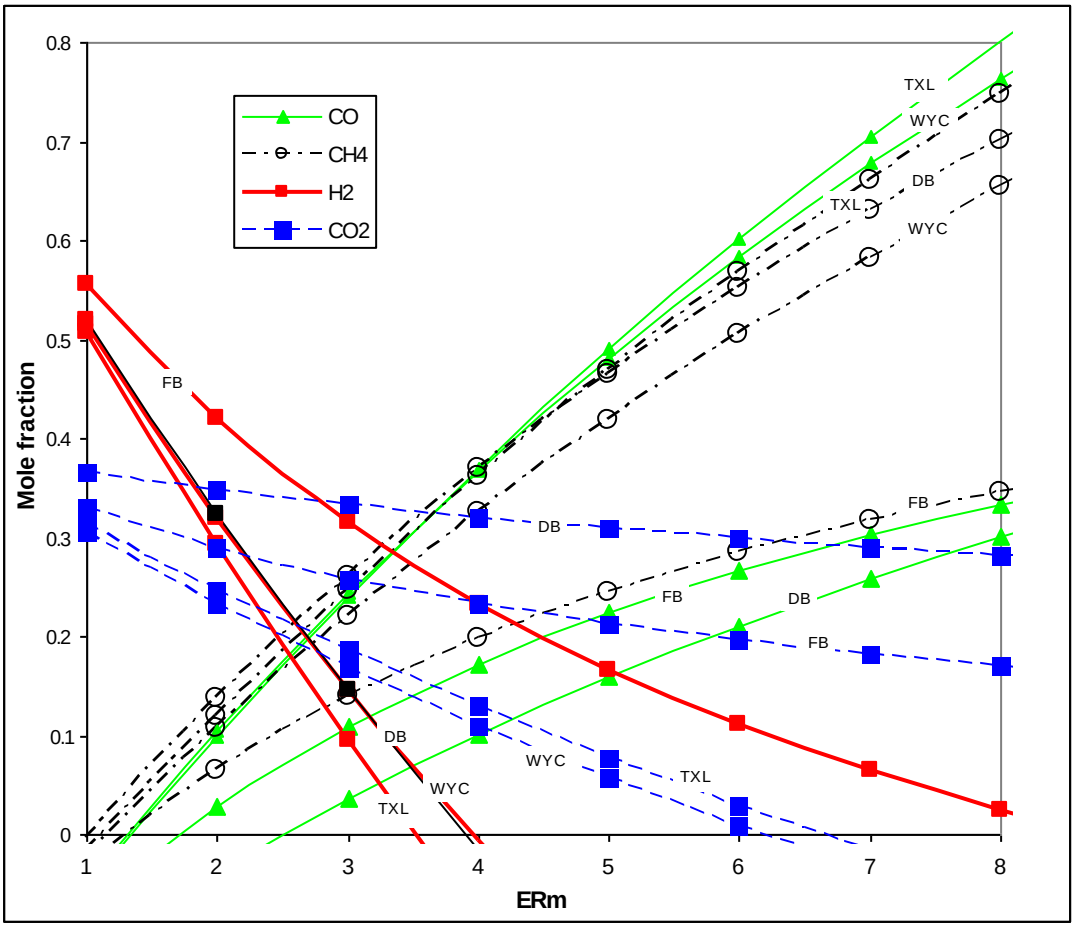

Figure 5.5.1: Effect of the ER_M on CO, CO2, CH4 and H_2 production for FB, DB, TXL, and WYC with AOF at 0.25 and temperature at 800 K, estimated with atom balance

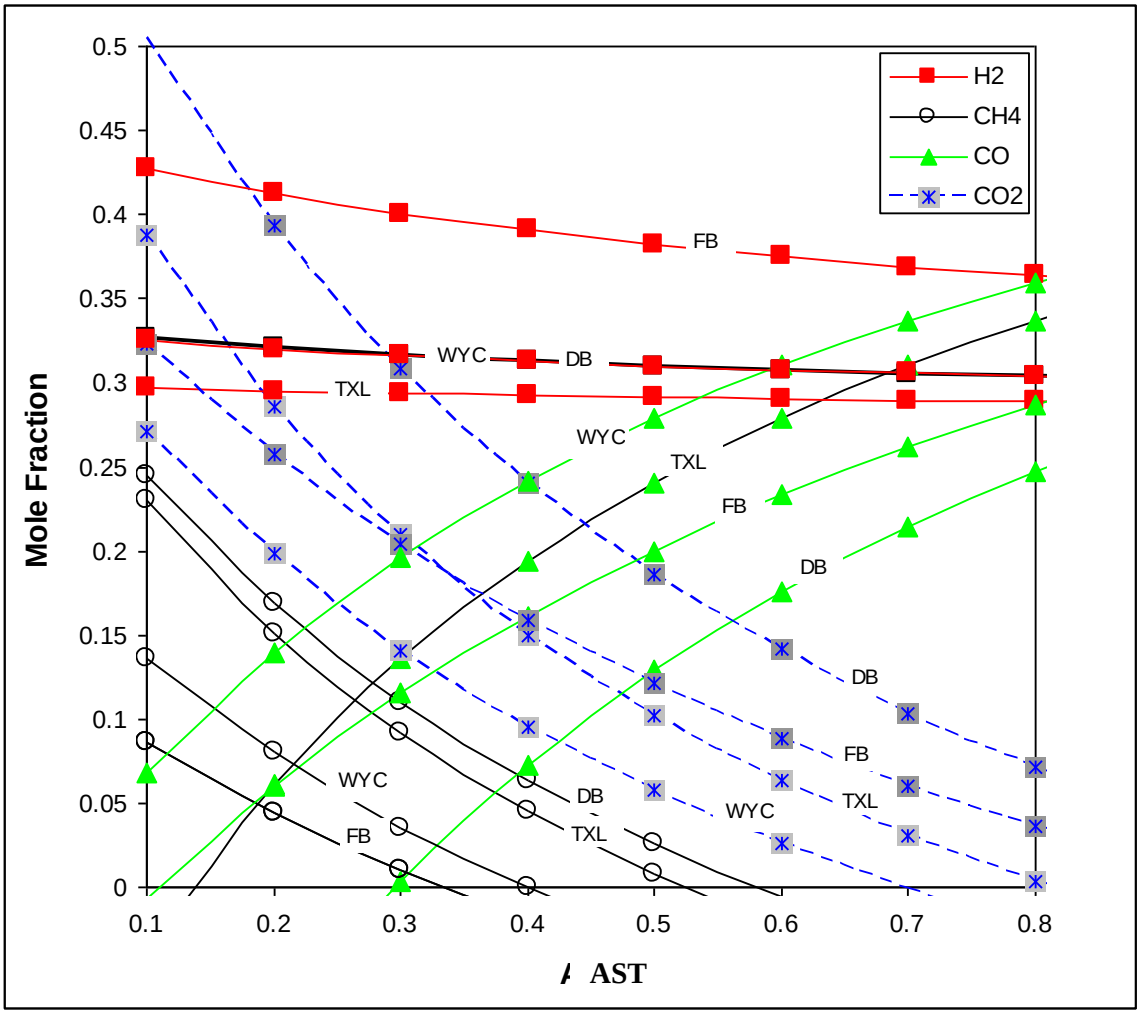

Figure 5.5.2: Effect of the ASTR on CO, CH_4, CO_2 and H_2 production for FB, DB, TXL, and WYC with ER_M at 2 and temperature at 800 K, estimated with atom balance

The HHV of the products estimated by equilibrium are illustrated in Figure 5.5.5 for TXL, DB, and FB at many ASTRs and ER_M =-2 and 8. As stated before, at constant ER decreased ASTRs produce mixtures richer in CH_4 and H_2, which have higher HHVs. While the HHV with steam and air gasification provides a measure of energy density, it does not provide a measure of degree of energy conversion (energy recovery) in gasification processes.

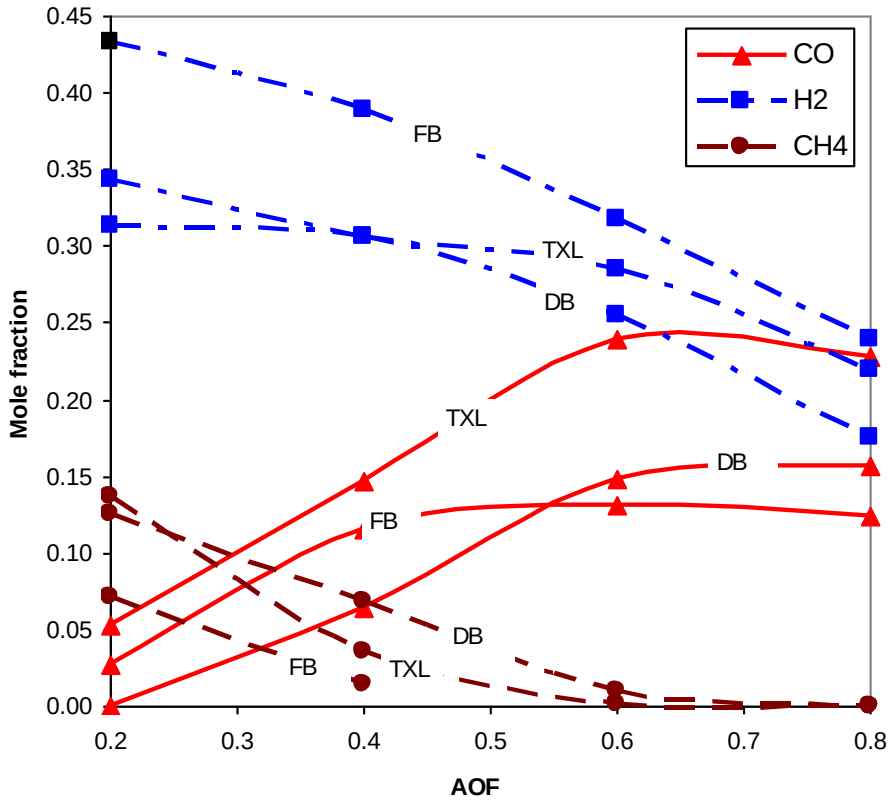

Figure 5.5.3: Effect of the ASTR on production of H_2, CO, and CH_4 for FB, DB, and TL with ER_M at 2, estimated with equilibrium model

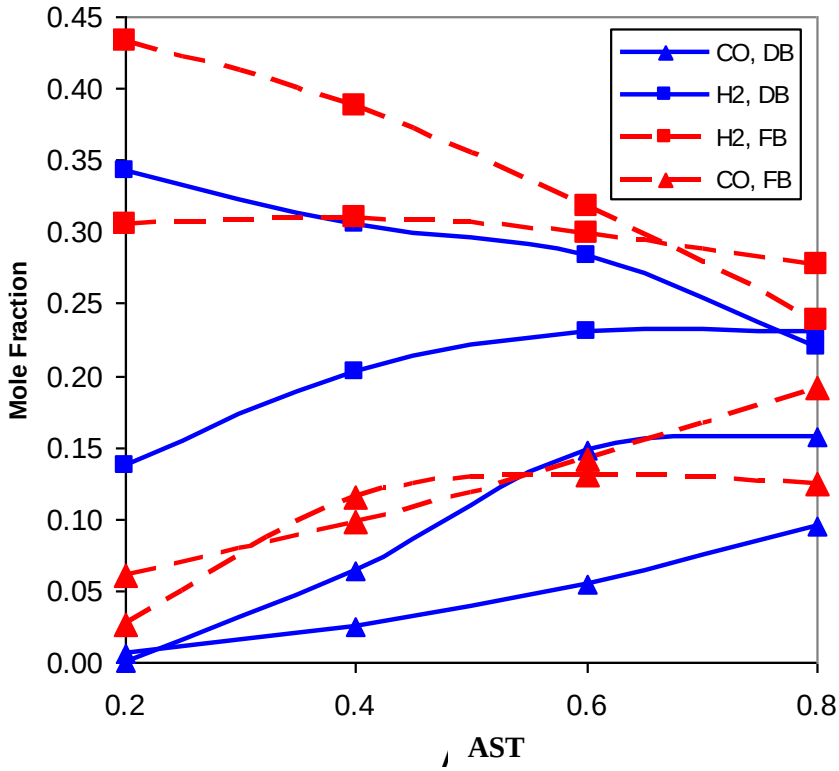

Figure 5.5.4: Effect of the ER and ASTR on production of H_2 and CO for DB and FB, estimated with equilibrium model

The rise of the ASTR results in decreased energy recovery (Figure 5.5.6), but at higher ER_M the decrease is not much. At constant ASTR, higher ER_M implies lesser mass flow of air to react with char and the process is almost pure pyrolysis (production of char), which produces a lesser mass of gases per kg of fuel resulting in lower energy recovery. Generally, methane and hydrogen rich mixtures have greater HHV and provide better energy conversion efficiency, since the methane is a gas with higher energy density (36,250 kJ m^{-3}) as compared to CO (11543 kJ m^{-3}).

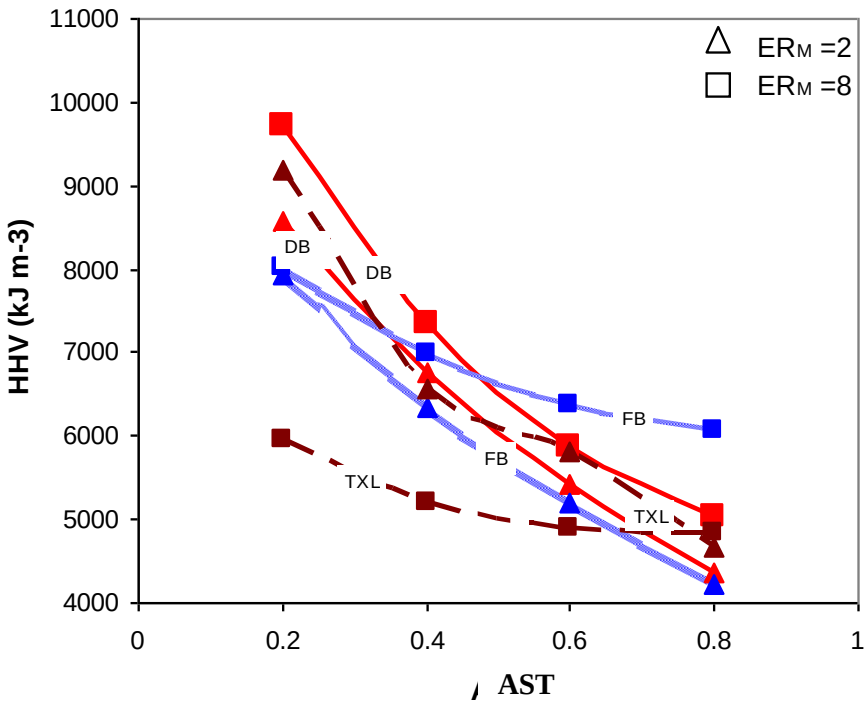

Figure 5.5.5: Effect of the ASTR and ER_M on HHV for DB, FB and TXL.

5.5.3. Experimental Results and discussion for air gasification

In this section, experimental results on bed temperature profile and gas composition are presented. To estimate the uncertainty in gas composition, standard deviation was determined for the data. The uncertainty for each gas was calculated as the ratio between the standard deviation and the average value measured. Additionally, the uncertainty of the temperatures was estimated as the ratio between the uncertainty of the device (±1.5 °C) and the measured value. In general, the gas composition values fluctuated within ~15% and the temperature values within ~0.55% of the average value measured.

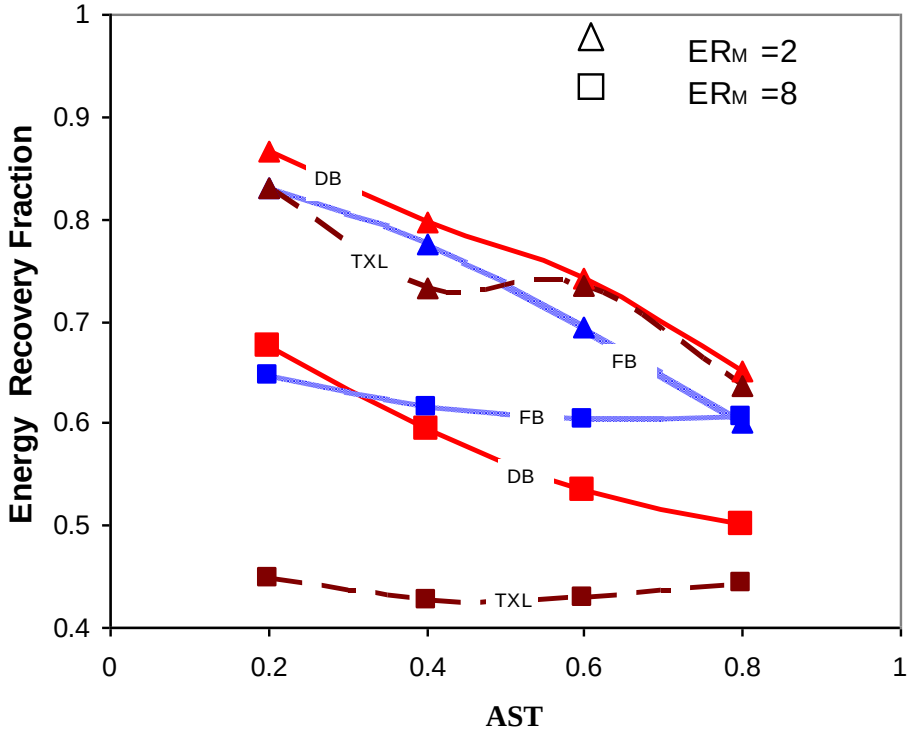

Figure 5.5.6: Effect of the ASTR and ER_M on energy recovery for DB, FB and TXL.

5.5.3.1. Temperature profiles

Temperature profiles are measured every 60 seconds along the gasifier axis. A typical gas analysis is presented in Figure 5.5.7a for an experiment at ER= 3.18 and S: F= 0.8. It is apparent that the temperature profile achieves almost state steady in the last ten minutes; therefore, it is appropriate to assume steady state conditions during the last 10 minutes of each gas analysis. The temperature profiles discussed in this paper correspond to the average measured during the last ten minutes. As discussed before, in a fixed bed gasifier, the oxidation of char (heterogeneous oxidations) occurs near to the bottom of the bed where mostly char reacts with the oxygen and steam to produce CO, CO_2, H_2, and the heat required for driving the gasification process is released. Due to the fact that under gasification conditions char oxidation of large particles is almost diffusion controlled, the char oxidation rate is dependent upon the availability of O_2 in the gas stream. The temperature in the combustion zone (T_{peak}) depends upon of

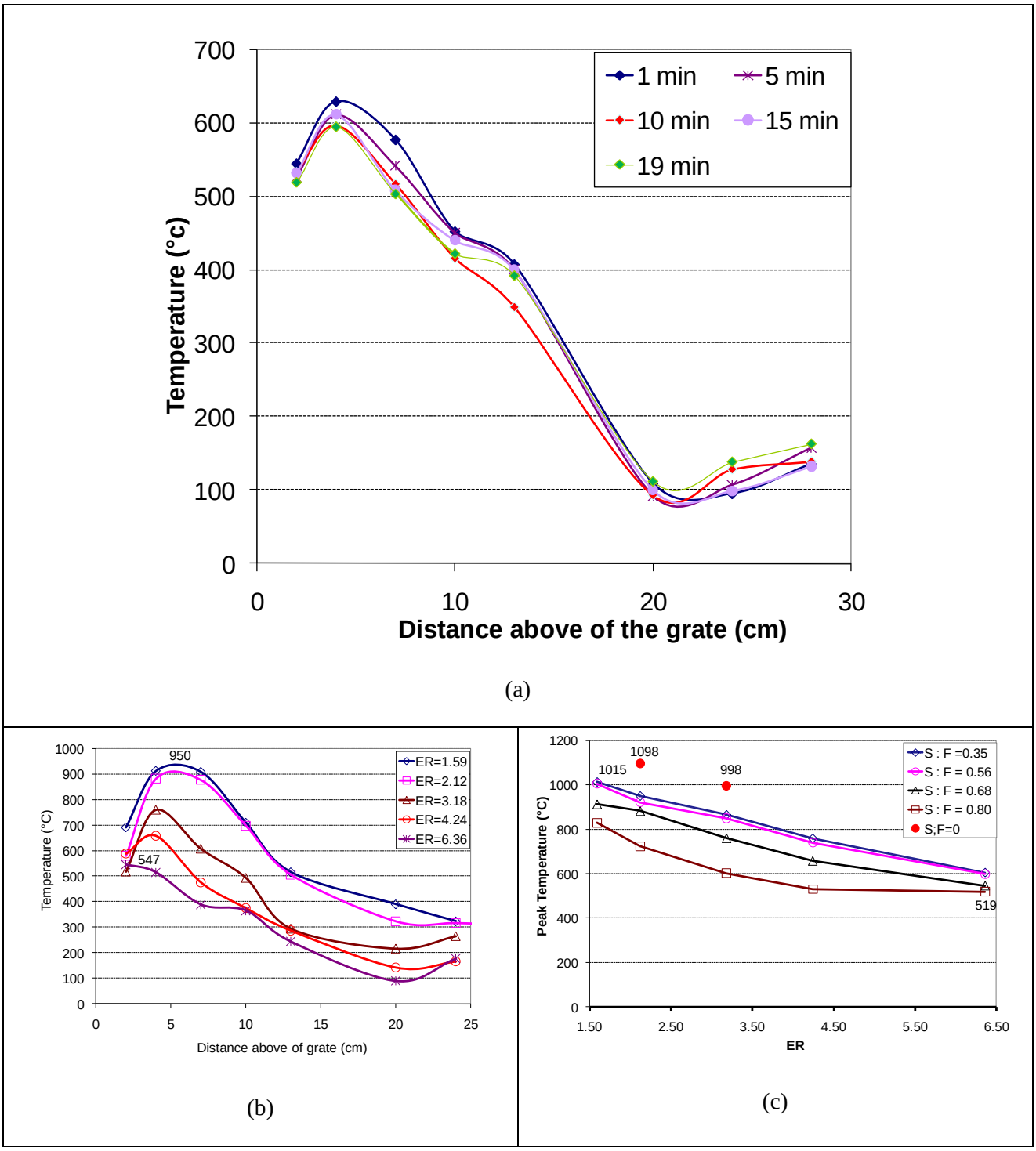

Figure 5.5.7 (a) Temperature Profile during a Typical Gas Analysis at ER=3.18 and SF=0.8 (b) Temperature Profile along of Gasifier Axis for Several ERs and S: F =0.68, (c) Peak Temperature Profile vs. ER for Several S: F ratios.

the concentrations of O_2, H_2O, and CO_2. Above the combustion zone, the temperature decreases since oxygen concentration is negligible and most of the reactions occurring there are endothermic. Below the combustion zone the temperature is lower because it corresponds to ash temperature. It is apparent

from Figure 5.5.7a that the peak temperature occurred at ~5 cm above of the grate indicating no ash accumulation.

Increase of ER, at fixed S: F ratio implies a decrease in the oxygen supplied; thus, heat generation due to char oxidation decreases resulting in lesser T_{peak} and hence results in lower temperature profile (Figure 5.5.7b). Due to the presence of oxygen at the bottom of the bed, the peak temperature occurs near the bottom. The temperature of the particle under the assumption of negligible char-steam reaction and diffusion controlled combustion can be derived as (Annamalai et al, 2006):

$$\frac{c_p(T_p - T_\infty)}{h_C} = B \tag{5.10}$$

Where h_c=$h_{c,I}$ for CO, h_c= $h_{c,II}$ for CO_2 produced, T_p= particle temperature, B= $\{Y_{O2\infty}/\nu_{O2}\}$, ν_{O2} = 1.33 for CO, 2.33 for CO_2 produced, $Y_{O2\infty}$= Oxygen mass fraction, and c_p specific heat of the gases. In particular, for ER=1.59 and S: F= 0.68 the peak temperature measured is about 950 °C (Figure 8b); however, this value is lower compared to (1191 °C) obtained with the equation 8 (c_p of air =1.15 kJ/kg K, c_p of the steam= 2.3 kJ/kg K, c_p of mixture =1.28 kJ/kg K, $YO_{2\infty}$ = 0.203, and $h_{c,I}$ = 9204 kJ/kg). The lower experimental temperature compared to that of the model indicates that i) the char may react with both O_2 and steam at the bottom of the bed to produce CO and H_2 and ii) combustion may not be diffusion controlled. On the other hand, if the steam carbon reaction was included in the model and if diffusion limited heterogeneous reactions was assumed, the estimated T_p would be lower than the estimated using equation 8.

Figure 5.5.7c shows the effect of change in ERs and S:F ratio on the peak temperature (combustion temperature zone). Also are presented two T_{peak} (1098 and 998 °C) obtained for gasification with only air at ER=2.12 and ER=3.18. At lower ERs, the effect of the S: F ratio is higher. For instance, at ER=1.59 the peak temperature difference between the curves of S: F =0.35 and 0.80 is 185 °C while at ER= 6.36 the difference between the same curves is 91 °C only since oxygen availability is limited. The curves from Figure 5.5.7c suggest that at constant S: F, the peak temperature is affected almost linearly by changes on the ER. Increased S: F causes the T_{peak} to decrease. This can occur due to i) decreased amount of air, ii) change in the c_p of the mixture, iii) regimes of combustion: kinetics vs. diffusion controlled, and iv) steam-char reaction.

At ER=2.12, the peak temperature for gasification with air only is 147 °C (15.45%) higher as compared to that of gasification with air-steam at ER=2.12 and S:F=0.35 while at ER=3.18, the difference in peak temperature between gasification with air and gasification with air-steam is ~ 132 °C (15.24%). In general, for the range of operating conditions (ER and S: F) investigated the T_{peak} ranged between 519 (ER=6.36, almost pure pyrolysis) and 1015°C (ER=1.59).

5.5.3.2. Gas composition results

The results on gas analysis obtained From MS for a typical experiment (ER=4.24 and S: F=0.35) are shown in the Figure 5.5.8a as a function of the time. The data on gas composition have a cyclic dynamic behavior in the vicinity of an average value. However, at first glimpse, it appears that the average is almost constant during the experimental period. Figure 5.5.8a shows the mole fraction of N2, H_2, CO_2, CO, CH_4, and C_2H_6 (on a dry basis) along with the average mole fraction and the standard deviation (STDEV) of the data. The data on H_2 presents the major standard deviation (3.2) about of the average value of 18.62% whereas the data on CH_4, CO_2, and C_2H_6 show the lower standard deviation and the data on CO shows a standard deviation of 1.53. As discussed earlier, in general for the set of experiments discussed in this paper, the composition value of the gases analyzed fluctuated within ±15 % of the average value.

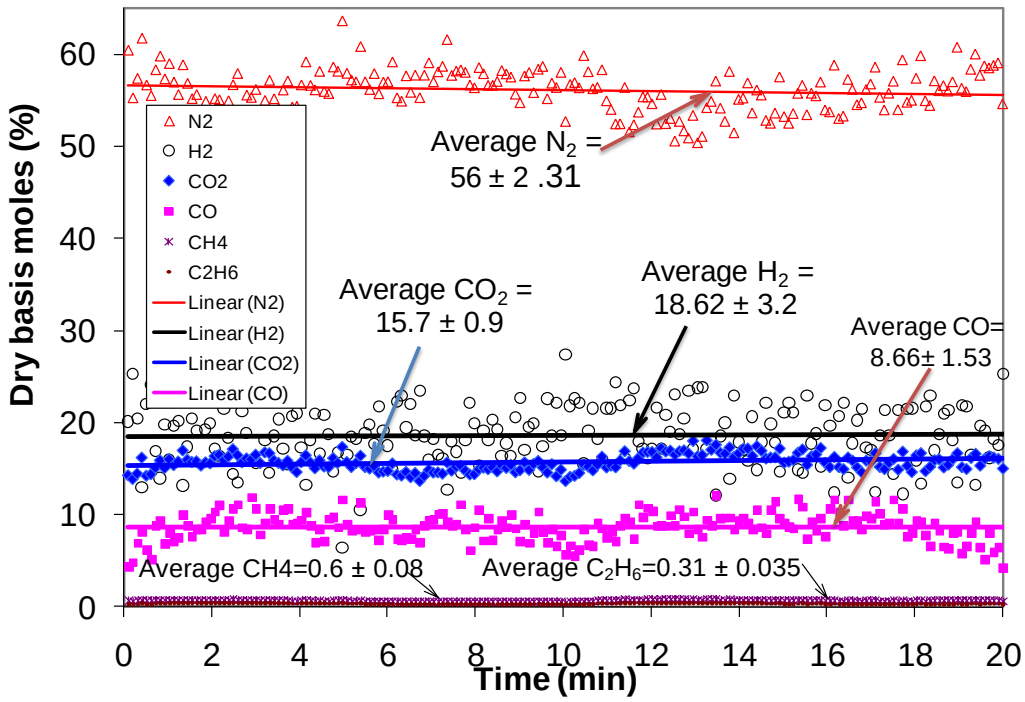

(a)

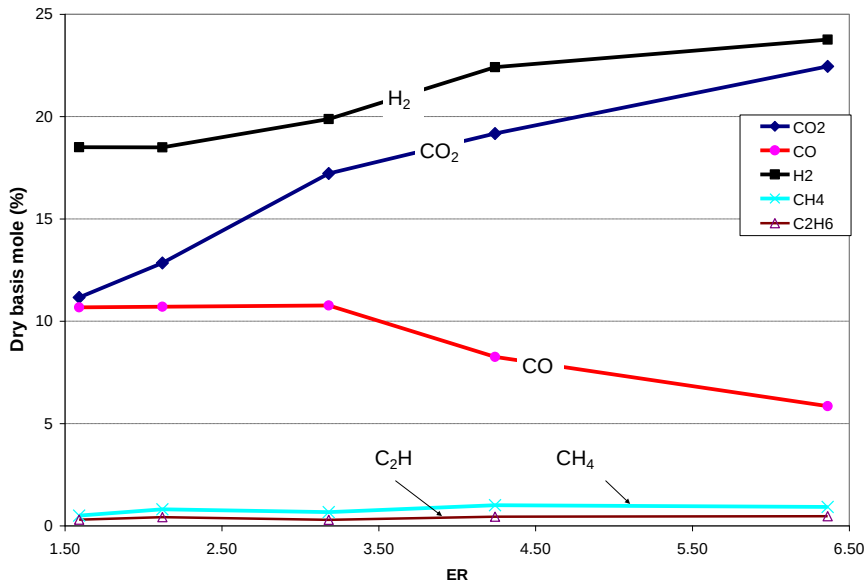

(b)

Figure 5.5.8 (a) Gas Composition vs. time for a Typical Experiment at ER= 4.24 and S: F=0.35, (b) Gas Composition for Several ERs and S: F=0.68

As discussed before, at constant S: F, increasing the ER decreases the O_2 supplied with the air at the bottom which implies decreasing T_{peak} in the combustion zone. Then, as the temperature is lowered, the reaction $C+O_2 \rightarrow CO_2$ is favored 0. CO_2 increases at lower temperatures. More production of CO_2 implies consumption of more O_2 via CO_2, thus, less O_2 is consumed via CO and hence less CO is produced (Figure 5.5.8b). Also, at constant S:F, increased ER increases steam-air ratio (S:A), which implies decreased air supplied and hence the combustion of char take place in a H_2O rich mixture which favors the heterogeneous reaction of char with H_2O to produce H_2. The rate of H_2 and CO produced by the heterogeneous reaction $C+H_2O \rightarrow CO+H_2$ becomes important when the reaction occurs at low O_2). On the other hand, the concentrations of CH_4 and C_2H_6 were lower ($0.43< CH_4< 1.75$ and $0.2<C_2H_6<0.7$) as compared with those of other gases and were almost not affected by the ER.

The effect of the ER and S: F on the concentrations of H_2, CO, and CO_2 are presented in Figure 5.5.9a, Figure 5.5.9b, and Figure 5.5.9c. At constant ER, higher S:F ratios signify more steam available to react with char to produce CO and H_2 (steam char reaction) in the high temperature reducing zone immediately above the combustion zone (i.e.O_2 deficient) near the bottom of the bed. The CO produced by the steam reforming reaction reacts with the surplus steam (shift reaction) in the upper zone (reduction) to produce more H_2 and CO_2 ; hence, more C atoms contained in the DB result in CO_2. It is evident from the graphs of Figure 5.5.9b that lower ERs have a lower effect on the CO production compared to higher ERs. Also, the results show that at constant ER, changing the S: F ratio affects the production of H_2 more than the production of CO. For instance, at ER=1.59 changing the S: F from 0.35 to 0.8 increases the production of H_2 by 57.5 % but decreases the production of CO by only 26.2 % (Figure 5.5.9a and Figure 5.5.9b). Since decrease in CO % is less than increase in H_2 % then there must be heterogeneous steam char reaction resulting in production of H_2. This is also evident from lowered T_{peak}. Under the operating conditions discussed ($1.59<ER<6.36$ and $0.35<S: F<0.80$), the CO ranged from ~4.77 to ~11.73 %, H_2 from 13.48 to 25.45%, CO_2 from 11 to 25.2%, CH_4 from 0.43 to 1.73 %, and C_2H_6 from 0.2 to 0.69%.

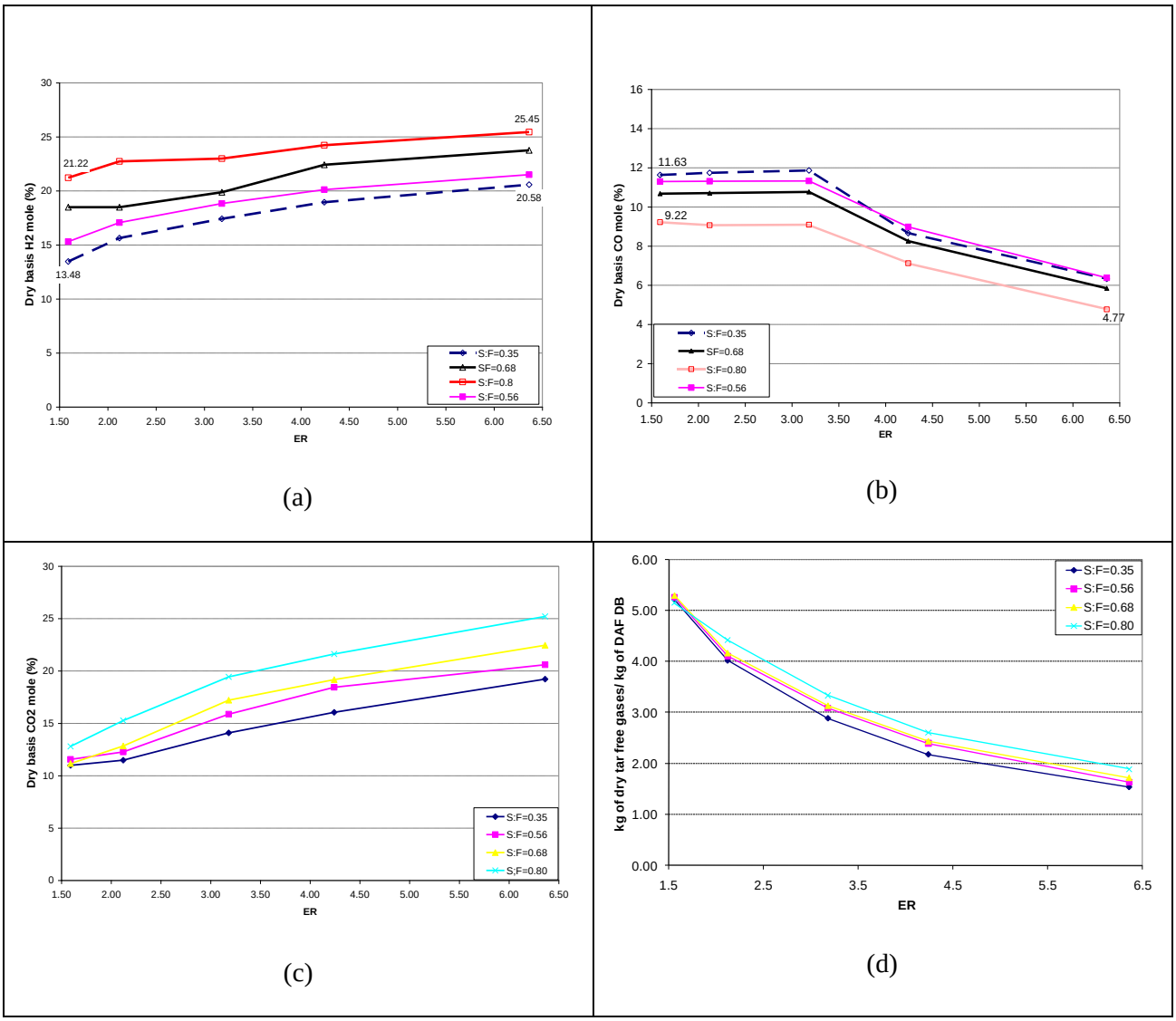

Figure 5.5.9 (a) Hydrogen % vs. ER for Several S: F ratios, (b) Carbon Monoxide % vs. ER for Several S: F ratios (c) Carbon Dioxide % vs. ER for several S: F ratios, (d) Mass of gases produced per kg of DAF DB on a dry tar free basis for gasification of pure DB

5.5.3.3. HHV of gases and energy conversion efficiency

The heat content of the combustible gases is computed on a dry tar free basis. The energy density (kJ/ m^3) of the gases is represented in Table 5.5.3 for several ER and S:F ratios. Increased ER or S:F tends to increase the energy density of the gases; this is due principally to the increase in the production of hydrocarbons (HC) and H_2. At constant S: F, increasing the ER tends to increase the HHV, due to more H_2 and HC, until certain ER beyond which the HHV starts to decrease. The energy density of the gases is strongly affected by the production of hydrocarbons such as CH_4 and C_2H_6 which have a high HHV as compared to the other gases (CO and H_2). For example, the HHV or energy density of the CH_4 is 36264 kJ/SATP m^3 while the HHV of CO and H_2 are 11550 and 11700 kJ/ SATP m^3 respectively. Although, the HHV of the H_2 (141800 kJ/kg) on mass basis is very high, its energy density is almost comparable to that of CO (only 1.08 % higher) due to its low density (~0.0857 kg/m^3). At constant ER, increased S: F increase the H_2/CO of the species produced (Figure 5.5.9a and Figure 5.5.9b), which implies increasing the energy density slightly. For the set of operating condition investigated the HHV of the gases ranged between 3268 and 4285 kJ/ SATP m3, which correspond to a range between 9 % and 12.6 % of the energy density of the CH_4 on volume basis.

Even although, the energy density of the gases give an idea of the energy content of the gases produced, it does not give information about the degree of energy conversion from biomass gasified. The fraction of energy recuperated in the gasifier can be calculated with Equation 7.

Table 5.5.3: Energy density of the gases (kJ /Standard temperature and pressure (SATP) m^3) for several ERs and S: Fs.

S:F (mole ratio)	**ER**				
	1.56	2.12	3.18	4.24	6.36
0.35	3280	3473	3787	3648	3666
0.56	3268	3835	4402	4245	4032
0.68	3762	3955	3993	4217	4079
0.80	3934	4116	4291	4378	4585

Ultimate analyses of samples of tar collected in the sample unit were obtained and were used to derive an empirical formula ($CH_2O_{0.48}N_{0.064}S_{0.0017}$). Because it was impossible to measure the mass of tar and H_2O produced during the experiments, the volumetric flow of gases, required to calculate the energy recovery, was estimated by mass balance using tar and gas compositions and with the knowledge of the char produced and the flows the air and steam. Table 5.5.4: Energy conversion efficiency (ECE) for several ERs and S:Fs estimated by tom balance presents the (ECE) estimated by atom balance and assuming gas composition on a dry tar free basis whereas figure 4d presents the yield of gases estimated using atom balance. Although, the energy density of the gases tends to increase with increased ERs, the ECE decreases, due to the fact that increased ERs produce more mass of tar and char but less mass of gases per kg of DB gasified. For the range of the operating conditions studied the ECE ranged from 0.24 to 0.69; the remaining fraction corresponds to the energy in char, tar, and sensible heat of gases leaving the gasifier. This agrees with the fact that in a fixed bed gasifier

the gases leave the gasifier at a lower temperature as compared to that of gases leaving a fluidized bed gasifier. Lower sensible heat of gases leaving the reactor implies higher gasifier efficiency, and hence more energy recovered in the gases.

Table 5.5.4: Energy conversion efficiency (ECE) for several ERs and S:Fs estimated by tom balance

S:F (mole ratio)	**ER**				
	1.56	2.12	3.18	4.24	6.36
0.35	0.65	0.56	0.45	0.33	0.24
0.56	0.60	0.59	0.53	0.41	0.27
0.68	0.69	0.60	0.47	0.41	0.29
0.80	0.69	0.64	0.53	0.44	0.35

5.5.4. Experimental results and discussion for enriched air gasification

5.5.4.1. Temperature Profiles for enriched air gasification

Experiments are carried out for different ER and different oxygen percentages. Temperature profile for equivalence ratio of 2.1 and for different oxygen percentages is shown in the Figure 5.5.10. From the profile it can be observed that the peak temperature increases with increase in oxygen concentration in the incoming air while the total oxygen entering the system still remains the same because of the same equivalence ratio. Note that total mass flow of gases into the reactor is reduced as the oxygen percentage increases at the same ER, thus the gas velocity is reduced.

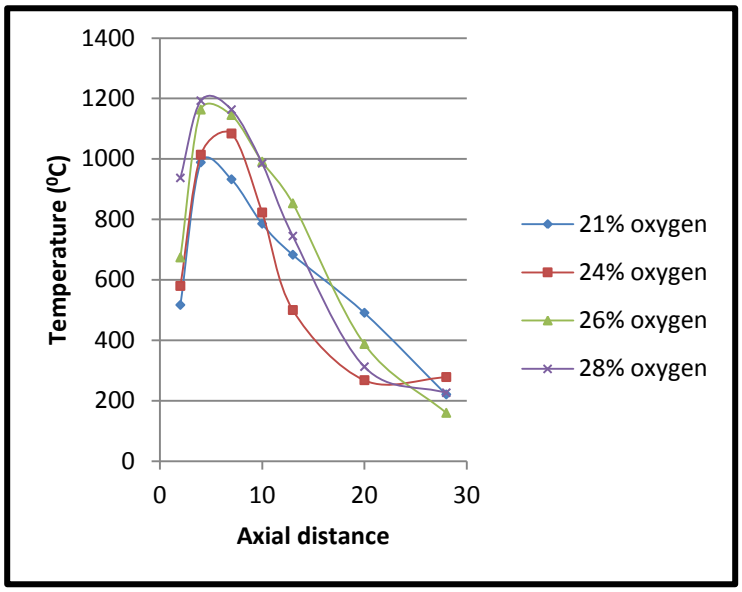

Figure 5.5.10. Temperature profile for ER = 2.1 and S:F = 0

Using the formula for calculating B number, assuming constant specific heat at constant pressure and the reaction $C + 0.5\ O_2 \rightarrow CO$, we can calculate the peak temperatures for different percentages of oxygen in the incoming air. Experimental values obtained are almost similar to the values calculated theoretically.

Table 5.5.5. Theoretical T_{peak} values.

O_2 %	T_{peak}(^{0}C)
24 %	1082.14
26 %	1170.24
28 %	1258.33

For a higher equivalence ratio of 4.2, it was observed that the peak temperature was almost similar for both 21% oxygen and 28% oxygen (Figure 5.5.11). However the temperature was higher at a height of 10 cm from the grate for 21% oxygen, compared to the 28% oxygen concentration.

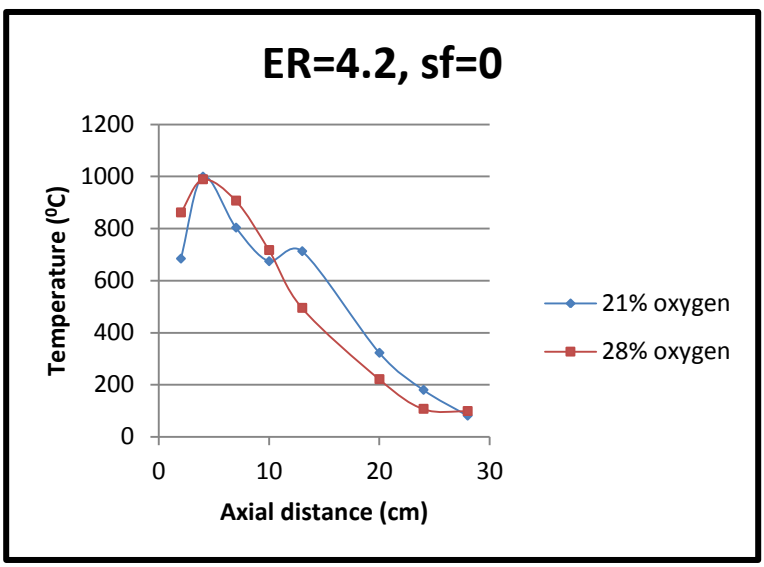

Figure 5.5.11. Temperature profile for ER = 4.2 and S:F = 0

This can be seen in Figure 5.5.11 where there is a slight rise in temperature at around 10 cm from the grate. However there is no such temperature rise for gasification of dairy biomass with air having 28% oxygen as the temperature profile is steady after having a peak at 2 cm from the top of the grate. Future experiments must be performed in order to verify the results.

With a steam fuel ratio (S:F) of 0.33 (or 0.55 kg/kg of DAF fuel) and ER = 4.2, the peak temperature decreased further in the case of air having 21% oxygen, however the peak temperature increased for air having 28% (Figure 5.5.12). The peak temperature for 28% oxygen mixture increases with increase in S:F. Hydrogen is produced in this case due to water gas shift reaction. It is hypothesized that the hydrogen produced oxidizes at higher oxygen concentration which causes an increase in peak temperature.

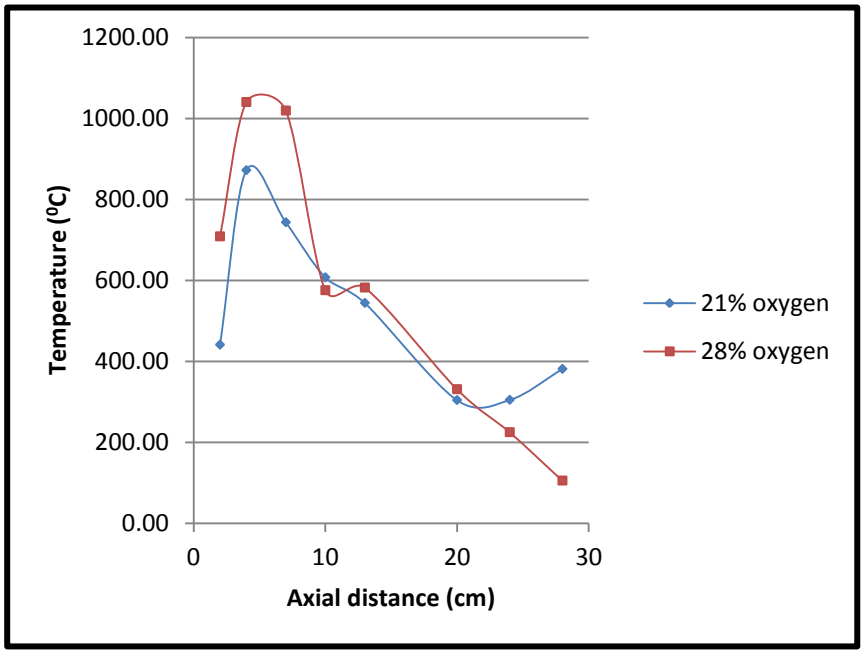

Figure 5.5.12. Temperature profile for ER = 4.2, S:F = 0.33

5.5.4.2. Gas composition for enriched air gasification

Gas composition for different oxygen percentages are determined using mass spectrometer. For ER = 2.11 and S:F =0, it has been observed that as the oxygen percentage increases the amount of carbon dioxide increases with the decrease in the amount of carbon monoxide (Figure 5.5.13). As the concentration of oxygen increases it reacts with carbon monoxide producing more carbon dioxide.

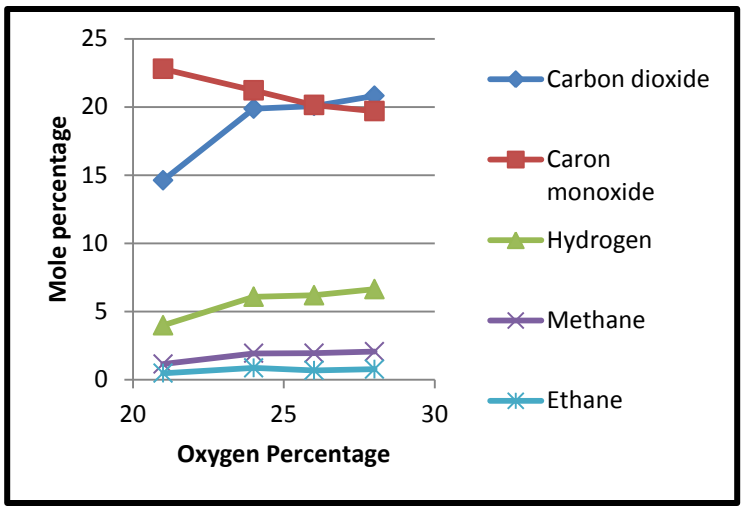

Figure 5.5.13. Gas composition for ER = 2.11, S:F = 0

For ER = 4.2, the amount of carbon monoxide produced increases with increase in oxygen percentage (Figure 5.5.14). Hence the heating value of the gas mixture also increases with increase in oxygen concentration. This may be due to increased concentration of oxygen with decrease in ER resulting in increased CO production.

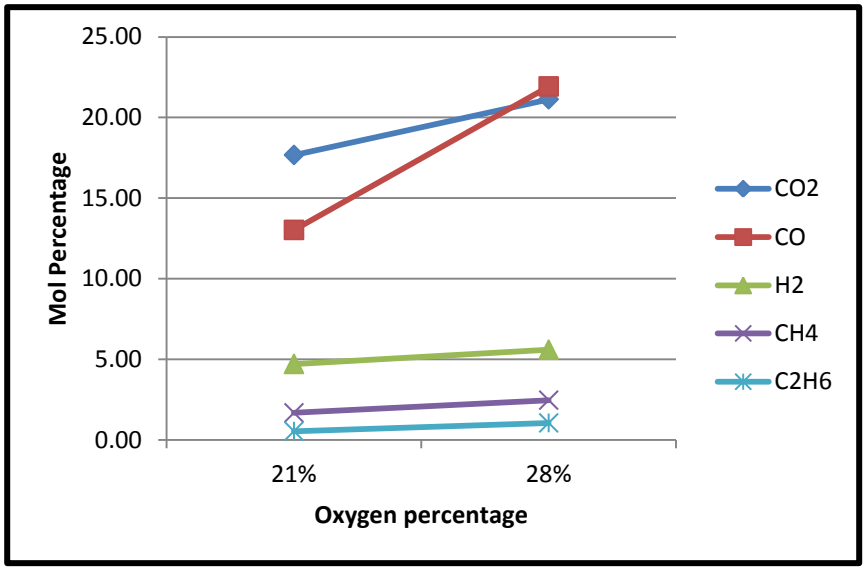

Figure 5.5.14. Gas composition for ER = 4.2 and S:F = 0

It was observed that with increase in S:F, the amount of hydrogen produced increases due to water gas shift reaction, $CO + H_2O \rightarrow CO_2 + H_2$. But the mass based heating value of the resulting mixture with higher S:F is less when compared to mixture obtained with S:F = 0 (Figure 5.5.15 and Figure 5.5.16).

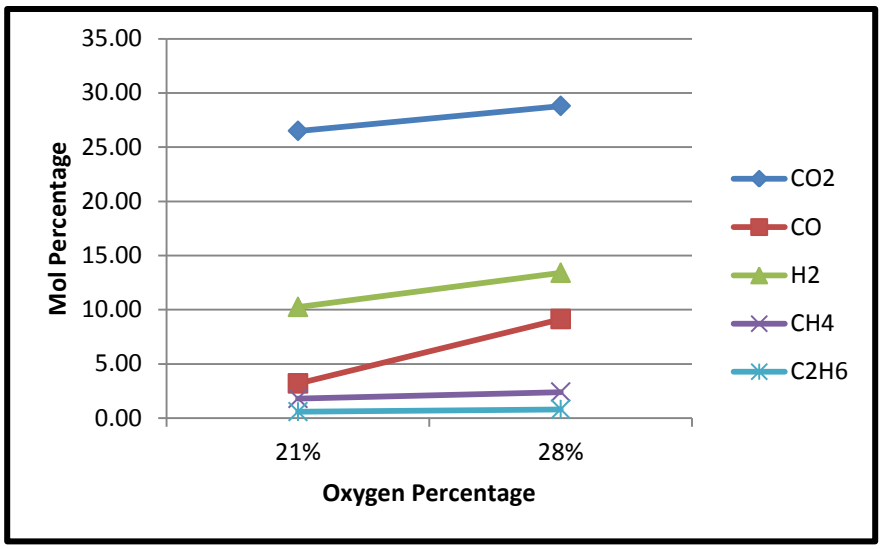

Figure 5.5.15. Gas composition for ER = 4.2 and S:F = 0.33

The heating value is low even with increased hydrogen percentage (higher mole percentage) for higher S:F. This may be due to low density of hydrogen and lower mass percentage in the resulting gas mixture.

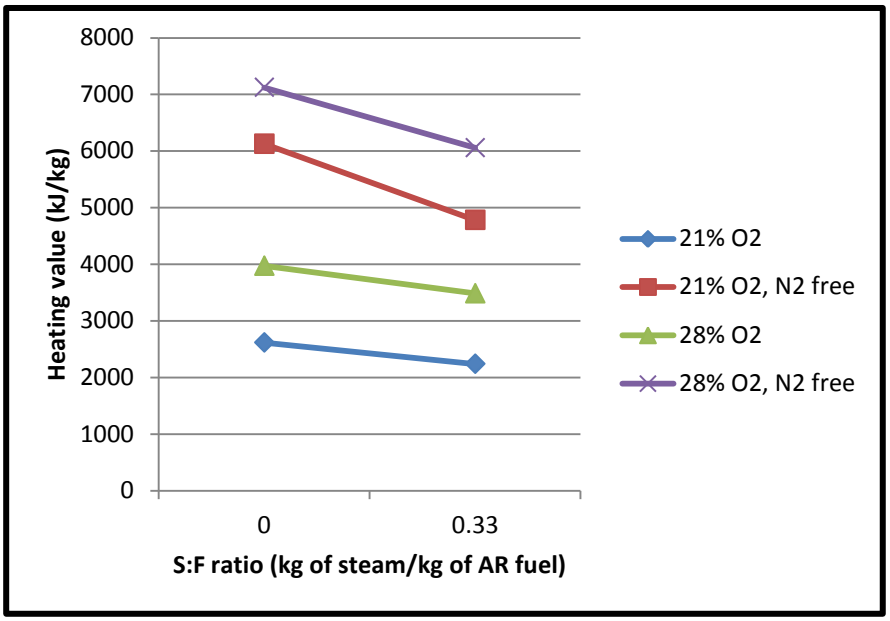

Figure 5.5.16. Gas heating value for ER = 4.2 and different S:F

From the experimental results, a decreased reactivity of fuel was observed for gasification with lower oxygen percentages i.e., with air having 21% oxygen.

5.6. Impact on Tasks due to Industrial Advisory Committee feed back

" Do not lose sight of the "FutureGen" opportunity in Central Texas; incorporate such a project, if it comes to pass, into the overall scheme of the DOE project, or at least capture data analogous to that of the Broumley Dairy digester study" Thus the renewal proposal, included a task to study steam gasification in order to produce more H2 for potential application to FutureGen (Task A-5).

5.7. Summary

Most of the tasks were completed except for using pure O2 for gasification due to safety reasons in the coal and biomass energy laboratory (CBEL) of TAMU and the problems with ash fouling due to high temperatures; instead enriched air was used with higher O2 % (> 21%) but less than 30 %. Further CO2+ O2 mixtures were studies even though not proposed. Results are included in MS thesis of Mr. Siva Thanapal (Dec. 2010) The results were presented at Applied Energy Conference [Thanapal et al 2011] and selected for Journal publication by the conference organizer. The summary and conclusions of this study on gasification of DB, DB-ash, and DB-WYC are presented in this section.

5.7.1. Gasification facility

A small scale (10 kW) gasification facility was rebuilt with the following modifications:

a An ash disposal system so that experiments could be run continuously with periodic ash disposal
b A steam generator to produce the steam for the gasifier
c A MS and the gas mixtures necessary to calibrate the MS were acquired
d A sampling system to prepare the gas samples before they are analyzed continuously and in real time by a mass spectrometer
e A data acquisition system to measure the temperature in different places of the gasification facility
f A control panel to control the flow of steam, air and heat to the heater elements of the steam generator and combustion chamber of the gasifier.
g A separate line to send in oxygen so that an enriched air mixture having higher oxygen percentages can enter the gasification chamber.

5.7.2. Modeling studies

Global modeling studies (atom balance and equilibrium) on gasification were performed in order to determine the operating conditions (ER and S:F). The effect of modified equivalence ratio ER_M and AOF on gasification of feedlot biomass (FB), dairy biomass (DB), Wyoming coal (WYC), and Texas Lignite coal (TXL) were also estimated by modeling.

a Decreased AOFs produce mixtures richer in CH_4 and H_2, which have higher HHVs. On the other hand, increased ER_M tends to produce mixtures with a higher HHV. Generally, mixtures

rich in methane and hydrogen have greater HHV and provide better energy conversion efficiency since methane is a gas with higher energy density (36250 kJ m-3) as compared to CO (11543 kJ/ m^3).

b The increase in the AOF results in decreased energy recovery, but at higher ER_M the decrease is not much. At constant AOF, higher ER_M implies lesser oxygen supplied in the oxidizers and the process is nearly pyrolysis (production of char), which produces a lesser mass of gases per kg of fuel resulting in lower energy recovery.

c At constant ER, increasing the S:F implies increased steam supplied with the oxidizing source ; thus, the reactions occur in a steam-rich ambient which favors the steam reforming reaction and the shift reaction producing mixtures rich in H_2, CO_2, and CH_4 but poor in CO.

d The increase in ER at constant S:F ratio implies decreased oxygen entering through the air and, hence, the reactions occurs in an ambient poor in O_2 but rich in H_2O, which favors the reactions of char and CO with steam to produce more CO_2 and H_2. More C atoms leaving the gasifier as CO_2 mean less C atoms leaving as CO. The curves of CO and H_2 show a peak. At ER<3.18, increasing ER improves the concentration of CO but at ER>3.18, the concentration of CO is decreased as ERs increase. Modeling results shows that the increase in ER produces rich mixtures in CH_4.

e Gasification under higher ERs produces CH_4 and H_2 rich mixtures which have high HHV due to the higher HHV of CH_4 and H_2. At ER<3.18, the gross heating value of the gases seems to not be affected by changes in the S:F. This can be due to the fact that at ER<3.18, the changes in the S:F do not affect the concentration of CH_4.

f Increasing the ER at constant S:F tends to increase the ECE until a value beyond which it starts to decrease. At ER<3.18, increased ERs increase the ECE until 0.87, at which point it stars to decrease. Gasification under ER>3.18 tends to produce char due to the lack of enough oxygen for the reaction of char.

5.7.3. Experimental studies

Experiments on gasification with air-steam were carried out and data on bed temperature profile and gas composition under various operating conditions were obtained. Additionally, chlorinate char was produced through the pyrolysis of DB using N_2 and N_2-steam blends.

a The adiabaticity of the reactor was checked by determining the overall heat transfer coefficient (U) and then estimating the heat loss; the U was measured by allowing the reactor to cool down after the experiment and storing the changes of temperature. The results showed that the global heat transfer coefficient is very low (U=6.37016E-6 kW/ m^2 k s) and almost constant along the gasifier axis.

b The bed temperature profile measured along the gasifier axis showed a peak in the combustion region where the char reacts with the oxidizer supplied. The peak temperature lies somewhere between 3 and 5 cm above the grate and depends upon the concentration of O_2, H_2O, and CO_2 in the combustion zone. Above the combustion zone in the reduction, pyrolysis, and dry zones, the temperature decreased because most of the reactions occurring there are endothermic.

c Increased ER and S:F ratios decrease the peak temperature. Operating at ER> 6.36 can lead to lower peak temperatures than that required for the combustion of char. Thus, under those operating conditions, the process becomes near pyrolysis which requires heat input. In general, for the set operating conditions, the peak temperature for gasification of DB ranged between 519 and 1015°. Gasification of DB-ash and DB-WYC blends showed the maximum peak temperatures (1032 and 1054 °C respectively).

d From the results, it is apparent that H_2 rich mixtures could be produced by adiabatic gasification of DB using mixtures of air-steam as an oxidizing source. Increased ER and S:F

ratios tend to produce H_2 and CO_2 richer mixtures but poor mixtures in CO. In general, the effect of the ER and S:F on the production of CH_4 and C_2H_6 is negligible. For gasification of DB under the set of operating conditions, the CO ranged from ~4.77 to ~11.73 %, H_2 from 13.48 to 25.45%, CO_2 from 11 to 25.2%, CH_4 from 0.43 to 1.73 %, and C_2H_6 from 0.2 to 0.69%.

e The addition of ash and WYC seems to affect the production of CO and H_2. The highest increase in CO (caused by the addition of ash) at S:F=0.35 and ER=6.36 was around 50%, while the highest increase in H_2 (~30%) was achieved at ER=1.5 and S:F=0.35. At ER>3.18, the effect of the addition of ash and WYC on the production of H_2 was insignificant. Gasification of DB–ash blends produced mixtures with CO ranging between 6.7 and 13 % and H_2 ranging between 17.5 and 25.3% while gasification of DB-WYC blends produced mixtures with CO from 6.5 to 13.6% and H_2 raging from 16 to 26.3 %.

f The effect of the S:F ratio on the HHV of the gases is more important than that of the ER. Although increased ER produces gases with higher gross heating value, the energy recovery decreases with increased ERs due to higher tar and char production.

g At constant S:F ratio, increasing ER increases the production of char while at constant ER, increased S:F ratios produce lower char. At ER=1.59, the char produced was almost zero. The highest yield of char (~0.18 kg per kg of DAF DB gasified) was reached for gasification of DB at ER=6.36 and S:F=0.35. This indicates that under those operating conditions only about 18% of the FC content in a kg of DAF DB is gasified; the remaining 82% corresponds to the char. Thus, gasification of DB at ER=6.36 and S:F=0.35 tends to be near pyrolysis.

h For all the cases, increased ER tends to produce gases with more concentration of tar while increased S:F reduces the production of tar.

i About 51% and 56% of the CL content in DB was volatilized during pyrolysis with N_2 and N_2-H_2O respectively while 68 % and 64% of the VM in DB were volatilized by pyrolysis with N_2 and N_2-H_2O. This indicates that the rates of volatilization of chlorine during pyrolysis are lower than those of VM. VM % to CL % pyrolyzed ratios were 1.34 and 1.12 during pyrolysis with N_2 and N_2-staam respectively.

For the experiments conducted with enriched oxygen mixture following conclusions can be drawn.

a. Peak temperature within the bed increases with increase in oxygen percentage. The theoretical values predicted using the B number calculations were verified experimentally and the values were approximately similar to the theoretical numbers.
b. Heating value of the gases produced during gasification increases with increase in oxygen percentage in the air while it decreases with increase in steam fuel ratio. However higher percentage of hydrocarbons and hydrogen is produced with increase in steam fuel ratio.

5.8. Acronyms

AOF	Oxygen from air to total oxygen from air and steam ratio
CB	Cattle Biomass
$CAFO_s$	Concentrated Feeding Operations
DAF	Dray ash free
DB	Dairy Biomass

DB-ash	Dairy biomass ash blend
ECE	Energy conversion efficiency
EIA	Energy Information Administration
ER	Equivalence ratio
FB	Feedlot Biomass
FC	Fixed Carbon
HHV	High heating value of gases
LA-PC-SepSol-DB	Low ash partial compost separated solids dairy biomass
LA-PC-FB	Low ash partial compost feedlot biomass
MS	Mass Spectrometer
SATP	Standard ambient temperature (25°C) and pressure (100 kPa)
SCFH	Standard feet cubic per hour
STDEV	Standard Deviation
TXL	Texas Lignite Coal
ER_M	Modified equivalence ratio
$C_{P,A}$	Air specific heat (kJ/kg.k)
$h_{k,p}$	Enthalpy of the products
$h_{k,R}$	Enthalpy of the reactants
HHV_{Gases}	High heating value of gases (kJ/m3)
HHV_i	High heating value of products (kJ/m3)
HHV_{Fuel}	High heating value of DB (kJ/Kmol)
$N_{k,p}$	Moles of the products
$N_{k,R}$	Moles of the reactants
S:A	Steam to air ratio
S:F	Steam to fuel ratio (mole basis)
T_p	Adiabatic temperature

T_{peak}	Peak Temperature
X_i	Moles fraction of each fuel product
$\eta_{Gas,E}$	Energy conversion efficiency
ρ	Air density (kg/m3)
λ	Latent heat of the water (kJ/Kg)

5.9. References

Annamalai, K.,Oh Hyukjin, Ben Lawrence, Siva Thanapal, and Joseph King, " Comparative evaluation of Catalytic and non-catalytic Pyrolysis Processes for Production of Bio-Fuel from Soy Seeds, " "ASME Turbo 2010, June 4-18,Glasgow, Scotland, UK, 2010

Annamalai K, Priyadarsan S, Arumugam S, Sweeten JM, 2007, "Energy conversion: principles of coal, animal waste, and biomass fuels", Encyclopedia Energy Eng Technol;1(1):476-97.

Annamalai, K and Puri, 2006, "Combustion Science and Engineering", CRC Press (Taylor and Francis).

Annamalai K, Sweeten JM, Freeman M, Mathur M, O'Dowd W, Walbert G, Jones S, 2003, "Co-firing of coal and cattle biomass (FB) fuels", Part III: Fouling result from a 500,000 Btu/h pilot plant scale burner. Fuel; 82:1195-1200**.**

Bridgwater AV, 1995, "The technical and economic feasibility of biomass gasification for power generation", Fuel; 74(5):631-653.

Carlin N, Annamalai K, Sweeten JM, Mukhtar S, 2007, "Thermo-chemical conversion analysis on dairy manure-based biomass through direct combustion", Int J Green Energy; 4:1-27.

Chen, Wei, Kalyan Annamalai1, R. James Ansley, and Mustafa Mirik, "Updraft Fixed Bed Gasification of Mesquite and Juniper Wood Samples , J of Energy, Positive Reviews Received.

Ferdous D, Dalai AK, Bej SK, Thring RW, 2001, "Production of H_2 and medium heating value gas via steam gasification of Lignins in fixed-Bed reactors", J Can Chem Eng;.79:913-922

Galloway T, Waidl J, Annamalai K, Sweeten JM, Tomlinson T, Weigle D, 2002, "Energy resources recovery applications using gasification and steam reforming", Bi-annual Incineration and Thermal Alternatives. New Orleans: Conference.

Gil J, Corella J, Azner MP, Caballero MA, 1999, "Biomass gasification in atmospheric and bubbling fluidized bed: effect of the type of gasifying agent on the product distribution", J Biomass and Bioenergy; 17:389-403.

Gerardo Gordillo and Kalyan Annamalai, “Dairy Biomass-Wyoming Coal Blends Fixed Gasification Using Air-Steam for Partial Oxidation , “ accepted, J of Combustion, 2011

Gordillo G, Annamalai K, and Arcot U, January 3-5, 2008, “Gasification of Coal and Animal Wastes Using an Air-mixture as Oxidizing Agent”, 19th National & 8th ISHMT_ASME Heat and Mass transference conference, JNTU Hyderabad, India

Gordillo G, Annamalai K, July 8-12, 2007, “Gasification of coal and Dairy manure with air steam as oxidizing agent”, Proceeding of HT 2007. 2007 ASME-JSME thermal Engineering Summer Heat Transfer Conference., Vancouver, British Columbia, CANADA

Gerardo G, 2009, “Fixed bed counter current low temperature gasification of dairy biomass and coal-dairy biomass blends using air-steam as oxidizer”, PhD Thesis, Texas A&M University.

Hobbs ML, Radulovic PT, Smoot LD, 1993, “Combustion and gasification of coals in fixed-Bed”, J Prog Energy Combust Sci; 19:505-586

Hobbs ML, Radulovic PT, Smoot LD,1992, “Modeling fixed-bed coal gasifier”, AIChe J; 38:681-702.

Hoffert MI, Caldeira K, Jain AK, Haites EF, Harvey LDD, Potter SD, Schlesinger ME, Schneider SH, Watts RG, Wigley TML, Wuebbles DJ, 1998, “Energy Implications of future stabilization of atmospheric CO_2 content”, Nature, 395:881-884.

Jangsawang W, Klimanek A, Gupta AK, 2006, “Enhanced yield of hydrogen from wastes using high temperature steam gasification”, J Energy Res Technol;128:179-185

Kalisz S, Lucas C, Jansson A, Blasiak W, Szewczyk D, 2004, “Continuous high temperature air/steam gasification (HTAG) of biomass”, Victoria, Canada: 6th Int. Conference on Science in Thermal and Chemical Biomass Conversion.

Klass DL, 1998, “Biomass for Renewable Energy, Fuels, and Chemicals”, San Diego: Academic press.

Lawrence, B, 2007, “Cofiring coal and dairy biomass in a 100,000 Btu/hr furnace”, Master’s Thesis. Texas A&M University.

Priyadarsan S, 2002, “Fixed bed gasification studies on coal-feedlot biomass and coal-chicken litter biomass under batch mode operation”, Master’s Thesis, Texas A&M University.

Priyadarsan S, Annamalai K, Sweeten JM, Mukhtar S, Holtzapple MT, 2005, “Fixed bed gasification of feedlot and poultry litter biomass”, Trans ASAE; 47:1689-1696.

Priyadarsan S, Annamalai K, Sweeten JM, Holtzapple M, 2005, “Co-gasification of blended coal with feedlot and chicken litter biomass”, Proc Combust Inst; 30:2973-2980

Raman KP, Walawender WP, Fan LT, 1980, ”Gasification of feedlot manure in a fluidized bed reactor. The effect of temperature”. J Ind Eng Chem Process Des Dev; 19: 623-629.

Rhinehart RR, Felder R, Ferrell J, 1987, “Coal gasification in pilot-scale fluidized bed reactor. Gasification of Texas Lignite”, J Ind Eng Chem Res; 26:2048-2057.

Sami M, Annamalai K, Wooldridge M, 2001, “Co-firing of coal and biomass fuel blends”, J Prog Energy Combust Sci; 27:171-214.

Schmidt GH, Van Vleck LD, Hutjens MF, 1988, “Principles of dairy science”, 2n edition. New Jersey: Prentice hall.

Sweeten JM, Heflin K, Annamalai K, Auvermann BW, McCollum FT, Parker DB, 2006, “Combustion-fuel properties of manure or compost from paved vs. un-paved cattle”, Portland, Oregon: ASBAE Annual Int Meeting.

Thanapal, Siva Sankar, Kalyan Annamalai, John Sweeten, and Gerardo Gordillo, “. “Fixed Bed Gasification of Dairy Biomass with Enriched Air Mixture,” Third International Conference on Applied Energy - 16-18 May 2011 , Perugia, Italy, pages 01-13

Siva Sankar Thanapal, Kalyan Annamalai, John Sweeten, and Gerardo Gordillo, “. “Fixed Bed Gasification of Dairy Biomass with Enriched Air Mixture**,”** *J of Applied Energy*, 2011

USD (2007) “Economics, Statistics, and market information system”, United States Dept. of Ag. Available on line C: http://usda.mannlib.cornell.edu

Young L, Pian C, 2003, “High temperature, air-blown gasification of dairy-farm wastes for energy production”, J Energy; 28:655-672.

Zhang J, 2004, “Research on gasification process of loose biomass material with oxygen-enriched air in fluidized bed gasifier”, Global energy issues; 21: 179-188.

5.10. Education and Training

Gerardo Gordillo Ariza, “ Fixed Bed Counter Current Low Temperature Gasification Of Dairy Biomass And Coal-Dairy Biomass Blends Using Air-Steam As Oxidizer, “Doctor Of Philosophy, Mechanical Engineering , Texas A&M, May 2009.

Siva Sankar Thanapal , “Gasification Of Low Ash Partially Composted Dairy Biomass With Enriched Air Mixture,, “ Master Of Science, Mechanical Engineering, Texas A&M University, College Station, TX, December 2010.

5.11. Other support

Kalyan Annamalai, Circulating Fluidized Bed Gasification and Combustion, "Confidential Project funded by unnamed Utilities, March 15-Dec, 2010, $ 80,000 (report not for public release)

Kalyan Annamalai, and Devesh Ranjan, "Torrefaction Studies On Agricultural Biomass Fuels," Biomass: Rice Straw ; AGNI Corporation, Ca , May, 18, 2010- Oct 31, 2010 $ 55,000; Report Confidential

Evaluation Of Catalytic Pyrolysis (Thermal Decomposition) Process For Production Of Bio-Fuels From Solid Biomass Fuels, Sustainable Energy Corporation (Baytown Green Energy Consortium, BGEC) , Highway 16 , Baytown, Texas, Kalyan Annamalai, 2009, $ 36,912 (Report accessible with permission from BGEC) [see conference paper under Annamalai, 2010]

5.12. Dissemination

Gordillo G, Annamalai K, 2010, "Adiabatic fixed bed gasification of dairy biomass with air and steam", Fuel; 89: 384-91.

Gordillo G, Annamalai K, Carlin N, 2009, "Adiabatic fixed-bed gasification of coal, dairy biomass, and feedlot biomass using an air-steam mixture as an oxidizing agent", Renewable energy;34: 2789-97.

Gerardo Gordillo And Kalyan Annamalai, "Air-Steam Gasification Of Dairy Biomass Using Small Scale Fixed Bed Gasifier, Proceedings of The ASME Turbo Expo 2009 June 8-12, Orlando, Florida, USA; GT2009-59218

Gordillo G, Annamalai K, July 8-12, 2007, "Gasification of coal and Dairy manure with air steam as oxidizing agent", Proceeding of HT 2007. 2007 ASME-JSME thermal Engineering Summer Heat Transfer Conference., Vancouver, British Columbia, Canada

Gerardo Gordillo, Kalyan Annamalai, Udayasarathy Arcot, Gasification of Coal and Animal Waste using an Air-Steam Mixture as Oxidizing Agent, "19th National & 8th ISHMT-ASME Heat and Mass Transfer Conference, January 3 - 5, 2008; Paper No: FBH-5 JNTU Hyderabad, India

Kalyan Annamalai, A Udayasarathy and G. Gordillo, " Coal and Biomass: Direct Combustion and Gasification, " Second International Conference, "2nd International Conference on Resource Utilization and Intelligent Systems (INCRUIS)–2008, Kongu Engineering College, Perundurai, January 3-5, 2008.pp 56-76, 2008;

6. PILOT SCALE TESTS ON COFIRING AND REBURN FOR HG REDUCTION

Task A-6 (KA, JS): Pilot-scale studies

Task A-6-1: As a sub-contract to TEES, a pilot-scale facility will be used to generate the reburn data

Task A-6-2: Pilot scale tests on Hg reduction using CB as "Hg-reburn" fuel and testing chlorinated activated carbon for Hg capture

Accomplishments: With cost sharing from Texas Commission on Environmental Quality (TCEQ) the pilot scale experiments were performed at Southern Research Institute , (SRI), Environment and Energy Department, Birmingham, AL and the results on Hg and NOx reduction are mixed due to pilot scale equipment limitation .The plot scale tests revealed two problems: i) the use of high Chlorine Choctaw coal as main fuel created problems in determining the reduction of Hg with use of high Cl CB as reburn fuel.; ii) the primary, secondary and overfire air controls were not satisfactory in adjusting the equivalence ratio in the primary zone. As such the primary burner operated line a low NOx burner with staged combustion. Thus the second pilot test was abandoned since it might require expensive modification of pilot scale facility.

{This section was modified form of report to TCEQ on pilot tests; TCEQ provided the cost sharing}.

ABSTRACT

The objective of this task is to validate the results of small-scale combustion tests that have shown significant reductions of NOx and moderate reduction of mercury emissions as a result of reburning feedlot biomass (FB) and coal: FB blends. Pilot scale tests were performed over 2.5 days during May 24, 25 and 30, 2007 in the Combustion Research Facility (CRF) at Southern Research Institute (SRI), Environment and Energy Department, AL in order to confirm the small-scale experiments performed at Texas A&M University Mechanical Engineering (TAMU/MENG) Department. The one mega watt (1 MW_{th}, thermal) pilot scale facility simulates the flue-gas path from the burner through the particulate collection devices, including a temperature-time profile that matches that of full-scale coal-fired power plants. The CRF has been designed to simulate the major boiler types in service today–specifically, wall-fired, tangentially-fired, tangentially-fired with overfire air, and low-NOx burner types. The NOx emissions were measured by continuous-emission monitors (CEMs), while the mercury speciation measurements were performed using a state-of-the-art semi continuous emission monitor, with an advanced spike and recovery system only featured at Southern Research Institute. The first set of data ever obtained from a facility simulating boiler burners indicated problems with modification of a large facility for safe injection of reburn fuel (FB and coal:FB blends) and operations. Thus the injection and operational parameters differed from those of small scale tests. Particularly the main burner operated near stoichiometry almost simulating a low NOx burner (LNB) instead of operating at 5% excess air as performed in small scale experiments. The preliminary data from SRI tests indicated NO_x reduction of about 75% for each of the different reburn fuel types, including the raw manure (LAFB-Raw or LA-RM) and low ash partially composted manure (LAFB-PC or LAPC) and almost independent of firing conditions tested so far. The NOx reduction of 75% is attributed due to almost staged combustion like behavior of the main burner and the reburner. The

fuel used for the main burner is Galatia coal, which had very low mercury content but somewhat higher Cl level compared with Wyoming Powder River Basin (PRB) coal used in the TAMU small-scale tests. The SRI results indicated negligible elemental Hg was emitted for most of the tests due to high Cl in the main burner and reburn fuel. The pilot scale tests demonstrated the difficulties in incorporating the changes in a large scale utility boiler and valuable experience was gained from these preliminary tests. It also indicated differences in performance using different baseline coal supply. As a result, the test procedure, operating conditions and injection geometry need to be improved for the future pilot scale tests. The second pilot test was abandoned since it might require expensive modification of pilot scale facility.

6.1. Introduction

The ultimate objective of this interdisciplinary and system-oriented research project involving professors across Texas Engineering Experiment Station (Mechanical Engineering) and Texas Agricultural Experiment Station (Biological and Agricultural Engineering) of the Texas A&M University System (TAMUS) is to develop environmentally benign and economically viable thermo-chemical and biological conversion technologies to convert low–value inventories of livestock biomass into renewable energy. The new enabling technologies will minimize the need for wastewater treatment lagoons and land applications, reduce reliance on high-rate land application of phosphorus-rich manure, and also provide new options for the disposal of livestock mortality. One of the objectives is energy conversion from animal wastes through co-firing, reburn and gasification in order to identify the best approach for energy conversion and reduction of emissions in coal fired systems.

Extensive research has been conducted by TAMUS on energy conversion from coal and animal waste over last two decades.

The investigators had obtained Texas Higher Education Coordinating Board (Texas ATP) grant in 1997 to conduct cofiring tests on coal:feedlot biomass (FB or known as Cattle manure) blends. The tests at TAMU 100, 000 BTU/hr facility at Mechanical Engineering Department surprisingly revealed lower NOx even though the N content in the fuel blends has increased. As a part of grant obligations and with TEES-DOE/FETC cooperative agreement (CRADA Cooperative Research and Development Agreement) with Annamalai as Principal Investigator and John Sweeten had performed pilot plant tests at DOE 500,000 BTU/hr facility in Pittsburgh in Jan 19-22, 2000 . The purpose of the tests were to combust a blend of 90 % pulverized Wyoming coal from the Powder River Basin (used by Southwestern Public Service Co.) and 10 % (weight basis) pulverized partially composted feedlot manure from Hereford Feedyards and North Plains Compost. The FETC combustion unit is operated continuously during a test with three shifts of experienced engineers and technicians, and it is extremely well instrumented with computers continually monitoring and displaying measurements of temperatures, fuel and air feed rates, air contaminant emissions, etc. In summary, this cofiring test was a very successful test of 90/10 coal/manure blends in that the NOx emission did not show any noticeable change when fuel was changed from coal to 90:10 coal:FB blend. The TAMU tests indicated that the N in FB originates from urea and hence it can be used to reduce NOx using FB as reburn fuel in existing power plants for reducing the NOx. Under the Texas ATP 99-02 grant, reburn tests with high ash FB and coal reburn fuels were performed at TAMU 100,000 BTU/hr facility. The results revealed that FB is twice more effective compared to coal in reducing the NOx. Thus a patent was filed with FB as reburn fuels. However the high ash content can result in increased ash disposal and fouling problems. Since the increased ash originates from soil collected along with FB, it was decided to decrease the ash by using ash paved feedlots. John and his group then prepared the low ash FB samples for testing which resulted in another patent application on fuel production. Low ash samples were shipped to A&M and also to DOE facility. Again under DOE/FETC CRADA program, reburn tests were performed at pilot scale DOE 500,000 BTU/hr facility with low ash FB as reburn fuels. Their system used vitiated air (low O2 %) for transporting the FB dust while TAMU system used air; thus the performance was expected to be better. Subsequently limited tests have been performed at 500,000 BTU/hr DOE-NETL-Pittsburg facility which confirmed TAMU data [US Patent # 6,973,883; TAMUS Disclosure # TAMUS Disclosure #

1997, 2003].With support from DOE Golden, more reburn tests were conducted with FB as reburn fuel (without overfire air) for reduction on NOx revealed significant reductions for NOx under certain operating conditions and injection methods. Further TAMU system used two opposite reburn injectors to spray laterally into the main stream while theirs used "sampling probes" as injectors injecting in a direction counter to the main stream with the result that DOE has to use water cooling for the injectors. Subsequently Kalyan , John and Mark Freeman of DOE and had a meeting on Thursday 5/23/02 and decided that the results were very good and another patent was filed in 2009 on fuel injection system .

Typically the heat rate contribution from the reburn fuel to the plant's total heat requirement ranges from 6-20%. In addition to NOx capture, the FB could also be used to reduce Hg emissions. It is apparent from Hg literature review that the current Hg capture technique involves the use of powdered activated (PAC) carbon either in pure form or halogenated PAC (HPAC) for the capture of Hg. Further the presence of Cl in CB l enhances the Hg capture as $HgCl_2$ which could be dissolved in water or wet scrubbers.

The chlorine contained in animal waste derived biomass fuel (called as AWDBF) may produce $HgCl_2$ (called oxidized form of Hg) particularly from low rank coals and hence capture the compound using water spray, chemical scrubbers or ESP. The method is ideally suitable for plants installed with wet scrubbers which capture SO2. The sludge from scrubbers is used for making Gypsum board. None of the existing methods presented thus far involve the use of trace amounts of Animal Waste Derived Biomass Fuels (AWDBF).

The small scale TAMU tests (TCEQ task Report on reburn by Annamalai et al, 2006) show a reduction of Hg by almost 60 % when a blend of Coal:FB (80:20) was fired as reburn fuel. The pilot scale tests are useful in providing additional data on NOx and Hg reduction and validating small scale test data,

6.2. Pilot scale facility selection

According to the original proposal, Task 3 dealt with pilot scale studies using the DOE-NETL facility at Pittsburgh, PA. A meeting was arranged on July 15, 2005, at the NETL facility in Pittsburgh, PA., to discuss the modalities of the pilot scale testing either to be conducted at NETL or a site to be recommended by DOE-NETL. John Sweeten and Kalyan Annamalai visited the DOE-NETL and met with DOE officials to discuss the pilot scale tests. Mr. Mark Freeman of DOE-NETL presented an overview of previous pilot tests on co-firing and reburn with AWDBF and KA made a presentation on the status of current research on AWDBF. Dr. Sweeten presented his work on biofuel properties of feedlot manure/biomass. After the presentations, Mr. Mark Freeman informed us that they did not get the required funding to hire sub-contractors for running the DOE-NETL pilot scale facility and hence recommended other vendors. 4) Based on recommendations from DOE-NETL, Dr. John Sweeten and Dr. Kalyan Annamalai then made trips to two of the suggested facilities (Vendors I and II) prior to possible selection of the site for pilot scale experiments. Vendor I's coal-fired unit (visited on June 29-30, 2006) is rated at 1 million BTU/hr (300 kW) vs. 100,000 BTU/hr (29 kW) for the lab-scale pilot plant in TAMU/MENG Department. Vendor I Energy Group has experience with several types of biomass fuels including sewage sludge/biosolids. However the Vendor I mentioned that they have a backlog of pilot scale test and informed us that the facilities would not be available until fall 2006. There is no doubt Vendor I could have conducted the pilot plant tests while TEES specified test conditions for combustion or reburn protocols. However, the administration of Vendor I waived off a non-disclosure agreement (NDA). So, the PIs and the personnel of Vendor I were circumspect in presentations, careful to stick to published or open literature material. Dr. Kalyan Annamalai outlined an ambitious test schedule. Vendor I said they could conduct some of the requested experiments, but would have to leave out many of the requested tests to have any hope of completing before the TCEQ grant expiration (including the final report date of Dec. 31, 2006). Further, Vendor I saw nothing in the presentations that was compelling enough for an NDA. Apparently, a NDA was expected to be a drawn out process with Vendor I and TAMUS administration and thus would likely cause further delays and uncertainty. 5) The PIs visited with Vendor II (Southern Research Institute) in July 19 and 20, 2006 and discussed the pilot scale tests. Vendor II had a facility rated at 3.5 million BTU/hr (thermal; 1.025 MW_{th}). The SRI Energy Group had experience with several types of fuels: such as coal, switch grass, etc. The facility was available for fall testing in fall 2006. The cost quoted by Vendor II was approximately $80,000 for one week (5 working days) of testing and report preparation. Vendor II was advised that feedlot biomass (FB) was unlikely to cause odor concerns, because when dried to less than 10% moisture, decomposition is very slow, and odor would be no more than Wal-Mart grade bagged compost. TAMUS mentioned that they required a 2-way NDA (Non-disclosure agreement). SRI agreed to sign the NDA (Non Disclosure Agreement).

Thus a request was made to the TCEQ to extend the ending date of the contract from the original date of June 30, 2006 to May 31, 2007. After receiving approval from TCEQ on no cost

extension officially in Dec 2006, bids were submitted to the Texas A&M/TEES Purchasing Office in January 2007 for processing and forwarding to two pilot scale vendors. A response was received from only one bidder. Another bidder did not respond, probably due to problems with signing non-disclosure agreements.

The selected vendor for pilot tests was Southern Research Institute, located at 2000 9th Ave South, Birmingham, AL 35205.

6.3. Problems and solutions regarding pilot test conditions

SRI originally planned to use low chlorine Choctaw America as the baseline coal (bituminous coal, Cl of about 15 ppm) as main burner fuel (Table 6.3.1 Choctaw America Coal) and thus generate NOx by burning coal. For the main burner, the firing condition was originally set at 5% excess air at the burner (ϕ_M= 0.95), which leads to excess oxygen of approximately 1%. Estimated feed rates for main feed rates and reburn feed rate are given in Table 6.3.2 SRI Pilot Scale Facility: Initially-estimated feed rates using Choctaw America Coal as baseline

Table 6.3.1 Choctaw America Coal

	As received %
C	78.92
H	4.77
N	1.89
O	5.96
S	0.9
Moisture	1.49
Ash	5.65
HHV	13,789 BTU/lb

Table 6.3.2 SRI Pilot Scale Facility: Initially-estimated feed rates using Choctaw America Coal as baseline

Pilot Facility Thermal Rating	3,500,000	BTU/hr		
Reburn Thermal Rating	10	%		
Hrs of operation/day	12	hrs/day		
days operation	3	days/week		
Period of test	1	week		
FUEL for Reburn:	PRB Coal	TX Lignite	LA PC FB	LA RM
HHV,BTU/lb	7820	6145	5705	5765
Total Hrs	36	hrs		
Input through reburn	***350,000***	***BTU/hr***		
	PRB Coal	TX Lignite	LA PC FB	LA RM
Reburn Feed rate, lb/hr	**44.8**	**56.9**	**61.3**	60.7
Reburn Fuel Needed, lb	1611	2050	2209	2186
Main Burner	90	%		
Total Hrs	36	hrs		
Input through main Burner	3,150,000	BTU/hr		
	PRB Coal	TX Lignite	Choctaw	
Main Burner Feed rate, lb/hr	402.8	512.6	228.4	
Main Burner Fuel Needed, lb	14,501.3	18,454.0	8,230.0	

Prior to discussing parametric cases, feedlot biomass (FB) and equivalence ratio ϕ will be defined. For FB, terminology is as follows:

LA = low ash from paved fly-ash feedlots,

HA = high ash from soil surfaced feedlots,

PC = partially composted solids (e.g. 30-60 days), and

RM = Raw manure as-collected (i.e. not composted).

Equivalence ratio ϕ, is defined as:

ϕ = Required stoichiometric oxygen for combustion divided by the actual oxygen supplied, given a fueling rate,

ϕ = Supplied fuel flow rate divided by the maximum fuel that could be burned for a given O_2 flow rate.

Hence, $\phi>1$ implies that the mixture is fuel-rich, and as such, the supplied O_2 is less than stoichiometric for a given fuel flow rate and will be completely consumed. However, for fuel-rich mixtures, the fuel may not be burned completely to CO_2 and H_2O. Moreover, note that there are four equivalence ratios (ER) involved in reburn systems:

1) Main Burner ER: Typically ϕ_M = 0.95 to 0.9
2) Reburn Pipe ER: $\phi_{Reb\ supp}$ = 2.3 (typically estimated so that Reburn Zone Equivalence Ratio, ϕ_{RBZ}, will be approximately 1.1; see item three below).
3) Reburn Zone ER:
$$\phi_{RBZ} = \frac{O_2\ required\ \ for\ stoichiometric\ combustion\ of\ \ reburn\ \ fuel}{O_2\ left\ in\ main\ combustion\ \ products + O_2\ supplied\ through\ reburn\ \ pipe}$$
4) Overall ER: $$\phi_{Overall} = \frac{O_2\ \ for\ complete\ combustion\ both\ reburn\ and\ main\ \ fuel}{\left(\begin{array}{l} O_2\ supplied\ by\ over\ \ fire\ air + O_2\ supplied\ by\ reburn\ \ pipe \\ \qquad\qquad\qquad\qquad + O_2\ supplied\ by\ main\ burner \end{array}\right)}$$
Typically $\phi_{overall}$ is 0.85 to 0.9. This is used to calculate over fire air (air fired downstream of reburners). Over fire temperatures are typically 1880 - 2240 F (1300- 1500 K) to complete combustion so that stack O_2 is about 2 - 3%.

Reburn Combustion conditions: Base Case: LA-PC-FB, Equiv Ratio 1.15 (SR= 0.87), Test variables: Two types of fuels: Low Ash Raw Manure (LARM), Low Ash Partially Composted (LAPC), Blend of Coal+ LAPC (Limited Test); Reduce % heat input by manure; Equivalence ratio: 1 to 1.15 , Emissions to be tested (NOx, SOx, Hg, $HgCl_2$).

There will be a log sheet on all experimental conditions.

<u>Problem 1</u>: Based on the extensive parameter testing required for two different reburn fuels (FB for TCEQ and Dairy biomass, DB for DOE-Golden), the vendor's proposal estimated two weeks of testing with a budget of almost $170,000. The number of parametric studies was reduced to perform the experiment within a week ($85,000); the amount requested even for one week is approximately twice the amount of the allocated funds from TCEQ and the ongoing DOE projects combined. In order to stay within the budget, it was decided split the cost approximately on equal basis between

TCEQ and the ongoing DOE-Golden projects. Thus negotiations were performed with SRI in the first week of March to reduce the number of conditions for testing so that tests could be performed within a week for both FB and DB and stay within budget. In addition there was a facility fee of over $3,000 per day by the parent Southern Company (SC) which built the facility in 1990 (so the company owns most of it) for all confidential work to be performed at the facility with clients. If Southern Company is allowed to have the report and pretest plans, then they are willing to waive the fees on this facility entirely. TEES/TAMUS requested SC to waive the use fees and we agreed to provide report to Southern Company and pre-test plans in order to reduce pilot scale test costs. Thus the contract negotiations between TAMUS-TEES and SRI continued till May 2007. Meanwhile TAES-Amarillo prepared the fuels, which were ground and shipped to SRI. Fuels prepared include PRB coal, TX lignite, LA-PC-FB, and LA-FB.

Problem 2: The pilot scale facility did not have an eductor large enough to handle the reburn fuel. A new eductor was acquired which delayed the start of experiment.

Problem 3: The pilot scale furnace is 3.5 feet in diameter, with an average upward flow of less than 10 feet/second. If the reburn fuel is injected at 50 ft/s across the furnace, it will blow the flame into the wall on the opposite side. The higher ash from FB in this facility may fall and may choke the main burner. The problem was minimized by using an opposed jet supplied with recirculated flue gases which will also aid in reducing the oxygen percentage in the reburn zone. However the selected injection configuration by SRI in order to stay within time constraint was different from the injection configuration used by TEES/TAMUS.

Problem 4: Meanwhile SRI faced a change in lab personnel, which caused delays of tests beyond May 31, 2007. Thus a conference call was scheduled on 4/26/07 with Ms Kate Williams to check whether no-cost contract extension was possible beyond May 31, 2007. TAMU and SRI were informed that the contract will end on May 31, 2007. The SRI hired/contracted new personnel in order to conduct tests within May 31st deadline. TAES shipped the experimental fuels in early May.

Problem 5: For the main burner, the desired firing condition is with 5% excess air at the burner (ϕ = 0.95) which leads to excess oxygen of approximately 1%. However pilot scale facility safety system required O_2 percentage above 1.5%. Thus the facility was modified for introduction of over fire air even for the base case.

6.4. Operating conditions

Part of the DOE funds, as well as internal funding, have been used to generate an EXCEL based program called REB-LOWNOX specifically for reburn methodology. The input data are main burner and reburn fuel properties, thermal rating of boiler, oxygen % in main burner air and reburn gas, % heat provided by reburn fuel, main burner (ϕ_M), reburn zone (ϕ_{RBZ}) and overall ($\phi_{overall}$) equivalence ratios. The outputs are:

i) derived fuel properties: chemical formulae for both main and reburn fuels, stoichiometric oxygen for main and reburn fuel, heating values per unit stoichiometric oxygen, A:F ratio in main burner

ii) operating conditions for main burner: fuel flow rate, air flow rate, expected CO2, O2 % in main burner products

iii) operating conditions for reburn system: fuel supply rate, oxygen supply rate and reburn gas supply rate to maintain desired equivalence ratio in reburn zone (ϕ_{RBZ}), required equivalence ratio in the reburn gas supply pipe (ϕ_{RB}) for specified $\phi_{RBZ,}$ CO and CO2 %

iv) operating conditions for over fire air: over fire air flow rate required to maintain $\phi_{overall}$ (in order to get desired stack oxygen % in stack):

The EXCEL program can be used to generate data for real scale boiler also. Sample input and output are presented in Table 6.4.1 and Table 6.4.2. Operating conditions were generated for different conditions using the REB-LOWNOX spread sheet based program. Sample conditions produced by TAMU Excel program are shown in Table 6.4.1 (Choctaw coal).

Table 6.4.1 Input data on reb-lownox excel based program

Equivalence Ratios (ϕ)	
Primary Burner Equiv	0.95
Reburn Zone equiv ratio	1.15
Primary Fuel gas	NO
Overall Equiv with overfire air	0.854

Primary Fuel : Input only on Atom basis

Primary Fuel	Choctaw coal
Element	% by mass
C	78.92
H	4.77
N	1.89
O	5.96
S	0.9
Moisture	1.49
Ash	5.65

HHV, BTU/lb	13790
Burner Rating	3.50E+06
Main Burner fuel	90
$x_{NO,MAINBURNER}$	400
Main AIR Properties	
Temp	78
$RH_{ambient}$	15
$O_{2,main,\ overfire,\ dry}$	20.9
P MAIN, overfire	101
Reburn Gas Properties	
$P_{ambient}$	101
Temp	78
$RH_{ambient}$	15
Preburn	101
$O_{2,\ reburn,\ dry}$	10

Reburn Fuel	3 WYPRB Sub bituminous Coal
Element	% Mass
C	46.523
H	2.730
N	0.657
O	11.293

S	0.273
Ash	5.640
Moisture	32.883
TOTAL	100.000
HHV (BTU/lb)	7,823.000

A chart has been developed for any generic fuel (C-H-O) for obtaining the desired RBZ (reburn zone) equivalence ratio (See TCEQ Monthly report, March 2007). The chart is applicable to almost any fuel. Using such a chart, one can select desired ϕ_{RB}, for specified reburn zone equivalence ratio (ϕ_{RBZ}) at various heat input ratios when main burner equivalence ratio operates at $\phi_M = 0.95$ (about 5% excess air).

If desired, $\phi_{RBZ} = 1.1$, then needed reburn gas equivalence ratio is (i.e. reburn injection pipe) is 2.3 at 10% heat input (See TCEQ Monthly report, March 2007). Since reburn zone is fuel rich overfire air (air fired downstream of reburners) is used to complete combustion. Further the $\phi_{Overall}$ can be controlled by adjusting the amount of over fire air. For $\phi_{Overall} = 0.9$, the stack O_2 or furnace exit oxygen (FEO) is about 2% and $\phi_{Overall} = 0.83$, the FEO is about 3.7%.

Fuel Requirements: The Vendor 2 facility will require approximately 3,500 lb of coal per day (with 10 hrs of operation per day; 350 lb/hr). For 5 days of tests and 2 weeks of test duration, the total coal required will be approximately 35,000 lb (17.5 short tons) and 7,000 lb of FB (90:10 blends on heat basis) for cofiring applications. For reburn applications with a maximum of 30%

Table 6.4.2 OUTPUT for Stack O_2 = 3% for 3,500,000 BTU/hr, 10% Heat Input via Reburn, Φmain = 0.95 (5% excess air) &

Exp #	**Φoverall**	**Main Air**	**Main Fuel**	**Main O_2 Exhaust**	**RB Fuel Type**	**RB Fuel Rate**	**RB Air**	**Φ RBZ**	**Φ RBF**	**RB O2**	**RB N2**	**RB Gas (Air+N2)**	**Overfire Air**	**CO2 Stack**
0.0	0.0	SCFH	lb/hr	%	0.0	lb/hr	SCFH	0.0	0.0	%	SCFH	SCFH	SCFH	%
1.0	0.8	31861.5	228.4	1.0	WY Coal	44.7	3346.8	1.1	2.2	10.0	3012.1	6359.0	6309.7	17.0
2.0	0.8	31861.5	228.4	1.0	WY Coal	44.7	3661.7	1.1	2.0	10.0	3295.5	6957.2	6182.3	16.9
3.0	0.9	31861.5	228.4	1.0	WY Coal	44.7	3059.3	1.2	2.4	10.0	2753.4	5812.7	6424.6	17.0

Note the expected CO2 % is without flue gas recirculation; the use of flue gas at reburn injection port will increase CO2 % at FEO

heat input with coal as reburn fuel, total coal fuel sample mass should be 12,250 lb (approx 6 short tons); for reburn with FB alone the required amount jumps to 21,000 lb (10.5 tons; FB feed: 65 lb/hr due to low heart value). Since coal will be fired only for baseline studies, the required amount could be reduced to about 3.5 short tons for coal but FB should still be about 10.5 tons.

Figure 6.4.1. Reburn Fuel Pallets Prepared and shipped by TAES-Amarillo/Bushland

With 10% reburn heat input; the highest feed rate for any reburn fuel is 62 lbs/hr. During the 3-day test, there is a maximum of 36 hours of testing. Therefore, the maximum amount of all fuels fuel that could be burnt as reburn fuel is only 2232 lbs. This is rather optimistic, given that one will not be able to do reburn all of the time since certain amount of time is required for heat up in addition to time between each fuel type to change the fuel in the feeder, etc.

Kevin Heflin (assistant to John Sweeten) prepared 800 lb of PRB coal LAPCFB; 3,150 lb LAPCFB from 2006 (samples #140-142). Texas Lignite: 2,100 lb ready; LAPCFB: 500 lb from 2005 samples and LA-Raw-FB: 500 lb from 2006 samples (Figure 6.4.1). He shipped the manure and coal in pallets on Friday, May 04, 2007. Each pallet weights ~1,200 lbs (~300 lbs/box); was shrink wrapped, and all fuels were double bagged and boxed for transportation by common freight carrier.

6.5. Pilot scale research facility

Facility

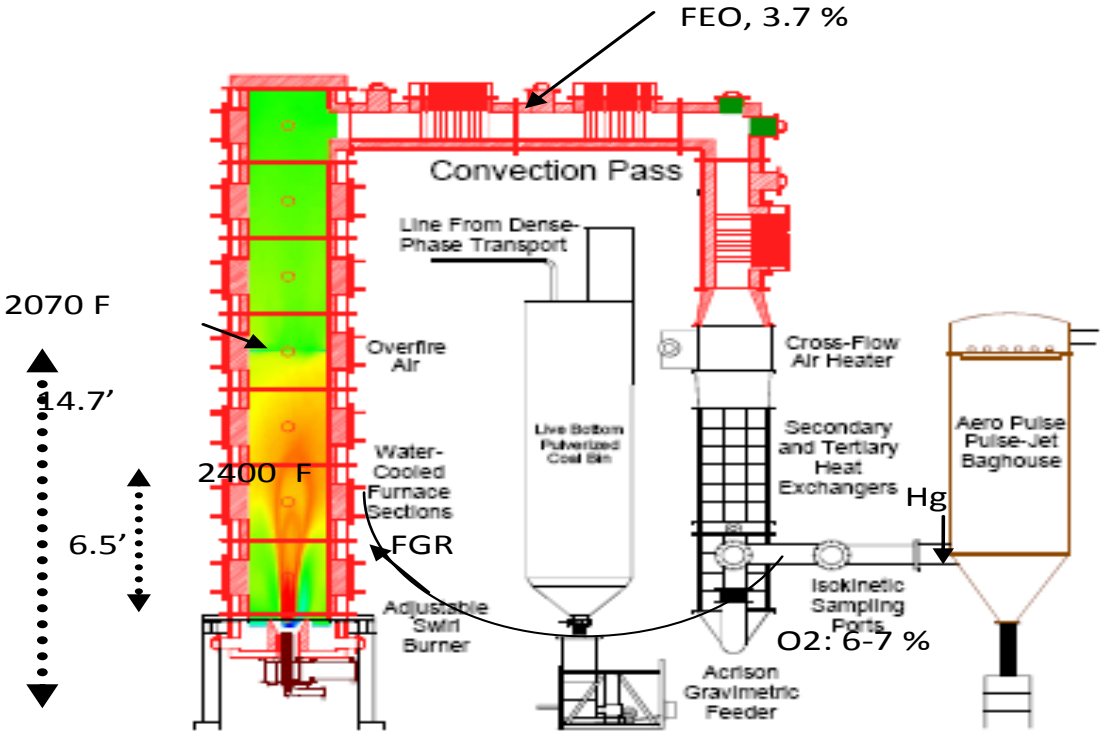

Figure 6.5.1. Combustion Research Facility (CRF) at SRI

The Combustion Research Facility (CRF) at Southern Research Institute (Southern Research) in Birmingham, AL, rated at 3.5 MMBtu/hr (1,025 MW_{th}) is a semi-industrial-scale, coal-fired facility, which mimics the thermal profile of a full-scale boiler from the burner through the economizer (Figure 6.5.1). The furnace is a vertical, up fired, 28-feet high cylinder, with an inner diameter of 3.5-feet.The thermal rating is 35 times the TAMU burner capacity, the fuel could be natural gas or coal. This allows gas velocities of 10 to 20 feet per second and residence times of 1.3 to 2.5 seconds, depending upon the firing rate. The design furnace exit gas temperature is 2200 °F. The secondary air (600 F) is given a swirl motion and the primary air-coal mixture enters through a refractory quarl with a 25° angle (half angle). The CRF is well suited for NO_x and mercury emission research relative to coal-fired power plants. Southern Research has operated the CRF for over 15 years and has performed extensive mercury speciation investigations and testing of technologies to mitigate mercury and NO_x emissions. The furnace is refractory lined to radiate heat back to the flame, simulating the radiant heat emitted from the surrounding burners in a full-scale boiler. However, water-cooled walls underneath the refractory allow steady consistent control of furnace temperatures. The refractory lining allows flame temperatures similar

to those in full-scale coal-fired boilers. The overfire air port may be fixed and approximately 1 s residence time between main burner and the over fire air port.

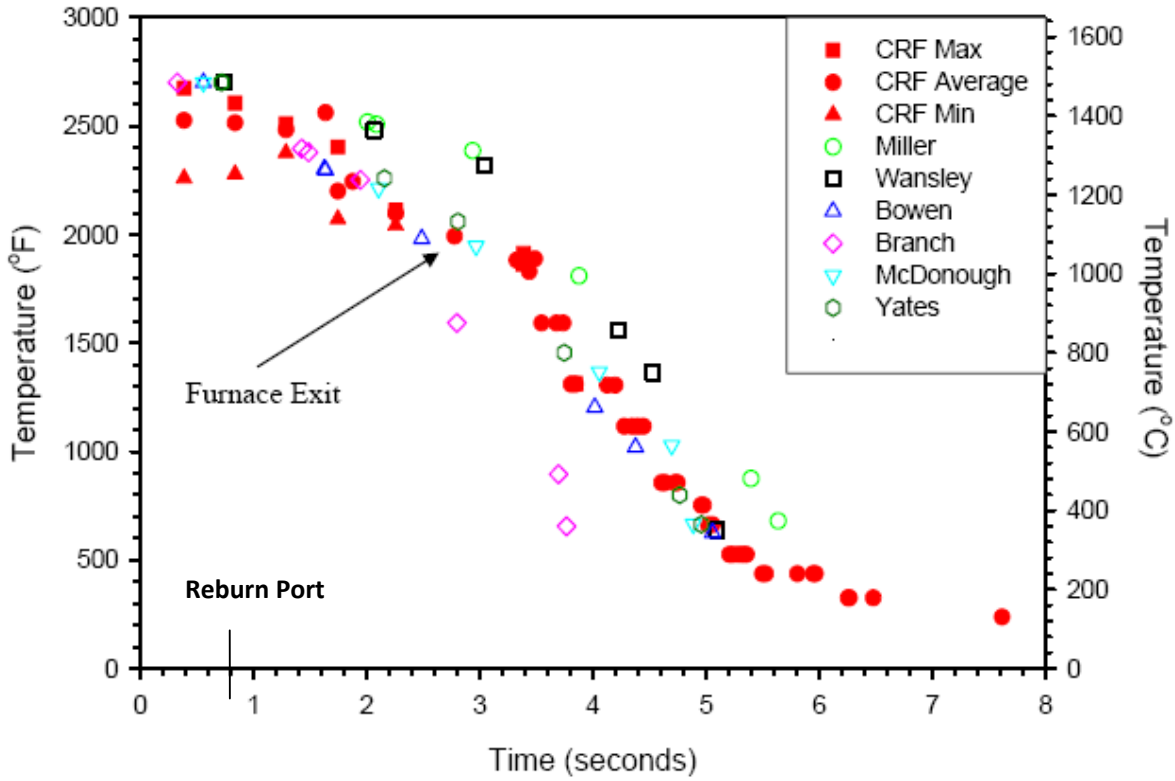

Figure 6.5.2. Temperature-time profile of the Combustion Research Facility (CRF).

As shown in Figure 6.5.2 the temperature-time history is similar to that of full-scale coal-fired boilers, for the entire seven second residence time, from the burner to the particulate collection devices. The peak flame temperatures are consistent with that of commercial boilers. The residence time in the furnace is between 2.5 and 3 seconds.

The facility is controlled and monitored by a networked combined digital control system (DCS) and data acquisition computers, managed by Yokogawa CS-1000 system software that runs under the Windows NT operating system. This DCS performs all process control for the facility and allows complex feed-forward and calculated variable control. This computer control also performs the safety monitoring needed for safe operation of combustion equipment, including Furnace Exit flame scanning and interlocks, automatic startup and automatic shutdown of the entire facility. Process data acquisition and storage is accomplished within the Yokogawa software.

Fuel Preparation

Fuel preparation includes on-site storage bins or open yard, rotary drum coal crusher, a CE Raymond bowl mill, and pulverized coal storage with 8 storage bins (capacity: 25 tons of solid fuel). The fuel is

crushed to a size of minus 3/8 inch which is then transported to one of two 125 ft3 storage bins mounted on load cells, equipped with vibrator/bridge-breakers, and rotary lock feeders. The fuel is further ground at a rated capacity of 2 tons per hour. The air for the pulverizer is preheated with a dedicated natural-gas burner.

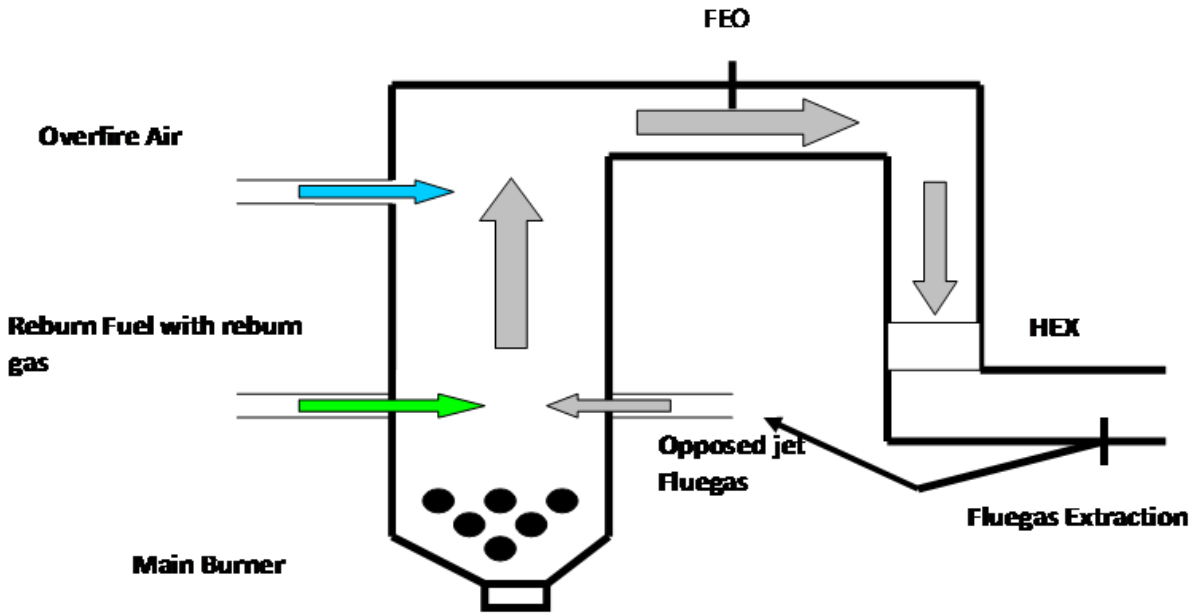

Figure 6.5.3. Schematic of Pilot Scale Facility

The primary air is maintained at 150 °F, and the secondary air enters the furnace at 600 °F. The coal mill is a refurbished and instrumented 1937 Model 352 CE-Raymond bowl mill, which has a rated capacity of 2 tons per hour. This type of mill provides representative milling simulations of the different air-swept table and roller mills normally used in power-plant service. During start up, the pulverized coal feed is diverted to a waste bin until the particle size has been established, after which the coal is dense-phase transported over to the pulverized-coal silo and feeder. The particle size of the coal is normally maintained at 70% passing 200 mesh, but other particle size ranges are easily obtained.

Reburning Configuration

Reburning took place at port two (Figure 6.5.1, Figure 6.5.2), approximately 0.8 seconds above the burner tip. An Acrison feeder was used to feed the reburn fuel into an eductor funnel at the rate desired. The eductor motive gas was in some cases pure nitrogen and in others house air, depending on the oxygen concentration desired in the reburn gas. Even when nitrogen was used for the motive gas, a significant amount of air (hence oxygen) was sucked into the transport gas through the funnel, with the reburn fuel. The sum of motive gas and aspirated air is called reburn gas. The O_2 percentage in reburn gas ranged from 7-21% O_2. In order to approach the oxygen concentrations desired for the transport gas, it was

necessary to mix the transport gas for the reburn fuel with recycled flue gas. The recycled flue gas extracted downstream of heat exchanger had some oxygen in it, between 6 and 7%. Mixing was accomplished in the furnace; using opposed jets of transport reburn gas and recycled flue gas. The recycled flue gas was taken just downstream from the last heat exchanger (Figure 6.5.3) pulling from a long pipe inserted axially along the duct, through an elbow, to minimize the recycle of fly ash. The flue-gas source was at 325 °F but was allowed to cool down some before being pulled through a blower and fired back into the furnace, opposite the reburn injection. The blower speed was controlled with a variac, and the flow was determined using a sonic orifice. In addition to providing greater control of the reburn-gas oxygen concentration, independent of the furnace oxygen concentration, the opposed-jet flow induced greater mixing of the reburn fuel and gas in the furnace. Further it also prevented reburn fuel flame impinging on the opposite wall.

Furnace Firing Parameters

SRI switched the baseline coal from Choctaw American coal to more readily available Galatia coal (see fuel analysis in Table 6.7.1 . The Galatia coal feed rate was 282 +/- 4 lbs/hr in the main burner at full load. See Table 6.5.1 for main burner operating condition. At this condition, without overfire air and 3.7% Furnace Exit Oxygen (FEO), approximately 400 ppm (actual) of NO_x were produced (this was approximately 555 ppm of NOx corrected to 3.0% O_2 in the flue gas). After this full-load NO_x level was established, the coal feed rate was reduced to 90% of full load. From then on, the Galatia coal feed rate to the main burner was 253 +/- 5 lbs/hr, and the secondary air was adjusted to provide 5% excess air at the main burner. The one exception to this was Condition 14, where 15% of the fuel was replaced with reburn fuel, and the coal feed rate was ~240 lbs/hr. Independent of the reburner, the overfire air (OFA) was adjusted for each test condition, to produce 3.7% FEO, thus matching that of the baseline condition. The primary and secondary air flows in the main burner were 120 SCFM and 452 SCFM, respectively, for all tests conducted, except condition 14.

The secondary air valve had problems sticking before and during the test. Consequently, the actual amount of secondary air was much higher than originally indicated by the readout. Hence, the flow settings for the main burner were obtained by adjusting the secondary air until the furnace exit oxygen reached the consistency with the desired amount of air in the main burner.

Table 6.5.1 SRI 1 MWth Pilot Scale Facility and Furnace Firing Parameters Main Burner, baseline firing conditions

MAIN BURNER	SRI
Swirl #	0.6
Thermal Power, BTU/hr	3.50E+06
Thermal Power, kW	1,025
Coal	Galatia (see table 6.1)

HHV, BTU/lb as is	12,694		
HHV, kJ/kg as is	29,526		
HHV-DAF, kJ/kg	33,434		
HHVO2, kJ/kg of O2	12,460		
HHVO2, BTU/lb of O2	5,589		
Main Burner Load	**100%**	**90%**	**85%**
Thermal Rating, MWth	**1,025**	**923**	**830**
Fuel Firing rate: lb/hr	282	254	240
Fuel Firing rate: lb/min	4.70	4.23	4
Fuel Fire rate, kg/min	2.13	1.920	1.814
O2 stoich rate kg/min	4.936	4.442	3.998
O2 stoich rate SCFM	127.720	114.948	103.453
Prim air, lb/min	9.256	9.256	9.256
Sec air(1), lb/min	34.863	30.451	28.245
Total main burner air(1),,lb/min	44.118	39.70648562	37.50056976
Prim air, SCFM	120	120	120
Sec air(1),, SCFM	452	394.8	366.2
Total main burner air(1),,SCFM	572	514.8	486.2
FEO (furnace ext Oxygen)	3.70%		
Estimated Overall Equiv ratio at 100 % load by main burner	0.826		
Stoich A:F	10.30		
Overall A:F include overfire	12.56		

Stoich airflow , lb/m	46.39	46.01633333	43.48
Req Air flow lb/m	56.09	55.626	52.56

(1): Set flow; however Sec. Air valve some time get stuck and hence the table values may be inaccurate; air flow estimated from FEO from its neighboring injector. In addition, the injectors were positioned with a 10° angle away from horizontal injection, to provide some swirl.

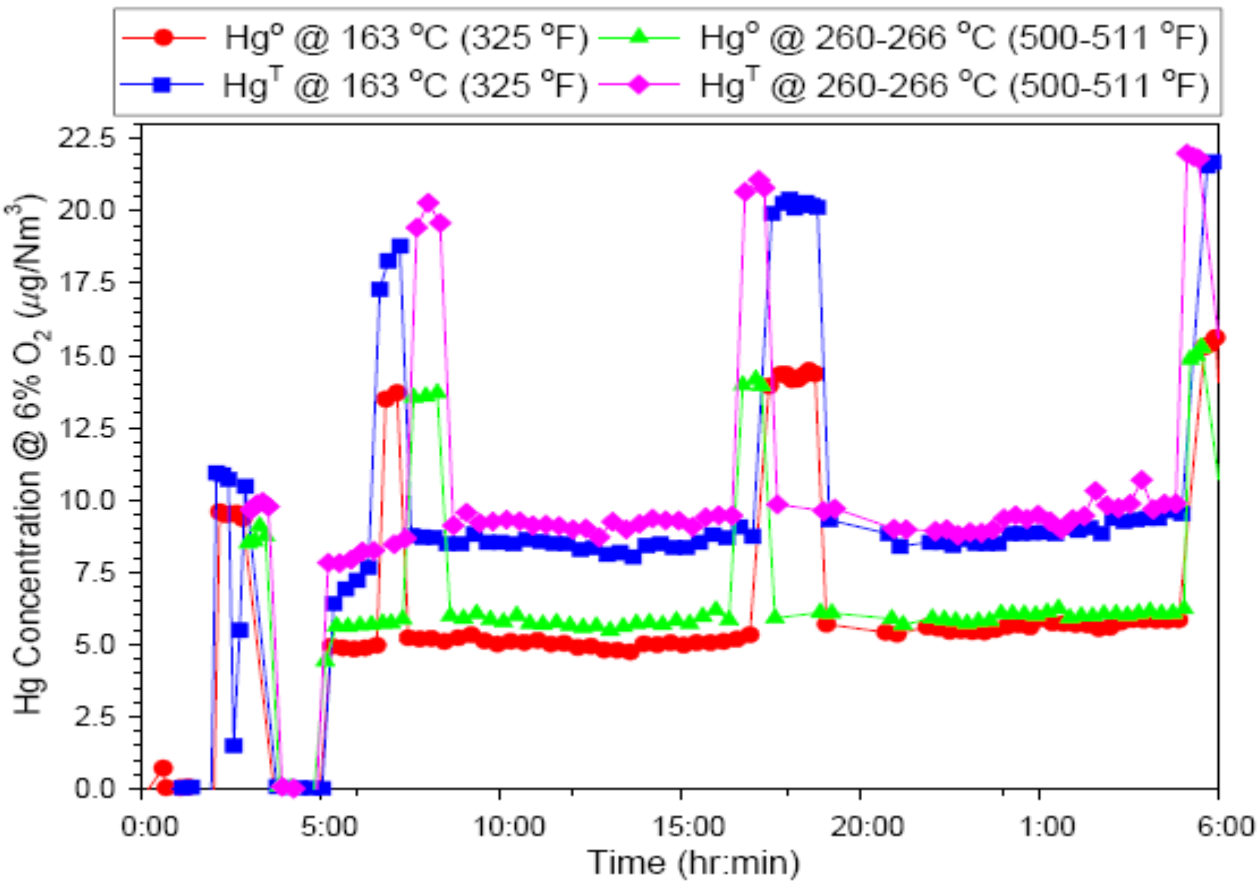

Figure 6.5.4. Mercury speciation data with spike and recovery.

In order to do this for the desired 5% excess air in the main burner, it was necessary to have the over fire air (OFA) on, because otherwise the furnace exit oxygen would drop down below 1.5% FEO, which would cause a furnace interlock to shut off the flame. Unfortunately, the secondary air valve did not

remain at the same *stuck setting*. Soon after the test started, the actual secondary air flow decreased somewhat, indicated by the amount of OFA necessary to obtain the FEO levels needed. Midway through the test plan, the flow to the main burner was readjusted, and the OFA required decreased. However, it appears that once the furnace was adjusted to the desired operating condition, the secondary air closed somewhat. The difficulty in adjusting the secondary air correctly, using the OFA and FEO, independent from the secondary air flow reading, was confounded by the fact that the OFA and secondary air originate from the same duct and are controlled by a damper between the two. The effect on the test was that instead of the main burner being continually fired at 5% excess air, it was more often near stoichiometric. More discussion is presented in the results section.

6.6. Diagnostics

Gas Analyzers

A complete extractive continuous emissions monitoring (CEM) system is installed in the facility and is interfaced to the computer control system. A set of gas analyzers, which analyze the flue gas for concentrations of O_2, NO_x, SO_2, CO_2, and CO, receives the dry flue gas sampled from a set of three extractive lines. The Combustion Research Facility has both pilot-scale baghouses and a pilot-scale ESP that may be used to extract the ash from the flue gas. Each of these devices has been designed and constructed to represent the full-scale baghouse and ESP devices in use today.

Hg

Mercury monitoring was performed with an advanced and customized mercury monitoring system, including a state-of-the-art gold-trap analyzer and an APOGEE Scientific QSIS probe for sampling from dust-laden flue gas. Southern Research also developed an advanced *spike and recovery* system to establish the validity of the mercury-speciation measurements. Because of these and other advancements, mercury speciation measurements within an uncertainty of ±5% are possible. This *continuous spike and recovery* system allows spiking at the tip of the APOGEE Scientific QSIS probe. The spike of mercury is introduced into the tip of the APOGEE Scientific QSIS probe far enough downstream from the inlet to prevent losses to the duct and far enough upstream of the porous annulus (coated with a monolayer of glass to inert the probe) to allow complete mixing before the sampled gas is pulled through the porous frit. A relatively small quantity of air is used to carry the mercury spike to the probe. Therefore, dilution is insignificant, and the general flue-gas composition is undisturbed. The main impact of the spike is simply to increase the concentration of mercury in the sampled gas. This is significant, since mercury-oxidation processes that interfere with speciation measurements can involve three and four component interactions of flue-gas species on catalytic ash sites.

Figure 6.5.4 illustrates the use of the *continuous spike and recovery system* for establishing total and oxidized mercury concentrations in the flue gas, while first burning natural gas (time 0:00 to 5:00) and then Black Thunder, a Powder River Basin (PRB) coal. As shown, the *spike recoveries* are observed on top of the measured initial mercury concentrations for both fuels. The concentration of mercury in the spike stream is generated by controlling the flow rate, pressures, and temperatures of air in and through a mercury-loaded support-packed flexible tube and the reservoir in which the tubing is enclosed. High-

precision mass-flow controllers are used to obtain the precise metering needed for high-certainty calibrated spikes. The proper use of *spike and recovery* provides a greater level of confidence in the resulting mercury speciation measurements than other methods currently in use.

6.7. Results

Fuel Properties

Main Burner Fuel

In order to reduce time for conducting pilot scale tests, the SRI selected readily available Galatia sub-bituminous Coal to produce 90 % of heat rate instead of Choctaw coal. Remaining 10 % of heat rate is provided by reburn fuel. Main burner fuel properties are presented in Table 6.7.1

Table 6.7.1 Galatia HvB Bituminous coal analysis (from coal feeder discharge).

Proximate		Ultimate, DAF	
% Moisture	5.10	% Carbon	82.60
% Ash	6.59	% Hydrogen	5.19
% Volatiles	31.70	% Nitrogen	1.90
% Fixed C	56.62	% Sulfur	1.48
HHV (Btu/lb)	12694	% Oxygen	8.83
HHV (kJ/kg)	29,526		
		Hg (μg/g)	0.107+/-0.001
		Cl (%)	0.4396 +/-0.0047
Chemical Formulae, DAF	$C_{6.877}H_{5.149}N_{0.136}O_{0.552}S_{0.0466}$		
St. O2, kg of O2/kg as received	2.37		

i) Reburn Fuel

Table 6.7.2 presents the reburn fuel properties

Table 6.7.2 Properties of Reburn Fuels.

RB Fuel	WY Sub bituminous Coal	TX Lignite Coal	LA PC FB	LA RM FB
Element	% Mass	% Mass	% Mass	% Mass
C	46.52	37.18	33.79	34.98
H	2.73	2.12	3.65	4.16
N	0.66	0.68	1.97	2.36
O	11.29	9.61	23.94	19.03
S	0.27	0.61	0.51	0.38
Mercury, Hg	0.00017	0.00014	0.00006	
Chlorine, Cl	0.010	0.009	0.73	0.85
Ash	5.64	11.46	16.50	9.57
Moisture	32.88	38.34	19.64	29.52
HHV (BTU/lb)	7,823	6,143	5,703	2,444
HHV (BTU/lb, DAF)			8,499	

Operating conditions

The baseline coal firing conditions were shown in Table 6.5.1. The reburn fuels include PRB coal, LAPCFB, LARMFB, and Texas lignite (TXL). The firing rates were adjusted to provide 10 % heat input. The required flow rates of reburn gas (9-28 SCFM) and opposed jet flue gas (24-79 SCFM), corresponding O_2 concentrations and overfire air flow rates for the various test runs were adjusted to yield FEO of 3.7 %. The injections include both lateral and 45 incline. The O2 % in reburn gas ranged from 7-21% while the % in flue gas ranged from 6-7 %.

Since equivalence ratio of main burner ϕ_M during operation is not exactly known, an analysis has been conducted to determine the oxygen input in the main burner using oxygen mass balance between main burner and the mass flow at furnace exit where O2 % is known.

From the combustion textbook by Annamalai and Puri (CRC Press, 2006), for any fuel operating with excess air, the equivalence ratio of a furnace can be given as:

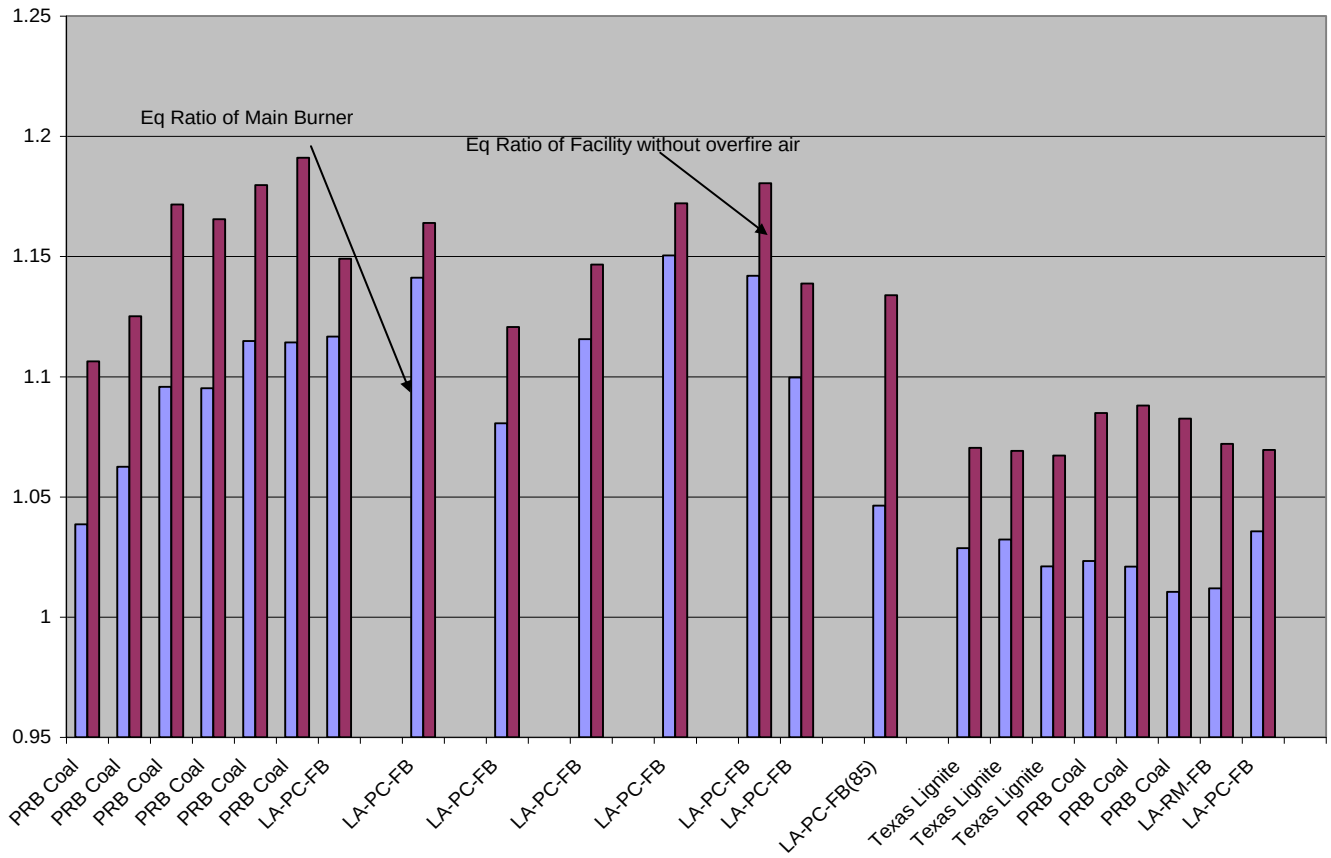

Figure 6.7.1. Estimated Equivalence Ratio (ϕ) of main burner and Equivalence Ratio the facility ; Note: there is no O2 supply from main burner; FEO: 3.7 %; Standard Flow at 60 F (376 SCF per lb mole)

$$\phi_{overall} = \frac{1}{SR} = 1 - 4.76 * \left(\frac{FEO\%}{100} \right)$$

And

$$Excess\ \%\ air = \{SR - 1\} * 100$$

Where $\phi_{overall}$ the equivalence ratio and SR is the stoichiometric ratio. If FEO % =3.7 and as such $\phi_{overall}$ = 0.826, SR= 1.21 and excess air including over fire air is 21%. However, the present furnace is supplied with air, N_2 and flue gas; thus ϕ_M= 0.826 is only approximate. Thus even this approximate result is very

close to exact values from 0.81 to 0.83. Figure 6.7.1 shows the estimated equivalence ratio of main burner from the knowledge of reburn gas, opposed jet gas flow O_2 percentage in reburn and opposed jet gas and FEO. Once the ϕ_M is known, the reburn equivalence ratio can be estimated without overfire air (Figure 6.7.1). Also from the knowledge of O_2 percentage in reburn gas and opposed jet gas and type of reburn fuel fired, the ϕ_{RBZ} was estimated (Figure 6.7.1); without over fire air; ϕ>1 implies that gas is oxygen deficient or mixture is rich; FEO: 3.7 % (with over fire air)

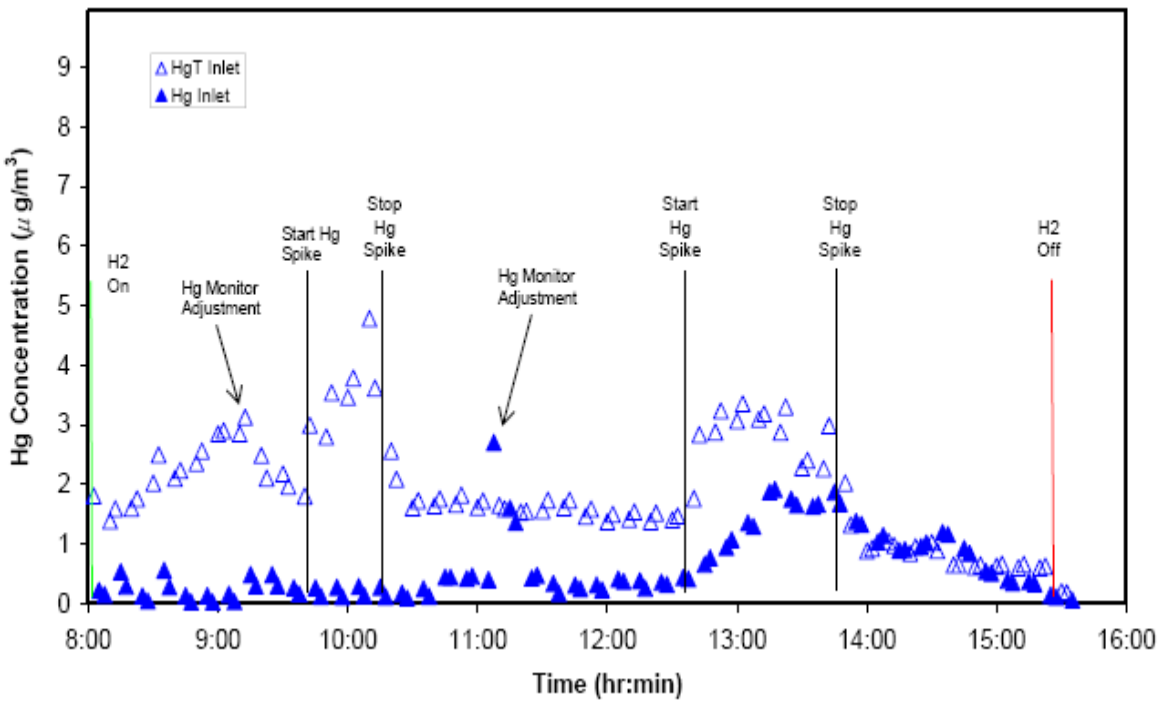

Figure 6.7.2. Mercury speciation data for the ESP inlet, taken Wednesday, May 30th

Emission Results

<u>NOx and SO2</u>

Table 6.7.3 Results on Flue Gas Composition shows a summary of results on emission of NOx, and SO2 along with measured values of CO2. Using more detailed set of data and Table 6.7.3, the % NOx reduction was plotted vs. estimated ϕ_{RBZ} for the three different reburn fuels (Figure 6.7.3). LA-RM-FB indicated similar results (67 % not shown) as that of LA-PC-FB. The % reduction was calculated for baseline NOx of 555 ppm for 3% FEO; this does not include the effect of lowering of NOx due to use of flue gas which supplies additional NOx in the reburn zone. The uncertainty in each measurement is much higher, illustrated by the difference in a few of the repeat condition results. The NO_x measurements for example, differ by as much as 40 ppm for some of the test conditions. The carbon monoxide levels at furnace exit did not significantly increase during any of the test conditions.

It is clear from Figure 6.7.3 that, the NO_x emissions were considerably lower (by as much as 75%) than the baseline test condition. However, it was also clear from the test that some of the NO_x reduction was simply due to staging. ***Nevertheless, the difference between the NO_x concentrations in the flue gas while at the condition (i.e., temperatures and gas flow rates were all stable at the given condition) but with the reburn fuel OFF, were consistently twice as high as when the reburn fuel was ON.***

It is noted that ϕ_{RBZ} is very rich due to operation of main burner near stoichiometry and as such as the temperature of reburn zone is affected due to incomplete combustion (i.e. not all reburn fuel is burnt in reburn zone). Most of the fuels seem to complete combustion near the overfire zone. However the ϕ_{RBZ} used in TAMU tests is considerably higher but still rich producing CO, CO_2, etc but there is enough O_2 to gasify all the reburn fuels to CO, CO_2 and H2O. Thus the reburn zone mixture temperatures are conducive for NOx reduction reactions.

Table 6.7.3 Results on Flue Gas Composition

Run Nos.	Reburn Fuel	NOx ppm	CO_2 ppm	SO_2 ppm
#1 - #6	PRB Coal	189.667 +/- 7.257	17.500 +/- 0.957	955.833 +/- 56.993
#7 - #14	LA PC FB	188.286 +/- 18.566	16.143 +/- 0.253	862.429 +/- 24.837
#15	LAPCFB/PRB	168	15.7	835
#16-#18	TX Lignite	165.000 +/- 6.245	16.1 +/- 0.100	937.000 +/- 18.248
#19 - #21	PRB Coal	177.8.083	NA	800-960
#22	LA RM FB	183	NA	800-960
#23	LA PC FB	163	NA	800-960

ii) Hg

As a result of the urgency of the test and the circumstances under which it was conducted, mercury data were only obtained on days two and three of the test campaign, and only at the ESP inlet. Figure 6.7.4 contain the elemental and total vapor-phase mercury measurements obtained on day two and day three of the test campaign, respectively. As illustrated in the figures, the total mercury concentration in the flue gas was very low, and the oxidation was high. This is consistent with the coal type that was burned, which had very low mercury content. Galatia coal produces about 250 ppm of HCl in the flue gas, along with a fairly high unburned carbon concentration in the ash, the combination of which tends to yield extensive mercury oxidation.

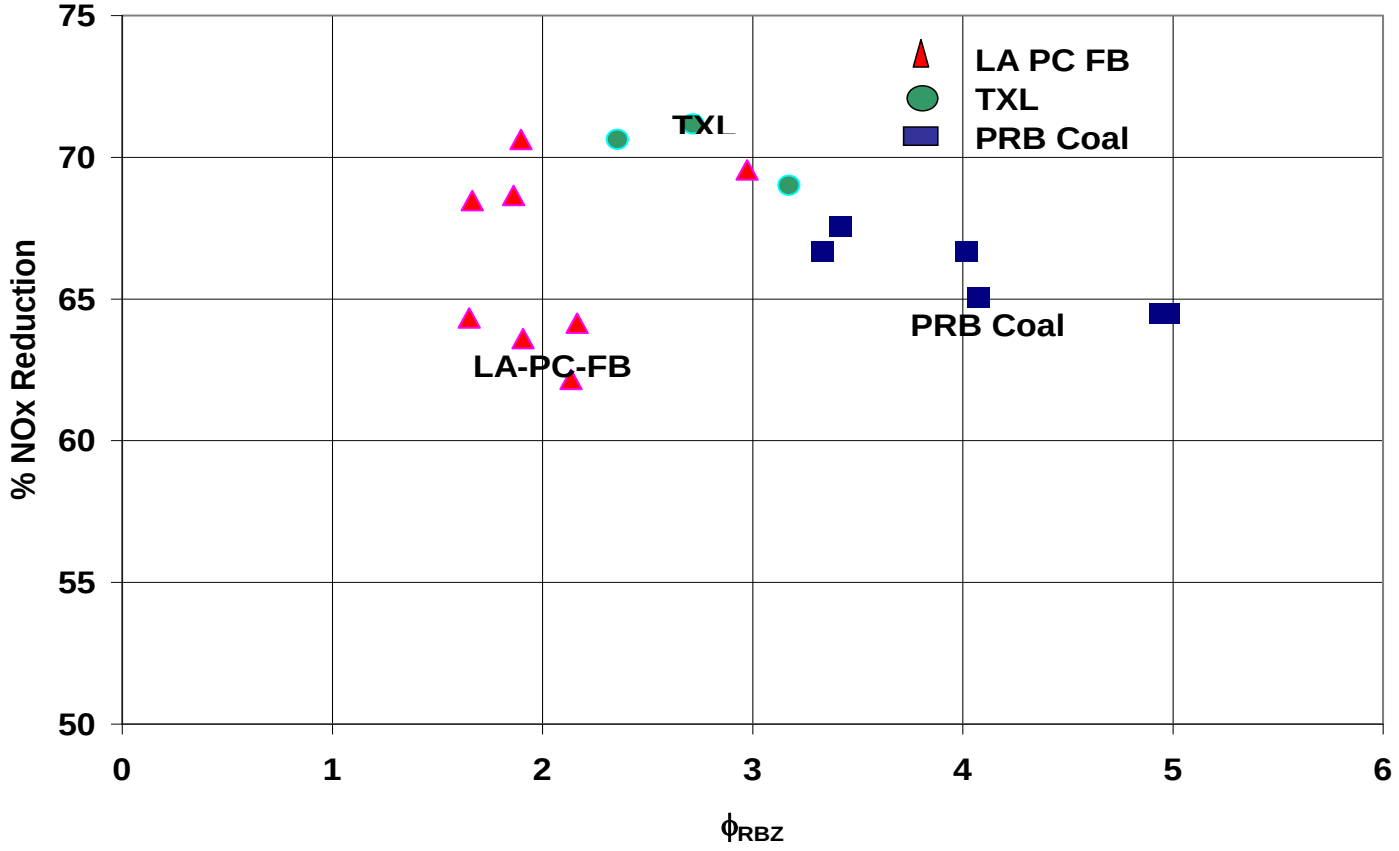

Figure 6.7.3. Estimated % NOx reduction vs. estimated Reburn Zone Equivalence ratio RBZ using Galatia baseline coal at SRI preliminary tests

The spike intervals are for QA/QC, and data regarding the reburn test cannot be extracted during

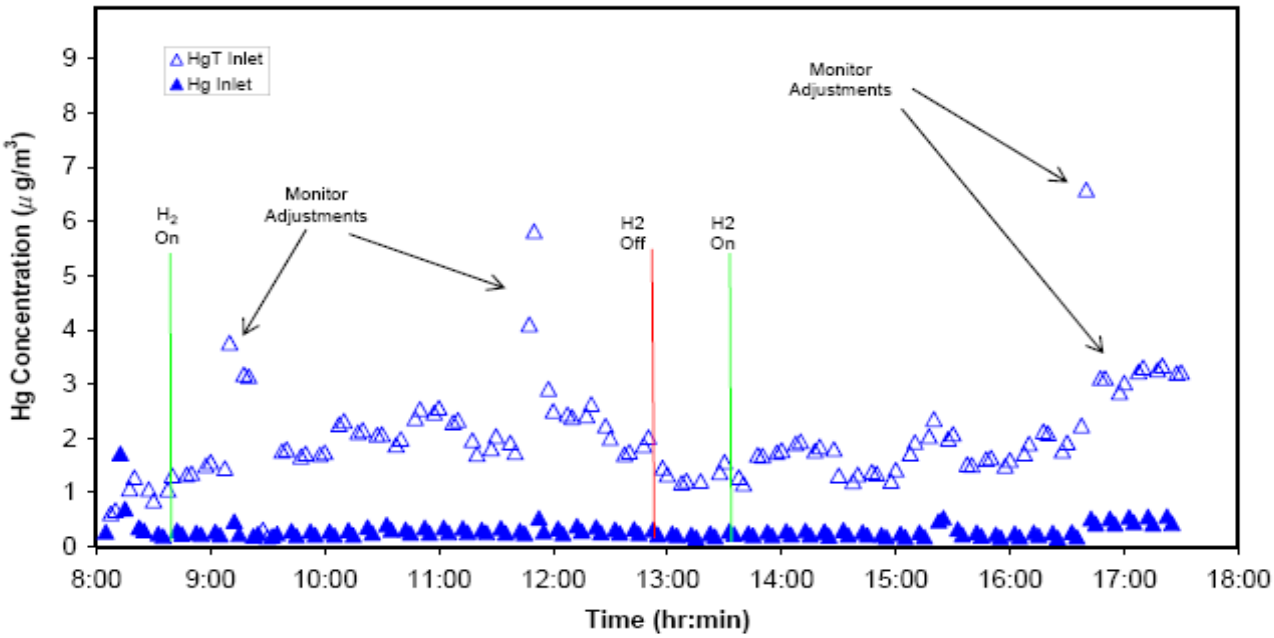

Figure 6.7.4. Mercury speciation data for the ESP inlet, taken Friday, May 25th.

these times. It appears that the total mercury concentration rose and fell with reburn injection. Perhaps because the main-burner coal had so little mercury in it, the addition of the mercury from the reburn fuel was significant enough to increase the total by a small amount. It is impossible to extract more information from these mercury data at this time, because each condition was very short, sometimes less than 15 minutes. Normally it takes at least 4 hours (and sometimes much more) for a condition to become stable in terms of total mercury and mercury oxidation state, given that mercury capture and oxidation is highly dependent on equilibrium conditions of low-temperature fly ash composition, temperature changes, and adsorption/desorption onto and off of fly ash, duct surfaces, and even the sampling systems. Further HCl+ Hg does not react fast enough; unburned C will provide chlorinated C sites for Hg absorption.

6.8. Summary

Originally we had proposed to conduct two pilot scale studies using DOE-Pittsburgh pilot scale facility. However DOE-Pittsburgh did not have funds to operate their facility and as such cost for pilot scale studies had gone up when we tried to look for private commercial facilities. Small scale commercial GE facility located in Ca was available but proprietary issues arose since GE wanted to retain all rights on invention and patents. Then we contacted Southern Services but the thermal rating of pilot scale facility was almost 10 times that of DOE-Pittsburgh Pilot scale facility. We had contracted with them to do first

pilot scale studies on Hg and NOx emission using feedlot biomass as reburn fuel. Since they did not have reburn system, they have to modify facility to install one and they were more expensive due to high thermal rating. Southern services had used Cl rich Alabama coal. Thus the reduction in Hg could not be attributed to Cl in feedlot biomass. Further the reburn fuel injection was not symmetric since they radially fired fuel only on one side while we wanted opposed radial injection. While we had NOx reduction almost 90 % in our TAMU-CBEL facilities, the reduction they achieved was considerably less. Due to problems at the large scale facility it operated the main burner slightly richer and further they had used Cl rich Alabama coal. Further due to problems in air injection, the main burner richer (almost like staged combustion). The second test required more modification to resolve air flow problems and opposed radial jet injection. Thus we replaced the second pilot scale test with a new task on the effects of asymmetric and symmetric injection on NOx reduction and effects of injection angles on NOx reduction (see PhD thesis of Oh 2008, listed under Task A-4). A paper submitted to Journal is under review.

The reburn tests at SRI were conducted as parametric experiments involving different operating conditions and reburn fuels, which included WY-PRB coal, TX lignite, low ash/partially composted feedlot biomass, and low ash raw feedlot biomass. The conditions of the SRI/CRF tests did not satisfactorily approximate the prior conditions for small scale TEES/TAMUS tests and this affects results which are as follows.

1. It is believed that the SRI/CRF facility seems to have operated as staged combustion facility with main burner with 90% heat input operating slightly rich or stoichiometric and that reburn fuel with 10% heat input operating extremely rich lowering NOx emission. The over fire is used to complete combustion.
2. Hence the reburning results indicated similar NOx reduction in the range of 62-75 % for each of the different reburn fuel types, including the low-ash raw FB and partially composted manure (LA-PC-FB).
3. The small scale TAMU tests used 30% of heat as reburn input while the present pilot scale used only 10% as heat input and as such i) there may not enough NH3 to reduce NOx from the main or ii) the extremely rich reburn zone did not have enough temperature to proceed with reactions.
4. The operational condition of reburn zone was different from TAMU tests, where larger NOx reductions from FB reburning were measured.
5. Further for same ϕ_{RBZ}, and heat % input by reburn fuel, the O2 flow in reburn system should not vary when fuel is switched from coal to FB since HHV_{O2} is roughly constant. However when PRB coal was fired as reburn fuel, the O_2 supply 2.5 SCFM for Cond #3 instead of 5.9 for same RBZ; as such the ϕ_{RBZ} increased for coal. In other words, reburn zone equivalence ratio is twice higher for coal compared to FB. As such coals operated under extremely rich conditions while FB operated under less rich conditions; still FB had the same reduction as coal indicating that FB is more effective even under less rich conditions.
6. Differences in NOx results can be attributed to difference in injection geometry of TEES/TAMUS and SRI. Depending on reburn gas jet velocity and opposed jet velocity, the reburn fuel may not have been uniformly spread across the cross section of the burner. Future work under DOE-Golden project funding will attempt to simulate TEES/TAMUS's geometry.
7. The secondary air valve had problems sticking before and during the test resulting in operation of main burner. The effect on the test was that instead of the main burner being continually fired at 5% excess air, it was more often near stoichiometric.
8. Most of the Hg seems to be oxidized since very little elemental Hg was detected. The oxidation is believed to be due to high Cl of Galatia coal, since introduction of PRB or TX lignite did not

affect elemental Hg emissions validating the hypothesis that high Cl content in fuels decrease elemental Hg. Future tests must use low-Cl coal as main burner fuel in order differentiate the effect of Cl in LAPCFB on Hg oxidation. Further tests must be performed first with coals as reburn fuels followed by FB nut not in other sequence.

9. The duration of each test was short (e.g. ~10-15 min each); while NOx results may be reasonable, Hg results could be affected. In the future test, fewer test conditions and longer duration per test must be adopted.
10. When biomass fuels are used as reburn fuels, emissions of di-oxins/furans (EPA method 23) , and trace heavy metals (EPA 29 method) must also be measured

6.9. Acknowledgements

Prof Annamalai and Sweeten gratefully acknowledge the help of Mr. Uday, Mr. Jin Oh, and Paul Goughnour, and Kevin Heflin in preparing for the pilot test and providing comments on the first draft of report; a part of this work is also supported by DOE-Golden project. The extraordinary diligence of Dr. Thomas Gale, Director of Power Systems Research, Environment and Energy Department, Southern Research Institute, in preparing for these tests during a time of personnel changes was greatly appreciated as well

6.10. Acronyms and symbols

A: Ash
AF: Air Fuel Ratio
ASTM: American Society for Testing and Materials
AW: Agricultural Wastes

AWDF: Animal Waste Derived Biomass Fuels

CB; Cattle biomass

CRADA : Cooperative Research and Development Agreement

DAF: Dry Ash Free
DB: Dairy Biomass

DOE: Department of Energy

DSC: Differential Scanning Calorimetry

EPA: Environmental Protection Agency
FB: Feedlot biomass (Cattle manure or Cattle Biomass CB)

FC: Fixed Carbon
FETC: Federal Energy Technology Center
HA-FB-PC: High Ash Feedlot Biomass Partially Composted

HA-FB-Raw: High Ash Feedlot Biomass Raw form

HHV: Higher or Gross heating value
HV: Heating value

LA-FB-PC: Low Ash Feedlot Biomass Partially Composted

LA-FB-Raw: Low Ash Feedlot Biomass

NETL: National Energy Technology Laboratory

NG: Natural gas

PC: Partially composted (45 days)

pf: pulverized fuel fired
ϕ: Equivalence ratio
ϕ_{RBZ}: Equivalence ratio in the reburn zone
ϕ_{RSZ}: Equivalence ratio in the reburn supply zone
PM: particulate matter

PRZ: Primary combustion zone

RBZ: Reburn combustion zone

RM; Raw Manure

SA: Secondary Air
SCFH: Standard Cubic Feet per Hour
SMD: Sauter mean diameter

SR: Stoichiometric ratio, Air: Fuel/ (Air: Fuel) $_{stoich}$

TAMU: Texas A&M University

TCEQ: Texas Commission on Environmental Quality

TEES: Texas Engineering Experiment Station

TGA: Thermo-Gravimetric Analysis
USDA: US Dept of Agriculture

VM: Volatile matter
VM: Volatile matter

6.11. References

Annamalai, Kalyan, Paul Gordon Goughnour, Hyukjin Oh, Udayasarathy Arcot V, and John M. Sweeten, "NOx And Hg Capture Using Coal, Feedlot Biomass (Cattle Manure) As Reburn Fuels,"

Task 2 Final Report: Reburn Experiments for NOx and Hg Reduction, Texas Commission on Environmental Quality, Aug. 1, 2006.

Annamalai, Kalyan and Puri, Ishwar, Combustion Science and Engineering, 18 Chapters, 1148 pages, Taylor and Francis: Orlando, Florida; ISBN: 0849320712; Dec., 2006.

Annamalai, Kalyan and John M. Sweeten, "Feedlot biomass: A reburn fuel for "maximum NOx" reduction in coal-fired power plants," Monthly Report for Mach 2007, TCEQ Grant #582-5-65591 0015.

6.12. Education and training

Kevin Heflin, Extension Associate for Texas AgriLife Extension Service and PhD Student , West Texas A&M University, Amarillo, Texas 79106

6.13. Other support if any

Only those involving reburn is presented here.

Feedlot Biomass: A Reburn Fuel For "Maximum NOx" Reduction In Coal-Fired Power Plants, Kalyan Annamalai, Dept. of Mechanical Engineering, Texas A&M University, and John Sweeten, Texas Agricultural Experiment station, Texas A&M Agricultural Research Extension Center, Amarillo, Texas, **Texas Commission on Environmental Quality**, 3/2005-5/2007; TCEQ Grant # 582-5-65591 0015 $ 341,933

6.14. Dissemination

None

6.15. Patents if any

None

7. REBURN MODELING

TASK A-7: Reburn modeling and exploratory studies.

ABSTRACT

Coal fired power plants will face many challenges in the near future as new regulations such as the Clear Sky Act are being implemented. These regulations impose much stricter limits on NO_x emissions from coal fired boilers. The current regulations on emissions of NO_x from coal power plants already require clean up technology, but the new regulations will require development of new cost competitive technologies

Reburn technology is a very promising technology to reduce NO_x emissions. Previous experimental research at TAMU reported that Feedlot Biomass (FB) can be a very effective reburn fuel, for reduction of NO_x up to 90%-95%; however little work has been done to model such a process with Feedlot Biomass as reburn fuel. The present work concerns with development of a reburn model to predict NO_x. The model accounts for finite rate of heating of solid fuel particles, mixing with NO_x laden hot gases, size distribution, finite gas phase and heterogeneous chemistry, and oxidation and reduction reactions for NO_x .

Once the model is validated by comparison with experimental findings, extensive parametric studies have been performed to evaluate the parameters controlling NO_x reduction. No experimental data are available currently.

The model recommends the following correlations for optimum reduction of NO_x: Equivalence Ratio should be above 1.05; mixing time should be below 100ms (especially for biomass); pure air can be used as carrier gas; the thermal power fraction of the reburner should be between 15% and 25%; residence time should be at least 0.5s and the SMD of the size distribution should be as small as possible, at least below 100 μm.

7.1. Introduction

In the United States, more than 50% of the electric power is generated from coal [1]. The year 2005 saw an increase in the coal consumption in the electric sector of 1.1% over the previous year [1].

Coal consumption in the power sector has been increasing in the recent years and there are no reasons to believe that this slow, but steady, growth will stop in the near future, as the electricity demand is growing

and other fossil fuels such as natural gas have become increasingly expensive. Besides, the USA has huge reserves of coal, which represent a very stable source of energy as it does not rely on imports from foreign countries such as for oil or natural gas. The combustion of coal, a solid fuel, poses many challenges as regulations about pollutant emissions become more stringent [2].

In fact exhaust from coal combustion normally contains many pollutants such as nitric oxides (NO_x), sulfur dioxide (SO_2), fly ash and particulate matter. In addition, coal emits a larger amount of carbon dioxide than the other fossil fuels (see Table 1), for the same amount of heat produced, and there is growing concern as CO_2 is believed to cause the phenomenon of global warming.

7.2. Literature review

7.2.1. NO_x formation

During the combustion process of hydrocarbons with air there is the possibility of forming, among many other pollutants, oxides of nitrogen in the exhaust. These oxides might be nitric oxide (NO), nitrous oxide (N_2O) or nitrogen dioxide (NO_2), and they are collectively called with the generic term of NO_x.

Theoretically, the formation of NO_x can take place in every part of the furnace, but often it is produced only in certain parts of the flame, and over 80% of the NO_x might be produced in only 10% of the flame volume.N_2O is not significant in the case of coal combustion and also NO_2 only represents a small fraction of the oxides of nitrogen emitted at the stack. The largest fraction is by far composed by NO. Typically, in the atmosphere most of the NO is then converted into NO_2.

EPA regulations on reporting emissions of NO on mass basis require the use of molecular weight of NO_2.The amount of NO_x formed depends on a variety of factors which include the fuel burned, the Stoichiometry, the temperatures, the mixing and the residence time.

The three main mechanisms of NO_x formation in the gas phase are: thermal NO_x, fuel NO_x and prompt NO_x (Smoot L.D.,et al,1985).Fuel NO is formed from the nitrogen contained in the fuel, and in the case of coal it can account for 60-80% of the total NO formed (Smoot L.D.,et al,1985). It is formed more readily than thermal NO as the bonds of nitrogen with coal or in the molecules emitted from coal (mainly HCN and ammonia) are much weaker than the triple bond of the molecular nitrogen present in the gas stream. Therefore the formation of fuel NO can be considered almost temperature independent.

Fuel nitrogen is normally emitted as molecular nitrogen, ammonia or HCN. Especially the last two species are the most significant, and their amount in the gas stream is a strong function of the kind of fuel (Karamba S,et al,1993). In general high rank coals tend to emit most of their nitrogen as HCN, while low rank coals have also a significant fraction of ammonia (Karamba S,et al,1993). It has been found that biomass emits a very large fraction of FN as ammonia (Zhou J.,et al,2000).

These species then react in the gas phase and they could either decay to NO or N_2, depending on the local stoichiometry, with more NO produced in the case of lean mixture (Smoot L.D.,et al,1985).

Thermal NO_x originates from the reaction of oxygen in the gas stream with nitrogen at high temperatures (Smoot L.D.,et al,1985). This pathway has a very strong dependence on the temperature and on the oxygen concentration. This pathway can be described by the widely accepted two-step Zeldovich mechanism:

$$N_2 + O \Leftrightarrow NO + N \qquad (7.1)$$

$$N + O_2 \Leftrightarrow NO + O \quad (7.2)$$

$$N + OH \Leftrightarrow NO + H \quad (7.3)$$

The third reaction is particularly important under rich flame conditions where the OH radicals are present in higher concentrations than atomic hydrogen or oxygen. At mean temperatures below 1800 K, thermal NO formation is very slow (Smoot L.D.,et al,1985). Figure II.1 presents the thermal NO_x equilibrium calculation for the combustion of methane according to the excess air provided (Annamalai K.,et al,2006). It is noted that if the excess air is low, the NO_x formation becomes significant only for temperature roughly above 1800 K.

In the case of coal flames, as flame temperature is normally below this threshold, the thermal NO_x formation is not very significant (Smoot L.D.,et al,1985). In the case of prompt NO_x, nitric oxide can be formed when hydrocarbons resulting from devolatilization process attack molecular nitrogen near the reaction zone of the flame (Smoot L.D.,et al,1985).

The main reaction in this process is:

$$N_2 + CH \rightarrow HCN + N \quad (7.4)$$

Then HCN reacts with oxygen to create NO. Prompt NO is more significant in fuel rich flames since it needs hydrocarbon to initiate the chain of NO formation (Smoot L.D.,et al,1985). Prompt NO_x is normally most significant in the case of clean fuels (that contain no nitrogen). In the case of coal combustion it is normally ignored (Smoot L.D.,et al,1985).

7.2.2. Control of NO_x emission

The techniques to reduce NO_x emissions can be in general divided into two categories: combustion control and post combustion control. In the combustion control the parameters of the combustion are optimized in order to avoid the formation of NO_x.

Reburning is a promising technique for NO_x reduction. In this case the furnace can be divided into three areas: main burner, reburner and burn out zone, (see Figure II.2) [4].

In the main burner, the main fuel is injected along with a slight excess of air, providing most of the thermal power of the furnace. Downstream there is the reburn zone where the reburn fuel is injected in the gas stream and burned under fuel rich conditions. Here it is possible to convert a certain fraction of the NO_x generated in the primary zone into molecular nitrogen through the reverse prompt NO_x mechanism (Smoot L.D..,et al,1998). The extent of this conversion is strongly dependent on the reburn parameters such as type of reburn fuel, the stoichiometry and the mixing achieved [4, 11]. Further downstream, there is the burn out zone where more air is injected in the stream in order to oxidize the unburned hydrocarbons still present in the gas. The conditions in this zone must be optimized in order not to produce any more NO_x.

Under conventional operating conditions, and natural gas as a reburn fuel, it is reasonable to expect reductions in the order of 40 – 60% [4, 11]. This reduction is good but is still not enough to compete with SCR, therefore this kind of process needs to be improved to gain a better NO_x reduction.

7.2.3. Parameters that influence the NO_x reduction in reburner process

One of the most important parameters that influence the NO_x reduction in the reburn process is the equivalence ratio: as the mixture becomes rich there is a significant decrease in the NO emission, as the lower concentration of oxygen does not favor its creation.

Another very important parameter is the residence time. Also the mixing process is very important in the reburn technique, as it has relatively fast chemistry if compared to the mixing times of the reburn installations.

7.2.4. Reburning with different fuels

The most widely used fuel in reburn process is methane (Smoot L.D..,et al,1998), because it is a clean fuel as it contains no fuel bound nitrogen, sulfur or particulate matter and it reacts faster than liquid or solid fuels. Still, virtually every kind of fuel can be fired in a reburner and strive to gain better performances and lower operating costs has pushed toward the study of different fuels. Also the increasing cost of natural gas has favored the research on different

The use of biomass as a reburn fuel is very interesting as it has the potential to lead to results better than with other fuel.

7.3. Objective and tasks

The overall objective is to develop a zero dimensional model in order to predict the reburn performance with coal, feedlot biomass (FB) and their blends. In order to achieve the overall objective the following tasks are performed:

1. Development of a simplified model for mixing of reburn gas stream with main gas.
2. Inclusion of nitrogen release model.
3. Incorporation of the heterogeneous and homogeneous reaction kinetics.
4. Take into account the size distribution of the particle.
5. Predict the NO_x emissions control performance.
6. Conduct parametric studies on NO_x reduction.

7.4. Explanation of model

The experimental reburn facility is a laboratory-scale, down-fired furnace, providing a rated throughput of 100,000 Btu/hr (29.3 kW), based on the higher heating value (HHV) of the fuel. This facility is used for testing the potential for NO_x reduction of various solid fuels.

The main burner fires natural gas, with excess of air. Also a certain amount of ammonia is sprayed in the flame in order to generate a significant amount of NO_x in the exhaust leaving the main burner, as done in

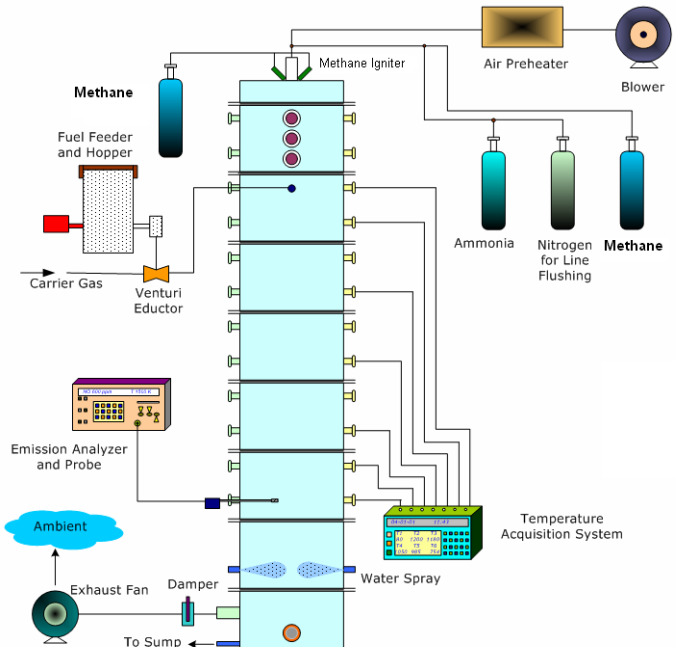

Figure 7.4.1 Facility Schematics

Zamansky (Zamansky V.M.,et al,1998) and Yang (Yang Y.B.,et al,1998). Downstream, the product gases, along with NO, enter the reburn zone (RZ). Here the reburn fuel is injected in the furnace along with carrier gas. The local stoichiometry in the RZ can be varied to study its effects on the performances. The facility is equipped with extensive diagnostics to keep track of the temperature along the furnace and to measure the gas composition at the exit of the furnace. A more detailed description of the facility can be found in Goughnour (Goughnour P.G.,et al,2006) and Arumugam (Arumugam S.,et al,2004).

7.4.1. General outline of the reburn model

Once the main burner and reburner thermal and heat input are fixed, it is possible to compute the mass flow of the main burner fuel as its heating value is known. The products of ammonia oxidation are assumed to be water and NO. Products from the main burner are computed assuming complete combustion. As shown in Figure IV.2, the hot gases, containing NO, then gradually mix with the reburn carrier gas, which contains the reburn fuel.

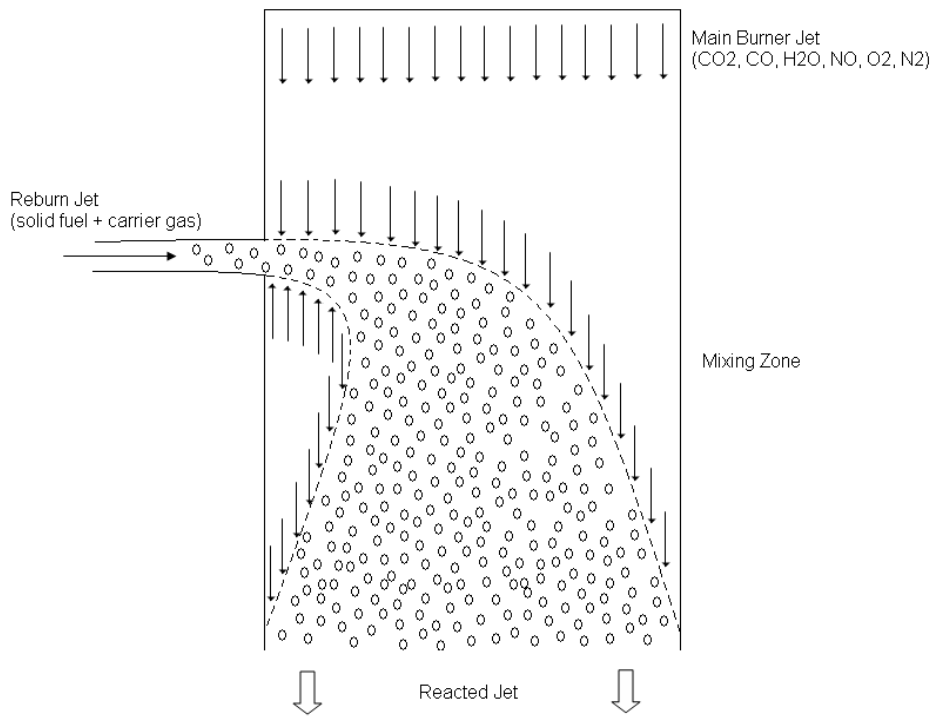

Figure 7.4.2 Schematics of the Reburner Zone

During the mixing with the hot gases, the reburn gases are heated up which in turn heat the solid particles. The particles release the volatiles and the fuel bound nitrogen, which undergoes homogeneous reactions. Simultaneously there is the combustion of the remaining fixed carbon and the heterogeneous reaction of nitrogen retained in the particles.

Volatiles originating from the pyrolysis process are composed of many different species; normally the important species are CO, CO_2 and CH_4 [27, 28], especially under the very fast heating that takes place in the burners.

The species coming from the fuel nitrogen (FN) pyrolysis are normally HCN, N_2 and NH_3 [8, 9]. The pyrolysis of FN is a process that is still not completely understood yet. The models for evolution of N are as follows: i) finite kinetics (Pohl J.H.,et al,1976) and ii) the emission of FN as proportional to the release of the volatiles (Nichols K.M.,et al,1986). Both these methods are discussed in the section on model description.

The reactions include four homogeneous reactions involving NO, three homogeneous reactions for the oxidation of CO, H_2 and CH_4, six heterogeneous reactions involving solid carbon and one heterogeneous reaction involving solid nitrogen. The code based on the model uses the following inputs:

Input to the code:

1. Main burner heat input, fuel characteristics, excess air, inlet temperature of fuel and air and initial NO_x.
2. Reburner thermal heat input, proximate and ultimate analysis of the reburn fuels, size distribution, density, specific heat and heating value, inlet temperature and composition of the carrier gas, heterogeneous and homogeneous kinetics parameters, FN products composition and equivalence ratio in the reburn area.

Output of the code:

1. Temperature (T) versus time (t) for the reburn gas and for each particle diameter (d_p).
2. Composition (Y_k) of the gas phase in the free stream and at the particle surface.
3. Mass (m_p), fixed carbon mass (FC), diameter (d_p) and density (ρ_p) of each class of particles.
4. Volatile matter (VM), rate of liberation of FN and elements left in the char.
5. The concentration of NO versus time.

7.4.2. Main burner modeling

The main burner fuel is assumed to be represented by the formula $CH_xO_yN_z$ which is burned along with some NH_3 to simulate the desired amount of NO. The amount of ammonia to be fired with the fuel is adjusted in order to achieve the desired amount of NO.

The solution for complete combustion of a general fuel is:

$$\begin{aligned} &CH_xO_yN_z + w\cdot NH_3 + \left(1+\frac{a}{100}\right)\cdot\left(1+\frac{x}{4}-\frac{y}{2}\right)\cdot\left(O_2+3.76\cdot N_2\right)\rightarrow CO_2+\left(\frac{x}{2}+\frac{3\cdot w}{2}\right)\cdot H_2O+ \\ &+\left(\frac{a}{100}\cdot\left(1+\frac{x}{4}-\frac{y}{2}\right)-\frac{5\cdot w}{4}\right)\cdot O_2+w\cdot NO+\left[\frac{z}{2}+3.76\cdot\left(1+\frac{a}{100}\right)\cdot\left(1+\frac{x}{4}-\frac{y}{2}\right)\right]\cdot N_2 \end{aligned} \quad (7.5)$$

where *a* is the percentage excess of air based on the main burner fuel only.

The excess air is fixed at 5%, therefore *a* is known. In the experiments, the NO_x local concentration at the exit of the main burner has been fixed at 400 ppm dry basis in which the reburn fuel is injected in a gas stream that contains a significant amount of NO. In the configuration of Goughnour (Goughnour P.G.,et al,2006), the main burner fuel is burned with 5% excess air. So the initial NO_x can be also expressed as

391 ppm (at 3% excess oxygen), or 0.43 lbm/MMBtu. This will be the reference, the starting condition to evaluate the effectiveness of the reburn process with the various fuels and conditions.

Therefore, on dry basis:

$$X_{NOx} = 400 \cdot 10^{-6} = \frac{w}{1 + \left(\frac{a}{100} \cdot \left(1 + \frac{x}{4} - \frac{y}{2} \right) - \frac{5 \cdot w}{4} \right) + w + \left[\frac{z}{2} + 3.76 \cdot \left(1 + \frac{a}{100} \right) \cdot \left(1 + \frac{x}{4} - \frac{y}{2} \right) \right]} \quad (7.6)$$

thus it is possible to compute *w* since *a* is known.

Now the amount of air and ammonia to be injected in the main burner fuel can be calculated and also the composition of the products coming from the main burner is known. In the experiments by Goughnour (Goughnour P.G.,et al,2006), the main burner fuel is natural gas which consists of over 95% of CH_4.

7.4.3. Natural gas composition

Therefore the main burner fuel can be approximated to be methane. In this case, there will be a complete combustion; besides the temperatures in the experiments are always below 1600K, therefore the NO at the exit of the main burner is generated mainly by ammonia.

As the thermal power coming from the main burner is fixed (70% of the total thermal power of the facility), it is possible to compute the mass flow of the main burner fuel:

$$\dot{m}_{fuelMB} = \frac{Thermal\,Rating_{MB}}{HHV_{fuelMB}} \left[\frac{kg}{s} \right] \quad (7.7)$$

Therefore the firing rate of ammonia is given by:

$$\dot{m}_{ammonia} = \frac{\dot{m}_{fuelMB} \cdot w \cdot M_{ammonia}}{M_{fuel}} \left[\frac{kg}{s} \right] \quad (7.8)$$

The components of the various species from the main burner are represented in vector form as:

$$\dot{m}_{MB} = \frac{\dot{m}_{fuel,MB}}{M_{fuel,MB}} \cdot \begin{Bmatrix} 0 \\ 0 \\ 1 \cdot M_{CO_2} \\ 0 \\ 0 \\ \left(\frac{x}{2} + \frac{3 \cdot w}{2}\right) \cdot M_{H_2O} \\ \left[\frac{z}{2} + 3.76 \cdot \left(1 + \frac{a}{100}\right) \cdot \left(1 + \frac{x}{4} - \frac{y}{2}\right)\right] \cdot M_{N_2} \\ 0 \\ w \cdot M_{NO} \\ \left(\frac{a}{100} \cdot \left(1 + \frac{x}{4} - \frac{y}{2}\right) - \frac{5 \cdot w}{4}\right) \cdot M_{O_2} \end{Bmatrix} = \begin{Bmatrix} \dot{m}_{CH_4} \\ \dot{m}_{CO} \\ \dot{m}_{CO_2} \\ \dot{m}_{H_2} \\ \dot{m}_{HCN} \\ \dot{m}_{H_2O} \\ \dot{m}_{N_2} \\ \dot{m}_{NH_3} \\ \dot{m}_{NO} \\ \dot{m}_{O_2} \end{Bmatrix} \quad \left[\frac{kg}{s}\right] \quad (7.9)$$

The temperature of the gases leaving the main burner zone can be computed by applying the energy conservation equation between the products and the reactants and considering a fraction of heat to be lost, proportional to the heating value of the main burner fuel.

7.4.4. Reburner modeling

Also the reburn fuel is known in the generic form of $CH_{x1}O_{y1}N_{z1}$. The reburn fuel is assumed to be a solid fuel, therefore it is necessary to model the release of volatiles and FN and the heterogeneous reactions at the particle surface. In the case of blends there are two different solid fuels, each one with its formula and chemical composition. The chemical formula is obtained from the ultimate analysis (dry ash free), normalizing the carbon atom content to one; the ultimate analysis gives the mass based composition of the fuel; so using the molar weight of each element it is possible to get the empirical formula:

$$CH_{x1}O_{y1}N_{z1} \rightarrow a \cdot C(s) + b \cdot CO + c \cdot CO_2 + d \cdot CH_4 + e \cdot HCN + f \cdot NH_3 + g \cdot N_2$$

$$\begin{cases} C: & 1 = a + b + c + d + e \\ H: & x_1 = 4 \cdot d + e + 3 \cdot f \\ O: & y_1 = b + 2 \cdot c + 4 \cdot d + e + 3 \cdot f \\ N: & z_1 = e + f + 2 \cdot g \\ FC: & FC = \dfrac{a \cdot M_C}{M_{fuel\,RB}} \\ FN: & NH_{3\,frac} = \dfrac{f \cdot M_{NH3}}{e \cdot M_{HCN} + f \cdot M_{NH3} + g \cdot M_{N2}} \\ FN: & HCN_{frac} = \dfrac{e \cdot M_{HCN}}{e \cdot M_{HCN} + f \cdot M_{NH3} + g \cdot M_{N2}} \end{cases} \quad (7.10)$$

In case of fuel blends this system has to be solved for the two fuels separately; from here it is possible to compute the compositions of the pyrolysis gases:

$$\dot{m}_{pyro_vect} = \dot{m}_{pyro} \cdot \bar{Y} = \dot{m}_{pyro} \cdot \begin{Bmatrix} Y_{CH_4} \\ Y_{CO} \\ Y_{CO_2} \\ Y_{H_2} \\ Y_{HCN} \\ Y_{H_2O} \\ Y_{N_2} \\ Y_{NH_3} \\ Y_{NO} \\ Y_{O_2} \end{Bmatrix} = \dot{m}_{pyro} \cdot \begin{Bmatrix} \dfrac{d \cdot M_{CH_4}}{b \cdot M_{CO} + c \cdot M_{CO_2} + d \cdot M_{CH_4}} \\ \dfrac{b \cdot M_{CO}}{b \cdot M_{CO} + c \cdot M_{CO_2} + d \cdot M_{CH_4}} \\ \dfrac{c \cdot M_{CO_2}}{b \cdot M_{CO} + c \cdot M_{CO_2} + d \cdot M_{CH_4}} \\ 0 \\ 0 \\ 0 \\ 0 \\ 0 \\ 0 \end{Bmatrix} \left[\frac{kg}{s}\right] \quad (7.11)$$

The mass flow rate of the reburn fuel is computed knowing the heat input of the reburner and the heating value of the fuel. For the general case of a blend, defining Y_{coal} and Y_{FB} as the mass fractions of the two fuels,

$$\dot{m}_{fuel\,RZ} = \frac{Thermal\,Power_{RZ}}{HV_{fuel\,FB} \cdot Y_{FB} + HV_{fuel\,coal} \cdot Y_{coal}} \qquad \left[\frac{kg_{fuel}}{s}\right] \qquad (7.12)$$

$$\dot{m}_{FB} = \dot{m}_{fuel\,RZ} \cdot Y_{FB} \qquad \left[\frac{kg_{FB}}{s}\right] \qquad (7.13)$$

$$\dot{m}_{coal} = \dot{m}_{fuel\,RZ} \cdot Y_{coal} \qquad \left[\frac{kg_{coal}}{s}\right] \qquad (7.14)$$

Where $Y_{FB} = 1 - Y_{coal}$.

Note that in the experiments by Goughnour (Goughnour P.G.,et al,2006), it has been assumed that the fractions of fuel represent mass fractions. The mass flow rate of the air at the reburner is computed as the reburn zone (RZ) equivalence ratio (Φ_{RZ}) is specified.

Let ν_{O2} be the stoichiometric oxygen to fuel ratio (mass basis) for a generic fuel $CH_{x1}O_{y1}N_{z1}$:

$$\nu_{O2} = \left(1 + \frac{x_1}{4} - \frac{y_1}{2}\right) \cdot \frac{MW_{O2}}{MW_{fuel}} \tag{7.15}$$

The reburn zone equivalence ratio is defined as:

$$\Phi_{RZ} = \frac{\dot{m}_{O2,stoi}}{\dot{m}_{O2}} = \frac{\dot{m}_{coal,DAF} \cdot \nu_{O2,coal} + \dot{m}_{FB,DAF} \cdot \nu_{O2,FB}}{\dot{m}_{O2,MB} + \dot{m}_{O2,RB}} \tag{7.16}$$

$$RB : reburner$$

Where $\dot{m}_{O2,MB}$ the flow of oxygen coming from the main burner is: as the combustion in the main burner is with excess air, there is some oxygen left in its exhaust; solving for the required $\dot{m}_{O2,RB}$ supplied with the reburn fuel in order to achieve Φ_{RZ}, the oxygen flow rate results:

$$\dot{m}_{O2,RB} = \frac{\dot{m}_{coal,DAF} \cdot \nu_{O2,coal} + \dot{m}_{FB,DAF} \cdot \nu_{O2,FB}}{\Phi_{RZ}} - \dot{m}_{O2,MB} \qquad \left[\frac{kg_{O2}}{s}\right] \tag{7.17}$$

Knowing the mass percentage of oxygen in the carrier gas at the reburner (which may be different from the atmospheric), it is possible to compute the mass flow rate of carrier gas that needs to be injected with the reburn fuel:

$$\dot{m}_{carriergas,RB} = \frac{\dot{m}_{O2,RZ}}{Y_{O2}} \qquad \left[\frac{kg_{RB,carriergas}}{s}\right] \tag{7.18}$$

The composition of the carrier gas could be different from pure air as it may be diluted with nitrogen in order to simulate the use of recirculation gases to test its effects on the NO_x reduction. In the case of vitiated air the oxygen content of the air is 12.5% (volume basis) (Goughnour P.G.,et al,2006).

The solid fuels are characterized by a size distribution. The size distribution has been measured at the Coal and Biomass Energy Laboratory, Texas A&M University, for each fuel used by Goughnour (Goughnour P.G.,et al,2006). See data in Chapter V. Each class is defined with its range of diameters. For the purpose of the modeling, each class is described with its mean diameter. For all the fuels there are 5 particle size groups. See Chapter V for details. All the properties (ultimate and proximate analysis) and kinetics of the solid fuels are assumed to be independent of the particle size. Let the mass percentage for each class of the size distribution be Y_j. If five size classes are taken in consideration, then:

$$Total\ initial\ mass = \begin{Bmatrix} Y_1 \\ Y_2 \\ Y_3 \\ Y_4 \\ Y_5 \end{Bmatrix} \cdot \dot{m}_{fuelRZ} \qquad \left[\frac{kg}{s}\right] \tag{7.19}$$

Similarly:

$$Initial\ VM = \begin{Bmatrix} Y_1 \\ Y_2 \\ Y_3 \\ Y_4 \\ Y_5 \end{Bmatrix} \cdot \dot{m}_{fuelRZ} \cdot VM \qquad \left[\frac{kg}{s}\right] \tag{7.20}$$

$$Initial\ FC = \begin{Bmatrix} Y_1 \\ Y_2 \\ Y_3 \\ Y_4 \\ Y_5 \end{Bmatrix} \cdot \dot{m}_{fuelRZ} \cdot FC \qquad \left[\frac{kg}{s}\right] \tag{7.21}$$

Where VM represents the volatile fraction of the fuel and FC represents the fixed carbon fraction. It is important to split all the components of the fuel in different classes according to the size distribution, as the behavior of the fuel during the combustion changes according to the size class taken under consideration, principally because the temperature profiles along the furnace are different for different particle sizes.

Assuming the particles to be spherical and calling d_j the mean diameter of class j, it is possible to compute the number of particles in each class:

$$n_{particles\,j} = \frac{Y_j \cdot \dot{m}_{fuelRZ}}{\frac{\pi}{6} \cdot d_j^3 \cdot \rho_{fuel}} \tag{7.22}$$

Also this is computed for each size class of fuel injected in the reburner. At each temporal step, the total mass of each species in reburn gas mixture is known as:

$$Total\ mass\ originating\ from\ reburner = \begin{Bmatrix} m_{CH_4} \\ m_{CO} \\ m_{CO_2} \\ m_{H_2} \\ m_{HCN} \\ m_{H_2O} \\ m_{N_2} \\ m_{NH_3} \\ m_{NO} \\ m_{O_2} \end{Bmatrix} \tag{7.23}$$

The mass and molar fractions and molar concentration at each temporal step are computed using:

$$Mass\ Fraction_i = Y_i = \frac{Mass\ of\ species_i}{\sum_{i=1}^{i=n\,species} Mass\ of\ species_i} \tag{7.24}$$

$$Mole\ Fraction_i = X_i = \frac{\dfrac{Mass\ of\ species_i}{M_i}}{\sum_{i=1}^{i=n\,species} \dfrac{Mass\ of\ species_i}{M_i}} \tag{7.25}$$

The mass of each species varies over time as some species are produced and others are consumed; therefore the data of the masses of the gas phase is stored in a matrix, in which the rows correspond to the species *i* and the columns correspond to a certain temporal step *t*.

$$\begin{aligned} Time &= \left\{ 0 \ldots\ldots\ldots\ldots t \ldots\ldots\ldots\ldots t_{fin} \right\} \\ Total\ mass &= \left\{ \begin{Bmatrix} m_{CH_4} \\ m_{CO} \\ m_{CO_2} \\ m_{H_2} \\ m_{HCN} \\ m_{H_2O} \\ m_{N_2} \\ m_{NH_3} \\ m_{NO} \\ m_{O_2} \end{Bmatrix} \ldots\ldots \begin{Bmatrix} m_{CH_4} \\ m_{CO} \\ m_{CO_2} \\ m_{H_2} \\ m_{HCN} \\ m_{H_2O} \\ m_{N_2} \\ m_{NH_3} \\ m_{NO} \\ m_{O_2} \end{Bmatrix} \ldots\ldots \begin{Bmatrix} m_{CH_4} \\ m_{CO} \\ m_{CO_2} \\ m_{H_2} \\ m_{HCN} \\ m_{H_2O} \\ m_{N_2} \\ m_{NH_3} \\ m_{NO} \\ m_{O_2} \end{Bmatrix} \right\} \end{aligned} \tag{7.26}$$

The same kind of matrix is built with the data regarding the fixed carbon and volatile matter over time. In this case there are two separate matrices for the two fuels (if using a blend) and the different rows indicate different particle sizes.

$$Time = \left\{ 0 \ldots\ldots\ldots\ldots t \ldots\ldots\ldots\ldots t_{fin} \right\}$$

$$Volatiles\ \ fuel_1 = \left\{ \begin{Bmatrix} VM_1 \\ VM_2 \\ VM_3 \\ VM_4 \\ VM_5 \end{Bmatrix} \ldots\ldots \begin{Bmatrix} VM_1 \\ VM_2 \\ VM_3 \\ VM_4 \\ VM_5 \end{Bmatrix} \ldots\ldots \begin{Bmatrix} VM_1 \\ VM_2 \\ VM_3 \\ VM_4 \\ VM_5 \end{Bmatrix} \right\} \tag{7.27}$$

And

$$Time = \left\{ 0 \ldots\ldots\ldots\ldots t \ldots\ldots\ldots\ldots t_{fin} \right\}$$

$$Fixed\ Carbon_1 = \left\{ \begin{Bmatrix} FC_1 \\ FC_2 \\ FC_3 \\ FC_4 \\ FC_5 \end{Bmatrix} \ldots\ldots \begin{Bmatrix} FC_1 \\ FC_2 \\ FC_3 \\ FC_4 \\ FC_5 \end{Bmatrix} \ldots\ldots \begin{Bmatrix} FC_1 \\ FC_2 \\ FC_3 \\ FC_4 \\ FC_5 \end{Bmatrix} \right\} \tag{7.28}$$

7.4.5. Mixing model

The mixing of the reburner gases with the main burner exhaust is a very important part of the reburn process; therefore it must be modeled carefully. Assuming the mixing to be instantaneous is far from reality, as this process takes time to be completed.

With respect to an observer traveling with the reburn mass, the total mass will be composed of the reburn mass and a fraction of the main burner mass that is added gradually over time, and will approach a total mass equal to the sum of reburn mass and main burner gases.

Considering exponential mixing model, the mass flow in the reburn zone due to mixing with main burner gases is:

$$\dot{m}_{RZ,t} = \dot{m}_{RZ,t=0} + \dot{m}_{prod,MB} \cdot \left(1 - \exp\left(-\frac{t}{\tau_{mix}} \right) \right) \qquad \left[\frac{kg}{s} \right] \tag{7.29}$$

Eq(7.30) satisfies the initial ($t \to 0$) and final ($t \to \infty$) condition. The mixing time τ_{mix} depends on the geometry of the furnace and the reburn gases velocity. It is estimated from experimental data for the furnace and reburn injection configuration used for the experiment. τ_{mix} is estimated to be around 40ms,

(Goughnour P.G.,et al,2006). In the discussion of the results from the simulation, it is shown that reasonable variations of this constant will not affect significantly the NO_x reduction, which is the most important parameter of this simulation and, most importantly, will hardly change the qualitative trend.

The elemental amount of mass coming from the main burner that will be added over a period of time dt is given as:

$$dm_{MB} = \frac{\dot{m}_{prod,MB}}{\tau_{mix}} \cdot \exp\left(-\frac{t}{\tau_{mix}}\right) \cdot dt \qquad (7.31)$$

The term dm_{MB} is a vector and contains the contribution of every gas species, and as well as contributes thermal energy to RB gases; the elemental mass dm decreases as time progresses as less and less mass is left to be mixed.

Since the composition of the gas coming from the main burner is known, it is possible to determine the quantity of each species at each temporal step of integration (considering only the contribution from the mixing process).

$$\dot{m}_{RZ,t+1} = \dot{m}_{RZ,t} + d\dot{m}_{MB,t} = \begin{Bmatrix} \dot{m}_{CH_4} \\ \dot{m}_{CO} \\ \dot{m}_{CO_2} \\ \dot{m}_{H_2} \\ \dot{m}_{HCN} \\ \dot{m}_{H_2O} \\ \dot{m}_{N_2} \\ \dot{m}_{NH_3} \\ \dot{m}_{NO} \\ \dot{m}_{O_2} \end{Bmatrix}_{RZ,t} + \frac{\exp\left(-\frac{t}{\tau_{mix}}\right)}{\tau_{mix}} \cdot \begin{Bmatrix} \dot{m}_{CH_4} \\ \dot{m}_{CO} \\ \dot{m}_{CO_2} \\ \dot{m}_{H_2} \\ \dot{m}_{HCN} \\ \dot{m}_{H_2O} \\ \dot{m}_{N_2} \\ \dot{m}_{NH_3} \\ \dot{m}_{NO} \\ \dot{m}_{O_2} \end{Bmatrix}_{MB} \cdot dt \qquad (7.32)$$

7.4.6. Chemical reactions

In order to reduce the computational effort, a simplified kinetics model has been adopted. The homogeneous reactions are the reactions that take place in the gas phase; for these reactions the species concentrations are directly computed knowing the composition of the gas phase stream.

7.4.6.1. NO reactions

A widely used model, for reduced NO reactions in the reburn process, is the one formulated by De Soete (De Soote G.G.,et al,2001). However, the simulations based on his kinetics have brought unsatisfactory results, especially with pure biomass or a blended fuel with a high content of biomass. It is speculated that the kinetics for ammonia reaction at low temperatures, plays a vital role in the case of reburn process with biomass. Further the De Soete's kinetics have been formulated based on data points at temperature mostly above 2000 K, while in this work, the temperatures are of the order of 1600 K. So

the two reaction rates from De Soete regarding ammonia will be substituted with the recent data by Brink et al. (Brink A.,et al,2001), which have been developed to describe the oxidation of volatile nitrogen in biomass combustion. The two reaction rates by De Soete regarding HCN will be substituted with the ones by He (He. R.,et al,2004), that are a very slight modification on De Soete's ones.

7.4.6.1.1 I_N Ammonia oxidation .

$$NH_3 + O_2 \rightarrow NO + H_2O + 0.5 \cdot H_2$$

$$\dot{w}_{NH3,I_N} = -1.21 \cdot 10^{11} \cdot T_g^2 \cdot [NH_3] \cdot [O_2]^{0.5} \cdot [H_2]^{0.5} \cdot \exp\left(\frac{-8000}{T_g}\right)\left[\frac{kmol}{m^3 \cdot s}\right] \qquad (7.33)$$

$$NH_3 + O_2 \rightarrow NO + H_2O + 0.5 \cdot H_2$$

$$\dot{w}_{NH3,I_N} = -1.21 \cdot 10^{5} \cdot T_g^2 \cdot [NH_3] \cdot [O_2]^{0.5} \cdot [H_2]^{0.5} \cdot \exp\left(\frac{-8000}{T_g}\right)\left[\frac{kmol}{m^3 \cdot s}\right]$$

7.4.6.1.2 II_N Ammonia reduction (Brink A.,et al,2001).

$$NH_3 + NO \rightarrow N_2 + H_2O + 0.5 \cdot H_2$$

$$\dot{w}_{NH3,II_N} = -\frac{8.73 \cdot 10^{20}}{T_g} \cdot [NH_3] \cdot [NO] \cdot \exp\left(\frac{-8000}{T_g}\right) \quad \left[\frac{kmol}{m^3 \cdot s}\right] \qquad (7.34)$$

$$NH_3 + NO \rightarrow N_2 + H_2O + 0.5 \cdot H_2$$

$$\dot{w}_{NH3,II_N} = -\frac{8.73 \cdot 10^{14}}{T_g} \cdot [NH_3] \cdot [NO] \cdot \exp\left(\frac{-8000}{T_g}\right) \left[\frac{kmol}{m^3 \cdot s}\right]$$

7.4.6.1.3 III_N HCN oxidation (He. R.,et al,2004).

$$HCN + O_2 \rightarrow NO + CO + 0.5 \cdot H_2$$

$$\dot{w}_{HCN,III_N} = -10^{11} \cdot X_{HCN} \cdot X_{O2}^{b} \cdot \frac{p}{R \cdot T_g} \cdot \exp\left(\frac{-280328}{R \cdot T_g}\right)\left[\frac{kmol}{m^3 \cdot s}\right] \qquad (7.35)$$

7.4.6.1.4 IV_N HCN reduction (He. R.,et al,2004).

$$HCN + NO \rightarrow N_2 + CO + 0.5 \cdot H_2$$

$$\dot{w}_{HCN,IV_N} = -3 \cdot 10^{12} \cdot X_{HCN} \cdot X_{NO} \cdot \frac{p}{R \cdot T_g} \cdot \exp\left(\frac{-251000}{R \cdot T_g}\right)\left[\frac{kmol}{m^3 \cdot s}\right] \qquad (7.36)$$

The *b* exponent (used in reaction IV_N) is calculated by a curve fit from the experimental data from De Soete (De Soete G.G., et al, 2001).

$$b = \begin{cases} 0 & if\ \ln X_{O2} \geq -3 \\ 233 \cdot \exp\left(\dfrac{28}{0.5 + \ln X_{O2}}\right) & if\ -5.67 < \ln X_{O2} < -3 \\ 1 & if\ \ln X_{O2} \leq -5.67 \end{cases} \tag{7.37}$$

7.4.6.2. Gas phase homogeneous oxidation reactions

These are other reactions, taking place in the gas phase, but in which NO is not involved.

7.4.6.2.1 I_G CO oxidation. Howard et al. (Howard J.B,et al,1973).

$$CO + 0.5 \cdot O_2 \rightarrow CO_2$$

$$\dot{w}_{CO,I_G} = -1.3 \cdot 10^{17} \cdot [CO] \cdot [O_2]^{0.5} \cdot [H_2O]^{0.5} \cdot \exp\left(\frac{-125580}{R \cdot T_g}\right)\left[\frac{kmol}{m^3 s}\right] \tag{7.38}$$

7.4.6.2.2 II_G H_2 oxidation. Jones et al. (Jones W.P.,et al,1988).

$$H_2 + 0.5 \cdot O_2 \rightarrow H_2O$$

$$\dot{w}_{H2,II_G} = -0.68 \cdot 10^{19} \cdot \left(\frac{Y_{H2}}{2}\right)^{0.25} \cdot \left(\frac{Y_{O2}}{32}\right)^{1.5} \cdot \rho_g^{1.75} \cdot \exp\left(\frac{-20130}{R \cdot T_g}\right)\left[\frac{kmol}{m^3 s}\right] \tag{7.39}$$

7.4.6.2.3 III_G CH_4 oxidation. Van der Vaart (Van Der Waart D.R.,et al,1992).

$$CH_4 + 2 \cdot O_2 \rightarrow CO_2 + 2 \cdot H_2O$$

$$\dot{w}_{CH4,III_G} = -5.74 \cdot 10^{10} \cdot [CH_4]^{-0.5} \cdot [O_2]^{1.5} \cdot \exp\left(\frac{-60000}{R \cdot T_g}\right)\left[\frac{kmol}{m^3 s}\right] \tag{7.40}$$

From the stoichiometry of the reactions, it is possible to compute the reaction rates of each species k:

$$\dot{n}_{\mathrm{homo},i} = \sum_{k=1}^{\mathrm{homo}\,react} \upsilon_{i,k} \cdot w_i \cdot \frac{R_{kg} \cdot m_{TOT,gas} \cdot T_g}{p} \qquad \left[\frac{kmol}{s}\right] \tag{7.41}$$

Where $\upsilon_{i,k}$ is the stoichiometric coefficient of species *i* in homogeneous reaction *k*, and it is positive if the species is being produced and negative if the species is being consumed. It is zero if the species *i* does not appear in the reaction *k*. Knowing the molecular weight of each species, it is possible to compute the mass variation rate.

$$\dot{m}_{\mathrm{homo},i} = \dot{n}_{\mathrm{homo},i} \cdot M_i \qquad \left[\frac{kg}{s}\right] \tag{7.42}$$

7.4.6.3. Heterogeneous reactions

These reactions take place at the particle surface between the solid carbon and the solid nitrogen and the gas phase. The kinetics of these reactions depend strongly on the characteristics of the solid fuel

(char porosity, dimension, condition of species diffusion etc). These kinetics have a way higher uncertainty than the reactions in the gas phase. When kinetics data are not available for specified biomass, they have been assumed to be the same as for lignite, as low rank coals are the closest to biomass in combustion characteristics.

7.4.6.3.1 I_{FC} Carbon complete oxidation. Annamalai et al. (Annamalai K..,et al,1993).

$$C + O_2 \rightarrow CO_2 \qquad \dot{w}_{C,I_{FC}} = 1.6 \cdot 10^5 \cdot \exp\left(\frac{-20000}{R \cdot T_g}\right) \qquad \left[\frac{m}{s}\right] \qquad (7.43)$$

7.4.6.3.2 II_{FC} Carbon partial oxidation. Smoot, et al. (Smoot L.D..,et al,1992) and Annamalai et al. (Annamalai K..,et al,1993).

$$C + 0.5 \cdot O_2 \rightarrow CO_2 \qquad \textit{for biomass}: \qquad \dot{w}_{C,II_{FC}} = 2.3 \cdot 10^7 \cdot \exp\left(\frac{-26000}{R \cdot T_p}\right)\left[\frac{m}{s}\right]$$

$$\textit{for lignite}: \qquad \dot{w}_{C,II_{FC}} = 1.22 \cdot T_p \cdot \exp\left(\frac{-10300}{R \cdot T_p}\right)\left[\frac{m}{s}\right] \qquad (7.44)$$

$$\textit{for subbitu}\,\min\,\textit{ous} \qquad \dot{w}_{C,II_{FC}} = 10.4 \cdot T_p \cdot \exp\left(\frac{-11200}{R \cdot T_p}\right)\left[\frac{m}{s}\right]$$

7.4.6.3.3 III_{FC} Carbon partial oxidation with CO_2. Smoot, et al. (Smoot L.D.,et al,1992).

$$C + CO_2 \rightarrow 2 \cdot CO \qquad \textit{for lignite} \qquad \dot{w}_{C,III_{FC}} = 3.42 \cdot T_p \cdot \exp\left(\frac{-15600}{R \cdot T_p}\right)\left[\frac{m}{s}\right]$$

$$\textit{for subbitu}\,\min\,\textit{ous} \qquad \dot{w}_{C,III_{FC}} = 6190 \cdot T_p \cdot \exp\left(\frac{-28900}{R \cdot T_p}\right)\left[\frac{m}{s}\right] \qquad (7.45)$$

7.4.6.3.4 IV_{FC} Steam carbon reaction: this reaction rate can be defined as a function of the previous kinetics. Yoon, H., et al., (Yoon H.,et al,1978).

$$C + H_2O \rightarrow H_2 + CO \qquad \dot{w}_{C,IV_{FC}} = 1.67 \cdot w_{C,III_{FC}} \left[\frac{m}{s}\right] \qquad (7.46)$$

7.4.6.3.5 V_{FC} Methane formation. Schoeters, (Shoeters J.G.,et al).

$$C + 2 \cdot H_2 \rightarrow CH_4 \qquad \dot{w}_{C,V_{FC}} = 3 \cdot 10^{-3} \cdot w_{C,III_{FC}} \left[\frac{m}{s}\right] \qquad (7.47)$$

7.4.6.3.6 VI_{FC}Solid carbon and NO reaction. Mitchel et al., (Mitchel J.W.,et al,1982).

$$C + NO \rightarrow CO + 0.5 \cdot N_2 \qquad w_{C,VI_{FC}} = 1.57 \cdot 10^5 \cdot \exp\left(\frac{-34000}{R \cdot T_p}\right)\left[\frac{m}{s}\right] \qquad (7.48)$$

7.4.6.3.7 I_{FN} Solid nitrogen oxidation. Mitchel et al., (Mitchel J.W.,et al,1982).

$$N + 0.5 \cdot O_2 \rightarrow NO \qquad \dot{w}_{C,VII_{FC}} = \frac{m_N}{m_P} \cdot w_{C,II_{FC}} \qquad \left[\frac{m}{s}\right] \qquad (7.49)$$

The FC consumption rate for the k-th heterogeneous reaction, for one particle of size *j*, can be computed as:

$$\dot{m}_{C,SP,k,j} = \rho_{w,j} \cdot k_{C,k,j} \cdot Y_{i,jw} \cdot \pi \cdot d_{p,j}^2 \qquad \left[\frac{kg}{s}\right]_{for\,each\,particle} \qquad (7.50)$$

All the variables in the formula depend on the particle size, as the temperature of the particle and the composition of the boundary layer will be different according to the size and this will affect the density, the mass fraction of the elements and the reaction rates as well.

Knowing the fixed carbon (FC) consumption rate and the stoichiometry of the heterogeneous reactions, it is possible to compute the amount of *i* species added to the gas phase:

$$\dot{m}_{i,hetero} = \sum_{j=1}^{J} \left[\sum_{k=1}^{heteroreact} \left(\upsilon_{k,i} \cdot \dot{m}_{C,k,j} \right) \cdot N_{particles,j} \right] \cdot \frac{M_i}{M_C} \qquad \left[\frac{kg}{s}\right] \qquad (7.51)$$

where J is the number of size groups (five).

7.4.6.4. Pyrolysis

For the release of volatiles it has been assumed a single reaction kinetics model, (Sami M.,et al,2001).

$$\left.\frac{dm_{pyro}}{dt}\right|_j = A_{pyro} \cdot VM_{remain,j} \cdot \exp\left(\frac{-E_{pyro}}{R \cdot T_{p,j}}\right), \qquad j = 1....5 \qquad \left[\frac{kg_{VM}}{s}\right] \qquad (7.52)$$

For the five size groups (j=1…5):

$$\begin{Bmatrix} \dot{VM}_1 \\ \dot{VM}_2 \\ \dot{VM}_3 \\ \dot{VM}_{4,} \\ \dot{VM}_{5,} \end{Bmatrix} = A_{pyro} \cdot \begin{Bmatrix} VM_{remain,1} \cdot \exp\left(\frac{-E_{pyro}}{R \cdot T_{p,1}}\right) \\ VM_{remain,2} \cdot \exp\left(\frac{-E_{pyro}}{R \cdot T_{p,2}}\right) \\ VM_{remain,3} \cdot \exp\left(\frac{-E_{pyro}}{R \cdot T_{p,3}}\right) \\ VM_{remain,4} \cdot \exp\left(\frac{-E_{pyro}}{R \cdot T_{p,4}}\right) \\ VM_{remain,5} \cdot \exp\left(\frac{-E_{pyro}}{R \cdot T_{p,5}}\right) \end{Bmatrix} \qquad \left[\frac{kg_{VM}}{s}\right] \qquad (7.53)$$

VM_{remain} represents the mass of volatiles left in a certain particle size group; its value needs to be updated at each integration step, as it drives the volatile emission kinetics. The activation energy E_{pyro} and the pre exponential factor A_{pyro} are different for coal and for biomass, but the same model is used. Note that T_p stands for particle temperature; as each size group has its own temperature, each group has a different rate of release of volatile matter. The VM content at the next temporal step can be computed as:

$$VM_{t+1} = \begin{Bmatrix} VM_{1,t+1} \\ VM_{2,t+1} \\ VM_{3,t+1} \\ VM_{4,t+1} \\ VM_{5,t+1} \end{Bmatrix} = \begin{Bmatrix} VM_{1,t} \\ VM_{2,t} \\ VM_{3,t} \\ VM_{4,t} \\ VM_{5,t} \end{Bmatrix} - \begin{Bmatrix} \dot{m}_{pyro1,t} \cdot dt \\ \dot{m}_{pyro2,t} \cdot dt \\ \dot{m}_{pyro3,t} \cdot dt \\ \dot{m}_{pyro4,t} \cdot dt \\ \dot{m}_{pyro5,t} \cdot dt \end{Bmatrix} \qquad (7.54)$$

The total mass flow of gases from the particles to the gas phase can be computed summing the contribution of the different size classes:

$$\dot{m}_{pyro,TOT} = \sum_{j=1}^{J} \dot{VM}_j \qquad (7.55)$$

The composition of volatile matter released is known (Eq. IV.11) and hence it is possible to compute species contribution to the gas stream. The pre exponential factors and activation energies have been selected from the literature paying attention to select data measured under very fast heating rate (1000 K/s – 10000 K/s) as this is close to the conditions the fuel encounters in the furnace.

7.4.6.5. Fuel Nitrogen pyrolysis

The two most used ways to model the FN release rate are to assume either the FN release rate to be proportional to the pyrolysis rate (Nichols K.M.,et al,1986) or to formulate a specific kinetics (Pohl J.H.,et al,1976).

In the case of N release proportional to pyrolysis rate, the FN release rate is given as:

$$\left.\frac{dm_{FN,pyro}}{dt}\right|_j = \left.\frac{dm_{pyro}}{dt}\right|_j \cdot \frac{N_{initial}}{VM_{initial}} \qquad \left[\frac{kg_N}{s}\right] \tag{7.56}$$

Where $\left.\frac{dm_{pyro}}{dt}\right|_j$ is the pyrolysis rate. Note that also in this case the FN release rate will vary depending upon the size group.

In the second model, the FN emission is described with a single reaction model.

$$\left.\frac{dm_{N-pyro}}{dt}\right|_j = A_{FN} \cdot N_{remain,j} \cdot \exp\left(\frac{-E_{FN}}{R \cdot T_{p,j}}\right) \qquad \left[\frac{kg_N}{s}\right] \tag{7.57}$$

These parameters have been provided by Pohl, (Pohl J.H.,et al,1976) and Peck (Peck R.E.,et al,1982). Both these studies were based on coal, for Peck A = 8300 s^{-1} and E = 69840 kJ/kmol. The FN kinetics data is not available for FB.

There is one important difference between the pyrolysis rate formulation and the FN release rate formulation: the first rate is expressed in kg of volatiles released per second, therefore, knowing the mass composition of the volatiles it is possible to compute the flow rate of each component. On the other side the FN pyrolysis rate is expressed in terms of kg of solid nitrogen being released per second through the FN volatiles, and not directly as kg of FN products released per seconds. For this reason the N consumption rate must be multiplied by a constant in order to switch to the FN total mass flow rate. This constant k_{FN} depends on the FN composition.

So now:

$$\dot{m}_{FN,TOT} = \sum_{j=1}^{N class} \left.\frac{dm_{N-pyro}}{dt}\right|_j \cdot k_{FN} \qquad \left[\frac{kg_{FN}}{s}\right] \tag{7.58}$$

This is the total mass flow of gases released from the pyrolysis of the fuel bound nitrogen. For biomass, as a base case, it is assumed that the FN pyrolysis rate is proportional to the volatiles release rate, while for coal the base case will be FN pyrolysis with a specific kinetics.

The N-bonds within a particle are very different for coal and biomass: in the case of animal waste biomass most of the nitrogen is in the form of urea and bond energy is low. So it is reasonable to assume the nitrogen to be released along with the volatiles; besides kinetics for N release from biomass is not available in literature, therefore it would have been necessary to assume the same kinetics as for coal. On the contrary, for coal, the bonds between the nitrogen and the particle are much stronger, therefore it is reasonable to describe the FN pyrolysis with its kinetic, especially because the activation energies are much higher than for the volatile release, so it would not be very accurate to describe coal FN pyrolysis to be simply proportional to the regular pyrolysis.

7.4.6.6. Gas stream mass conservation equations

The species concentrations in the free stream change with time due to various processes: they are produced / consumed by the homogeneous or heterogeneous reactions, mass is added from the main burner, the volatiles, the FN and species from the heterogeneous reactions.

In general it is possible to state:

$$\left.\frac{dm}{dt}\right|_{i,gas} = \dot{m}_{pyro,TOT} \cdot y_{pyro,i} + \dot{m}_{FN,TOT} \cdot y_{FN,i} + \dot{m}_{hetero,i} + \dot{m}_{\mathrm{homo.},i} + \dot{m}_{MB} \cdot y_{MB,i} \qquad (7.59)$$

With the following formula it is possible to compute the variation of each species *i* at each temporal step of the integration:

$$m_{RZ,t+1} = m_{RZ,t} + \left.\frac{dm}{dt}\right|_{RZ} \cdot dt = \begin{Bmatrix} m_{CH_4} \\ m_{CO} \\ m_{CO_2} \\ m_{H_2} \\ m_{HCN} \\ m_{H_2O} \\ m_{N_2} \\ m_{NH_3} \\ m_{NO} \\ m_{O_2} \end{Bmatrix}_{RZ,t} + \dot{m}_{pyro,TOT} \cdot \begin{Bmatrix} y_{CH_4} \\ y_{CO} \\ y_{CO_2} \\ 0 \\ 0 \\ 0 \\ 0 \\ 0 \\ 0 \\ 0 \end{Bmatrix}_{pyro} \cdot dt + \dot{m}_{FN,TOT} \cdot \begin{Bmatrix} 0 \\ 0 \\ 0 \\ 0 \\ y_{HCN} \\ 0 \\ 0 \\ y_{NH_3} \\ y_{NO} \\ 0 \end{Bmatrix}_{FN} \cdot dt +$$

$$+ \begin{Bmatrix} \dot{m}_{CH_4} \\ \dot{m}_{CO} \\ \dot{m}_{CO_2} \\ \dot{m}_{H_2} \\ \dot{m}_{HCN} \\ \dot{m}_{H_2O} \\ \dot{m}_{N_2} \\ \dot{m}_{NH_3} \\ \dot{m}_{NO} \\ \dot{m}_{O_2} \end{Bmatrix}_{Hetero} \cdot dt + \begin{Bmatrix} \dot{m}_{CH_4} \\ \dot{m}_{CO} \\ \dot{m}_{CO_2} \\ \dot{m}_{H_2} \\ \dot{m}_{HCN} \\ \dot{m}_{H_2O} \\ \dot{m}_{N_2} \\ \dot{m}_{NH_3} \\ \dot{m}_{NO} \\ \dot{m}_{O_2} \end{Bmatrix}_{Homo} \cdot dt + \frac{\exp\left(-\frac{t}{\tau_{mix}}\right)}{\tau_{mix}} \cdot \begin{Bmatrix} 0 \\ 0 \\ y_{CO_2} \\ 0 \\ 0 \\ y_{H_2O} \\ y_{N_2} \\ 0 \\ y_{NO} \\ y_{O_2} \end{Bmatrix}_{MB} \cdot dt \qquad (7.60)$$

7.5. Results and discussion

7.5.1. Discussion of the numerical model

After the data has been entered, and the condition of the main burner has been solved and the composition of the volatiles has been determined, the integration over time can start. First the contribution of the mixing process is considered at the particular temporal instant, afterwards it is possible to consider the effect of the mixing on the temperatures, then the devolatilization and the chemical reactions are taken in consideration,

Subsequently it is possible to compute the temperature of the gas and the particles at this temporal step. The temporal instant is then updated and it is checked whether the end of the integration has been reached or not. In this model all the differential equations are integrated with an explicit scheme, in order to reduce the computational effort. A critical aspect in this kind of studies is the choice of the temporal step for the integration. A large temporal step would lead to short computational time but would also bring to a bad solution or even to divergence as this is an explicit method and therefore is not always stable. On the other side, a very small temporal step would bring to a good solution but would require a massive computational effort. Therefore the temporal step must be carefully chosen to produce a good solution, but still not make the computational time excessively long.

In general the temporal step has to be smaller than the shortest characteristic time of the processes present in the model: it has to be small enough to guarantee a good accuracy even for the fastest events occurring in the simulation.

Figure shows the NO_x profiles versus the equivalence ratio with different temporal steps as parameter.

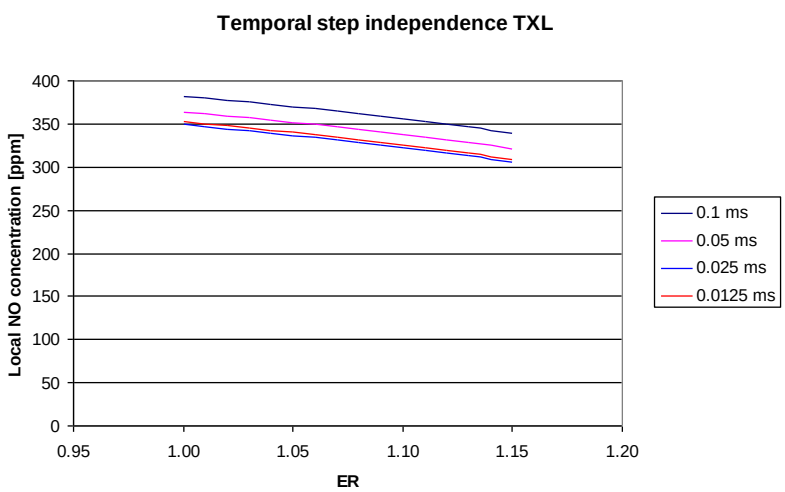

Figure 7.5.1 Choice of Temporal Step, Texas Lignite

As the temporal step is gradually reduced, the difference between two successive solutions becomes smaller and after the temporal step is 0.025ms the difference becomes negligible. So the 0.025ms is used as temporal step.

The same study has been repeated also for biomass and blends and in all the cases this temporal step has turned out to be similar.

7.5.2. NO_x results

The data from literature is directly used, without any changes to match with the experimental data. An alternative way is to adjust the kinetics to minimize the discrepancy between experiments and model, but this requires massive computational efforts, and besides, the experimental data available cannot be considered to be accurate enough to develop kinetics data based on them.

The residence time in the furnace is estimated to be of the order of 0.85s, and hence the numerical result for the NO emission is the value of the NO concentration considered at the residence time t = 0.85s. It is important to note that the only purpose of the residence time in the simulation is to know at what instant to select the results from the simulation and compare it with the experimental data. It might be argued that the method adopted to determine residence time (=Distance/velocity) is too simplistic; to compute more accurately the residence time it would be necessary to go for complete fluid dynamic simulation. In fact the main result from this code is the NO concentration at the end of the furnace; since temperatures are already low all the NO reactions are already almost frozen well before the end of the furnace. Hence the NO concentration vs. time flattens well before the end of the furnace as the temperatures are decreasing. Under these circumstances it would make hardly any difference assuming a residence time of 0.7s or 1s.

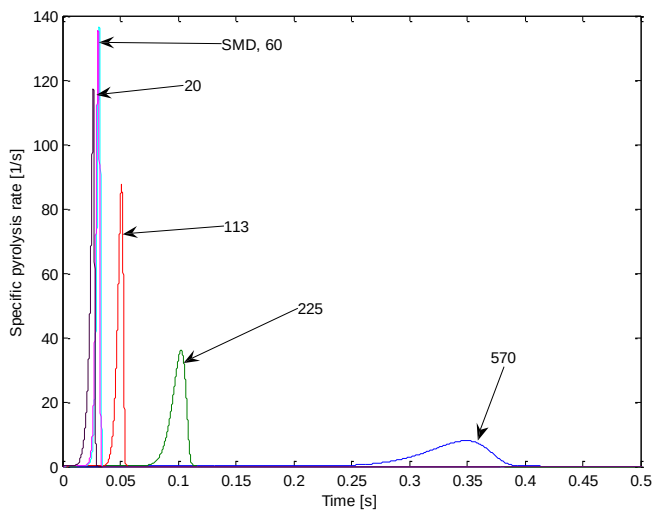

Figure 7.5.2 Effect of class size distribution on devolatilization rate

Figure presents the specific devolatilization rate for LAPC, ER = 1, and it is here presented to show the effect of a discrete number of size classes on this variable, the spikes are identified with the diameter of the corresponding class in micron.

This is due to the description of the particle size distribution with a finite number of size groups. The solid fuel size distribution is continuous, but in this model it is described by five size groups. This

number has been chosen because this is the number of sieves used in the standard coal sieving machine in the laboratory; therefore a more detailed distribution was not available. Besides, more size groups would have resulted in more computationally intensive code.

With a finite size distribution, the process of release of the volatiles occurs when a certain size group reaches a certain temperature (e.g. pyrolysis temperature), its release rate becomes significant at that time. Correspondingly in the reactions that involve those species, there is a spike as now there are more reactant species in the gas phase. With an infinite number of classes the release of volatiles would be a continuous function and hence the spikes can disappear. However using five size groups is a better description of reality than using just the SMD of the distribution and describing the reburn fuel with SMD: in that case there would be only one large spike and it is not possible to predict the effect of size distribution on the final NO concentration.

Many times small scale test data cannot be directly scaled to a large scale combustion system; however the ratios of reburn performance of fuel of interest to selected standard fuel which is coal, is typically scalable. Then Texas Lignite is selected as standard fuel for the purpose of evaluating comparative reburn performance of LAPC biomass.

7.5.2.1. Low Ash Partially Composted biomass (LAPC)

Figure shows the predicted temperature profiles of the gas and the various particle size groups for LAPC biomass.

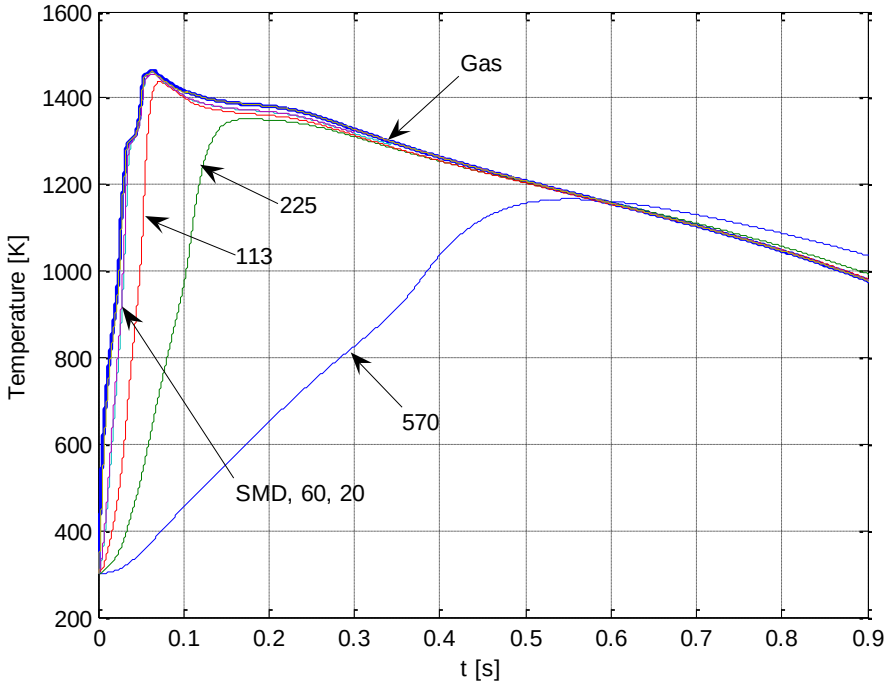

Figure 7.5.3 Temperature profile for LAPC, pure air, ER = 1

It is seen that there is hardly any difference between the 20 micron, 60 micron and SMD classes, while the other larger classes have different temperature profiles.

As the main burner gases start mixing with reburn gases, the temperature of the reburn gas increases very rapidly; it reaches a peak and then it decreases as time passes and the gas moves down the furnace. As expected, the small particles heat up very rapidly, having curves that are hardly distinguishable from that of gas. On the other hand the large particles heat up slowly. It is possible to see that the temperatures of the particles always remain below the gas temperature since the fixed carbon content in biomass is very low and when particles reach a temperature where the heterogeneous reactions become fast, most of the oxygen has already been consumed by the combustion of the volatile gases; therefore the lack of oxygen at the particle surface tends to shift the reactions toward the endothermic gasification reactions which tend to cool the particles down.

The only exception is at the end of the furnace when the temperature of the gas is dropping: the temperature of the largest particles goes above the gas temperature, but this only happens due to the larger thermal inertia of these particles with respect to the small ones. The heat exchange coefficient h for large particles is smaller than for small particles (i.e. heat is transferred more rapidly out of particle with small d_p, than from the ones with large d_p).

Figure V.21 shows the difference between the temperature profile of Texas Lignite and LAPC.

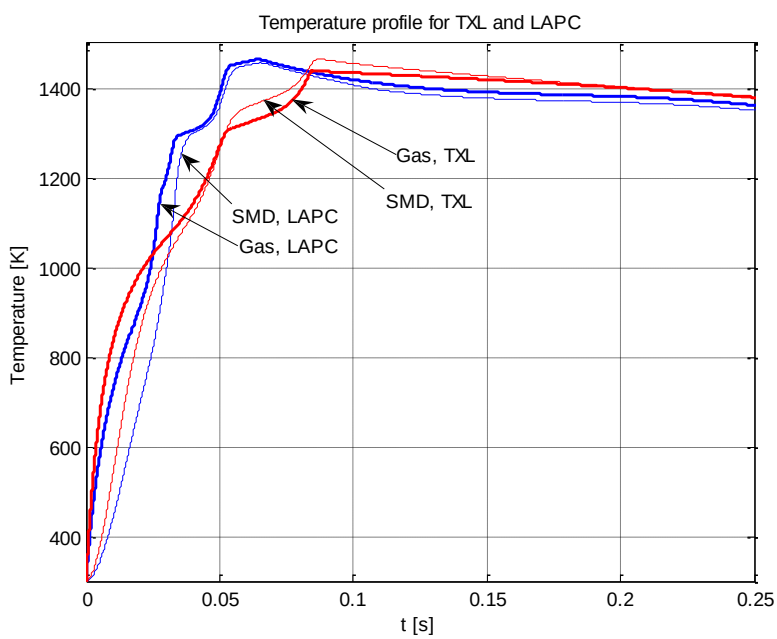

Figure 7.5.4 Comparison between temperature profile for Texas Lignite and LAPC, pure air, ER = 1

From this graph the delay between the combustion of LAPC and TXL is apparent.

Figure V.22 shows the predicted temperature profile along the furnace for biomass with vitiated air.

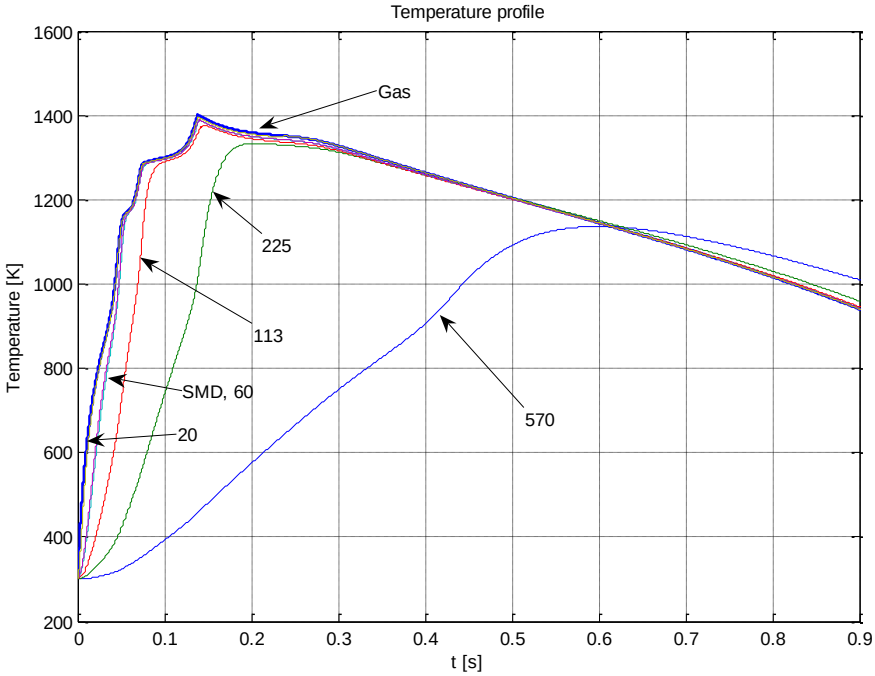

Figure 7.5.5 Temperature profile for LAPC, vitiated air, ER = 1

The differences between the case of pure and vitiated air become apparent plotting the gas profile and the SMD profile for the two cases on the same figure, see Figure V.23.

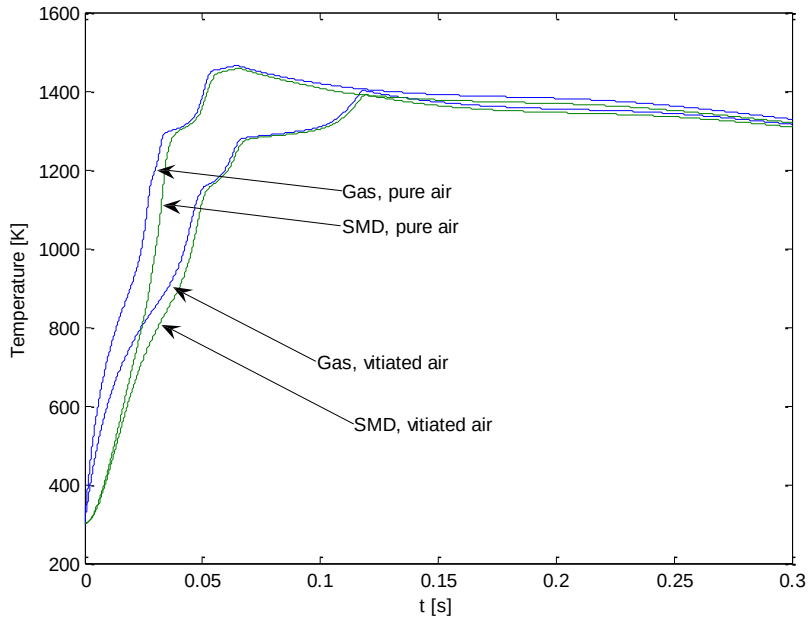

Figure 7.5.6 Comparison of temperature profiles for pure and vitiated air, LAPC, ER = 1

The rate of heating up is slower and all the temperatures are lower than those with pure air. Note that the comparison is made at same Φ_{RZ}; since in the case of vitiated air the oxygen concentration is 12.5% more gas must be supplied to maintain the same Φ_{RZ}. Thus the mass of inert gas at the reburner is almost the double than before; so there is a large amount of inert gas to be heated up without giving any contribution to the combustion and this drives down the temperatures.

It is also interesting to study the effect of the size distribution on the temperature profile: Figure V.24 shows this effect. In this figure the temperature profile for gas is plotted for the case of real distribution (five size groups) and in the case of monosized suspension with d_p = SMD. On the same plot T_p of the particle with d_p = SMD is plotted for both cases.

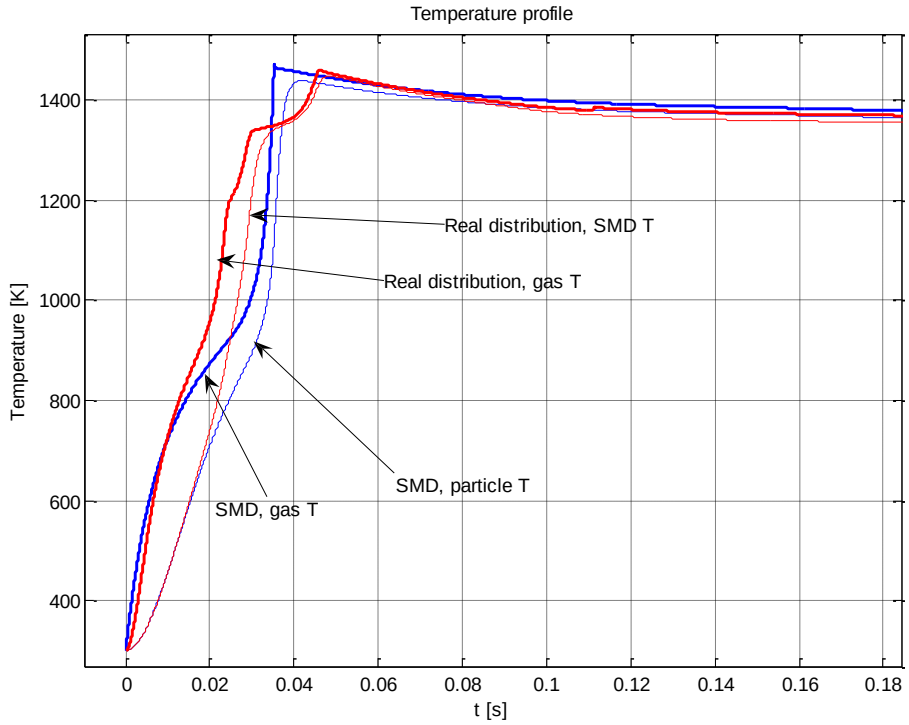

Figure 7.5.7. Comparison between temperature profile with real distribution and monosize, LAPC, pure air, ER = 1

It is possible to see some differences in the temperature profiles: in the very first part the gas temperature in the case of real distribution increases faster than for the monosized distribution because in the case of real distribution there are particles smaller than the SMD that become combustible at earlier times. As these particles are burned out the rate of increase of T slows down, as now it is necessary to wait for the larger particles to burn. In the case of the monosized distribution, the particles are larger than the smallest particles of the real distribution, and hence it takes a longer time to heat up. Once they are combustible the temperature rise becomes much steeper than in the case of the real distribution, because the whole fuel becomes reactive at the same time. It is apparent that it is possible to reach the maximum temperature faster for monosized distribution than with the real distribution, because in the case of real distribution the small particles do not provide enough energy to reach the highest temperature.

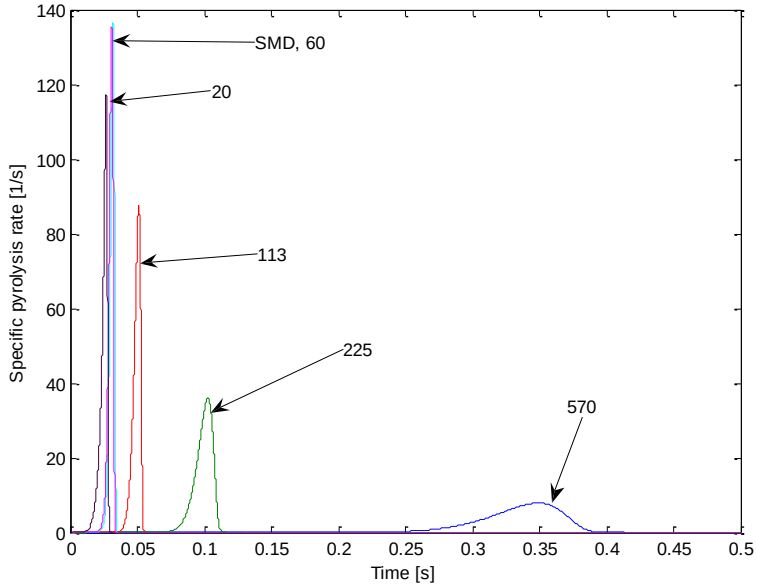

Figure 7.5.8 Volatile emission rate LAPC, pure air, ER = 1

LAPC biomass releases its volatiles at a very high rate which then oxidize in the gas phase, consequently the gas stream is heated up very rapidly. The rapid release of volatiles consumes a large amount of oxygen in a very short time; this is one of the reasons why biomass is so effective in NO reduction: the higher is VM, the lower O_2 and higher the NO_x reduction.

The shape of Figure V.25 is clearly dependent on the finite number of size groups: the spikes correspond to the five size groups. The SMD spike has been included to show the hypothetical behavior of particles with the SMD diameter. Discretizing the size distribution has forced the volatiles to evolve at some specific times. In a model with monosized fuels, there would be only one spike. The release of FN follows similar pattern.

As expected, the small particles are the first to release their volatiles as they are heated up first. It is interesting to compare the behavior of the same fuel when fired with pure and vitiated air for the SMD.

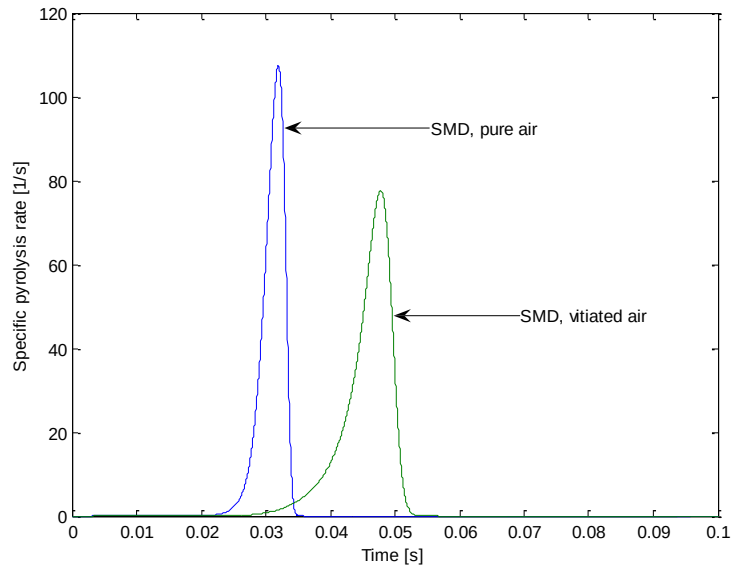

Figure 7.5.9 Comparison of normalized pyrolysis rate for pure and vitiated air, LAPC, ER = 1

In Figure V.26 the difference between the two cases is clearly seen. The pyrolysis process is delayed and the rate of release is reduced. This is due to the lower temperatures due to the reduced oxidation rate and increased inert mass and hence slower heating rate.

It is also interesting to consider the specific mass of the various particle size groups versus time; the mass is divided by the initial particle mass. See Figure V.27.

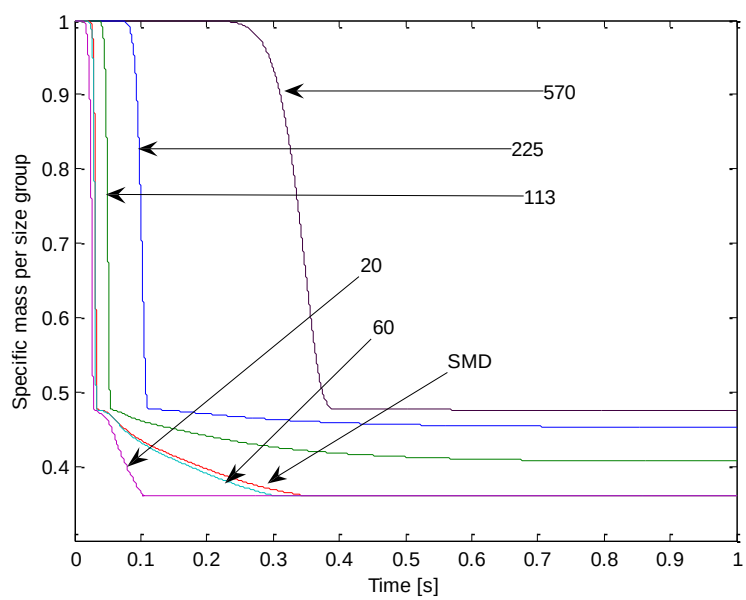

Figure 7.5.10 Specific mass per Particle LAPC, pure air, ER = 1.

In Figure above it is possible to see that all the small particles show a first sharp decrease in their mass due to the loss of volatile matter. The largest size group presents the release of volatile matter at much later times than all the other classes.

The curves show a sharp decrease in mass loss rate due to slower heterogeneous reactions rates of fixed carbon; further this process is much slower, and occurs after the peak temperature. For the largest particles the second loss is almost negligible. It is also possible to see the different amplitude of the two losses: the first one is much larger because the volatile content in the biomass is much larger than the fixed carbon content.

Figure below shows the fixed carbon fraction versus time, and it is clear that the fixed carbon consumption depends strongly on the particle size.

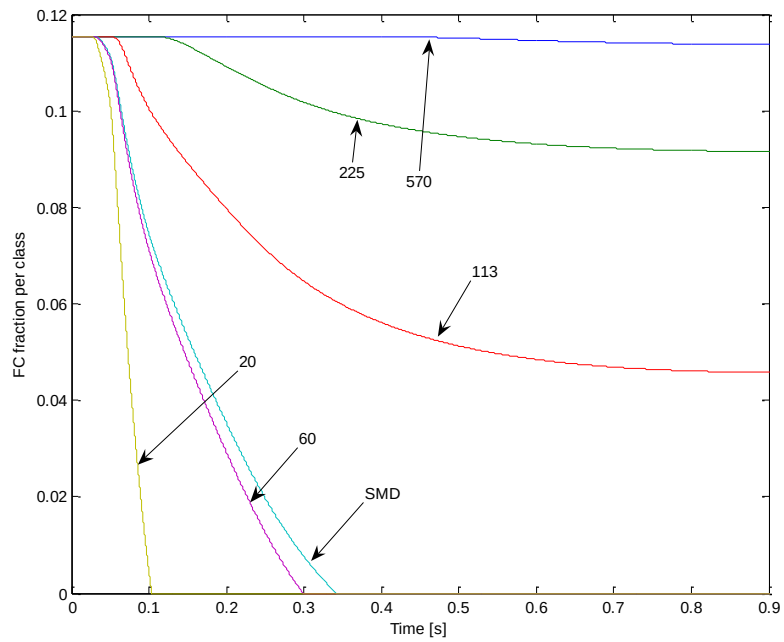

Figure 7.5.11 Fixed Carbon fraction LAPC, pure air, ER = 1

Only the two smallest size groups are able to burn out their fixed carbon; the SMD would be able to burn out all its fixed carbon. Particles with diameter of 113 μm and 225 μm consume only a part of their fixed carbon, while particles with diameter of 570 μm hardly consume their fixed carbon. This happens because it takes longer time for the largest particles to be heated up; they never reach temperatures high enough for the heterogeneous reactions to become significantly fast.

- Comparison with experimental data

Let us now compare the results from the simulation with the results from the experiment from Goughnour, (Goughnour P.G.,et al,2006).

Figure 29 and Figure 30 present a comparison of experimental data with numerical prediction for NO_x at the end of the reburn process, with the main burner providing 70% of the thermal power. In Figure 29 pure air is used as a carrier gas, while in Figure 30 vitiated air is used as a carrier gas.

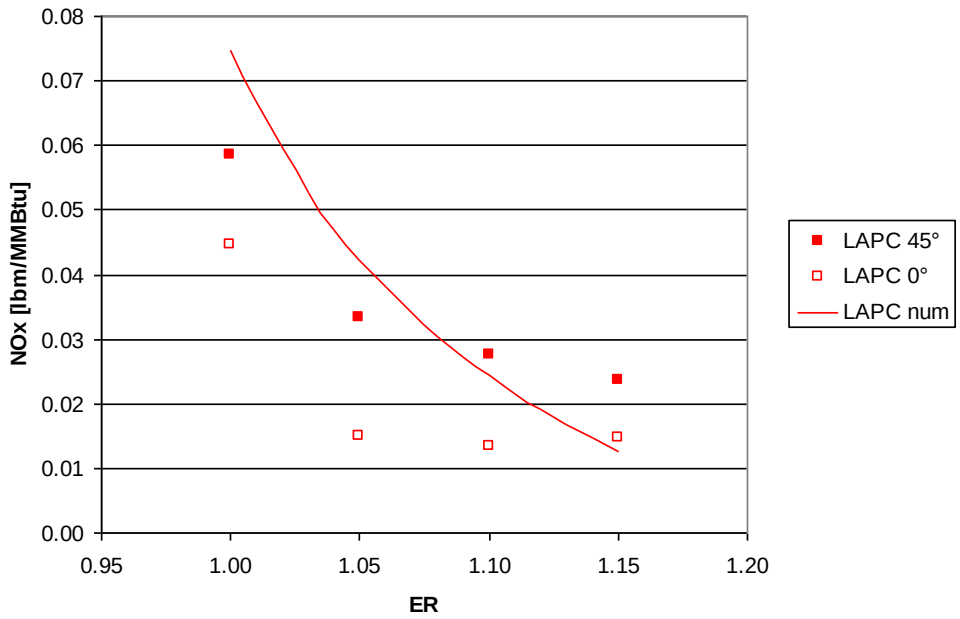

Figure 7.5.12 Comparison with experimental data LAPC, pure air

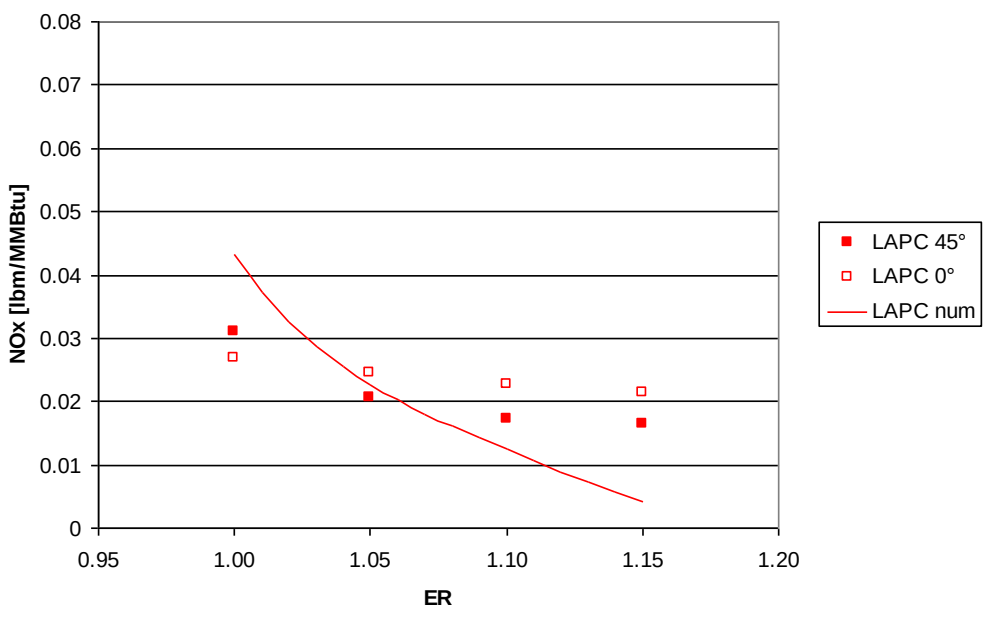

Figure 7.5.13 Comparison with experimental data LAPC, vitiated air

In both cases (pure air and vitiated air) there is a good agreement between the experimental data and the numerical solution, which lends some credence to the present NO_x model. The model predicts the dependence of NO_x reduction on the ER and on the presence of vitiated air.

- NO data

The NO and O_2 concentrations along the furnace are plotted when reburn gas is pure air, in order to gain a better understanding of the process (see Figure V.31).

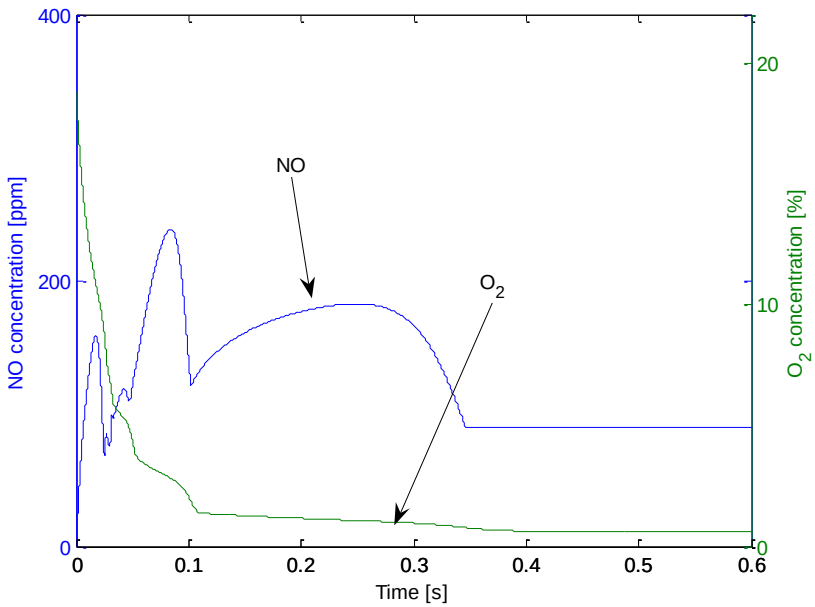

Fig.7.5.14. NO and oxygen concentration along the furnace, LAPC, pure air, ER = 1

The NO concentration raises very quickly during the initial period, mainly due to the mixing of gases from the main burner which contains much NO and, partly due to the reactions of the FN that in this very first part might tend to produce NO instead of destroying it (this will be verified later). With increase in time, a sharp decrease in NO concentration occurs when some FN is released by a size group. The concentration increases again due to the contribution from the main burner gases. It is interesting to note that at the same time the oxygen concentration is rapidly decreasing and this is important in making the NO reduction even more effective; in this case, the ER is set at 1, so at the end of the process there should be no oxygen left. Actually there is a small fraction of oxygen left as it was shown that not all the fixed carbon is consumed.

The effect of ER on the NO concentration along the furnace is shown in Figure V.32 for pure and vitiated air.

The NO concentration for the case of vitiated air is lower than the case of regular air simply because there is the dilution effect due to a larger amount of carrier gas; Figure V.29 and V.30 have shown that the use of vitiated air does not lead to any significant improvement on the NO reduction. The shape of all the curves is somehow similar, characterized by the NO reduction when the FN is being released by a size group. The main difference between the stoichiometric and rich mixture cases is that the NO reductions due to the FN coming from the large particles (therefore reductions to take place at later times) are larger in the case of rich mixture because in the case of rich mixture there is less oxygen and so it goes down to very small concentration faster.

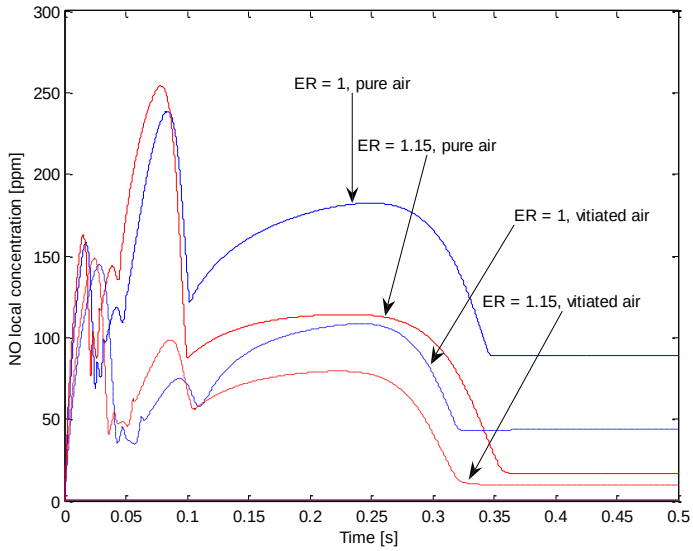

Figure 7.5.15 Comparison of NO concentration along the furnace, pure and vitiated air, LAPC

It is useful to study the rate of the reactions for different reactions outlined in chapter IV that affect the NO_x chemistry in order to gain a better understanding of the NO_x reduction process.

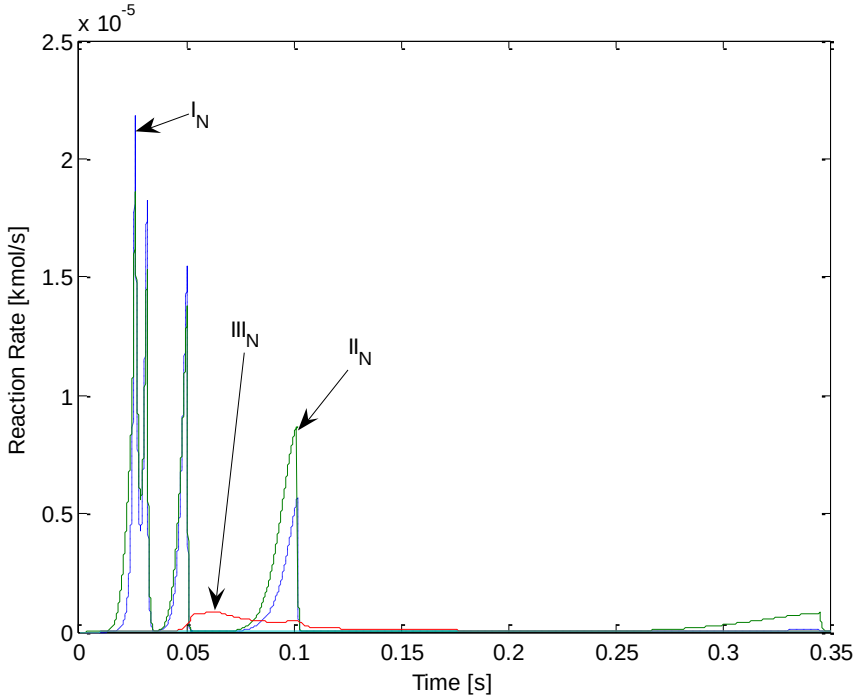

Figure 7.5.16 Reaction rate involving NO, LAPC, pure air, ER = 1

Figure V.33 shows the relative importance of the reactions: at the temperatures and conditions used in these experiments, the ammonia reactions are much more important than the reactions regarding HCN. The ammonia content in biomass is roughly the double of the HCN content, but ammonia reaction rates are much higher than double that of HCN. Thus reduction of the NO is driven by the presence of ammonia in the FN volatiles.

This plot explains the shape of the curve of the NO concentration in Figure V.31. Initially there is still much oxygen in the gas phase, therefore when the FN is released it tends to react through oxidation reaction I_N producing more NO. It is seen from Figure V.33 there exist three spikes reaction I_N which are faster than reaction II_N. After one tenth of a second the concentration of oxygen has decreased to a low value; so NO reduction reaction II_N becomes faster than I_N and so NO is being reduced. Also around 0.35s, when the largest size group releases FN, reaction II_N is dominant and at this point the oxygen concentration has become so low that oxidation reaction I_N is negligible. Among the reactions regarding HCN, the IV_N is absolutely negligible under these conditions. Reaction III_N, by which HCN reacts with oxygen to create NO, is present but its importance is not comparable with the ammonia reactions and as the oxygen is depleted the reactions becomes even slower.

7.5.3. Fuel Nitrogen emission modeling

The release of the fuel bound nitrogen is a very important part of the reburn process; therefore it is worth studying how different models would have affected the results. The base case that was chosen was to model the FN release from biomass as proportional to the pyrolysis, since no kinetic data for FN release from biomass was available from the literature. For the purpose of this study the base case for

biomass is compared with those results with kinetics scheme similar to those of coal. Note that these kinetics have been developed for coal, so their applicability to biomass is questionable [29, 49, 57].

Figure V.76 shows the NO emissions for the various cases of release of FN.

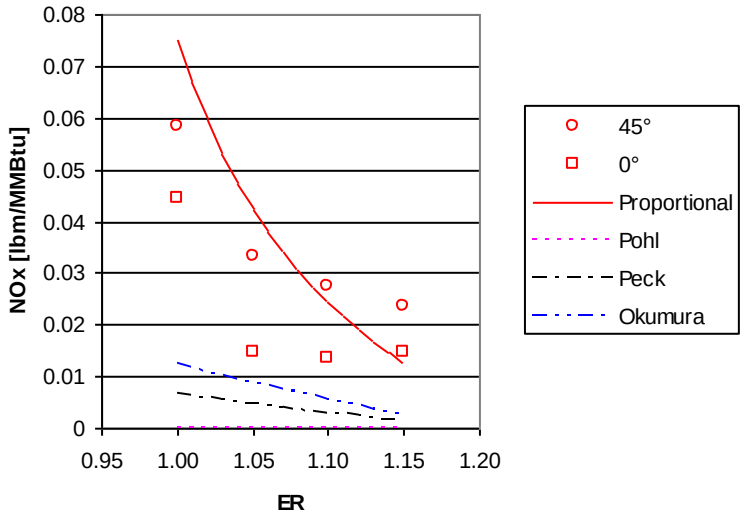

Figure 7.5.17 Effect of different FN models

Figure reveals that the assumption of having the FN to be released in proportion to the pyrolysis leads to better comparison with experimental data. The assumption of kinetics similar to coal leads to an overestimate of the NO reduction. This is expected as these kinetics have been formulated for coal, in which case nitrogen has strong bonds with the char structure; therefore the FN is released later than the pyrolysis; so when the N is released, the oxygen concentration in the gas phase is lower, leading to a more effective NO reduction.

Consider Texas Lignite. For the base case, it is assumed to model the FN release using dedicated kinetics by Peck (Peck R.E.,et al,1982), which was developed for coal. It is interesting now to compare these results with the results that it would have been possible to get using other kinetics (Pohl (Pohl J.H., et al,1976), Okumura (Okamura Y., et al,2002)) or by assuming the FN to be emitted along with the volatiles (Karamba S,et al,1993). Figure below shows the comparison.

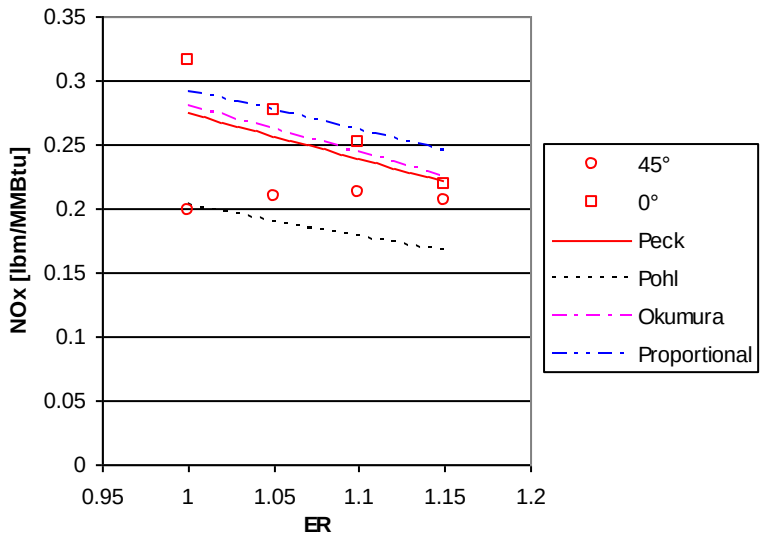

Figure 7.5.18 Effect of different FN emission model, Texas Lignite

It is seen that the kinetics by Peck leads to better comparison with the experimental data. Still in this case also the other models would have performed reasonably well. Modeling FN to be released along with the volatiles would have led to an underestimation of the NO reduction because in this case FN would have been released very early when there is still much oxygen in the gas phase.

With this brief analysis, it is shown that the base case choice seems to be the one that best match the experimental results.

7.5.4. NO reaction kinetics

The kinetics parameters for the reactions involving NO are probably the most vital parameters in the whole model, in order to get a good prediction of the NO reduction. Several kinetics data are available from literature, but sometimes their applicability to cases different from the ones in which they were formulated or for different fuels is questionable. Previously it has been said that one of the most used reduced kinetics formulation for this kind of model is the one by De Soete (De Soete G.G.,et al,2001); still this kinetics has not led to good results in the current case, probably because those kinetics were based on data points at temperatures above 2000 K, while in the current experiments the temperature is never above 1600 K. Therefore the kinetics for ammonia were substituted with the ones by Brink (Brink A.,et al,2001), that have been formulated specifically for biomass, and the kinetics for HCN were substituted with the ones by He (He. R.,et al,2004), which are slight corrections on the De Soete's ones, to adapt them for lower temperatures. Figure V.78 compares the NO_x predictions for different NO kinetics from literature adopted for LAPC biomass.

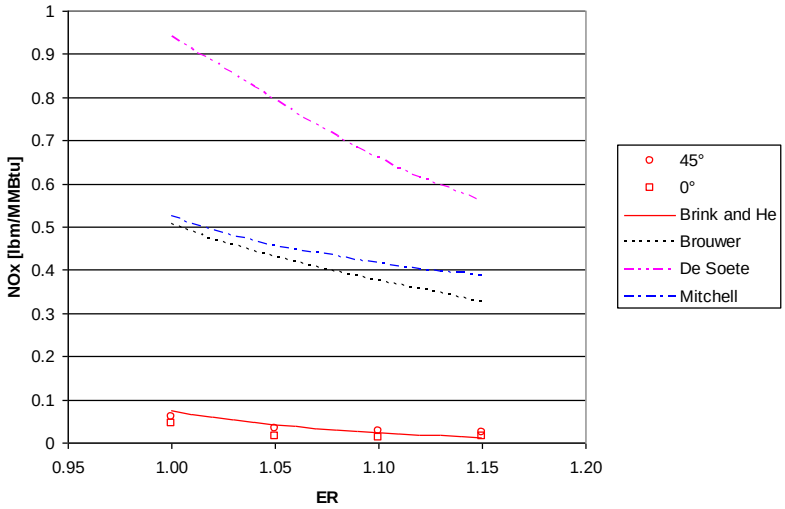

Figure 7.5.19 Effect of different NO kinetics on the results, LAPC biomass

From Figure V.78 it is evident that the choice of the proper NO kinetics is vital in matching with the experimental results. The base case proves to be the one that best matches with the experimental point. De Soete's kinetics leads to the worst results. All the kinetic data predict correct dependency on the ER, but all, except the base case kinetics, fail to lead to results comparable with those from experiments.

Figure V.79 shows the same plot for Texas Lignite; the base case kinetics are the same as used for the LAPC biomass.

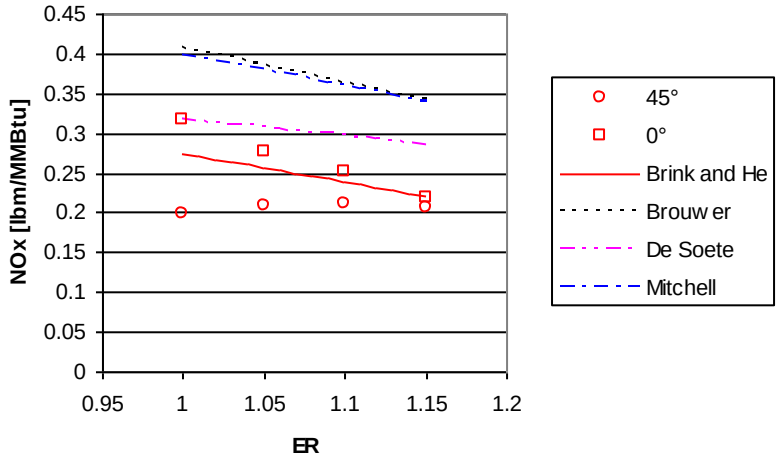

Figure 7.5.20 Effect of different NO kinetics on the results, Texas Lignite

The case for Texas Lignite is very different from the one for biomass; in this case, the base kinetics are still the ones that best match with the experimental results, but now the other kinetics are not so far away from the experimental points.

This is interesting, and it means that the most uncertainties are about the reaction rate for ammonia, as the amount of ammonia and HCN released in the gas stream is what is really different between the two cases: coal and biomass.

The choices of the NO reaction rates are vital in modeling the reburn process, especially when there is a significant amount of ammonia in the gas stream.

7.5.5. Ammonia content

Another parameter that plays an important role in determining the NO reduction is the N based compounds in the volatiles. Coal normally releases significant amount of its FN as HCN and a small fraction as ammonia (Karamba S,et al,1993). The amount of ammonia released depends on the rank of the coal: the higher the rank, the smaller the fraction of ammonia.

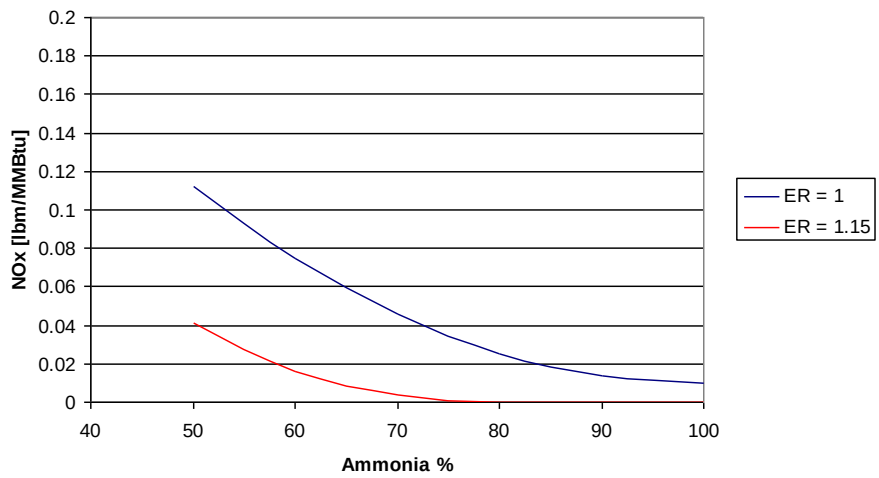

Figure 7.5.21 Effect of ammonia fraction, LAPC biomass

From Figure V.80 it is clear that the ammonia fraction plays an important role in determining the level of NO emission, therefore it is important to know the composition of FN with a good accuracy.

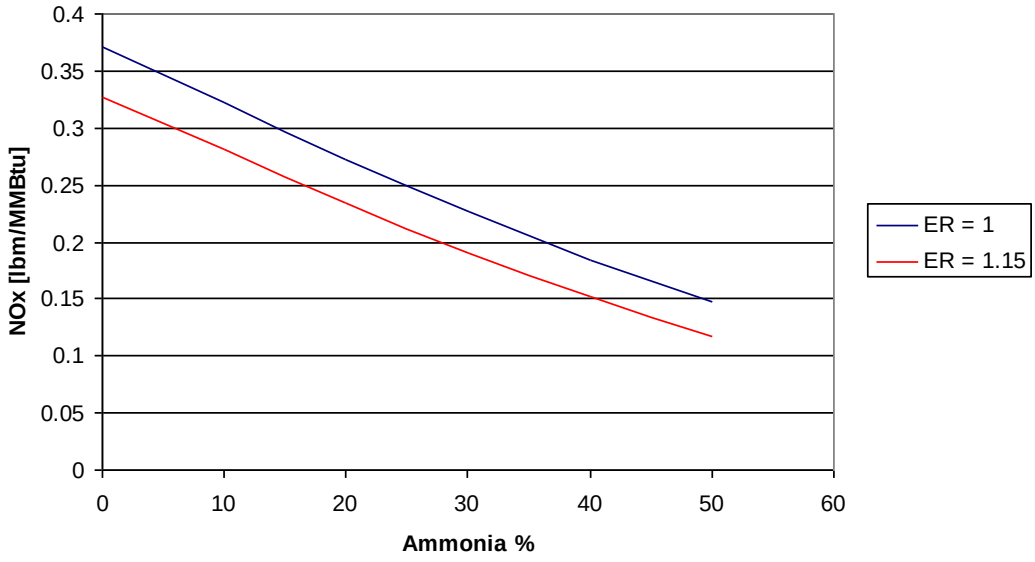

Figure 7.5.22 Effect of ammonia fraction, Texas Lignite, pure air, ER = 1

Also for coal it is evident that the composition of the FN is important in determining the NO emission.

7.5.6. Particle size distribution

Finally it is interesting to evaluate the effect of the particle size distribution on the NO emission: the base case is the one with the real size distribution that divides the particles in five groups.

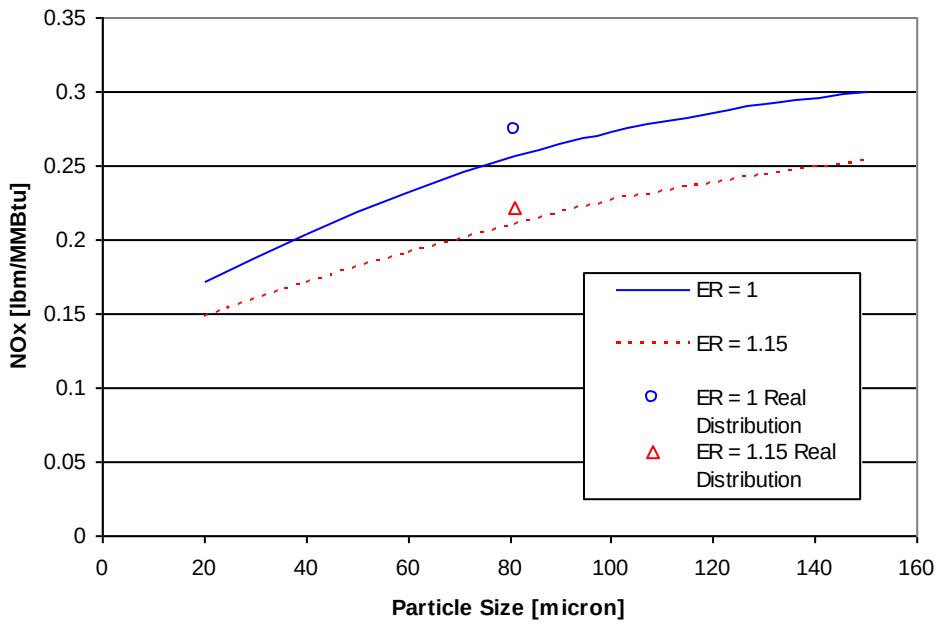

Figure 7.5.23 Effect of SMD or real distribution on NO emission, Texas Lignite

In Figure V.82 two open symbols represent the NO_x obtained from the real distribution and they are placed along the X – axis in correspondence of the SMD value of that distribution. The solid lines represent the NO emission according to the SMD size of that distribution (monosized suspension).

7.5.7. Reburn Thermal Energy

The fraction of thermal energy contributed by the reburner normally lies between 10% and 30% of the total thermal rating of the furnace.

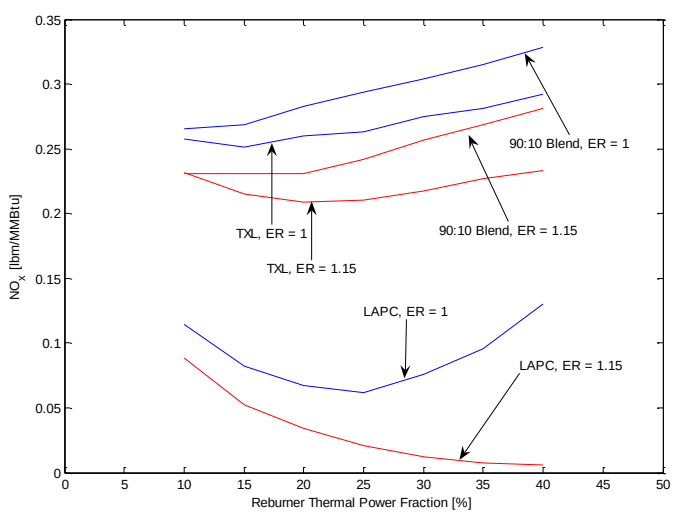

Figure 7.5.24 Effect of reburner thermal power fraction

7.5.8. Reburner Inlet Temperature

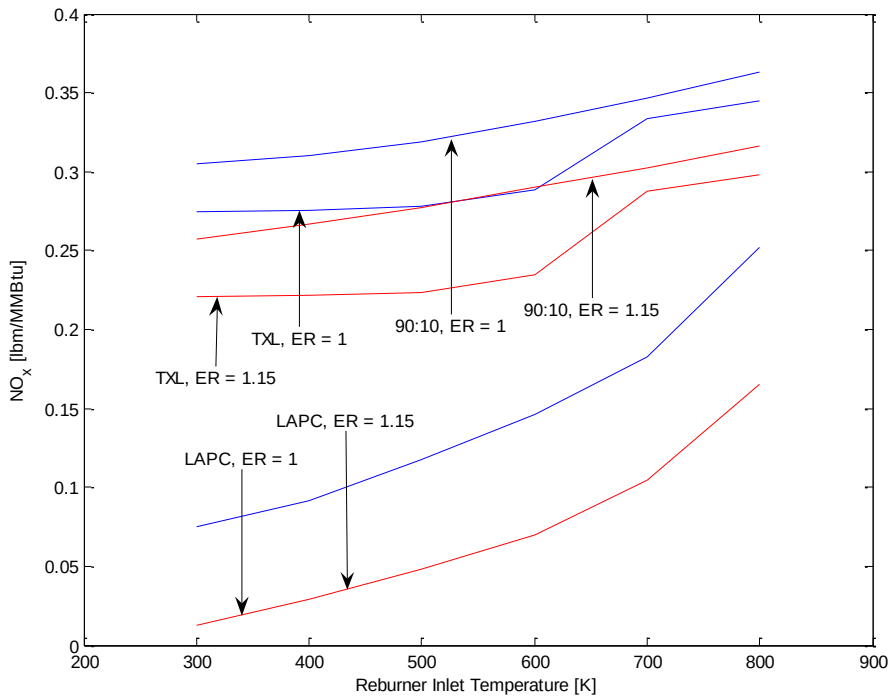

Figure 7.5.25 Effect of the Reburner Inlet Temperature on the NO_x emissions

Figure shows that the inlet temperature affects the NO reduction and in particular the higher the temperature, the larger the NO emission.

7.6. Summary

The model supports the impressive NO_x reduction using pure LAPC biomass as reburn fuel. All the other fuels have led to poorer results and this conclusion can be drawn both from the experiments and from the model. We had performed the zero D reburn models. Though not proposed, we had performed an additional modeling study on "Comparisons of Energy potentials of Gases produced from various Gasification Technologies using Coal and Biomass Fuels,"[Annamalai et al 2007] and an EXCEL based software were developed to predict the results from proximate and ultimate analyses.

The other conclusions are summarized below:

1. LAPC biomass is very effective in the reburn process due to the higher amount of volatiles and the large fraction of ammonia in the fuel nitrogen.
2. The accuracy of the model is strongly dependent on the selection of kinetics applicable to the present condition.
3. The model has confirmed that higher equivalence ratios (richer mixture) reduce NO_x levels to a greater extent than lower equivalence ratios (leaner mixture).
4. The model has also confirmed that the use of finer ground fuel can lead to better NO_x reduction.

5. Blends present NO_x reduction levels somewhere between the performance of pure coal and LAPC biomass, but in general closer to coal than to biomass.
6. Some parameters such as the reburn thermal fraction might be optimized to improve the performance of the system.
7. The use of vitiated air, in this case, does not lead to significant improvements.
8. Increase of ER from 1 to 1.1 results in reduction of NOx from 0.07 lbm/MMBtu to 0.02 lbm/MMBtu for LAPC biomass and from 0.27 lbm/MMBtu to 0.24 lbm/MMBtu for Texas Lignite, with pure air.
9. When SMD is decreased from 80μm to 40μm at ER = 1, for Texas Lignite, NOx decreased from 0.27 lbm/MMBtu to 0.2 lbm/MMBtu.

7.7. Acronyms

LAPC	Low ash partially composted biomass
HHV	Higher heating value
SMD	Sauter mean diameter
FN	Fuel nitrogen
CO	Carbon monoxide
H_2O	Water
O_2	Oxygen
NO	Nitrous oxide
NH_3	Ammonia
HCN	Hydrogen cyanide
H_2	Hydrogen
Φ	Equivalence ratio
VM	Volatile matter
FC	Fixed carbon
Y_i	Mass fraction
X_i	Mole fraction
RZ	Reburn zone
MB	Main Burner

7.8. References

Annamalai K. and Ryan W., Prog. Energy Combust. Sci., 19:383-446, (1993)

Annamalai, K., Udayasarathy Arcot John M. Sweeten and Kevin Heflin, "Comparison Of Energy Potential Of Gases Produced From Various Gasification Technologies Using Coal And Biomass Fuels, " Internal Report , Mechanical Engineering, Texas Engineering Experiment Station, Texas A&M University, College station, TX 77843 , June, 7, 2007

Annamalai K. and Puri I., Combustion Science and Engineering, Florida: Taylor and Francis, 2006

Arumugam S., "Nitrogen Oxides Emission Control Through Reburning with Biomass in Coal-Fired Power Plants", MS Thesis, Texas A&M University, 2004

Brink A., Kilpinen P and Hupa M., Energy & Fuels, 15:1094-1099, (2000)

De Soete G. G., ., in Fifteenth Symposium (International) on Combustion, The Combustion Institute, Pittsburgh, 1975, pp. 1093-1102

Goughnour P. G., "NOx Reduction with the Use of Feedlot Biomass as a Reburn Fuel", MS Thesis, Texas A&M University, 2006

Han D., Mungal M. G., Zamansky V. M. and Tyson T. J., Combustion and Flame, 119 (1999) 483-493

He R., Suda T., Takafuji M., Hirata T. and Sato J., Fuel, 83:1133-1141, (2004)

Howard J. B., Williams G. C. and Fine D. H., in Fourteenth Symposium (International) on Combustion, The Combustion Institute, Pittsburgh, 1973, pp. 975-986

Jones W. P. and Lindstedt R. P., Comb. Flame, 73:233-249, (1988)

Karamba S., Takarada T., Yamamoto Y. and Kato K., Energy & Fuels, 7 (1993) 1013-1020.

Mitchel J. W. and Tarbell J. M., AIChE Journal, 28:302-311, (1982)

Nichols K. M., Hedman P. O. and Smoot D. L., "Release and Reaction of Fuel – Nitrogen in a High Pressure Entrained Coal Gasifier", Western States Section of the Comb. Inst., 1986.

Okumura Y., Sugiyama Y. and Okazaki K., Fuel, 81:2317-2324, (2002).

Peck R. E., Midkiff K. C. and Altenkirch R. A., "Fuel Nitrogen Transformations in one – dimensional Coal Dust Flames", Western States Section of the Combustion Inst., 1982

Pohl J. H. and Sarofim A. F., Sixteenth Symposium (International) on Combustion, The Combustion Institute, Pittsburgh, 1976, pp. 491-501.

Sami M., "Numerical Modeling of Coal – Feedlot Biomass Blend and NOx emission in Swirl Burner", PhD Thesis, Texas A&M University.

Schoeters J. G., "The Fundamentals of Wood Gasification", Proc. of the Symposium on Forest Products Research International – Achievements and the Future, Pretoria, South Africa, Apr. 22-26.

Smoot L. D., Hobbs M. L. and Radulovic P. T., AIChE Journal, 38:681-702, (1992).

Smoot L. D. and Smith P. J., Coal Combustion and Gasification, Plenum Press, New York, 1985

Smoot L. D., Hill S. C. and Xu H., Prog. Energy Combust. Sci., 24 (1998) 385-408

Van der Vaart D. R., Ind. Eng. Chem. Res., 31:999-1007, (1992).

Wojtowicz M. A., Miknis F. P., Grimes R. W. Smith W. W. and Serio M. A., Journal of Hazardous Materials, 9 (2000) 74-81.

Yang Y. B., Hampartsoumian E. and Gibbs B. M., Twenty-Seventh Symposium (International) on Combustion, The Combustion Institute, 1998, 3009-3017.

Yoon H., Wei J. and Denn M. M., AIChE Journal, 24:885-903, (1978).

Zamansky V. M., Maly P. M., Sheldon M. S., Moyeda D., Gardiner W. C. and Lissianski V. V., Second generation Advanced Reburning for High Efficiency NOx Control, DOE, Quarterly Report No. 6 for period January 1 – March 31, 1997.

Zamansky V. M., Sheldon M. S. and Maly P. M., Twenty-Seventh Symposium (International) on Combustion, The Combustion Institute, 1998, 3001-3008.

Zhou J., Masutani S. M., Ishimura D. M., Turn S. Q. and Kinoshita C., Ind. Eng. Chem. Res, 39 (2000) 626-634

7.9. Education and Training

Giacomo Colmegna, Masters, "MODELING OF THE REBURN PROCESS WITH THE USE OF FEEDLOT BIOMASS AS A REBURN FUEL" May 2007.

7.10. Other support

None

7.11. Publications

None

8. DIRECT COMBUSTION

TASK A-8: Exploratory Overall Energy Conversion Studies

Abstract

Manure-based biomass (MBB) has the potential to be a source of green energy at large coal-fired power plants and on smaller-scale combustion systems at or near confined animal feeding operations. Although MBB is a low quality fuel with an inferior heat value compared to coal and other fossil fuels, the concentration of it at large animal feeding operations can make it a viable source of fuel. A base case run of a mathematical model describing a small-scale, on-the-farm MBB combustion system that can completely incinerate high-moisture (over 90%) manure biomass was developed and completed. If all of the energy or steam produced by the MBB combustion system were to bring revenue to the animal feeding operation either by avoided fueling costs or by sales, the conceptualized MBB combustion system has the potential to be a profitable venture.

8.1. Introduction

The industrialization of American agriculture has come about due to low commodity prices, federal funding, high competition between farmers, and a large fast food industry. Currently, fewer than five million Americans live on farms, and only about half of them keep any farm animals on their land. However, for those who do house dairy cows, beef cattle, hogs, chickens, and other traditional farm animals, the amount of manure produced from the hundreds, sometimes thousands, of animals on the farm is a significant undertaking (Centner, 2004) These Confined Animal Feeding Operations (CAFOs) show the potential for water, soil, and air pollution, yet the concentration of the manure makes this low heat value feedstock a viable source of fuel for combustion and emission control systems either at nearby power plants or in smaller energy conversion systems on or near the farm.

8.2. Literature Review

Review of Designs for Small-scale, On-the-farm Manure-based Biomass Combustion Systems

Manure-based biomass can also be considered a possible feedstock for smaller, on-the-farm combustion systems designed to properly dispose of manure solids and wastewater. Using commercially available equipment like solid separators, augers, and dryers, MBB can be prepared for smaller combustion processes. If these systems are constructed on or near a CAFO, the benefits of reducing tremendous amounts of waste and avoiding potential environmental misfortunes can be realized without much of the transportation and processing costs required to burn cattle biomass in large electric utility boilers.

There have been several patents and design studies of small scale, combustion systems meant to burn manure on or near large animal farms. One such design was the gasification system discussed earlier by Young *et al*. (2003) for dairy manure biomass. The dairy manure is first reduced to about 70% moisture with an auger press and then sent through a high-temperature, entrained-flow air gasification system. A patent by Kolber (2001) was an elaborate design of an energy conversion system that could treat solid and liquid manure from confined animal feeding operations. The motivation of this study was to reduce the need for anaerobic treatment lagoons at large pig farms in North Carolina. The design is illustrated in Figure 8.2.1. Flushed manure wastes from growing buildings enter a waste holding tank, where the manure is either sent to a covered waste processor or held if the rest of the system is backed up. The components of the covered waste processor are shown in Figure 8.2.2. Wastewater is homogenized

and then sent to a solids separator, after which the solids are dried and then burned or gasified in a combustor. The liquid from the separator is treated or deodorized in an ozonation tank, where organic material left in the liquids is oxidized. The liquids are then sent to a flush water reservoir. Air and hot flue gases from the manure combustion are used to dry the separated solids. Any waste gases generated from the other components of the system would also be burned in the combustor.

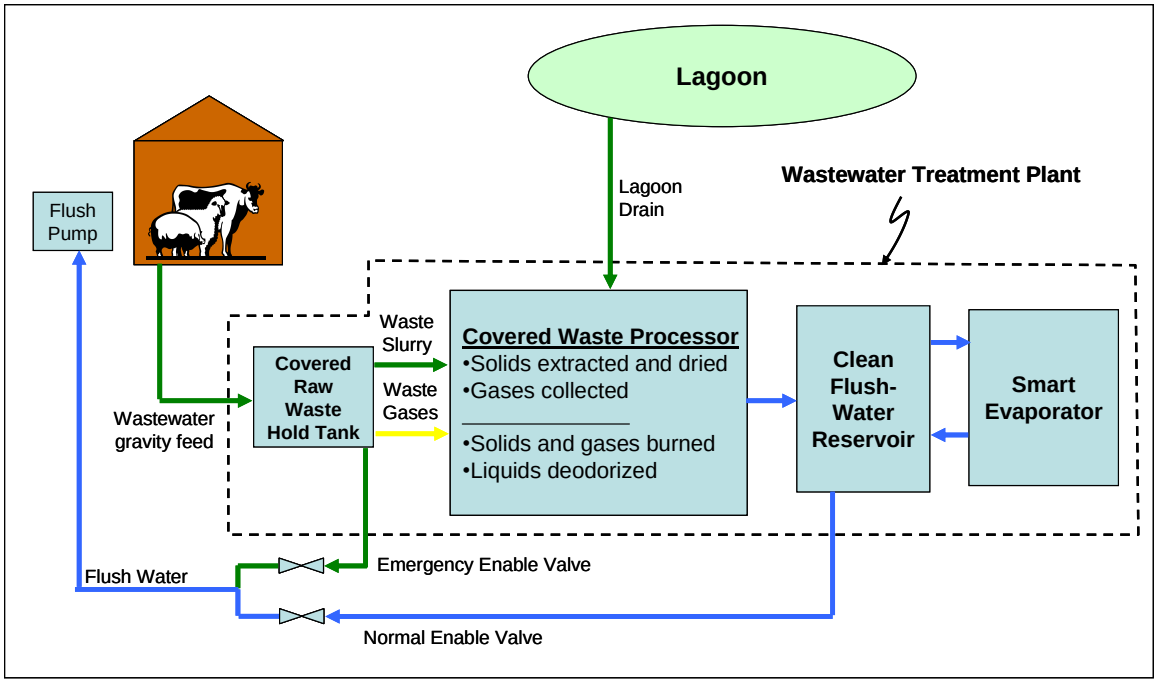

Figure 8.2.1 Design for a wastewater treatment plant for large confined animal feeding operations and drainage of anaerobic treatment lagoons (Kolber, 2001)

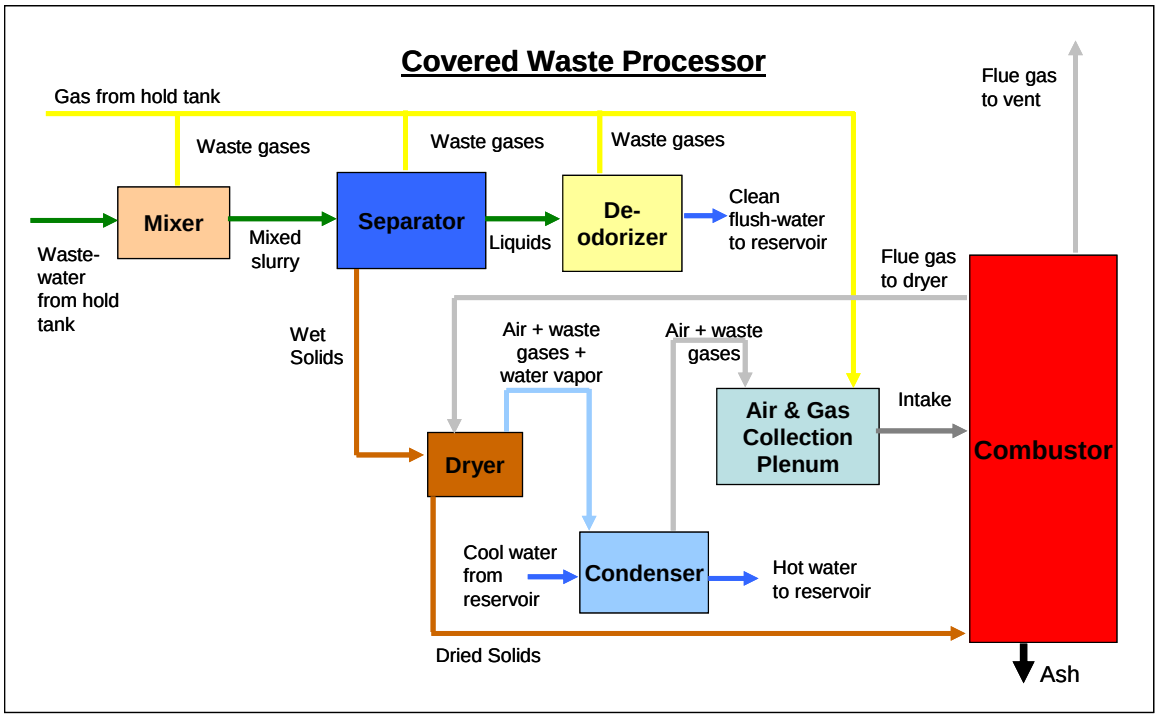

Figure 8.2.2 Components of the covered waste processor in the wastewater treatment plant discussed by Kolber (2001)

A solar drying system, which Kolber called a "Smart Evaporator", would evaporate any wastewater that is not treated in the covered waste processor and keep the system from overflowing. Each of these components, as well as a control system and alternative embodiments, are discussed in greater detail in Kolber's patent.

There is also a prototype system developed by Skill Associates, Inc. called Elimanure™ that can eliminate both the liquid and solids of any animal manure. The system is pictured in Figure 8.2.3. Waste manure up to 95% moisture enters large drying units and is mixed by large augers with hot air. The temperature in the drying units reaches 82 °C (180 °F) and the manure is dried to about 40% moisture. The water vapor is ventilated out of the drying unit, while the 40% moisture solid manure is sent to a thermal gasification boiler where it is burned at 1090 °C (2000 °F). The boiler generates steam which runs turbines to generate electricity. During the first two hours of operation, the system uses propane or some other fuel to start up, but after that, the dried manure can sustain the process. Besides water vapor from the drying process, the only byproduct is a grey powdery ash which contains the inorganic or noncombustible material in the manure. The facility was constructed at an animal farm in Greenleaf, Wisconsin in 2005 (Skill Associates, 2005), which houses 4,000 animal units (dairy cows, horses, and other animals) and produces 1,007 dry kg (2,220 dry lbs) of manure per hour. At this animal farm, the boiler produces 4500 kg (10,000 lb) of steam per hour at 2,000 kPa (300 psi). The turbine is sized to produce 600 kW_e of electricity.

An update of the Elimanure system, installed in Greenleaf, was written in Ag Nutrient Management Magazine (Caldwell, 2008). During early operation of the combustor, Skill Associates assumed that dried manure would burn (gasify) much like sawdust, however, they soon found that the higher ash content of the manure created plugging in the boiler and heat exchangers. Moreover, the ash formed "lava" in the burning bed of the combustor. In July 2008, however, Skill Associates claimed they had solved the ash problem with the combustor by "modify[ing] and improve[ing] the combustor, making it more robust." A "new, larger, and state-of-the-art" combustor replaced the original one. The cost estimates for the system were also updated to $4.5 million initial investment with a 3.5 year payback period. Part of the reason for the quick payback period was the fact that the animal farm originally

produced 94.6 million liters (25 million gallons) of liquid manure per year, which needed to be hauled away from the farm at an annual cost of $400,000. Reducing the liquid manure to just ash greatly reduced the waste disposal cost of the farm.

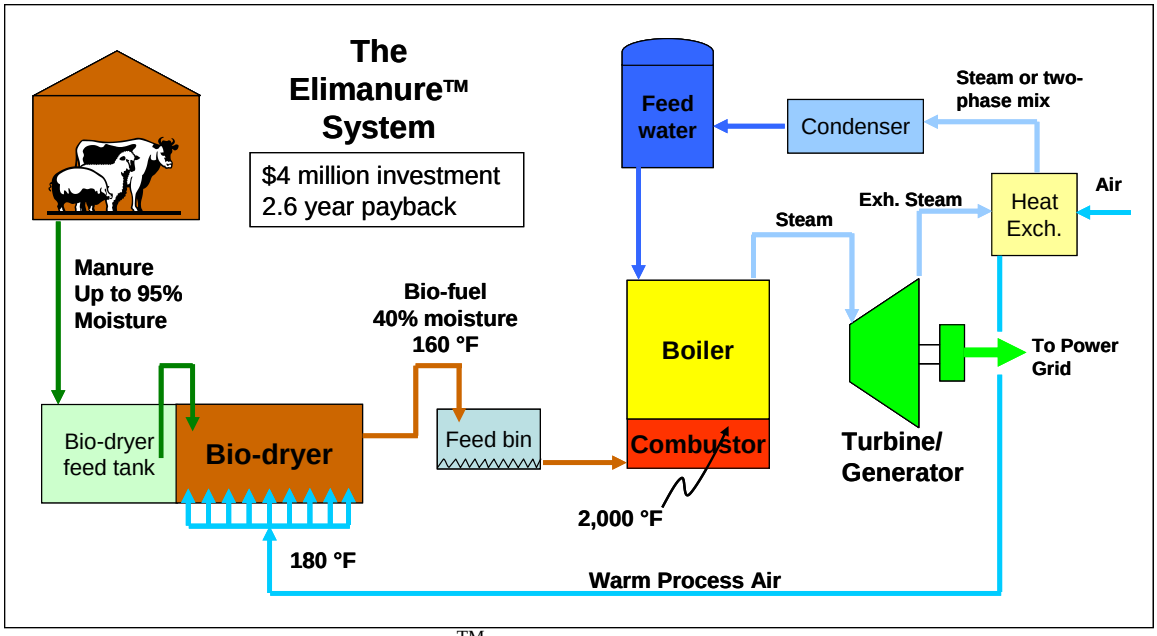

Figure 8.2.3 The Elimanure™ System developed by Skill Associates (2005)

On-the-farm combustion systems were also modeled by Carlin (2005) and Carlin *et al*. (2007a). Thermodynamically, a black box method was utilized to determine the greatest amount of waste that could be converted into the desired end products. This method is shown in Figure 8.2.4, with the inputs and outputs to the system crossing through the control volume (CV) fixed around the combustion system. A complete mass and energy balance of the system was conducted. The ash and moisture percentages were treated as variables in order to determine their required values to convert all material to combustion gases, water vapor, dry ash, and to maintain a desired system temperature (for example, 373 K).

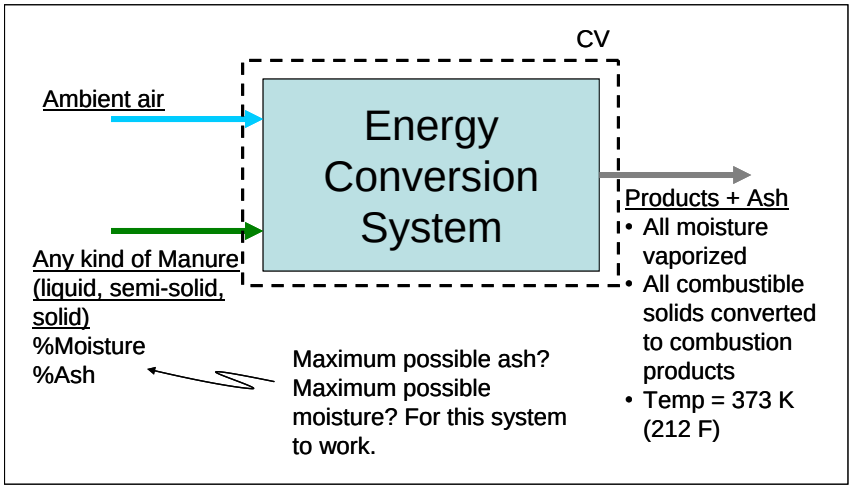

Figure 8.2.4 Black box thermodynamic model of a manure energy conversion system (Carlin, 2005)

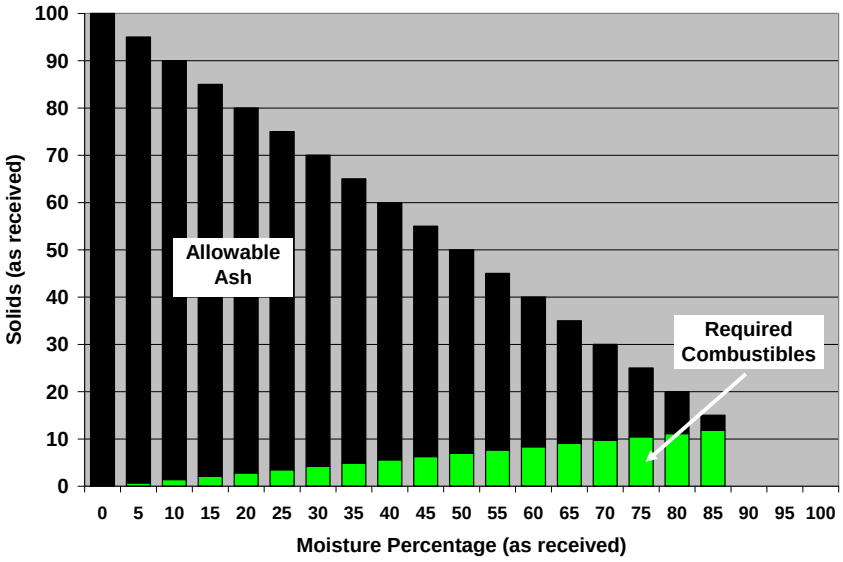

Figure 8.2.5 Required manure biomass solids composition needed to completely convert manure waste to combustion gases, water vapor, dry ash, and to maintain a desired system temperature of 373 K (Carlin, 2005)

Figure 8.2.5 displays the results of the black box methodology. According to the figure, if the flushed manure emanating from a dairy or feedlot has a moisture percentage of more than 85%, then no amount of combustible material in the solids can produce enough heat during combustion to fully vaporize all of the moisture portion (wastewater) of the manure. However, ash also plays a limiting role in the effectiveness of independent manure combustion systems. Depending on the manure collection process, the bedding used in the dairy free stalls, or the pavement surfacing of the feed yards and open lots, the ash content of the solid manure material can make direct combustion impossible due to fowling and inadequate fuel heating value.

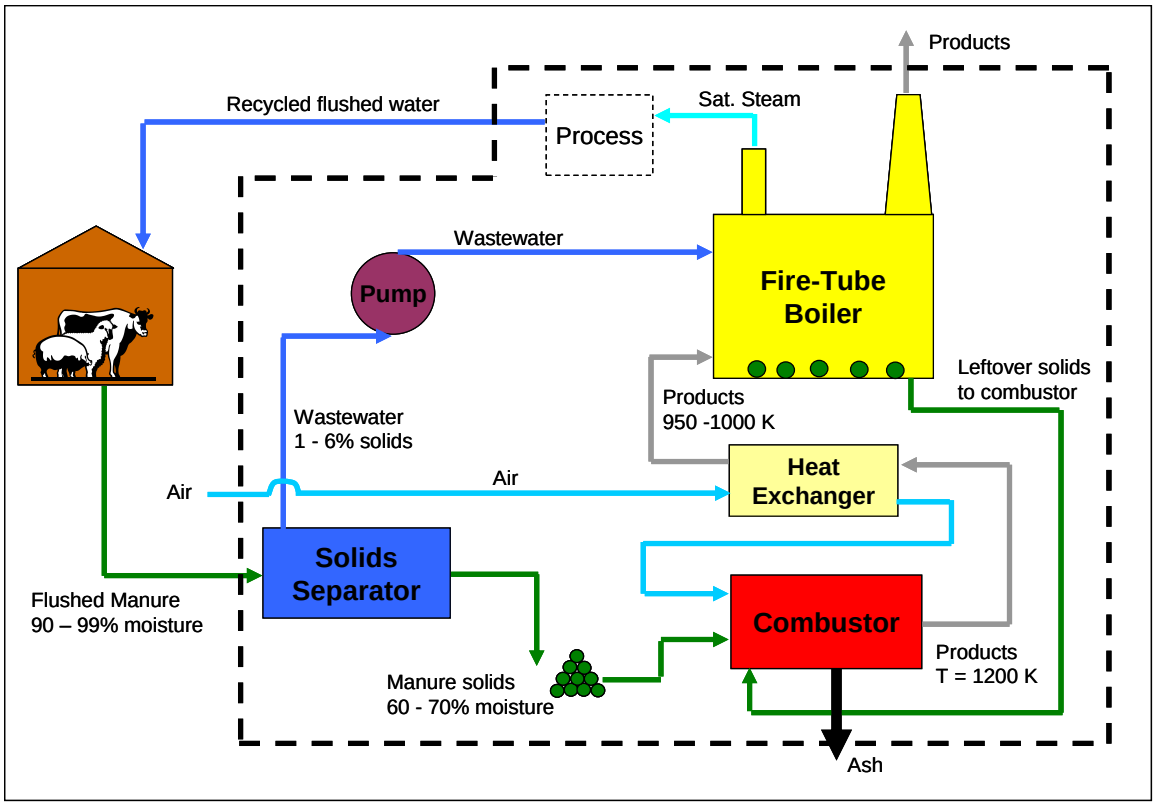

Figure 8.2.6 Conceptualized model for manure biomass thermo-chemical energy conversion system for a CAFO (Carlin, 2005)

The conceptualized system shown in Figure 8.2.6 has the potential to burn most of the manure solids and vaporize at least a portion of the wastewater stream. Again, the flushed manure is mechanically separated into solid and liquid streams. The solids are injected into a combustor, furnace, or perhaps a gasifier with a subsequent product gas burner. The combustion air is preheated in a heat exchanger by the hot products of combustion. Meanwhile, some of the remaining wastewater is sent to a fire-tube boiler where it is sprayed onto heat pipes containing the combustion gases. The remaining solids from the wastewater can be removed periodically from the boiler (similar to blow down in conventional fire-tube boilers) and either sent back to the combustor or used as fertilizer.

This system was modeled by Carlin (2005) and Carlin *et al*. (2007a). Carlin *et al.* (2007b) added the effects of combustion air pre-heating. The steam could be used as a general heat commodity for the farm or it can be used to dry the manure solids. Figure 8.2.7 shows some of the results of the modeling of the system in Figure 8.2.6. Here, the waste disposal percentage is defined as the heat released by the combustion process, divided by the heat required to evaporate all of the manure wastewater. Waste disposal was plotted against the added amount of fuel injected into the combustor. Methane, coal and addition composted manure solids were all modeled. As can be seen, if no additional fuel is used, then the combustion process only releases about 32% of the heat required to incinerate the manure wastes. From this plot it can be seen how much additional fuel would be required to eliminate all of the manure wastes.

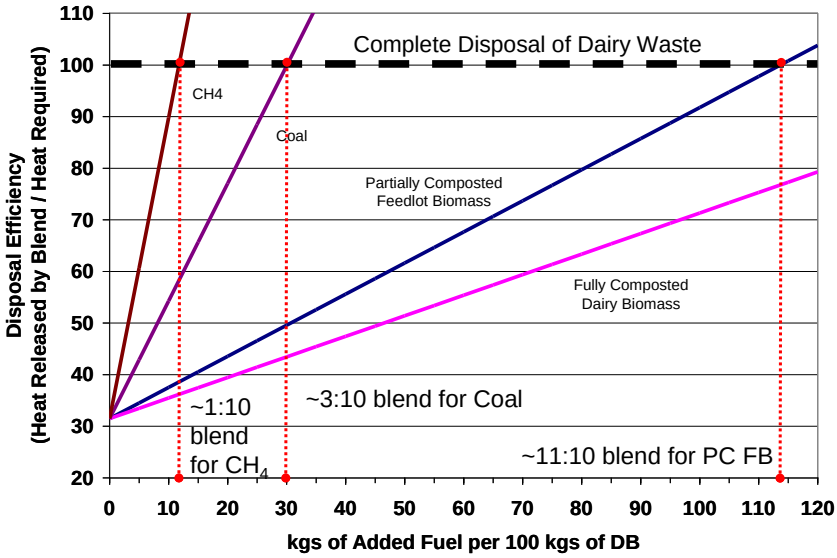

Figure 8.2.7 Waste disposal efficiency of conceptualized manure biomass energy conversion system vs. mass of additional fuel used for combustion (Carlin, 2005)

In addition to the combustor, one of the main design challenges of the conceptualized system in Figure 8.2.6 is the fire-tube boiler. There are numerous designs for wastewater evaporators such as the patented design by Gregory (1993). These evaporation tanks can handle most sludge and liquid waste streams. Kamen *et al*. (2008) patented a locally powered water distillation system for converting any wastewater, even raw sewage, to clean, potable water. The inspiration for this invention was the lack of available clean water to millions of people in developing countries in Southeast Asia, the Middle East, and Africa. The pressure vapor cycle liquid distillation system is about the size of a residential washing machine and designed to provide enough water for a family or small rural village. The design is meant to be relatively affordable for governments and individuals of third world countries, about $1,000 to $2,000 each when mass production is established. The distillation system was designed to be powered locally with easily obtainable fuels, such as "cow dung" (Schonfeld, 2006). Such a system may be scaled-up in size to handle the larger amount of wastewater from a CAFO.

For most of the energy conversion systems discussed in this section, designers assumed that high temperature gasification would be the most appropriate means by which the manure solids would be burned. However, there are some claims to directly firing manure solids such as a patent for a moving grate combustor by Mooney *et al*. (2005). See Figure 8.2.8. However, most of these systems are essentially two-stage gasification systems in which the released volatile gases are immediately fired, in this case, by a natural gas pilot burner. In this sense, these systems become co-firing furnaces, only now the manure is the primary fuel and the fossil fuel is an igniter.

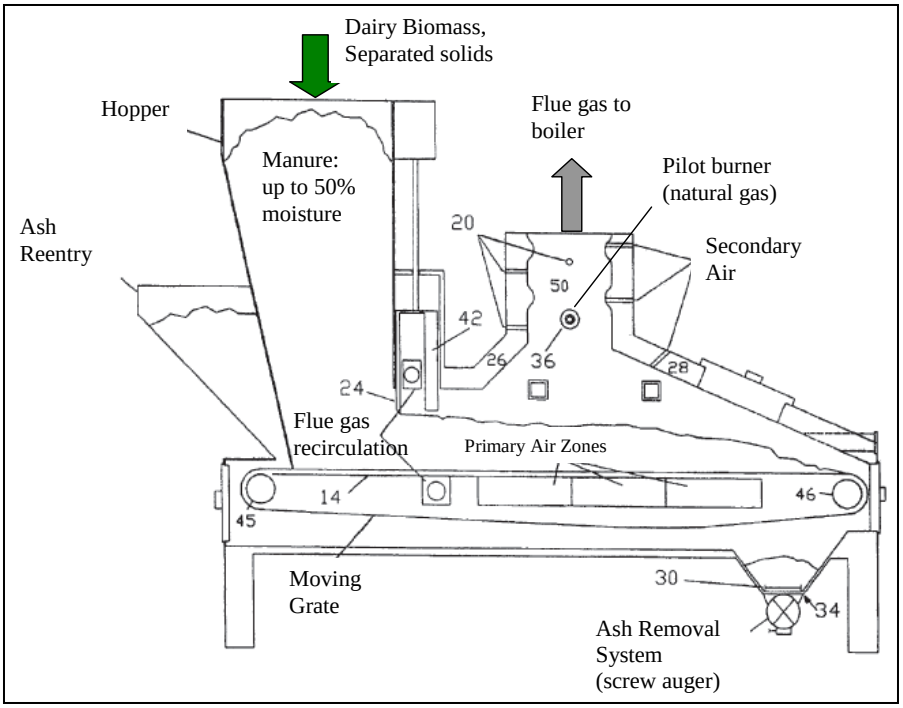

Figure 8.2.8 Schematic of a moving grate manure biomass combustor (adapted from Mooney *et al*., 2005)

On-the-farm MBB gasification systems might also solve many of the economic and practical issues with reburning and co-firing on larger coal-fired power plants discussed earlier. For example, synthesis gas from MBB gasification may be a viable and effective reburn fuel itself. Synthesis gas can be piped to the power plant from CAFOs or centralized gasification facilities, instead of hauled by truck. Plus, no additional ash loading would be incurred by the coal plant. Moreover, reburning with gas requires significantly less capital costs compared to solid fuel reburning systems; although, the capital cost of constructing enough gasifiers to supply a suitable amount of synthetic gas to the coal plant must be taken into account. Studies by Rudiger *et al*. (1996) and Rudiger *et al*. (1997) investigated the fuel nitrogen content in pyrolysis gases from both coal and wood and grass-based biomass that could possibly be used as reburn fuel. Future investigation into the nitrogen content and reburn effectiveness of pyrolysis gases from MBB should also be undertaken.

8.3. Objectives

A. Investigate and suggest values for design parameters of heat exchangers, biomass dryers, combustors, and boilers, so that future experimentation and pilot-tests may be conducted.

B. Estimate economic costs of installing and operating a MBB combustion system on an animal feeding operation (either solid fuel burners or gasifiers with subsequent producer gas firing). Determine if on-site combustion of biomass would provide any long term financial benefits to the animal feeding operation owners.

C. Compare the viability of burning MBB on smaller scale, on-the-farm combustion systems to the possibility of burning in larger scale reburn or co-fired system on existing coal-fired power plants.

8.4. Experiential Procedure

8.4.1. Modeling Small-Scale, On-the-farm Manure-Based Biomass Combustion Systems

Manure-based biomass may also be utilized on smaller scale combustion systems located on or very near large animal feeding operations. The primary purpose of these combustion systems would be to incinerate manure wastes not used for fertilizer, compost, or other external purposes. These systems would be particularly useful in situations were few application fields or crop lands exist near the feeding operation or when there are local environmental laws or mandates that restrict the size of manure storage structures such as anaerobic treatment lagoons. Combustion systems can also alleviate odor problems on large animal feeding operations.

There have been several designs, and even at least one demonstration system, for local thermo-chemical conversion of MBB. In these systems, there have been several common aspects such as: (1) the separation of high moisture manure streams into a solid manure portion and a liquid wastewater portion, (2) aggressive usage of waste heat, (3) drying of high moisture solids, and (4) the recycling of wastewater. In addition to previous work conducted by Carlin (2005) and Carlin *et al*. (2007), these facets can be added to form a revised conceptual design that is inclusive of most of these aspects. Although most of the discussion here will center on the disposal of high moisture MBB, simpler systems with much of the same design characteristics can also be designed to handle lower moisture solid MBB from feedlots, large corrals, and open lot dairies.

8.4.2. Combustion System for High Moisture Manure-based Biomass

A revised conceptualized thermo-chemical conversion system for high moisture MBB is shown in Figure 8.4.1. This system, if installed at or near a large animal feeding operation, has the potential to burn most of the manure solids and vaporize at least a portion of the wastewater generated from the feeding operation. The flushed manure can be mechanically separated into solid and liquid streams. The solids can then be dried, in this case using an indirect rotary steam-tube dryer, which was discussed earlier. The dried solids can then be injected into a combustor, which can be a solid fuel burner but probably would have to be a gasifier-burner system due to ash fouling. However, the mass and energy balances for both these systems are equivalent The combustion air may be preheated before it is injected along with the manure solids. Meanwhile, some of the wastewater from the solids separator may be sent back to the animal housing units for further flushing or to storage or treatment lagoons for later irrigation or fertilizer uses. The rest of the wastewater would be pumped to a fire-tube boiler where it can be vaporized by heat pipes containing the hot gaseous products of combustion. The remaining solids that were contained in the vaporized wastewater can be removed periodically from the boiler (similar to blow down in conventional fire-tube boilers) and either sent back to the combustor or used as fertilizer. The steam produced in the fire-tube boiler can be used for drying solids, preheating combustion air, or for external uses such as hot water generation for milking center cleanup, space heating at feeding operations located in northern states, production of cattle feed in steam flaking mills, or any other process on or near the farm that may require steam and make the combustion system profitable.

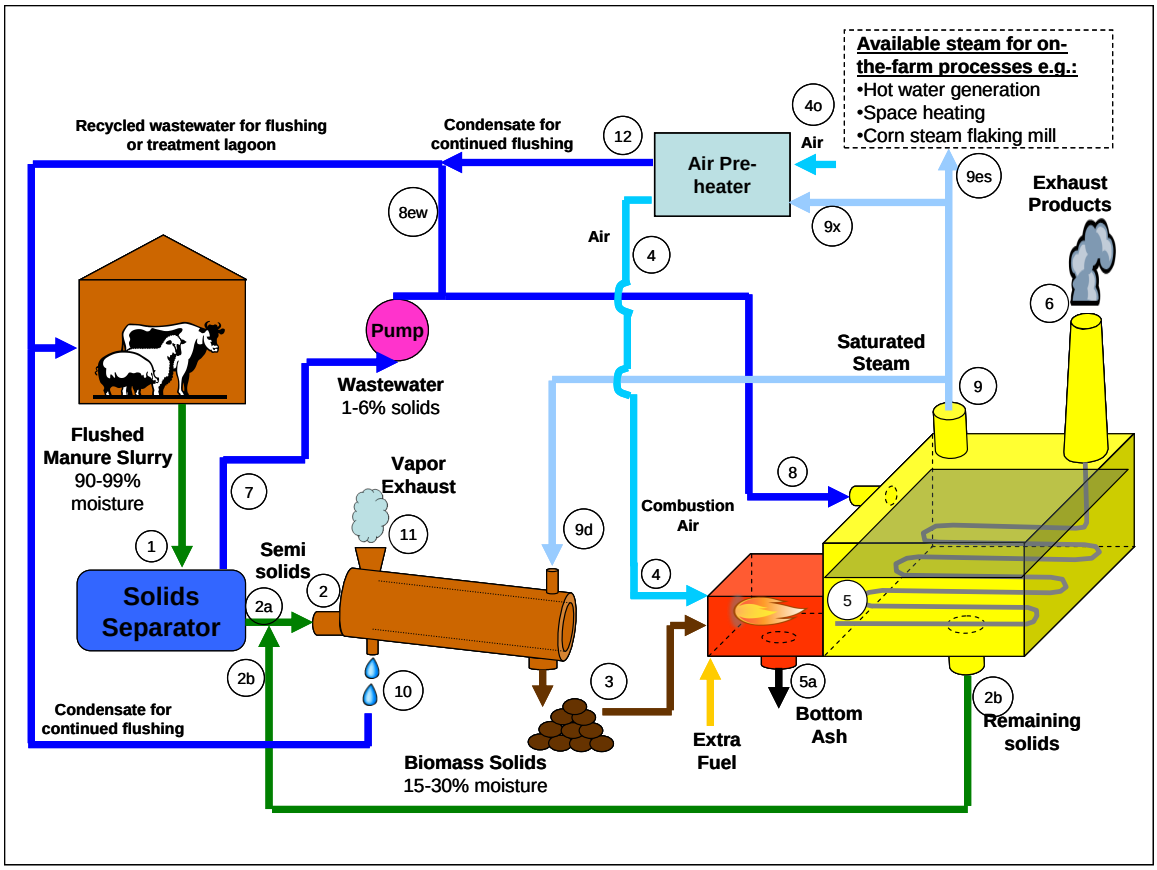

Figure 8.4.1 Conceptualized design of MBB thermo-chemical energy conversion system for large free stall dairies or large indoor piggeries with flush waste disposal systems

The generalized equations presented earlier for drying and burning biomass can be applied to this system, but the mass and energy balances can become complicated. Moreover, if extra fuel is added to the combustor, the analysis becomes slightly more complicated.

The analysis of this system can begin with a mass balance about the solids separator. It is important to remember that the MBB flows at points 1, 2a, and 7 in Figure 8.4.1 all contain solid and moisture fractions. The solid separator will probably not remove all of the solids from the flushed manure. The mass balance of dry solids entering and exiting the separator can be expressed as the following:

$$\dot{m}_{MBB,dry,1} = \dot{m}_{MBB,dry,7} + \dot{m}_{MBB,dry,2a} \qquad (8.2.1)$$

where $\dot{m}_{MBB,dry,1}$ is the flow rate of dry biomass entering the solid separator, $\dot{m}_{MBB,dry,7}$ is the relatively small amount of biomass solids remaining in the wastewater exiting the solids separator, and $\dot{m}_{MBB,dry,2a}$ is the dry fraction of the separated solids. But each of these points also has a moisture fraction. The flow of moisture in and out of the separator can be expressed as:

$$\dot{m}_{MBB,dry,1}\omega_{MBB,1} = \dot{m}_{MBB,dry,7}\omega_{MBB,7} + \dot{m}_{MBB,dry,2a}\omega_{MBB,2a} \qquad (8.2.2)$$

where $\omega_{MBB,i}$ is the moisture content of the MBB in each point, i. Also note that:

$$\dot{m}_{MBB,i} = \dot{m}_{MBB,dry,i}\left(1+\omega_{MBB,i}\right)$$
$$= \dot{m}_{MBB,dry,i}\left(\frac{1}{1-\%M_i/100}\right) \tag{8.2.3}$$
$$= \dot{m}_{MBB,DAF,i}\left(\frac{1}{1-\%A_{dry,i}/100}\right)\left(\frac{1}{1-\%M_i/100}\right)$$

Usually, $\dot{m}_{MBB,dry,1}$ and $\omega_{MBB,1}$ will be known from fuel analyses and knowledge of the number of animals on the farm or how much liquid manure must be incinerated. Moreover, $\omega_{MBB,2a}$ and $\omega_{MBB,7}$ will be known from design specifications of the solids separator.

The remaining unknowns, $\dot{m}_{MBB,dry,2a}$ and $\dot{m}_{MBB,dry,7}$, may be found by combining equations (8.2.1) and (8.2.2):

$$\dot{m}_{MBB,dry,2a} = \dot{m}_{MBB,dry,1}\left(\frac{\omega_{MBB,7}-\omega_{MBB,1}}{\omega_{MBB,7}-\omega_{MBB,2a}}\right) \tag{8.2.4}$$

$\dot{m}_{MBB,dry,7}$ is simply the difference between $\dot{m}_{MBB,dry,1}$ and $\dot{m}_{MBB,dry,2a}$.

Now, the prime mover for this system is the combustor. In order to determine how much wastewater can be vaporized, it is necessary to know how much heat is released during combustion, but the tools for these computations have already been discussed. The only exception might be for cases in which additional fuel such as propane, coal, or additional composted biomass is used. For this case, the same concept that was discussed for co-firing in large coal plants in can be utilized. Namely, equations (8.2.1) through (8.2.4) will be based on the combined blend of the two fuels:

$$\begin{aligned}
\%M_{blend} &= \left(1-mf_{EF}\right)\%M_{MBB} + mf_{EF}\%M_{EF} \\
\%A_{blend} &= \left(1-mf_{EF}\right)\%A_{MBB} + mf_{EF}\%A_{EF} \\
C_{blend} &= \left(1-mf_{EF}\right)C_{MBB} + mf_{EF}C_{EF} \\
H_{blend} &= \cdots \\
N_{blend} &= \cdots \\
O_{blend} &= \cdots \\
S_{blend} &= \cdots \\
HHV_{blend} &= \cdots
\end{aligned} \tag{8.2.5}$$

Here, mf_{EF} is defined as:

$$mf_{EF} = \frac{\dot{m}_{EF}}{\dot{m}_{fuel}} \tag{8.2.6}$$

where, $\dot{m}_{EF}$ is the mass flow rate of extra fuel and $\dot{m}_{fuel}$ is the total amount fuel consumed by the combustor.

$$\dot{m}_{fuel} = \dot{m}_{MBB,3} + \dot{m}_{EF} \tag{8.2.7}$$

It is also important to distinguish time rate flows of mass through the combustion system ($\dot{m}$) as opposed to mass flows per 100 kg of fuel fired (m). This distinction can be described by the following general equation:

$$\dot{m}_{k,i} = m_{k,i} * \dot{m}_{fuel} = N_{k,i} * \frac{MW_k}{100} * \dot{m}_{fuel} \tag{8.2.8}$$

for each species k = O_2, N_2, CO_2, etc. and point in Figure 8.4.1 i = 1, 2a, 2b, 3, etc.

Next, the adiabatic flame temperature, T_5, can be found.

$$
\begin{aligned}
& N_{CO_2,5}\left\{\bar{h}^0_{f,298,CO_2}+\Delta\bar{h}^{T_5}_{t,CO_2}\right\}+N_{H_2O(g),5}\left\{\bar{h}^0_{f,298,H_2O(g)}+\Delta\bar{h}^{T_5}_{t,H_2O(g)}\right\} \\
& +N_{N_2,5}\left\{\Delta\bar{h}^{T_5}_{t,N_2}\right\}+N_{SO_2,5}\left\{\bar{h}^0_{f,298,SO_2}+\Delta\bar{h}^{T_5}_{t,SO_2}\right\}+N_{O_2,5}\left\{\Delta\bar{h}^{T_5}_{t,O_2}\right\} \\
& +m_{ash,5}\left\{c_{p,ash}\left(T_5-298\right)\right\}+m_{ash,5a}\left\{c_{p,ash}\left(T_{5a}-298\right)\right\} \\
& =\left\{HHV_{fuel,DAF}MW_{fuel}+C\bar{h}^0_{f,CO_2}+\frac{H}{2}\bar{h}^0_{f,298,H_2O(l)}+S\bar{h}^0_{f,298,SO_2}\right. \\
& \quad \left.+c_{fuel,DAF}MW_{fuel}\left(T_3-298\right)\right\}+w\left\{\bar{h}^0_{f,298,H_2O(l)}+\bar{c}_{p,H_2O(l)}\left(T_3-298\right)\right\} \\
& \quad +m_{ash,3}\left\{c_{p,ash}\left(T_3-298\right)\right\}+N_{O_2,air,4}\left\{\Delta\bar{h}^{T_4}_{t,O_2}\right\}+N_{N_2,air,4}\left\{\Delta\bar{h}^{T_4}_{t,N_2}\right\} \\
& \quad +N_{H_2O(g),air,4}\left\{\bar{h}^0_{f,298,H_2O(g)}+\Delta\bar{h}^{T_4}_{t,H_2O(g)}\right\}
\end{aligned}
\tag{8.2.9}
$$

This equation must be iterated for T_5. Note that if there is extra fuel added to the combustor, it is simply lumped with the MBB fuel at point 3. Here, the inert solid byproduct of combustion (ash) can be divided into fly ash, which will travel with the other gaseous products of combustion, through point 5, and bottom ash or slag, which will exit the combustor at point 5a. So, if the fly ash percentage of the solid byproduct is $\%FA$, and the total amount of ash produced per 100 kg of fuel fired in the combustor is $m_{ash,3}$, then:

$$m_{ash,5}=\left(\frac{\%FA}{100}\right)m_{ash,3} \tag{8.2.10}$$

$$m_{ash,5a}=\left(1-\frac{\%FA}{100}\right)m_{ash,3} \tag{8.2.11}$$

Next, the heat generated from the combustion, that in turn heats the wastewater entering the boiler to produce steam.

$$
\begin{aligned}
Q_{comb}\left[\frac{kJ}{100\ kg\ as\ rec\ \ fuel}\right]= & \sum_{products,6}N_k\bar{h}_k+m_{ash,6}\left\{c_{p,ash}\left(T_6-298\right)\right\} \\
& +m_{ash,5a}\left\{c_{p,ash}\left(T_{5a}-298\right)\right\} \\
& -N_{fuel,DAF,3}\bar{h}_{fuel,DAF,3}-w\bar{h}_{H_2O(l),fuel,3} \\
& -m_{ash,3}c_{p,ash}\left(T_3-298\right)-\sum_{air,4}N_k\bar{h}_k
\end{aligned}
\tag{8.2.12}
$$

Here T_6 is the stack temperature, which is usually a known design variable, dependant on the operating conditions of the boilers.

Once the quantity of heat transferred to the wastewater is known, the amount of wastewater that can possibly be vaporized in the boiler can be computed. This analysis can begin by isolating the wastewater in the boiler and conducting a mass and energy balance of that system. See Figure 8.4.2.

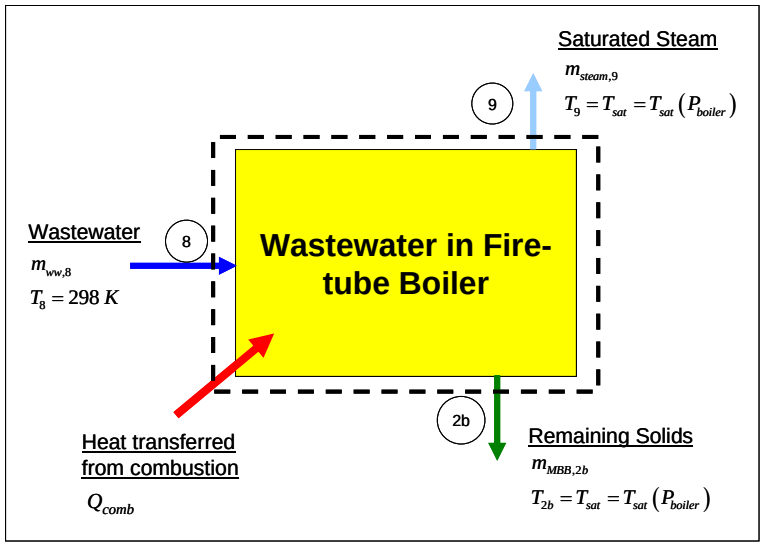

Figure 8.4.2 Mass and energy balance of wastewater in fire-tube boiler

So, the objective of this analysis is to find the amount of wastewater entering the fire-tube boiler per 100 kg of fuel burned in the combustor, $m_{ww,8}$. An energy balance of the wastewater system provides the following.

$$\begin{aligned} &Q_{comb} + m_{MBB,DAF,8}c_{MBB,DAF}T_8 + m_{ash,8}c_{ash}T_8 + m_{H_2O(l),8}c_{H_2O(l)}T_8 \\ &\quad = m_{steam,9}h_{sat,steam}\left(P_{boiler}\right) + m_{MBB,DAF,2b}c_{MBB,DAF}T_{2b} + m_{ash,2b}c_{ash}T_{2b} \\ &\qquad + m_{H_2O(l),2b}c_{H_2O(l)}T_{2b} \end{aligned}$$

Noting that $m_{MBB,DAF,8} = m_{MBB,DAF,2b}$ and that $m_{ash,8} = m_{ash,2b}$

$$\begin{aligned} Q_{comb} &= m_{steam,9}h_{sat,steam} + m_{H_2O(l),2b}c_{H_2O(l)}T_{2b} - m_{H_2O(l),8}c_{H_2O(l)}T_{2b} \\ &\quad + m_{MBB,DAF,8}c_{MBB,DAF}\left(T_{2b} - T_8\right) + m_{ash,8}c_{ash}\left(T_{2b} - T_8\right) \end{aligned} \tag{8.2.13}$$

The ash and moisture percentages at points 8 and 2b are known. The moisture percentage at 2b, which is the remaining amount of moisture in the solids coming out of the boiler in the blow down process, will be considered a design variable dependant on the specifics of the boiler's operation. In equation (8.2.13), $m_{MBB,DAF,8}$, $m_{ash,8}$, $m_{H_2O(l),2b}$, $m_{H_2O(l),8}$, and $m_{steam,9}$, must be expressed in terms of moisture percentage, ash percentage, and one unknown variable, such as $m_{ww,8}$, the flow of wastewater into the boiler per 100 kg of fuel burned in the combustor. The ash and the dry ash free portions of the incoming wastewater can be shown to be:

$$m_{MBB,DAF,8} = m_{MBB,DAF,2b} = \left(1 - \frac{\%A_{dry}}{100}\right)\left(1 - \frac{\%M_8}{100}\right)m_{ww,8} \tag{8.2.14}$$

$$m_{ash,8} = m_{ash,2b} = \left(\frac{\%A_{dry}}{100}\right)\left(1 - \frac{\%M_8}{100}\right)m_{ww,8} \tag{8.2.15}$$

where $\%A_{dry}$ is the ash percentage on a dry basis. The moisture percentage of the wastewater at 2b can be defined as:

$$\frac{\%M_{2b}}{100} \equiv \frac{m_{H_2O(l),2b}}{m_{MBB,DAF,2b} + m_{ash,2b} + m_{H_2O(l),2b}}$$

Inserting equations (8.2.14) and (8.2.15) into this definition provides the following:

$$m_{H_2O(l),2b} = \frac{\%M_{2b}}{\left(100-\%M_{2b}\right)}\left(1-\frac{\%M_8}{100}\right)m_{ww,8} \tag{8.2.16}$$

The moisture percentage of the incoming wastewater is simply:

$$m_{H_2O(l),8} = \frac{\%M_8}{100}m_{ww,8} \tag{8.2.17}$$

The steam production rate is simply the difference between $m_{H_2O(l),8}$ and $m_{H_2O(l),2b}$:

$$m_{steam,9} = \left[\frac{\%M_8}{100} - \frac{\%M_{2b}}{\left(100-\%M_{2b}\right)}\left(1-\frac{\%M_8}{100}\right)\right]m_{ww,8} \tag{8.2.18}$$

Now, inserting equations (8.2.14) through (8.2.18), the ratio of heat produced by the combustion to the amount of wastewater entering the boiler can be solved in terms of the moisture and ash percentages of the wastewater stream and the temperatures.

$$\begin{aligned}\frac{Q_{comb}}{m_{ww,8}} = &\left[\frac{\%M_8}{100} - \frac{\%M_{2b}}{\left(100-\%M_{2b}\right)}\left(1-\frac{\%M_8}{100}\right)\right]h_{sat,steam} \\ &+\left(\frac{\%M_{2b}}{100-\%M_{2b}}\right)\left(1-\frac{\%M_8}{100}\right)c_{H_2O(l)}T_{2b} - \frac{\%M_8}{100}c_{H_2O(l)}T_8 \\ &+\left(1-\frac{\%A_{dry}}{100}\right)\left(1-\frac{\%M_8}{100}\right)c_{MBB,DAF}\left(T_{2b}-T_8\right) \\ &+\left(\frac{\%A_{dry}}{100}\right)\left(1-\frac{\%M_8}{100}\right)c_{ash}\left(T_{2b}-T_8\right)\end{aligned} \tag{8.2.19}$$

Since, Q_{comb} has already been computed, $m_{ww,8}$ can now be found. Subsequently, values can be found for equations (8.2.14) through (8.2.18). However, it is also required to find all of these mass flows on a time rate basis, but since all of the values so far are on a "per 100 kg fired" basis, it is now necessary to compute the time rate of fuel fired in the boiler. The calculation of fueling rate involves a rather complicated mass balance since the burned separated solids, extra fuel, wastewater for the boiler, and steam used to dry the separated solids are all interconnected in the system. The following is an explanation of this mass balance.

Just before the rotary dryer, the separated solids are combined with the remaining solids from the wastewater boiler so that:

$$\dot{m}_{MBB,dry,2a} + \dot{m}_{MBB,dry,2b} = \dot{m}_{MBB,dry,2} \tag{8.2.20}$$

$$\dot{m}_{MBB,dry,2a}\omega_{MBB,2a} + \dot{m}_{MBB,dry,2b}\omega_{MBB,2b} = \dot{m}_{MBB,dry,2}\omega_{MBB,2} \tag{8.2.21}$$

The combined biomass solids will then go through the dryer, where moisture will be removed, but the dry solid fraction will remain the same. That is:

$$\dot{m}_{MBB,dry,2} = \dot{m}_{MBB,dry,3} \tag{8.2.22}$$

On an as received basis, the mass balance through the dryer can be expressed as the following:

$$\dot{m}_{MBB,3} = \dot{m}_{MBB,2} - \dot{m}_{vapor,11} \tag{8.2.23}$$

Inserting expression (8.2.20) for $\dot{m}_{MBB,2}$, along with an expression for the flow of vapor exhaust leaving the dryer, equation (8.2.23) becomes:

$$\dot{m}_{MBB,3} = \dot{m}_{MBB,2a} + \dot{m}_{MBB,2b} - \dot{m}_{MBB,dry,3}\left(\omega_{MBB,2} - \omega_{MBB,3}\right) \tag{8.2.24}$$

Next, inserting this expression for $\dot{m}_{MBB,3}$ into equation (8.2.7) for the total fuel entering the combustor:

$$\dot{m}_{fuel} = \dot{m}_{MBB,2a} + \dot{m}_{MBB,2b} - \dot{m}_{MBB,dry,3}\left(\omega_{MBB,2} - \omega_{MBB,3}\right) + \dot{m}_{EF} \tag{8.2.25}$$

Rearranging this equation:

$$\begin{aligned}\frac{\dot{m}_{MBB,dry,3}\left(\omega_{MBB,2} - \omega_{MBB,3}\right) - \dot{m}_{MBB,2a}}{\dot{m}_{MBB,3} + \dot{m}_{EF}} &= \frac{\dot{m}_{MBB,2b}}{\dot{m}_{fuel}} + \frac{\dot{m}_{EF}}{\dot{m}_{fuel}} - 1 \\ &= m_{MBB,2b} + mf_{EF} - 1\end{aligned} \tag{8.2.26}$$

Before solving for the biomass flow rate at point three, $\omega_{MBB,2}$ and $\dot{m}_{EF}$ must be replaced with known variables. If equations (8.2.20) and (8.2.21) are combined, the following expression for $\omega_{MBB,2}$ can be found:

$$\omega_{MBB,2} = \frac{\dot{m}_{MBB,dry,2a}}{\dot{m}_{MBB,dry,3}}\omega_{MBB,2a} + \omega_{MBB,2b} - \frac{\dot{m}_{MBB,dry,2a}}{\dot{m}_{MBB,dry,3}}\omega_{MBB,2b} \tag{8.2.27}$$

Next, with equations (8.2.7) and (8.2.8) $\dot{m}_{EF}$ can be eliminated by finding the following expression:

$$\dot{m}_{EF} = \frac{mf_{EF}\left(1 + \omega_{MBB,3}\right)}{1 - mf_{EF}}\dot{m}_{MBB,dry,3} \tag{8.2.28}$$

Finally, plugging equations (8.2.27) and (8.2.28) into (8.2.26) and noting that $\dot{m}_{MBB,3} = \dot{m}_{MBB,dry,3}\left(1 + \omega_{MBB,3}\right)$, the following formula for $\dot{m}_{MBB,dry,3}$ can be obtained.

$$\dot{m}_{MBB,dry,3} = \frac{\dot{m}_{MBB,dry,2a}\left(1 + \omega_{MBB,2b}\right)\left(1 - mf_{EF}\right)}{\left(1 - mf_{EF}\right)C_2 - mf_{EF}\left(1 + \omega_{MBB,3}\right)C_1} \tag{8.2.29}$$

where,

$C_1 = m_{MBB,2b} + mf_{EF} - 1$

$C_2 = \left(\omega_{MBB,2b} - \omega_{MBB,3}\right) - \left(1 + \omega_{MBB,3}\right)C_1$

All the moisture contents in this equation are known, or have been computed. Thus, the time rate mass flow of wastewater and left over solids flowing in and out of the fire-tube boiler can also be found, along with each reactant entering the combustor and each product of combustion exiting the stack, along with the ash production using equation (8.2.8).

Now, some discussion should be articulated as to the limits of applicability of the formulae derived for this model; namely, the maximum amount of extra fuel that can be added to the combustor before all of the wastewater is vaporized in the boiler. Once $\dot{m}_{fuel}$ is known, a value for the amount of wastewater that can be vaporized, $\dot{m}_{ww,8}$, can be computed, but the total amount of liquid manure coming from the solids separator, $\dot{m}_{MBB,7}$, may be computed with the following expression.

$$\dot{m}_{MBB,7} = \dot{m}_{ww,8} + \dot{m}_{ww,8ew} \tag{8.2.30}$$

where $\dot{m}_{ww,8ew}$ is the amount of extra wastewater from the solids separator that could not be handled by the boiler because the combustion of the fuel blend could not provide enough heat. But as mf_{EF} increases, $\dot{m}_{ww,8ew}$ will eventually become zero and $\dot{m}_{ww,8}$ will be greater than $\dot{m}_{MBB,7}$. If this is the case, then additional wastewater, not produced from the confined animal units, can be handled by the system, or the steam produced in the boiler can be superheated and not simply saturated vapor.

There are two main factors that may be used to gage the effectiveness of this conceptualized MBB combustion design. The first is the boiler efficiency, which is defined as the total amount of heat transferred to the boiler water divided by the heat released by the fuel. However, since in this case the boiler water is wastewater emanating from the solid separator, there will be a great deal of solids in the

boiler water as it is being vaporized. Thus the equation for boiler efficiency must be modified to account for these solids.

$$\eta_{boiler} = \frac{\dot{Q}_{comb} - \left(\dot{m}_{MBB,BD,2b} c_{MBB,BD} - \dot{m}_{H_2O,2b} c_{H_2O_{(l)}}\right)\left(T_{2b} - T_8\right)}{\dot{m}_{fuel,3} HHV_{fuel}} \tag{8.2.31}$$

Finally, the disposal efficiency is an indication of how much of the liquid flushed manure from the animal housing was incinerated. Since there will always be ash leftover from the combustion, the disposal efficiency can never be unity, but high disposal efficiencies are achieved when all of the water in the liquid manure is vaporized and all of the combustible material in the manure has been burned.

$$\eta_{disposal} = \frac{\dot{m}_1 - \dot{m}_{8,ew} - \dot{m}_{5a}}{\dot{m}_1} \tag{8.2.32}$$

8.4.3. Combustion System for Scraped Solids and Lower Moisture Biomass

Not all manure waste from large CAFOs is handled as a liquid or is even high in moisture. Scraped manure from open lots and feedlots, especially in areas with dry climates, will usually be lower than 30% (Heflin, 2008). For these cases, solids separators and dryer would not be needed. See Figure 8.4.3. Plus, instead of using wastewater in the boiler, a standard vapor-power cycle would suffice, in order to utilize heat from biomass combustion to generate steam for external processes.

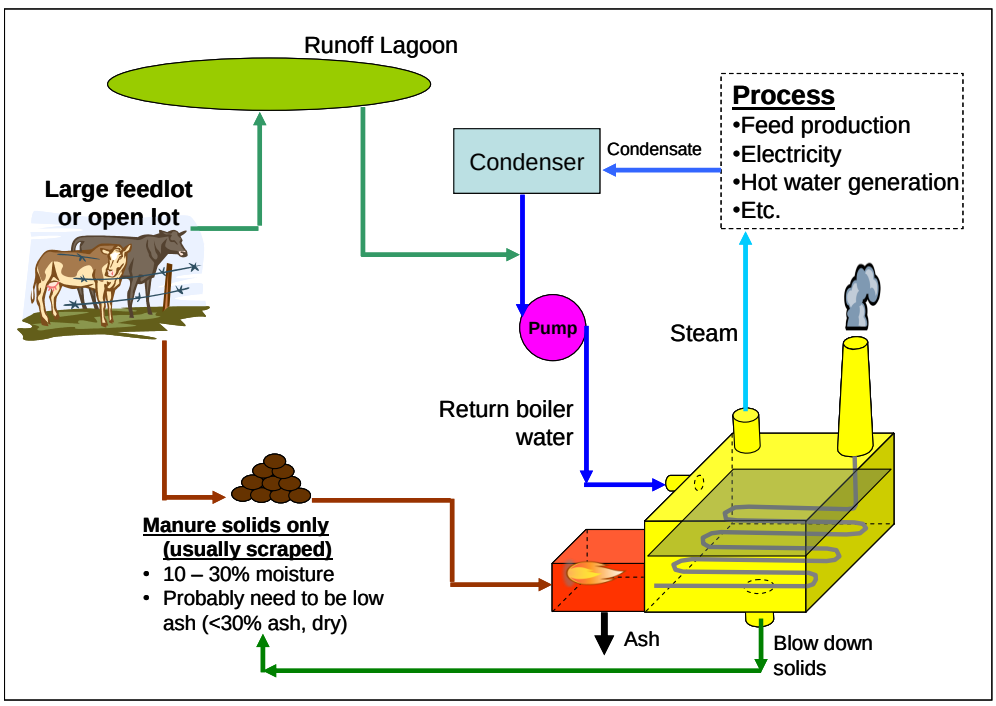

Figure 8.4.3 Conceptualized design of MBB thermo-chemical energy conversion system for large feedlot corrals or open lot dairies that produce low moisture manure

There are of course different ways a MBB combustion system could be designed. For instance, if the large feedlot has a lagoon that stores wastewater runoff, a fire-tube boiler could be used in a similar way to that of the flushed manure design. Also, it is possible to avoid producing steam at all, and still generate useful energy. If the MBB is gasified then the producer gas can be burned in a modified internal combustion engine or a gas turbine to produce electrical energy. All of these possibilities can be modeled

with the equations presented throughout this section. The use of a vapor-power cycle in manure biomass energy conversion systems, shown in Figure 8.4.3, was discussed by Carlin (2005) for cases where lower moisture biomass was present. However, in that report, it was thought that vacuumed manure solids would have similar moisture contents to scraped manure solids. Yet, based on the data reported this assumption may not be true for most cases. The moisture content of manure, that is not flushed or washed with water, is probably more dependent on the climate of the local geographic area.
Moreover, it should be noted that for all of these small-scale combustion systems, low-ash manure is preferred. High ash contents in manure make direct combustion processes very difficult, if not impossible. Even for gasification processes, the cost of continuously removing ash and increased maintenance to equipment can become very costly.

8.5. Results And Discussion

Mass and energy balances were conducted to predict the combustion system's effectiveness at incinerating the manure and the amount of steam that can be generated for use as a thermal commodity for operations at or near the feeding operation.

8.5.1. Base Run

The base case parameters chosen for the small-scale combustion system are listed in Chapter 10. Suppose the combustion system is installed at a 500-cow dairy with each cow excreting about 8 dry kg of manure per day. The manure from all 500 animals is flushed from the free stall housing to the solid separator and is 95% moisture when it reaches the separator. The fire-tube boiler produces saturated steam at 300 kPa(gage). Ten percent, preheated excess air is used to burn the dried manure solids. The base case parameters for the dryer are similar to those discussed earlier in Table 8.5.1.

The equations for the combustion model were, once again, compiled into a computer spreadsheet program. The resulting mass flows and temperatures at each point in the system for the base run are shown in Figure 8.5.1. The spreadsheet program helped tremendously in visualizing the mass flows of the system during parametric analyses.

Table 8.5.1 Base case values for modeling the small-scale on-the-farm MBB combustion system

Parameter	Base Value (unit)
Moisture percentage of flushed manure	95%
Type of biomass	low-ash dairy biomass, 20% ash, (dry basis)[c]
No extra fuel	--
Number of animals	500
Manure production	7.73 dry kg/cow/day
Moisture percentage of separated solids	80%
Percent solids remaining in the separated wastewater	3%
Desired moisture percentage of dried solids[a]	20%
Excess air percentage	20%
Pre-heated combustion air[b]	Yes
Boiler pressure	300 kPa,gage
Stack temperature	420K

Parameter	Base Value (unit)
Moisture percentage of remaining solids from boiler (blow down solids)	70%

[a]Please see Carlin (2009) for base case values for rotary dryer
[b]Heat exchanger for pre-heating air is 99% effective
[c]For base run, all ash is assumed to exit the combustion system as bottom ash

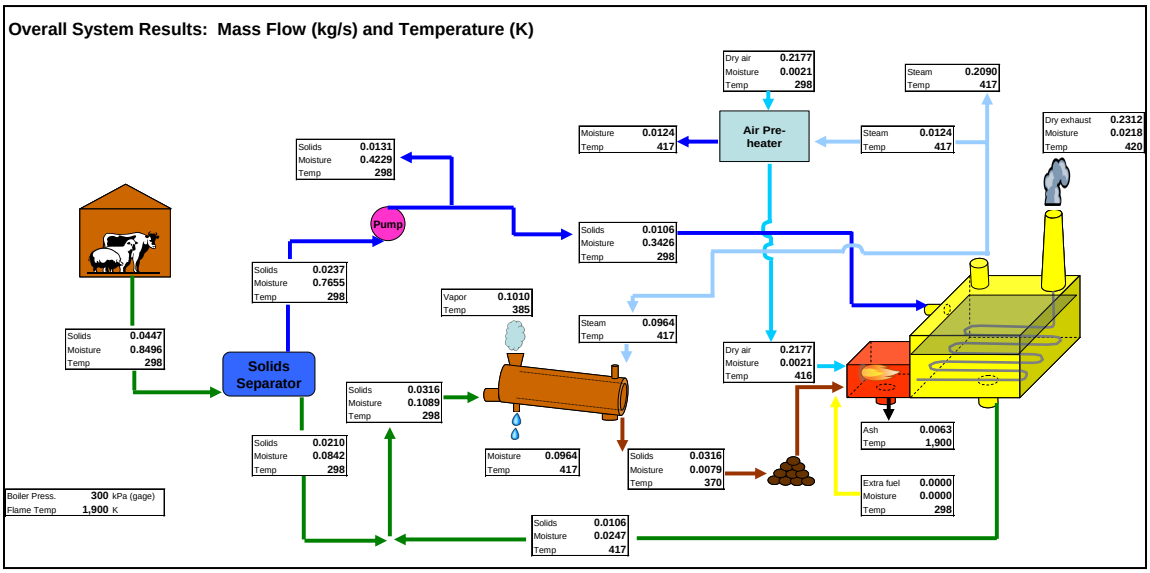

Figure 8.5.1 Sample output from computer spreadsheet model of small-scale on-the-farm manure biomass combustion system

For the base case, the system was found to produce 753 kg/hr of steam that would be available for thermal processes at or near the farm. The adiabatic flame temperature was found to be 1900 K and the corrected boiler efficiency was found to be 82%. The disposal efficiency was found to be about 50% during the base case run when the only fuel that was burned was the dried separated MBB solids. This disposal efficiency is much improved from the 34% reported by Carlin (2005) and Carlin *et al*. (2007a). This improvement is attributed mostly to the drying of the separated solids and the pre-heating of combustion air in this revised system. However, as was discussed by Carlin et al., since the moisture of the flushed solids was so high, at 95%, obtaining disposal efficiency close to 100% was not possible without the help of additional fuel. Aside from the additions of drying and pre-heating, the analysis of the system is much improved from these earlier studies. Carlin *et al*. estimated that the water leaving the solid separator was pure water and that the remaining solids in the boiler water were negligible. Thus the boiler efficiency was not adjusted for the possibility of having more solids remaining in the separated wastewater stream. Moreover, constant specific heats of combustion gases and dry combustion air were also assumed under the earlier studies. Here both those assumptions were not made.

The system can be scaled for different sized animal feeding operations and for different manure excretion rates per animal, as can be seen in Figure 8.5.2.

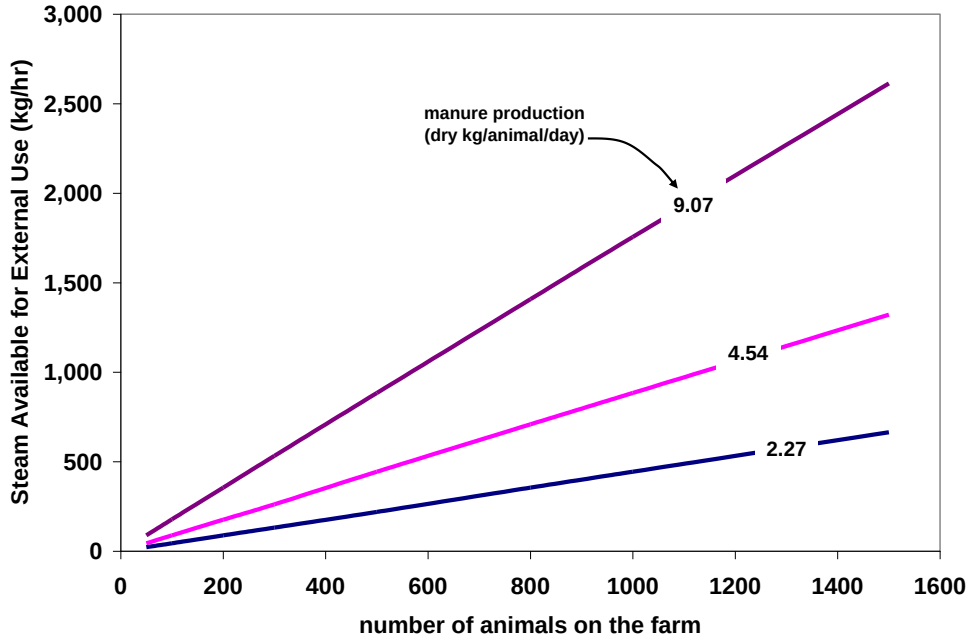

Figure 8.5.2 Usable steam produced from combustion system vs. number of animals housed at the feeding operation

The steam production, boiler efficiency and disposal efficiency can vary greatly when the base values are altered. The following discussion will be of parametric studies in which some of the base values were changed in order to view the sensitivity of the steam production, disposal efficiency and other important parameters.

8.5.2. Flushing Systems and Solids Separation

First, the performance of the combustion system is greatly dependant on how much moisture is in the flushed manure to begin with. The amount of wastewater that cannot be incinerated by the combustion system can increase greatly if the moisture percentage of the flushed manure approaches 99%. See Figure 8.5.3. Not only is the load on the boiler greater, but the amount of fuel is depleted when the flushed moisture percentage is extremely high.

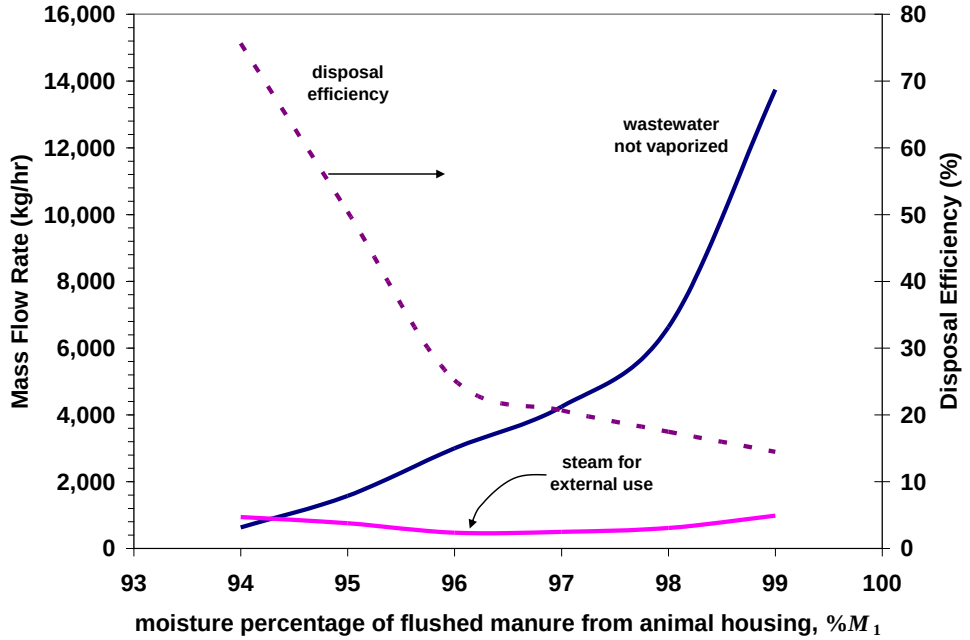

Figure 8.5.3 Usable steam, remaining wastewater, and disposal efficiency vs. moisture percentage of the flushed manure

The effectiveness of the combustion system is also dependant on the ability of the solid separator to screen out solids from the flushed stream. Figure 8.5.4 is a representation of how steam production and disposal efficiency change with increasing moisture percentage of the separated solids. Although the steam production decreases for wetter separated solids, the disposal efficiency actually increases. This is because the rotary dryer must consume more steam and transfer more heat to the separated solids in order to dry them to the desired moisture percentage of 20%. So, less steam is available for external use. However, essentially more of the wastewater is exiting the system at the vapor exhaust valve of the rotary dryer and less is being sent to the boiler. This may indicate that the rotary dryer is more effective at removing moisture from the solids than the steam tube boiler, since the net effect is greater disposal efficiency.

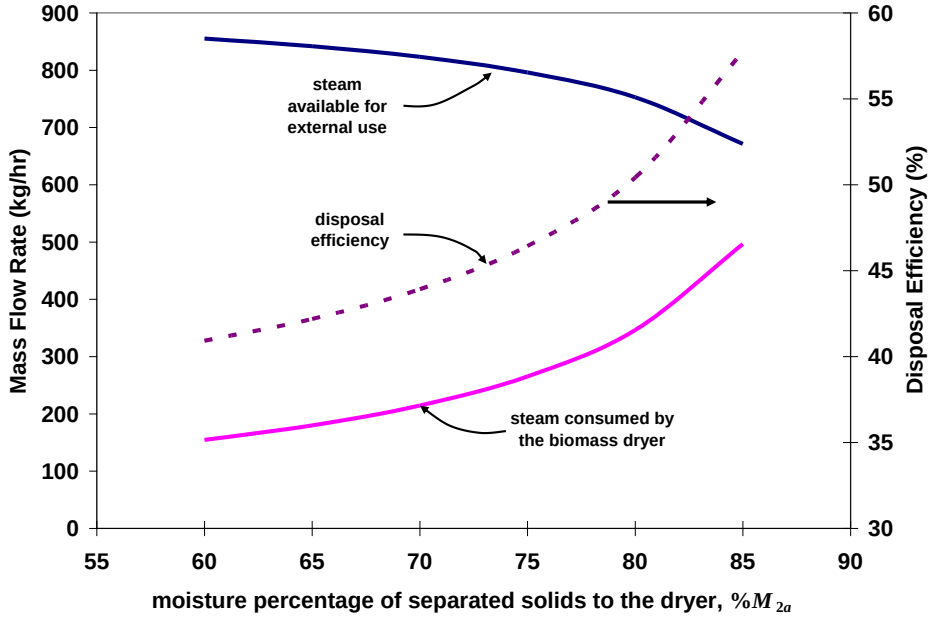

Figure 8.5.4 Disposal efficiency and steam production vs. moisture content of the separated MBB solids

The solids remaining in the flushed manure are mostly detrimental to the boiler efficiency. When more solids enter the drying chamber at point 8, more heat from the combustion goes to heating up these remaining solids, which are eventually sent back to the dryer, but the heat energy used to bring them to the steam temperature is essentially wasted. Thus, having more solids in the boiler water is detrimental to both boiler efficiency and the disposal efficiency as can be seen in Figure 8.5.5

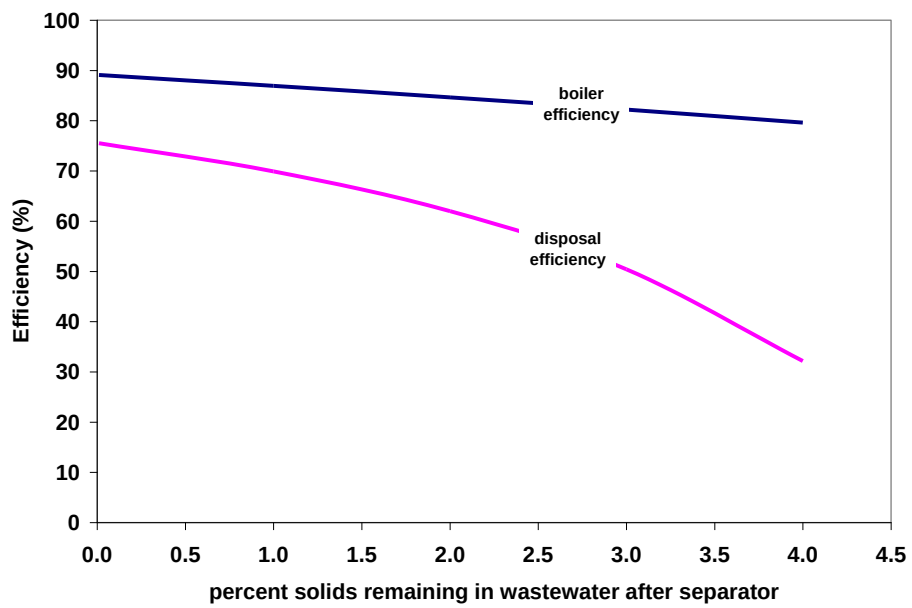

Figure 8.5.5 Boiler and disposal efficiency vs. the amount of solids remaining in the wastewater after the solid separator

8.5.3. Effect of Drying Solids Before Combustion

Drying the manure separated solids before combustion was the most significant addition to the small-scale system discussed by Carlin (2005). Figure 8.5.6 shows how drying the solids can improve flame temperature and increase the amount of wastewater that is vaporized in the boiler. Although the dryer must consume more steam to dry the manure to lower moisture percentages, the overall amount of steam that is generated in the boiler increases, causing a net increase in usable steam for external thermal processes. See Figure 8.5.7.

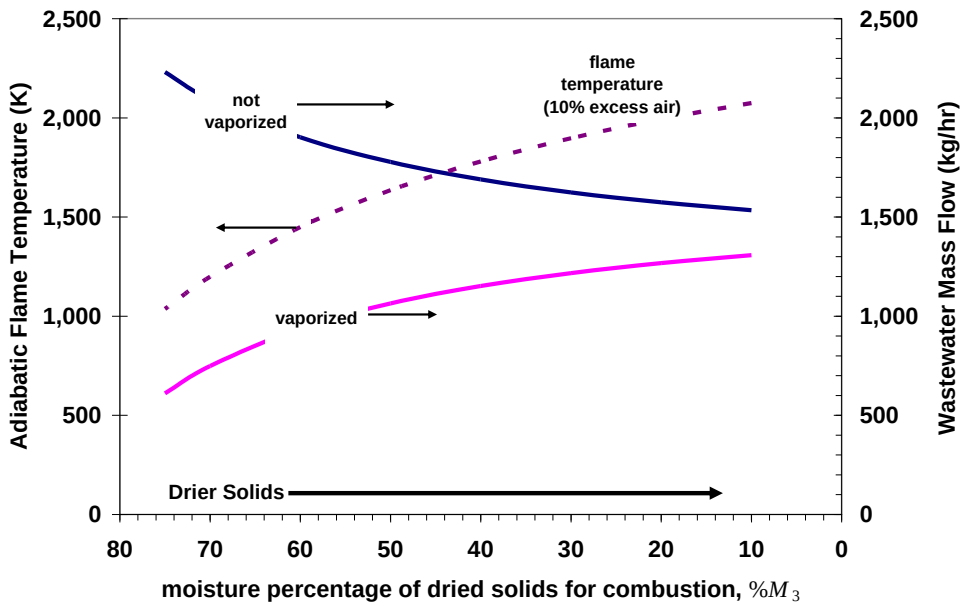

Figure 8.5.6 Adiabatic flame temperature and wastewater mass flow vs. moisture percentage of the dried solids

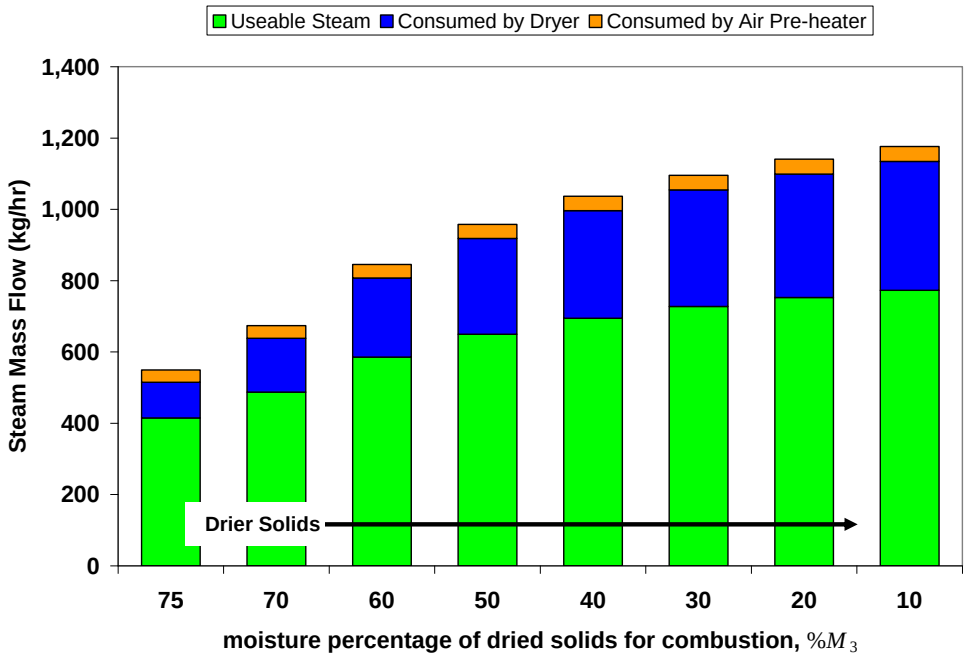

Figure 8.5.7 Steam production and use vs. moisture percentage of the dried solids

8.5.4. Combustion of Dried Biomass Solids

The addition of combustion air preheating was not quite as significant as drying, but still made some difference to the boiler and disposal efficiencies as can be seen in Figure 8.5.8. The effects of pre-heating the air are really limited by the steam temperature (and thus the boiler pressure, if the steam is saturated). The effectiveness of the heat exchanger heating the air was assumed to be 99% for the base case run. This assumption provides the hottest air possible for the combustion as the air cannot exceed the steam temperature due to the Second Law of Thermodynamics.

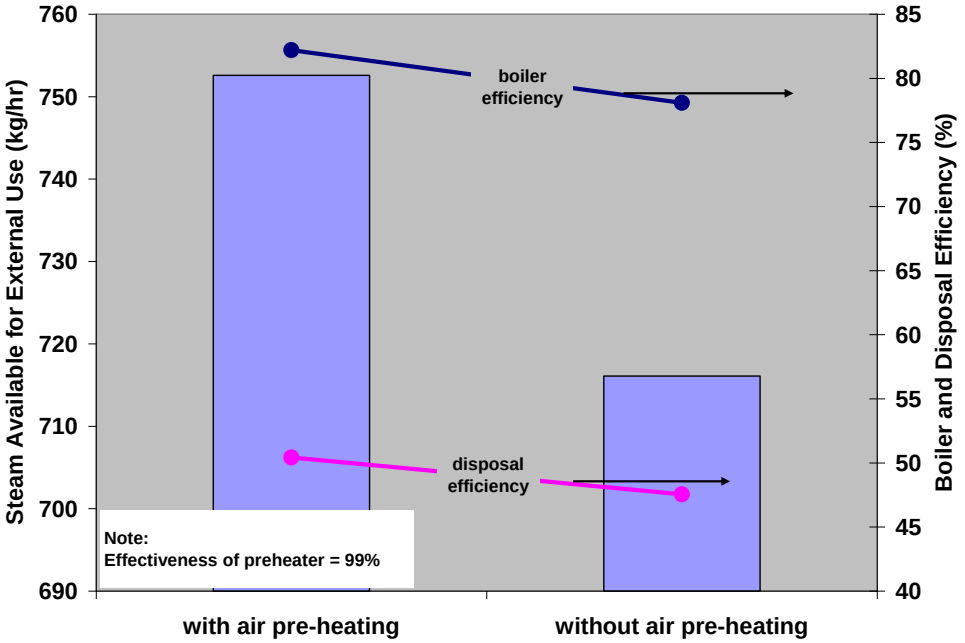

Figure 8.5.8Effects of preheating combustion air

However, the pre-heating of combustion air did have a peculiar effect on both boiler efficiency (Figure 8.5.9) and disposal efficiency (Figure 8.5.10). At lower stack temperatures, both of these efficiencies actually increased with excess air percentage. Typically, both efficiencies drop with excess air percentage; however, due to the way they were defined for this study, the heat energy added to the combustion air is seen as an addition to the system. However, at higher stack temperatures, the efficiencies were found to drop with excess air percentage as usual.

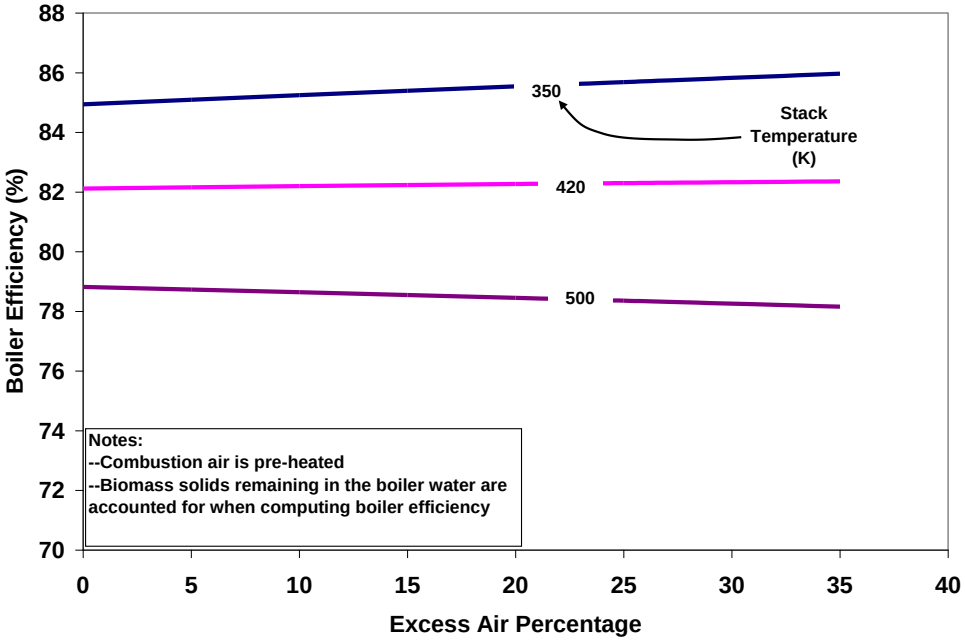

Figure 8.5.9Boiler efficiency vs. excess air percentage and stack temperature

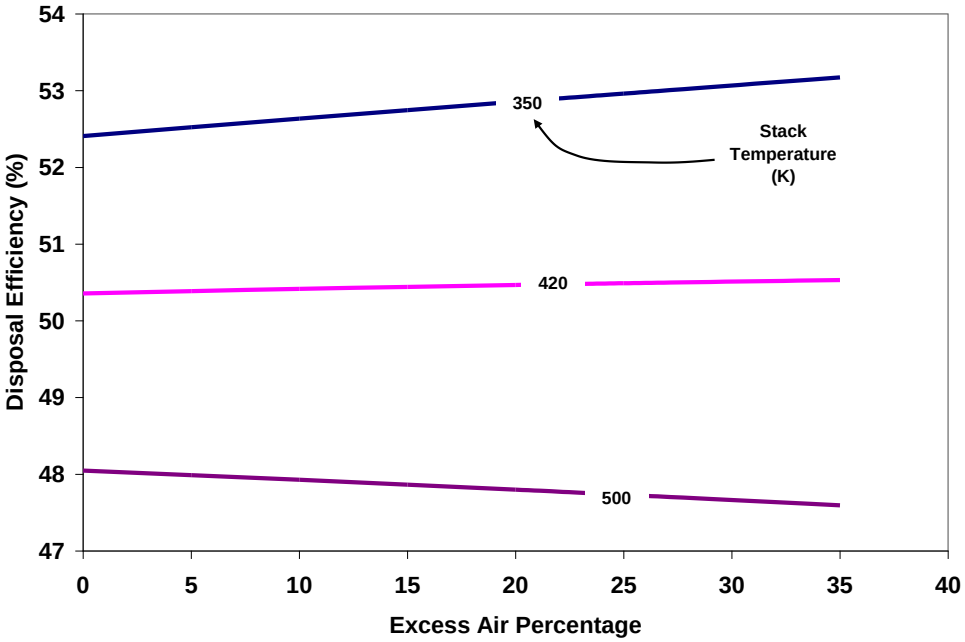

Figure 8.5.10 Disposal efficiency vs. excess air percentage and stack temperature

As has been the case throughout this study of MBB combustion, the ash content in the biomass fuel is detrimental to the system in every aspect. Figure 8.5.11 is a graph of flame temperature, steam production, and steam consumption plotted against the ash percentage of the biomass. Figure 8.5.12 is a plot of disposal efficiency and the remaining amount of wastewater against ash percentage. If the manure biomass has an ash content of 40%, disposal efficiency drops to about 35%, which negates the improvements obtained from drying solids and pre-heating air.

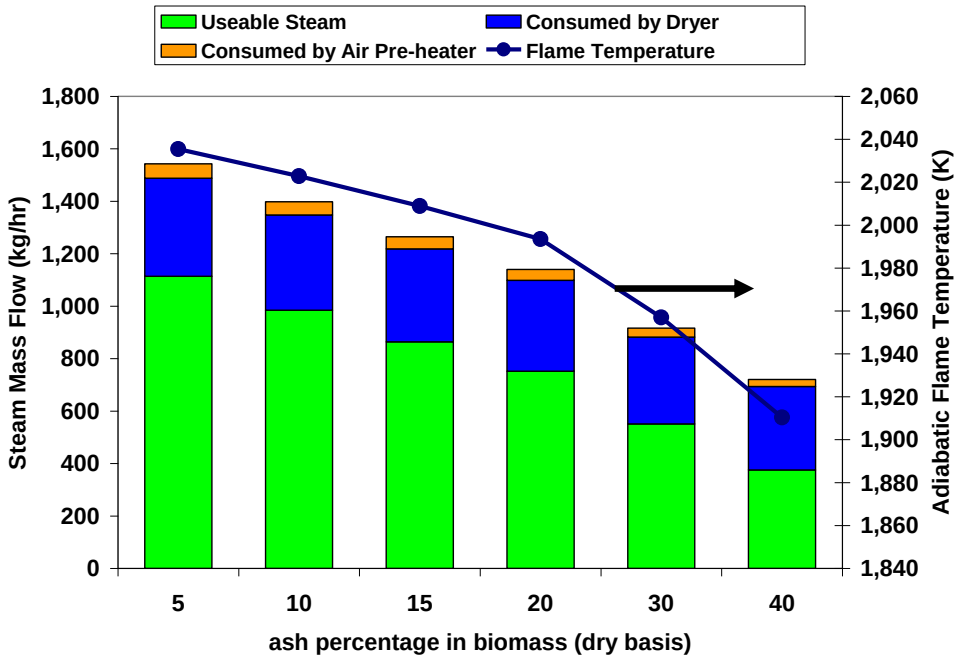

Figure 8.5.11 Flame temperature, Steam production, and steam usage vs. ash percentage in the MBB solids

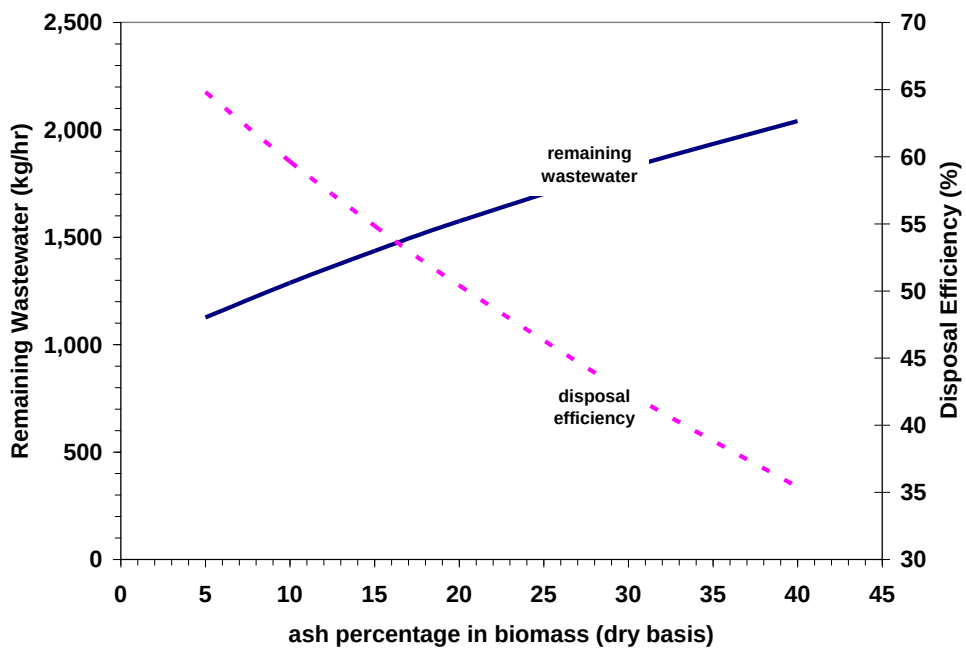

Figure 8.5.12The effect of ash percentage in the MBB solids on disposal efficiency

8.5.5. Operation of Fire-tube Boiler

The greatest design issue of the conceptualized combustion system is the fire-tube boiler, which must accept heat from the combustion of a low grade fuel (MBB) and vaporize wastewater that many times can be heavy in impurities and solid material that would otherwise be used to further fuel the

boiler's burner. The mechanical design of the boiler, as well as other design issues such as fowling and scaling of the fire-tube, are unfortunately not covered here. These issues are left to future work.

However, one parameter pertaining to the operation of the boiler can be investigated, and that is the degree to which the remaining solids and impurities in the boiler water (wastewater) are dried in the boiler's chamber. Figure 8.5.13 is a plot of usable steam and the disposal efficiency against the moisture percentage of the remaining solids (or the blow down solids). If the remaining solids leave the boiler high in moisture, then a lesser amount of wastewater was converted to steam. Thus, the amount of usable steam decreases. However, once again, the disposal efficiency was found to increase as the remaining solids are returned to the dryer, and the wastewater is eventually vaporized there instead of the boiler. This finding suggests that if disposal efficiency is the only important parameter, the operator of this system may be better served to simply produce just enough steam to run the dryer and vaporize as much of the wastewater in the dryer as possible. However, doing this (i.e. allowing the moisture percentage of the blow down solids to be left high) would greatly reduce the amount of usable steam produced by the boiler.

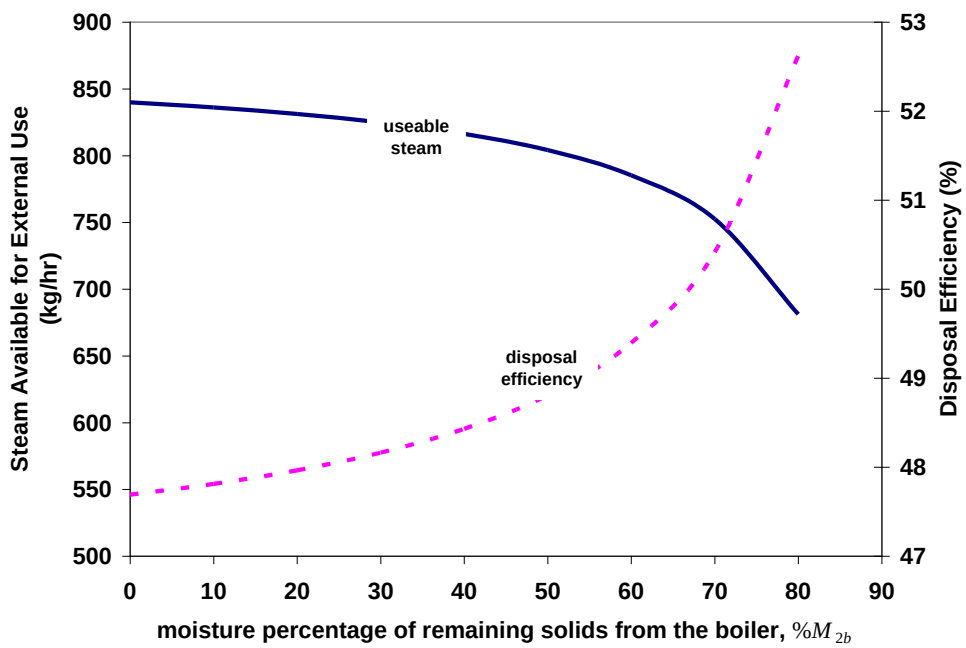

Figure 8.5.13 Steam production and disposal efficiency vs. moisture percentage of boiler blow down solids

8.5.6. Additional Fueling for Complete Wastewater Disposal

For high moisture flushed systems, all of the wastewater drained from the free stall barn cannot be incinerated if the only fuel that is used to generate heat energy is the separated MBB solids. In order to completely incinerate the waste coming from the barn, additional fuel must be burned in the furnace or gasifier. Figure 8.5.14 is a plot of disposal efficiency against a growing amount of additional fuel injection into the boiler burner. Methane, propane, and Texas lignite were modeled, but there did not seem to be much difference between these fuels as far as disposal efficiency. Due to the way disposal efficiency is defined, an efficiency of 100% can never be obtained because there will always be some ash from the biomass combustion remaining. However, for all fuels modeled, the maximum disposal efficiency was found to be obtained when the additional fuel was about 18 to 20% of the total fuel burned.

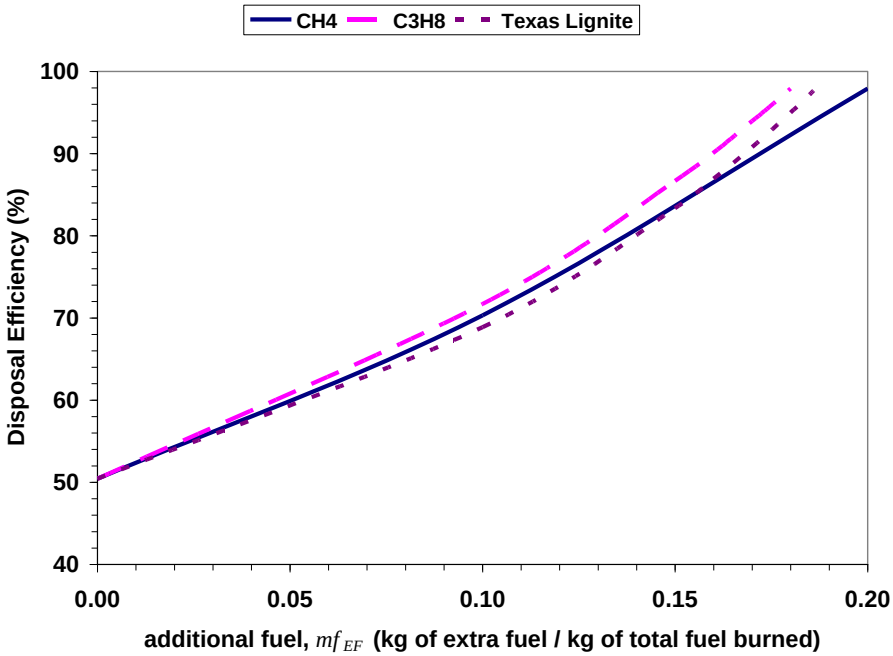

Figure 8.5.14 The effect of additional fueling on the disposal efficiency

8.6. Summary And Conclusions

Given the high cost of transporting and preparing MBB for combustion in large scale coal plants, as well as the lack of available low-ash biomass, burning MBB in smaller scale combustion facilities on or near animal feeding operations may be preferable at this time. The discussion of small scale on-the-farm combustion of MBB may be summarized with the following main points:

1. A base case run of a mathematical model describing a small-scale, on-the-farm MBB combustion system that can completely incinerate high moisture (over 90%) manure biomass was completed. In the conceptualized model, liquid manure is sent to a solid separator where the separated solids are dried and then burned. The remaining wastewater is sent to a fire-tube boiler and vaporized to produce steam that can then be consumed by the dryer or a combustion air pre-heater. Some remaining steam can also be used for external thermal processes on or near the farm to make the system profitable.
2. The conceptualized MBB combustion system, under base assumptions, could potentially incinerate about 50% of all the high moisture manure waste emanating from a 500-cow dairy, while producing over 750 kg/hr of 300 $kPa_{(gage)}$ saturated steam that could be used for external thermal processes.
3. The ability of the solid separator to strain solids out of the wastewater was found to be critical, as remaining solids in the wastewater reduce the boiler efficiency and ability of the combustion system to vaporize the wastewater.
4. Drying separated solids and pre-heating combustion air greatly improve the efficiency of the MBB combustion system and increase the amount of usable steam that can be produced.
5. Higher ash contents in the MBB solids (greater than 30% on a dry basis) were found to be detrimental to the performance of the small-scale combustion system.
6. Interestingly, the results from the parametric study of the small-scale MBB combustion system seem to suggest that the rotary steam-tube dryer removes moisture from the manure waste stream more effectively than the fire-tube boiler.

7. Co-firing the dried MBB separated solids with 20% natural gas, propane, or coal can generate enough heat to completely incinerate all of the wastewater from the animal feeding operation.

8.7. Acronyms

β	TGA Heating Rate
μm	Micrometer or Micron
B	Pre-exponential Factor
ºC	Degree Celsius
C_2H_6	Ethane
CB	Cattle Biomass (either FB or DB)
CH_4	Methane
CO	Carbon Monoxide
CO_2	Carbon Dioxide
DAF	Dry Ash Free
DB	Dairy Biomass
DEAM	Distributed Activation Energy Model
DSC	Differential Scanning Calorimetry
DTA	Differential Thermal Analysis
E	Activation Energy
$E(X_n)$	Exponential Integral of the nth Order
FB	Feedlot Biomass
FC	Fixed Carbon
FTIR	Fourier Transform Infra Red
H_2	Hydrogen
HA-PC-DB-SoilSurf	High Ash Partially Composted Dairy Biomass Soil Surface
HA-PC-FB	High Ash Raw Manure Feedlot Biomass
HA-RM-FB	High Ash Raw Manure Feedlot Biomass
HR	Heating Rate
HHV	Higher Heating Value
K	Degree Kelvin
LA-PC-DB-SepSol	Low Ash Partially Composted Dairy Biomass Separated Solids
LA-PC-FB	Low Ash Partially Composted Feedlot Biomass
LA-RM-FB	Low Ash Raw Manure Feedlot Biomass
MVRR	Maximum Volatile Release Rate
min	Minute
mL	Milliliter
m_v	Volatile Mass
N_2	Nitrogen
PRB	Powder River Basin Coal (a sub bituminous coal)
RM	Raw Manure
R_u	Universal Gas Constant
SMD	Sauter Mean Diameter
SRM	Single Reaction Model
t	Time
T	Temperature
T_e	Empty Pan Thermocouple
T_s	Sample Pan Thermocouple
TC	Thermocouple

TGA	Thermogravimetric Analysis
TXL	Texas Lignite

8.8. References

Caldwell E. (2008). Roast your compost: EcoCombustion Energy Systems Corporation has commercialized a manure-burning system dubbed Elimanure. *Ag Nutrient Management* Magazine by Progressive Dairy Publishing. August 2008.

Carlin, N. T. (2005). Thermo-chemical conversion of dairy waste based biomass through direct firing. MS Thesis. Texas A&M University: College Station, Texas.

Carlin, N., Annamalai, K., Sweeten, J., and Mukhtar, S. (2007a). Thermo-chemical conversion analysis on dairy manure-based biomass through direct combustion. *International Journal of Green Energy* 4(2): 133-159.

Carlin, N., Annamalai, K., Sweeten, J. M., and Mukhtar,S. (2007b). Utilization of latent heat derived from vaporized wastewater in high moisture dairy manure combustion schemes. International Symposium on Air Quality and Waste Management for Agriculture, September 15-19, 2007: Broomfield, Colorado.

Centner, T. J. (2004). *Empty pastures: confined animals and the transformation of the rural landscape*. Urbana and Chicago, Illinois: University of Illinois Press.

Gregory M. W. (1993). Wastewater evaporation system. US Patent No. 5,240,560.

Heflin K. (2008). Personal contact. Extension Associate. Texas AgriLife Extension Service, Amarillo and Bushland, Texas.

Kamen D., Demers J. A., and Owens K. (2008). Locally powered water distillation system. US Patent No. 7,340,879 B2.

Kolber, S. N. (2001). Treatment of waste produced by farm animals raised under confined conditions. United States Patent #6,190,566.

Mooney, R., Mooney, D., and Latulippe, D. (2005). Method and apparatus for the gasification and combustion of animal waste, human waste, and/or biomass using a moving grate over a stationary perforated plate in a configured chamber. United States Patent #6,948,436 B2.

Rudiger, H., Kicherer, A., Greul, U., Spliethoff, H., and Hein, K. R. G. (1996). Investigations in combined combustion of biomass and coal in power plant technology. *Energy and Fuels* 10: 789-796.

Rudiger, H., Greul, U., Spliethoff, H., and Hein, K. R. G. (1997). Distribution of fuel nitrogen in pyrolysis products used for reburning. *Fuel* 76(3): 201-205.

Schonfeld E. (2006). Segway creator unveils his next act: Inventor Dean Kamen wants to put entrepreneurs to work bringing water and electricity to the world's poor. Business 2.0 Magazine and CNNMoney.com. 16 February 2006.

Skill Associates. (2005). Elimanure™. Available online at: http://www.burnmanure.com/management/elimanure.html. (Accessed on February 2008).

Young, L. and Pian, C. C. P. (2003). High-temperature, air-blown gasification of dairy-farm wastes for energy production. *Energy* 28: 655-672.

8.9. Student's & Training

This work was used in part to fulfill the Doctoral requirements Nicholas Carlin.

8.10. Other support

None

8.11. Dissemination

Carlin NT, Annamalai K, Harman W, Sweeten JM. (2009). The economics of reburning with cattle manure-based biomass in existing coal-fired power plants for NO_x and CO_2 emissions control. Accepted by *Biomass & Bioenergy* in March 2009. In press.

Carlin NT, Annamalai K, Oh H, Gordillo Ariza G, Lawrence B, *et al*. (2008). Co-combustion and gasification of coal and cattle biomass: a review of research and experimentation. Accepted by *Progress in Green Energy* in January 2008. In press.

Carlin NT, Annamalai K, Sweeten JM, and Mukhtar S. (2007). Thermo-chemical conversion analysis on dairy manure-based biomass through direct combustion. *International Journal of Green Energy* 4(2):133-159.

Carlin NT, Annamalai K, Sweeten JM, and Mukhtar S. (2007). Utilization of latent heat derived from vaporized wastewater in high moisture dairy manure combustion schemes. International Symposium on Air Quality and Waste Management for Agriculture, September 15-19, 2007: Broomfield, CO.

Annamalai K, Carlin NT, Oh H, Gordillo Ariza G, Lawrence B, *et al*. (2007). Thermo-chemical energy conversion using supplementary animal wastes with coal. Proceedings of the IMECE, 2007 ASME International Mechanical Engineering Congress and Exposition, November 11-15, 2007: Seattle, WA, USA

9. ASH CHARACTERIZATION

TASK A-9: Ash characterization for value-added uses.

See Vol II for report on this task

10. ECONOMIC MODELING OF CATTLE BIOMASS ENERGY SYSTEMS

ABSTRACT: Cattle biomass (cattle manure) has been proposed as a reburn fuel to reduce nitrogen oxide (NOx) emissions in coal-fired power units. Coal plants that reburn with catttle biomass (CB) can reduce CO2 emissions and save on coal purchasing costs while reducing NOx emissions by 60 to 90% beyond levels achieved by low-NOx burners. Reductions from reburning coal with CB are comparable to those obtained by other secondary NOx technologies such as selective catalytic reduction (SCR). The objective of this study is to model the potential fueling, emission, and economic savings from reburning coal with CB and compare those savings against competing technologies. A spreadsheet program was developed to compute capital, operation, and maintenance costs for CB reburning, SCR and selective non-catalytic reduction (SNCR). An initial run of the economics modeling program, with input parameters found in research and literature review, showed that a CB reburn system retrofitted on an existing 500 MW coal plant (9,750 Btu/kWh and 80% capacity factor) was found to have a net present worth (NPW) of $43.7 million with a rate of return of 15.6% and a six year seven month simple payback period. Comparatively, an SCR system under the same base case input parameters was found to have a NPW of $6.45 million with a rate of return of 6.59% and a 13 year six month simple payback period. An SNCR system, under the same conditions, would not generate enough revenue from NOx credits to payoff initial investments. The profitability of a CB reburning system retrofit on an existing coal-fired power plant can decrease with lower coal prices, shorter operation periods, lower values on NOx emission credits, and more efficient primary NOx controllers. However, a future carbon tax or avoided sequestration cost of only $10 per ton of CO2 would more than double the NPW of a CB reburn system retrofit and reduce the payback period by almost three years. Biomass transport distances and the unavailability of suitable, low-ash CB may require future research to concentrate on smaller capacity coal-fired units between 50 and 300 MW. Construction of lower capacity plants near areas dense in agricultural biomass could improve the outlook of biomass reburn and cofiring facilities and boost rural economies.

10.1. Introduction

Recently, CO_2 emissions from fossil fuel combustion have garnered the most attention due to the threat of global warming caused by higher concentrations of CO_2 in the atmosphere. In the US, 36% of CO_2 emissions in 2006 came from the combustion of coal. Ninety-one percent of all CO_2 emissions from burning coal are emitted from electric power plants. Currently, there are no commercially available technologies that can reduce CO_2 emissions after combustion. The only feasible way to reduce CO_2 emissions, at this time, is to obtain electricity from alternative sources such as nuclear, hydro-electric, solar, wind, and biomass combustion or to burn other fossil fuels that emit less CO_2 per unit energy, such as natural gas. However, in most parts of the country, coal is both cheaper and more available than any alternative form of energy. Plus, coal is generally cheaper than most other fossil fuels per unit energy. The average price of natural gas for electricity producers in 2006 was $6.74/GJ$_{th}$ ($7.11/MMBtu) (EIA, 2007b). However the price of coal in all states is much lower than this price.

Based on these understandings of large industrial CAFOs and fossil fueled power plants, there seems to be an opportunity for a more symbiotic relationship between animal farmers and energy producers, or at least for animal farmers to become energy producers themselves. If burning MBB can

alleviate the waste disposal issues found on some large animal farms and generate more jobs and activity to rural economies, while at the same time displacing a fraction of the fossil fuels that are burned for energy generation, then perhaps MBB can be added to the list of renewable and carbon-neutral energy production technologies that will eventually supplement fossil fuel combustion.

Co-combustion of coal and MBB has been found to reduce NO_x emissions, increase the oxidation of elemental mercury emissions, and reduce the amount of nonrenewable CO_2 emissions from coal combustion. This claim will be warranted and explained in the following sections of this dissertation. However, the primary purpose of this study is to investigate the economic feasibility of processing and transporting MBB to existing energy production facilities and subsequently burning the biomass.

10.2. Literature Review

10.2.1. Co-firing Coal with Biomass

Although there have not been many studies on burning manure biomass in large combustion facilities, there have been co-combustion studies of other solid biomass fuels such as wood-based biomass. In fact, there have even been several recent biomass co-firing tests and proposals. For example, in 2005, American Electric Power, the largest electric generator and coal consumer in the US, successfully displaced 10% of the coal consumed at the 100 MW Picway coal plant near Columbus, Ohio with wood chips and wood waste-based biomass (Electric Power Daily, 2005). In 2007, as part of a proposal to approve the construction of a 750 MW plant, LS Power proposed to co-fire switch grass, cornstalks, and ethanol production wastes to supplement coal (Waterloo Courier, 2007). In the United Kingdom, the electric generator, Drax, is aiming to co-fire coal with 10% olive cake and elephant grass biomass at a 4,000 MW power plant in Yorkshire by 2009. Doing so would displace 1 million tons of coal and save 2 million tons of CO_2 per year. It was estimated that the delivery cost of the biomass would be 2 to 5 times that of coal, but benefits from renewable obligation certificates (ROCs) would justify the additional fueling costs (Froley, 2007).

In 2004, the US Department of Energy (DOE) conducted a fairly expansive study on co-firing coal with biomass. The study centered on the success of a pilot co-firing test at the DOE Savannah River Site in Aiken, South Carolina. The DOE facility is composed of two stoker boilers that generate steam for heating applications. The facility is relatively small compared to most utility coal steam electric power plants, and consumes about 11,145 tons of coal per year. At the time of the study, the as delivered price of coal was $50 per ton. The facility also generated about 280 tons of scrap paper and cardboard per year. The waste paper and wood products were converted to “process engineered fuel” cubes and co-fired along with the coal. Twenty percent of the coal was offset by the biomass cubes. The project resulted in a net annual savings of about $254,000. These savings were computed after subtracting the cost of processing the wood and paper wastes. The total investment of the project was $850,000, which was paid back in approximately four years. The 10-year, net present worth of the system was determined to be $1.1 million (DOE, 2004).

There are several reasons why this specific co-firing application was so profitable. First, the cost of coal was relatively high. Secondly, the biomass that was used was generated from the facility itself, so the avoided costs of discarding the paper and wood waste in a landfill were added to the overall savings of the project. Although the DOE study sites various examples of successful co-firing applications on all types of boilers, it did say that stoker boilers are uniquely suited for co-firing because very little investment is required to accommodate most biomass fuels (DOE, 2004). Moreover, unlike manure biomass, wood biomass generally has very little moisture, ash, and sulfur, making it much more suitable for many direct combustion applications. Overall the study seemed to suggest that the eastern part of the US is particularly suited for co-firing applications because as delivered coal prices tend to be higher in eastern states,. Also landfill tipping fees are generally more expensive in eastern states, giving added incentive to utilize waste-based biomasses in alternative ways.

For the purposes of this study, the most difficult cost to estimate is the capital investment cost of making the necessary modifications to the power plant site to process and handle the new biomass fuel. Several studies of biomass co-firing have quoted estimates of the investment costs of a co-fire project. Some of these studies are listed in Table 10.2.1. Note that capital costs are listed as dollars per kW_e generated from the biomass.

Table 10.2.1 Capital investment costs of installing a biomass co-firing system on an existing coal-fired power plant, taken from various sources

Capital Cost, η ($/kW$_e$ from biomass)	**Source**	**Notes**
	CO-FIRING	
60	(Robinson *et al*, 2003)	Mode co-firing rate for <2% biomass on an energy basis. Range: 40 - 100 $/kW biomass. Wood and agriculture residue
200	(Robinson *et al*, 2003)	Mode co-firing rate for >2% biomass on an energy basis, separate stream and injection required. Range: 150 - 300 $/kW biomass. Wood and agriculture residue
175 - 200	(Hughes, 2000)	Co-firing with separate feeder. Wood waste, short rotation crops, and switch grass biomass
109	(USEPA, 2007c)	>500 MWe pulverized coal plant. Probably wood and crop based biomass
218	(USEPA, 2007c)	201 - 500 MWe pulverized coal plant. Probably wood and crop based biomass
251	(USEPA, 2007c)	<200 MWe pulverized coal plant. Probably wood and crop based biomass

Robinson *et al*. (2003), along with the DOE (2004) study, suggested that a major factor in the capital investment cost of a co-firing project was the percentage of biomass that the boiler would use. If less than 2% biomass were to be utilized, then the investment costs would be significantly lower because existing equipment used to process the coal may also be used at the same time to process the biomass. The coal and biomass would be directly mixed before grinding and conveying to the burner. Figure 10.2.1 illustrates the new equipment that would be required to process the biomass under this scenario. However, this may not be true for some pulverized coal power plants, which have equipment specifically designed to micronize coal and not biomass, which may be more difficult to grind.

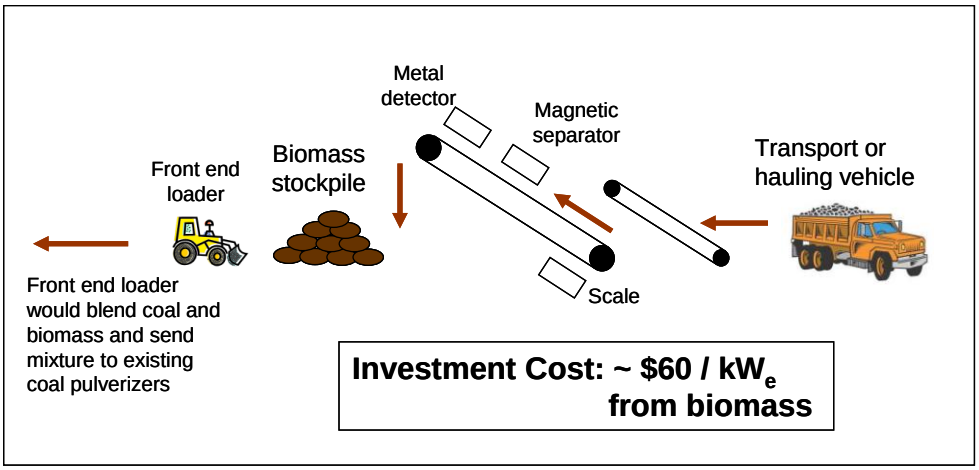

Figure 10.2.1 Schematic of a blended-feed co-firing arrangement for a pulverized coal boiler (adapted from DOE, 2004)

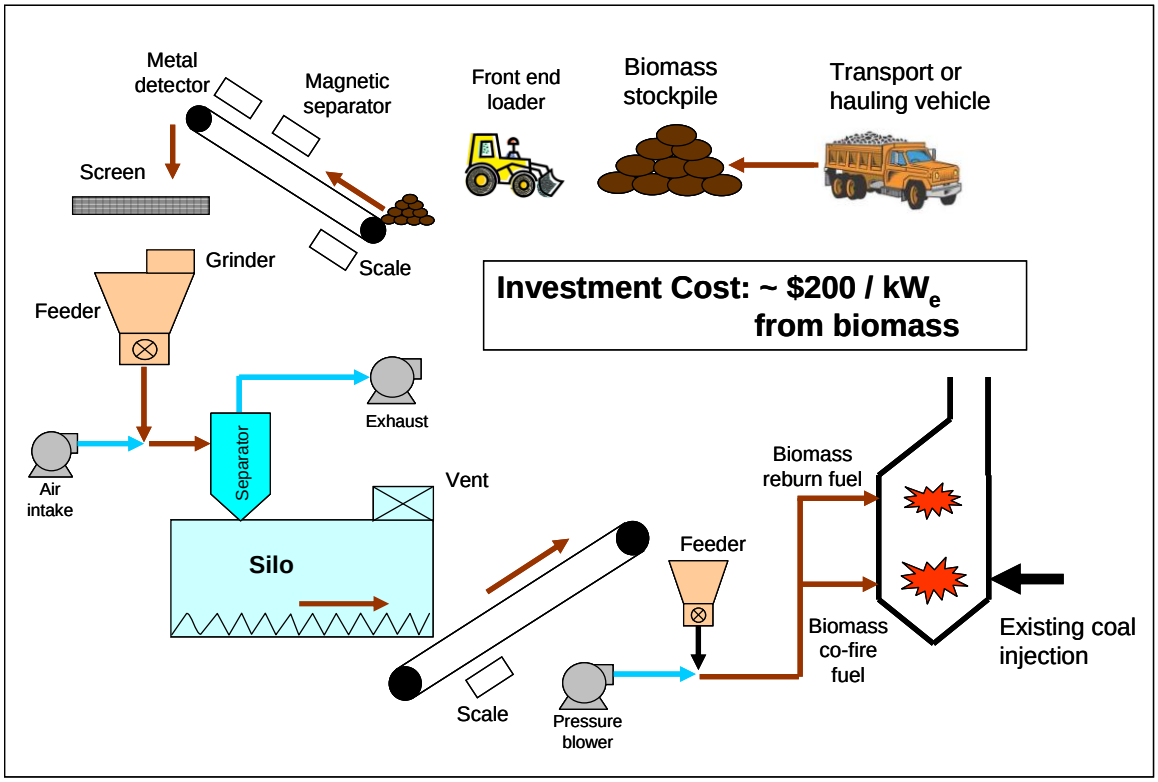

Figure 10.2.2 Schematic of a separate-feed co-firing arrangement for a pulverized coal boiler (adapted from DOE, 2004)

If more than 2% biomass were to be utilized, then additional processing equipment would be necessary, adding to the overall investment cost. Figure 10.2.2 illustrates the greater amount of new equipment that must be purchased if separate equipment were used to handle the biomass. However, keep in mind that these projected additions to coal-fired facilities are for wood-based biomass. Manure-based biomass may require different equipment.

The USEPA (2007c) study, listed in Table 10.2.1, also provided estimates for the annual operation and maintenance costs. According to the study, the fixed operation and maintenance cost for

operating the additional biomass processing equipment was estimated to be approximately \$7.63 per kW_e from biomass per year. Additional values were given to estimate the cost of transporting the biomass to the combustion facility.

10.2.2. Reburning Coal with Biomass

As discussed earlier, there have been relatively few reburn tests at coal-fired power plants in the US. Most of these tests included reburning coal with natural gas and only four or five power plants reburned coal with more micronized coal. Thus, one of the challenges of this study was to estimate the cost performance of a MBB reburning system at a coal plant, even when only experimental results and pilot scale tests have been conducted for MBB reburning, and few applications of gas and coal reburning systems existed for comparison. Work by Zamansky *et al*. (2000) suggested that reburn systems utilizing furniture wastes, willow wood, and walnut shell biomass as reburn fuel have similar capital costs to coal reburning systems. An earlier USEPA (1998) report for the Clean Air Act Amendment, which was also cited by Biewald *et al*. (2000), modeled both gas and coal reburn systems, although the coal reburn model was meant only for cyclone boiler types. And since gas reburning costs are generally lower than coal reburning costs, the reburn capital cost model presented by the USEPA (1998) would only be applicable for cyclone boilers. Cyclone boilers burn coarsely crushed coal, but coal reburn systems typically require pulverized or micronized coal to avoid unburned carbon emissions. Hence, purchasing pulverizing equipment is generally required for cyclone boiler plants that wish to install coal, or other solid fuel, reburn systems.

Table 10.2.2 Capital investment costs of installing a reburning system on an existing coal-fired power plant, taken from various sources

Capital Cost, η (\$/kW_e total plant capacity)	**Source**	**Notes**
	REBURNING	
35	(Zamansky *et al*, 2000)	Same cost for both coal and biomass reburning. 300 MWe plant. Furniture, willow wood, and walnut shell biomass.
45	(Zamansky *et al*, 2000)	Same cost for both coal and biomass reburning. 300 MWe plant. Advanced reburn process.
$70.7\left(\frac{300}{P}\right)^{0.388}$	(USEPA, 1998)	Coal reburning in cyclone boilers only. P = plant capacity in MW_e
60	(Smith, 2000)	Coal reburning in cyclone boilers, 40% NO_x reduction from an 0.86 lb/MMBtu baseline emission
6 - 13	(Smith, 2000)	Pulverized coal configurations using some existing equipment for coal reburn fuel preparation
66 and 43	(Mining Engineering, 2001)	For 110 MW and 605 MW plants, respectively. 50% NO_x reduction on cyclone burners with pulverized coal for reburn fuel

Some estimates of coal and biomass reburn capital costs are presented in Table 10.2.2. Unlike co-firing, reburning costs are usually expressed on a "dollar per kW_e of total plant capacity" basis. Smith (2000) reported that coal reburn capital costs may be as low as \$6/kW_e for pulverized coal plants with

existing equipment available for preparing the reburn fuel. However, MBB is significantly different from most wood and plant-based biomasses, as well as coal. The moisture and ash contents in MBB vary to greater degrees than wood biomass, although low ash cattle biomass has a comparable heat value to the biomass discussed by Zamansky *et al*. (2000). Moreover, reburn systems usually require 15 – 20% of the power plant's heat rate to be supplied by the reburn fuel. If biomass were to be used as the reburn fuel, additional processing equipment would almost certainly be required, based on the previous discussion of biomass co-firing.

Also note that capital costs for reburning in Table 10.2.2 do not include the capital cost of dryers and biomass hauling vehicles which will be needed for manure biomass reburning but not coal reburning. These costs must be computed separately. As for fixed operation and maintenance costs of the reburn fuel's processing equipment, the model presented by the USEPA (1998), for reburning coal with micronized coal, may be used for the current study; however, an additional correction factor that accounts for the MBB's poorer heat value, and hence greater required fueling rate, should be implemented.

10.2.3. Competing NO_x Control Technologies

In addition to modeling the economics of reburning coal with biomass, comparative estimates of other competing NO_x control technologies should also be computed. Fortunately, the economics of more common NO_x control technologies such as low-NO_x burners, SCR, and SNCR are modeled by the US EPA. The USEPA Integrated Planning Model (IPM) is a multi-regional, dynamic, deterministic linear programming model of the US electric power sector. The results from the IPM are meant to compare energy policy scenarios and governmental mandates concerning electric capacity expansion, electricity dispatch and emission control strategies. The model and base case inputs to the model are updated annually. The latest update, as of the writing of this dissertation, may be found on the USEPA (2006) website. Since a section of the IPM is concerned with evaluating the cost and emission impacts of proposed policies, it is possible to adopt these emission models to describe the economics of common primary and secondary controls, and then compare them to results for MBB reburning. However, since reburn technologies are not a significant part of the current efforts to reduce NO_x at coal-fired power plants in the US, their associated investment and operating costs were not included in the latest version of the IPM.

The NO_x control technology options modeled by the EPA IPM are low-NO_x burners (with and without over fire air), SCR, and SNCR. Capital and fixed operation and maintenance costs were set as functions of power plant capacity, while variable operation and maintenance costs were set as functions of heat rate. Models presented by Mussatti *et al*. (2000 a & b) offer more detailed and comprehensive representations for SCR and SNCR cost components, but require more detailed inputs. The cost equations in the IPM for NO_x control technologies are based on costs for 300 MW_e sized boilers. These costs are then translated to costs for different boiler sizes with scaling factors. The cost equations and scaling factors of IPM will be discussed further in the modeling section of this dissertation.

10.2.4. Dollar Values of Emissions

Annual monetary values pertaining to NO_x, SO_x, nonrenewable CO_2, and ash revenues are also required. Values for NO_x and SO_x emission credits can be found by the South Coast Air Quality Management District (SCAQMD) (2007). In 2006, trading credits for NO_x were $2,353/ton for the 2005 compliance year and as high as $15,698/ton for the 2010 compliance year. For compliance years beyond 2010, the NO_x credit values were $11,100/ton. SOx credits were traded at $882/ton for the 2005 compliance year and $966/ton for the 2006 compliance year. In a white paper prepared for TXU Energy (now Luminant Energy) by NERA Economic Consulting in 2004, the NO_x permit price assumption for long term strategic fuel planning was $4,000/ton NO_x with a sensitivity range of $2,000 to $6,000/ton NO_x. The permit price assumption for SO_2 was $250/ton SO_2 with a sensitivity range of $150 to $500/ton SO_2 (NERA, 2004).

Although most coal-fired plants in the US are currently not required to reduce CO_2 emissions, speculations may be made as to how emission taxes, cap and trade-based CO_2 allowances, or avoided

sequestering costs may affect the profitability of a MBB co-fire or reburn system. The same NERA report to TXU estimated that the cost of reducing CO_2 by capture and storage would range between \$50 and \$80/ton CO_2. Comparatively, the report showed that the cost of reducing CO_2 by co-firing coal with biomass ranged between \$5 and \$15/ton CO_2. However, the biomass referred to in this study was undoubtedly wood or plant-based biomass, and was probably based on a similar report to the DOE (2004) study on biomass co-firing discussed earlier. Moreover, ongoing results of the Regional Greenhouse Gas Initiative (RGGI, 2008) can provide some basis of the monetary value put on CO_2 in the US, even though the RGGI is in its infancy and only has jurisdiction in the northeastern part of the US. According to the RGGI website, the clearing price of CO_2 allowances in its inaugural auction in September 2008 was \$3.07/ton CO_2.

Finally, the ability of plant managers to find suitable uses for ash produced from biomass combustion as well as local buyers, could greatly affect a MBB co-fire or reburn system's overall profitability. Preliminary studies on the possible usage of ash produced from manure combustion have provided mixed results. Ash produced from manure combustion is a suitable sub-grade material for road construction, and if mixed with 10% Portland cement, can be used as a light weight concrete material with about one-third of the compressive strength of concrete. Yet the manure ash is not self-cementing and is not a suitable replacement for Portland cement. Also, chemical analyses show that manure ash is a non-hazardous, possibly reactive industrial waste which could be used for feedlot surfacing, road base, some structural building projects, and possibly fertilizer (Megel *et al*, 2006 and Megel *et al*, 2007). More information about the uses of fly ash from coal combustion was provided by the USDOT (2006). If ash is not sold, then it must be discarded, typically in local landfills, which require tipping fees.

10.3. Objectives

a. Determine capital expenditures for a MBB reburn and/or co-firing system including the cost of installing the reburner on an existing coal-fired power plant, the cost of purchasing transportation vehicles, and the cost of purchasing biomass processing equipment such as dryers.
b. Determine the operation and maintenance costs that would be inherent to a MBB reburn and/or co-firing system.
c. Estimate the economic impacts of reducing NO_x and CO_2 and increasing ash.
d. Determine the capital, operation and maintenance costs for other, more common NO_x control technologies such as low-NO_x burners and selective catalytic reduction (SCR), and compare to findings for MBB reburning.
e. Compute the overall annualized cost of reducing NO_x for each NO_x control technology. Moreover, estimate the net present worth and simple payback period of a MBB reburn retrofit project on an existing coal-fired power plant.
f. Conduct a full sensitivity analysis of the annualized cost and/or the net present worth to all significant parameters in the economic model.
g. Determine optimum conditions for a MBB reburn system including maximum acceptable biomass transportation distance and minimum required dollar values of CO_2 and NO_x emissions.

10.4. Experimental Procedure

10.4.1. Biomass Drying Models

The following equations ((10.1) – (10.17)) describe the overall heat and mass balance of the drying system chosen to dry the MBB (Figure 10.4.1), and are applicable to both the perpendicular flow conveyor belt dryer and the parallel flow conveyor belt dryer.

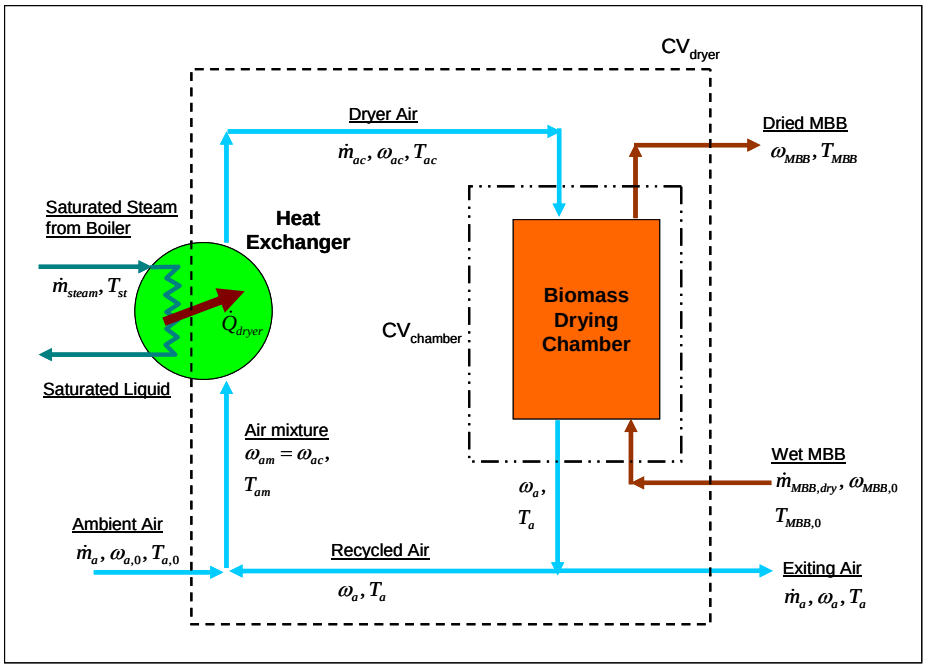

Figure 10.4.1 Mass and energy flow diagram for conveyor belt dryers (adapted from Kiranoudis et al., 1994)

The total enthalpy of air as a function of temperature, T, and humidity ratio, ω, can be written as:

$$h_{air,i} = c_{p,air} T_i + \omega_i \left(h^0_{f,H_2O_{(g)}} + c_{p,H_2O_{(g)}} T_i \right) \tag{10.1}$$

Where $c_{p,air}$ is the specific heat of dry air, $c_{p,H_2O_{(g)}}$ is the specific heat of water vapor in the air, and $h^0_{f,H_2O_{(g)}}$ is the enthalpy of formation of water vapor, which is approximately 2501.6 kJ/kg. The total enthalpy of the wet MBB can also be expressed as:

$$h_{MBB} = c_{MBB,dry} T_i + \omega_i c_{H_2O_{(l)}} T_i \tag{10.2}$$

Here, $c_{MBB,dry}$ is the specific heat of dry MBB, and $c_{H_2O_{(l)}}$ is the specific heat of liquid water, which is about 4.20 kJ/kg K. T_i is in degrees K. Note that relative humidity, ϕ, is usually known, and ω can be computed from ϕ and the temperature with the following expression:

$$\omega_{air,i} = 0.622 \frac{\phi_i P_g(T_i)}{P_{air} - \phi_i P_g(T_i)} \tag{10.3}$$

P_{air} is the air pressure (for this case approximately ambient pressure, 101,325 Pa), and P_g is the saturation pressure as a function of temperature. The Antoine Equation may be used to compute P_g from a known air temperature (Pakowski *et al*., 1991).

$$P_g = 133.322 * \exp\left[18.3036 - \frac{3816.44}{(T_i - 46.13)} \right] \tag{10.4}$$

where P_g is in Pascal (Pa) and T_i is in degrees K.

Now, a mass and energy balance can be conducted about CV_{dryer}. From the mass balance, the following expression can be found:

$$\dot{m}_a \left(\omega_a - \omega_{a,0} \right) = \dot{m}_{MBB,dry} \left(\omega_{MBB,0} - \omega_{MBB} \right) \tag{10.5}$$

And from the energy balance:

$$\dot{Q}_{dryer} = \dot{m}_a \left(h_a - h_{a,0} \right) + \dot{m}_{MBB,dry} \left(h_{MBB} - h_{MBB,0} \right) \tag{10.6}$$

A mass and energy balance can also be conducted about $CV_{chamber}$. The mass balance provides the following expression:

$$\dot{m}_{ac} \left(\omega_a - \omega_{ac} \right) = \dot{m}_{MBB,dry} \left(\omega_{MBB,0} - \omega_{MBB} \right) \tag{10.7}$$

And from the energy balance:

$$\dot{m}_{ac} \left(h_{ac} - h_a \right) = \dot{m}_{MBB,dry} \left(h_{MBB} - h_{MBB,0} \right) \tag{10.8}$$

From Figure 10.4.1, the following expression can also be generated from the mixing of ambient air and recycled air for the air mixture that will be sent to the drying chamber.

$$\dot{m}_{ac} h_{am} = \dot{m}_a h_{a,0} + \left(\dot{m}_{ac} - \dot{m}_a \right) h_a \tag{10.9}$$

For this analysis, the following are usually considered known parameters:

- the initial moisture content and the temperature of the MBB entering the dryer, $\omega_{MBB,0}$ and $T_{MBB,0}$,
- the desired moisture content of the MBB, ω_{MBB},
- the $\dot{m}_{MBB,dry}$ can be found from equation (10.3), and
- the properties of the ambient air entering the dryer, $\omega_{a,0}$ and $T_{a,0}$.

The following parameters are typically considered design variables for the dryer:

- the moisture content and temperature of the air exiting the dryer chamber, ω_a and T_a, and
- the air temperature drop over the drying chamber, $\Delta T_{chamber}$.

The dryer's temperature drop is defined as:

$$\Delta T_{chamber} = T_{ac} - T_a \tag{10.10}$$

Now, the following parameters must all be computed from equations (10.5) through (10.10): $\dot{m}_a$, T_{ac}, T_{MBB}, $\dot{Q}_{dryer}$, ω_{ac}, $\dot{m}_{ac}$, and T_{am}. The mass flow of air entering and exiting CV_{dryer}, $\dot{m}_a$, can be computed from equation (10.5). The temperature of the air exiting the heat exchanger and entering the drying chamber, T_{ac}, can be computed from the defined temperature drop in equation (10.10). The solution for T_{MBB} depends on how exactly the MBB is dried in the chamber. For example, if the conveyor belt dryer is a perpendicular flow dryer then T_{MBB} will be approximately equal to T_a. However, if the dryer is a parallel flow dryer, then T_{MBB} is approximately equal to the wet bulb temperature, T_{wb}, which is a function of T_a and ω_a.

$$T_{MBB} \cong \begin{cases} T_a, & \text{if perpendicular flow dryer} \\ T_{wb}, & \text{if parallel flow dryer} \end{cases} \tag{10.11}$$

With temperatures $T_{a,0}$, T_a, $T_{MBB,0}$, and T_{MBB} either known or computed along with the moisture contents, ω, of both the MBB and air, the enthalpies can be computed at each point in Figure 10.4.1 with equations (10.10) and (10.2), and $\dot{Q}_{dryer}$ may be computed from equation (10.3).

Now, in order to find ω_{ac}, and $\dot{m}_{ac}$, the remaining equations (10.7)and (10.8) must be combined:

$$\frac{h_{ac} - h_a}{\omega_a - \omega_{ac}} = \frac{h_{MBB} - h_{MBB,0}}{\omega_{MBB,0} - \omega_{MBB}}$$

and arranged as:

$$h_{ac} + \frac{h_{MBB} - h_{MBB,0}}{\omega_{MBB,0} - \omega_{MBB}} \omega_{ac} = \frac{h_{MBB} - h_{MBB,0}}{\omega_{MBB,0} - \omega_{MBB}} \omega_a + h_a$$

From equation (10.1) the enthalpy of the air entering the dryer is $h_{ac} = c_{p,air}T_{ac} + \omega_{ac}\left(h^0_{f,H_2O_{(g)}} + c_{p,H_2O_{(g)}}T_{ac}\right)$. Plugging this equation into the expression above, and solving for ω_{ac}, an equation for ω_{ac} can be obtained:

$$\omega_{ac} = \frac{\left(\dfrac{h_{MBB} - h_{MBB,0}}{\omega_{MBB,0} - \omega_{MBB}}\right)\omega_a + h_a - c_{p,air}T_{ac}}{h^0_{f,H_2O_{(g)}} + c_{p,H_2O_{(g)}}T_{ac} + \left(\dfrac{h_{MBB} - h_{MBB,0}}{\omega_{MBB,0} - \omega_{MBB}}\right)} \tag{10.12}$$

With ω_{ac} computed, $\dot{m}_{ac}$ can be found with either equation (10.7) or (10.8). The enthalpy, and hence the temperature, of the air mixture, T_{am}, can be computed from equation (10.8).

Thus far, the analysis has produced solutions for drying parameters that are essential for computing operation costs of drying. For example, the value determined for $\dot{Q}_{dryer}$ can now be used to determine how much steam will be required for the heat exchanger. If the boiler is operated at a pressure, P_{boiler}, and produces saturated steam, then the steam temperature, T_{st} can be computed by rearranging the Antoine Equation:

$$T_{st} = \frac{3816.44}{18.3036 - \ln\left(P_{boiler}/133.322\right)} + 46.13 \tag{10.13}$$

The steam consumption is thus,

$$\dot{m}_{steam} = \frac{\dot{Q}_{dryer}}{\Delta h^{T_{st}}_{H_2O,fg}} \tag{10.14}$$

where $\Delta h^{T_{st}}_{H_2O,fg}$ is the latent heat of vaporization, which is a function of T_{st}. Pakowski *et al*. (1991) suggested the following polynomial equation to compute $\Delta h^{T_{st}}_{H_2O,fg}$:

$$\begin{aligned}\Delta h^{T_{st}}_{H_2O,fg} = {} & 2504.65 - 2.80701*\left(T_{st} - 273.15\right) + 1.21884e-2*\left(T_{st} - 273.15\right)^2 \\ & -1.25205e-4*\left(T_{st} - 273.15\right)^3 + 4.50499e-7*\left(T_{st} - 273.15\right)^4 \\ & -6.67186e-10*\left(T_{st} - 273.15\right)^5\end{aligned} \tag{10.15}$$

Here, $\Delta h^{T_{st}}_{H_2O,fg}$ is in kJ/kg and T_{st} is in K. The amount of fuel required, in kJ_{th}/s, to produce this steam can be computed as:

$$\dot{F}_{dryer\ fuel} = \frac{\dot{m}_{steam}\left(h_{steam}\left(T_{st}\right) - h_{fw}\left(T_{a,0}\right)\right)}{\eta_{boiler}} \tag{10.16}$$

Here, η_{boiler} is the boiler efficiency, h_{steam} is the enthalpy of the steam entering the heat exchanger, and h_{fw} is the enthalpy of the boiler feed water, which is usually a function of the ambient temperature. The capital cost of the dryer's boiler is usually a function of $\dot{m}_{steam}$.

The electrical energy consumed by the dryer's fans can be computed, in kW, with the following expression:

$$\dot{E}_{fans} = \frac{\Delta P_{chamber} * \dot{m}_{ac}}{\rho_{air}} * \left(\frac{1\,kN}{1{,}000\ N}\right) \tag{10.17}$$

where $\Delta P_{chamber}$ is the pressure drop in the drying chamber, in Pa, and ρ_{air} is the air density.

Two main parameters that are computed from these equations are the air mass flow rate in the drying chamber ($\dot{m}_{ac}$) and the dryer's heat consumption rate ($\dot{Q}_{dryer}$). These parameters are particularly important for economic analyses. First, $\dot{m}_{ac}$ largely determines the air velocity in the drying chamber (U_{∞}) which in turn affects the pressure drop ($\Delta P_{chamber}$) and the electricity consumption ($\dot{E}_{dryer}$) of the dryer. On the other hand, $\dot{Q}_{dryer}$ exclusively determines the steam consumption of the dryer, and if conventional fuels such as natural gas or propane are used to generate this steam, then the dryer's fuel consumption (equation (10.16)) is greatly dependant on $\dot{Q}_{dryer}$.

The variables in equations (10.1) through (10.17) that are typically known are the ambient temperature, ambient relative humidity ($T_{a,0}$ and $\phi_{a,0}$, respectively), and the initial temperature of the MBB ($T_{MBB,0}$), which can usually be assumed to be equal to $T_{a,0}$. The dry mass flow of MBB traveling through the dryer will, in this case, be determined by how much biomass is needed to fuel a co-fire or reburn system at a particular power plant of a known electric capacity and heat rate. The initial moisture content of the MBB will also be considered a known input value in this analysis. Moreover, the desired moisture content of the MBB ($\%M_{MBB,0}$) is also determined by the needs of the power plant.

However, there are three main design variables, inherent to the dryers themselves, which greatly affect the air mass flow rate and the heat consumption. These variables are: the temperature drop in the drying chamber ($\Delta T_{chamber}$); the temperature of the air exiting the drying chamber (T_a); and the relative humidity of the air exiting the drying chamber (ϕ_a). Ideally, in order to reduce fan power costs and fueling costs, it is necessary to find a combination of these three design variables that will lower both $\dot{m}_{ac}$ and $\dot{Q}_{dryer}$ as much as possible. Beginning with $\dot{m}_{ac}$, is a plot of the air mass flow rate in the chamber vs. T_a and ϕ_a at a fixed value for $\Delta T_{chamber}$ of 10 K. Increasing T_a and ϕ_a will decrease the flow rate. Similarly, Figure 10.4.2 is a plot of $\dot{m}_{ac}$ vs. T_a and $\Delta T_{chamber}$ at a fixed value for ϕ_a of 20%. Again here, $\dot{m}_{ac}$ decreases with higher values of T_a and $\Delta T_{chamber}$.

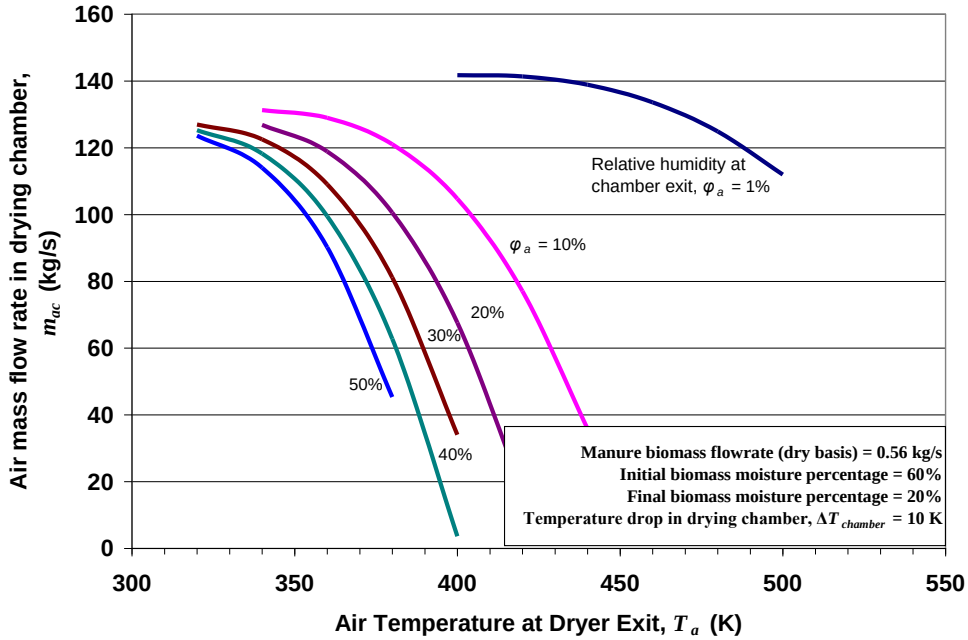

Figure 10.4.2 Dryer air flow rate vs. air exit temperature and exit relative humidity at fixed chamber temperature drop, ΔTchamber = 10 K. MBB being dried from 60% to 20% moisture at a rate of 0.56 kg/s (2 metric tons/hour)

However, in practice a person operating a dryer does not have direct control of T_a, ϕ_a, and $\Delta T_{chamber}$. Instead, the air flow rate and the amount of air that is recycled through the heat exchanger and drying chamber, $(\dot{m}_{ac} - \dot{m}_a)$, can be controlled with dampers and controlling the air fans. But in the context of designing the dryer (or dryers) for providing a predetermined amount of biomass at a required moisture content to a power plant, T_a, ϕ_a, and $\Delta T_{chamber}$ can be treated as the variables, similarly to the analysis by Kiranoudis *et al*. (1994). For example, suppose that two metric tons/hour of biomass is required per dryer, and that the biomass must be dried from 60% moisture to 20% moisture. From the above figures, a set of base case values can be selected. A low flow rate is desired; therefore, $\Delta T_{chamber}$ should be at least 20 K. The temperature of the exiting air cannot be too high since MBB, which is assumed to leave the dryer at a temperature equal to T_a ((10.11)), may begin to rapidly de-volatilize at temperatures over 470 K (386 °F) (Lawrence, 2007). Rodriguez *et al.* (1998) reported that there was a 4.6% loss in heating value when drying cattle manure at 377 K (219 °F) for 360 minutes. Therefore, T_a should certainly be lower than 470 K, and if it is between 370 and 470 K, then the residence time of the MBB in the dryer should be as limited as possible.

To reduce energy costs, a significant amount of the exiting drier air should be mixed with incoming fresh air and recycled back to the heat exchanger and drying chamber. Doing this will keep ϕ_a high, at least to 20%, but recycling the process air will also increase T_a between 360 K and 380 K. The plot of recycled air flow vs. T_a and $\Delta T_{chamber}$ (Figure 10.4.3) shows that this recycled flow rate peaks between 360 and 380 K for $\Delta T_{chamber}$ greater than 10 K.

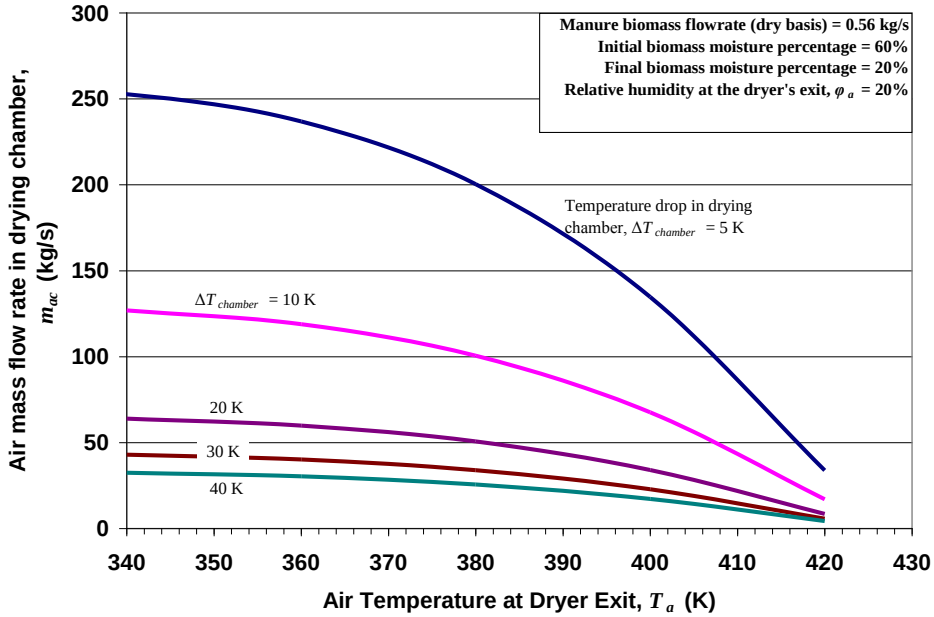

Figure 10.4.3Dryer air flow rate vs. air exit temperature and drying chamber temperature drop at fixed exit relative humidity = 20%. MBB being dried from 60% to 20% moisture at a rate of 0.56 kg/s (2 metric tons/hour)

However, in practice a person operating a dryer does not have direct control of T_a, ϕ_a, and $\Delta T_{chamber}$. Instead, the air flow rate and the amount of air that is recycled through the heat exchanger and drying chamber, $\left(\dot{m}_{ac} - \dot{m}_a\right)$, can be controlled with dampers and controlling the air fans. But in the context of designing the dryer (or dryers) for providing a predetermined amount of biomass at a required moisture content to a power plant, T_a, ϕ_a, and $\Delta T_{chamber}$ can be treated as the variables, similarly to the analysis by Kiranoudis *et al*. (1994). For example, suppose that two metric tons/hour of biomass is required per dryer, and that the biomass must be dried from 60% moisture to 20% moisture. From the above figures, a set of base case values can be selected. A low flow rate is desired; therefore, $\Delta T_{chamber}$ should be at least 20 K. The temperature of the exiting air cannot be too high since MBB, which is assumed to leave the dryer at a temperature equal to T_a (10.11), may begin to rapidly de-volatilize at temperatures over 470 K (386 °F) (Lawrence, 2007). Rodriguez *et al.* (1998) reported that there was a 4.6% loss in heating value when drying cattle manure at 377 K (219 °F) for 360 minutes. Therefore, T_a should certainly be lower than 470 K, and if it is between 370 and 470 K, then the residence time of the MBB in the dryer should be as limited as possible.

To reduce energy costs, a significant amount of the exiting drier air should be mixed with incoming fresh air and recycled back to the heat exchanger and drying chamber. Doing this will keep ϕ_a high, at least to 20%, but recycling the process air will also increase T_a between 360 K and 380 K. The plot of recycled air flow vs. T_a and $\Delta T_{chamber}$ shows that this recycled flow rate peaks between 360 and 380 K for $\Delta T_{chamber}$ greater than 10 K.

Yet, there is a greater reason why T_a should be kept between 360 and 380 K. Ultimately, the most important parameter that must be found from equations (10.1) through (10.17) is $\dot{Q}_{dryer}$, which is independent of the physical dimensions of the dryer such the conveyor belt area (A_{belt}) and only weakly dependant on whether the air flow is perpendicular or parallel to the conveyor belt by equation (10.11). Moreover, $\dot{Q}_{dryer}$ is independent of $\Delta T_{chamber}$. In Figure 10.4.4, $\dot{Q}_{dryer}$ decreases asymptotically below 2,000 kW at exit temperatures above 380 K, for ϕ_a greater than 10%. Fixing T_a at 380 K or above ensures that a minimum amount of heat will be consumed by the dryer.

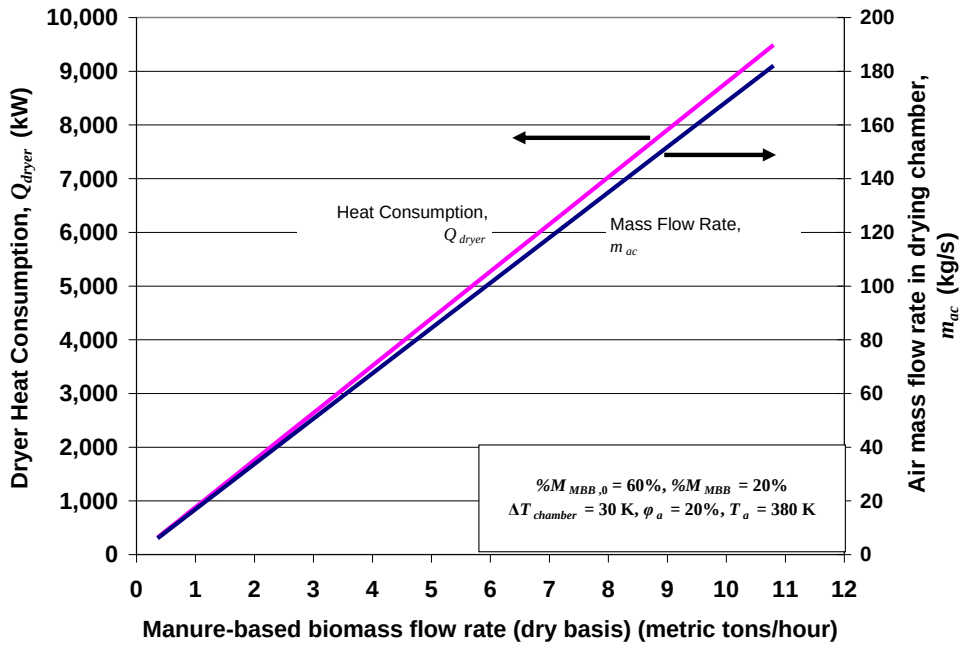

Figure 10.4.4 Dryer heat consumption and air mass flow rate in drying chamber vs. rate of manure-based biomass

Thus, base values for T_a, ϕ_a, and $\Delta T_{chamber}$ of 380 K, 20%, and 30 K, respectively, can be chosen so that $\dot{Q}_{dryer}$ and $\dot{m}_{ac}$ remain low. Next, the MBB handling capacity of the dryer can be increased to investigate how heat consumption and air flow rate will change. This plot is shown in Figure 10.4.5.

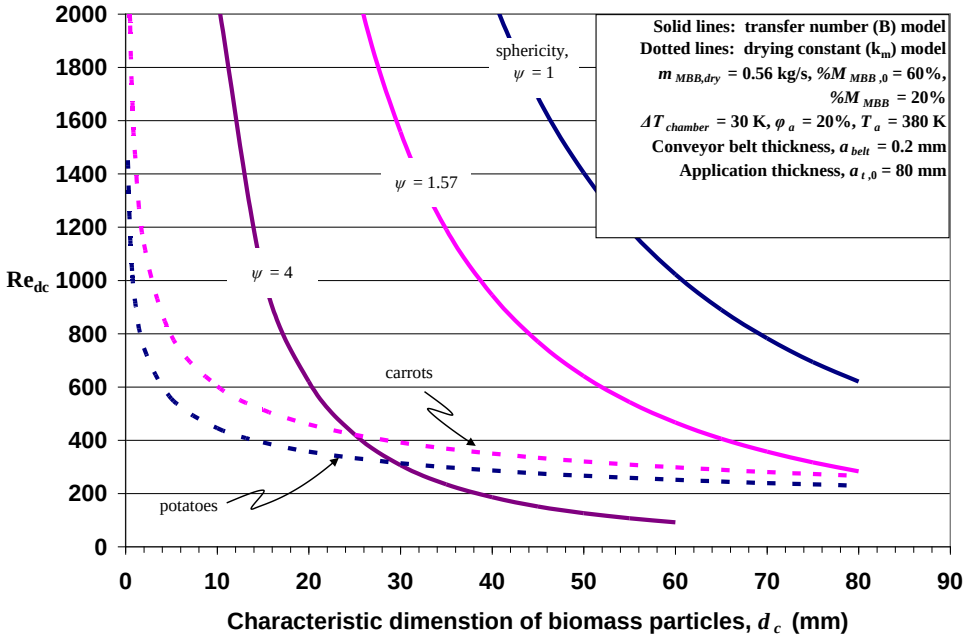

Figure 10.4.5 Comparison of two drying models for perpendicular air flow dryers by monitoring Reynolds number against characteristic biomass particle size and sphericity. Biomass application thickness on conveyor belt = 80 mm

After finding the heat consumption and air flow rate in the drying chamber, the next step in the drying analysis is to find the pressure drop over the conveyor belt, $\Delta P_{chamber}$, and the required area of the conveyor belt, A_{belt}. The pressure drop is needed to compute the electrical energy consumption of the fans while A_{belt} is needed to compute the capital investment cost of the dryer. Both of these parameters are significant when computing the overall cost of drying MBB. Other parameters such as the MBB residence time in the dryer (t) and the velocity of the dryer air (U_∞) can be computed after finding A_{belt}.

The conveyor belt area, unlike $\dot{Q}_{dryer}$ and $\dot{m}_{ac}$, is dependent on whether the dryer air flows perpendicular or parallel to the conveyor belt. For the economic analysis that will follow later in this part of the report, the focus will be on perpendicular flow dryers.

Within the discussion of perpendicular flow dryers in two separate models were presented for determining A_{belt}: one based on a drying rate constant (k_m) defined by:

$$\frac{d\omega_{MBB}}{dt} = k_m\left(\omega_{MBB,E} - \omega_{MBB}\right) \tag{10.18}$$

where $\omega_{MBB,E}$ is the equilibrium moisture percentage of the MBB. Another based on a transfer number (B) defined by:

$$B = \frac{mf_{H_2O,\infty} - mf_{H_2O,s}}{mf_{H_2O,s} - 1} \tag{10.19}$$

The drying constant (k_m) model requires empirical constants. The following table is a list of these constants for several drying experiments on different processed foods.

Table 10.4.1 Empirical constants required for drying constant (km) model for perpendicular air flow dryers

	onions	**peppers**	**potatoes**	**carrots**	**tomatoes**
k_0 (s^{-1})	5.83E-08	1.11E-08	1.72E-07	9.44E-08	NR
k_l	-0.8080	-0.9820	-1.5100	-1.4800	NR
k_T	1.5500	1.5400	0.3210	0.5710	NR
k_ω	0.2480	0.0903	0.0359	0.1110	NR
k_U	-0.1190	0.2930	-0.1440	-0.0624	NR
ω_m (dry basis)	0.2020	0.2110	0.0870	0.2120	0.1820
C_0	2.30E-05	1.46E-05	1.86E-05	5.94E-05	1.99E-05
$\Delta\bar{H}_C$ (kJ/kmol)	32,500	33,400	34,100	28,900	34,500
K_0	5.79E-02	5.56E-02	5.68E-02	8.03E-02	5.52E-02
$\Delta\bar{H}_K$ (kJ/kmol)	6,430	6,560	6,750	5,490	6,700

NR: Not reported
Data adopted from Kiranoudis *et al*. (1992) and Kiranoudis *et al*. (1993)

On the other hand, the transfer number (B) model is dependent on non-dimensional numbers such as the mass transfer Stanton number (St_m) and the Colburn j factor ($\bar{j}_m$) and relationships between these numbers. Both the k_m and the B-models are highly dependent on the characteristic particle size of the MBB (d_c) and the initial manure application thickness on the conveyor belt at the dryer's entrance ($a_{t,0}$). In order to choose which model should be integrated into the overall economic model, these models should be compared against each other to see if there is any agreement between them. One way to compare the two models is by plotting Reynolds number (Re_{d_c}) for each of them. This plot can be seen in Figure 10.4.6. The solid-lined data are results from the B-model, while the dotted-lined data are results from the k_m-model. The Reynolds number is plotted against d_c and the sphericity factor, ψ , for the B-model, and for the k_m-model, it is plotted against d_c for carrots and potatoes.

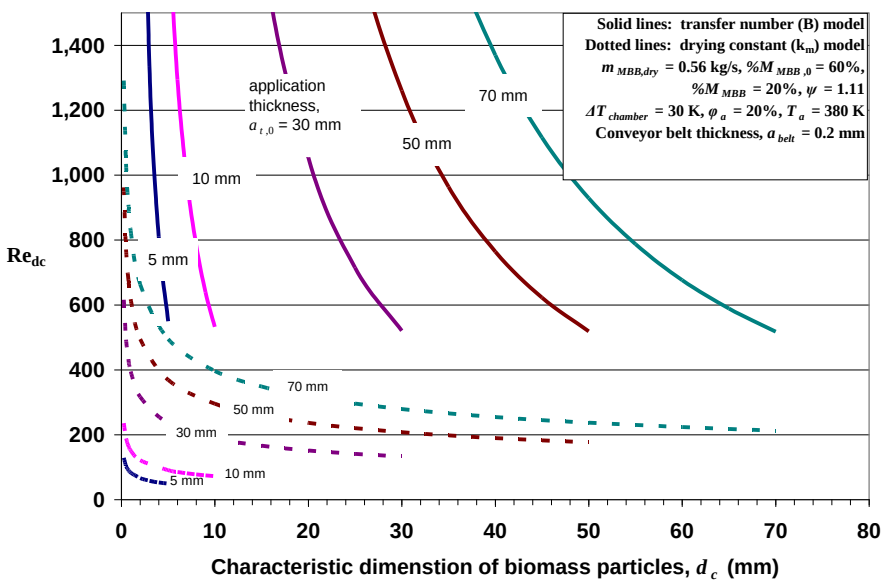

Figure 10.4.6 Comparison of two drying models for perpendicular air flow dryers by monitoring Reynolds number against characteristic biomass particle size and biomass application thickness on conveyor belt

First of all, the curves seem to have the same general shape for both models, indicating that Re_{d_c} increases steeply as d_c decreases. This relationship may seem counter-intuitive at first, since Re_{d_c} is directly proportional to d_c; however, Re_{d_c} is also inversely proportional to A_{belt} (= l * w). It may be shown that A_{belt} is also proportional to not only d_c, but also $\dot{m}_{ac}$. Thus d_c and $\dot{m}_{ac}$ cancel out of the Reynolds equation when equation. The reason why Re_{d_c} still changes with d_c is because the wetted surface area of the biomass particles (A_{MBB}) is inversely proportional d_c as well. Subsequently plugging equation it can be shown that:

$$\mathrm{Re}_{d_c} \propto \left(\frac{1}{\psi \cdot d_c} \right)^{40/23} \tag{10.20}$$

Thus, Re_{d_c} increases quickly with lower d_c, especially for spherical particles ($\psi \approx 1$). Physically, this relationship means that collections of smaller particles with greater surface areas dry quicker, and thus require a smaller conveyor belt area and residence time.

These smaller belt areas in turn increase the air velocity (U_∞). Ultimately, for this drying problem, high Reynolds numbers suggest high air velocities in the dryer. High velocities are problematic however, because manure particles would be blown off of the conveyor belt as they travel through the dryer and hit the fans. The Rosin Rammler characteristic particle size of dried cattle manure is 2.18 mm (0.086 inches). At this particle size, the Re_{d_c} is beyond the 4000 limit. However, for the k_m-model assuming constants for potatoes, the Reynolds number is predicted to be 726 and U_∞ is predicted to be 9 m/s (about 20 mph).

There are two possible reasons for the quantitative disagreement of the models in Figure 10.4.6. (1) Perhaps the food particles studied by Kiranoudis *et al*. truly had high sphericity factors. Higher values of ψ dampen the relationship between Re_{d_c} and d_c in equation (10.20), and bring the curves of the two models to better agreement (see curve for ψ = 4 in Figure 10.4.6). However, such high values for ψ in all of the foods tested by Kiranoudis *et al*. are unlikely. A cubic particle has a sphericity factor of 1.08; a cylindrical particle with an axial ratio of 10 has a sphericity of 1.58, at most (Hinds, 1999). (2) The disagreement between the empirical k_m-model and the *B*-model are more likely due to the inherent limits to the Colburn j factor relationships. These equations are probably more suited to flows over larger particle sizes. Thus the constants and exponents may need to be altered, in effect changing the exponent of 40/23 in equation (10.20). Thus, for the remainder of this discussion and the discussion of the economics model, the k_m-model will be used to estimate A_{belt}. The models did not vary significantly between the different foods listed in Table 10.4.1, so, for brevity in the remaining figures, the constants for potatoes will be used from now on. However, there is still value in the *B*-model in that a greater physical understanding of the drying problem is gained as the k_m-model simply a fit to experimental data.

The Reynolds number, and hence the air velocity, is also a function of the application thickness of the manure on the conveyor belt at the dryer's entrance ($a_{t,0}$). Figure 10.4.7 is a plot of Re_{d_c} against d_c and $a_{t,0}$ at a constant ψ = 1.11. According to the plot, Re_{d_c} increases with $a_{t,0}$. The quantitative disagreement between the k_m and the *B* models can be seen here as well.

During the operation of the conveyor belt dryer, it is necessary to determine the appropriate manure application thickness ($a_{t,0}$). Thicker applications increase the required U_∞ and the pressure drop

in the chamber ($\Delta P_{chamber}$) which in effect increase the electrical consumption of the dryer fans. However, thicker applications also reduce the required conveyor belt area, which reduces the capital investment cost of the dryer (i.e. smaller dryers require thicker applications of manure in order to handle the same throughput and achieve the desired moisture percentage). Thus, a compromise must be made between the two costs. In Figure 10.4.7, A_{belt}, $\Delta P_{chamber}$, and U_∞ are plotted against $a_{t,0}$. The data for this case, suggests that an application thickness of 30 to 50 mm (1.18 to 1.96 inches) would be most appropriate, because both A_{belt} and $\Delta P_{chamber}$ are relatively low at this range. At a 40 mm thickness, the k_m-model for potatoes predicts a required belt area of 9.55 m^2 (about 100 ft^2), an air velocity of 4.89 m/s (about 11 mph), a MBB residence time of about 5 minutes, and a required fan power of 331 kW.

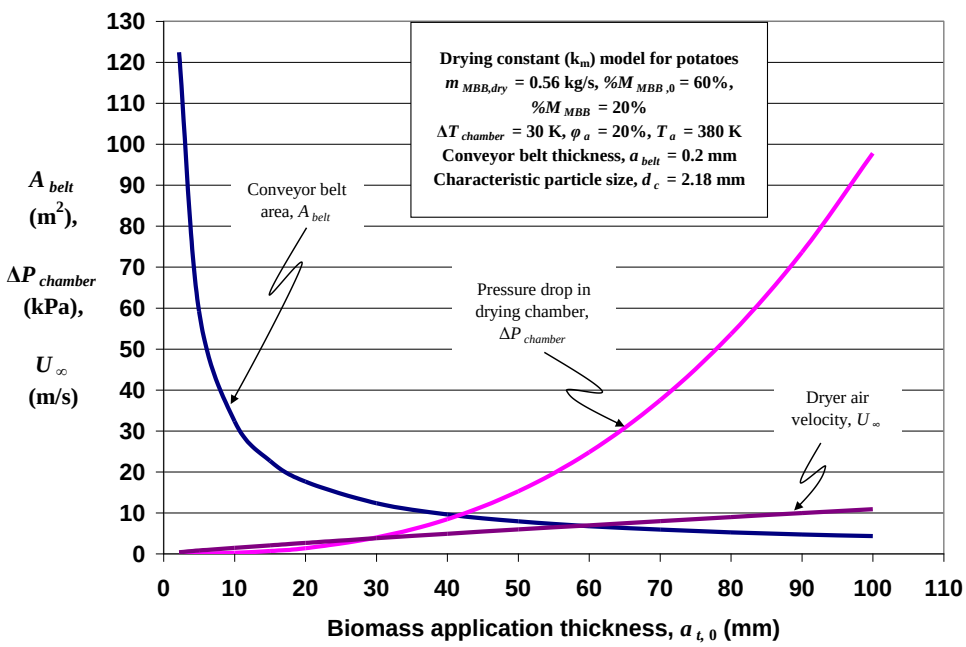

Figure 10.4.7 Determination of appropriate manure-based biomass application thickness

Another option for drying the MBB would be to use a conveyor belt dryer with air blowing parallel to the belt. However, for the manure throughput and moisture reduction required for this drying problem, extremely large belt areas even at very thin application thicknesses ($a_{t,0}$) are predicted. These large areas may be reduced if the cross sectional area of the drying chamber is reduced. However, if cross-sectional area is decreased, the air velocity becomes too great. From these results, perpendicular flow conveyor belt dryers may be more appropriate for drying manure at a scale large enough to supply coal-fired power plants than parallel flow dryers.

The one advantage to parallel dryers is that the conveyor belt does not have to be a screen, since air flows over the belt and biomass and not through them. Solid, non-screen conveyor belts may be helpful since the biomass particles have a wide range of sizes; smaller particles may fall through the screen causing major design issues for the dryer when handling granular solids of non-uniform size.

However, as stated before, conveyor belt size becomes an issue with these parallel flow conveyor belt dryers. An alternative to conveyor belt dryers are rotary dryers. Rotary dryers can handle granular solids with smaller particle sizes such as powders (< 100 mesh) (Brammer *et al*. (1999)), and remain relatively compact compared to conveyor belt dryers. The performance of the rotary dryer can still be compared to the conveyor belt dryer. A list of base parameters for running the rotary dryer model is presented in Table 10.4.2. Again, a biomass throughput of 2 metric tons/hour (dry basis) can be assumed,

as was done for the conveyor belt dryer. The same initial and desired moisture percentages are also assumed for this case.

Table 10.4.2 Base case parameters for rotary steam-tube manure-based biomass dryer

Parameter	Base Value (unit)
Mass flow of MBB through the dryer	0.56 kg/s (2 metric tons/hr)
Initial moisture percentage of biomass	60%
Desired moisture percentage of biomass	20%
Dryer drum diameter	1 m
Drying zone length to drum diameter ratio	5 (m/m)
Rotation speed of drum	35 rpm
Steam tube diameters	0.04 m
Number of steam tubes[a]	36
Characteristic particle size of MBB	2.18 mm
Sphericity factor	1.11
Holdup	5%
Molar fraction of steam in vapor phase	0.9
Boiler pressure	350 kPa, gage
Boiler efficiency	85%

[a]The steam tubes are arranged in two concentric rings around the drum's center. The first is half the distance from the center of the drum to the steam shell, the second is located 80% of the distance from the center of the drum to the shell.

From the base case results it was found that at 2 metric tons/hour, a rotary steam-tube dryer would consume about 16% less heat energy, and thus consume 16% less fuel a if similar 350 kPa (gage) boiler were to provide steam to both dryers. Figure 10.4.8 is a graph of fuel consumption versus biomass flow rate for both a conveyor belt dryer and a rotary dryer. Energy savings become more noticeable at higher biomass throughputs, according to the results of the dryer models. Moreover, the length of the rotary dryer was computed to be 5.29 m (about 17.5 ft). With a rotation speed of 35 rpm, the drum would need to be tilted 0.8 degrees (0.014 m/m) from horizontal and the biomass particles would travel through the drum at about 0.03 m/s (about 6 ft/minute) and have a residence time in the rotary dryer of 2.7 minutes.

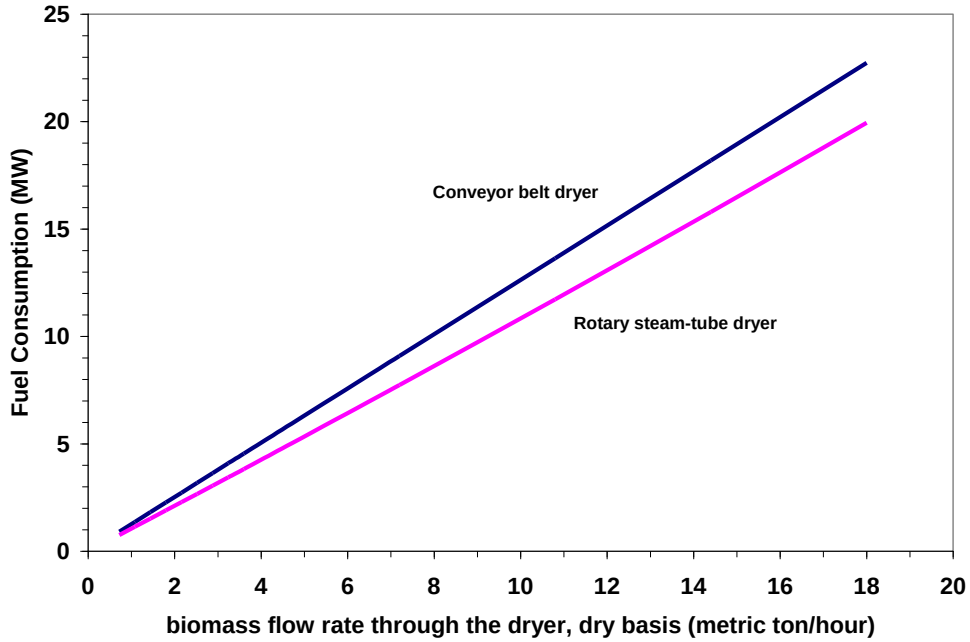

Figure 10.4.8 Comparison of fuel consumption between conveyor belt dryer and rotary steam-tube dryer

Another point of interest for these dryers may be the vapor temperature and the temperature of the biomass in drying zone. For this model, the temperature at which the biomass dries is solely determined by the molar fraction of steam in the vapor phase, $Y_{steam,\ vapor}$. The drying temperature of the biomass is then used to determine the vapor temperature, the length of the heat-up zone of the dryer, and the steam consumption. Figure 10.4.9 is a plot of these temperatures versus $Y_{steam,vapor}$. This plot agrees fairly well with a similar plot made by Canales *et al*. (2001); however, the vapor temperature computed here seems to be two or three degrees below what Canales *et al*. computed. This difference is probably due to a slightly lower boiler pressure (and thus lower steam temperature) for this case.

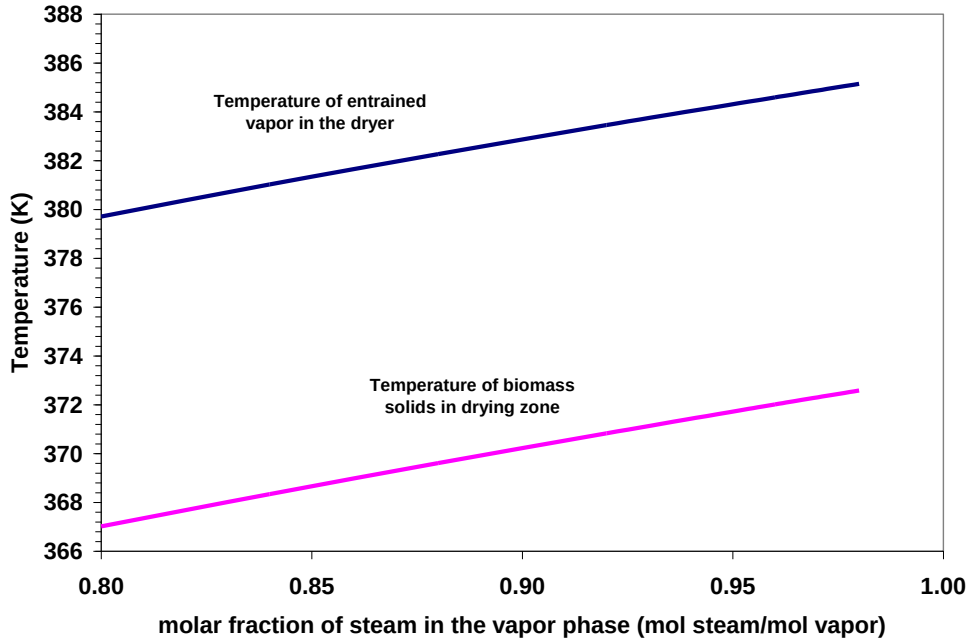

Figure 10.4.9 Temperature of entrained vapor and temperature of biomass solids in the drying zone vs. molar fraction of steam in vapor phase

The vapor temperature is also very dependent on biomass particle size, as can be seen in Figure 10.4.10. Larger particles require more time to heat up to the biomass drying temperature, thus the required length of the dryer is predicted to be slightly longer for larger particles. Since the flow rate of the vapor is fixed by the desired moisture percentage, the vapor spends slightly more time in the dryer heated by the steam tubes and steam shell, and the vapor's temperature begins to approach the temperature of the steam tubes and shell.

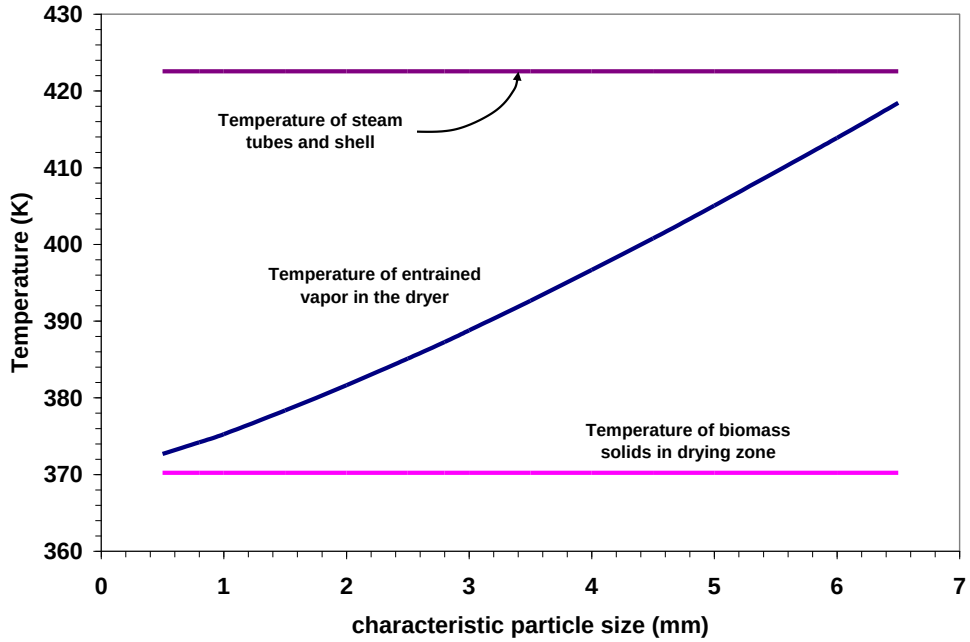

Figure 10.4.10 Temperature of entrained vapor vs. characteristic particle size of biomass solids

One other parameter unique to the rotary dryer is the holdup. Increasing the holdup in the dryer changes most of the operating conditions of the dryer. For example, in Figure 10.4.11, the slope of the drum, the residence time of the biomass and the linear speed at which the biomass solids travel through the drum are plotted against holdup. A greater holdup means that there are more solids in the dryer at any given time. More solids require longer residence times, thus the slope of the dryer must decrease and the biomass must move through the dryer slower.

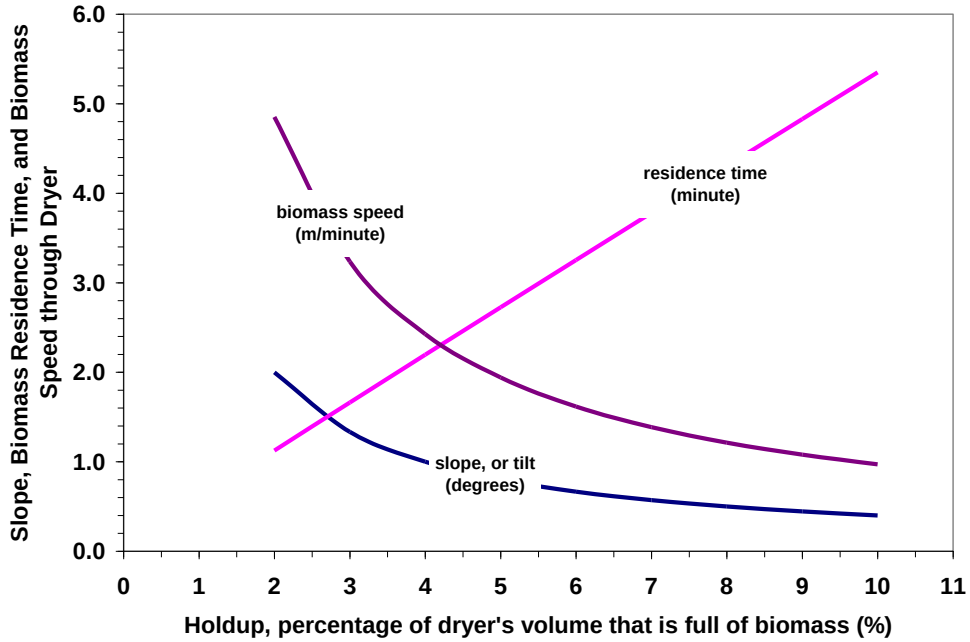

Figure 10.4.11 The effect of holdup on the slope, biomass residence time, and biomass speed through a rotary steam-tube dryer

10.4.2. Biomass Transportation Model

The manure based biomass (MBB) may be transported before or after drying. The decision of when to dry the MBB may greatly affect the transportation costs because the liquid water in the manure is added weight that must also be transported and because the bulk density of the manure is a function of the moisture percentage. The benefit of transporting wet MBB and drying it at the power plant is that waste heat from the plant's combustion processes may be used for drying manure instead of using natural gas or propane. The transportation analysis discussed here was first presented in a USEPA (2001) report for transporting composted solids from feeding operations. However, changes in density were not mentioned in that report and are unique to the analysis presented here. In the USEPA report, densities were assumed to be roughly the same as the density of water (998 kg/m^3).

So, there are seemingly two components when considering transportation costs vs. MBB moisture percentage: if the manure is transported when it is high in moisture, more weight must be carried from the feeding operations to the combustion facility, but the manure will be denser, hence hauling vehicles with fixed carrying volumes (see Figure 10.4.12) can carry more of it. On the other hand, if the manure is transported after drying, when moisture is low, less weight must be transported, but the dried solids will not be as dense and each truck with a fixed carrying volume will not be able to carry as much biomass (assuming no compaction or compression equipment is used to artificially increase the density of the dried MBB).

Figure 10.4.12 Montone 33.6 m3 (44 yd3) dump trailer (Montone Trailers, LLC., 2008)

For example, suppose that 76,000 dry metric tons per year is required by a particular power plant. This is approximately the amount of low-ash dairy biomass that would be required for a 300 MW_e coal plant co-firing a 95:5 blend of Wyoming sub-bituminous coal and MBB. Moreover, suppose the biomass must be transported 50 km (31 miles) to the power plant, that each truck has a carrying volume of 30.6 m^3 (40 yd^3), and that the average truck speed is 80.5 km/hr (50 mile/hr). Manure hauling is assumed to be conducted 16 hours per day and 320 days per year, and loading and unloading times are assumed to be 25 minutes each. In Figure 10.4.14, the number of trucks required and the hauling weight per truck are plotted against the moisture percentage of the MBB when it is transported. These results seem to suggest that even with more liquid mass being hauled for high moisture biomass, the number of trucks required to haul this additional mass will not change significantly due to the increase of bulk density. There is no significant difference in capital or purchasing costs for hauling vehicles once the MBB has been dried below 70% moisture. However, the figure does show that hauling liquid manure, such as flushed manure from free stalls, at 90% moisture would be significantly more expensive.

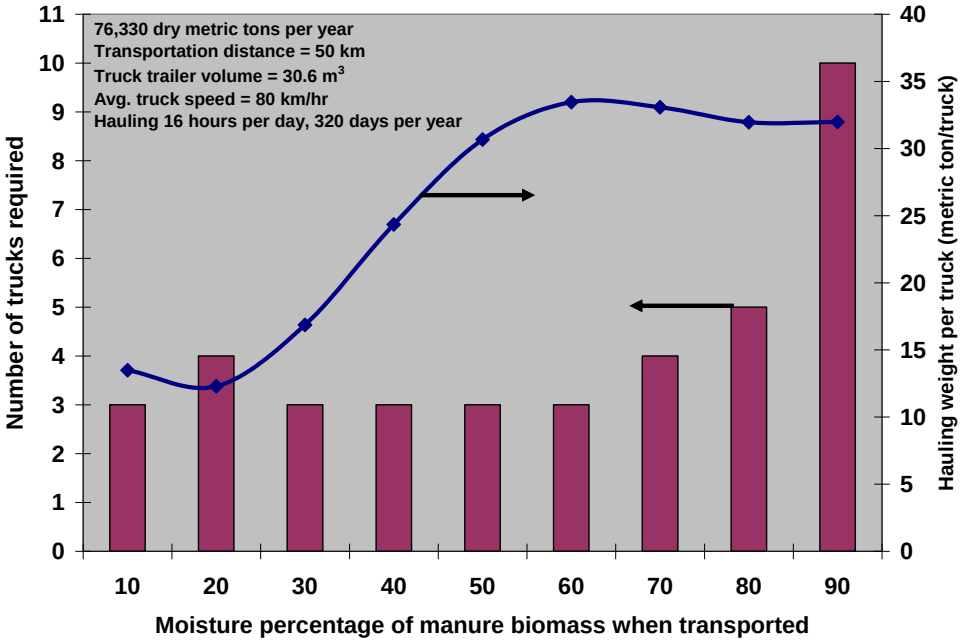

Figure 10.4.13 Number of hauling vehicles and hauling weight vs. moisture percentage of transported manure based biomass

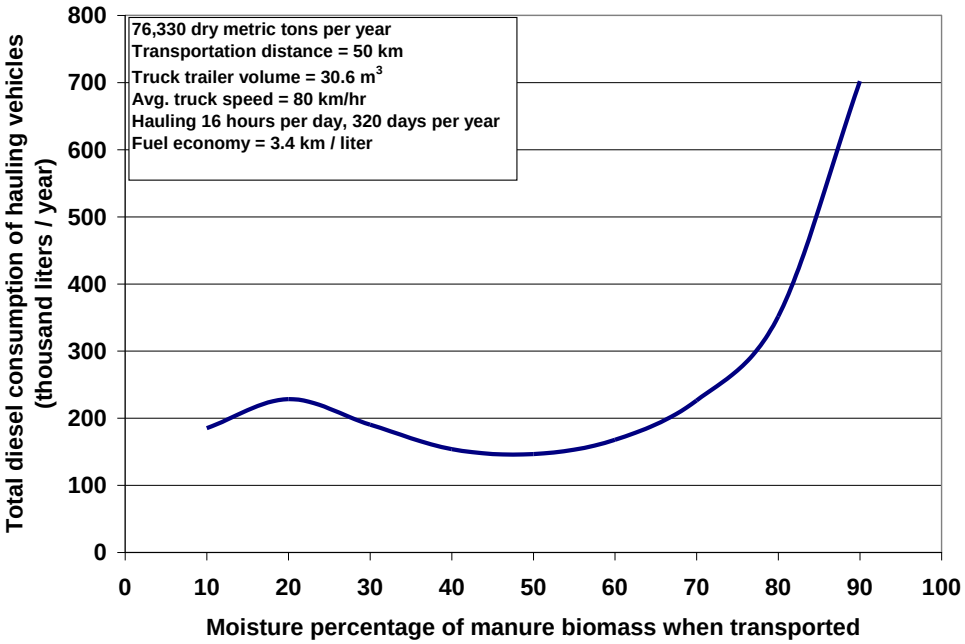

Figure 10.4.14 Total diesel fuel consumption from hauling vehicles vs. moisture percentage of transported manure based biomass

The same analysis can be extended to the fueling costs of the transport vehicles. Figure 10.4.14 is a plot of total diesel consumption of the vehicles vs. the moisture percentage of the MBB when it is hauled. This curve is similar to the data in the previous figure for the number of required trucks. Again, there seems to be no significant difference in fuel consumption between hauling manure with 10%

moisture and hauling manure with 70% moisture. In fact, there seems to be a slight minimum in fuel consumption at approximately 50% moisture. However, fuel consumption does increase dramatically if the moisture content is above 85 or 90%. It should also be noted that these calculations do not take into account any difference in fuel economy for vehicles hauling heavier loads when the manure has higher moisture content, but the aerodynamics and mechanics of the vehicle usually have a greater influence on fuel economy than the haul weight.

Moreover, there are other factors, aside from the number of vehicles required and the fuel consumption that may affect the decision of when to transport the manure. Power plant operators may have reservations to the idea of accepting wet, as-received MBB and drying it at or near the plant due to odor, health, and environmental issues. Also loading and unloading times, as well as the general ease of handling the MBB when it is wet instead of dried, will certainly play into the decision making. Composting and outdoor drying can reduce the MBB's moisture content to an equilibrium value between 20 and 30%. However, natural composting and drying without external heat may not be able to produce enough dried biomass to consistently supply a co-combustion operation at a large coal-plant. This may be especially true for reburn systems, which would require at least 10% of the plant's heat rate to be supplied by biomass reburn fuel, although, biomass storage or stockpiling operations may be a solution. For the base case run of the economics calculations, which will be discussed later in this section, manure will be assumed to be dried with natural gas before transport to the power plant. During sensitivity analysis, cases where it is not necessary to dry MBB with fossil fuel combustion will also be considered.

Other aspects can affect the transportation cost of hauling MBB to power plants. Figure 10.4.15 is a graph of total diesel fuel consumption vs. the distance between the animal feeding operations supplying the MBB and the power plant for the same general conditions described above. Biomass moisture percentage was set at 20%. The number of trucks that would be required to transport all of the biomass is also indicated. As expected, both the fuel consumption and the number of trucks that must be utilized increase when the biomass must be hauled greater distances. These calculations were also conducted for different trailer volumes: 30.6 m^3 (40 yd^3), 19.11 m^3 (25 yd^3), and 11.47 m^3 (15 yd^3) trailers.

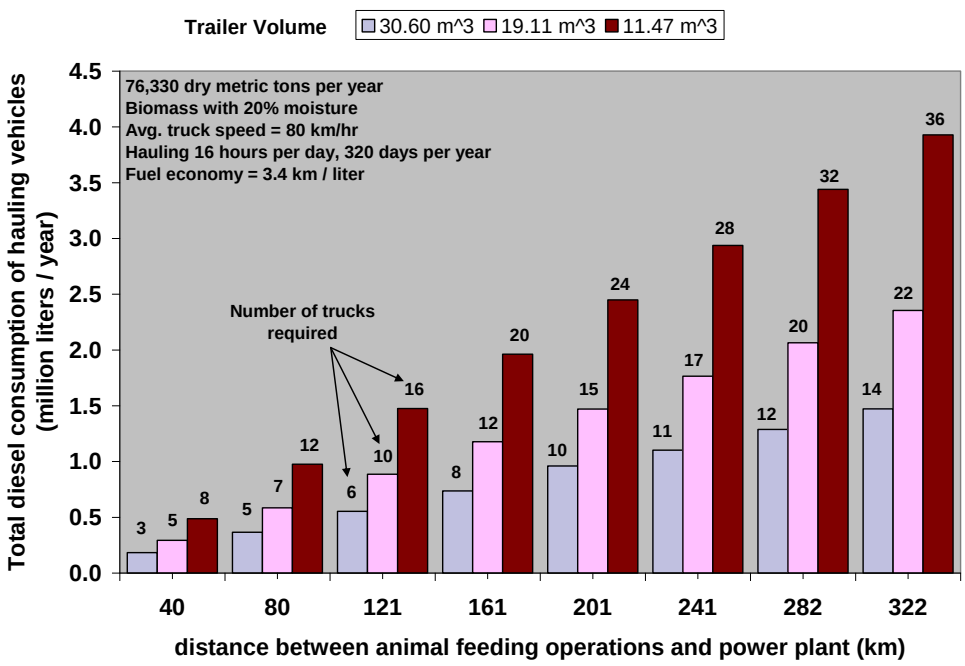

Figure 10.4.15 Total diesel fuel consumption and number of trucks required vs. biomass transport distance and trailer volume

One other major factor in determining the expense of transporting MBB from animal feeding operations to power plants is the time spent hauling the manure. Large electric utility coal-fired boilers generally run constantly; 24 hours per day, 365 days per year; as they provide the base load of the electrical grid. These power plants only make scheduled stops in operation for maintenance and up-grades. However, the transportation system that supplies MBB to the power plants may not run constantly, and may only run a small fraction of each day or each year. Figure 10.4.16 is a plot of the number of trucks required vs. the number of hours spent hauling manure each day and the number of days per year spent hauling. Again, the same other conditions were assumed for this plot as in the previous figures. One interesting result from this plot is that there seems to be a greater difference between hauling for one 8-hour shift and two 8-hour shifts (i.e. 16 hours) versus the difference between hauling for two shifts and three 8-hour shifts (i.e. 24 hours per day). This larger margin between these three hauling schedules is probably due to the fact that in the calculations, the total annual amount of MBB required and the volume of each truck are fixed. Thus, in some cases for the shorter hauling schedules, some of the trucks at the end of the schedule may be hauling below their capacity.

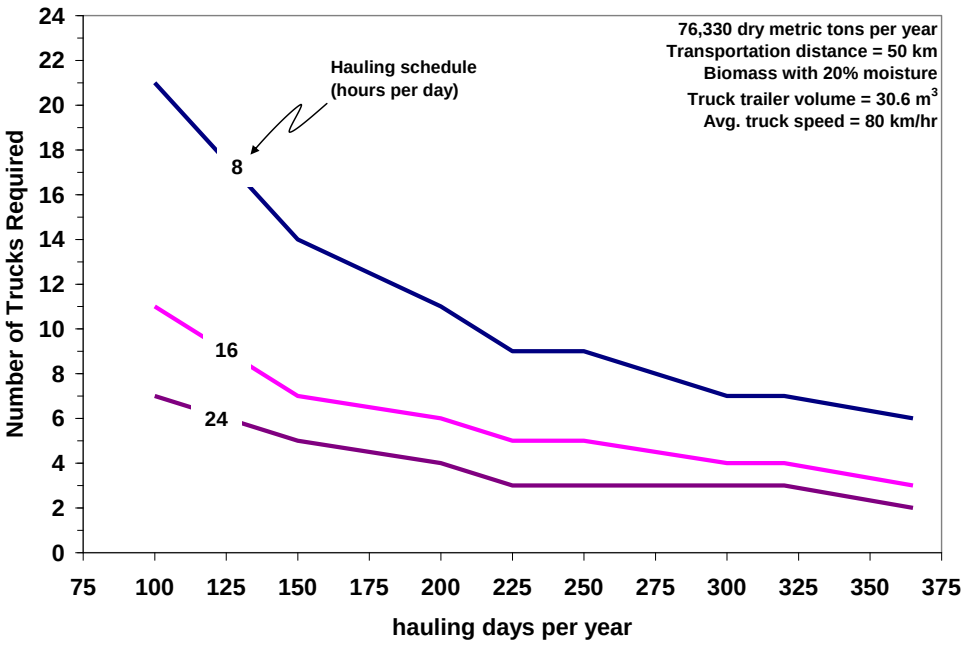

Figure 10.4.16 Number of trucks required for hauling MBB vs. hauling schedule and annual number of hauling days

10.5. Economics of Manure-based Biomass Combustion in Large-scale Coal-fired Power Plants

The equations presented in the modeling section of this paper were integrated into three large computer spreadsheet programs: one for computing the overall economics of co-firing coal with MBB at an existing coal plant, another for the overall economics of reburning coal with MBB, and a third for computing the general performance of a small-scale system operating at a concentrated animal feeding operation. These spreadsheet programs were useful tools for studying the feasibility and cost of utilizing MBB in combustion systems. They were also used for parametric studies to determine the limiting factors that may reduce the success of manure biomass combustion. First, in this part of the dissertation, the results of the co-fire model will be discussed, followed by the reburn model.

10.5.1. Co-firing

An outline of the co-fire model is presented in Figure 10.5.1. The program can be divided into three main computing blocks: (1) for estimating the fueling, emissions and costs when burning coal alone, before any co-firing, (2) for computing the same costs when co-firing coal with biomass plus any addition O&M, transporting and drying costs, and (3) for comparing the two operating conditions with an economic analysis.

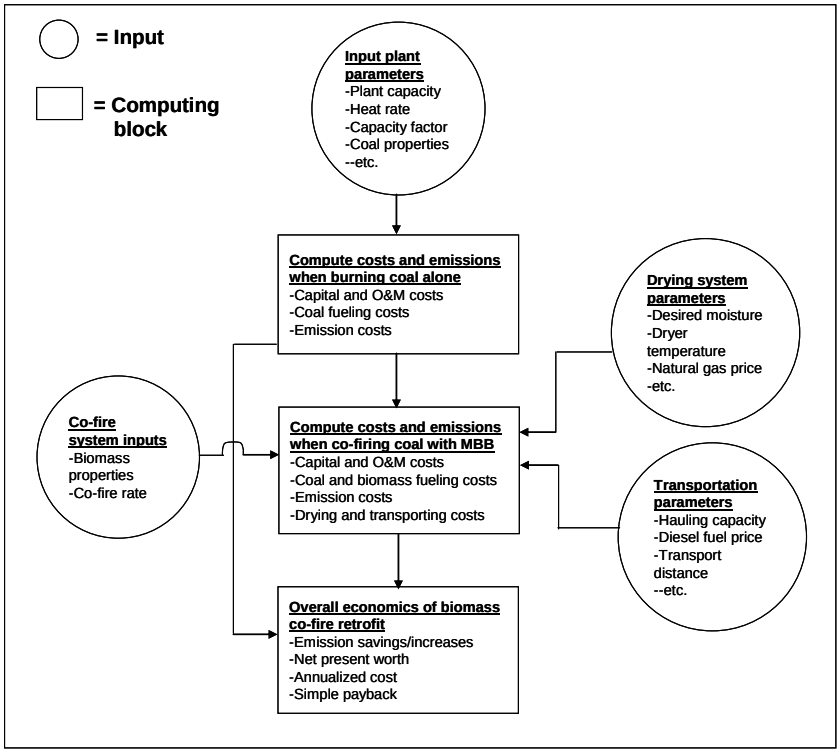

Figure 10.5.1 Flow diagram of computer spreadsheet model for coal/manure-based biomass co-firing system on an exiting coal-fired power plant.

10.5.1.1. Base case inputs and results

To demonstrate the usage of the economic spreadsheet model for co-firing, some base case input parameters were chosen. Most of these parameters are best guess values taken from research and literature review. This set of inputs acted as a reference point for parametric study and sensitivity analysis. Table 10.5.1 through Table 10.5.5 are lists of all base case input parameters pertinent to modeling the installation and the operation of the MBB co-firing system. However, these base case inputs are not set. These numbers can and should be changed to accommodate different situations and facilities. In fact, variations of many of these input parameters were made to study the sensitivity of the overall net present worth and annualized cost. This discussion will follow a brief review of the base case findings.

Table 10.5.1 Base case input parameters for coal-fired power plant operating conditions and emissions

Input	Value (unit)	Source	Notes
Plant capacity	300 MW_e		

Input	Value (unit)	Source	Notes
Heat rate	10,290 kJ_{th}/kWh_e (9750 Btu/kWh)		About 35% plant efficiency, average for most coal-fired power plants
Capacity factor	80%		
Operating hours[a]	8760 hr/yr		1 year = 8760 hours. Non-stop utility operation.
Primary fuel	WYPRB coal	(TAMU, 2006)	Moisture percentage for coal when fired is 30%
Boiler type	Tangentially-fired		
Coal cost	$38.58/metric ton	(EIA, 2007d)	As delivered cost for WY Powder River Basin Sub-bituminous coal in Texas.
Farmer's asking price for MBB	$0/dry metric ton		For the base case, the MBB will be assumed to be free of charge.
CO_2 price	$3.85/metric ton	(RGGI, 2008)	Slightly higher than the clearing price of CO_2 allowances at the September 2008 auction of the Regional Greenhouse Gas Initiative.
SO_x credit/allowance	$970/metric ton	(SCAQMD, 2007)	Average annual price for Compliance Year 2005.
Ash sale price	$27.56/metric ton	(Robl, 1997)	Range: $27.56 - 33.07/metric ton
Ash disposal cost	$33.07/metric ton	(ACAA, 2006)	Range: $22.05 - 44.09/metric ton. Landfill tipping fees for non-hazardous waste.
Percentage of ash sold[b]	20%	(Robl, 1997)	For coal, 61% of solid byproduct is fly ash which can be sold for outside use. On average, only 11% of solid byproduct is sold.

[a]For base case, reburn, SCR and SNCR systems are assumed to operate during all plant operating hours

[b]For base case run, ash sold during reburning is the same, by mass, as that sold when only primary controls are used

Note: metric tons = 1,000 kg = 1.1 ton

Table 10.5.2 Base case input parameters for co-firing and SOx controls

Input	Value (unit)	Source	Notes
Co-fired fuel	LADB	(Sweeten *et al*, 2006)	
Co-firing Rate	5% (by mass)	(DOE, 2004), (USEPA, 2007c)	Range: 2 - 15%. Generally power plants greater than 500 MW capacity co-fire at 2% biomass. Plants with capacities between 201 and 500 MW co-fire at 10% biomass. And smaller plants, less than or equal to 200 MW co-fire at 15% biomass.
Co-fire capital cost	Variable, See Notes	(USEPA, 2007c)	If capacity of power plant is >500 MW_e, then \$109/kW_e supplied by biomass. If capacity is 201 - 500 MW_e, then \$218/kW_e. If capacity is <200 MW_e, then \$251/kW_e.
Co-fire fixed O&M	\$7.63/kW supplied by the co-fired fuel per year	(USEPA, 2007c)	Does not include transportation costs of biomass if co-firing rate is larger than the standard rate. For example, if a 500 MW plant has a co-firing rate greater than 2%, then additional transportation costs must be added to the total O&M costs since more biomass is required to satisfy the desired co-firing rate. In the case of manure-based biomass, this does not include drying costs.
SO_x control	Flue gas desulphurization system **is** installed		
SO_x reduction efficiency[a]	95%	(USEPA, 2004)	Typical for Limestone Forced Oxidation (LSFO), which can reduce SO_x down to about 0.06 lb SO_x/MMBtu and is applicable to plants with greater than 100 MW capacities

[a]For the base case run, the SO_x reduction efficiency during co-firing is assumed to be the same, by percent, as the reduction efficiency during normal operations when only coal is burned.

Table 10.5.3 Base case input parameters for manure-based biomass drying system

Input	Value (unit)	Source	Notes
Biomass moisture percentage before drying	60%	(Carlin, 2005)	Typical for partially composted separated dairy biomass solids from flushing system
Biomass moisture percentage after drying	20%	(Annamalai *et al*., 2003a), (Annamalai *et al*., 2005)	Approximate moisture percentage of biomass during co-firing and reburn experiments
The biomass is dried before it is transported to the power plant	--		The biomass can possibly be dried at the power plant by using waste heat from the combustion processes at the plant. However, this may increase the cost of transporting the biomass and it may not be allowable to have as received manure biomass at the power plant.
Capacity of single biomass dryer	2 metric tons (2.2046 tons)		Smaller scale dryer such as those discussed by Brammer *et al*. (2002)
Height of drying chamber	0.5 m (1.64 ft)	(Brammer *et al*, 2002)	
Width of drying chamber	0.5 m (1.64 ft)	(Brammer *et al*, 2002)	
Number of drying days	300 days/yr		Approximately 6 days per week, minus holidays
Drying schedule	20 hrs/day		2 1/2 eight hour shifts
Dryer operators	0.4 employees/dryer		Employees operate loaders and maintain the dryers
Number of loaders	0.2 loaders/dryer	(GSNet.com, 2007)	3.86 - 4.63 m^3 (5 - 6 yd^3) capacity per loader. Loaders carry biomass from dryer to transport vehicles. Capital cost of each loader is about $200,000.
Characteristic particle size of manure	2.18 mm (0.09 inches)	(Houkum, 1974)	Characteristic size for Rosin-Rammler distribution of low moisture beef cattle biomass

Input	Value (unit)	Source	Notes
			particles
Temperature of biomass entering the dryer	25 °C (77 °F)		Same as ambient air temperature, see next item
Ambient air temperature	25 °C (77 °F)		Annual average day time temperature for central Texas
Ambient relative humidity	50%		Annual average day time relative humidity for central Texas
Temperature of air exiting the dryer	107 °C (224 °F)	(Rodriguez *et al*., 1998)	Can be, at most, 195 °C (383 °F) before rapid de-volatilization occurs. Moreover, at drying temperatures over 100 °C (212 °F), drying times should also be limited to less than five minutes to preserve the biomass's heating value.
Relative humidity of air exiting the dryer	20%		
Air temperature difference in dryer	30 °C (54 °F)		Difference between temperature of air entering and exiting the drying chamber. Generally determined by the air flow through the dryer.
Boiler pressure	345 kPa (gage) (50 psig)		Capital cost of each boiler is approximately $44/(kg/hr) or $20/(lb/hr) of steam production
Boiler efficiency	85%		
Labor cost for dryer operators	$15/hr		
Cost of electricity	$0.09/kWh$_e$	(EIA, 2007e)	Average retail price for 2006 commercial consumers
Natural gas price	$7.36/GJ ($7.76/MMBtu)	(EIA, 2007b)	Average 2006 price for electricity producers

Input	Value (unit)	Source	Notes
Land requirement	4 hectares per drying site		Note: 1 hectare = 10,000 m^2. It was estimated that one drying site of this size could house 5 dryers
Land cost	$12,350/hectare ($5,000/acre)		This cost may also include general overhead costs such as small office buildings and parking lots at the drying sites.
Extra storage structures	four 30.6 m^3 storage trailers		122.3 m^3 (160 yd^3) of total extra biomass storage (about 2 days extra capacity) in case of inclement weather.

Table 10.5.4 Base case input parameters for manure-based biomass transportation system

Input	Value (unit)	Source	Notes
Loading & unloading times	25 min each	(USEPA, 2001)	
Average distance between plant and animal feeding operations	80 km (50 miles)		This distance should be an average distance weighted by the amount of biomass from each animal feeding operation contributing to the power plant's fueling
Number of hauling days	300 days/yr		Approximately 6 days per week, minus holidays
Hauling schedule	16 hrs/day		2 eight hour shifts
Truck capacity	30 m^3 (40 yd^3)	(GSNet.com, 2007)	30 m^3 (40 yd^3) trailers cost roughly $40,000 each, and the truck tractors hauling the trailers cost approximately $150,000 each.
Truck maintenance	$0.31/km ($0.50/mile)	(USEPA, 2001)	
Labor cost for biomass haulers	$15/hr		
Diesel fuel price	$0.79/liter ($3.00/gal)		
Average truck speed	80.5 km/hr (50 mph)	(Krishnan *et al.*, 2005)	Fuel economy for the hauling vehicles was assumed to be 3.4 km/liter (8 mpg)
Rated truck horse power	373 kW (500 hp)	(Peterbilt.com, 2009)	
Truck load factor	70%	(Krishnan *et al.*, 2005)	
Truck SCR cost	$3,120/yr	(Krishnan *et al.*, 2005)	Includes O&M and annualized capital costs. SCR can meet 74.5 g/GJ (0.2 g/bhp hr) NO_x levels; 2007 standards

Table 10.5.5 Base case economics input parameters

Input	Value (unit)	Source	Notes
Book Life	30 years	(USEPA, 2004)	Balance sheet for corporate financing structure for environmental retrofits
Real (non-inflated) Discount Rate	5.30%	(USEPA, 2006)	"
Inflation Rate	4.00%		
Capital Charge Rate	12.10%	(USEPA, 2006)	Balance sheet for corporate financing structure for environmental retrofits
Tax Rate	34.00%	(Turner, 2001)	Omnibus Reconciliation Act of 1993: Marginal tax rate for taxable incomes between $335,000 and $10,000,000
Assumed annual rates of price escalation based on data from the US Bureau of Labor Statistics from 1998 to 2007			
Transport vehicles	0.00%	(US Bureau of Labor Statistics, 2008)	Estimated from the combined average annual rate of price increase for truck tractors and trailers between 1998 and 2007 (computed from Producer Price Commodity Indexes). Truck trailers increased in price by about 2.66% annually, but truck tractors decreased in value by about 0.73% between 1998 and 2007.
Dryers	3.90%	(US Bureau of Labor Statistics, 2008)	Estimated from the average annual rate of price increase for industrial food production machinery (e.g. dryers) between 1998 and 2007 (computed from Producer Price Commodity Indexes)
Coal	3.77%	(US Bureau of Labor Statistics, 2008)	Estimated from the average annual rate of price increase for bituminous coal and lignite between 1998 and 2007 (computed from Producer Price

Input	Value (unit)	Source	Notes
			Commodity Indexes)
Natural gas	5.00%		The prices of natural gas and propane have increased by about 10% and 20% annually, respectively on average, from 1998 to 2007. The assumed values are more optimistic because such high annual price increases would certainly make any co-fire or reburn project economically unfeasible if prices were to increase at these rates throughout the life of the project.
Propane	5.00%		"
Electricity	3.71%	(US Bureau of Labor Statistics, 2008)	Estimated from the average annual rate of price increase for industrial electrical power between 1998 and 2007 (computed from Producer Price Commodity Indexes)

Table 6.7, continued

Diesel fuel	5.00%		The price of diesel has increased by 20% annually, on average from 1998 to 2007. The assumed value of 5% is more optimistic because such a high annual price increase would make transporting biomass unfeasible if the price were to increase at this rate throughout the life of the project. Moreover, the rate computed from the Producer Price Commodity Indexes is somewhat skewed due to the large price increase of oil and petroleum products in 2007.
Labor	1.50%	(US Bureau of Labor Statistics, 2008)	
CO_2 allowances	5.25%	(Sekar *et al*., 2005)	The estimated annual increase of the value of CO_2 under the proposed

Input	Value (unit)	Source	Notes
			McCain-Libermann bill of 2003
SO_2 allowances	4.00%	(SCAQMD, 2007)	
Ash sales	1.00%		
Ash disposal (tipping fees)	1.00%		

From the base case inputs, a resulting reference run was completed. The base case results for fueling and emission rates for a 300 MW_e coal-fired power plant, before any co-fire or reburn system is implemented, are summarized in Table 10.5.6 These rates may be compared to those in Table 10.5.7 for fueling and emissions when the same power plant is fueled with a 95:5 blend (by mass) of coal and MBB. The annual energy consumption was found to increase by about 259,000 GJ per year when co-firing with MBB. This includes the energy consumed by drying equipment and transportation vehicles. The heat energy released by the MBB when burned at the power plant (i.e. 794,800 GJ/yr in Table 10.5.7) was found to be 535,000 GJ more than the energy needed to dry it and transport it to the plant.

Table 10.5.6 Base case fueling and emissions results for a 300 MWe coal plant operating before any co-firing or reburning system is installed

		Coal only (burned with primary NO_x controls and FGD)
Fueling rate	GJ/yr	21,625,812
	metric ton/yr	1,137,322
CO_2 emission	g/GJ	93,497
	metric ton/yr	2,021,983
SO_2 emission	g/GJ	15
	metric ton/yr	324
Ash emission	g/GJ	3,093
	metric ton/yr	66,897
NO_x emission	g/GJ	84
	metric ton/yr	1,822

Total CO_2 emissions when co-firing with MBB, including carbon emissions from biomass drying and transportation, were found to be 58,600 metric tons per year less than CO_2 emissions before implementing co-firing. However, this estimate assumes that all of the electricity used to run the dryer's fans was generated completely from coal combustion. Moreover, SO_2 emissions were found to increase slightly when co-firing, but this is mostly because a flue gas desulphurization system was assumed to be installed whether MBB was being burned or not. Otherwise, higher sulfur contents in the biomass compared to the Wyoming sub-bituminous coal may have been more of a factor. Finally, ash emissions were found to increase by about 10% when co-firing with only 5% MBB under the base case run, even though the MBB was of the low-ash variety.

Table 10.5.7 Base case fueling and emissions results for a 300 MWe coal plant operating while co-firing manure-based biomass (5% by mass)

Number of drying sites	1
Number of dryers (each rated at 2 dry metric tons/hr)	5
Number of dryer operators	2
Total hectares required for drying site(s)	4
Total extra storage trailers	4
Number of hauling vehicles required (30.6 m^3 each)	3
Number of cows required (6.35 dry kg/cow/day)	21,000

		Primary fuel (coal)	Co-fired fuel (MBB)	Dryers (natural gas)	Dryers (electricity for fans)[a]	Hauling vehicles (diesel)	Total
Fueling rate	GJ/yr	20,831,030	794,782	213,423	36,931	9,091	21,885,256
	metric ton/yr	1,095,524	57,693	4,268	2,169	189	n/a
CO_2 emission	g/GJ	90,063	3,681	55,005	93,497	64,290	n/a
	metric ton/yr	1,947,672	79,655	11,709	3,453	584	1,963,418[b]
SO_2 emission	g/GJ	14.43	1.23	n/a	n/a	n/a	n/a
	metric ton/yr	312	27	n/a	n/a	n/a	338
Ash production	g/GJ	2,980	426	n/a	n/a	n/a	n/a
	metric ton/yr	64,439	9,220	n/a	n/a	n/a	73,659

[a]Electricity for fan operation is assumed to come entirely from coal. Fueling and emission rates are for the equivalent amount of coal required to produce the electricity in a power plant with an overall efficiency of 35%.

[b]Excluding CO_2 emissions from renewable fuels such as the MBB co-fired fuel

Yet economically, co-firing coal and MBB was found to be 2.3% more expensive than burning coal alone, under base case assumptions. A list of cost components at Year 1 and the overall sum of these costs and revenues for both firing coal alone and burning coal with MBB under the base case assumptions are juxtaposed in Table 10.5.8. The major increase in cost of co-firing MBB comes from the variable O&M increase, largely due to biomass drying operations. However, this is partly offset by combined (coal and biomass) fuel delivery savings of about $990,000. Yet, increased fixed O&M cost and $223,700 more in ash disposal costs (even when the co-fire rate is only 5%, by mass) make co-firing coal with MBB more expensive, at Year 1, under base case assumptions.

Table 10.5.8 Comparison of base case Year 1 costs for power plant operation before and during manure-based biomass co-firing (300 MWe plant, 5% biomass by mass)

Year 1 Costs	**Coal Combustion only**	**Co-firing Coal with Biomass**
Fixed O&M Cost	0	67,261
Variable O&M Cost[a]	0	2,155,166
Biomass Delivery Cost	0	620,100
Coal Delivery Cost	43,878,448	42,265,847
CO_2 Penalty	7,800,913	7,574,966
SO_2 Penalty	314,864	329,081
Ash Revenue	(368,704)	(368,601)
Ash Disposal Cost	1,769,781	1,993,493
Annualized Capital Cost	0	594,887
TOTAL COST (w/o capital)	53,395,301	54,637,314

[a]For MBB, variable O&M includes the cost of drying the biomass

In order to compute the net present worth (NPW) of a MBB co-fire implementation project, the cash flows throughout the life of the project must be computed. This analysis requires knowledge of the discount (non-inflated) rate, inflation rate, price escalation rates, and the project life. The base case values of these parameters are listed in Table 10.5.5. Usually an economically attractive project would generate annual revenue in order to pay off the initial investment of the project. In the case of the co-fire project, the hope is that avoided CO_2 emission costs (allowances, taxes, avoided sequestering and/or storage costs) and avoided coal fueling costs will overrule the additional costs of drying and transporting the biomass, grinding and burning the biomass at the plant, and the cost of disposing ash emitted when burning MBB. However, at least for the base case run, this payoff was found not to occur. The total operating cost (or revenue) at year one can be computed by taking the difference of the total costs listed in Table 10.5.8 (i.e. $54,600,000 – $53,400,000 = $1,200,000). Even though the value of carbon and the price of coal were assumed to escalate annually by 5.25% and 3.77%, respectively; the price of natural gas, electricity, and diesel fuel, which are all necessary to supply the biomass under the base case assumptions, escalate as well at similar rates.

Thus, the operating cost of the co-fire project only grows throughout the project life without any return, as can be seen in Figure 10.5.2 The discounted values of the operating costs are also displayed in present dollars. The total initial investment of the project was found to be $5.9 million dollars. After adding the discounted operating costs throughout the project, the 30-year NPW for the base case run was found to be negative $22.6 million (i.e. net present cost). Distributing this NPW evenly through all 30 years showed that the annualized cost of co-firing would be $2.30 million per year. Also the specific CO_2 reduction cost was found to be $35.68/ton CO_2. Dividing the annualized cost by the electricity output of the plant showed that co-firing coal with MBB would cost 0.11 ¢/kWh$_e$.

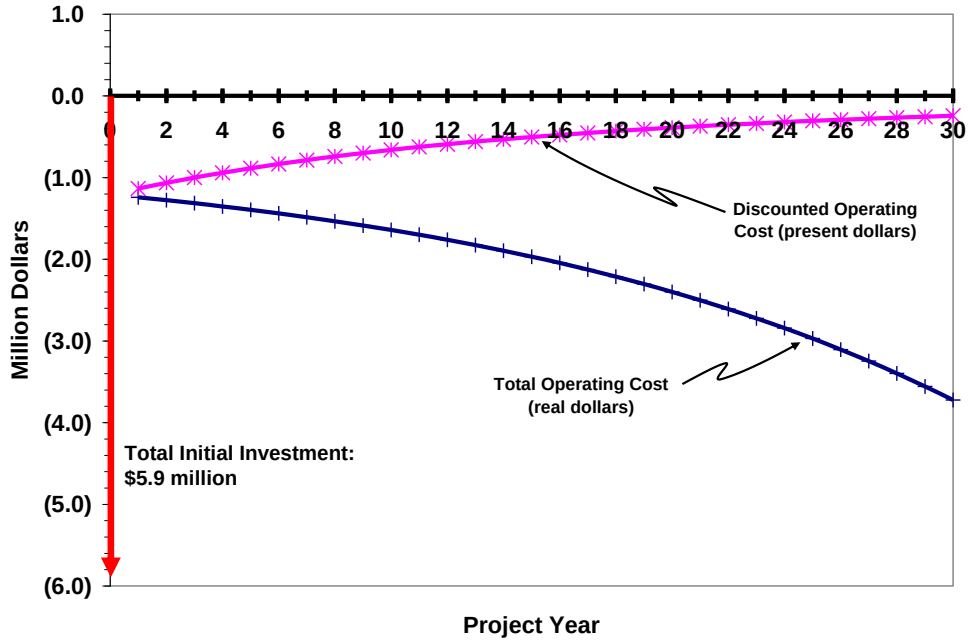

Figure 10.5.2 Overall cash flows for the base case run of the manure-based biomass co-fire economics model

These results will act as the base case for the remainder of this discussion on the economics of co-firing coal and MBB. Each parameter will be varied while holding all other parameters fixed at their respective base values. Some of the more significant parameters such as transport distance and diesel price will be discussed presently.

10.5.1.2. Biomass and coal fueling

The amount of MBB burned along with the coal can greatly influence the overall cost of the system. However, whether an increase in co-fire rate will increase or lower the overall cost may not be intuitively clear, since transport and drying costs will go up, but revenue from avoided CO_2 and avoided coal will also increase. Yet in Figure 10.5.3, drying and transport cost seem to dominate even at higher co-fire rates. The annualized cost of the co-fire system rises steadily with higher co-fire rates.

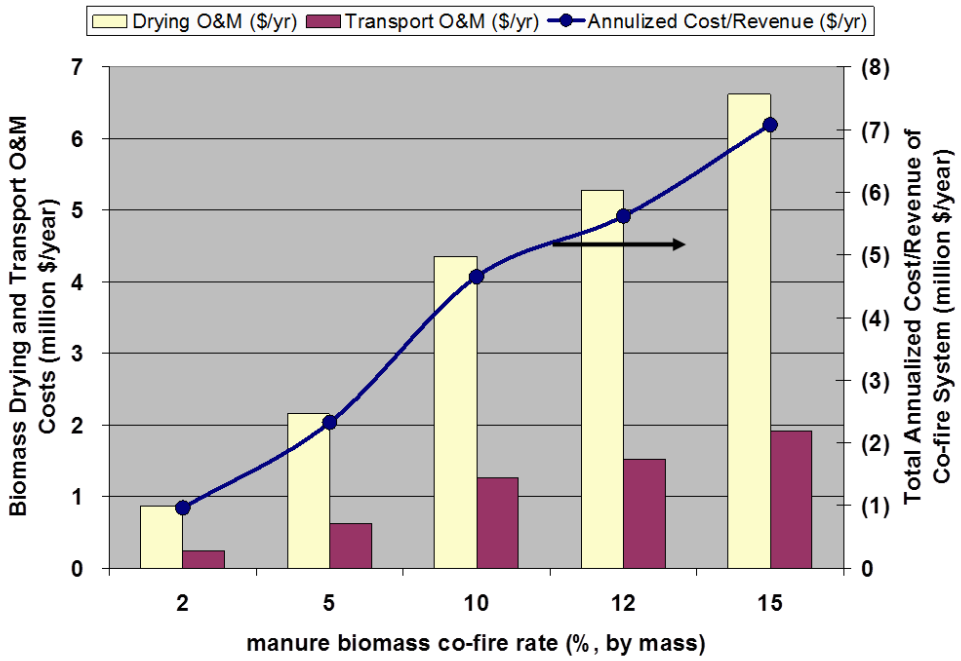

Figure 10.5.3 Biomass drying and transportation cost and annualized cost/revenue of biomass co-fire system vs. the biomass co-fire rate

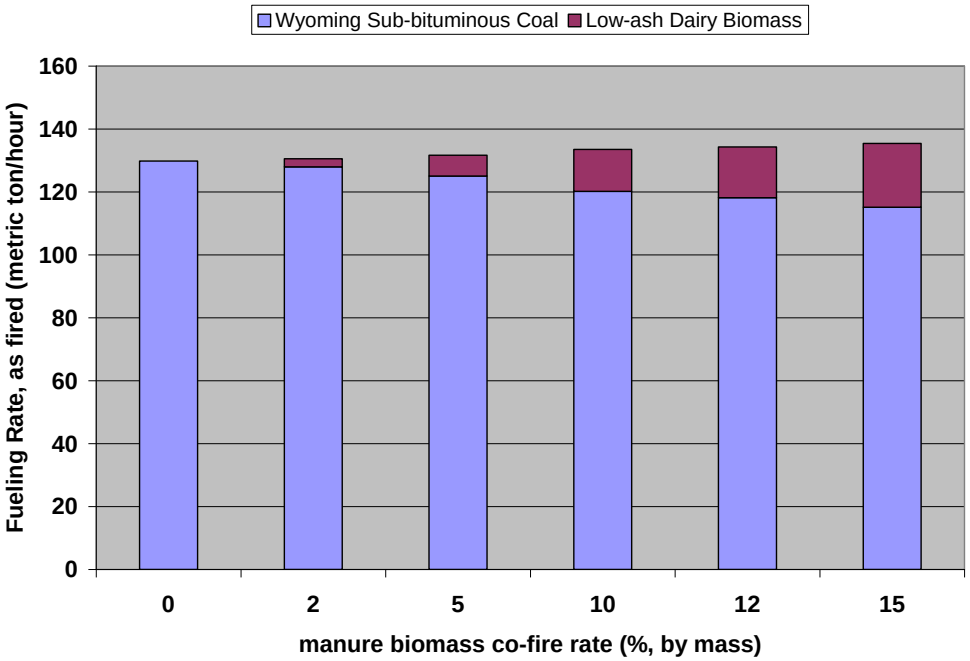

Figure 10.5.4 Fueling rates for Wyoming sub-bituminous coal and low-ash dairy biomass vs. co-fire rate

The MBB displaces some of the coal that must be purchased by the plant operator as seen in Figure 10.5.4; although, the overall fuel mass injected into the boiler increases with higher co-fire rates. For this reason, the profitability of co-firing coal with MBB is extremely sensitive to the price of the displaced coal as may be seen in Figure 10.5.5. If the coal is inexpensive, then there is little economic return on its displacement. This may be particularly troublesome when co-firing MBB in a plant that

exclusively fires relatively cheap sub-bituminous or lignite coals from nearby mines. However, displacing higher rank, more expensive coals or even lower rank coals that must be transported long distances to the plant that consumes them may provide a better situation for MBB combustion. Coals obtained from underground mines also tend to be more expensive than coals taken from surface mining. The base case year 1 value of coal was $38.58/metric ton ($35/ton), but if the value of coal at year 1 were to be $60.63/metric ton ($55/ton), then the annualized cost would drop by 56%.

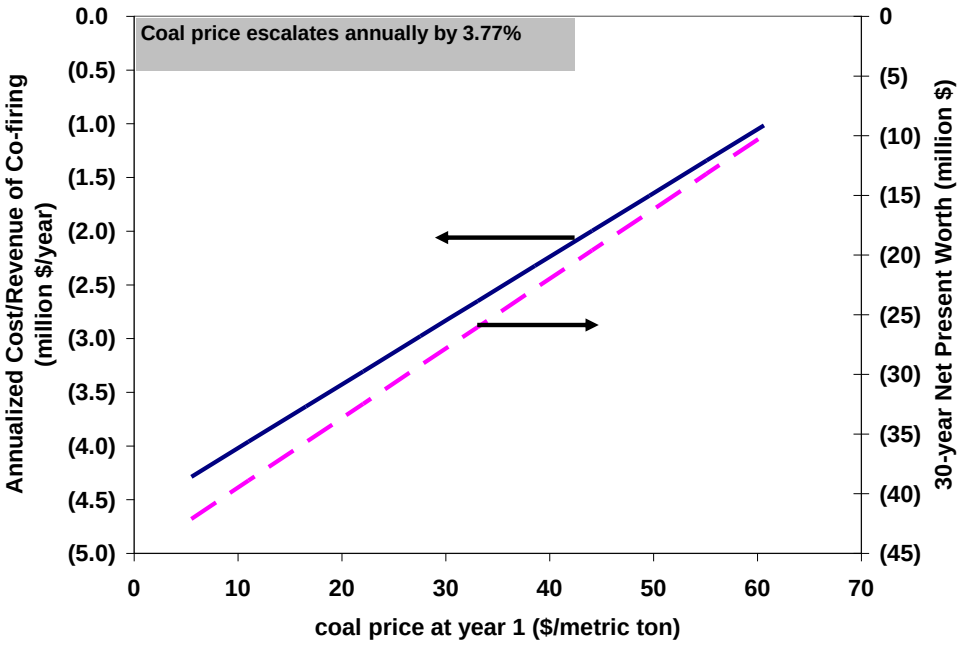

Figure 10.5.5 Annualized cost/revenue and net present worth vs. year 1 coal price

For the base case, the MBB was assumed to be given to the power plant facility free of charge by the farmer; however, if this is not the case, then the additional cost of buying manure from animal farm operators will adversely affect the NPW of the co-fire system, as can be seen in Figure 10.5.6. A MBB price of $10/dry metric ton can decrease the NPW of co-firing by 29%, if the price is also assumed to escalate by 3% annually.

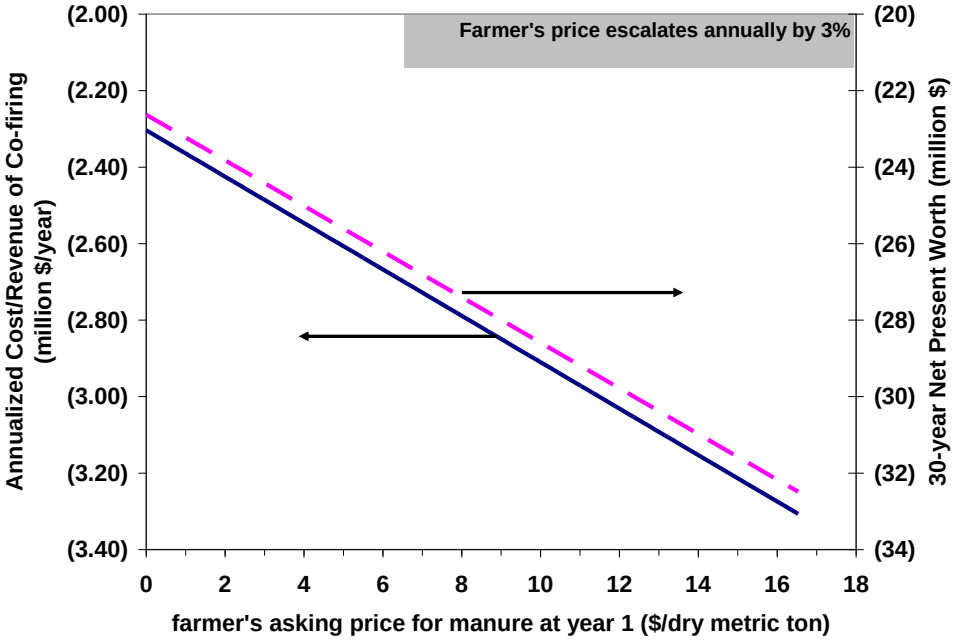

Figure 10.5.6 Annualized cost/revenue and net present worth vs. year 1 farmer's asking price for manure

10.5.1.3. CO_2, SO_x, and ash emissions

Changes in fueling also bring changes in the plant's emissions. Since co-firing with MBB was assumed not to significantly affect NO_x emissions for this study (although some current experimentation at the Texas A&M Coal and Biomass Laboratory on co-firing manure with coal in a low-NO_x burner may prove otherwise), the primary source of revenue for co-firing must come from avoided CO_2 emissions. If the dollar value placed on CO_2 is large enough from taxes, cap and trade policies, or capture and sequestering operations, then the overall worth of a co-firing installation project may prove to be acceptable. Figure 10.5.7 is a plot of annualized cost and net present worth against the year 1 dollar value of a metric ton of CO_2. At the base case value of $3.85/metric ton ($3.50/ton), the net present worth and annualized value are decidedly negative, making a co-firing retrofit project economically undesirable. However, if all other base values remain the same, and the value of CO_2 were to increase to about $25/metric ton, then a breakeven point may be met. CO_2 values higher than $25/metric ton would make the investment of co-firing with MBB in an existing coal plant profitable.

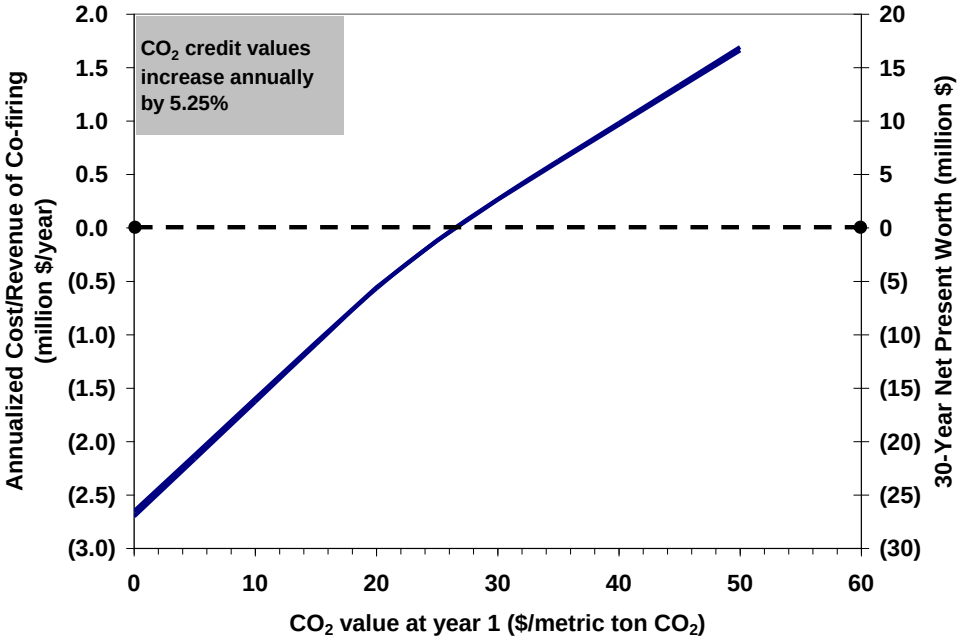

Figure 10.5.7 Annualized cost/revenue and net present worth vs. the value of CO2

Another way to view the relationship between the value of CO_2 and the net present worth of the system is to divide the annualized cost/revenue by the total reduction of nonrenewable CO_2 from co-firing with MBB. Thus, a dollar per metric ton value can be obtained that is representative of every aspect of installing and operating a co-fire system. This value can then be compared to the going market value of CO_2. This comparison is illustrated in Figure 10.5.8. The plot can be divided into three different sections. If the specific CO_2 reduction value falls under Section 1, then the cost of reducing CO_2 through co-firing with MBB is more expensive than simply paying the market value of CO_2. If the results from the co-fire model fall under Section 2, then the cost of reducing CO_2 through co-firing is less than the market value. Finally, in extremely fortunate cases, the specific cost of reducing CO_2 by co-firing with MBB could under Section 3, which suggests that co-firing with MBB would be even more profitable than selling CO_2 allowances; hence the going market value would be considered too low.

The plot was also generated at different CO_2 escalation rates. If the price of CO2 is expected to increase throughout the life of the co-firing project, then co-firing with MBB would become more profitable. The base case escalation rate of CO_2 was 5.25%. At this rate, a year-1 CO_2 value of over $17/metric ton would be considered enough to stimulate a profitable MBB co-firing project at an existing power plant.

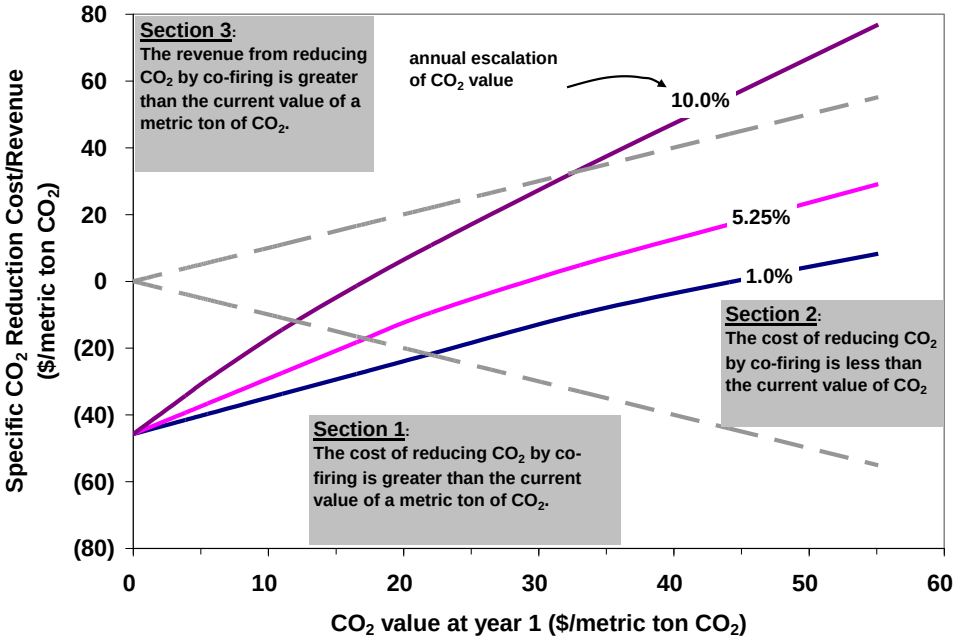

Figure 10.5.8 Specific CO2 reduction cost/revenue vs. the value of CO2

Another emission that can affect the profitability of a co-firing project is SO_2. However, the significance of sulfur depends on two issues: (1) the amount of sulfur contained in the MBB compared to the coal this being replaced and (2) whether or not there is a flue gas desulphurization (FGD) system installed at the power plant. The effect these two issues have on the annualized cost of co-firing coal with MBB is illustrated in Figure 10.5.9. The amount of sulfur in low-ash dairy biomass can be found to be 32.6 kg/GJ, whereas Wyoming sub-bituminous coal contains 13.5 kg/GJ. Therefore, when substituting Wyoming coal with low-ash dairy biomass, having a FGD system reduces the annualized cost by about 17%. On the other hand, Texas lignite contains about 42.2 kg sulfur/GJ. Not having a FGD seems to actually benefit a MBB co-fire system if the biomass were to replace Texas lignite. However, usually power plants that burn low-sulfur coals such as Wyoming sub-bituminous do not have FGD systems, whereas many plants that burn Texas lignite do have FGD systems to reduce SO_2 emissions post combustion.

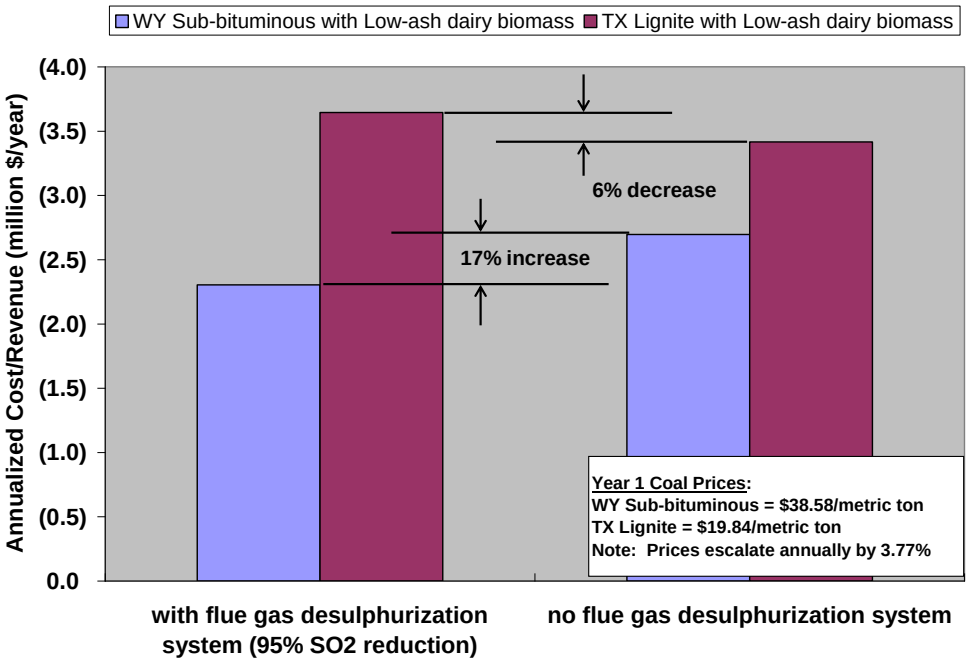

Figure 10.5.9 Effect of flue gas desulphurization on the annualized cost/revenue of co-firing manure-based biomass with coal

Moreover, the price of the coal is usually related to the amount of sulfur it contains. For example, Wyoming sub-bituminous coal is transported long distances to power plants in Texas such as Tolk Station, Harrington, and WA Parish because those plants do not have FGD (USEPA, 2007a). These long transport distances make Wyoming sub-bituminous coal expensive, at least in Texas. However, any dollar savings from replacing the Wyoming coal with MBB might be partly overruled by the additional cost of SO_2 emissions from burning manure instead of low-sulfur coal.

Another emission that will certainly be detrimental to co-firing with MBB is ash. Ash in MBB is a drag on the co-firing system (or reburning system) at every level. Ash adds to transportation costs as it means moving more mass for less energy content. Ash is also a heat sink during drying, making drying high ash biomass slightly more expensive than drying low ash biomass. Most significantly, ash adds to the O&M cost of co-firing because it must be removed from the power plant and then sold or disposed of offsite. Figure 10.5.10 is a diagram of ash emission from coal and biomass for different co-fire rates when Wyoming coal is replaced by low-ash biomass. Figure 10.5.11 is a similar graph for Texas lignite replacement with low-ash biomass, and Figure 10.5.12 is for Texas lignite replacement with high-ash feedlot biomass.

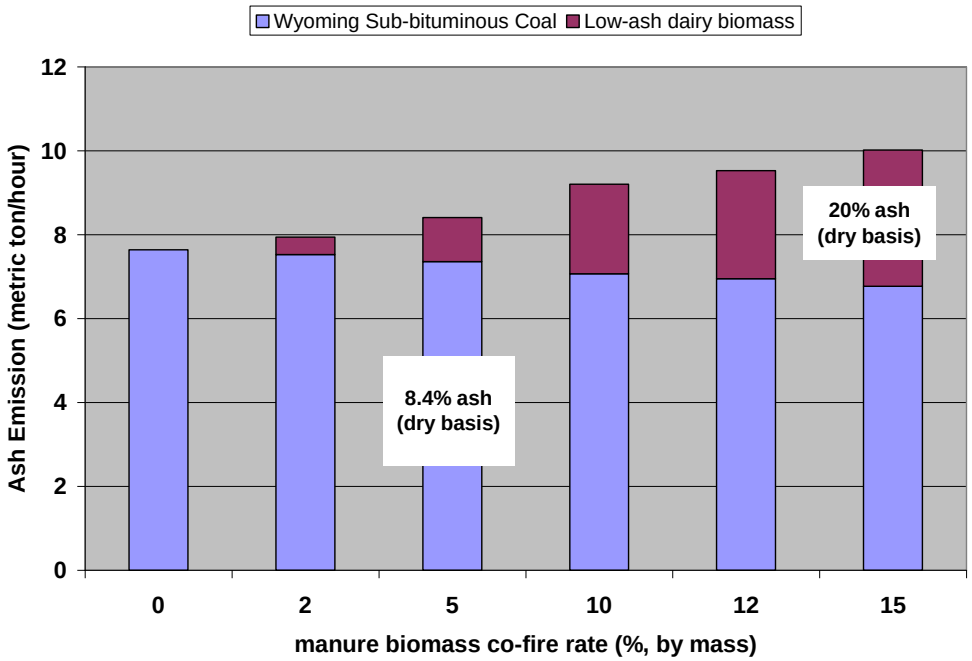

Figure 10.5.10 Ash emission vs. co-fire rate when replacing Wyoming sub-bituminous coal with low-ash dairy biomass

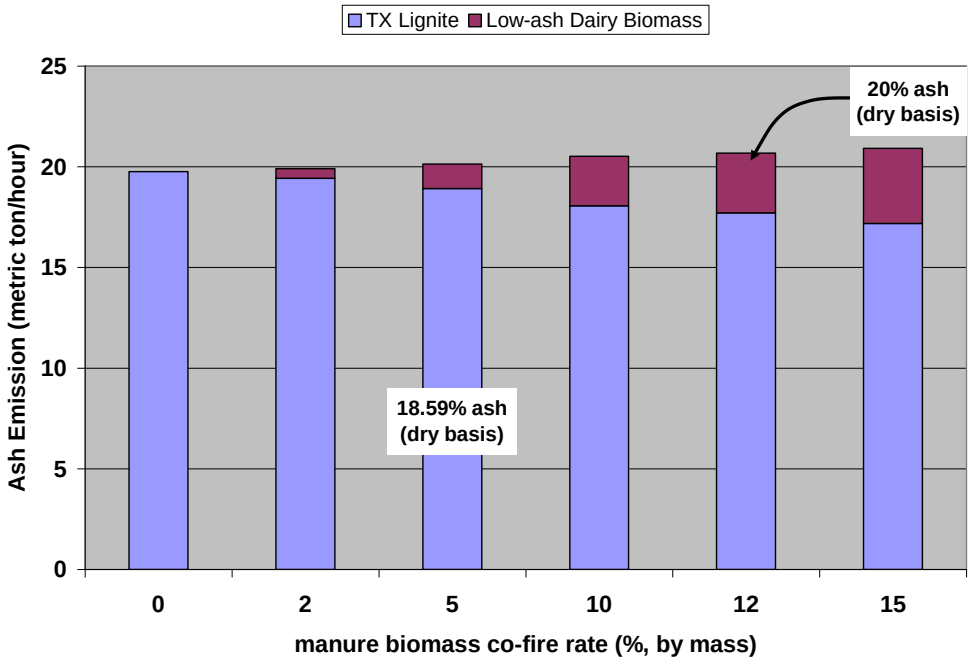

Figure 10.5.11 Ash emission vs. co-fire rate when replacing Texas lignite with low-ash dairy biomass

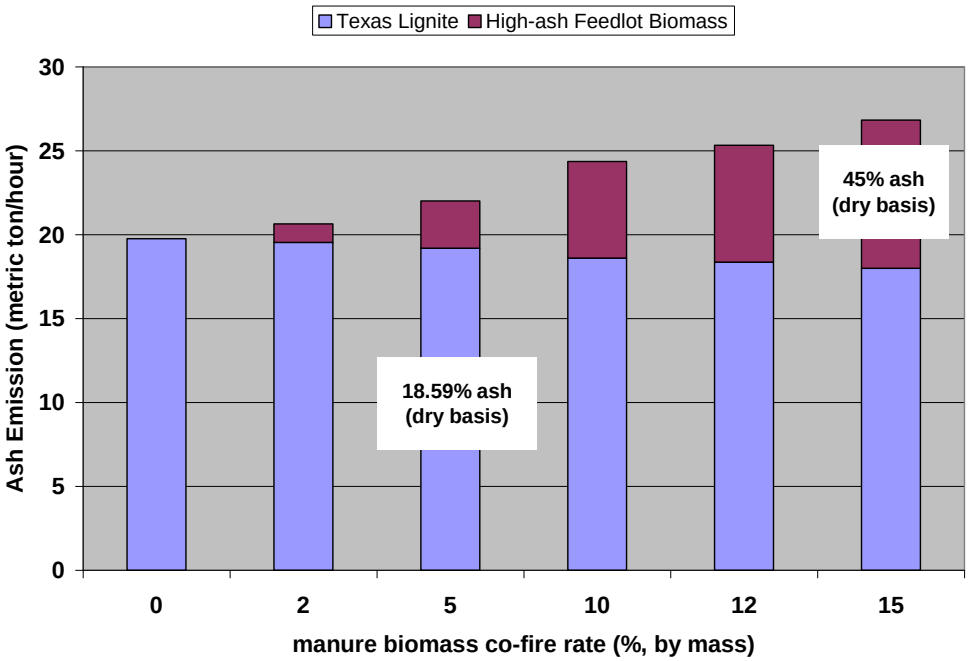

Figure 10.5.12 Ash emission vs. co-fire rate when replacing Texas lignite with high-ash feedlot biomass

Just as with sulfur, the significance of ash content on the profitability of co-firing with MBB is heavily dependent on the amount of ash in the MBB relative the ash content in the coal it is replacing. If low ash MBB replaces the relatively low ash Wyoming coal, ash emissions would increase from 7.64 metric tons/hr to 8.41 metric tons/hr (about 10%) when co-firing 5% biomass. However, if low-ash MBB were to replace lignite, which is higher in ash than Wyoming coal, at the same 5% rate, ash emission would increase from 19.76 metric tons/hr to 20.13 metric tons/hr (only about 1.9%).

These high ash emissions are troubling, given that studies by Megel *et al*. (2006 and 2007) reported that manure ash was not suitable as a cement replacement on its own. However, it is not clear if the same problems would occur when manure is fired with coal, as would be the case with co-firing MBB. Also, manure ash may be utilized in other ways, as discussed previously. The responsibility of finding local markets and buyers for the ash produced by MBB would probably fall on plant operators and managers.

10.5.1.4. Biomass drying and transporting

In order to co-fire coal with MBB at an existing power plant, some important logistical issues should be considered. An important logistical parameter was found to be the average distance between the plant and the animal feeding operations that supply the biomass. The power plant should be near or in a geographical area of high agricultural biomass density. Figure 10.5.13 is an illustration of how power plant facilities and possible supply regions of MBB fuel can be matched. Goodrich *et al*. (2007) studied manure production rates and precise rural transportation routes between coal plants and feeding operations in Texas.

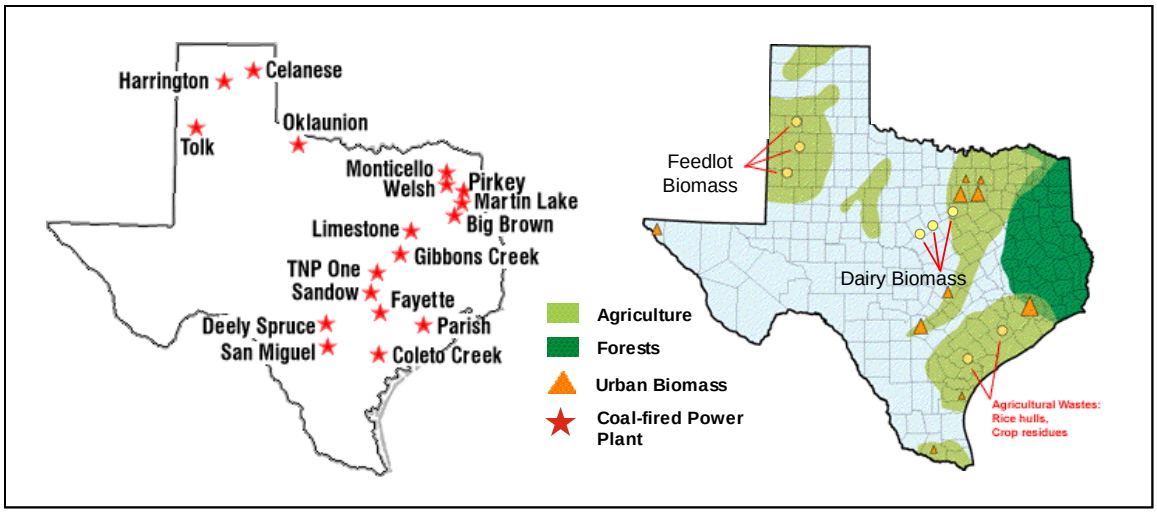

Figure 10.5.13 Matching coal-fired power plants and areas with high agricultural biomass densities, adapted from (Virtus Energy Research Associates, 1995) and (Western Region Ash Group, 2006)

The importance of logistics can be seen further in Figure 10.5.14 and Figure 10.5.15. These figures depict the co-firing O&M (grinding and other associated costs of burning biomass at the plant), the transportation O&M, the drying O&M, and the respective capital costs versus the distance to the feeding operations. Drying MBB was found to be the dominate O&M cost. However, if the average distance between the plant and the feeding operations that supply it were to be over 160 km (100 miles), then transportation costs would become as significant. For longer transport distances, the number of possible round trips to and from the feeding operations that hauling vehicles must make per day decreases. Hence, more trucks must be purchased for longer distances to adequately maintain the desired co-fire rate.

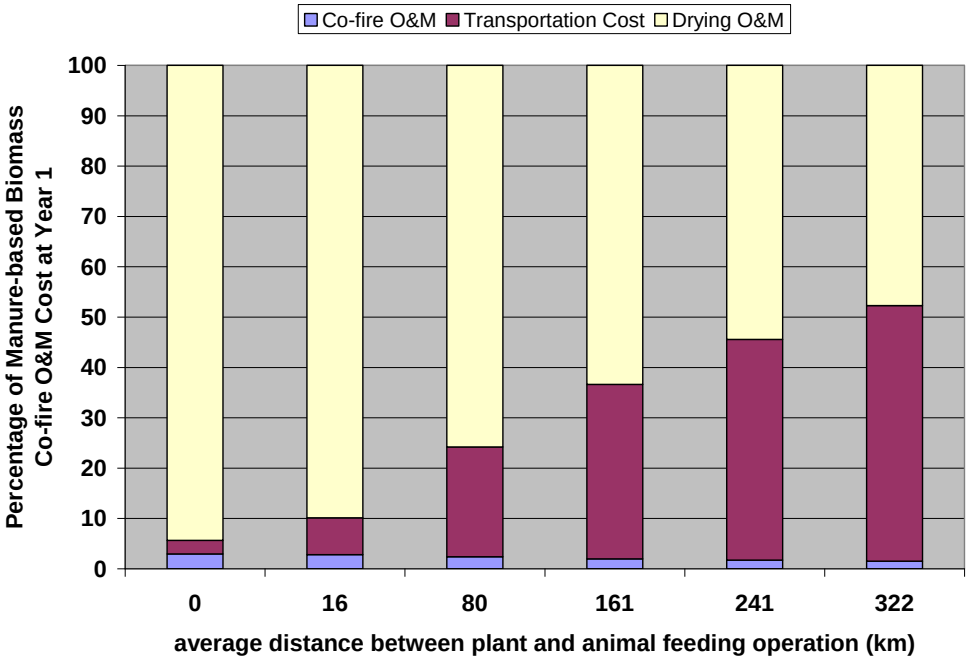

Figure 10.5.14 Manure-based biomass co-fire O&M cost components vs. distance between plant and animal feeding operations

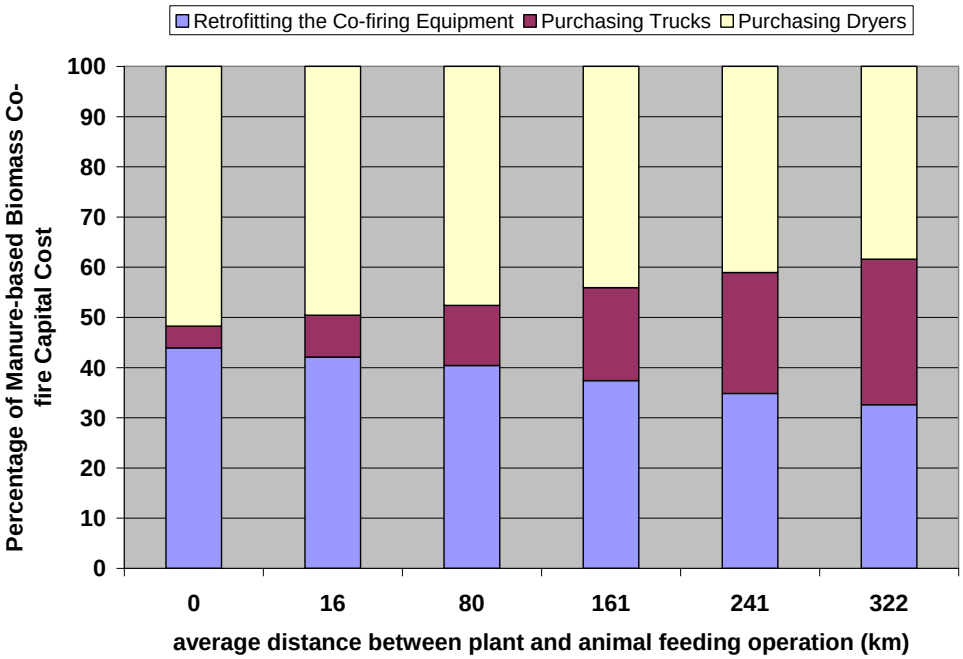

Figure 10.5.15 Manure-based biomass co-fire capital cost components vs. distance between plant and animal feeding operations

Figure 10.5.16 is a plot of annualized cost and net present worth against MBB transportation distance. If the cost of drying biomass were less significant, the transportation distance could be the deciding factor of whether co-firing with MBB was profitable or not. The most effective MBB transport systems should be closely knit networks of animal feeding operations surrounding one or two coal plants in areas within a 160 km (100 mile) radius. Short transport distances would also allow some flexibility to some of the other base case input parameters such as coal cost and ash disposal cost. Moreover, it may be possible to use ash from coal and biomass combustion to pave more feed yards in nearby feedlots which would increase the amount of low-ash feedlot biomass available for reburning facilities and other combustion processes. Currently, the only realistic CB feedstock would have to come from free stall dairies with composted manure-based bedding and flushing systems. For many cases, there may simply not be enough low-ash biomass near the plant to sustain a co-fire rate of more than a few percent.

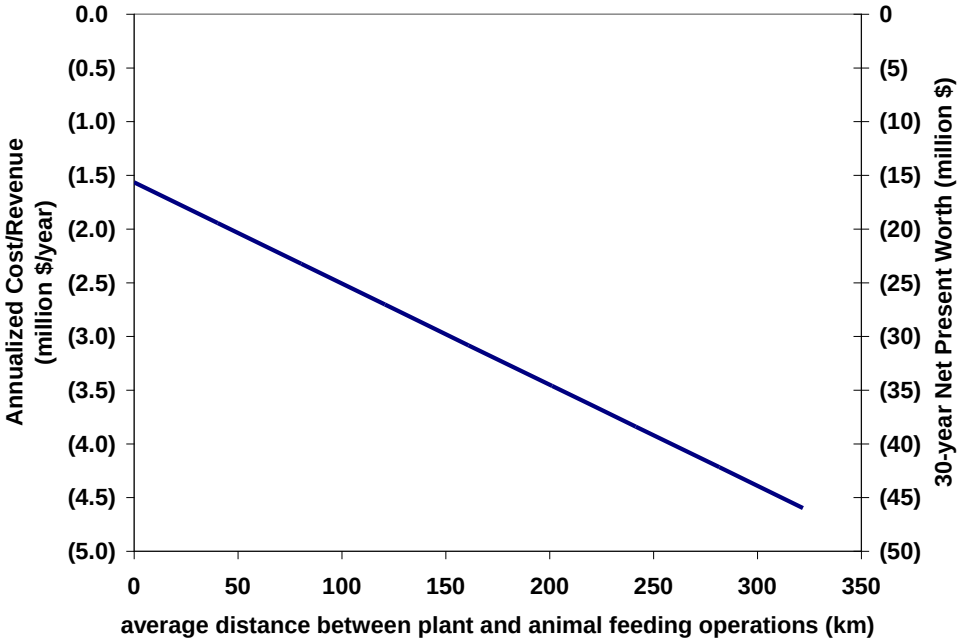

Figure 10.5.16 Annualized cost/revenue and net present worth vs. manure-based biomass transport distance

Yet for shorter transportation distances, the O&M cost of co-firing is dominated by the cost of drying the biomass. For the base case run of the co-firing model, drying constitutes 76% of the total cost. Of this cost, 73% is due to purchasing natural gas for generating steam for the biomass dryers. Another 15% is due to running the dryers' fans. Moreover, if the biomass must be dried before being sent to the power plant, natural gas is probably the cheapest fuel to use. Both propane and electric driers would probably be more expensive. Figure 10.5.17 is a plot of annualized cost against natural gas price and annual escalation of gas price. If natural gas was free, or not needed, to dry the biomass, then a breakeven point for the cost of co-firing would be reached, that is if all other base case values remained the same. If the price of natural gas is too high, or if the escalation is expected to be high, then a profitable scenario may be out of reach.

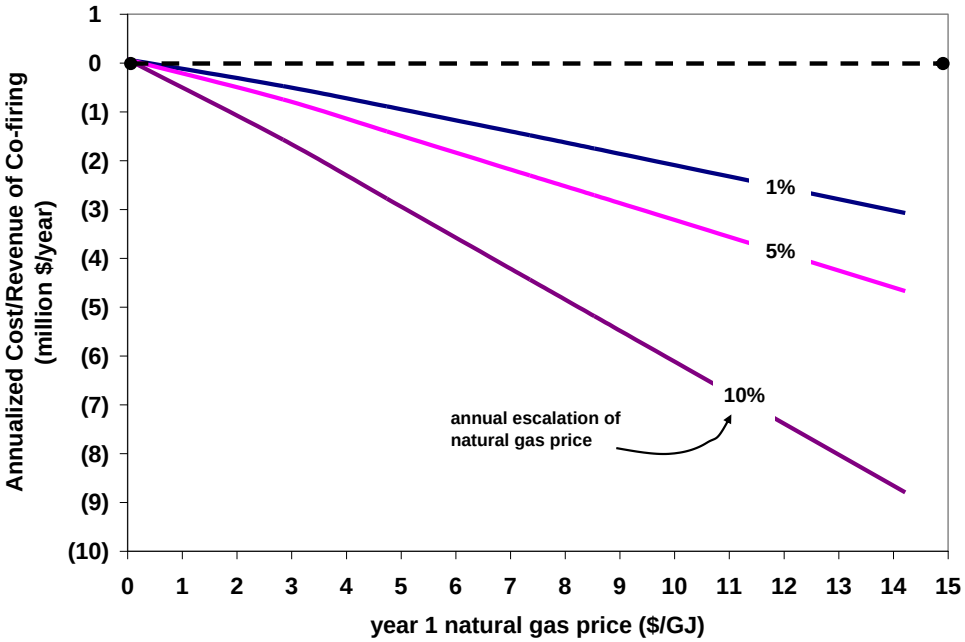

Figure 10.5.17 Annualized cost/revenue vs. natural gas price

However, there may not always be a need to use expensive conventional fuels to dry MBB. If power plant operators are willing to receive wet MBB, then waste heat from coal combustion could be used to dry the biomass instead natural gas. Or if the MBB is from a more arid region where the relative humidity is low, the moisture content of the biomass, when harvested, might be low enough to forgo any drying at all. According to Heflin (2008), the moisture percentage of scraped feedlot biomass collected in the Texas Panhandle is rarely over 30%, as harvested, even after heavy rainfall. This is particularly true for low-ash solids from paved feedlots. Figure 10.5.18 is a graph of overall delivery cost for Texas lignite, Wyoming sub-bituminous, and low-ash dairy biomass at three drying scenarios. The first scenario is such that the biomass is dried using natural gas, just like the base case. The overall as-delivered cost of the biomass for this case is $3.95/GJ ($4.16/MMBtu), over twice the price of Wyoming sub-bituminous. If the MBB is transported to the power plant and then dried with waste heat, then the delivery price of the biomass was found to drop by 55%. If the biomass is inherently dry, say less than 30% moisture, and no additional drying is required, then the delivery price drops by 81% to $0.76/GJ ($0.80/MMBtu), which is actually cheaper than the Wyoming and Texas lignite coals.

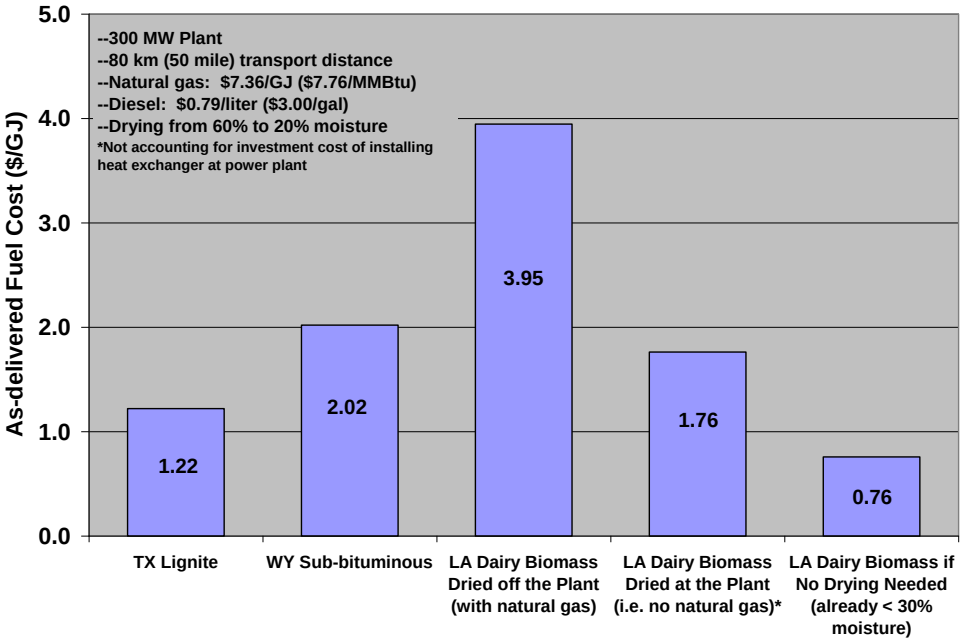

Figure 10.5.18 Overall fuel costs for coals and low-ash dairy biomass at different drying requirements

Yet, as stated before, currently the greatest supply of low-ash MBB may be from dairies with flushing systems or perhaps from indoor swine farms. Separated solid manure from these facilities would probably be high in moisture and require drying before combustion. Most scraped manure from feedlots and open dairy lots is high in ash since most of these lots are unpaved.

For the base case 300 MW power plant, if each cow, on average, were to produce 6.35 dry kg of manure per day (14 lb/cow/day), then about 21,000 dairy cows would be required to sustain a co-fire rate of 5% (by mass). The Bosque and Leon River Watersheds in north central Texas have about 150,000 dairy cows in over 150 dairies. Therefore, one 300 MW_e plant would require approximately 14% of all cattle manure produced by these farms. Hence, the availability of suitable, low-ash MBB, as well as the coordination between farmers, centralized composting facilities, and plant operators easily come into question when trying to apply this low heat value biomass to large electric boilers.

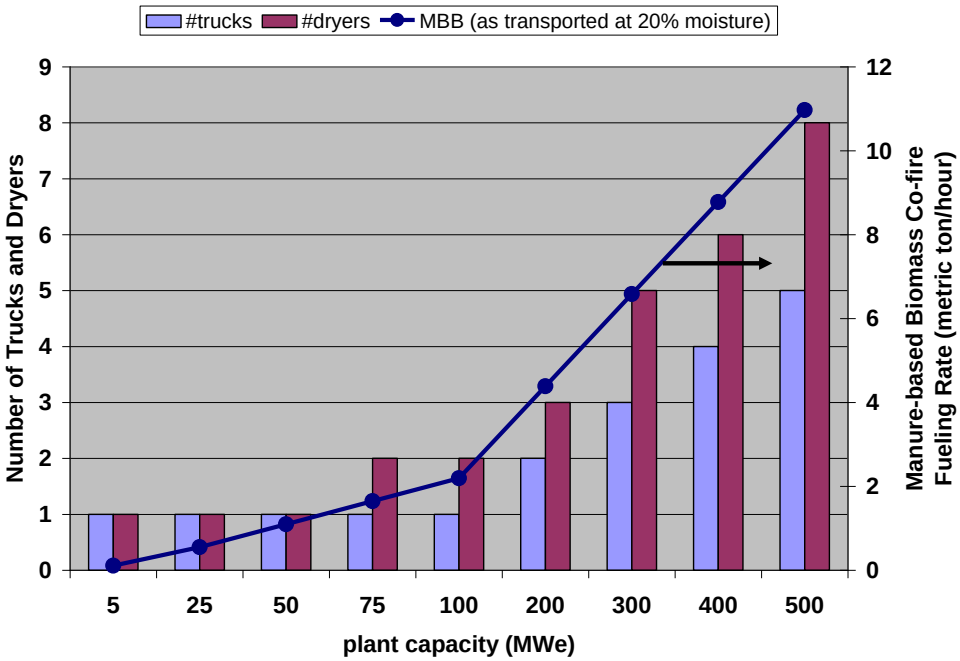

Figure 10.5.19 Number of trucks and dryers and manure-based biomass fueling rate vs. power plant capacity

To handle these issues, several methods such as storage and reserve stockpiles of ready-to-fire MBB can be kept near the power plant. In Figure 10.5.19, the number of required trucks and dryers are plotted against power plant capacity. A 500 MW_e plant would require at least 8 two-metric ton conveyor belt dryers where as a 100 MW_e plant would only require 2 dryers. Concentrating research and development of animal biomass utilization on smaller, more dispersed power facilities may be more helpful. Power plants with 50 to 100 MW_e capacities would seem to be the best candidates for co-firing coal with MBB.

10.5.2. Reburning

Modeling a MBB reburn system is very similar to the previous model for co-firing. The main difference is NO_x emissions. The revenue generated from avoided NO_x emissions adds another dimension to the analysis, and in theory makes a MBB reburn system more profitable than a simple co-firing operation. However, reburn systems require anywhere between 10 and 20% reburn fuel (in this case, biomass) on a heat basis. For the case of replacing Wyoming sub-bituminous coal with low-ash dairy biomass at 20% moisture, this range is equivalent to about 13 and 26% by mass, which is far greater than the 5% co-fire rate discussed for the base case in the previous section.

An outline of the reburn computational model is presented in Figure 10.5.20. The layout of the program is similar to the co-firing model, except that baseline NO_x levels must be computed both for cases with primary NO_x controls and without primary controls. Then, NO_x emission reductions can be computed for secondary controls such as reburning, SCR, and SNCR. The biomass drying and transportation sections of the model are left relatively unchanged, except for the fact that more biomass must be dried, transported, and processed at the power plant.

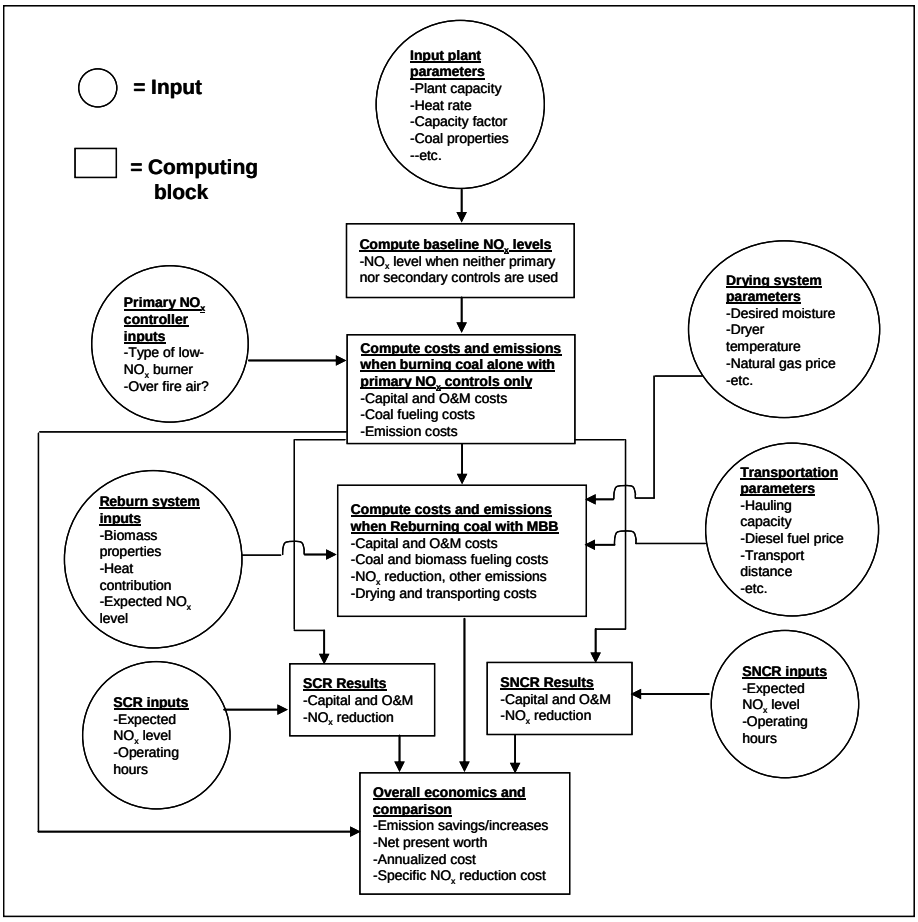

Figure 10.5.20 Flow diagram of computer spreadsheet model for reburning coal with manure-based biomass in an exiting coal-fired power plant along with comparisons to SCR and SNCR systems

10.5.2.1. Base case inputs and results

All base case inputs will remain the same for the reburning discussion except for those listed in Table 10.4.1. For the base case, the 300 MW_e coal power plant will be equipped with a primary NO_x controller (low-NO_x burner with closed coupled over fire air) capable of lowering NO_x levels to 84.2 g/GJ (0.196 lb/MMBtu). The secondary NO_x controls such as MBB reburning and SCR will be installed and operated along with the primary controls. The reburn model can be set up so that the coal is reburned with MBB without any primary controls present; however for this discussion, since low-NO_x burners, over fire air and other primary controllers are presently installed in most existing coal plants, the secondary technologies will add to the NO_x reductions already achieved by the primary controls. Thus, all dollar savings for NO_x are acquired for reductions from the 84.2 g/GJ level.

Table 10.5.9 base case inputs for reburning coal with manure-based biomass

Input	Value (unit)	Source	Notes
Primary NO_x control	Low-NO_x coal and air nozzles with closed-coupled OFA		See primary control NO_x level (next item)
Primary NO_x control level	84.23 g/GJ (0.1959 lb/MMBtu)	(Srivastava, 2005)	about 50% average reduction efficiency for these primary controls when burning sub-bituminous coals
Reburn fuel	LADB	(Sweeten *et al*, 2006)	
Heat contribution from reburn fuel	10%		Range: 10 – 30%
Reburn NO_x control level	25.9 g/GJ (0.06 lb/MMBtu)	(Colmegna *et al*, 2007), (Oh, *et al*., 2008), (Annamalai *et al*., 2005)	
Reburn capital cost	$35/kWe	(Zamansky *et al*., 2000)	
Reburn fixed O&M	$1.07/kWe yr	(Biewald, *et al*., 2000), (USEPA, 1998)	Scaled for different plant capacities and firing cattle biomass
SCR NO_x control level	25.9 g/GJ (0.06 lb/MMBtu)	(USEPA, 2004)	>90% reduction, but current commercial systems are usually limited to 25.9 g/GJ
SNCR NO_x control level	64.6 g/GJ (0.15 lb/MMBtu)	(Srivastava, 2005)	~35% reduction for larger coal plants
NO_x credit/allowance	$2,590/metric ton reduced	(SCAQMD, 2007)	Average annual price for Compliance Year 2005. Assume credits gained for reductions beyond primary control levels
NO_x allowances	4.50%	(SCAQMD, 2007)	

For the reburn base case, the reburn fuel was pure low-ash dairy biomass, which contributed 10% of the power plants overall heat rate (about 13% by mass). The reburn model can be setup so that blends

of coal and MBB can be the reburn fuel; however, according to Oh *et al*. (2008) and Annamalai *et al*. (2005), the greatest NO_x reductions are achieved when pure biomass is used as the reburn fuel. Manure-based biomass reburning and SCR were presumed to achieve the same NO_x level of 25.9 g/GJ (0.06 lb/MMBtu), whereas SNCR was assumed to only achieve a level of 64.6 g/GJ (0.15 lb/MMBtu). Both SCR and SNCR use ammonia or urea as reagents, which do not contribute to the overall heat rate of the power plant; therefore, coal consumption and other emissions aside from NO_x are presumed to be the same for SCR and SNCR as for the case of burning pure coal alone.

Just as with the co-fire model, the base case inputs for reburning were used to generate a reference run of the reburn model. The base case results for fueling and emission rates for burning coal alone with primary NO_x controls are listed in Table 10.5.6. These rates may be compared to those in Table 10.5.10 for fueling and emissions when reburning coal with MBB. Again, the total annual fueling (energy) consumption was found to be about 709,000 GJ more per year when reburning with MBB. This increase in total fueling is almost three times that for the co-firing base case. Yet this is predominantly due to the fact that more diesel and natural gas are required to prepare enough biomass for reburning. The heat energy released by the MBB in the reburn zone of the boiler burner (i.e. 2.16 million GJ/yr in Table 10.5.10) was found to be 1.46 million GJ more than the energy needed to dry and transport it to the plant. However, this may not be the case if transportation distances were greater, or if more biomass was required to obtain desired NO_x levels.

Table 10.5.10 Base case fueling and emissions results for a 300 MWe coal plant operating while reburning coal with manure-based biomass (10% by heat)

Number of drying sites	2
Number of dryers (each rated at 2 dry metric tons/hr)	12
Number of dryer operators	5
Total hectares required for drying site(s)	8
Total extra storage trailers	8
Number of hauling vehicles required (30.6 m^3 each)	8
Number of cows required (7.7 dry kg/cow/day)	47,000

		Primary fuel (coal)	Reburn fuel (MBB)	Dryers (natural gas)	Dryers (electricity for fans)[a]	Hauling vehicles (diesel)	Total
Fueling rate	GJ/yr	19,463,231	2,163,816	582,264	100,510	24,800	22,334,620
	metric ton/yr	1,023,590	157,400	11,644	5,046	515	n/a
CO_2 emission	g/GJ	84,147	10,043	55,005	93,497	64,290	n/a
	metric ton/yr	1,819,785	217,316	31,944	9,398	1,594	1,862,721[b]
SO_2 emission	g/GJ	13.48	3.34	n/a	n/a	n/a	n/a
	metric ton/yr	291	72	n/a	n/a	n/a	364
Ash production	g/GJ	2,784	1,162	n/a	n/a	n/a	n/a
	metric ton/yr	60,208	25,154	n/a	n/a	n/a	85,361
NO_x emission	g/GJ	26	n/a	n/a	n/a	74,501	n/a
	metric ton/yr	557	n/a	n/a	n/a	2	559

[a]Electricity for fan operation is assumed to come entirely from coal. Fueling and emission rates are for the equivalent amount of coal required to produce the electricity in a power plant with an overall efficiency of 35%.

[b]Excluding CO_2 emissions from renewable fuels such as the MBB reburn fuel

Total CO_2 emissions for reburning, including carbon emissions from MBB drying and transportation, were found to be 159,000 metric tons/yr less than emissions for primary control operation only. Again, since much more biomass would be required for reburning than the 5% (by mass) for the co-fire base case, CO_2 reduction was almost 3 times as much as carbon reduction from co-firing. However, ash emissions greatly increased for the MBB reburn system under the base case run by 27.6%. Lastly, since the hauling vehicles were assumed to meet 2007 NO_x standards with catalytic converter systems, the NO_x emitted by the vehicles only inhibited MBB reburn NO_x reductions by about two metric tons/year, compared to a 1,260 metric ton/year reduction beyond primary control levels.

Despite the increase in ash emissions, economically, the MBB reburn system was found to be only 0.61% more expensive for the first year than operating with primary controls alone, under base case assumptions. The full list of cost components and the overall annualized results for the four possible NO_x reduction scenarios are compared in Table 10.5.11. The major increase in overall cost for the MBB reburn system, was found again to come from the variable O&M increase, largely due to biomass drying operations. However, this increase was offset by combined (coal and biomass) fuel delivery savings of $2.70 million/yr, avoided CO_2 penalty of $615,000/yr, and $3.71 million/yr in additional NO_x credits (or savings).

Table 10.5.11 Comparison of base case Year 1 costs of selected NOx control technology arrangements (300 MWe plant, 10% biomass by heat for reburn case)

Year 1 Costs	**Primary control only**	**Primary control + manure-based biomass reburn**	**Primary control + SCR**	**Primary control + SNCR**
Fixed O&M Cost	63,000	506,995	272,657	119,664
Variable O&M Cost[a]	56,765	5,876,452	1,433,709	2,118,293
Biomass Delivery Cost	0	1,691,040	0	0
Coal Delivery Cost	43,878,448	39,488,099	43,878,448	43,878,448
NO_x Credits[b]	0	(3,271,151)	(3,275,800)	(1,106,857)
CO_2 Penalty	7,800,913	7,186,025	7,800,913	7,800,913
SO_2 Penalty	314,864	353,717	314,864	314,864
Ash Revenue	(368,704)	(368,550)	(368,704)	(368,704)
Ash Disposal Cost	1,769,781	2,380,425	1,769,781	1,769,781
Annualized Capital Cost	531,647	2,735,890	4,481,734	1,007,622
TOTAL COST (w/o capital)	53,515,066	53,843,052	51,825,867	54,526,402

[a]For MBB, variable O&M includes the cost of drying the biomass
[b]NO_x credits are assumed to be earned for all reductions beyond those obtained from primary controls

Compared to the other secondary control options, MBB reburning was found to be more expensive than SCR, yet cheaper than SNCR. In fact, SCR was found to be about 3.2% cheaper for the year 1 total cost, than sole primary control operation. However, SCR was found to have the highest annualized capital cost, mostly due to the catalyst installation, which can constitute up to 20% of the

initial investment of this type of control system (Mussatti *et al*., 2000b). SNCR was found to have the most expensive year 1 total cost mostly due to a poorer NO_x level than that achieved by either MBB reburning or SCR. Since SCR and MBB reburning were assumed to have similar NO_x reductions, the comparisons made in this section will mostly be made between these two.

The same discount, inflation, and escalation rates, as well as project life, were assumed for the reburn model. The overall cash flow diagram for the base case run of the MBB reburn model is presented in Figure 10.5.21. The overall operating income begins as a net cost from years 1 through 7, but as the combined escalation of coal, CO_2 and NO_x prices overtakes that of natural gas, electricity, and other prices and costs, the operating income becomes positive after year 7. However, after adjusting the operating income for depreciation of capital, a net positive income is not seen until after year 23, thus income tax does not become a factor until this time. The major difference in this analysis compared to simple co-firing is the dollar savings from avoided NO_x emissions. Despite the requirement of larger amounts of MBB, along with more trucks and dryers needed to process it, the net present worth of the MBB reburn system, under base case assumptions, was found to be negative $19.1 million (i.e. net present cost), which is a slightly lower cost than for the simpler co-firing case discussed earlier. However, the NO_x credits are still not enough to achieve a positive net present worth or a payback under base case assumptions.

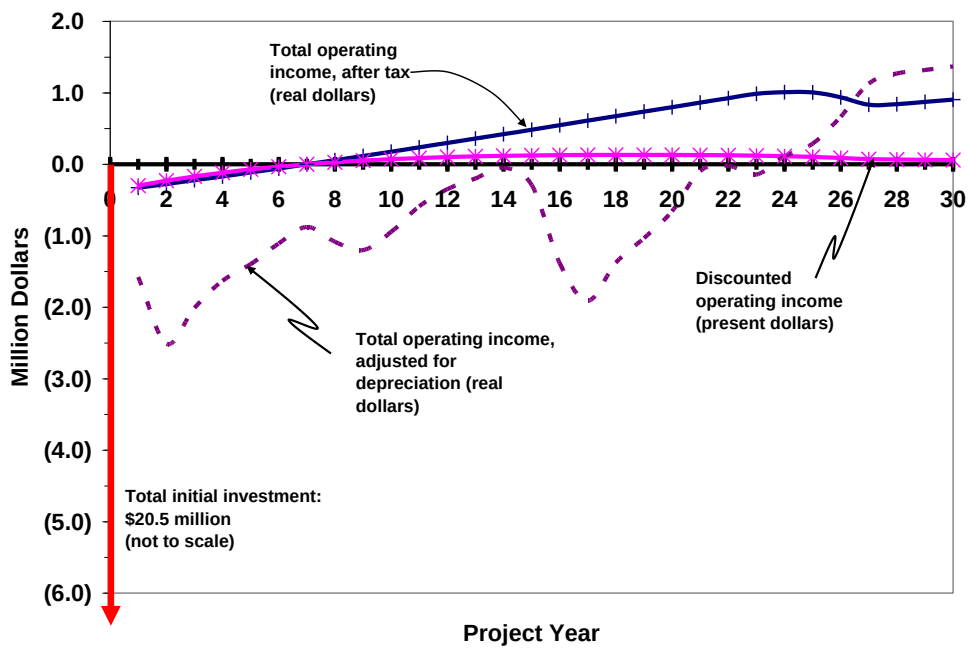

Figure 10.5.21 Overall cash flows for the base case run of the manure-based biomass reburn economics model

On the other hand, the total operating income for SCR was found to be positive throughout the 30 year life of the project, as can be seen in Figure 10.5.22. Yet, the net present worth of the SCR system, for the base case, was still found to be slightly negative at minus $4.6 million. The simple payback period, which does not account for the time value of money, was found to be about eight and half years and the rate of return for SCR at the base case was found to be 8.2%. The main reason for the relative success of SCR compared to MBB reburning at the base case is due to the fact that the same NO_x reductions can be achieved with SCR without having to pay high variable O&M costs of importing MBB. However, in the remaining part of this section, the net present worth of the MBB reburn system will be monitored for variations of certain base values to determine if reburning with MBB could ever be as

profitable as SCR, or justifiable as a NO_x reduction technology on an exiting coal-fired power plant with primary NO_x controllers.

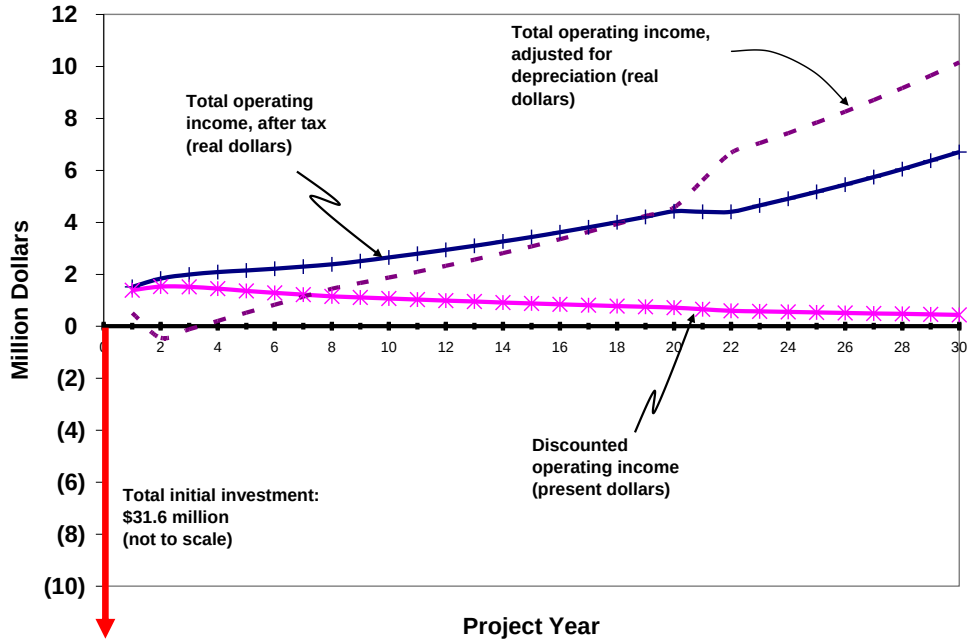

Figure 10.5.22 Overall cash flows for the base case run of the SCR economics model

10.5.2.2. Biomass and coal fueling

The overall negative net present worth for MBB reburning was mostly attributed to the relative expense of importing biomass, with an inferior heat value, to meet a set percentage of the plant's heat rate (for the base case, 10% by heat). Since the ammonia, urea, or other reagents imported for SCR do not add to the fueling of the plant, O&M costs for this competing technology can stay relatively low for the same targeted NO_x level. If MBB reburn systems are ever to be installed in coal plants, plant operators and engineers must find a perfect balance between lowering the biomass contribution to the heat rate, saving on coal, and still maintaining targeted NO_x levels. In Figure 10.5.23, the rise in MBB drying and transport O&M can be seen as more of the plant's heat rate is supplied by the biomass reburn fuel. Also, the annualized costs of MBB reburning steadily increases with greater biomass reburn contributions.

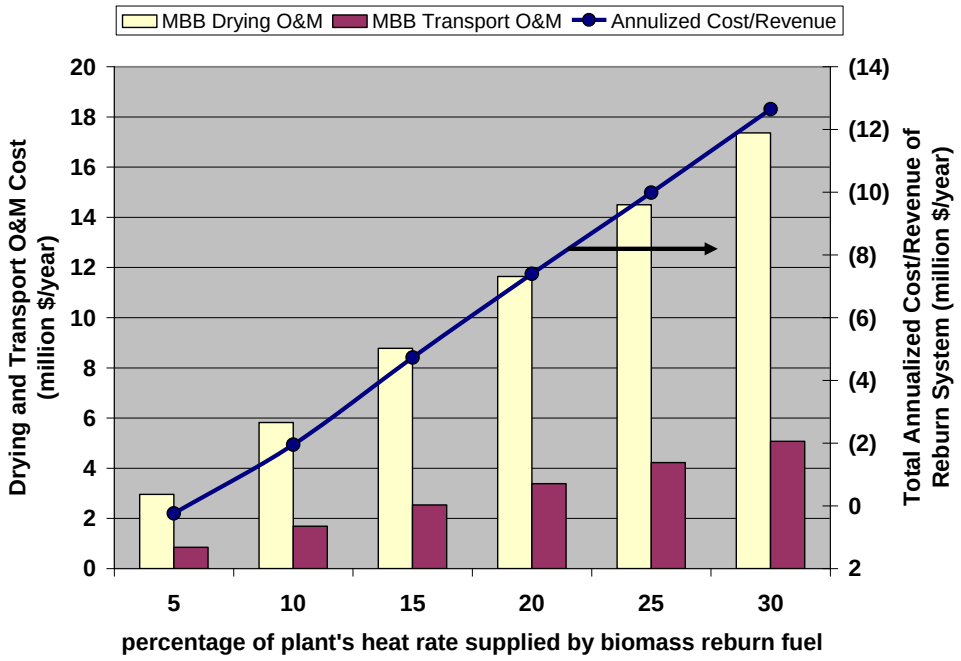

Figure 10.5.23 Drying and transport O&M costs and annualized cost/revenue vs. percentage of plant's heat rate supplied by manure-based biomass reburn fuel

The displacement of coal by the biomass is even more significant during reburning. The decrease of coal consumption, along with the overall increase in total fuel injection into the power plant can be seen in Figure 10.5.24 for different heat rate contributions from the biomass. Moreover, the significance of coal price is displayed in Figure 10.5.25. If the price of coal were to increase to $50/metric ton for the first year of the project, then the net present worth and annualized cost of the reburn system would be the same as SCR's.

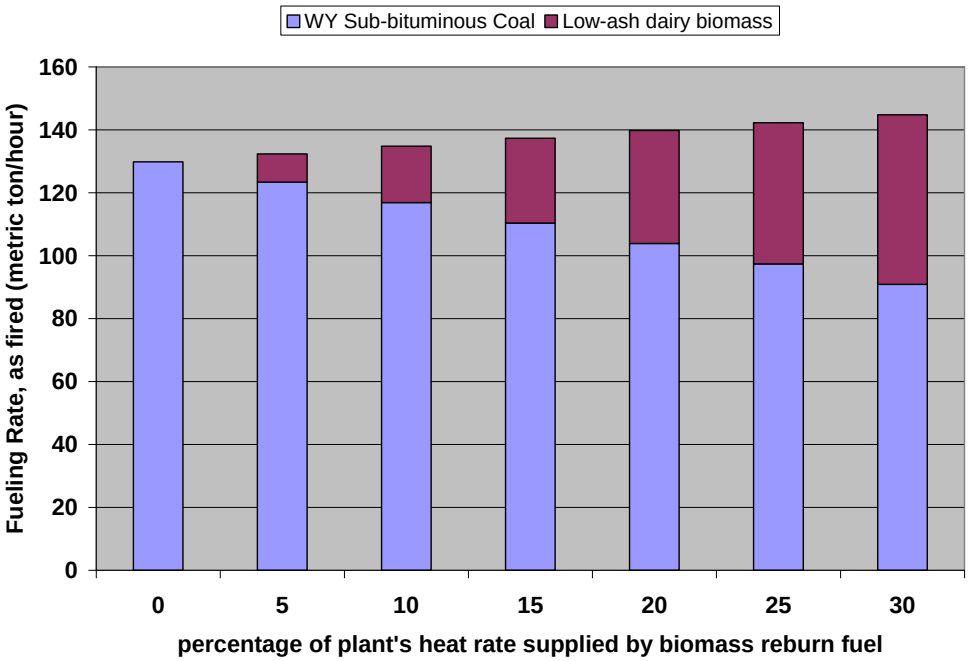

Figure 10.5.24 Fueling rates of Wyoming sub-bituminous coal and low-ash dairy biomass vs. percentage of plant's heat rate supplied by the biomass reburn fuel

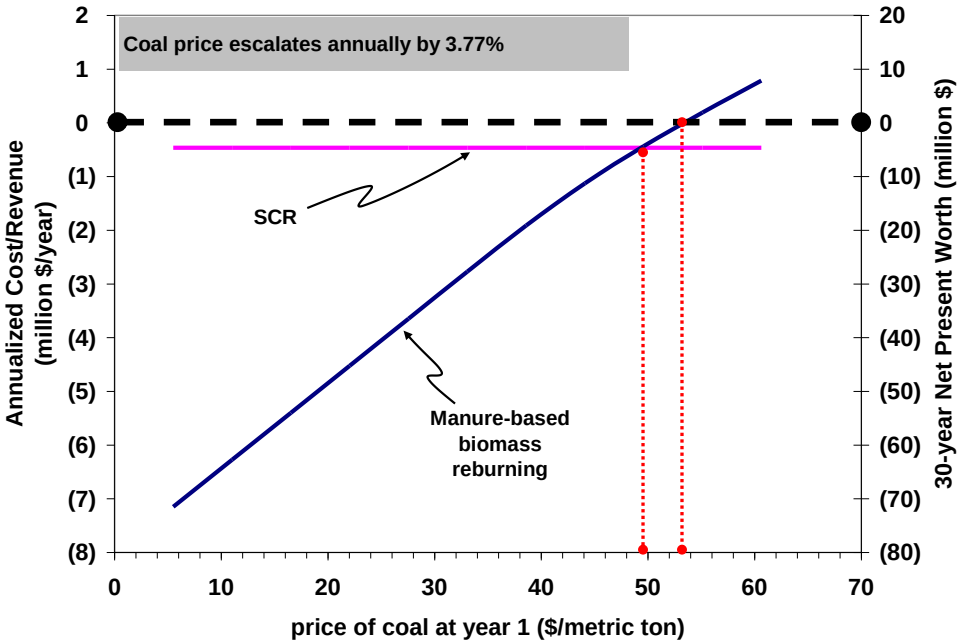

Figure 10.5.25 Annualized cost/revenue and net present worth of manure-based biomass reburning and SCR vs. coal price

10.5.2.3. CO_2, NO_x, SO_x, and ash emissions

Carbon emissions affect the net present worth of the MBB reburn system just like avoided coal costs. An increase in the value of CO_2 improves the profitability of a MBB reburn system tremendously,

perhaps more than any other parameter other than the dollar value of NO_x. A CO_2 value beginning at $12/metric ton would make reburning coal with MBB economically competitive to SCR. See Figure 10.5.26

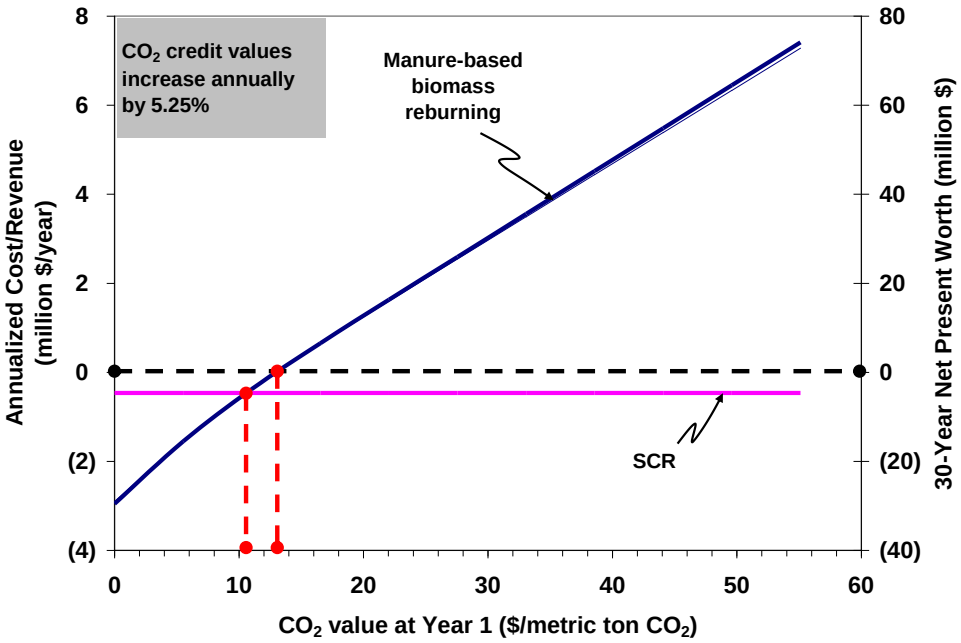

Figure 10.5.26 Annualized cost/revenue and net present worth vs. the value of CO2

A similar plot is shown in Figure 10.5.27 for the dollar value of NO_x. If the escalation rate of the dollar value of NO_x remains the same as the base value, 4.5%, then SCR reaches an economic breakeven point at a year 1 NO_x value of a little less than $3,000/metric ton, whereas MBB reburning would require a year 1 value of about $4,000/metric ton.

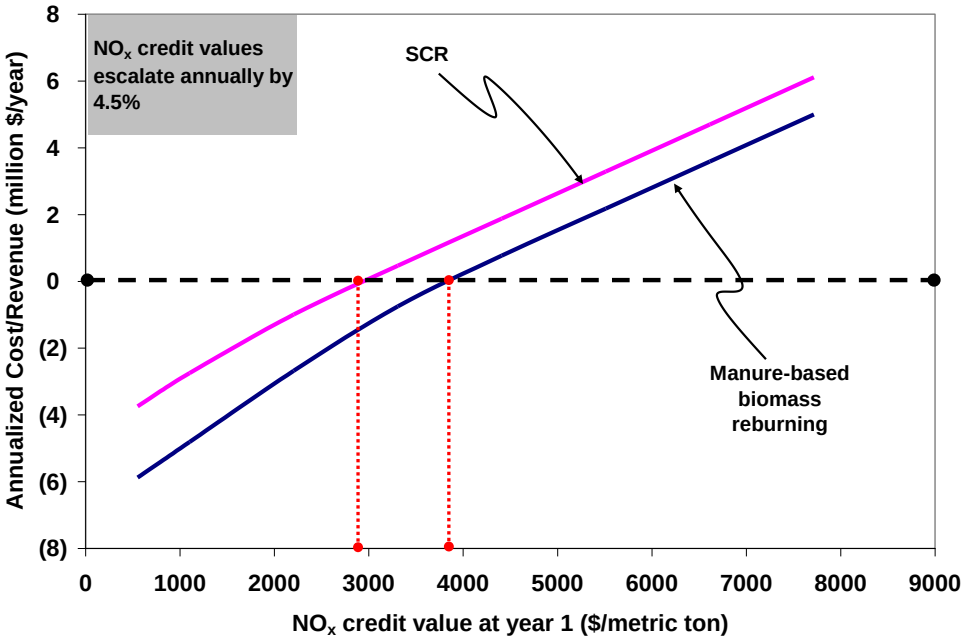

Figure 10.5.27 Annualized cost/revenue for both MBB reburning and SCR vs. the value of NOx

Yet more importantly, the profitability of MBB reburning was found to be very sensitive to the effectiveness of the primary NO_x control technology already installed at the power plant. On top of competing with SCR, MBB reburning must also compete with these existing low-NO_x burners and over fire air. Figure 10.5.28 is a plot of annualized cost against the NO_x level achieved by primary controls. In many instances, coal-fired power plants have already installed very effective low-NO_x burners that can achieve levels as low as 60.2 g/GJ (0.14 lb/MMBtu) (Srivastava *et al*, 2005). For these plants, gaining enough revenue from NO_x credits to payoff the capital of drying and transporting biomass reburn fuel would be difficult.

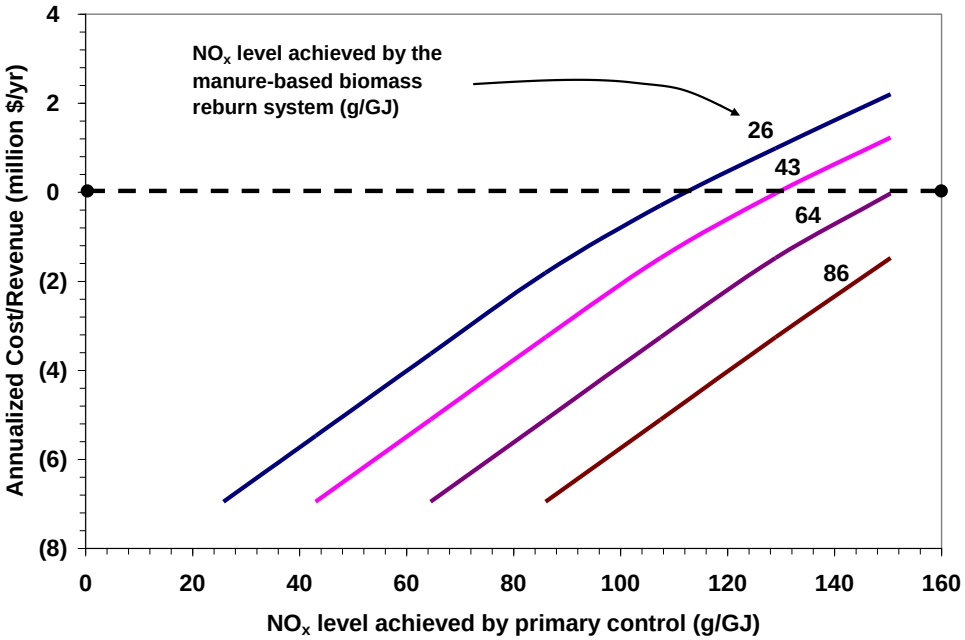

Figure 10.5.28 Annualized cost/revenue vs. NOx levels achieved by primary NOx controllers

Moreover, the success of a MBB reburn system can also be tested against the going value of NO_x, just as co-fire systems were tested against the current value of CO_2. Figure 10.5.29 is a similar plot to Figure 10.5.10, only for NO_x values. At an escalation rate of 4.5%, a current NO_x value of $2,500/metric ton would justify a MBB reburn system if this standard were to be used. However, reburning would still not be as attractive as SCR.

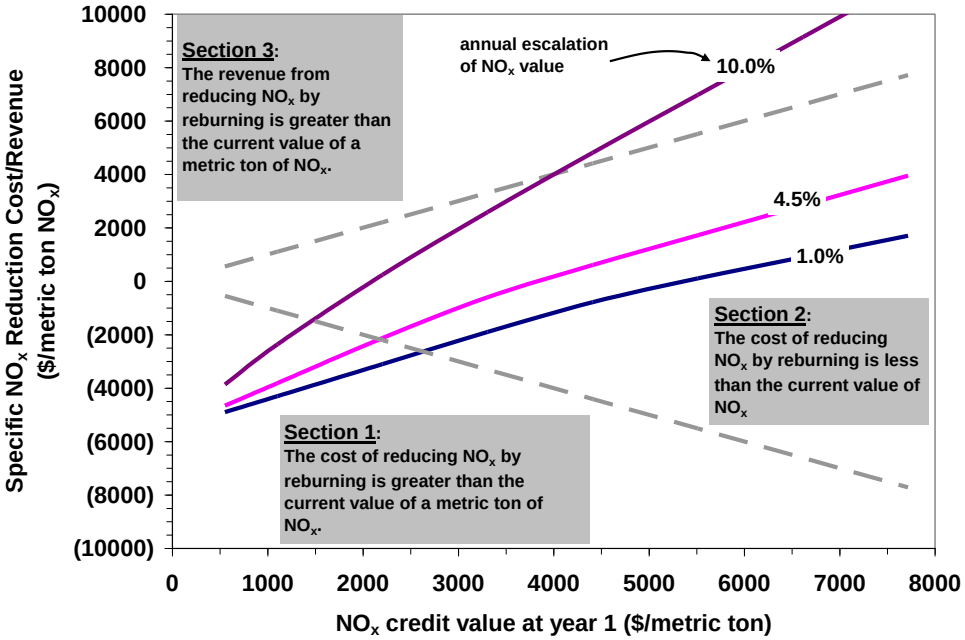

Figure 10.5.29 Specific NOx reduction cost/revenue for manure-based biomass reburning vs. the value of NOx

Emissions of SO_2 (Figure 10.5.30) and ash (Figure 10.5.31) were found to affect a reburn system in much the same way as they would a co-fire system. Supplying 10% of the heat rate through MBB reburning was found to increase ash production from 7.6 metric tons/hr (when burning coal only) to 9.7 metric tons/hr (about a 28% increase). If the heat contribution from biomass reburn fuel were to be higher at 20%, the ash level would exceed 11.8 metric tons/hr, with almost half of the ash coming from the MBB reburn fuel. Again, the high ash emissions are troubling, given the studies on the salability of manure ash by Megel *et al*. (2006 and 2007).

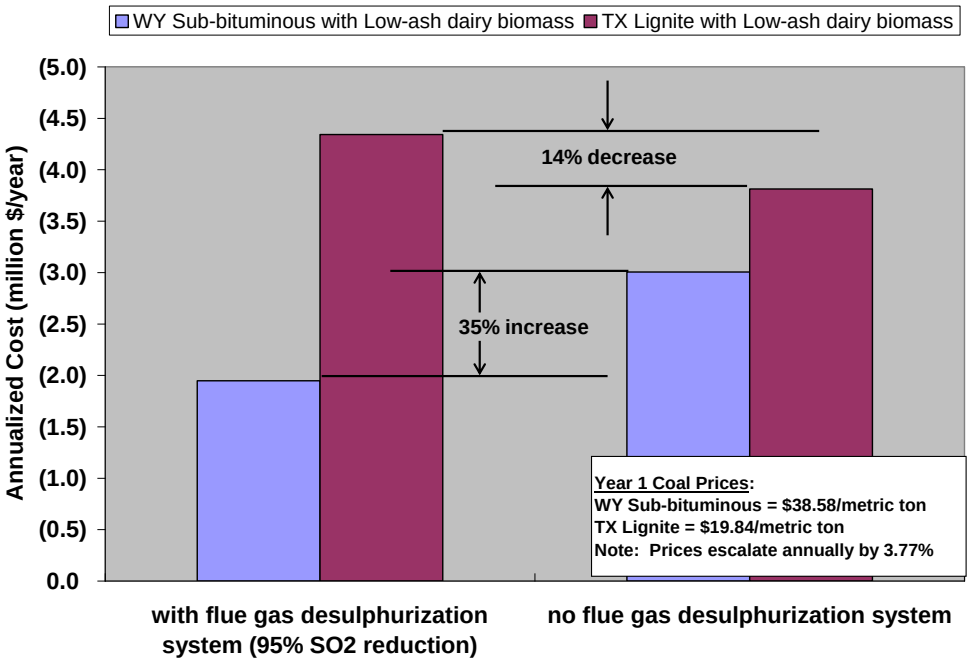

Figure 10.5.30 The effect of sulfur emissions on annualized cost during reburning

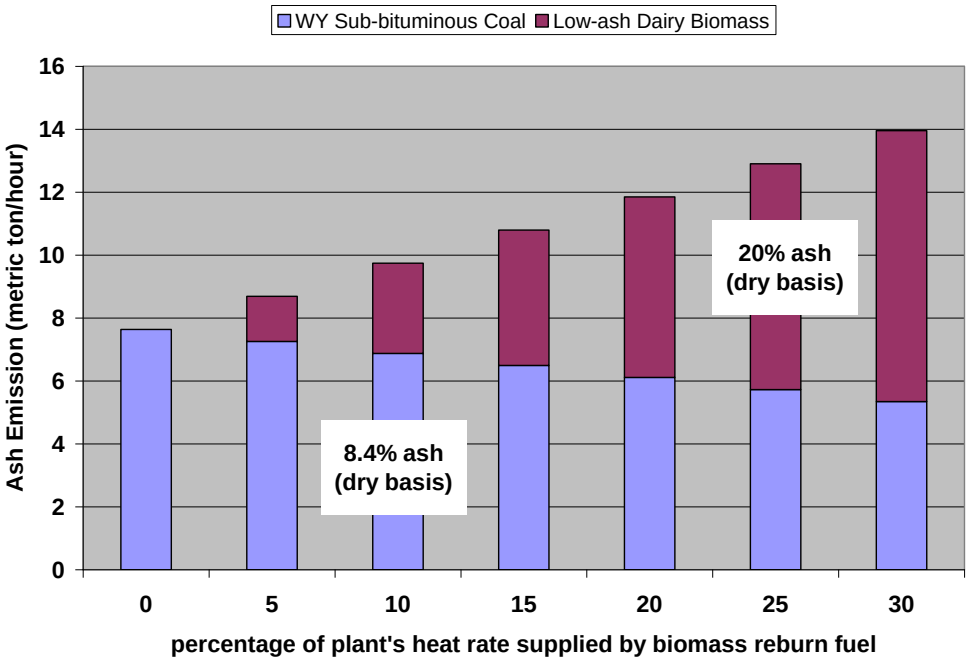

Figure 10.5.31 Ash emission vs. heat rate supplied by biomass reburn fuel for Wyoming sub-bituminous coal being replaced by low-ash dairy biomass

10.5.2.4. Biomass drying and transporting

The same discussion about MBB drying and transporting can be made for reburning as was done for co-firing. Since the only change for the drying and transportation sections of the economics model was the amount of biomass required for reburning, the trends during sensitivity analysis remain largely

the same. However, the relationship of parameters, such as transport distance, to reburning's competitiveness to SCR should be noted. For example, in Figure 10.5.32, MBB reburning was found to have a similar net present worth if transport distances were shorter than 20 km (12 miles), despite the same high natural gas fueling costs involved with drying the biomass.

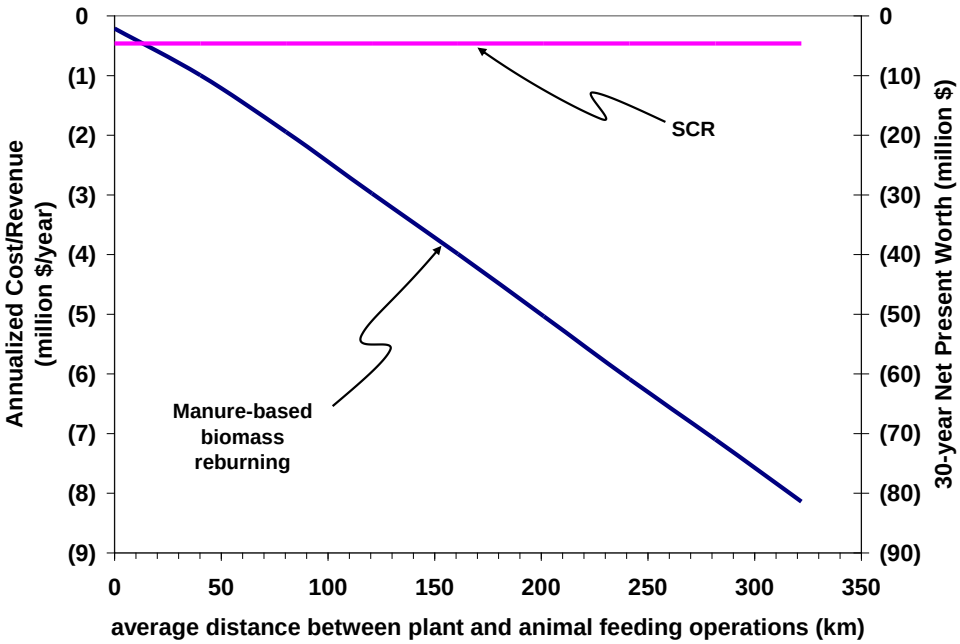

Figure 10.5.32 Annualized cost and net present worth of both reburning and SCR vs. manure-based biomass transport distance

During co-firing operations, the plant operator is free to burn coal with any fraction of MBB, so long as the combustion can be maintained and there is an adequate supply of co-fire fuel. However, with reburning, the amount of reburn fuel that is required is essentially fixed due to the desired NO_x emission levels. According to Oh *et al*. (2008), lower amounts of reburn fuel will hinder NO_x reductions. Thus, the problem of finding enough low-ash biomass suitable for burning in a power plant may be an even greater challenge for reburning. For the base case 300 MW power plant, about 57,000 dairy cows, each producing about 6.35 dry kg of manure per day would be required to supply the reburn facility if the biomass reburn fuel supplied 10% of the overall heat rate. This amount of manure is roughly 38% of all the manure produced in the Bosque and Leon River Watersheds in Texas. So, even though the economics models presented for this research predict that MBB reburning would be a better investment than MBB co-firing, the feasibility of reburning coal with MBB is seemingly more doubtful.

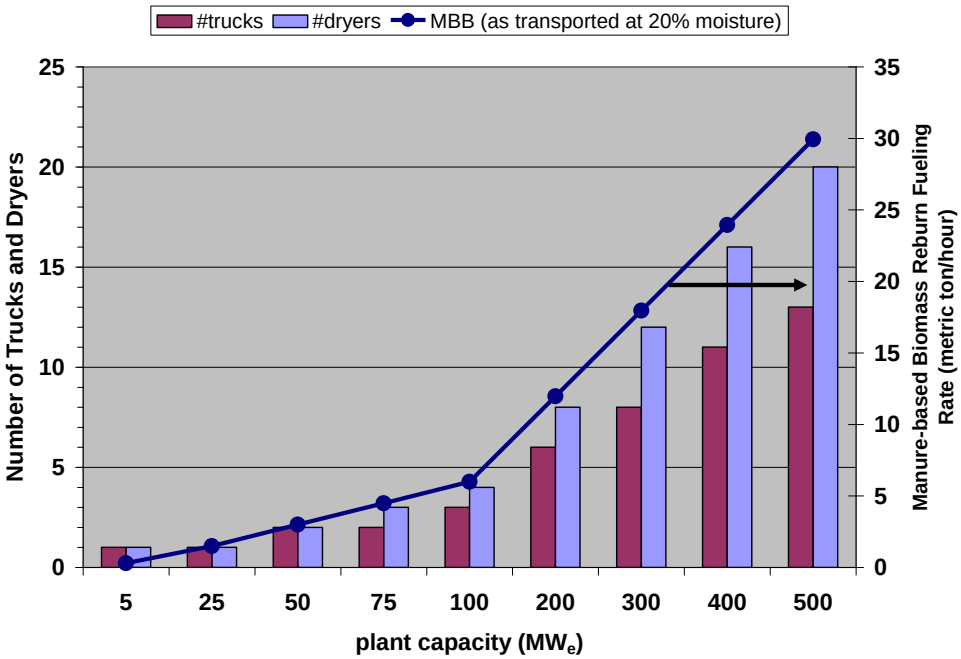

Figure 10.5.33 Number of required trucks and dryers and biomass fueling rate vs. plant capacity

In Figure 10.5.33, the number of trucks and dryers required to supply the biomass reburn fuel are plotted against power plant capacity. A 500 MW plant would require at least 20 two-metric ton/hr conveyor belt dryers where as a 100 MW plant would only require 4 dryers. Once again, the applicability of MBB reburn technology may be limited to smaller sized power plants. As state and federal governments decide how to increase the overall electrical power capacity in the country, instead of constructing extremely large power plants dependant on nonrenewable (although readily available) fossil fuels, steps ought to be made to construct a greater number of smaller plants. These new plants can be strategically placed near areas with higher concentrations of agricultural biomass to promote reburning and co-firing coal with carbon neutral feedstock, such as MBB. Infrastructure such as smaller sized power plants could curb NO_x and CO_2 emissions, boost rural economies, minimize the environmental load from large concentrated animal feeding operations, and develop stronger business ties between the agriculture and energy sectors of the US.

10.5.3. Economic Estimations for Small-scale Manure-based Biomass Systems

The discussion of economics for small-scale MBB combustion systems will not be covered as extensively here as the economics for large-scale co-fire and reburning projects on existing coal-fired power plants. However, the results of the modeling equations will be shown here. Under the base case input parameters, the capital cost of the rotary dryer was found to be about $1 million. If the combustor in the conceptualized model is assumed to be a gasifier and subsequent producer gas burner, then the capital investment cost of a gasifier capable of handling the amount of manure from a 500-cow farm was found to be $924,000. The air pre-heater was found to be about $11,000 when the overall heat transfer coefficient was set at 3.5 kJ/s m^2 K.

The circumstance of how these investments would be paid off depends greatly on the procedures of the animal feeding operation before the combustion system is installed. The Elimanure System is said to be profitable partly because the animal farm was transporting many gallons of liquid wastewater off the farm before the installation of the disposal system. The avoided cost of hauling manure plus the profits from electricity generation were claimed to be enough to pay off the $4.5 million investment and have a 3.5 year simple payback period.

This scenario can be roughly tested for the conceptual system presented here. Keeping with the same input parameters in Chapter 8, suppose that a 500-cow dairy hauls all of its liquid manure, at 95% moisture, 50 km (about 30 miles) off site. Moreover, assume that the animal farm, or a nearby business, can somehow use the steam generated in the fire-tube boiler and avoid having to pay a fueling cost (for example propane) to generate the steam. If the conceptualized MBB combustion system is installed it will save on manure transportation costs and generate revenue from the sale or avoided fueling cost of the steam. Also assume that a solid separator is already available at the dairy and that the boiler runs continuously every day of the year. Perhaps the greatest unknown is the capital cost of the fire-tube boiler, but for now, assume that it will cost $1 million just like the dryer. The total capital cost of the system is then about $2.9 million for a system disposing waste from 500 animals. The Elimanure System was said to be $4.5 million for a 4,000-head animal farm which included dairy cows, horses, and pigs (Skill Associates, 2005), (Caldwell, 2008).

The results of this base case run are presented in Table 10.5.12. The combustion system was found to save the animal feeding operation $137,000 per year, even without the use of additional fuel to completely incinerate the wastewater. The manure transportation equations were used here to estimate the cost of hauling manure (both before and after installation of the combustion system) and the resulting ash from the combustion. The labor cost was computed such that 1.5 workers were operating the combustion system at $15 per hour; that is, there was always one or two workers monitoring and maintaining the combustion system throughout the year.

Table 10.5.12 Base case run for the economics of the small-scale MBB combustion system when no additional fuel is burned

Cash flows before installation	
Hauling liquid manure--labor	(37,655)
Hauling liquid manure--diesel	(20,654)
TOTAL ($/yr)	(58,309)
Cash Flows after installation	
Fixed O&M of system	(118,300)
Hauling remaining liquid manure--labor	(18,403)
Hauling remaining manure--diesel	(10,094)
Hauling ash--labor	(255)
Hauling ash--diesel	(140)
Fuel Savings from boiler	423,470
Labor for system operation	(197,213)
System extra fuel (propane) cost	0
TOTAL ($/yr)	79,066
ANNUAL SAVINGS	137,375
Total capital cost of the system ($)	2,957,506
Simple Payback (years)	21.53

The payback for this base run was found to be 21 ½ years, which is usually unacceptable for a small scale project such as this. However, suppose that additional propane is injected into the burner so that all of the wastewater and MBB from the dairy is incinerated. This was the case for the Elimanure System as well. These results are presented in Table 10.5.13. For this case, the payback period was found to be only four year, much more comparable to the 3.5 payback period for the Elimanure System.

Table 10.5.13 Economic results for the small-scale MBB combustion system when additional fuel is used to completely vaporize all waste from the animal feeding operation

Cash flows before installation	
Hauling liquid manure--labor	(37,655)
Hauling liquid manure--diesel	(20,654)
TOTAL ($/yr)	(58,309)
Cash Flows after installation	
Fixed O&M of system	(137,221)
Hauling remaining liquid manure--labor	0
Hauling remaining manure--diesel	0
Hauling ash--labor	(340)
Hauling ash--diesel	(186)
Fuel Savings from boiler	1,129,805
Labor for system operation	(197,213)
System extra fuel (propane) cost	(400,885)
TOTAL ($/yr)	794,845
ANNUAL SAVINGS	853,154
Total capital cost of the system ($)	3,430,537
Simple Payback	4.02

However, these findings are all dependant the presumptions and estimations that were made, none of which is probably more significant than the capital cost of the fire-tube boiler, as can be seen in Figure 10.5.34

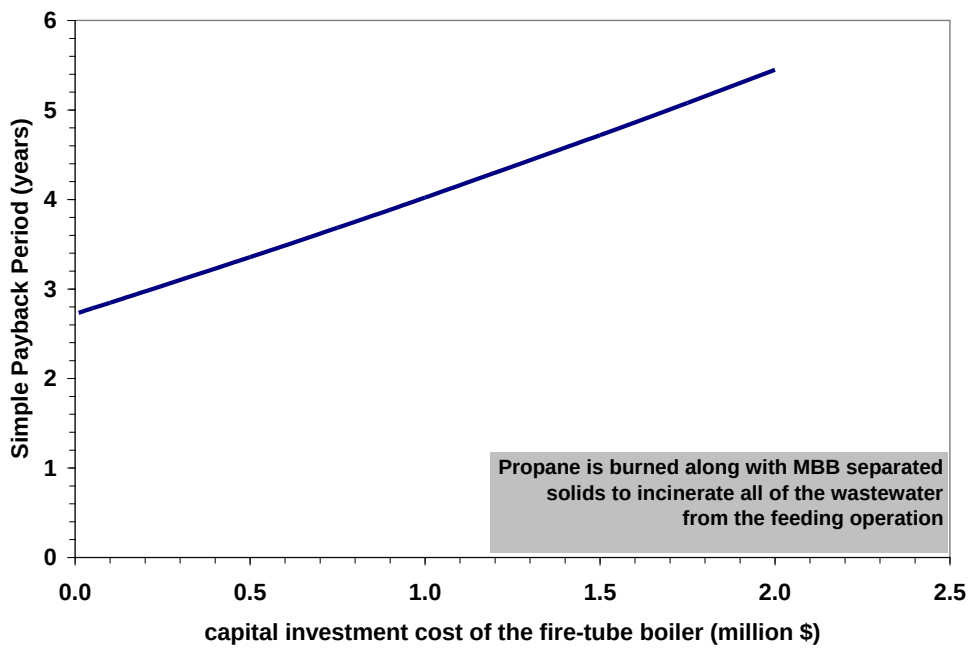

Figure 10.5.34 Simple payback period vs. the capital investment of the fire-tube boiler of the small-scale MBB combustion system

- Develop models for field-scale system (e.g. Panda Project and transportation models).

10.6. Impact on Tasks due to Industrial Advisory Committee feed back

1. "Develop models for field-scale system (e.g. Panda Project and transportation models)" . "Transporting coal vs. manure; relationship need to be better defined. Geography equals with manure as biofuel. Have to compete with coal as gold standard". "Trading allowances for Hg, NOx etc" . "Different characters of fuel – energy density is important here. Want properties with higher BTU. My biggest cost is transportation of that fuel. Some of what is taken to market, may have to look at further processing to tailor it to a market to sell." Hence the current model incorporates a transportation model for estimation of allowable distance .
2. "Nick Carlin's model is a good model; The best he has seen; Add a water treatment/reuse model". The direct combustion approach (task A-8) presents a model for water evaporation
3. The research must pursue other venues of revenue streams regarding animal waste. High energy prices cause alternative energy to be reasonably high.
4. There is more uncertainty in FB and DB and hence research "can remove through scientific knowledge" and it will help them (industries).
5. "This project has been extremely valuable….. The studies you have done will lead to new uses of manure. …..The carbon credit concept is shedding a new light on the situation". As a result the carbon credit was added in the economics modeling.

10.7. Summery and Conclusions

10.7.1. Economics of Co-firing

Co-firing MBB in large coal-fired power plants can be profitable, but a lot has to happen. The manure must be low in ash, coal prices must be high, CO_2 values must be high and expected to escalate, and the use of high-grade fuels such as natural gas during drying operations should be avoided. The following points summarize the discussion of co-firing coal with MBB.

1. A base case run of the MBB co-fire economics model for a MBB co-fire system installed on an existing 300-MW_e coal-fired power plant burning a 95:5 blend of coal to biomass showed that overall fuel energy consumption (including coal, biomass, diesel fuel, natural gas for drying, and electricity) would increase by 259 GJ/yr.
2. Burning a 95:5 blend of coal to low-ash MBB was found to lower CO_2 emissions by 58,600 tons/year (this value was calculated when accounting for CO_2 emitted during drying and transporting of MBB to the coal plant).
3. However, ash production from the plant was found to increase by 10% when burning a 95:5 blend, even when low-ash biomass was fired.
4. From base case parameters, an overall net present cost of $22.6 million was computed for the co-fire system at the 300-MW_e power plant. Operating income was never positive throughout the 30-year life of the co-fire project, causing zero return on investment, at least for the base case run. The most significant cost that hindered the profitability of the co-fire project was the cost of natural gas needed to fuel biomass dryers that could reduce the MBB's moisture content from 60% to 20%.

5. However, a higher value on avoided nonrenewable CO_2 emissions could overrule exorbitant costs of drying and transporting the MBB to power plants. A CO_2 value of $17/metric ton was found to be enough for the MBB co-fire project to reach an economic break even point.
6. The price of coal was also found to be significant to the overall profitability of the co-fire project. Since the biomass partly displaces the coal burned at the power plant, more expensive coal was found to lead to greater savings.
7. Although monetary compensation for the MBB would certainly benefit the owner of the animal feeding operation, a payment for obtaining biomass from farms could significantly decrease the profitability of a co-fire system. A MBB price of $10/dry metric ton can decrease the NPW of co-firing by 29%, if the price is also assumed to escalate by 3% annually.
8. Depending on the relative sulfur content of the MBB compared to the coal it is replacing, SO_2 emissions can become a significant factor in the economics of the co-firing project, especially if a flue gas desulphurization system is not installed at the coal plant. Sulfur is a greater detriment to the profitability when the biomass must replace a coal with very low sulfur content, such as Wyoming sub-bituminous coal.
9. Ash in MBB is a drag on the co-firing system (or reburning system) at every level. Ash adds to transportation costs as it means moving more mass for less energy content. Ash is also a heat sink during drying, making drying high ash biomass slightly more expensive than drying low ash biomass. Most significantly, ash adds to the O&M cost of co-firing because it must be removed from the power plant and then sold or disposed of off site.
10. For the base case run of the co-firing model, drying constituted 76% of the total cost. Of this cost, 73% was due to purchasing natural gas for generating steam for the biomass dryers. Another 15% was due to running the dryers' fans.
11. If scraped MBB can be both low in ash and low in moisture due to dry weather and low relative humidity, the ability to use MBB as a co-fire fuel at coal-fired power plants greatly increases.
12. Due to the low amount of suitable low-ash MBB, simply finding enough biomass to satisfy desired co-fire rates or required reburn rates for co-combustion projects at large coal-fired power plants may be challenging.

10.7.2. Economics of Reburning

The discussion on reburning coal with MBB in large coal-fired power plants can be summarized by the following three points.

1. Emitting NO_x is expensive. Therefore, a retrofit project in which coal is reburned with MBB (10% heat rate supplied by MBB) to reduce NO_x emissions can theoretically be more profitable than a co-fire project. However, the problem of finding enough suitable low-ash biomass becomes even more problematic for reburn systems because in order for NO_x reductions to be maintained, 10 to 25% of the plant's heat rate must be satisfied by the reburn fuel, and the highest reductions have been found to occur when the reburn fuel is pure MBB.
2. Under base case assumptions the net present cost of a MBB reburn project for an existing 300-MW_e coal-fired power plant was found to be $19.1 million. Comparatively, a selective catalytic reduction (SCR) project for a similar sized power plant with the same base case assumptions was found to be $4.6 million.
3. If the value of NO_x were to escalate annually at 4.5%, a current NO_x value over $2500/metric ton would justify installing a MBB reburn system. However, a reburn project would not be more justified, at least economically, than an SCR retrofit. In order for MBB reburning to be more profitable than SCR, a CO_2 tax or avoided cost of over $10/metric ton would be needed if the value of CO_2 was expected to escalate at 5.25% annually

10.8. Acronyms

β	TGA Heating Rate
μm	Micrometer or Micron
B	Pre-exponential Factor
ºC	Degree Celsius
C_2H_6	Ethane
CB	Cattle Biomass (either FB or DB)
CH_4	Methane
CO	Carbon Monoxide
CO_2	Carbon Dioxide
DAF	Dry Ash Free
DB	Dairy Biomass
DEAM	Distributed Activation Energy Model
DSC	Differential Scanning Calorimetry
DTA	Differential Thermal Analysis
E	Activation Energy
$E(X_n)$	Exponential Integral of the nth Order
FB	Feedlot Biomass
FC	Fixed Carbon
FTIR	Fourier Transform Infra Red
H_2	Hydrogen
HA-PC-DB-SoilSurf	High Ash Partially Composted Dairy Biomass Soil Surface
HA-PC-FB	High Ash Raw Manure Feedlot Biomass
HA-RM-FB	High Ash Raw Manure Feedlot Biomass
HR	Heating Rate
HHV	Higher Heating Value
K	Degree Kelvin
LA-PC-DB-SepSol	Low Ash Partially Composted Dairy Biomass Separated Solids
LA-PC-FB	Low Ash Partially Composted Feedlot Biomass
LA-RM-FB	Low Ash Raw Manure Feedlot Biomass
MVRR	Maximum Volatile Release Rate
min	Minute
mL	Milliliter
m_v	Volatile Mass
N_2	Nitrogen
PRB	Powder River Basin Coal (a subbituminous coal)
RM	Raw Manure
R_u	Universal Gas Constant
SMD	Sauter Mean Diameter
SRM	Single Reaction Model
t	Time
T	Temperature
T_e	Empty Pan Thermocouple
T_s	Sample Pan Thermocouple
TC	Thermocouple
TGA	Thermogravimetric Analysis
TXL	Texas Lignite

10.9. References

ACAA. (2006). Frequently asked questions. American Coal Ash Association. Available online at: http://acaa.affiniscape.com/displaycommon.cfm?an=1&subarticlenbr=5. (Accessed on September 2007).

Annamalai, K. and Sweeten, J. M. (2005). Reburn system with feedlot biomass. U. S. Patent #6,973,883 B1.

Biewald B, Cavicchi J, Woolf T, Allen D. (2000). Use of selective catalytic reduction for control of NO_x emissions from power plants in the US. Prepared for the OntAlRio Campaign.

Brammer J.G. and Bridgwater A.V. (1999). Drying technologies for an integrated gasification bio-energy plant. *Renewable and Sustainable Energy Reviews* 3: 243-89.

Brammer J.G. and Bridgwater A. V. (2002). The influence of feedstock drying on the performance and economics of a biomass gasifier-engine CHP system. *Biomass & Bioenergy* 22: 271-81.

Caldwell E. (2008). Roast your compost: EcoCombustion Energy Systems Corporation has commercialized a manure-burning system dubbed Elimanure. *Ag Nutrient Management* Magazine by Progressive Dairy Publishing. August 2008.

Canales E. R., Borquez R. M. and Melo D. L. (2001). Steady state modeling and simulation of an indirect rotary dryer. *Food Control* 12: 77-83.

Carlin, N. T. (2005). Thermo-chemical conversion of dairy waste based biomass through direct firing. MS Thesis. Texas A&M University: College Station, Texas

Carlin, N., Annamalai, K., Sweeten, J., and Mukhtar, S. (2007a). Thermo-chemical conversion analysis on dairy manure-based biomass through direct combustion. *International Journal of Green Energy* 4(2): 133-159.

Colmegna G., K. Annamalai, and Udayasarathy A.V. (2007). Modeling of Hg reduction during reburn process with the use of cattle biomass as a reburn fuel. Third International Green Energy Conference (IGEC-III), June 17-21, Västerås, Sweden.

DOE. (2004). Biomass co-firing in coal-fired boilers, federal technology alert: A new technology demonstration publication. Federal Energy Management Program (FEMP) of the United States Department of Energy. Paper No. DOE/EE-0288. Available online at: http://www1.eere.energy.gov/femp/pdfs/fta_biomass_cofiring.pdf. (Accessed on December 2008)

EIA. (2007b). Natural gas: US price data. Energy Information Administration of the US Department of Energy. Available online at: http://www.eia.doe.gov/oil_gas/natural_gas/info_glance/natural_gas.html. (Accessed on February 2009).

EIA. (2007d). Average price of coal delivered to end use sector by census division and state: US price data. Energy Information Administration of the US Department of Energy. Available online at: http://www.eia.doe.gov/cneaf/coal/page/acr/table34.html. (Accessed on February 2009)

EIA. (2007e). Average retail price of electricity to ultimate customers: total by end-use sector: US price data. Energy Information Administration of the US Department of Energy. Available online at: http://www.eia.doe.gov/cneaf/electricity/epm/table5_3.html. (Accessed on February 2009).

GSNet.com. (2007). The largest source of machinery listings online. Available online at: http://www.gsnet.com. (Accessed on November 2007).

Goodrich L. B., Mukhtar S., Capareda S., Harman W. (2007). Characterization and transportation analysis of dairy biomass for co-firing in coal-fired power plants. Texas A&M University. Unpublished paper.

Heflin K. (2008). Personal contact. Extension Associate. Texas AgriLife Extension Service, Amarillo and Bushland, Texas.

Hinds W. C. (1999). *Aerosol technology: properties, behavior, and measurement of airborne particles, second edition*. New York: John Wiley & Sons, Inc.

Houkom R. L., Butchbaker A. F., and Brusewitz G. H. (1974). Effect of moisture content on thermal diffusivity of beef manure. *Transactions of the ASABE* 17: 973-977.

Kiranoudis C. T., Maroulis Z. B., Marinos-Kouris D. (1994). Modeling and design of conveyor belt dryers. *Journal of Food Engineering* 23: 375-96.

Krishnan R. and Tarabulski T. J. (2005). Economics of emission reduction for heavy duty trucks. DieselNet Technical Report. Available online at: http://www.dieselnet.com/papers/0501krishnan/. (Accessed on October 2007).

Lawrence, B. D. (2007). Co-firing of coal and dairy biomass in a 100,000 Btu/hr furnace. MS Thesis. Texas A&M University: College Station, Texas.

Megel A. J., Parker D. B., Mitra R., Sweeten J. M. (2006). Assessment of chemical and physical characteristics of bottom, cyclone, and baghouse ashes from combustion of manure. Presented at the ASABE Annual Meeting, Portland, Oregon, June 2006.

Megel, A. J., DeOtte, R. E., and Robinson, C. A. (2007). Investigation of economically viable coproducts developed from ash from the combustion of manure. 2007 ASABE Annual International Meeting, Minneapolis Convention Center, Minneapolis, Minnesota, June 17-20, 2007.

Mussatti D. C., R. Srivastava, P. M. Hemmer, and R. Strait. (2000b). EPA Air Pollution Control Cost Manual – Sixth Edition. Section 4, Chapter 2, Selective Catalytic Reduction. Available online at: http://www.epa.gov/ttn/catc/products.html. Scroll down to "EPA Air Pollution Control Cost Manual Chapters & Information". (Accessed on June 2006).

Oh, H. (2008). Reburning renewable biomass for emissions control and ash deposition effects in power generation. Ph.D. Dissertation. Texas A&M University: College Station, Texas.

Pakowski Z., Bartczak Z., Strumillo C., and Stenstrom S. (1991). Evaluation of equations approximating thermodynamic and transport properties of water, steam and air for use in CAD of drying processes. *Drying Technology* 9(3): 753-773.

Peterbilt.com. (2009). Trucks by Peterbilt: a PACCAR Company. Company headquarters in Denton, Texas. More information online at: http://www.peterbilt.com/showroom.aspx. (Accessed on February 2009).

RGGI. (2008). Regional greenhouse gas initiative: an initiative of the Northeast and Mid-Atlantic states of the US. Information available online at: http://www.rggi.org/home. (Accessed on September 2008).

Robl T. L. (1997). We are running out of fly ash: the nature of regional supply problems. Prepared for NETL of the DOE. Third Annual Conference on Unburned Carbon on Utility Fly Ash, Available online at: http://www.netl.doe.gov/publications/proceedings/97/97ub/robl.pdf. (Accessed on June 2006).

Rodriguez, P., Annamalai, K., and Sweeten, J. (1998). Effects of drying on heating values of biomass. *Society of Agricultural Transactions* 41: 1083-1087

SCAQMD. (2007). Annual RECLAIM audit report for 2005 compliance year. South Coast Air Quality Management District. March 2, 2007 board meeting. Available online at: http://www.aqmd.gov/hb/2007/March/070334a.html. (Accessed on May 2007).

Sekar, R. C., J. E. Parsons, H. J. Herzog, and H. D. Jacoby. (2005). Future carbon regulations and current investments in alternative coal-fired power plant designs. MIT Joint Program on the Science and Policy of Global Change. Report No. 129, December 2005. Available online at: http://mit.edu/globalchange/www/MITJPSPGC_Rpt129.pdf. (Accessed on May 2006).

Skill Associates. (2005). Elimanure™. Available online at: http://www.burnmanure.com/management/elimanure.html. (Accessed on February 2008).

Srivastava, R. K., Hall, R. E., Khan, S., Culligan, K., and Lani, B. W. (2005). Nitrogen oxides emissions control options for coal-fired electric utility boilers. *Journal of Air & Waste Management Association* 55: 1367-1388.

Sweeten.J. M., Heflin K., Annamalai K., Auvermann B. W., McCollum F. T., and Parker D. B. (2006). Combustion-fuel properties of manure or compost from paved vs. un-paved cattle feedlots. Presented at the 2006 ASBAE Annual International Meeting, Portland, Oregon.

TAMU. (2006). TAMU Fuel Data Bank. Texas A&M University Coal and Biomass Energy Laboratory. Available online at: http://www1.mengr.tamu.edu/REL/TAMU%20FDB.htm. (Accessed on January 2007).

Turner W. C. (2001). *Energy management handbook, fourth edition*. Chapter 4, Economic Analysis. Liburn, GA: The Fairmont Press, Inc.

US Bureau of Labor Statistics. (2008). Producer price indexes: archived producer price index detailed report information. United States Bureau of Labor Statistics of the US Department of Labor. Available online at: http://www.bls.gov/ppi/ppi_dr.htm. (Accessed on November 2008).

USEPA. (2007a). Integrated planning model. Clean Air Markets Division of the United States Environmental Protection Agency. Available online at: http://www.epa.gov/airmarkt/progsregs/epa-

ipm/index.html. Scroll down to about two-thirds of the page to National Electric Energy Data System (NEEDS) 2006. Download Microsoft Excel Spreadsheet database file. (Accessed on June 2007).

USEPA. (2007c). EPA's updates to EPA base case v3.01 from EPA base case 2006 (v3.0) using the integrated planning model (IPM). Carbon assumption enhancements. Available online at: http://www.epa.gov/airmarkets/progsregs/epa-ipm/. Scroll down to "Documentation Supplement for EPA's Base Case (v3.01)". (Accessed on June 2007).

USEPA. (2006). Documentation for EPA base case 2006 (V.3.0) using the integrated planning model. Clean Air Markets Division of the United States Environmental Protection Agency, EPA Contract No. 430-R-05-011. Available online at: http://www.epa.gov/airmarkets/progsregs/epa-ipm/. (Accessed on June 2007).

USEPA. (2004). Standalone documentation for EPA base case 2004 (V.2.1.9) using the integrated planning model, chapter 5, emissions control technologies. Clean Air Markets Division. September 2005, EPA Contract No. 430-R-05-011. Available online at: http://www.epa.gov/airmarkets/progsregs/epa-ipm/past-modeling.html. Scroll down to the 2004 update. (Accessed on June 2006).

USEPA. (2001). Cost methodology report for beef and dairy animal feeding operations. Engineering and Analysis Division. EPA Contract No. 821-R-01-019. Available online at: http://www.epa.gov/waterscience/guide/cafo/pdf/BDCostReport.pdf. (Accessed on June 2006).

USEPA. (1998). Analyzing electric power generation under the CAAA. Appendix No. 5.

Zamansky, V. M., Sheldon, M. S., Lissianski, V. V., Maly, P. M., Moyeda, D. K., et al. (2000). Advanced biomass reburning for high efficiency NOx control and biomass reburning – modeling/engineering studies. USDA Phase II SBIR, Contract #97-33610-4470 and DOE-NETL, Contract #DE-FC26-97FT-97270. Available online at: http://www.osti.gov/bridge/servlets/purl/786516-Dddr9I/native/786516.pdf. (Accessed on May 2006).

10.10. Education and Training

This work was used in part to fulfill the Doctoral requirements of Nicholas Carlin.

10.11. Other support

None

10.12. Dissemination

Carlin NT, Annamalai K, Harman W, Sweeten JM. (2009). The economics of reburning with cattle manure-based biomass in existing coal-fired power plants for NO_x and CO_2 emissions control. Accepted by *Biomass & Bioenergy* in March 2009. In press.

Carlin NT, Annamalai K, Oh H, Gordillo Ariza G, Lawrence B, *et al*. (2008). Co-combustion and gasification of coal and cattle biomass: a review of research and experimentation. Accepted by *Progress in Green Energy* in January 2008. In press.

Carlin NT, Annamalai K, Sweeten JM, and Mukhtar S. (2007). Thermo-chemical conversion analysis on dairy manure-based biomass through direct combustion. *International Journal of Green Energy* 4(2):133-159.

Carlin NT, Annamalai K, Sweeten JM, and Mukhtar S. (2007). Utilization of latent heat derived from vaporized wastewater in high moisture dairy manure combustion schemes. International Symposium on Air Quality and Waste Management for Agriculture, September 15-19, 2007: Broomfield, CO.

Annamalai K, Carlin NT, Oh H, Gordillo Ariza G, Lawrence B, *et al*. (2007). Thermo-chemical energy conversion using supplementary animal wastes with coal. Proceedings of the IMECE, 2007 ASME International Mechanical Engineering Congress and Exposition, November 11-15, 2007: Seattle, WA, USA

11. CO-FIRE AND REBURN FOR HG REDUCTION

Task A-3 (KA): Co-firing (by Ben)
Task A-3-2: Co-fire the CB with low grade TXLC and chlorinated carbon
Task A-4 (KA): Reburn Process (by Jin)

Abstract

Mercury is a leading concern among the air toxic metals addressed in the 1990 Clean Air Act Amendments (CAAA) because of its volatility, persistence, and bioaccumulation as methyl mercury in the environment and its neurological health impacts. Unlike other trace metals that are emitted in particulate form, mercury is released in vapor phase in elemental or oxidized form. As on date, there is no post combustion treatment which can effectively capture elemental mercury vapor, but oxidized form of mercury can be captured in traditional emission control devices such as wet flue gas desulfurization (WFGD) units, since oxidized mercury is soluble in water. The chlorine concentration present during coal combustion plays a major role in mercury oxidation, which is evident from the fact that plants burning coal having high chlorine content have lesser elemental mercury emissions. For Wyoming coal the concentration of chlorine is 100 ppm, while for Low Ash Partially Composted Dairy Biomass it is 1,400 ppm. Since increase in chlorine concentration increase mercury oxidation, blending higher fractions of cattle biomass with coal increases the probability of mercury oxidation

Cofiring (2008)

To increase the chlorine content during combustion, a novel method of co-firing blends of coal with high chlorine content cattle manure/biomass was used to increase mercury oxidation and hence mercury capture. The current research, co-firing experiments were performed in 100,000 BTU/hr Boiler Burner facility located in Coal and Biomass Energy laboratory (CBEL); where coal and biomass blends in proportions of 80:20, 90:10, 95:5 and 100:0 were investigated. A wet chemical set up was assembled and appropriate chemicals were acquired. Both elemental Hg0 and total HgT (elemental + oxidized Hg which was converted into elemental Hg) were measured and the oxidized Hg was evaluated as the difference between the two. The % reduction of Hg with 95:5, 90:10 and 80:20 blends were measured to be 28-50%, 42-62% and 71-75% respectively. Percentage reduction for WYC and LAPCFB blends varied from 28-71% with increase in biomass proportion; for WYC and HA LA-PC varied from 14-71% with increasing biomass proportion. For TXL and LA PC-DB blends reduction in elemental Hg varied from 50-75% and for TXL and HA PC-DB it was 37-50%. A methodology has been developed to estimate flue gas volume per GJ heat input. Using such an analysis, total Hg as a percentage of input Hg is estimated to be 7-14%. The difference is believed to be capture by unburnt combustibles in ash.

Though cattle biomass serves as an additive to coal, to increase the chlorine concentration, it leads to higher ash loading. Low Ash and High Ash Partially Composted Dairy Biomass have 164% and 962% more ash than Wyoming coal respectively. As the fraction of cattle biomass in blend increases in proportion, ash loading problems increase simultaneously. Beyond a certain blend ratio, adding excess biomass to the blend does not cause any significant reduction in elemental mercury but causes other problems related to increased fuel feed rate and increased ash deposition. Hence an optimum blend ratio is arrived and suggested as 90:10 blend with good reduction in mercury emissions without any compromise on ash loading.

Cofiring (2009)

More co-combustion studies using cattle biomass (CB) and coals were conducted in 2008 on Hg reductions in the coal-fired power plants. A small-scale 30 kWt (100,000 Btu/h) downward fired boiler burner facility was used for the co-firing experiments. The results show that the pulverized CB can serve as a supplementary fuel for the coal-fired boilers, and the co-firing CB with coals shows reductions in NOx and Hg emissions depending on blending ratios and equivalence ratios (ϕ).

Reburn

Reburning of cattle manure-based biomass (CB) with coals is performed to investigate the reduction of Hg . A small-scale (30 kWth) down-fired boiler burner facility has been used is designed for burning most types of pulverized solid fuels including coal and biomass. Coal was used as main fuel. Blends of cattle biomass (CB) and coals are used as reburn fuels. The CB contains larger amounts of chlorine (Cl) than most types of coals. Gaseous mercury (Hg) in the flue gas is oxidized by large amounts of Cl species mainly from the CB combustion. Consequently, the results indicate that the CB can serve as is a very effective fuel supplementing coals on Hg reductions in pulverized coal-fired boilers.

Bench Scale Experiments

Chlorinated carbons (DB-CH) have been produced by pyrolysis, using biomass in a fixed bed gasifier. The effectiveness of DB-CH in capturing elemental mercury (Hg) has been experimentally measured using bench scale test rig. A permeation tube was used as Hg source. The DB-chars were packed in a U-tube and Hg laden gases were passed through the DB-CH in the U-tube. Parametric studies on mass (10g, 20g) and temperature (15°C, 90°C, 150°C) were performed. Also mercury sorption for flue gas, produced by a 30kW small-scale furnace firing Texas Lignite Coal, was investigated.

Mercury adsorption rates over time show decreasing adsorption for both chlorinated carbons investigated. This happens due to a saturation process on the surface of DB-CH used. Two types of DB-CH were used: DB-CH produced using N_2 and DB-CH produced by N_2 and H_2O. No significant differences between the two DB-CH used were observed. Investigating the effects of mass and temperature on the adsorption rate, the influence of temperature is much stronger than the influence of mass. Raising the temperature leads to smaller adsorption rates, hence the driving mode of adsorption for the chlorinated carbons used is physisorption, which compared to chemisorption is much more temperature dependent. Comparing the results of mercury sorption for a nitrogen flow to the case where flue gas was used, the adsorption over time shows no significant difference

11.1. Introduction

The 1165 coal fired utilities in USA produce about 48 tons of Mercury (Hg) every year [Feeley III et al, 2005]. EPA's Clean Air Mercury Rule (CAMR) calls for reduction of Hg emissions in two phases: from 48 tons/yr to 38 tons/yr in Phase I and to 15 tons/yr in Phase II [EPA Website]. The Phase I control begins in 2010 with 38 Tons/yr as the cap while Phase II begins in 2018. Phase I is based on co-benefit reductions of Hg through conventional Air Pollution Control Devices (APCD) for reduction of SO2 (e.g. wet scrubbers), particulate matter (PM) emissions from coal fired flue gases required under Clean Air Interstate Rule (CAIR). For example, the Selective Catalytic Reduction (SCR) used for NOx control can also oxidize elemental Hg.

Typically the Hg in coal (Lignites: 10-350 parts per billion or ppb; Sub-Bituminous 10-440 ppb; Bituminous: 20-820 ppb) is vaporized as elemental Hg, yielding Hgo vapor while the Hg in the flue gas exists in three different forms: elemental Hg^o (elemental) and Hg^{2+} (oxidized form, e.g. HgCl2) [Linak, 2001] and Hg in particulates. Typically the proportions are about 20-50% in elemental forms, 50-80% in oxidized forms and 5% in particulate forms [Carpi, A., 1997]. The elemental form is an insoluble and volatile metal which cannot be captured by traditional pollution control devices. On the contrary, the oxidized and particulate forms can easily be captured by electrostatic precipitators (ESP), fabric filters (FF), or wet flue gas desulphurization (WFGD) systems. Thus technologies which are able to convert more elemental forms into oxidized forms need to be developed in order to control the Hg emissions. The predominant form of the oxidized Hg in the flue gas is believed to be HgCl2.

The elemental Hg^o does not dissolve in water and is not usually captured in APCD (advanced Pollution Control Device) while the Hg in particulates is captured in particulate control devices (PCD) (Electro static precipitator {ESP} or fabric filter {FF}, other appropriate devices). The oxidized form dissolves in water and can be captured with water spray or in flue gas desulphurization (FGD) unit. In fact the relative solubility of Hgo and Hg2+ are 1 and 1,400,000 respectively [Wilhelm, 1999]. The oxidized mercury compounds are also known to form complexes with fly ash aerosols.

The Cl content in Bituminous coals ranges from 200 to 2000 ppm (dry basis) while for low rank coals (sub-bituminous and lignite) Cl ranges from 20 to 200 ppm an order of magnitude lower. Typically elemental Hg content in coal is inversely proportional to Cl content of coal. Thus the low rank Sub-bituminous and lignite coals reveal lower Hg capture (3-72 %) in "co-benefit" systems than higher rank bituminous coal (9-98 %) [Feeley III et al, 2005]. Hg removal plotted against coal chlorine content reveals increasing Hg capture with Cl due to HgCl2 formation [Senior and Alfonso, 2001]. Typically, when Cl concentration exceeds 200 ppm, Hg is captured primarily in the particulate phase. TXU Energy uses Texas Lignite and the Texas Municipal Power Agency (TMPA) near College Station uses Wyoming sub-bituminous coal as fuel. As Cl is low in sub-bituminous and lignite coals, the Hg exists primarily as elemental Hg, which is difficult to capture. The particles are captured using either ESP to capture the particulate containing carbon along with Hg compounds or using wet scrubbers. In order to form oxidized Hg, Chlorine (Cl) is required.

Numerous studies on the Hg emissions or oxidations have been investigated using boiler facilities and flow reactors ; see following references: Agarwal, H., et al; Gibb, W. H.,et al. 2000; Cao, Y. et al., 2005; Hall, B. et al. 1991; Laudal, D. L. et al.
2003; Sable, S. P. et al 2007a; Sable, et al. 2007b]. Their results can be summarized as follows: 1) The Hg released during combustion is mainly influenced by the type of boiler, type of fuel, temperature,

equivalence ratio (ϕ), amount of Cl, amount of UBC, other species present in the flue gas, and the type of emission control system, 2) Most of the Cl in coals is released as HCl which oxidize Hg, thus firing high-Cl fuels typically reduces the emissions of elemental Hg, 3) Retention of Hg in the fly ash increases with an increase of UBC in the ash or in fuel-rich conditions (ϕ > 1) because the carbon adsorbs Hg, and 4) Selective catalytic reduction (SCR) catalysts or active carbons increase Hg reductions by capturing elemental Hg.

Figure **11.1.1**shows a schematic of a typical coal fired power plant. The coal is ground (pulverized) to a fine powder, so that less than 2% is +300 µm and 70-75% is below 75 µm, for a bituminous coal. The powdered coal is then blown into a combustion chamber of a boiler, where it is burned at temperatures around 1,400ºC. Surrounding the walls of the boiler room are pipes filled with high pressure water. Because of the intense heat, the water vaporizes into superheated high-pressure steam. The steam passes through a turbine (which is similar to a large propeller) connected to a generator. The incoming steam causes the turbine to rotate at high speeds, creating a magnetic field inside wound wire coils in the generator. This pushes an electric current through the wire coils out of the power plant through transmission lines. After the steam passes through the turbine chamber, it is cooled down in cooling towers and it again becomes part of the water/steam cycle. During the combustion of coal, products as a result of combustions result (CO_2, SO_2, NO_x, ash, slag, gypsum). Initially, the nitrogen oxides contained in the flue gas are reduced to harmless N_2, CO_2 and H_2O either in a SCR or SNCR kind of NO_x removal device. Subsequently, the flue gas is made dust free where particulate matter is removed in an electrostatic precipitator (ESP) or fabric filter, and finally to remove SO_2 from stack gas, the flue is passed through a wet flue gas desulphurization (Wet FGD) unit where SO_2 dissolves in water when water is sprayed over it. The ash removed from the steam generator and the electro filter can be used in the construction industry, e.g. cement making.

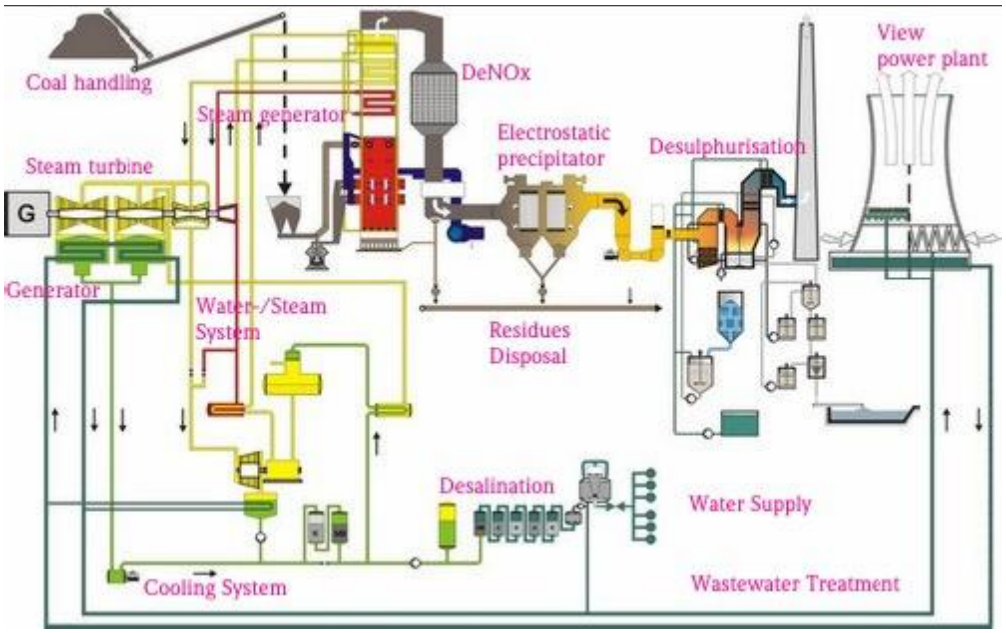

Figure 11.1.1. Layout of a coal fired power plant [Endress+Hauser, Coal Fired Power Plant, http://www.endress.com, August 2007]

Mercury may be controlled to limited success using existing control technologies, for instance, many power plants have existing mercury capture as co-benefit of air pollution control technologies for NOx, SOx and particulate matter. This includes capture of oxidized mercury in WFGD units. Use of selective catalytic reduction (SCR) units used for NOx control enhances oxidation of elemental mercury (Hg^0) to its soluble ionic form Hg^{2+} resulting in removal at WFGD system. Alternative technologies which emerged recently include use of activated carbon injection (ACI) and advanced sorbents to capture mercury from flue gases at the fabric filters used to collect ash.

It is apparent that apart from "co-benefit" method (phase I) , other methods are required to meet the CAMR Phase II regulations; a few of the methods under development are as follows: i) Blended Coals: a blend of high Cl and low Cl coals, ii) Activated Carbon Injection (ACI): powdered activated carbon (PAC) injected downstream of the air preheated and upstream of APCD and capture of Hg along with fly ash in APCD , and iii) patented "thief process" by DOE where small % (< 1 %) of partially burnt char is captured near the coal burner and then injected downstream of the boiler to capture Hg . Recent experimental data indicate that the patented Activated Carbon Injection technique removes almost 90 % of Hg.

11.2. Literature review

The literature review presents an overview of mercury emissions, its health effects, control technologies present and an insight to cattle biomass.

Mercury Emissions

While Mercury is one of the most useful of the heavy metals found in our daily lives, it is also one of the most deadly. The calculated atmospheric lifetime of elemental mercury is computed as the inverse of the net removal rate of mercury based on global measurements of deposition, balanced against the sum of sources (anthropogenic, terrestrial and oceanic). There is wide range of estimated of amount of mercury present in the atmosphere. Based upon the recent findings several researchers report that the amount of mercury in the atmosphere at any time may be in the range of 6000 to 7000 tons [Lindquist el al 1994;Levin 2004, Puchakayala, 2006; Udayasarathy, 2007]. Table 2.1 provides global totals as estimated by various authors. As can be seen, these estimates of overall global burden of mercury vary widely.

Table 11.2.1 Estimates of total release of mercury to the global environment [L. Levin, 2004]

Process	Lindquist *et al.* 1984	Nriagu & Pacyna 1988,Nriagu 1989	Fitzgerald 1986	Lindquist *et al.* 1991	Mason *et al.*, 1994	Pirrone *et al.*, 1996	Lamborg *et al.*, 2002
Anthropogenic releases	2000-10,000	3560 (910-6200)	2000	4500 (3000-6000)	5550 *1	2200	3000 *2
Natural releases	<15,000	2500 (100-4900)	3000-4000	3000 (2000-9000)	1650	2700	1400
Total present releases	2000-<25,000	6060 (1010-11,100)	5000-6000	7500 (5000-15,000)	7200	4900	4400

The mercury emitted from the power plants is not harmful; however, in the natural environment the mercury can go through a series of chemical transformations that convert the mercury to a highly toxic form that is concentrated in fish and birds. Of 158 tons of mercury being emitted by anthropogenic sources annually, coal fired power plants contribute about 33%, taking the largest share. Table 2.2 shows the source of mercury from various anthropogenic sources and their corresponding contribution in the US. Mercury is a natural constituent of coal and generally associated with pyrite (iron sulfide), commonly secondary arsenic-bearing pyrite, or is present in clay and the organics, or in coal with low iron content (pyrite) it occurs as a selinide [Finkelman,2003]. The reported average mercury concentrations of 0.087 μg/g (ranging from0.03–0.25μg/g) in Australian coal, 0.22 μg/g (ranging from 0.09–0.51 μg/g) in eastern U.S. coal, 0.04 μg/g in Colombian coal and 0.72 μg/g (ranging from 0.14–1.78 μg/g) in Polish coal [Chu, 1995]. The average mercury concentrations of 0.070 μg/g in bituminous coal, 0.027 μg/g in sub-bituminous coal and 0.118 μg/g in lignite coal [Chu 1995]. It was estimated that typically 0.24 μg/g of mercury occurs in Appalachian coals, 0.14 μg/g in Interior Eastern coals and 0.21 μg/g in Illinois Basin coals [Chu 1993]. Table 2.3 shows mercury values in selected U.S. coal areas from the U.S. Geological Survey Coal Quality (COALQUAL) database [Bragg, 1998]. This is the way that mercury data are presented in most publications. This may be misleading because, in order to obtain similar energy outputs, more low-rank coal has to be burned than a higher-ranked coal. This can result in a net mobilization of more total mercury to the environment. A better way to compare mercury data for coal is on an equal energy basis. Table 2.4 shows mercury on equal energy basis, mean values for samples in selected U.S. coal areas [Finkelmann,2003]. Figure **11.2.1** shows the map, generated from the U.S. Geological Survey COALQUAL database compiled on mercury loading over the United States atmosphere [http://igs.indiana.edu/Geology/]. It clearly shows that mercury loading over the Texas region is very high compared to others. Out of the top ten power plants which contribute to mercury pollution, five are present in Texas.

Table 11.2.2 Sources of mercury in US [www.iit.edu/~ipro356s05/bg_sources.html]

Sources	Tons/yr	% Total
Utility boilers	52	32.8%
Municipal waste incenerators	29.6	18.7%
Commercial/industrial boilers	28.4	17.9%
Medical waste incenerators	16	10.1%
Hazardous waste incenerators	7.1	4.4%
General lab use	1.1	0.7%
Others	23.9	15.4%

Table 11.2.3. Mercury values in selected U.S. coal areas from the COALQUAL database [Finkelmann,2003]

	mean (ppm)	maximum (ppm)	number of samples
Appalachian	0.2	2.9	4,399
Eastern interior	0.1	0.4	301
Fort Union	0.13	1.2	300
Green River	0.09	1	418
Gulf Coast	0.22	0.6	29
Hams Fork	0.09	1	142
Pennsylvania anthracite	0.18	1.3	52
Powder River	0.1	1.4	616
Raton Mesa	0.09	0.5	40
San Juan River	0.08	0.9	194
Southwest Utah	0.1	0.5	42
Uinta	0.08	0.6	271
Western interior	0.18	1.6	311
Wind River	0.18	0.8	42

Table 11.2.4. Mercury on equal energy basis, mean values for samples in selected U.S. coal areas [Finkelmann, 2003]

	mercury (pounds / 10^{12} BTU)	mean (ppm)
Appalachian	15.4	0.2
Eastern interior	8.2	0.1
Fort Union	21.8	0.13
Green River	6.6	0.09
Gulf Coast	36.4	0.22
Hams Fork	4.8	0.09
Pennsylvania anthracite	15.4	0.18
Powder River	12.6	0.1
Raton Mesa	6.6	0.09
San Juan River	7.7	0.08
Southwest Utah	11	0.1
Uinta	7.3	0.08
Western interior	16.1	0.18
Wind River	18.7	0.18

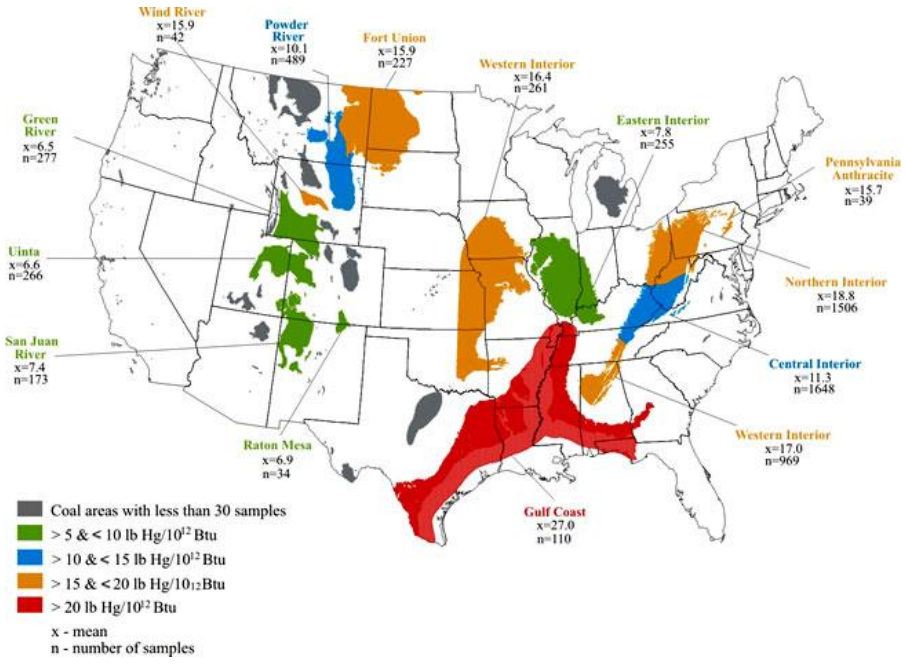

Figure 11.2.1. Mercury loadings (in pounds of Mercury per 1012 British thermal units (lbs Hg/1012 Btu) [http://igs.indiana.edu]

Health Effects

Mercury is a naturally occurring heavy metal, classified as a toxic metal emitted both by natural and anthropogenic sources. It can exist in elemental, inorganic and organic forms. Elemental mercury though being a metal is highly volatile, especially at high temperatures like coal combustion or incinerators. They escape into the atmosphere without being captured in the any pollution control devices. Inorganic mercury may exist in mercuric or mercurous forms, which combines with other elements to form inorganic metal compounds or salts such as mercuric chloride, mercuric sulfide, mercuric oxide, mercuric selenide, etc. The inorganic mercury enters the atmosphere from mining of coal, coal combustion or during incineration of waste. Organic mercury can be formed from either elemental or inorganic compounds, and exist in various species such as methyl mercury, phenyl mercury, merthiolate, etc. In mercury contaminated soil or water, the micro-organisms can organify the mercury into methyl mercury, which concentrates in the food chain. The health effects of mercury are diverse and it may depend on the form of mercury encountered and severity and the length of exposure.

Elemental Mercury

Intoxication may occur in workers excessively exposed to mercury or to its compounds. The exposure may be due to mercury vapor, mist, dust, or fume, by inhalation, ingestion, or through skin. The current Occupational Safety and Health Administration (OSHA) permissible exposure limit (PEL) for mercury vapor is 100 microgram per cubic meter ($\mu g/m^3$) of air as a ceiling limit. Two general types of mercury intoxication exist, chronic and acute. Chronic mercury intoxication is caused by exposure to a low concentration of mercury over an extended period of time. Acute mercury intoxication is due to a greater exposure and is unrelated to time factors. Definite symptoms of chronic mercurialism may not appear

until after six months of exposure, or longer. The symptoms are primarily of the nervous and digestive systems. The symptoms of overexposure to mercury may include such personality manifestations as: irritability, excitability, or excessive timidness. Other symptoms include: headaches, drowsiness or insomnia, and weakness. Many cases also include reports of sore mouths, excessive salivation, and perspiration. In mercury intoxication, a common symptom is a tremor which is aggravated by emotion or excitement [http://www.epa.gov/hg/effects.htm]

Inorganic Mercury

Exposure to inorganic mercury is mostly through ingestion. The most prominent effect is on kidneys, where mercury accumulates, leading to tubular necrosis. High exposures to inorganic mercury may also result in damage to the gastrointestinal tract, the nervous system. Symptoms of high exposures to inorganic mercury include: skin rashes and dermatitis; mood swings; memory loss; mental disturbances; and muscle weakness [http://www.epa.gov/hg/effects.htm]

Organic Mercury

Organic mercury is more toxic than inorganic mercury. Organic mercury compounds, also called organomercurials, are those containing covalent bonds between carbon and mercury. Examples are methyl mercury, dimethylmercury and methylmercury chloride (methylmercuric chloride). The effects of organic mercury especially methylmercury are acute which include changes in vision, sensory disturbances in the arms and legs, cognitive disturbances, dermatitis, and muscle wasting. The developing nervous systems of the fetus and infants are considered to be susceptible to the effects of methyl mercury. Exposure of childbearing-aged women is of particular concern because of the potential adverse neurological effects of Hg in fetuses [http://www.epa.gov/hg/effects.htm]. Outbreaks of methylmercury poisonings have made it clear that adults, children, and developing fetuses are at risk from ingestion exposure to methylmercury. During these poisoning outbreaks some mothers with no symptoms of nervous system damage gave birth to infants with severe disabilities, it became clear that the developing nervous system of the fetus may be more vulnerable to methylmercury than is the adult nervous system [Mahaffey,1999]. Table 2.5 shows the percentage of women with blood mercury concentration greater than 5.8 μg/L (this is an estimated level assumed to be with no appreciable harm).

Table 11.2.5. Percentage of women aged 16-49 years with blood mercury (Hg) levels ≥ 5.8μg/L, by race/ethnicity − National Health and Nutrition Examination Survey, United States, 1999-2002 [Mhaffey, 1999]

Race/Ethnicity	No.	% with Hg levels ≥5.8 μg/l	(95% CI*)
Mexican American	1,106	1.70	(1.04–2.79)
White, non-Hispanic	1,377	5.77	(3.71–8.97)
Black, non-Hispanic	794	4.82	(2.55–9.11)
Total	**3,637**	**5.66**	**(4.04–7.95)**

* Confidence Interval

Mercury Behavior during Combustion

Mercury (Hg) forms in the flue gas from coal-fired power plants; they are typically classified to elemental form (Hg^0), oxidized form (Hg^{2+}) and particulate form (Hg_p). This is technically termed as mercury speciation. Mercury speciation generally depends on coal properties, combustion conditions, reaction temperatures, flue gas composition, and fly ash composition. Mercury in coals is completely vaporized as elemental form at high temperatures during combustion. The vaporized Hg is released into the atmosphere as Hg^0 by the direct emission, Hg^{2+} by the catalytic oxidation and $HgCl_2$ by the chlorination. Fly ash formed during the combustion absorbs some gaseous Hg to produce particulate forms. The Hg_p is easily captured by electrostatic precipitators (ESP) and fabric filters (FF), and the Hg^{2+} is water soluble and likely to be absorbed by the fly ash. However, the Hg^0 is insoluble and difficult to capture. Therefore, the technology for the conversion of Hg^0 into an oxidized form plays an important role in Hg removals. Table 2 presents some of Hg conversion studies and their operating conditions. The majority of the oxidized form is believed to be $HgCl_2$. The main reactions are shown in Eqs. (4), (5) and (6). The most important species for Hg oxidation is the chlorine-containing species such as HCl and Cl_2. It was found that the reaction of Hg with atomic Cl is very fast when compared to the other forms of chlorine species [20]. The CB contains higher amounts of chlorine (Cl) than most coals and thus releases Cl-rich compounds (mainly HCl) when burned, which oxidizes Hg^0 to $HgCl_2$.

$$2Hg^0 + 4HCl + O_2 \rightarrow 2HgCl_2 + 2H_2O \qquad (4)$$

$$Hg^0 + Cl_2 \rightarrow HgCl_2 \qquad (5)$$

$$Hg^0 + 2Cl \rightarrow HgCl_2 \qquad (6)$$

In general, emissions of mercury from coal combustion sources are approximately 20–50% elemental mercury (Hg_) and 50–80% divalent mercury (Hg(II)), which may be predominantly HgCl2, while particulate mercury constitutes less than 5% [Carpi 1996]. Experiments [Meiji 2002] conducted to study the fate and behavior mercury in power plants showed that 43% of Hg present in the coal is found in the flue gases in the vapor phase. With the presence of HCl, Hg^0 (partly) is converted into $HgCl_2$ at temperatures less than 500-800^{0}C. According to the one of the test conducted it was found that 53% of the Hg presented in a water soluble form, mostly in the form of $HgCl_2$. However, it is still in the vapor phase due to the high temperature of flue gases (140-150^{0}C).

Distribution of mercury species in coal combustion flue gases has been calculated using equilibrium calculations by Mojtahedi et al. [Mojtahedi ,1987] and Senior et al , [2000] which shows that all of the Hg exists in the form $HgCl_2$ below 450^{0}C. And above 700^{0}C, 99% of the Hg exist as gaseous Hg as shown in Figure **11.2.2**. The rest is in the form of HgO. Equilibrium is not attained in flue gas since the environment is highly transient and also due to fact that flue gas cools rapidly as heat is transferred from water to steam. Though experiments conducted by Lindqvist et al. validated that mercury exists in elemental form only at temperatures above 700^{0}C .

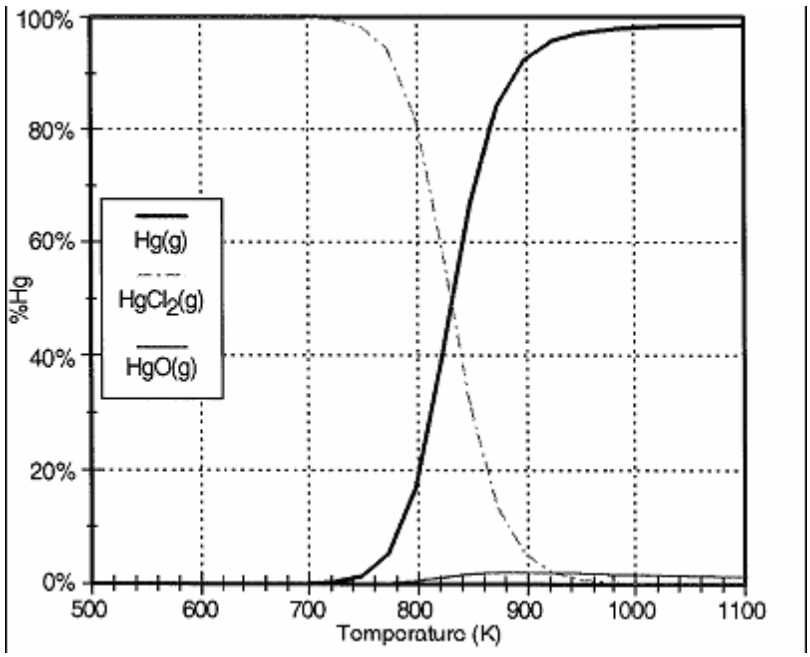

Figure 11.2.2. Equilibrium speciation of mercury in flue gas as a function of temperature [14]

In Hall.B (thesis) [16], the re-oxidation reaction is stated to occur rapidly at about 500^0C and is described as:

$2Hg(g) + 4HCl + O_2 \Leftrightarrow 2HgCl_2\ (g,s) + 2H_2O\ (g)$

This occurs between 400 to 700^0C. Below 400^0C, the atomic chlorine is responsible for further Hg oxidation.

$Hg + Cl_2 \rightarrow HgCl + Cl$

$HgCl + Cl_2 \rightarrow HgCl_2 + Cl$

However, in case of flow reactor, where the temperature is very high at the upstream, stable HCl decomposes supplies atomic chlorine which aids in formation of intermediate HgCl. As these species move downstream, HgCl oxidizes further to form stable $HgCl_2$ which is favored at lower temperatures.

$Hg + Cl \rightarrow HgCl$

$HgCl + HCl \rightarrow HgCl_2 + H$

$HgCl + Cl_2 \rightarrow HgCl_2 + Cl$

$HgCl + Cl \rightarrow HgCl_2$

It can be said that for oxidation of Hg in presence of HCl, high temperatures is required to decompose HCl to produce atomic chlorine, and occurrence of intermediate HgCl. While lower temperatures are required to further oxidize HgCl to $HgCl_2$.

Thus the extent of oxidation depends on the concentration of chlorine in flue gases. As shown in the Figure **11.2.3**, the fraction of elemental Hg emission of coal-fired boilers decreases with increase in Cl content of coal [18]. The Cl content in Bituminous coals range from 200 to 2000 ppm (dry basis) while for low rank coals (sub-bituminous and lignite) it ranges from 20 to 200 ppm an order of magnitude lower. Thus the low rank Sub-bituminous and lignite coals reveal lower Hg capture (3-72 %) in co-benefit systems than higher rank bituminous coal (9-98 %) [19]. Hg removal plotted against coal chlorine content reveals increasing Hg capture with Cl due to HgCl2 formation. As Cl is low in sub-bituminous and lignite coals, the Hg exists primarily as elemental Hg, which is difficult to capture.

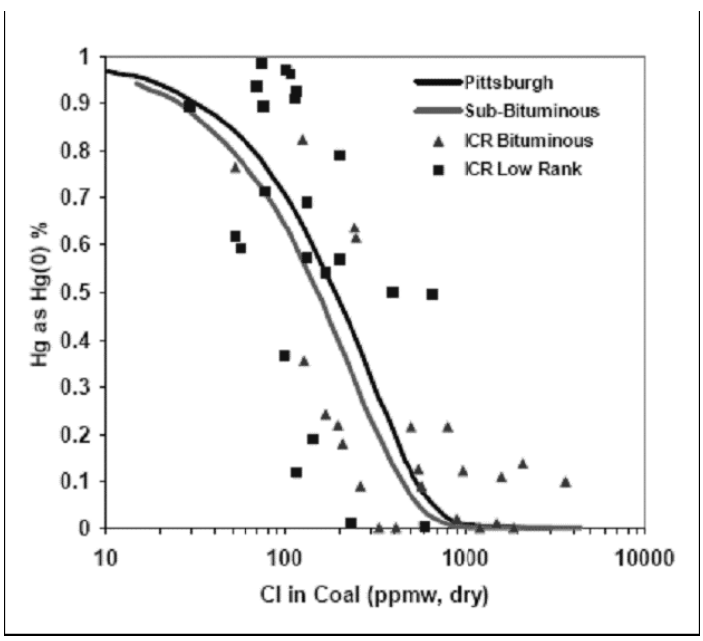

Figure 11.2.3. Effect of chlorine in coal with mercury emissions [18]

Mercury Control Technologies

Mercury is difficult to remove because it is present in vapor form since it is highly volatile. A variety of control approaches that address mercury during pre- and post-combustion can achieve reductions in mercury emissions from power generation facilities fueled by coal. Precombustion strategies essentially involve pollution prevention measures, such as fuel management by coal cleaning, or selection of lower mercury content fuels. These measures may achieve reductions in mercury concentrations in the fuel prior to the fuel entering the combustion zone. Post-combustion methodologies are generally absorption or conversion techniques focused on removal of one or more of the mercury species incorporated in the boiler exhaust stream. Many existing controls for gaseous and particulate pollutants can secondarily reduce mercury emissions through simultaneous "co-control" physical and chemical reactions. The various Hg control technologies are summarized in S thesis of Uday 2007.

Pre-combustion Mercury Control Techniques

Pre-combustion techniques for reducing mercury emissions are focused at lowering mercury concentrations prior to combustion. Pre-combustion approaches are principally fuel cleaning techniques, although fuel-switching or management strategies have also been investigated.

The cleaning techniques normally considered for pre-combustion control reductions are coal washing/cleaning with either an aqueous solution or with a magnetic medium as the separation medium. Other cleaning techniques, such as K-Fuel, have been developed that remove mercury through heat, although data for these non-aqueous cleaning approaches are limited.

Coal cleaning or washing is a physical technique that can remove coal contaminants that are bound with particulates or soils (commonly the pyritic fraction) associated with the coal. The degree of association of coal mercury with the mineral fraction has been estimated by several researchers as up to 50% of the total mercury content. Mercury that is bound organically to the carbon structure or absorbed onto internal carbon structures is little affected by cleaning. Mercury compounds associated with the particulate fraction (Hg^0 and Hg^{2+}) may be removed; however, a residual mineral content (from 8-15%) is typically retained in the cleaned coal. Cleaned coals also generally lose BTU content with a gain in moisture content. Toole-O'Neil et al. (1999) evaluated the tendency of coal cleaning to preferentially remove mercury. Of the 24 cases of coal cleaning cited, the average decrease in mercury concentration was 37% on an energy basis, ranging from 12% to 78% overall. On a mass basis, the average mercury reduction from coal cleaning was 30%, which indicates a coal cleaning factor of 0.70, a higher rate of mercury removal than that applied by EPA in 1997 (21%) (Brown et al. 1999).

In general, effective removal of coal contaminants may be enhanced when coals is finely ground and subjected to intense agitation. In practice, coal cleaning efficiencies vary considerably with multiple factors such as coal type, rank, ash content and mineral composition. Although these methods appear to reduce mercury, further post-combustion treatment must be performed to control remaining mercury. Some additional benefits of coal cleaning include a reduction in the sulfur content, which translates into lower $S0_2$ emissions, as well as reduced ash loading.

Coal cleaning is widely used on high rank coals in east such as bituminous and anthracite coals, to reduce ash and sulfur compounds. There is less experience with cleaning in lower rank western coals such as sub-bituminous and lignite.

Another pre-combustion technique considered is by strategically managing fuel used for combustion. Mercury emissions can be lowered for a distinct facility by selecting and burning fuels of lower mercury

concentration. Within a given coal type, current data suggests that many deposits exhibit a high degree of variability in mercury content on a seam to seam basis. The ability to selectively mine lower mercury concentration seams has not been demonstrated repetitively, nor have the business economics been quantified to encourage such mining efforts. While shifting coal types could impact mercury emissions, the economic and physical impacts of differing fuel types onto generation capabilities and the boiler and fuel handling complex are likely to exceed costs associated with direct controls.

Post-combustion Mercury Control Techniques

Mercury capture in existing emissions control equipment offers a cost effective mercury control option for coal-fired power plants. The incidental capture of mercury from coal-fired power plants varies significantly depending on the existing emissions control configuration and type of coal being burned. In post-combustion technique, there are three basic methods of flue gas treatment to capture mercury: first, capture of particulate-bound mercury in particulate matter (PM) control devices; second, adsorption of elemental and oxidized mercury onto sorbents for subsequent capture in PM control devices, and; third, removal of soluble oxidized mercury in wet scrubbers (including processes to convert elemental to oxidized mercury for subsequent capture in wet scrubbers).

Mercury speciation along the convective flue gas path determines the mode of mercury capture using these traditional pollution control devices. Figure **11.2.4** shows the various species of mercury present at different stages of a plant layout.

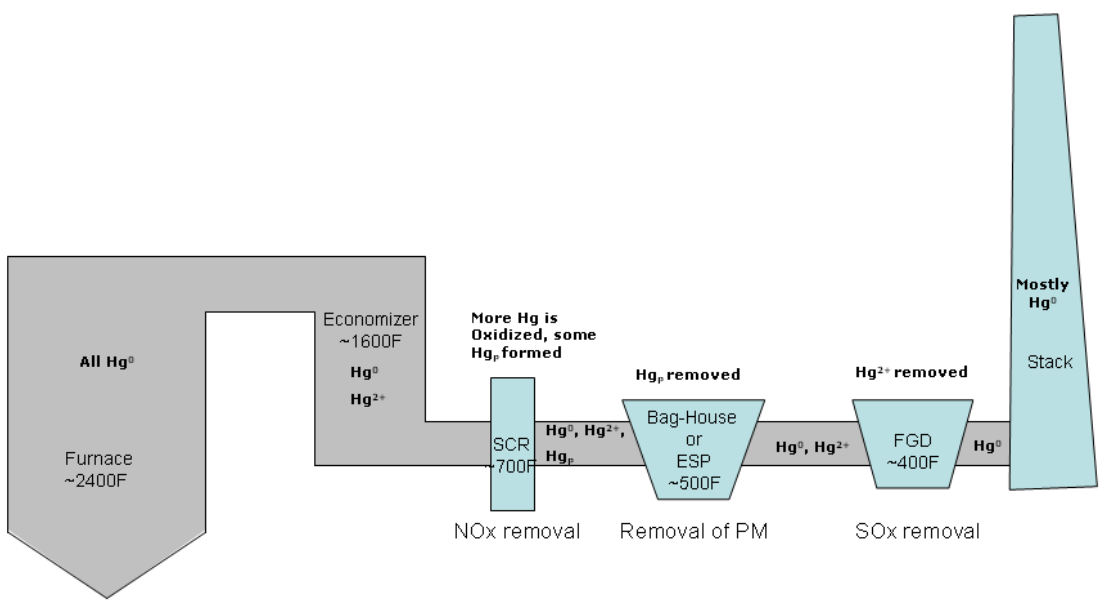

Figure 11.2.4. Mercury in flue gas path [32]

More than 20 percent of coal-fired utility boiler capacity in the United States uses wet FGD systems to control SO_2 emissions. Wet FGD systems remove gaseous SO_2 from flue gas by absorption. For SO_2

absorption, gaseous SO_2 is contacted with a caustic slurry, typically water and limestone or water and lime. Gaseous compounds of Hg^{2+} are generally water-soluble and can absorb in the aqueous slurry of a wet FGD system. However, gaseous Hg^0 is insoluble in water and therefore does not absorb in such slurries. When gaseous compounds of Hg^{2+} are absorbed in the liquid slurry of a wet FGD system, the dissolved species are believed to react with dissolved sulfides from the flue gas, such as H_2S, to form mercuric sulfide (HgS); the HgS precipitates from the liquid solution as sludge. The capture of Hg in units equipped with wet FGD scrubbers is dependent on the relative amount of Hg^{2+} in the inlet flue gas and on the PM control technology used. ICR data reflected that average Hg captures ranged from 29 percent for one ESP plus FGD unit burning sub bituminous coal to 98 percent in a FF plus FGD unit burning bituminous coal [10]. The high Hg capture in the FF plus FGD unit was attributed to increased oxidization and capture of Hg in the FF followed by capture of any remaining Hg^{2+} in the wet scrubber.

More than 10 percent of the U.S. coal-fired utility boiler capacity uses spray dryer absorber (SDA) systems to control SO_2 emissions. An SDA system operates by the same principle as a wet FGD system using a lime scrubbing agent, except that the flue gas is mixed with a fine mist of lime slurry instead of a bulk liquid (as in wet scrubbing). The SO_2 is absorbed in the slurry and reacts with the hydrated lime reagent to form solid calcium sulfite and calcium sulfate. Hg^{2+} may also be absorbed. Sorbent particles containing SO_2 and Hg are captured in the downstream PM control device (either an ESP or FF). If the PM control device is a FF, there is the potential for additional capture of gaseous Hg^0 as the flue gas passes through the bag filter cake composed of fly ash and dried slurry particles. ICR data reflected that units equipped with SDA scrubbers (SDA/ESP or SDA/FF systems) exhibited average Hg captures ranging from 98 percent for units burning bituminous coals to 24 percent for units burning sub bituminous coal.

There has been increasing number of generators installing selective catalytic reduction (SCR) or selective non-catalytic reduction (SNCR) systems to reduce NOx emissions. SCR devices for reduction of NOx emissions have long been expected to enhance mercury capture by particulate collection devices and SO_2 scrubbers through increased oxidation of mercury. Conversion of more of the elemental mercury to Hg^{2+} would increase the potential removal in a wet FGD, but is not expected to significantly increase removal by precipitators and fabric filters.

The catalyst in SCR system provides sites for mercury oxidation, and the effect of oxidation of elemental mercury by SCR catalyst may be affected by the following:

- The space velocity of the catalyst;
- The temperature of the reaction;
- The concentration of ammonia;
- The age of the catalyst; and
- The concentration of chlorine in the gas stream.

Confounding issues that surround SCR usage in quantifying the degree of oxidation are that when SCR is in place, increase of both unburned carbon (LOT in ash, due to low NOx burner applications) and of excess ammonia (ammonia slip) are both generally present. The increase in unburned carbon may function as a synthetic “activated carbon” that results in direct “carbon” capture of both Hg^0 and Hg^{2+} species. Un-reacted ammonia (slip) is adsorbed onto particulate surfaces and may also enhance sulfur mercury reactions, again with the result being that Hg_P bound onto ash particulates is subjected to more effective removal by particulate control devices. A negative aspect impacting SCR usage is that de-activation, or poisoning, of catalytic function of SCR has been reported associated with lignite coals.

Summary of post combustion type of mercury emission control devices are presented in table 2.6.

Table 11.2.6.Average mercury capture by existing post-combustion control configurations used for PC-fired boilers [20]

Post-combustion Control Strategy	Post-combustion Emission Control Device Configuration	Average Mercury Capture by Control Configuration		
		Coal Burned in Pulverized-coal-fired Boiler Unit		
		Bituminous Coal	Subbituminous Coal	Lignite
PM Control Only	CS-ESP	36 %	3%	0 %
	HS-ESP	9 %	6 %	not tested
	FF	90 %	72 %	not tested
	PS	not tested	9 %	not tested
PM Control and Spray Dryer Adsorber	SDA+CS-ESP	not tested	35 %	not tested
	SDA+FF	98 %	24 %	0 %
	SDA+FF+SCR	98 %	not tested	not tested
PM Control and Wet FGD System[(a)]	PS+FGD	12 %	0 %	33%
	CS-ESP+FGD	75 %	29 %	44 %
	HS-ESP+FGD	49 %	29 %	not tested
	FF+FGD	98 %	not tested	not tested

CS-ESP = cold-side electrostatic precipitator
HS-ESP = hot-side electrostatic precipitator
FF = fabric filter
PS = particle scrubber
SDA = spray dryer absorber system

(a) Estimated capture across both control devices

Emerging Technology for Mercury Control

Post combustion mercury control options are relatively expensive to implement. One reason for the expense is that large flue gas volumes must be treated to capture very small amount of mercury; typical mercury concentrations in untreated flue gas are in the range of few $\mu g/m^3$. One of the dry control technologies that are emerging for mercury emissions reduction is the use of activated carbon injection (ACI). ACI is used upstream of a particulate control device, and under most conditions, if the carbon achieves good contact with the gaseous mercury for a sufficient amount of time, it will adsorb the mercury, both elemental and oxidized forms of mercury. The resulting mercury-laden carbon could then be collected by the downstream particulate control. The amount of mercury adsorbed is dependent upon the mercury adsorption capacity of the activated carbon and the mass transfer characteristics of the system, where the mercury removal will increase with increasing sorbent capacity up to the mass transfer limit of the system.

The capacity of activated carbons can be affected by flue gas composition and temperature depending on the mercury species present. For elemental mercury, lack of halides such as chloride/chlorine in the flue gas can reduce the carbon capacity significantly. A temperature effect can be seen when conditions exist where the carbon capacities may decrease below the threshold levels, such as where high levels of oxidized mercury exist and the temperature is significantly greater than 300°F (150°C) [10].

Cattle Biomass

There is considerable concern regarding the potential global environmental impact of fossil fuels used for power generation. By increasing the fraction of renewable energy in the national energy supply, some of the impact can be mitigated. Co-firing biomass with coal in traditional coal-fired boilers or using biomass as a reburn fuel in advanced coal-fired boiler configurations represent two options for combined renewable and fossil energy utilization. To add to the above, it can also be considered the best solution to combat the challenging waste disposal problem, with 110 million tons of dry animal manure produced annually in the United States. National Agricultural Statistics Service (NASS) reports that cattle in US grew from 98.2 million in 1990 to 971 million in 2006. With an estimate of each animal fed leaving approximately 1 ton collectable cattle manure in 5 months, the bio-waste can contribute to surface or ground water contamination and air pollution problems with the release of CH_4 (a greenhouse gas), NH_3, H_2S, amides, volatile organic acids, mercaptans, esters, and other compounds [21].

The sole source biomass as fuel for combustion application have limitations primarily due to highly variable properties (high ash, high moisture, salt composition, etc.) of manure and the associated flame stability problems. By blending biomass with coal and firing it in existing boiler burners the problems can be eliminated since cattle manure can be readily combusted in the presence of high heating value coal. It is known from previous works of Annamalai et al. on co-firing cattle biomass with coal that, it has great potential in reducing fossil fuel based CO_2, reduction in NO_x, reduction in fuel costs since biomass is cheaper than coal, and minimization of soil, water, and air pollution.

Apart from the above, cattle biomass has very high amounts of chlorine content compared to coal with relatively good heating value. For instance, low ash partially composted dairy biomass contains 13% higher chlorine content compared to Wyoming sub bituminous coal, while its heating value is almost 70% as that of the coal. This gives a potential use for blending coal with biomass and co-firing it in existing boilers to increase the chlorine content in the fuel, and hence achieve higher mercury oxidation and hence its capture to reduce elemental mercury emissions.

Recent research activities of reburning cattle biomass with coal [23] have shown remarkable results of reducing NOx emissions by almost 90%. Simulation studies conducted previously by Puchakayala [22], predicted very effective mercury oxidation when coal is fired with biomass. He showed that presence of high chlorine concentration in flue gases substantially reduces elemental mercury emissions. Figure **11.2.5** shows results of blending feedlot biomass with coal in proportions of 10:90 and 20:80, by which 65-80% of mercury was converted to mercuric chloride, while for pure coal only 9% mercury was oxidized.

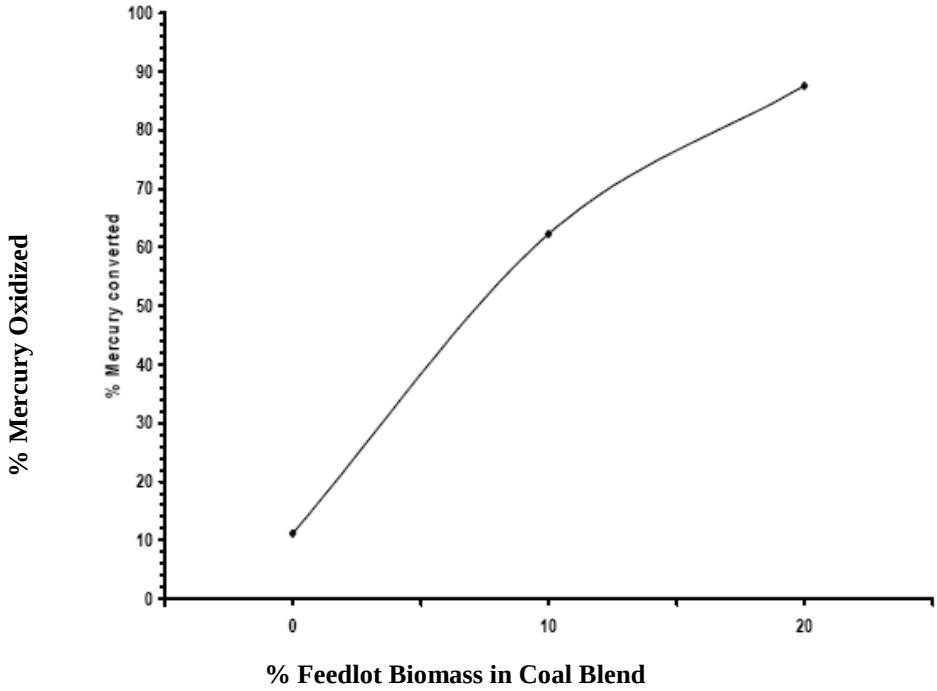

Figure 11.2.5. Effect of blending coal with biomass on mercury oxidation [22]

11.3. Objectives

Cofiring

The CB also contains higher amounts of Cl and thus releases Cl rich compounds (mainly HCl) when burned, which oxidizes elemental Hg to HgCl2 that can be captured by SOx and particulate control devices such as wet scrubbers. The overall objective of the current study is to develop environmentally friendly thermo-chemical energy conversion technologies for utilizing CB to reduce Hg emissions from traditional pulverized coal-fired power plants. The specific objectives are to investigate combustion and emission behaviors during combustion of CB and coals in conventional coal-fired boilers and to study the effects of equivalence ratios (ϕ) and blending ratios on Hg reductions.

Reburn

The objective is to use CB as reburn fuel for reducing Hg emissions since it is hypothesized that Cl in the CB will help in oxidizing Hg to water soluble reduce Hg Cl_2.

Bench Scale Experiments :

The overall objective of this work is, to test chlorinated carbon (DB-CH), made of dairy biomass via gasification, for its effectiveness in capturing the elemental mercury out of a gaseous flow. The properties

of the carbons used are presented in the experimental setup. Furthermore several parameters affect the total mercury capture. They include temperature (15°C, 90°C – cold side of ESP (Electrostatic Precipitator), 150°C – hot side of ESP), mass of chlorinated carbon (10 g, 20 g) and two different types of chlorinated carbon (DB-CH-N2 and DB-CH-N2-H2O, the different types will be classified further in the experimental setup).The following tasks were performed, in order to achieve the objective : Determination of particle size and Sauter mean diameter of Texas Lignite coal using sieve analysis, Ultimate and proximate analyses of Texas Lignite and DB-CH and Parametric studies on temperature, mass and type of DB-CH

11.4. Experimental facility and procedure

In order to validate reduction in mercury emission, co-firing experiments were conducted on a 100,000 BTU/hr small scale coal fired boiler burner at the Coal and Biomass Energy Laboratory, Texas A&M University. This section briefly describes the facilities used and modifications made to report the results.

Boiler Burner Facility

The furnace consisting of a 15.24 cm (6 in) diameter, 182.88 cm (6 ft) long downward fired combustor, is made with a steel frame containing a two inch layer of insulation and a two inch section of refractory (Dimensions are shown in Figure **11.4.1** and Figure **11.4.2**. The top section of the furnace is the main burner which has a swirl burner (or injector) and a quarl section. The swirl injector consists of a swirler and a nozzle. The swirling jet of the primary air is generated by the swirler and mixed with the primary fuel and air from the injection nozzle. The quarl is a diffusing section molded with the top section of the refractory which aids to stabilize the recirculation zone. A swirl number of 0.69 to 0.82 and quarl half angle of 24^0 are achieved during the boiler operation.

Along the walls of the furnace are several gas sampling ports and temperature measurements ports. There are also three wall temperature measurement locations. Water jets at the near bottom are used to cool the hot exhaust gasses before they enter the exhaust system. Solid fuel is fed using commercial Acrison feeder system, where fuel is carried to the furnace by carrier air (also called primary air) through an eductor. Secondary air is supplied to the furnace by an air compressor and controlled by an electronic air flow meter. The furnace is operated at slight negative pressure to ensure flames are within the furnace and no exhaust gas leaks to the laboratory. A vacuum of 2.5 cm (0.1 inch) is achieved through an exhaust fan and a damper on the exhaust line.

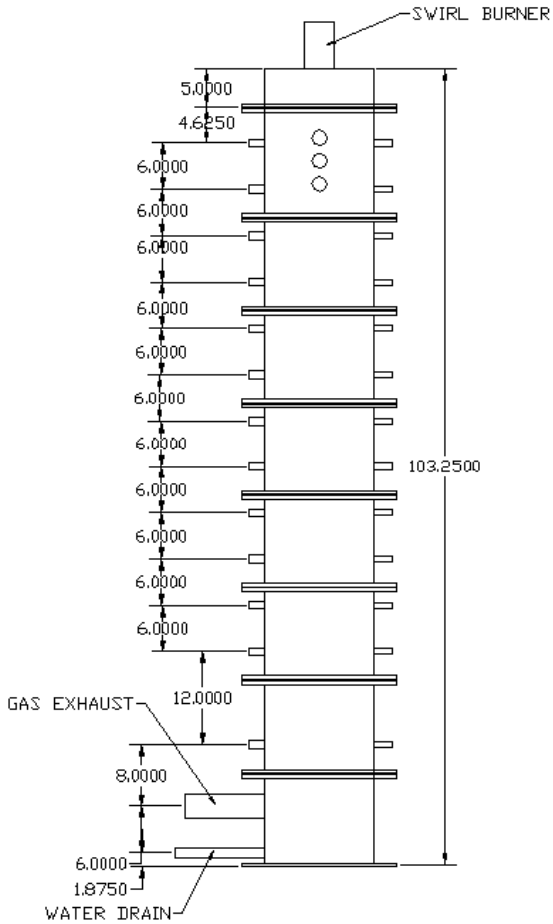

Figure 11.4.1. Dimensions of the furnace

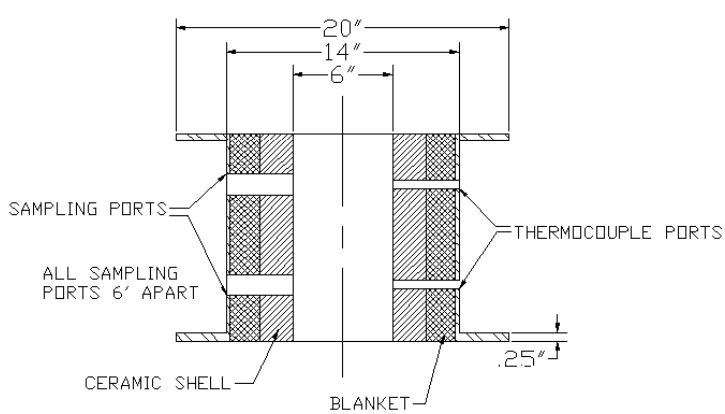

Figure 11.4.2. Vertical section of the boiler

A portable commercial GreenLine 6000 flue gas analyzer is used to measure different gas species such as CO, CO_2, O_2, NO_x, SO_x and C_xH_y, while Mercury Instrument VM 3000 is used to measure

mercury in the flue gas using cold vapor atomic absorption (CVAA) principle. The schematic of the experimental layout is shown in Figure ***11.4.3***.

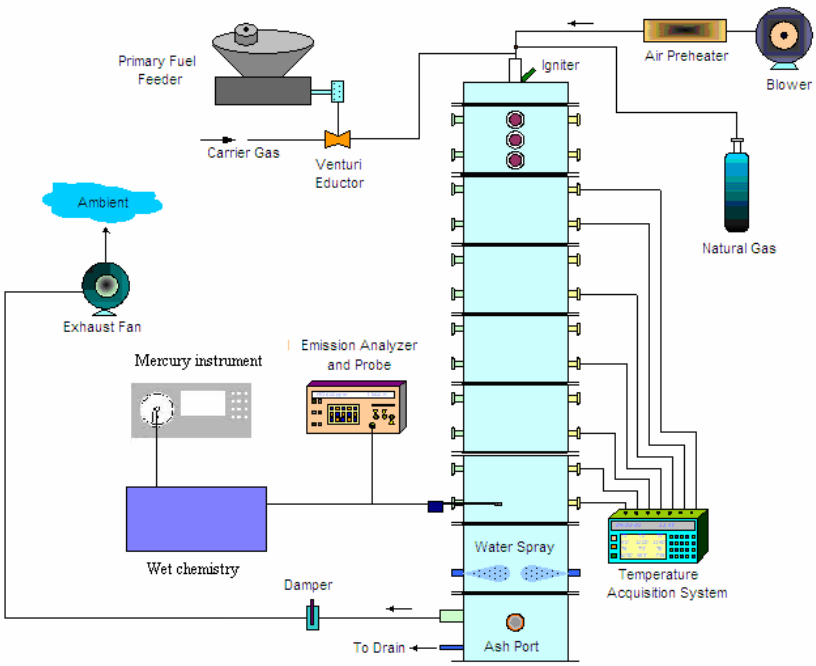

Figure 11.4.3. Schematic layout of the furnace and accessories

Mercury Measurement and Wet Chemistry System

Mercury measurement technologies in flue gas have been speculated and have been listed as a challenge due to its very low concentration (less than 10ug/m3), and also the inherent complications in reading oxidized mercury. At Coal and Biomass Energy Lab, Texas A&M University, mercury measurement is done using VM3000, Mercury Instrument which adopts CVAA principle. The CVAA method determines the mercury concentration in the gas by measuring the attenuation of the light produced by a mercury vapor lamp as it passes through a cell that contains the sample gas. The mercury atoms in the cell absorb UV light at their characteristic wavelength of 253.7 nm. Other flue gas constituents such as SO2 absorb light across a wide spectrum including the 243.7 wavelength, thus acting as an interferant. Water vapor and particulate are also broadband absorbers that must be dealt with in CVAAS measurement [24].

Mercury is present in three different forms in flue gas, viz., elemental mercury (Hg^0), oxidized mercury (Hg^{2+}) and particulate mercury (Hg^P). Particulate form of mercury in flue gases of utility boilers or any coal combustion process is in the range of 3% to 8%, which is considered negligible. Moreover, particulate mercury can be easily trapped in conventional ash removal devices such as baghouse or ESP, and hence does not create any potential toxic emission threat. Since the intention in this research is to convert as much elemental mercury into oxidized form, it is essential to measure both the elemental and oxidized mercury concentration in the flue gas, which would enable us compare results with the relation of each fuel used to effective mercury oxidation and hence evaluate its efficiency in mercury capture.

The instrument is limited to read only elemental mercury, and not the total mercury. There are several ways to condition the flue gas to read both elemental and total mercury. To list them, they are Wet

Figure 11.4.4. VM 3000 Mercury Vapor Monitor

Chemistry method, Dry Sorbent method and Thermocatalytic converter. The Dry Sorbent method and Thermocatalytic converter are highly expensive methods, hence Wet Chemistry based flue gas conditioning is used for this research. The U.S. Environmental Protection Agency (EPA) Methods 101A and 29, and the Ontario Hydro method have been validated for measuring total mercury emissions from coal-fired boilers, though the Ontario Hydro method has become a standard for mercury speciation measurements in coal combustion flue gas. However, these wet-chemistry methods are difficult to perform, costly, time-consuming, and labor-intensive.

Several on-line analyzers have been developed primarily for measuring mercury emissions. One such method based on modified Ontario-Hydro method was constructed and used in this study, which was adopted by University of Utah previously. In this system the sample gas is pulled in two streams directly from sampling port of the existing 100,000 BTU/hr small scale boiler into a set of conditioning impingers. One stream is bubbled through 10% stannous chloride solution to reduce oxidized mercury species to elemental mercury. The stream then contacts a solution of 10% sodium hydroxide (caustic solution) to remove acid gases. This stream represents the total mercury concentration in the reactor.

The second stream is first treated with 10% potassium chloride solution to remove oxidized mercury species and then is also treated in 10% caustic solution for acid gas removal. This stream is representative of the elemental mercury concentration in the reactor. Oxidized mercury species is calculated as the difference between total and elemental mercury concentrations. Water is removed from the sample gas by a chiller and then each stream is intermittently sent to the analyzer by a valve box connected to the analyzer [25]. The complete circuit of mercury wetted path is made through Tygon R3603 tubing which has low mercury memory. To ensure the reagents' active reaction in the impingers with flue gas, fresh chemicals are replenished into the system and spent chemicals are removed using two different 4 channel peristaltic pumps. The schematic of the wet chemistry system is shown in Figure ***11.4.5***

A quick silver inertial separation (QSIS) filter manufactured by Apogee Scientific Inc., was originally planned to be used in the flue gas conditioning system to negate the effects of particulate matter, which could cause unpredictable speciation between elemental and oxidized mercury. After the construction of filtration system it was realized that it would not be suitable for the application such as this study owing to relatively smaller size of boiler used. Moreover, since mercury bound particulate matter constitutes only 3 to 8% of the total mercury, and its extremely small concentration, the filtration system was deployed.

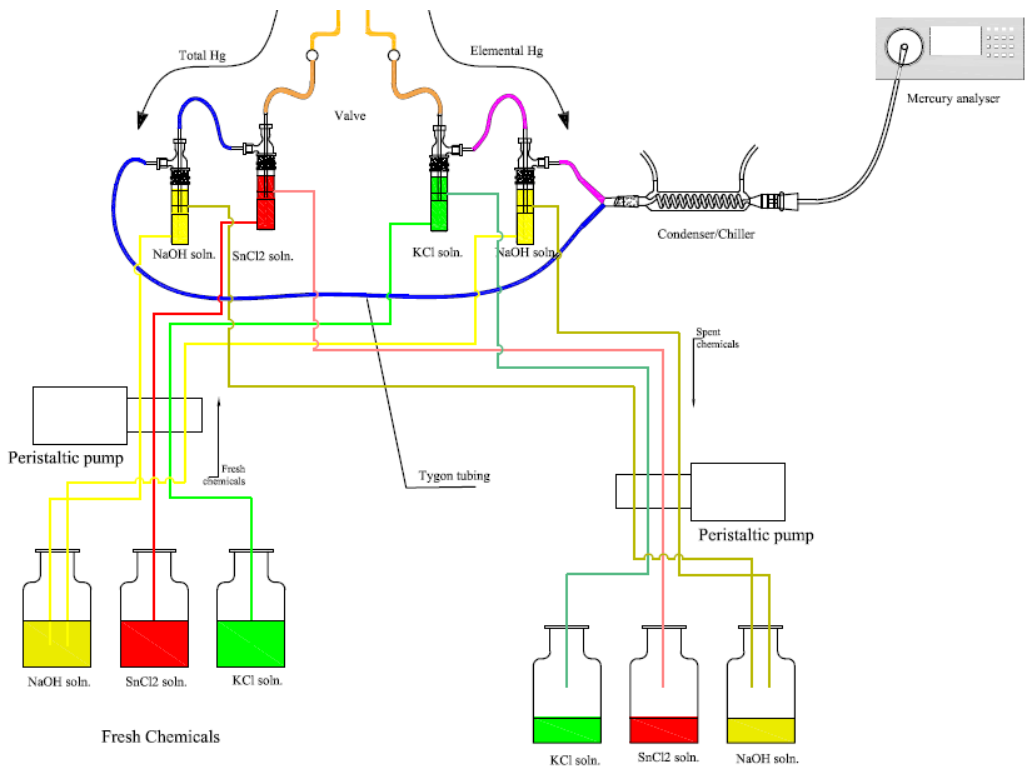

Figure 11.4.5. Wet chemistry based flue gas conditioning system

Procedure

Conducting experiments during coal and fuel blend combustion followed three distinct steps: preparation phase, firing phase and measurement phase. In preparation phase, the furnace is preheated to a temperature of about 2000 F by burning natural gas only at near stoichiometric condition with air being supplied from secondary air supply channel. This process of preheating takes about 3 to 4 hours until

steady state is attained. In the meantime, the fuel feeder is loaded with required solid fuel, and feed rate is calibrated manually by measuring mass of fuel flow in specific amount of time (normally in 1 minute). Once steady state is attained, the second phase of firing solid fuel can begin. The natural gas supply is turned off and feeder motor is started to feed solid fuel which is carried by carrier air (also called primary air) to the furnace. Air flow rates are adjusted by varying the secondary air flow rate, the means by which desired equivalence ratios are achieved (from lean to rich combustion). Once steady state is attained (which takes roughly 10 minutes), measurement phase begins, when sampling probe is plugged into the sampling port to make measurements of flue gas species using GreenLine analyzer. Once these readings are taken, mercury measurements are made using VM3000 analyzer and wet chemistry system. This measurement step is followed for every equivalence ratio. Finally on completing the set of experiments at the end of the day, fuel supply is turned off and the furnace is allowed to cool down.

Bench Scale Experiments:

The experimental setup consists of a nitrogen source (nitrogen cylinder) and a valve to control the flow rate of nitrogen. The nitrogen passes through a first u-shaped tube containing a permeation tube, which releases mercury. Since the amount of mercury released by the tube is strongly temperature dependent, the tube is placed in a container, which is filled with water and is kept at a constant temperature as assured by a thermocouple. The temperature of the water is adjusted, using a heating plate. The mercury flow rate varied between 45µg/m3 and 55µg/m3 but was kept almost constant for the duration of one experiment. For direct measurement without adsorption of mercury the other end of the u-shaped tube, containing the permeation tube, was connected to the Mercury Monitor. However, for the experiments, DB-CH was packed in another u-shaped tube, wrapped with heating tape (Figure 12). The heating tape was connected to an automatic temperature control device and the temperature of DB-CH was checked using a thermocouple. For the cases with higher temperature, cooling of the nitrogen flow was necessary prior to analysis of Hg by the mercury monitor. Also steam would interfere with the mercury measurements, so the flow was cooled down, letting the gas path through an ice bath before it enters the mercury measuring instrument. The H2O was condensed from the flow. A schematic of the experimental setup is shown in Figure 10. The experimental setup may be seen in Figure ***11.4.6***.

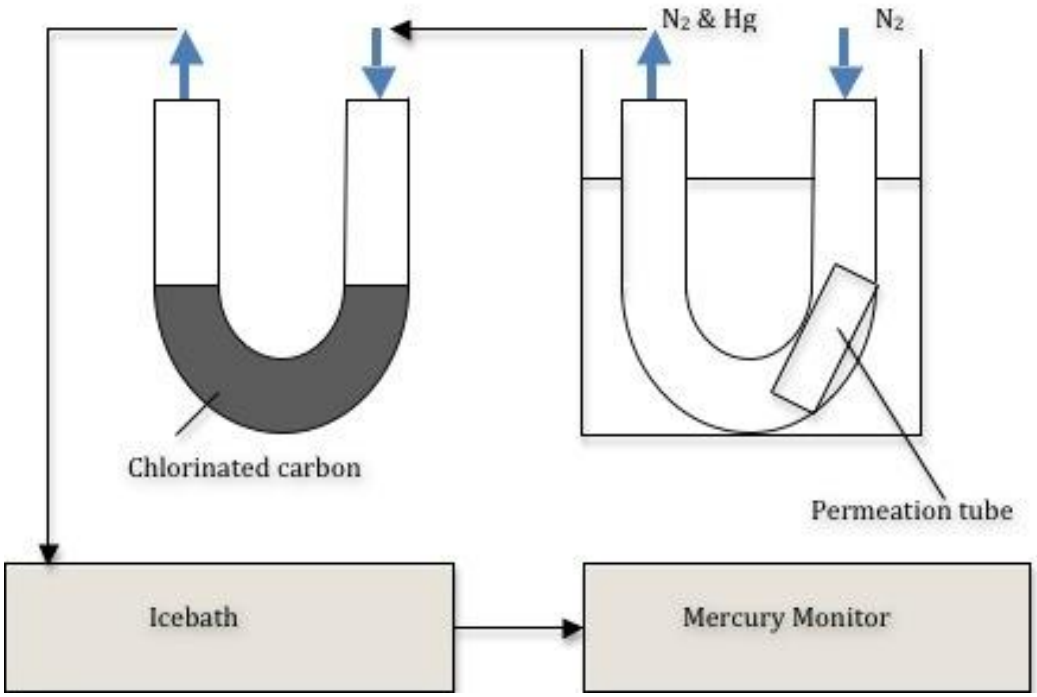

Figure 11.4.6. Schematic of experimental setup

Two types of DB-CH were used. Both carbons were produced via gasification. The chlorinated carbon in the following referred to as “DB-CH-N2” was produced using a flow of five SCFH of N2 and the chlorinated carbon referred to as “DB-CH-N2-H2O” was produced using a flow of five SCFH of N2 and an additional flow of 1.85cm3/min of steam. The most remarkable difference between the two DB-CH: DB-CH-N2-H2O has slightly lower chlorine content compared to DB-CH-N2. For more information about the DB-CH used and the procedure to produce them, see [11].

11.5. Results and discussion

This chapter reports the fuels used during experiments, their proximate and ultimate analysis results, base case mercury measurements, results of mercury measurement from each case conducted, discussion of extent of mercury oxidation under different operating conditions, and other observations.

Fuels and Proximate and Ultimate Analysis

Proximate and ultimate analyses were used to determine the basic fuel properties, mercury and chlorine content of each type of fuel used.

Fuels used during experiments were Texas Lignite Coal (TXL), Wyoming Sub bituminous Coal (WYC), Separated Solids Partially Composted Dairy Biomass (Sep. Sol. PC-DB), High Ash Partially Composted Dairy Biomass (HA PC-DB), and their blends. Dairy Biomass (DB) fuels used in this study

Table 11.5.1. Proximate and Ultimate Analysis of fuels used– Hg Cofiring Experiments

	Txlig-3 samples	Wy Coal-3 samples	DB-Sep solids-PC-2006	DB-HA-PC
Fuel Source	Texas Lignite and Wyoming Powder River Basin Coal provided by TXU Energy, Dallas		Dairy Farm in Comanche County, Texas	
Reference	Combustion-Fuel Properties of Manure or Compost from Paved vs. Un-paved Cattle Feedlots, by Sweeten.JM, Heflin.K, Annamalai.K, Auvermann.BW, McCollum.FT, Parker.DB, presented at the 2006 ASBAE Annual Intl meeting, Portland, Oregon		Preliminary Interpretation of Data from Proximate, Ultimate and Ash Analysis, by John M. Sweeten & Kevin Heflin. Results of June 7, 2006 Samples Taken from Feedlot and Dairy Biomass BioFuel Feedstocks at TAES/USDA-ARS, Bushland, TX. Oct 23, 2003	
Ananlysis Lab	Hazen research inc., Golden, CO	Hazen research inc., Golden, CO	Hazen research inc., Golden, CO	Hazen research inc., Golden, CO
Sample ID	TXL 113-115	PRB 116-118	128-130	131-133
Date of sampling	10/10/2005	10/10/2005	5/15/2006	5/15/2006
Date of analysis	11/29/2005	11/29/2005	10/23/2006	10/23/2006
Ash	11.46	5.64	14.93	59.91
Dry Loss (% Moisture)	38.34	32.88	25.26	12.21
FC	25.41	32.99	12.95	3.85
VM	24.79	28.49	46.86	24.04
Carbon, C	37.18	46.52	35.21	18.04
Hydrogen, H	2.12	2.73	3.71	1.45
Nitrogen, N	0.68	0.66	1.93	1.15
Oxygen, O (diff)	9.61	11.29	18.60	7.07
Sulfur, S	0.61	0.27	0.43	0.19
HHV (kJ/kg)	14,287	18,193	12,844	4,312
Chlorine, Cl %, (ppm)	0.01 (100ppm)	0.009 (90 ppm)	0.14 (1400 ppm)	0.23 (2300 ppm)
Mercury, Hg g/kg (ppb)	0.00017 (170 ppb)	0.00014 (140ppb)		

Separated Solids Partially Composted Dairy Biomass (Sep. Sol. PC-DB) and High Ash Partially Composted Dairy Biomass (HA PC-DB), were supplied by Texas Agricultural Experiment Station, Amarillo, TX. Prior to shipping, the DB fuels sourced from dairy farm in Comanche County, TX were composted partially (half the complete composting time) for 45 days involving successive wetting and turning cycles and then placed in a green house to facilitate drying. Once the DB were dried to >10%, bulk samples were processed with a hammer mill and the Vortec impact mill to grind them to particle size convenient to burn in the existing 100,000 BTU/hr facility at Texas A&M University, College Station.

The blends of fuels fired were mixed on weight basis, in following proportion:

- 95:5 – Coal:Biomass
- 90:10 – Coal:Biomass
- 80:20 – Coal:Biomass

Overall, 13 different fuel blends were fired (all combinations of fuels and ratios as stated above, except 80:20 – TXL:HA PC-DB).

The fuels used for experimentation were tested for their combustible properties and elemental constituents. It can be seen that DB has much higher chlorine content (1400 ppm to 2300 ppm), which is 13 to 25% higher compared to coal (90 ppm to 100 ppm), while its heating value ranges from 23 to 70% to that of the coal. When DB is blended with coal in different proportions, it tends to increase the chlorine content in the coal based fuel, but decreases the heating value. Figure ***11.5.1*** shows the variation of chlorine content and change in heating value of the fuel blend compared to pure 100% coal.

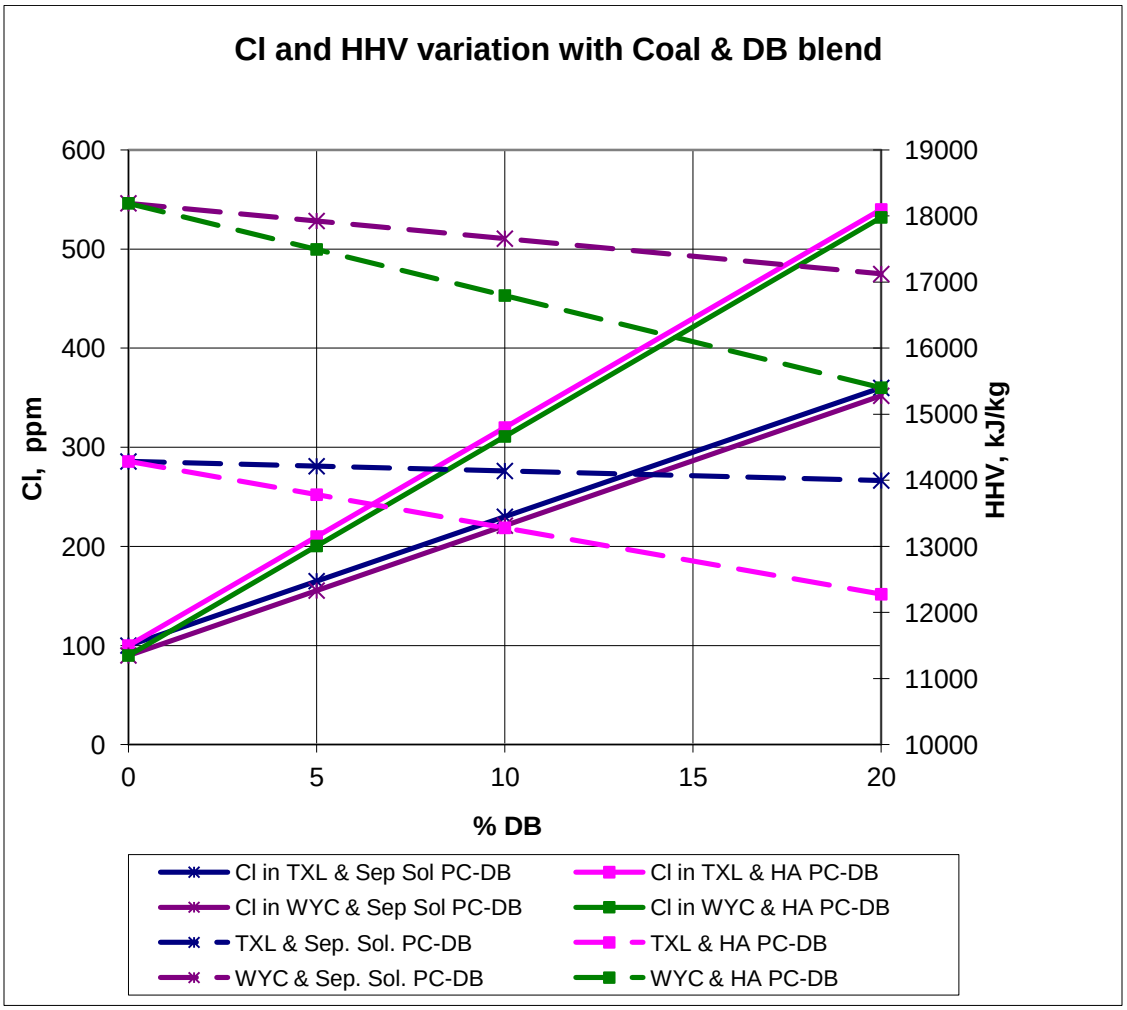

Figure 11.5.1. Variation of Cl and Heating values for different blends

Decreasing the fuel's heating value leads to increasing the firing feed rate. This in turn increases ash loading, more because DB has higher ash content compared to coal.

Base Case Mercury

Mercury measurements made when 100% coal fired is reported in this section and is termed base case with which other blend ratios will be compared to judge the reduction in mercury emissions. Figure ***11.5.2*** shows the variation of elemental and total mercury at various equivalence ratios for TXL and WYC. The elemental mercury for TXL and WYC is 0.8 and 0.7 $\mu g/m^3$ at stoichiometry, and it fluctuates to a maximum of 1.2$\mu g/m^3$ for TXL. It is interesting to note that total mercury for TXL is higher than that for WYC, which means the oxidized fraction of mercury is greater for TXL than that for WYC, which is evident from the Figure ***11.5.3***.

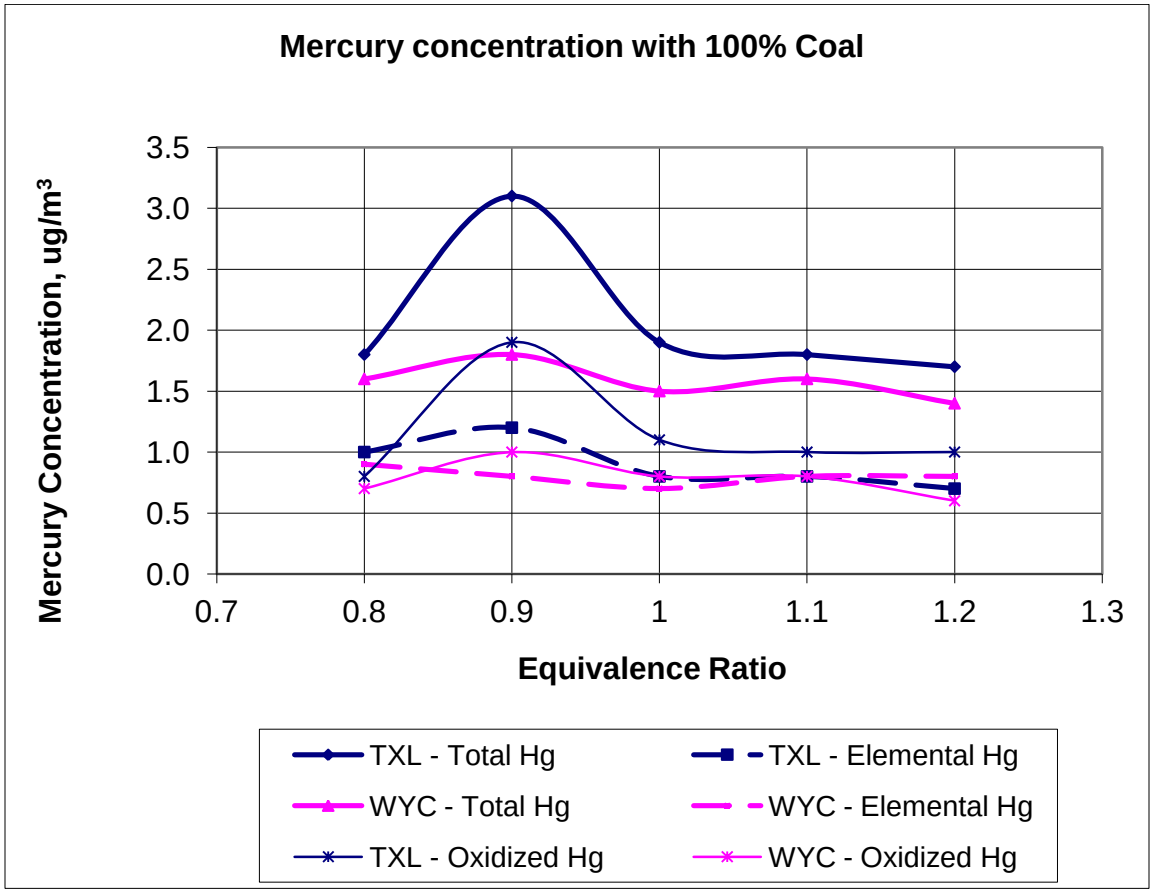

Figure 11.5.2. Base case mercury results for Coal

Blending TXL with DB

TXL when blended with DB, causes increased chlorine content in the fuel which aids mercury oxidation and hence reduction in elemental mercury. Figure ***11.5.3*** show the variation of elemental mercury for TXL with different blends of DB at various equivalence ratios.

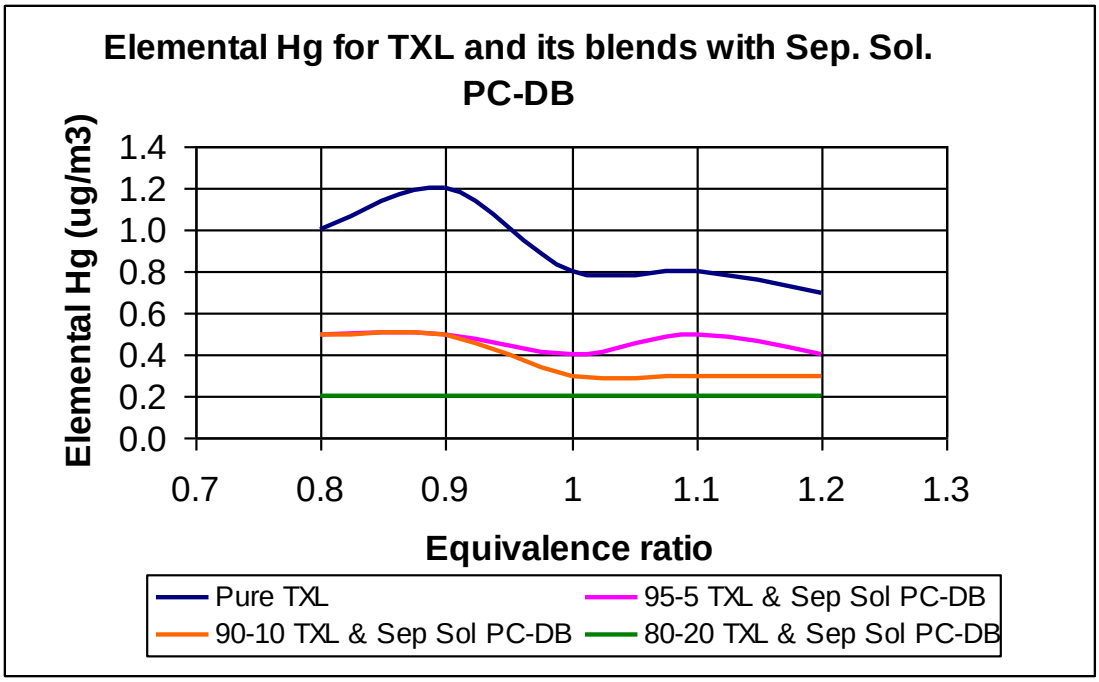

Figure 11.5.3. Elemental Hg for TXL and its blends with Sep. Sol. PC-DB

Blending WYC with DB

When WYC is blended with DB, similar reduction in elemental mercury occurs due to increase in chlorine content in the fuel. Figure ***11.5.4*** and **Error! Reference source not found.** show the elemental mercury for WYC when mixed with DB at different ratios and various equivalence ratios.

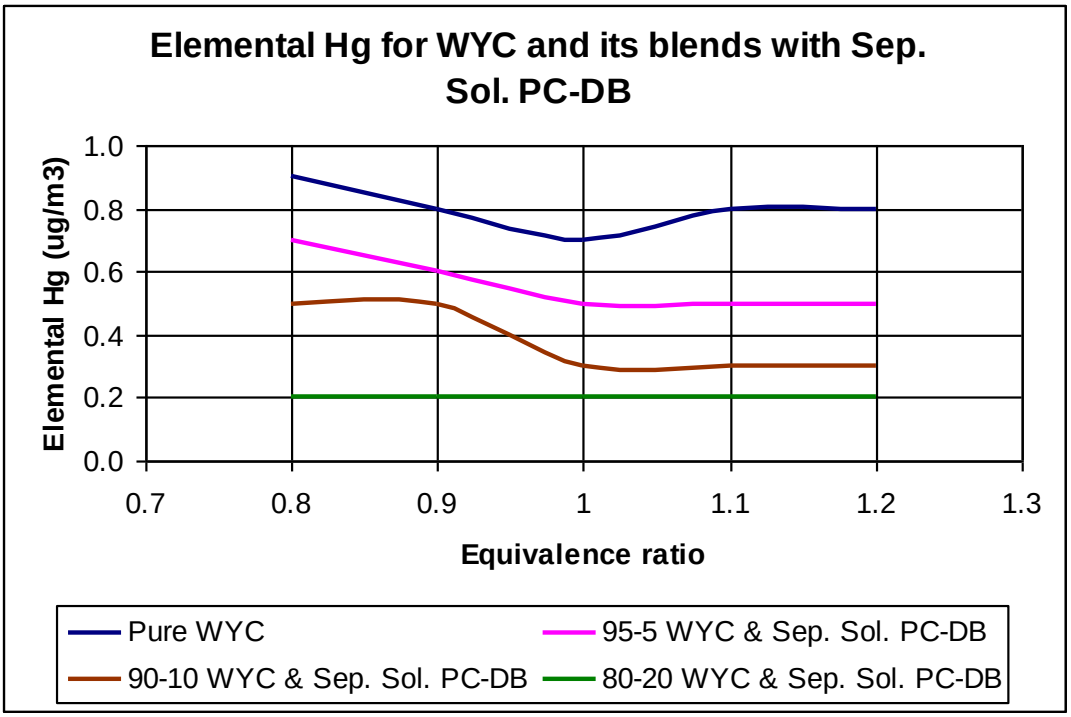

Figure 11.5.4. Elemental Hg for WYC and its blends with Sep. Sol. PC-DB

From figures Figure ***11.5.3***,Figure ***11.5.4*** Figure ***11.5.5*** and Figure ***11.5.6*** a very obvious trend can be easily observed, which is, as DB ratio in the blend increases, the elemental mercury concentration falls. And also seen is that, for 80-20 blend of any coal with any DB, the elemental mercury is at its least value ($0.2\mu g/m^3$). This level of mercury concentration is very low and near the resolution of the mercury measuring instrument. It can be deduced that at 80-20 blend of coal and DB, there is more than sufficient chlorine in the blend to almost completely oxidize all elemental mercury to oxidized mercury during or immediately after combustion.

Effect of Blend ratios

As discussed in the previous section, increasing fractions of DB in blended mixtures of coal and DB, increases the chlorine content which causes increased mercury oxidation, hence reduction in elemental mercury. This result is presented in Figure ***11.5.5***. It can be observed that elemental mercury is least for 80-20 blend of coal and DB, and though elemental mercury concentration falls rapidly from pure coal firing to 90-10 coal and DB blend, beyond 90-10 blend until 80-20 blend the change is not very much.

The reduction in elemental mercury concentration due to blending of DB to coal could occur for two reasons, the first being presence of more chlorine species in the fuel blend which causes increased mercury oxidation and hence reduction in elemental mercury, and secondly due to reduced mercury input during firing. DB has very low mercury content compared to coal; hence in 80-20 coal and DB blend, the mercury input from coal is reduced by 20% which may yield reduced mercury emissions. To understand this fact, a plot of mercury emitted on energy basis (mg/GJ) is presented in Figure ***11.5.6*** which shows not much significant change from the trend as discussed on mercury concentration levels with blend ratios.

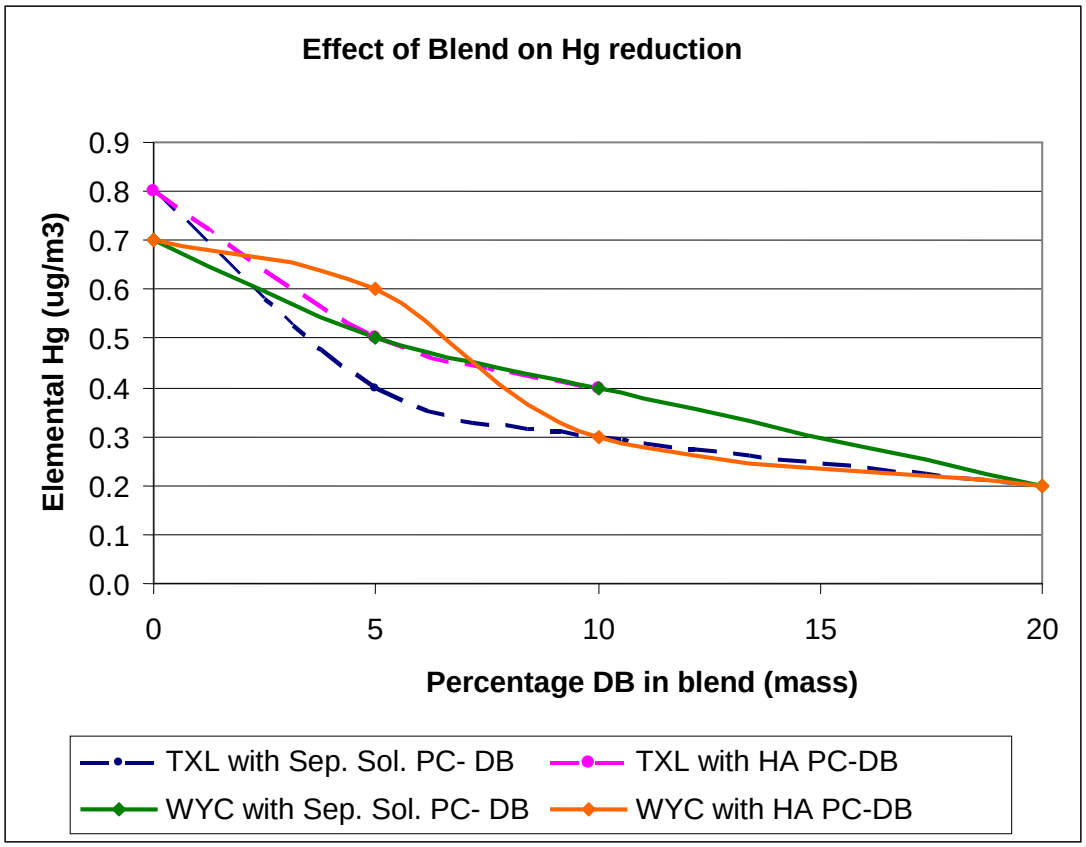

Figure 11.5.5. Effect on elemental mercury (μg/m^3) when blending DB with coal on flue gas concentration basis

Figure ***11.5.6*** shows the effect of elemental mercury with amount of chlorine in the fuel. As DB in fuel blend increases, the chlorine content increases linearly which increases oxidation of mercury and hence reduce elemental mercury concentration.

Effect of NOx on mercury

It is stated that NOx inhibits mercury oxidation. Figure ***11.5.7*** shows the variation of elemental mercury with NOx under for selected fuels and equivalence ratio. The trend of mercury variation is not very clear with varying NOx in the flue gas.

Other Observations

Mercury speciation depends on lot of factors such as presence of ash, ash constituents, refractory type used in boiler, unburnt carbon during combustion and several others which is yet to be investigated and reasoned. The factors though found to play a role, due to unpredictable behavior of mercury in presence of innumerous factors, it still remains a mystery.

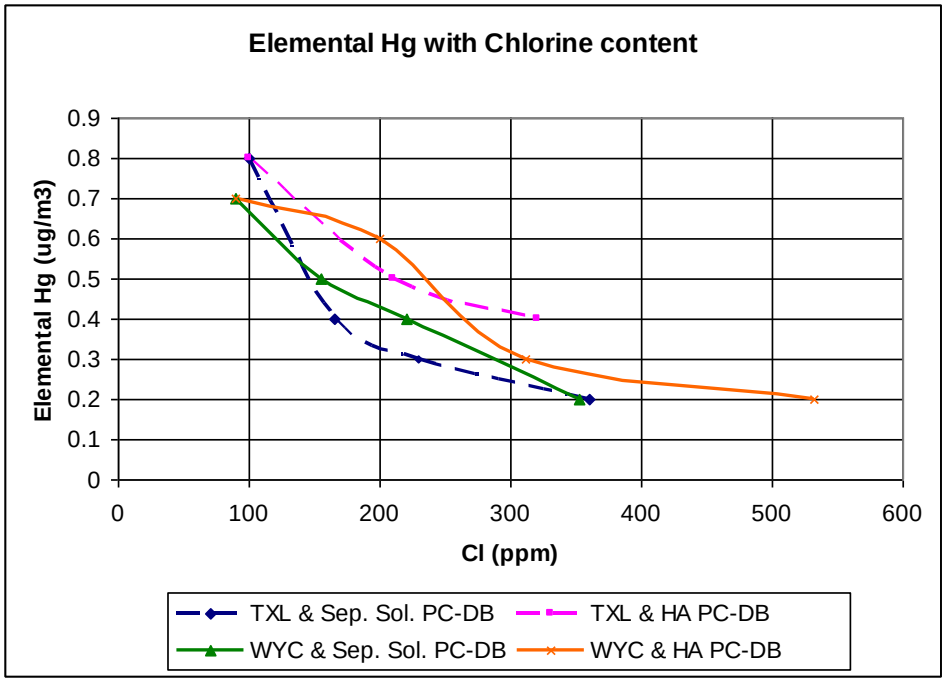

Figure 11.5.6. Effect on elemental mercury with chlorine content in fuel

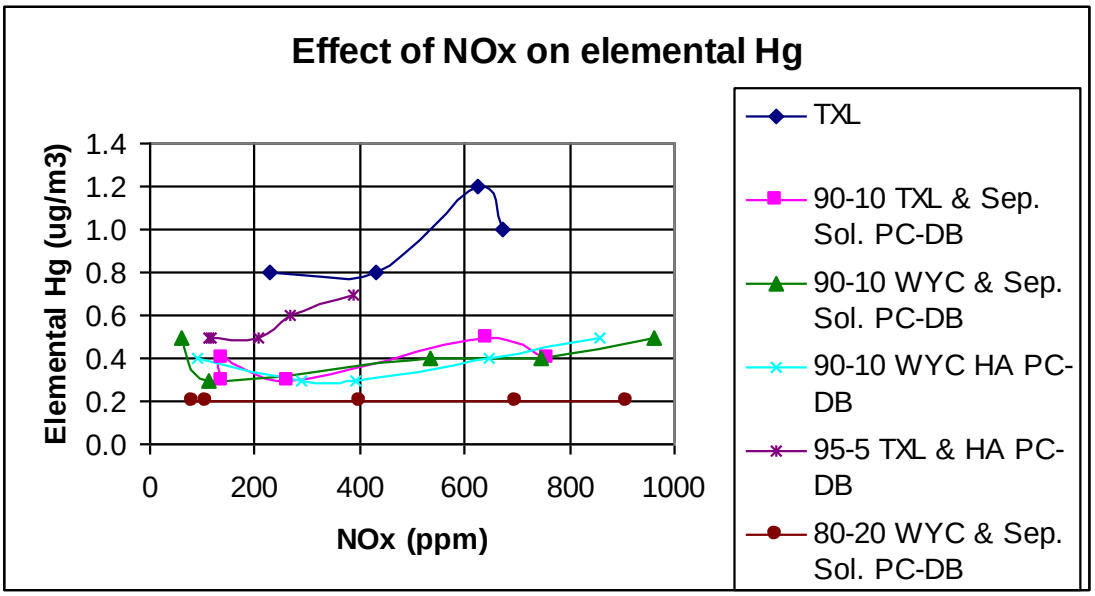

Figure 11.5.7. Effect of NOx on elemental mercury

During one day of co-firing experiments, 4 different blends of were tested in period of 6 hours. The summary of results of elemental mercury with respect to time is reported in table 5.2. It is seen that with change of fuel from 95-5 WYC and HA PC-DB blend to 80-20 blend there is significant reduction in elemental mercury from 0.8 $\mu g/m^3$ to 0.2 $\mu g/m^3$ as expected, which is assumed to be largely due to

presence of chlorine and hence mercury oxidation. The next fuel fired was 100% pure WYC, for which mercury measured was around 0.4 μ/m^3, but pure WYC burned all day on another day measured 0.8 $\mu g/m^3$. This difference in measured value may be due to firing of high ash fuels during previous cases which might have deposited ash on the refractories which has the possibility to capture elemental mercury on its surface and re-emit at a later point of time. However the prediction is not certain.

Table 11.5.2. Mercury measurements with time

	Equivalence ratio	Time	Total Hg	Elemental Hg
95:5 WYC-HA PC-DB	1	10:32	1.8	0.6
	0.9	10:44	1.7	0.8
	0.8	10:58	2.0	0.7
	1.1	11:18	1.3	0.7
	1.2	11:34	1.3	0.7
90:10 WYC-HA PC-DB	1	13:20	1.0	0.3
	0.9	13:32	1.1	0.4
	0.8	13:44	0.9	0.5
	1.1	13:56	1.3	0.3
	1.2	14:12	1.2	0.4
80:20 WYC-HA PC-DB	1	15:02	1.5	0.2
	0.9	15:15	1.0	0.2
	0.8	15:25	1.3	0.2
	1.1	15:48	1.3	0.2
100% WYC	0.9	16:22	1.5	0.3
	1	16:30	1.3	0.4
	1.2	16:42	1.4	0.4

Hg Emissions during Reburn

{ Reader must refer to Chapter/Section on Reburn for more details on reburn process; more details on Hg reduction with reburn is given in Hyukjin et al [2011]}

Emissions, captures and removals of Hg^0 are studied under the variation of reburn fuels and equivalent ratios in the RBZ. WYC was used as the primary fuel, and the mixtures of DB and WYC were used as the reburn fuels. The baseline concentration of Hg^0 in the PRC was found to be between 5.3 and 6 $\mu g/m^3$ (or 1.47 and 1.67 mg/GJ). Figure ***11.5.7*** and Table. 7 present the Hg^0 emissions and removals with various equivalence ratios (ϕ_{RCR}) during the

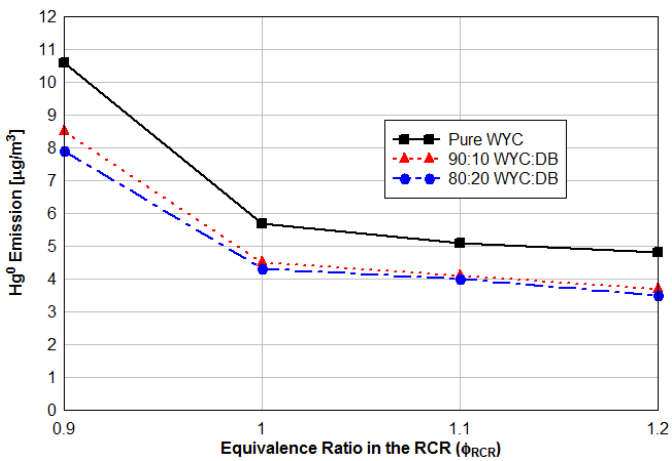

Figure 11.5.8.. Hg emissions using dairy biomass (db) and prb/wyc as reburn fuels

The results show the Hg^0 emissions at $\phi_{RCR} = 0.9$ are higher than the baseline Hg^0 concentration ((Figure 11.5.8). Complete combustion is expected in the fuel-lean combustion or excess of oxygen, and thus almost all of the Hg in WYC is released resulting in high Hg^0 concentration. In addition, the excess air can burn the unburned carbons (UBCs) present on the refractory walls in the furnace and causes the release of even more Hg^0. At $\phi_{RCR} \geq 1.0$, the combustion is incomplete and large amounts of the UBC are presented in the flue gas, which indicates a higher retention of gaseous Hg^0 and therefore the Hg^0 removals. As a result, the more amounts of the UBC, the more captures of Hg^0 in the flue gas and the higher Hg^0 removals. Thus, it was found that the effect of the UBC on the Hg^0 removals was significant.

The peak concentrations of the Hg^0 were observed at $\phi_{RCR} = 0.9$ and about 10.6 $\mu g/m^3$ for pure WYC. With an increase in the proportion of the DB in the reburn fuels, the amounts of Cl increase while those of Hg decrease, hence the Hg emissions were reduced. However, it appears that the effect of the UBC is much stronger on Hg removals than that of Cl. The Hg emissions on a heat basis [mg/GJ] were used for obtaining the Hg removals (%) in the fuel-rich conditions during the reburn process as presented in

Table 11.5.3. The mixture of 10% DB and 90% WYC achieved 20 ~ 36% of Hg removals, and the addition of 20% DB achieved 28 ~ 43% of Hg removals. It can be expected that the results of TXLC cases show higher Hg emissions than those of WYC cases because TXLC contains more amounts of Hg and less amounts of Cl than WYC. Consequently, the use of the DB as a reburn fuel is effective on Hg removals in addition to NO_x reduction.

Table 11.5.3. Hg removals in fuel-rich conditions with wyc as the primary fuel-reburn[Hyukjin et al 2011]

Reburn fuel	Hg removals [%]		
	ϕ_{RCR} = 1.0	ϕ_{RCR} = 1.1	ϕ_{RCR} = 1.2
Pure WYC	8.0	21.4	25.2
90:10 WYC:DB	19.6	28.5	36.3
80:20 WYC:DB	28.0	34.9	42.9

Bench Scale Experimental Results with DB char

As indicated in Figure 11.5.9, the adsorption rates for both types of chlorinated carbon almost match and therefore remain within the range of uncertainty. The 20g of chlorinated carbon would have been expected to have a higher storage capacity for mercury adsorption and therefore show better results for mercury adsorption over time. But especially during period I the 10g sample yields a better mercury adsorption than using 20g. At a certain point of time (in this case roughly 25min) a change occurred and from then for 20g the adsorption rate was better compared to 10g (Period II). One reason for this phenomenon might be, that canals formed inside the chlorinated carbon, through which the nitrogen flow passed through. So only the chlorinated carbon, which formed the walls for the canals was able to adsorb mercury. This effect is considered to be stronger for 20g of chlorinated carbon, since nearly the whole tube was filled with chlorinated carbon. A possible explanation that the 20g do better in the end might be, that as time goes by and more and more carbon accumulates on the surface of the canals diffusion becomes more important. The mercury disperses over the whole chlorinated carbon and when the 10g of carbon were almost completely saturated and this effect continued for 20g. It can also be concluded, that Sauter mean diameter doesn't seem to have a significant influence. Sauter mean diameter of DB-CH-N2 for the 20g at 15°C case was the lowest of all determined (221.2µm) and Sauter mean diameter of DB-CH-N2-H2O for 20g at 15°C was the highest of all determined (410.5µm). But further investigations would have to be made to prove this. The mercury adsorption at 15°C was much lower compared to the adsorption at 15°C. For the 15°C case, mercury adsorption rate started off at almost 100% whereas for 150°C the initial mercury adsorption varied between 20% and 40%, depending on the case (Figures not shown; more details in report by Jaeger, 2008] . It can be seen from Figure 16 and Figure 17, that for the 150°C case mercury adsorption was always lower, compared to the adsorption rates at 15°C.

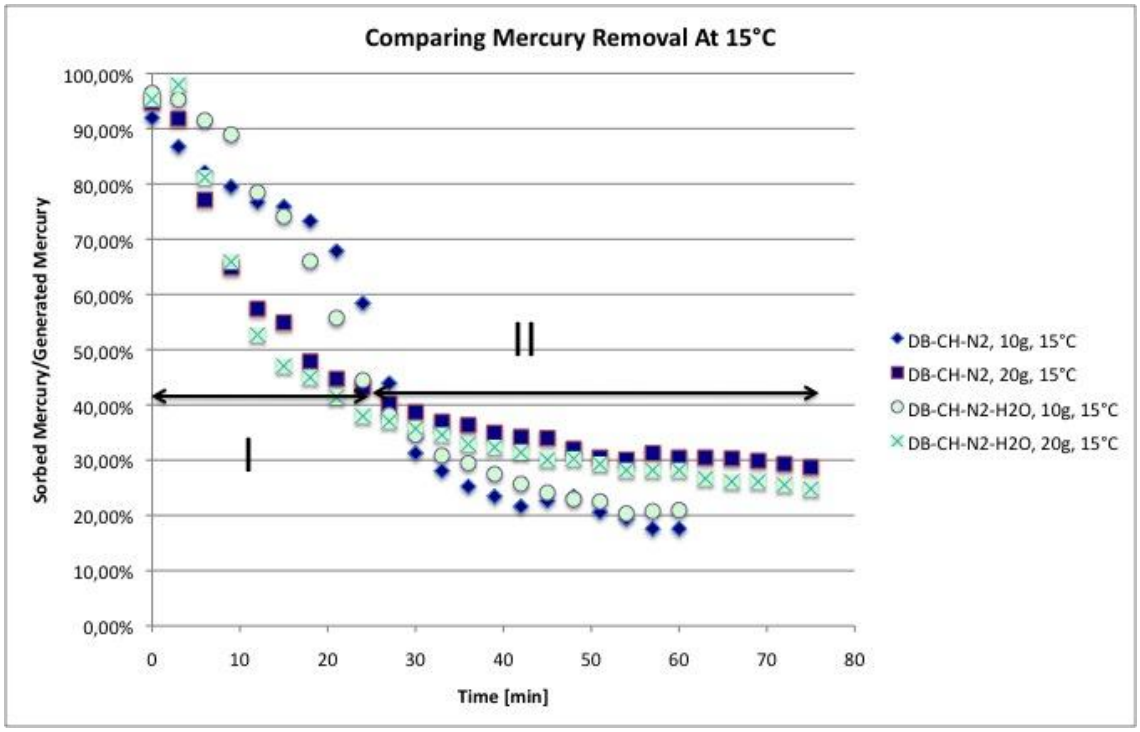

Figure 11.5.9. Sorbed Hg Fraction: 15°C case for both chlorinated carbons

11.6. Impact on Tasks due to Industrial Advisory Committee feed back

1. "Investigating the idea to create higher value –manure over coal is value of Cl to remove Hg from exhaust streams; High Hg chlorine manure equals high Cl in powdered concentrated carbon. New driver is potential to remove Hg using FB" .The current task is based on this feed back in order to increase the potential of FB and DB as fuel in power plants.
2. "Probably will be CO2 regulations added to Hg regulations.." The present work presents results on the effect of adding FB and DB in coal fired systems and the reduction of Hg

11.7. Summary and conclusions

After conducting the study of mercury reduction using dairy biomass blends in coal, it was determined that increase in biomass to coal-biomass blends aids in mercury oxidation. To summarize, elemental Hg reduces by

i) 75% from pure TXL to 80:20 blend of TXL:LA PC-DB, where oxidized Hg is as high as 88%
ii) 72% from pure WYC to 80:20 blend of WYC:LA PC-DB, where oxidized Hg is as high as 87%
iii) Increasing in biomass causes increased ash loading, which is evident from the following:
iv) 80:20 blend of TXL:LA PC-DB increases ash by 6% to pure TXL
v) 80:20 blend of TXL:HA PC-DB increases ash by 85% to pure TXL
vi) 80:20 blend of WYC:LA PC-DB increases ash by 33% to pure WYC

vii) 80:20 blend of WYC:LA PC-DB increases ash by 192% to pure WYC

The optimum fuel blend would be coal and Sep. Sol. PC-DB in a blend ratio of 90:10 on mass basis without much compromise on ash while achieving good mercury reduction, which is evident from the following:

viii) 80:20 blend of TXL:LA PC-DB increases ash by 6% to pure TXL
ix) 80:20 blend of TXL:HA PC-DB increases ash by 85% to pure TXL
x) 80:20 blend of WYC:LA PC-DB increases ash by 33% to pure WYC
xi) 80:20 blend of WYC:LA PC-DB increases ash by 192% to pure WYC
xii) NOx and SOx do not any evident effect in mercury oxidation
xiii) Ash plays a role in aiding mercury oxidation which is evident from low elemental Hg in 100% WYC seen immediately after burning 80-20 WYC high ash blend.
xiv) During reburn tests, the effect of unburned carbon (UBC) on Hg emissions was found to be significant. The more amounts of the UBC, the more captures of Hg0 in the flue gas and the higher Hg0 removals
xv) During reburn tests, with an increase in the proportion of the DB in the reburn fuels, the amounts of Cl increase while those of Hg decrease; hence the Hg emissions were reduced.

11.8. Acronyms and symbols

A	Ash
AF	Air Fuel Ratio
ASTM	American Society for Testing and Materials
BF	Burnt Fraction
CB	Cattle biomass
CBEL	Coal and Biomass Energy Laboratory
DAF	Dry Ash Free
DB	Dairy Biomass
DOE	Department of Energy
DSC	Differential Scanning Calorimetry
EPA	Environmental Protection Agency
FB	Feedlot biomass (Cattle manure or Cattle Biomass CB)
FC	Fixed Carbon
HA-FB-PC	High Ash Feedlot Biomass Partially Composted
HA-FB-Raw	High Ash Feedlot Biomass Raw form
HHV	Higher or Gross heating value
HV	Heating value
LA-FB-PC	Low Ash Feedlot Biomass Partially Composted
LA-FB-Raw	Low Ash Feedlot Biomass

LAHP	Low ash/High Phosphorus feedlot biomass
LALP	Low ash/Low Phosphorus feedlot biomass
LOI	Loss on ignition or % carbon in bottom and fly ash
mmBTU	million BTU
NETL	National Energy Technology Laboratory
NG	Natural gas
PC	Partially composted (45 days)
Pf	pulverized fuel fired
ϕ	Equivalence ratio
ϕ_{RBZ}	Equivalence ratio in the reburn zone
ϕ_{RSZ}	Equivalence ratio in the reburn supply zone
PM	particulate matter
PRZ	Primary combustion zone
RBZ	Reburn combustion zone
RM	Raw Manure
SA	Secondary Air
SCFH	Standard Cubic Feet per Hour
SMD	Sauter mean diameter
SR	Stoichiometric ratio, Air: Fuel/ (Air: Fuel) $_{stoich}$
TAMU	Texas A&M University
TCEQ	Texas Commission on Environmental Quality
TEES	Texas Engineering Experiment Station
TGA	Thermo-Gravimetric Analysis
TXL	Texas lignite coal
USDA	US Dept of Agriculture
VM	Volatile matter
WYC	Wyoming coal

11.9. References

Agarwal, H., Stenger, H. G., Wu, S., and Fan, Z., 2006, "Effects of H2O, SO2 and NO on Homogeneous Hg Oxidation by Cl2," Energy & Fuels, 20, pp. 1068-1075.

Annamalai, K and Sweeten, J M, A Reburn System with Feedlot Biomass, TAMUS 1726, patent to be issued by US Patent Office, July 2005

Bragg, L.J., Oman, J.K., Tewalt, S.J., Oman, C.L., Rega, N.H., Washington, P.M., and Finkelman, R.B., 1998, The U.S.Geological Survey Coal Quality (COALQUAL) Database -- Version 2.0: U.S.Geological Survey Open-File Report 97-134

Cao, Y., Duan, Y., Kellie, S., Li, L., Xu, W., Riley, J. T., Pan, W. P., Chu, P., Mehta, A. K., and Carty, R., 2005, "Impact of Coal Chlorine on Mercury Speciation and Emission from a 100-MW Utility Boiler with Cold-Side Electrostatic Precipitators and Low-NOx Burners," Energy & Fuels, 19(3), pp. 842-854.

Carpi, A., 1997, "Mercury from Combustion Sources: A Review of the Chemical `254

Carpi, Anthony , MERCURY FROM COMBUSTION SOURCES: A REVIEW OF THE CHEMICAL SPECIES EMITTED AND THEIR TRANSPORT IN THE ATMOSPHERE, June 1996

Chu, P., D. B. Porcella, Water, Air, Soil Pollut. 80 (1995) 135-144.

Chu,P., B. Nott, W. Chow, Results and Issues from the Pisces Field Tests, in: 2nd International Conference on Managing Hazardous Air Pollutants, Washington, DC, 1993.

Endress+ and Hauser, Coal Fired Power Plant, http://www.endress.com, August 2007

EPA website: http://www. EPA.gov/ttn/atw/utility/utiltoxpg.html

Feeley, III, T J, Brickett, L A, O'Palko, B A and Murphy, J T, " Field testing of Hg Control Technologies for Coal Fired Plants," DOE/NET Hg R&D Program Review, May 2005.

Finkelman, Robert B. , Joseph E. Bunnell ,Health Impacts of Coal, U.S. Geological Survey Reston, Virginia, September 21, 2003

Gibb, W. H., Clarke, F., and Mehta, A. K., 2000, "Fate of Coal Mercury during Combustion," Fuel Processing Technology, 65, pp. 365-377;

Hall, B., Schager, P., and Lindqvist, O., 1991, "Chemical Reactions of Mercury in Combustion Flue Gases," Water Air & Soil Pollution, 56, pp. 3-14.

http://igs.indiana.edu/Geology/coalOilGas/mercuryInCoal/index.cfm
http://www.epa.gov/hg/effects.htm

Hyukjin Oh, Kalyan Annamalai, John Sweeten, Witold Arnold, " Reburning Of Cattle Manure-Based Biomass With Coals In A Small Scale Boiler Burner Facility For Nox And Mercury Reduction, " Proceedings of the ASME/JSME 2011 8th Thermal Engineering Joint Conference, AJTEC2011-44182, March 13-17, 2011, Honolulu, Hawaii, USA

Jaeger, Andreas, “Sorption Of Elemental Mercury By Chlorinated Carbons Made of Dairy Biomass,” Report submitted to Department of Mechanical Engineering, Texas A&M University, Advisor : Kalyan Annamalai Fa 2008.

Laudal, D. L., Thompson, J. S., Pavlish, J. H., Brickett, L., Chu, P., Srivastava, R. K., Kilgroe, J., and

Lee, C. W., 2003, “Mercury Speciation at Power Plants Using SCR and SNCR Control Technologies,” EM: Air and Waste Management Association's Magazine for Environmental Managers, pp. 16-22.

Levin, Lindqvist, O., Wang, J., and Xiao, Z., Water, Air and Soil Pollution, 80: 1217-1226, 1995L., Atmospheric Mercury Research Update, Final Report, EPRI, March 2004

Linak, W. P., Ryan, J. V., Ghorishi, B. S., Wendt, J. O. L., 2001, Issues Related to Solution Chemistry in Mercury Sampling Impingers, J. Air & Manage. Assoc., 51, 688-698.
Lindqvist, O., Wang, J., and Xiao, Z., Water, Air and Soil Pollution, 80: 1217-1226, 1995

Mahaffey, Kathryn R. Robert P. Clickner, Catherine C. Bodurow, Blood organic mercury and dietary mercury intake: National Health and Nutrition Examination Survey, 1999 and 2000

Meji,R., H. J. V. Leo, W. Henk, J. Air Waste Manage. Assoc. 52 (2002) 912-917

Mojtahedi, W., Backman, R., and Larjava, K., Technical Research Center of Finland, Publications 42, 1987

Puchakayala, Madhu Babu , “Mercury Emission Behavior During Isolated Coal Particle Combustion, “ Doctor Of Philosophy (PhD) , Mechanical Engineering , Texas A&M, December 2006.

Sable, S. P., de Jong, W., Meij, R., and Spliethoff, H., 2007a, “Effect of Secondary Fuels and Combustor Temperature on Mercury Speciation in Pulverized Fuel Co-Combustion: Part 1,” Energy & Fuels, 21(4), pp. 1883-1890.

Sable, S. P., de Jong, W., Meij, R., and Spliethoff, H., 2007b, “Effect of Air-Staging on Mercury Speciation in Pulverized Fuel Co-combustion: Part 2,” Energy & Fuels, 21(4), pp. 1891-1894]

Senior, C. L. , A. F. Sarofirm, T. Zeng, J. J. Helble, R. Mamani-Paco, Fuel Process. Technol. 63 (2000) 197-213.

Senior, C.L., and Alfonso, R.F.: “Validation of Fundamentally based Model for Mercury Emission from Coal-fired Power Plants Using ICR Data,” Proceedings of the 94th A&WMA Annual Meeting and Exhibition, Air & Waste Management Association, Pittsburgh, PA, USA, 2001.

Udayasarathy, A, “Mercury Emission Control for Coal Fired Power Plants using Coal and Biomass” Hg Emissions from Coal and Animal wastes, “Master Of Science (MS), Mechanical Engineering, Texas A&M University, College Station, TX, Dec. 2007

Wilhelm, S. M., 1999, Generation and Disposal of Petroleum Processing Waste that contains Mercury, Environ. Prog, 18 (2), 130-143.

www.iit.edu/~ipro356s05/bg_sources.html

11.10. Education and training

1. Madhu Babu Puchakayala , "Mercury Emission Behavior During Isolated Coal Particle Combustion, " Doctor Of Philosophy (PhD) , Mechanical Engineering , Texas A&M, December 2006.
2. Udayasarathy, A, "Mercury Emission Control for Coal Fired Power Plants using Coal and Biomass" Hg Emissions from Coal and Animal wastes, "Master Of Science (MS), Mechanical Engineering, Texas A&M University, College Station, TX, Dec. 2007
3. Christopher Rynio," Impact Of Co-Firing Coal/Biomass Blends On Elemental Mercury Emission," German Exchange Student MEEN 685 Report, Fa. 08

11.11. Other support if any

Only those Hg reduction presented here.

{ This list is same as those listed under Reburn task report since the projects deal with both NOx and Hg}

Feedlot Biomass: A Reburn Fuel For "Maximum NOx" Reduction In Coal-Fired Power Plants, Kalyan Annamalai, Dept. of Mechanical Engineering, Texas A&M University, and John Sweeten, Texas Agricultural Experiment station, Texas A&M Agricultural Research Extension Center, Amarillo, Texas, Texas Commission on Environmental Quality, 3/2005-5/2007; TCEQ Grant # 582-5-65591 0015
$ 341,933

Development And Application Of New Optical Sensors For Measurements Of Mercury Concentrations, Speciation, And Chemistry, Department of Energy, Robert Lucht of Purdue University, J. Caton and K. Annamalai of TAMU, 2004-2008, ($ 400,000 from DOE); Subcontract to TAMU: J. Caton and Annamalai, $135,480

11.12. Dissemination

{ A few publications are also cross listed under other Sections/Chapters}

Book/ Chapters

1. Combustion Science and Engineering, 18 Chapter book on "Combustion Science and Engineering," by Annamalai, Kalyan and Puri, Ishwar, pages: 1121, Taylor and Francis, Orlando, Florida; ISBN: 0849320712; Dec 2006

2. Annamalai, A. Udayasarathy, Hyukjin and Sweeten, JM, ," Mercury Emission And Control For Coal Fired Power Plants, pp 205-217, ISBN 978-81-8487-014-5, Book Edited Agarwal, AK, Kushari, A, Aggarwal, S K and Ruchai , AK, Narosa Publishing House, New Delhi,2009.

Journal Publications printed, accepted, {subject area in parenthesis}

19. Magnuson, Jesse; Anderson, Thomas; Lucht, Robert, Vijayasarathy, Udayasarathy; Oh, Hyukjin; Annamalai, Kalyan; Caton, Jerald Title: "Application of a Diode-Laser-Based Ultraviolet Absorption Sensor for In Situ Measurements of Atomic Mercury in Coal Combustion Exhaust", Energy & Fuels, 22, pp 3029–3036, 2008

Full paper refereed Conference Proceedings and Publications

20. Hyukjin Oh, Annnamalai, K., John M. Sweeten, Christopher Rynio, and Witold Arnold, "Combustion Of Cattle Biomass As A Supplementary Fuel In A Small Scale Boiler Burner Facility For Nox And Mercury Reduction, " IMECE2009-12626, Proceedings of IMECEC2009, 2009 ASME International Mechanical Engineering Congress and Exposition, November 13-19, Lake Buena Vista, Florida, USA.
21. Kalyan Annamalai, , "Thermo-chemical Energy Conversion of Coal, Animal Waste Based Biomass, and Coal:Biomass Blends, " 19th National & 8th ISHMT-ASME Heat And Mass Transfer Conference, January 3 - 5, 2008, ASME -ISHMT, Hyderabad, India , Jan 3-5, 2008.
22. K. Annamalai, N.T. Carlin, H. Oh, G. Gordillo Ariza, B. Lawrence, And U. Arcot V, J.M. Sweeten K. Heflin, W.L. Harman " Thermo-Chemical Energy Conversion Using Supplementary Animal Wastes With Coal , ", Invited Key Note Presentation, 2007 ASME International Mechanical Engineering Congress and Exposition, November 11-15, 2007 Seattle, Washington, USA; IMECE2007-43386; CROSS LISTED UNDER INVITED LECTURE
23. Giacomo Colmegna, Kalyan Annamalai, Udayasarathy Arcot V , "Hg Reduction During Reburn Process With The Use Of Cattle Biomass As A Reburn Fuel, " The 3rd International Green Energy Conference, IGEC-2007, Västerås, Sweden, June 17-20, 2007.

Conference Publications Under review , {subject area in parenthesis}

24. Hyukjin Oh, Kalyan Annamalai, John Sweeten, Witold Arnold, " Reburning Of Cattle Manure-Based Biomass With Coals In A Small Scale Boiler Burner Facility For Nox And Mercury Reduction, " Proceedings of the ASME/JSME 2011 8th Thermal Engineering Joint Conference, AJTEC2011-44182, March 13-17, 2011, Honolulu, Hawaii, USA (NOx and Hg Reduction)

Abstract reviewed Conference Publications and other non-reviewed Proceedings

25. Hyukjin Oh, Kalyan Annamalai1*, John M. Sweeten, Christopher Rynio(Ruhr-Universität-Bochum, Bochum, Germany 44780) , "Co-Combustion of Animal Wastes and Coals in a 30 kWt Boiler Burner Facility for Reductions of NOx and Mercury Emissions, " 11E4, US national Combustion Meeting, Ann Arbor, MI , May 17-20, 2009.
26. Kalyan Annamalai Invited participant for Combustion Work shop," Mercury Emission And Control For Coal Fired Power Plants, " Dec 31-Jan 2, 2008, Indian Inst of Technology (IIT), Kanpur, India. (CROSS LISTED UNDER INVITED SEMINARS)
27. Jesse K. Magnuson, Thomas N. Anderson, Robert P. Lucht, School of Mechanical Engineering, Purdue University , Udayasarathy A. Vijayasarathy, Hyukjin Oh, and Kalyan Annamalai,Texas A&M University, "Application of a diode-laser-based ultraviolet absorption sensor for in situ measurements of atomic mercury in coal combustion exhaust, "Paper G02 – Diagnostics, 5th US Combustion Meeting, March 25-28, 2007.

11.13. Patents/disclosures if any

1.Disclosure of Invention # 04-TAMUS Disclosure # 2300, 2005 - Hg Reduction in Coal Fired Plants Using Trace Amounts of Animal Waste Derived Biomass Fuels (AWDBF)